

Hong-Wu He · Hao Peng
Xiao-Song Tan

Environmentally Friendly Alkylphosphonate Herbicides



Chemical Industry Press



Springer

Environmentally Friendly Alkylphosphonate Herbicides

Hong-Wu He · Hao Peng
Xiao-Song Tan

Environmentally Friendly Alkylphosphonate Herbicides



Chemical Industry Press



Springer

Hong-Wu He
Hao Peng
Xiao-Song Tan
Key Laboratory of Pesticide and Chemical
Biology, Ministry of Education
Institute of Pesticide Chemistry
College of Chemistry
Central China Normal University
Wuhan
China

ISBN 978-3-662-44430-6 ISBN 978-3-662-44431-3 (eBook)
DOI 10.1007/978-3-662-44431-3

Library of Congress Control Number: 2014947653

Springer Heidelberg New York Dordrecht London

Jointly published with Chemical Industry Press, Beijing
ISBN: 978-7-122-21381-5, Chemical Industry Press, Beijing

© Chemical Industry Press, Beijing and Springer-Verlag Berlin Heidelberg 2014

This work is subject to copyright. All rights are reserved by the Publishers, whether the whole or part of the material is concerned, specifically the rights of translation, reprinting, reuse of illustrations, recitation, broadcasting, reproduction on microfilms or in any other physical way, and transmission or information storage and retrieval, electronic adaptation, computer software, or by similar or dissimilar methodology now known or hereafter developed. Exempted from this legal reservation are brief excerpts in connection with reviews or scholarly analysis or material supplied specifically for the purpose of being entered and executed on a computer system, for exclusive use by the purchaser of the work. Duplication of this publication or parts thereof is permitted only under the provisions of the Copyright Law of the Publishers' location, in its current version, and permission for use must always be obtained from Springer. Permissions for use may be obtained through RightsLink at the Copyright Clearance Center. Violations are liable to prosecution under the respective Copyright Law. The use of general descriptive names, registered names, trademarks, service marks, etc. in this publication does not imply, even in the absence of a specific statement, that such names are exempt from the relevant protective laws and regulations and therefore free for general use.

While the advice and information in this book are believed to be true and accurate at the date of publication, neither the authors nor the editors nor the publishers can accept any legal responsibility for any errors or omissions that may be made. The publishers make no warranty, express or implied, with respect to the material contained herein.

Printed on acid-free paper

Springer is part of Springer Science+Business Media (www.springer.com)

Foreword

Agrochemicals are used to safeguard our agricultural products from damages caused by weeds, diseases, or insects. The use of herbicides enables us to optimize the labor utilization and to ensure both high yields and good quality of crops. After repetitive application of herbicides over many years, the appearance of herbicide-resistant weeds has become a difficult problem confronting us. Currently, hundreds of herbicides have been available on the market, but their modes of action toward target weed species are rather limited. This situation calls for further research to discover highly active, environmentally friendly herbicides with novel modes of action.

Pyruvate dehydrogenase complex (PDHc) is one of the most important oxidoreductases in living organisms. It catalyzes the oxidative decarboxylation of pyruvate to form acetyl CoA, which is a pivotal process in cellular metabolism. PDHc has been reported as a potential target enzyme affected by some herbicidally active compounds. Regrettably, the PDHc inhibitors reported so far were not as active as other commercial herbicides. Therefore PDHc as a potential herbicidal target needs further investigation.

Professor Hong-Wu He is a renowned scientist in the field of pesticide science in China. She is an expert in phosphorus chemistry and pesticide innovation, for which she has received many national honors. She is the first one in China to initiate research projects in the field of novel PDHc inhibitors as potential herbicides. Through the systematic studies on molecular design, synthetic methodology, structural optimization, bioscreening, modeling etc., Professor He's group discovered a new environmentally friendly herbicide, namely clacyfos (HW02), which has the characteristics of low toxicity, low residue, and is highly safe to bees, birds, fishes, and silkworm etc. As a new PDHc inhibitor, clacyfos exhibits a different mode of action and shows no cross-resistance toward other conventional herbicides. Clacyfos has been approved in 2007 as a new post-emergence herbicide by the Ministry of Agriculture of China. It is expected that clacyfos will play a significant role in weed control.

In this book, Prof. Hong-Wu He and co-authors systematically introduce their work on the PDHc inhibitor clacyfos, from its discovery, development to commercialization. This monograph is hereby highly recommended to our colleagues and graduate students in the fields of pharmaceutical and pesticide research, phosphorus chemistry, chemical biology, life sciences, and etc. It will bring new insights into the discovery of a novel herbicide, and the complex interdisciplinary work involved. I thank the authors for sharing their expertise and experience with us, which will surely be valuable for our future research.

A handwritten signature in black ink, reading "Zhengming Li". The signature is written in a cursive style with a large, stylized initial "Z" and a long horizontal stroke at the end.

April 2013

Zheng-Ming Li
Nankai University

Preface

With the human population explosion, the safeguarding of the world's present and future food supplies is a major problem facing mankind. Therefore enhancing the crop yields is becoming increasingly necessary. Herbicides as one of the important tools for crop protection have made a major contribution to the advancement of agriculture around the world including China. The widespread and overuse of herbicides for weed control over the past few decades has resulted in the rapid development and proliferation of herbicide-resistant weeds. It is worthy noting that there are more than 290 commercial herbicides on the market, but only a limited number (only 25) of target sites for those herbicides to work on. Biotypes of numerous susceptible weed species are now resistant to one or more herbicides. The advent of genetic engineering is currently revolutionizing this paradigm by enabling the use of nonselective herbicides on crops, that have been genetically altered to be resistant to certain compounds. The benefit, such as ease of use is obvious. However agricultural practices relying on the use of herbicide-resistant crops are leading to shifts in weed populations to naturally resistant species and the transgenic crops are not generally accepted by some countries. Therefore, the need to discover new herbicides continues to be urgent.

To cope with the increasing resistant weeds problem, numerous compounds were generated by modifying the commercial products and hope some of analogs are more potent than their parents. Unfortunately, these new compounds still target on the same sites as their parents do. New herbicides with novel mechanisms of action are hence highly desired to combat with the evolution of resistance in weeds. Finding an environment-friendly herbicide with a novel structure and new target is another challenge.

The pyruvate dehydrogenase complex (PDHc) is one of the most important oxidoreductases in organisms. It catalyzes the oxidative decarboxylation of pyruvate to form acetyl CoA, which is a pivotal process in cellular metabolism. Therefore, targeting on plant PDHc is an interesting approach from the biorational design point of view. PDHc has been reported to be one of the target enzymes affected by some herbicidal compounds. Some acetylphosphinates and acetylphosphonates, which were prepared as potential mechanism-based inhibitors for

plant PDHc E1, showed modest herbicidal activity. However, none of these PDHc inhibitors have been further developed as a herbicide due to either lack of activity, poor selectivity, or unfavorable human toxicity.

Attempts to design desirable PDHc inhibitors as herbicides have been performed in my laboratory for more than 15 years. Previous research showed that some OP compounds could be a powerful PDHc inhibitor. *O,O*-diethyl 1-(substituted phenoxyacetoxy)alkylphosphonates were later identified as the scaffolds for lead structures. Different kinds of alkylphosphonate derivatives including their optically active isomers were then synthesized and tested for their inhibitory potency against PDHc and herbicidal activities. Some alkylphosphonates with excellent herbicidal activity were then found. The binding modes of the alkylphosphonates to PDHc are in good agreement with the theoretical study reported earlier. Through the systematic R&D work, clacyfos, *O,O*-dimethyl 1-(2,4-dichlorophenoxyacetoxy)ethylphosphonate turned out to be the best herbicide candidate against broadleaf weeds and with a safe toxicity profile for mammals and non-target species. Clacyfos received the temporary registration from ICAMA of China in 2007.

This book presents many years of research on environment-friendly alkylphosphonate herbicides designed to inhibit the plant PDHc using biochemical reasoning. The most recent research on pyruvate dehydrogenase complex inhibitors is discussed in this book. Systematic studies from basic research to field application of the novel alkylphosphonate herbicidal candidates are also discussed in this book. It contains certain details about the molecule design, synthesis, biological screening, structure–activity relationship analysis, structural optimization, biochemical mechanism, field trial results, residual analysis, toxicology, and environmental fate. Data suggested that clacyfos could be an environment-friendly herbicide with low toxicity, low residue, and desirable selectivity. The R&D of clacyfos exemplifies how to use biorational design and traditional method to come up with a novel herbicide targeting on plant's PDHc. We hope this book can provide you some valuable information on chemistry, chemical biology, and practical application of alkylphosphonates.

The research introduced in this book was carried out in the Key Laboratory of Pesticide and Chemical Biology, Ministry of Education; Institute of Pesticide Chemistry, College of Chemistry, Central China Normal University, by my research team that includes Associate Professor Xiao song Tan and Dr. Hao Peng, Associate Professor Junlin Yuan, Dr. Shuqing Wan, and Ms. Aihong Lu. Many data cited in this book are from my students' dissertations, including doctoral students: Tao Wang, Ting Chen, Hao Peng, Wei Wang, Chubei Wang, Chuanfei Jin, and Junbo He; and Master students: Xia Hong, Jun Wang, Siquan Wang, Liang Xu, Xufeng Liu, Liping Mong, Meiqiang Li, Guihong Liao, Gangliang Huang, Ping Shen, Yanjun Li, Na Zuo, Xijun Sheng, Gao Ling and Xu Chao. The contributions from my colleagues and students to this book are highly appreciated.

I gratefully acknowledge the financial support for my research work from the following grant funding agencies:

1. National Basic Research Program of China (“973” Program No: 2003CB114400; 2010CB126100).
2. National Natural Science Foundation of China (No: 29572045; 20072008; 20372023; 20772042 and 21172090).
3. National Key Technologies R&D Program of China (No: 97-563-02-05, 2001BA308A02-15; 2004BA308A22-9; 2004BA308A24-9; 2006BAE01A04-07; 2006BAE01A02-9; 2006BAE01A01-10 and 2011BAE06B03).
4. Science and Technology Research Project of Ministry of Education (No. 214607 and 230532).
5. Natural Science Foundation of Hubei Province (No. 90J26; 94J40).

Finally, I am greatly indebted to Prof. Zhaojie Liu for his guidance, advice and encouragement for my research in Central China Normal University. I am very grateful to Prof. Morifusa Eto, who was my advisor when I studied at Laboratory of Pesticide Chemistry, Kyushu University, Japan in 1989. His kind encouragement, guidance, and advice on research work continue to inspire my life. I wish to express my heartfelt appreciation to Prof. Eiichi Kuwano from the Laboratory of Pesticide Chemistry, Kyushu University for his kind suggestions and guidance for my doctoral thesis.

Here I would like to thank Prof. Mitsuru Sasaki from the Department of Bio-functional Chemistry, Kobe University, Japan for his contributive advice for revising the manuscript. I wish to express special appreciation to Prof. Philip W. Lee from DuPont Crop Protection (1978–2008) for his advice on the organization of this book. Many thanks to Prof. Eddie Chio from Eli Lilly and Company (1977–2006) and Prof. Adam Hsu from Rohm and Haas (1982–2002) for their very helpful suggestions for revising the manuscript. Last but not least, my special thanks go to Ms. Carol Ashman (USA) for her efforts in revising and editing the manuscript.

The author hopes that this book would be helpful to researchers, teachers, and students in organic chemistry, pesticide science, and other related fields.

May 2014

Hong-Wu He

Contents

1	Overview	1
1.1	Introduction	1
1.1.1	Mode of Action of Herbicide	5
1.1.2	Herbicide Resistance	5
1.1.3	New Opportunity for Novel Herbicides	6
1.1.4	Basic Methodology for Discovery of Hit/Lead Compounds	9
1.2	Pyruvate Dehydrogenase Complex (PDHc)	10
1.2.1	Function of PDHc	10
1.2.2	Distribution of PDHc	11
1.2.3	Plant PDHc E1 as Site of Action of Herbicide	12
1.3	Progress in the Research of PDHc Inhibitors	13
1.3.1	OP Compounds as Inhibitors of <i>E. coli</i> PDHc	13
1.3.2	OP Compounds as Inhibitors of Plant PDHc	20
1.3.3	Enzyme-Selective Inhibition of OP Compounds	22
1.4	Design of Novel PDHc E1 Inhibitors as Herbicides	23
1.4.1	Selecting Plant PDHc E1 as Target of New Herbicide	23
1.4.2	PDHc E1 Inhibitor Acylphosphonate as Hit Compound	24
1.4.3	Finding Lead Structure IA	25
1.4.4	Optimization Strategy	28
1.5	Book Chapter Organization	36
	References	39
2	Alkylphosphonates	45
2.1	(Alkyl or Substituted Phenyl)Methylphosphonates IA–IF	46
2.1.1	Introduction	46
2.1.2	Synthesis of <i>O,O</i> -Dialkyl 1-Hydroxyalkylphosphonates M2	48

2.1.3	Synthesis of Substituted Phenoxyacetic Acids M4 and Substituted Phenoxyacetyl Chlorides M5	49
2.1.4	Synthesis of IA–IF	51
2.1.5	Spectroscopic Analysis of IA–IF	56
2.1.6	Crystal Structure Analysis of IC-7.	63
2.1.7	Herbicidal Activity of IA–IF	65
2.1.8	Structure–Herbicidal Activity Relationships	87
2.1.9	Herbicidal Activity of IC-22.	89
2.1.10	Summary	90
2.2	Heterocyclymethylphosphonates IG–IJ	91
2.2.1	Introduction	91
2.2.2	Synthesis of IG–IJ	92
2.2.3	Spectroscopic Analysis of IG–IJ	94
2.2.4	Crystal Structure Analysis of IH-18 and IG-21	98
2.2.5	Herbicidal Activity of IG–IJ.	102
2.2.6	Structure–Herbicidal Activity Relationships	111
2.2.7	Herbicidal Activity of IG-21	112
2.2.8	Summary	116
2.3	(1-Phenyl-1,2,4-Triazol-3-yloxyacetoxy) Alkylphosphonates IK	116
2.3.1	Introduction	116
2.3.2	Synthesis of IK	116
2.3.3	Spectroscopic Analysis of IK	118
2.3.4	Herbicidal Activity of IK	119
2.3.5	Summary	119
	References.	119
3	Salts of Alkylphosphonates	123
3.1	Alkali Metal Salts of <i>O</i> -Alkyl Alkylphosphonic Acids IIA–IIE	125
3.1.1	Introduction	125
3.1.2	Synthesis of IIA–IIE	126
3.1.3	Spectroscopic Analysis of IIA–IIE	130
3.1.4	Crystal Structure Analysis of IIB-20	133
3.1.5	Herbicidal Activity of IIA–IIE	133
3.1.6	Summary	149
3.2	Alkali Metal Salts of Alkylphosphonic Acids IIF, IIG and IIH	154
3.2.1	Introduction	154
3.2.2	Synthesis of IIF, IIG and IIH	155
3.2.3	Spectroscopic Analysis of IIF, IIG and IIH	157
3.2.4	Herbicidal Activity of IIF, IIG and IIH	159
3.2.5	Summary	166

3.3	<i>t</i> -Butylammonium Salts of Alkylphosphonates IIIJ	166
3.3.1	Introduction	166
3.3.2	Synthesis of IIIJ	167
3.3.3	Spectroscopic Analysis of IIIJ	169
3.3.4	Crystal Structure Analysis of IIIJ-24	169
3.3.5	Herbicidal Activity of IIIJ	172
3.3.6	Summary	177
	References	177
4	Alkylphosphinates	179
4.1	Alkylphosphinates IIIA–IIIG	180
4.1.1	Introduction	180
4.1.2	Synthesis of Dichloro(Methyl)Phosphine M10	183
4.1.3	Synthesis of <i>O</i> -Methyl (1-Hydroxyalkyl)- Methylphosphinates M12	183
4.1.4	Synthesis of IIIA–IIIG	184
4.1.5	Spectroscopic Analysis of IIIA–IIIG	187
4.1.6	Crystal Structure Analysis of IIIE-9	190
4.1.7	Herbicidal Activity of IIIA–IIIG	191
4.1.8	Summary	204
4.2	Sodium Salts of Alkylphosphinic Acids IIIH	205
4.2.1	Introduction	205
4.2.2	Synthesis of IIIH	206
4.2.3	Spectroscopic Analysis of IIIH	207
4.2.4	Herbicidal Activity of IIIH	209
4.2.5	Summary	213
4.3	[(5-Methylisoxazol-3-yloxyacetoxy)Alkyl]- Methylphosphinates IIIJ	213
4.3.1	Introduction	213
4.3.2	Synthesis of IIIJ	214
4.3.3	Spectroscopic Analysis of IIIJ	215
4.3.4	Herbicidal Activity of IIIJ	216
4.3.5	Summary	218
	References	218
5	Cyclic Phosphonates and Caged Bicyclic Phosphates	221
5.1	Cyclic 1-Hydroxyalkylphosphonates IVA and IVB	222
5.1.1	Introduction	222
5.1.2	Synthesis of IVA and IVB	222
5.1.3	Spectroscopic Analysis of IVA and IVB	224
5.1.4	Crystal Structure Analysis of IVA-3	226
5.1.5	Herbicidal Activity of IVA and IVB	228
5.1.6	Summary	230

5.2	Cyclic Alkylphosphonates IVC–IVF	230
5.2.1	Introduction	230
5.2.2	Synthesis of IVC–IVF	231
5.2.3	Spectroscopic Analysis of IVC–IVF	234
5.2.4	Crystal Structure Analysis of IVC-19	239
5.2.5	Herbicidal Activity of IVC–IVF	241
5.2.6	Summary	259
5.3	Caged Bicyclic Phosphates IVG and IVH	261
5.3.1	Introduction	261
5.3.2	Synthesis of IVG and IVH	261
5.3.3	Spectroscopic Analysis of IVG and IVH	264
5.3.4	Crystal Structure Analysis of IVG-10	266
5.3.5	Herbicidal Activity of IVG and IVH	268
5.3.6	Summary	273
	References.	275
6	Optically Active Alkylphosphonates	279
6.1	Optically Active 1-Hydroxyalkylphosphonates IVB and M2	281
6.1.1	Introduction	281
6.1.2	Asymmetric Synthesis of 1-Hydroxyalkylphosphonates IVB and M2 via Hydrophosphonylation	282
6.1.3	Asymmetric Synthesis of 1-Hydroxyalkylphosphonates M2 via Hydroxylation	289
6.1.4	Summary	291
6.2	Optically Active (Substituted Phenyl)methylphosphonates IA, IE and IF	292
6.2.1	Introduction	292
6.2.2	Synthesis of Optically Active IA, IE and IF	292
6.2.3	Herbicidal Activity of Optically Active IA, IE and IF	296
6.2.4	Summary	308
6.3	Optically Active Substituted Ethylphosphonates IA and IC	310
6.3.1	Introduction	310
6.3.2	Synthesis of Optically Active IA and IC	310
6.3.3	Herbicidal Activity of Optically Active IA and IC	314
6.3.4	Aquatic Toxicity of Optically Active IA and IC	316
6.3.5	Summary	318
	References.	319

7	Biochemical Mechanism of Alkylphosphonates	323
7.1	Molecular Docking and 3D-QSAR Studies	324
7.1.1	Introduction	324
7.1.2	Binding Conformational Analysis	325
7.1.3	CoMFA and CoMSIA Analysis	325
7.1.4	Validation of the 3D-QSAR Models	330
7.1.5	Molecular Docking	330
7.1.6	Molecular Alignment and 3D-QSAR Modeling	331
7.1.7	CoMFA Analysis and CoMSIA Analysis Modeling	331
7.1.8	PLS Calculations and Validations	334
7.1.9	Summary	334
7.2	Enzyme Inhibition	335
7.2.1	Introduction	335
7.2.2	Inhibitory Potency Against Plant PDHc	336
7.2.3	Kinetic Experiment of PDHc	338
7.2.4	Selective Enzyme Inhibition	339
7.2.5	Structure-Activity Relationships	341
7.2.6	Assay of PDHc from Plant	350
7.2.7	Assay of PDHc from <i>E. coli</i> and Pig Heart	352
7.2.8	Assay of Other Enzymes	354
7.2.9	Summary	354
	References	355
8	Evaluation and Application of Clacyfos and HWS	359
8.1	Evaluation of Clacyfos	359
8.1.1	Introduction	359
8.1.2	Physiochemical Properties	360
8.1.3	Stability of Clacyfos	361
8.1.4	Herbicidal Activity in Greenhouse	363
8.1.5	Systemic Property of Clacyfos	366
8.1.6	Rainfast Characteristics of Clacyfos	366
8.1.7	Field Trials of Clacyfos	367
8.1.8	Toxicity Evaluation	377
8.1.9	Environmental Fate	378
8.1.10	Residues	379
8.1.11	Adsorption of Clacyfos on Soils	379
8.1.12	Ecological Effects	380
8.1.13	Summary	380
8.2	Evaluation of HWS	381
8.2.1	Introduction	381
8.2.2	Physiochemical Properties	381
8.2.3	Herbicidal Activity in Greenhouse	382
8.2.4	Systemic Property of HWS	385
8.2.5	Rainfast Characteristics of HWS	385

8.2.6	Field Trials of HWS	386
8.2.7	Toxicity Evaluation	388
8.2.8	Ecological Effects	389
8.2.9	Summary	389
	References	390
9	General Methodology	391
9.1	General Synthetic Procedure	391
9.1.1	Chemicals, Reagents, and Solvents	391
9.1.2	<i>O,O</i> -Dialkyl Phosphonates M1	391
9.1.3	<i>O,O</i> -Dialkyl 1-Hydroxyalkylphosphonates M2	392
9.1.4	<i>O,O</i> -Dialkyl 1-(Chloroacetoxy)- Alkylphosphonates M3	393
9.1.5	Substituted Phenoxyacetic Acids M4	393
9.1.6	Substituted Phenoxyacetyl Chlorides M5	396
9.1.7	<i>O,O</i> -Dialkyl 1-(Substituted Phenoxyacetoxy)- Alkylphosphonates IA–IJ	398
9.1.8	Phenylhydrazinecarboxamide M6 and Sodium Triazol-3-olate M7	405
9.1.9	(1-Phenyl-1,2,4-Triazol-3-yloxyacetoxy)- Alkylphosphonates IK	406
9.1.10	Alkali Metal Salts of <i>O</i> -Alkyl Alkylphosphonic Acids IIA–IIE	407
9.1.11	<i>O,O</i> -Bis(Trimethylsilyl) Alkylphosphonates M8 and Alkylphosphonic Acids M9	410
9.1.12	Alkali Metal Salts of Alkylphosphonic Acids IIF–IIH	411
9.1.13	<i>t</i> -Butylammonium Salts of Alkylphosphonates IJJ	413
9.1.14	Dichloro(Methyl)Phosphine M10	414
9.1.15	<i>O</i> -Methyl Methylphosphinate M11	415
9.1.16	<i>O</i> -Methyl (1-Hydroxyalkyl)Methylphosphinates M12	415
9.1.17	Alkylphosphinates IIIA–IIIG	416
9.1.18	Sodium Salts of Alkylphosphinic Acids IIIH	419
9.1.19	3-Hydroxy-5-Methylisoxazole Derivatives M13–M16	420
9.1.20	<i>O</i> -Methyl [1-(5-Methylisoxazol-3-yloxyacetoxy)- Alkyl]Methylphosphinates IIJJ	421
9.1.21	1-Phenyl-2,2-Dimethyl-1,3-Propanediol M17	422
9.1.22	Cyclic Phosphonates M18	423
9.1.23	Cyclic 1-Hydroxyalkylphosphonates IVA and IVB	423
9.1.24	Substituted Phenoxypropionic Acids M19	425
9.1.25	Substituted Phenoxypropionyl Chlorides M20	425
9.1.26	Cyclic Alkylphosphonates IVC–IVF	426

9.1.27	4-(Hydroxymethyl)-2,6,7-Trioxa-1-Phosphabicyclo- [2.2.2]Octane-1-One/Thione M21/M22	429
9.1.28	Caged Bicyclic Phosphates IVG and IVH	429
9.1.29	Optically Active Cyclic 1-Hydroxyalkylphosphonates IVB	431
9.1.30	<i>O,O</i> -Diethyl (Substituted Benzyl)Phosphonates M23	432
9.1.31	Optically Active 1-Hydroxyalkylphosphonates M2 . . .	433
9.1.32	Optically Active (Substituted Phenyl)- Methylphosphonates IA, IE, and IF.	435
9.1.33	1-Keto Phosphonates M24 and Vinylphosphonates M25	437
9.1.34	Optically Active 1-Substituted Ethylphosphonates IA and IC	441
9.2	General Information of Structural Characterization	442
9.3	Herbicidal Activity Assay	443
9.3.1	Test in Petri Dishes.	444
9.3.2	Test in Greenhouse	445
	References.	446
Index	449

Abbreviations

Abbreviations	Common Name	Latin name
Abu	Chingma abutilon	<i>Abutilon theophrasti</i>
Aca	Asian copperleaf	<i>Acalypha australis</i>
Ach	Pig's knee	<i>Achyranthes bidentata</i>
Alj	Japanese alopecurus	<i>Alopecurus japonicus</i>
Alo	Shortawn foxtail	<i>Alopecurus aequalis</i>
Alt	Alligatorweed	<i>Alternanthera philoxeroides</i>
Ama	Slender amaranth	<i>Amaranthus blitum</i>
Amm	Monarch redstem	<i>Ammannia baccifera</i>
Amr	Common amaranth	<i>Amaranthus retroflexus</i>
Ams	Spiny amaranth	<i>Amaranthus spinosus</i>
Amt	Chinese spinach	<i>Amaranthus tricolor</i>
Ave	Wild oat	<i>Avena fatua</i>
Bec	American sloughgrass	<i>Beckmannia syzigachne</i>
Bet	Sugar beet	<i>Beta vulgaris</i>
Bra	Rape	<i>Brassica campestris</i>
Brc	Field mustard	<i>Brassica rapa</i>
Brj	Leaf mustard	<i>Brassica juncea</i>
Brn	Cabbage type rape	<i>Brassica napus</i>
Bro	Ball cabbage	<i>Brassica oleracea</i>
Brp	Chinese cabbage	<i>Brassica pekinensis</i>
Caa	Chili	<i>Capsicum annum</i>
Cap	Shepherd's purse	<i>Capsella bursa-pastoris</i>
Car	Hairy bittercress	<i>Cardamine hirsute</i>
Cas	Sickle senna	<i>Cassia tora</i>
Cay	Japanese cayratia	<i>Cayratia japonica</i>
Cer	field chickweed	<i>Cerastium arvense</i>
Che	Goosefoot	<i>Chenopodium album</i>
Chl	Feather finger grass	<i>Chloris virgata</i>

Abbreviations	Common Name	Latin name
Chs	Small goosefoot	<i>Chenopodium serotinum</i>
Cir	Setose thistle	<i>Cirsium japonicum</i>
Cis	Creeping thistle	<i>Cirsium setosum</i>
Com	Dayflower	<i>Commelina communis</i>
Con	Field bindweed	<i>Convolvulus arvensis</i>
Cuc	Cucumber	<i>Cucumis sativus</i>
Cyp	Ricefield flatsedge	<i>Cyperus iria</i>
Cym	Asian flatsedge	<i>Cyperus microiria</i>
Cyn	Bermudagrass	<i>Cynodon dactylon</i>
Cyr	Nut grass	<i>Cyperus rotundus</i>
Dap	Water flea	<i>Daphnia magna</i>
Dau	Carrot	<i>Daucus carota</i>
Des	Flixweed tansymustard	<i>Descurainia Sophia</i>
Dic	Southern crabgrass	<i>Digitaria ciliaris</i>
Dig	Crab grass	<i>Digitaria sanguinalis</i>
Ech	Barnyard grass	<i>Echinochloa crusgalli</i>
Ecl	White eclipta	<i>Eclipta prostrata</i>
Ele	Goose grass	<i>Eleusine indica</i>
Eri	Flaxleaved fleabane	<i>Erigeron bonariensis</i>
Esc	Colon bacillus	<i>Escherichia coli</i>
Eul	Aper spurge	<i>Euphorbia lathyris</i>
Eum	Spotted spurge	<i>Euphorbia maculata</i>
Eup	Wolf's milk	<i>Euphorbia humifusa</i>
Fes	Tall fescue	<i>Festuca arundinacea</i>
Gal	Cleavers	<i>Galium aparine</i>
Gly	Soybean	<i>Glycine max</i>
Gos	Cotton	<i>Gossypium hirsutum</i>
Ipn	Morning glory	<i>Ipomoea nil</i>
Ipo	Lobedleaf pharbitis	<i>Ipomoea hederacea</i>
Ixe	Chinese ixeris	<i>Ixeris chinensis</i>
Lac	Lettuce	<i>Lactuca sativa</i>
Lam	Henbit deadnettle	<i>Lamium amplexicaule</i>
Lap	Common nipplewort	<i>Lapsanastrum apogonoides</i>
Lin	Prostrate false pimpernel	<i>Lindernia procumbens</i>
Lyc	Tomato	<i>Lycopersicon esculentum</i>
Mal	Water chickweed	<i>Malachium aquaticum</i>
Med	Clover	<i>Medicago sativa</i>
Mon	Pickerel weed	<i>Monochoria vaginalis</i>
Oen	Water dropwort	<i>Oenanthe javanica</i>
Ory	Rice	<i>Oryza sativa</i>
Oxa	Creeping woodsorrel	<i>Oxalis corniculata</i>

Abbreviations	Common Name	Latin name
Pis	Pea	<i>Pisum sativum</i>
Poa	Annual bluegrass	<i>Poa annua</i>
Pob	Bunge's smartweed	<i>Polygonum bungeanum</i>
Poc	Pinkhead smartweed	<i>Polygonum capitatum</i>
Pof	Asia minor bluegrass	<i>Polyogon fugax</i>
Pol	Knotgrass	<i>Polygonum aviculare</i>
Pop	Water pepper	<i>Polygonum flaccidum</i>
Por	Common purslane	<i>Portulaca oleracea.</i>
Ran	Tall buttercup	<i>Ranunculus japonicus</i>
Rap	Radish	<i>Raphanus sativus</i>
Rot	Indian toothcup	<i>Rotala indica</i>
Rum	Curled dock	<i>Rumex crispus</i>
Sef	Giant foxtail	<i>Setaria faberi</i>
Sep	Yellow bristlegrass	<i>Setaria pumila</i>
Set	Green bristlegrass	<i>Setaria viridis</i>
Sin	White mustard	<i>Sinapis alba</i>
Sol	Black nightshade	<i>Solanum nigrum</i>
Ste	Bog chickweed	<i>Stellaria alsine</i>
Stm	Chickweed	<i>Stellaria media</i>
Tri	Wheat	<i>Triticum aestivum</i>
Trp	Cucumber-herb	<i>Trigonotis peduncularis</i>
Ver	Gray field speedwell	<i>Veronica polita</i>
Vic	Common vetch	<i>Vicia sativa</i>
Vig	Wild vetch	<i>Vicia gigantea</i>
Vir	Mung bean	<i>Vigna radiata</i>
Xan	Siberian cocklebur	<i>Xanthium strumarium</i>
Zea	Maize	<i>Zea mays</i>

About the Authors

Hong-Wu He obtained her Doctoral Degree in Agricultural Science from Kyushu University, Japan. She is currently a full-time Professor at the Key Laboratory of Pesticide and Chemical Biology, Ministry of Education of China, and the Director of Institute of Pesticide Chemistry, College of Chemistry, Central China Normal University, Wuhan, China. She is also a Member of the Council of Pesticide Society of China and the Director of Pesticide Professional Committee and Chemical Industry Society of Hubei province.

Prof. He has more than 33 years of teaching and research experience in the field of pesticide chemistry, especially in the design, synthesis, and development of novel herbicide based on pyruvate dehydrogenase. She has devoted herself to the research and development of novel herbicide named clacyfos and several other OP insecticides. She is the author of more than 230 scientific articles and 6 books. Besides that Prof. He holds more than 30 patents related to pesticide chemistry. She has received multiple Scientific and Technological Progress Awards and Technological Invention Awards in agrochemical research from the Ministry of Education of China and the Government of Hubei province. She was the winner for the award of Outstanding Contribution to the Pesticide Industry of China in 2009 and the title “National Outstanding Scientific and Technological Worker” in 2001.

Hao Peng currently is an Associate Professor at the Key Laboratory of Pesticide and Chemical Biology, Ministry of Education of China, College of Chemistry, Central China Normal University (CCNU), Wuhan, China. He obtained his Ph.D. in Pesticide Science from CCNU under the supervision of Prof. Hong-Wu He.

His current research focuses on the research and development of novel agrochemicals, especially on the design of organophosphorus compounds with herbicidal and fungicidal activity based on pyruvate dehydrogenase and pyrroline-5-carboxylate reductase. He has been involved in the research and development of novel herbicide clacyfos since 2003. He has received two Scientific and Technological Progress Awards and Technological Invention Awards in agrochemical research from the Government of Hubei province and Wuhan city. He has published more

than 45 scientific articles and serves as an active reviewer for a number of scientific journals.

Xiao-Song Tan currently is an Associate Professor at the Key Laboratory of Pesticide and Chemical Biology, Ministry of Education of China, College of Chemistry, Central China Normal University (CCNU), Wuhan, China. He obtained his M.S. degree in Chemistry from CCNU.

He has worked on the synthesis, structural identification, and analysis of new bioactive chemicals for 30 years including the development of novel herbicide clacyfos since 2000. He has received multiple Scientific and Technological Progress Awards and Technological Invention Awards in agrochemical research from the Ministry of Education of China and Government of Hubei province. He has co-authored more than 50 scientific articles and several book chapters in the field of pesticide chemistry.

Chapter 1

Overview

1.1 Introduction

Chemical control which is a critical component in Integrated Pest Management (IPM), provides sustainable support to world food production. Agrochemicals have made great contribution to the advancement of agriculture in the world. In general, 30–40 % crop yield loss can be avoided by use of agrochemicals. Applying herbicide is relatively efficient and economical in controlling weeds in the world. In China, weed control has also highly depended on herbicide use in most cropping systems in recent years. Currently, more than 290 herbicides have been developed and are widely used. In 2006, the global herbicide market was valued at \$15 billion, equivalent to approximately 50 % of the global agrichemicals market. In 2011, the global agrichemicals market increased to about \$44 billion, while the herbicides market was about \$14.86 billion, or 48 % of the total. Over the last decade, the herbicide market for both crop and noncrop usage captured over 40 % of the global agrochemical market.

The major use of herbicides is for field crops. The major field crops are cereals, maize, soybean, rice, rape, sugarbeet, cotton, sugarcane, and sunflower followed by potato, vine, pome fruit, citrus, and other crops. Post-emergence application, which is the leading method for weeds control, gains even more momentum as Genetically Modified (GM) crops such as maize and soybeans are getting popular. Leading herbicides in the market are shown in Table 1.1.

Among those leading herbicides, many are nonselective, such as glyphosate, paraquat, glufosinate, and sulfosate. They are used mainly for post-harvest treatment, pre-plant treatment, and incorporated pre- and post-emergence against both grasses and broadleaf weeds. The 2,4-D that is recommended as a post-emergence herbicide against broad leaved weeds, is a mature, commodity herbicide. However, 2,4-D is still an important product due to its low-cost and broad spectrum against many broadleaf weed in a wide range of crops. Among many different forms of 2,4-D, the most common formulation is an ester in an emulsifiable concentrate. Many of those

Table 1.1 Leading herbicides on the market

No.	Active ingredient	Chemical class	Site of actions	Mode of action	Launch date	Application		Main pest and rate g ai/ha
						Pre or post	Main crop usage	
1	Glyphosate	Amino acid	Inhibition of EPSP synthase	Inhibition of amino acid synthesis	1974	Pre- and post-emergence	Nonselective	Grasses, broadleaf weeds, 550–4500
2	Paraquat	Bipyridyl	PS I electron diversion	Photo-system-I-electron diversion	1962	Pre- and post-emergence	Non-crop, Plantation	Grasses, broadleaf weeds, 150–1000
3	Metolachlor	Acet-amide	Cell division or VLCFA	Inhibition of cell division	1975	Pre-emergence	Maize, soybean	Grasses, 1000–3000
4	Acetochlor	Acet-amide	Cell division or VLCFA	Inhibition of cell division	1985	Pre-emergence	Maize, soybean	Grasses and broad-leaf weeds, 1750–2500
5	Mesotrione	Other	4-Hydroxy-phenyl-pyruvate-dioxy-genase or 4-HPPD	Inhibition of 4-hydroxy-phenyl-pyruvate-dioxy-genase (4- HPPD)	2001	Pre- and early post-emergence	Maize	Broadleaf weeds, 70–225
6	2,4-D	Phenoxy	Synthetic auxins	Synthetic auxins. Action like indole acetic acid	1945	Post-emergence	Cereals, maize, potato, peanuts, fruit, noncrop use, sugarcane, rice, citrus, sunflower	Broadleaf weeds, 200–2000

(continued)

Table 1.1 (continued)

No.	Active ingredient	Chemical class	Site of actions	Mode of action	Launch date	Application		Main pest and rate g ai/ha
						Pre or post	Main crop usage	
7	Atrazine	Triazine	Photosynthesis PS II	Inhibition of photo-synthesis at photo-system II	1957	Pre- and post-emergence	Maize, cereal	Broadleaf weeds, 450–4500
8	Glufosinate	Amino acid	Glutamine synthetase	Inhibition of amino acid synthesis	1986	Pre- and post-emergence	Nonselective	200–750
9	Sulfosate	Amino acid	EPSP synthase	Inhibition of amino acid synthesis	1989		Nonselective	550–4500
10	Fenoxaprop	Aryloxypropionate	Acetyl CoA carbox-ylase (ACCase)	Inhibition of acetyl CoA carbox-ylase in fatty acid synthesis pathway	1984	Post-emergence	Cereals	Grasses, 200–500
11	Pendimethalin	Dinitro-anilines	Micro-tubule assembly	Micro-tubule assembly inhibition	1976	Pre- and post-emergence	Soybean, maize	Grasses, broadleaf weeds, 560–2250
12	Picloram	Pyridine	Synthetic auxin	Synthetic auxin	1963	Post-emergence	Noncrop, Cereals	Broadleaf weeds, 70–560

(continued)

Table 1.1 (continued)

No.	Active ingredient	Chemical class	Site of actions	Mode of action	Launch date	Application		Main pest and rate g ai/ha
						Pre or post	Main crop usage	
13	Trifluralin	Dinitro-aniline	Micro-tubule assembly inhibition	Micro-tubule assembly inhibition	1964	Pre-emergence	Soybean, cotton	Grasses, 580–1100
14	Clodinafop	Aryloxypropionate	Acetyl CoA carbox-ylase (ACCase)	Inhibition of acetyl CoA carbox-ylase in fatty acid synthesis pathway	1991	Post-emergence	Cereals	Grasses, 40–80
15	Nicosulfuron	ALS-Sulfonylurea	Aceto-lactate synthase (ALS)	Inhibition of branched chain amino acid synthesis	1991	Post-emergence	Maize	Grasses, broadleaf weeds, 35

leading herbicides on the list are already off-patent. Their sales have been in decline due to the unfavorable regulatory actions against them, chemical resistance issue, and new competitive products.

1.1.1 Mode of Action of Herbicide

Although several hundreds of herbicides have been widely used, they only affect a limited number of target sites in plants. According to the Herbicide Resistance Action Committee (HRAC, <http://www.hracglobal.com/>), herbicides can be classified into 18 groups according to their target sites or sites of action (Table 1.2). Herbicides as a group, captures over 40 % of the global agrochemical market.

Six of the most important sites of actions of herbicides including EPSP synthase, ALS, photosynthesis PS II, synthetic auxin, ACCase and cell division (VLCFA), and their chemical class are listed in Table 1.3. It is worth mentioning noticing that six modes of action of herbicides accounted for almost 75 % of the total herbicides used in the market (Fig. 1.1) [1].

Table 1.3 shows the targets of actions of most leading herbicides belong to those six sites of actions.

Application and mode of action of several leading herbicides are shown in Table 1.1. Among those leading herbicides, glyphosate is currently the largest-selling single product in the global crop protection market. Although this nonselective product was originally developed for noncrop use, it is now widely used for crops due to the application of genetically modified seed and the associated technologies. Despite increasing generic competition, glyphosate continues to deliver significant growth in sales, year after year.

1.1.2 Herbicide Resistance

Herbicides play a very important role in modern agriculture. However, resistance becomes a big issue because approximately 75 % of the commercial herbicides are working on only six action sites. The repeated use of the same herbicide or repeated treatment with herbicides having the same mode of action, has resulted in the wide spread evolution of herbicide resistance in populations of agricultural weeds.

According to the International Survey of Herbicide Resistant Weeds (www.weedscience.org) report, there are currently 434 unique cases of herbicide resistant weeds globally, involving 237 species (138 dicots and 99 monocots). Herbicide resistant weeds have been reported in 82 crops in 65 countries. Multiple resistances also have been observed. Weeds have evolved resistance to 22 of the 25 known herbicide sites of action and to 155 different herbicides. The evolution of herbicide-resistant weeds for selected herbicides of six leading sites of actions is shown in Table 1.4.

Table 1.2 Mode of action and site of action of herbicides

Mode of action of herbicide	Sites of action of herbicides	Number of herbicides
Inhibition of acetyl CoA carboxylase in fatty acid synthesis pathway	Acetyl CoA carboxylase (ACCase)	19
Inhibition of branched chain amino acid synthesis	Acetolactate synthase (ALS)	57
Inhibition of photosynthesis at photo-system II	Photosynthesis PS II	50
Photosystem I electron diversion	PS I electron diversion	2
Inhibition of protoporphyrinogen oxidase	Protoporphyrinogen oxidase (PPO)	28
Inhibition of pigment synthesis (bleaching)	Carotenoid biosynthesis at the phytoene desaturase step (PDS)	24
Inhibition of pigment synthesis (bleaching)	4-Hydroxyphenyl-pyruvate-dioxygenase (4-HPPD)	
Inhibition of amino acid biosynthesis	EPSP synthase	2
Inhibition of amino acid biosynthesis	Glutamine synthetase	2
Inhibition of DHP (dihydropteroate) synthase	DHP	1
Inhibition of microtubule assembly	Microtubule assembly	14
Inhibition of mitosis/microtubule organisation	Mitosis/Microtubule organization	2
Inhibition of cell division (VLCFA)	Cell division (VLCFA)	23
Inhibition of cell wall (cellulose) synthesis	Cellulose synthesis	6
Uncoupling (Membrane disruption)	Uncoupler of oxidative phosphorylation	3
Inhibition of lipid synthesis (not ACCase)		19
Synthetic auxin action	Synthetic auxin	18
Auxin transport inhibition	Auxin transport	2
Unknown mode of action		18

Herbicide-resistant weed forces us to increase the application frequency and rate to get them under control. More frequency and higher rate in application would cause contamination and pollution in our environment. Therefore, it urgently needs to develop new herbicides as an alternative measure to control weeds.

1.1.3 New Opportunity for Novel Herbicides

The evolution of herbicide-resistant weeds due to repeated use of herbicides with the same site of action has become a challenge in modern agriculture. A different target-site herbicide can aid in the management of herbicide resistance by

Table 1.3 Important sites of actions and chemical class of herbicides

Sites of action for herbicides	Chemical class
EPSP synthase	Glycine (Amino acid)
ALS	Sulfonylurea
	Imidazolinone
	Triazolopyrimidine
	Pyrimidinyl(thio)benzoate
	Sulfonylaminocarbonyl-triazolinone
Photosynthesis PS II	Urea
	Amide
	Nitrile
	Benzothiadiazinone
	Phenyl-pyridazine
	Bipyridylum
Synthetic auxin	Phenoxy-carboxylic-acid
	Benzoic acid
	Pyridine carboxylic acid
ACCCase	Aryloxyphenoxy-propionate
	Cyclohexanedione
	Phenylpyrazoline
	Quinoline carboxylic acid
	Other
Cell division (VLCFA)	Chloroacetamide
	Acetamide
	Oxyacetamide
	Tetrazolinone
	Other

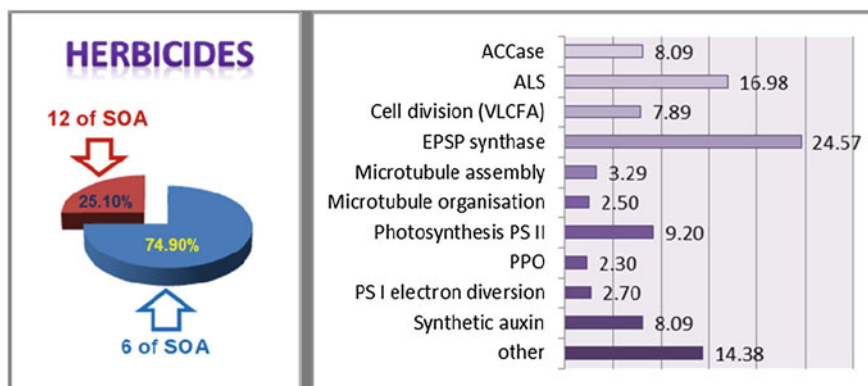
**Fig. 1.1** Sites of action for 75 % herbicides

Table 1.4 Herbicide-resistant weeds grouped by leading sites of action

Herbicides group	Sites of action	Example herbicides	Dicots weed	Monocots weed	Total
ALS inhibitors	Inhibition of ALS (branched chain amino acid synthesis)	Chlorsulfuron	88	57	145
Photosystem II inhibitors	Inhibition of photosynthesis PS II	Atrazine	49	23	72
ACCCase inhibitors	Inhibition of acetyl CoA carboxylase (ACCCase)	Sethoxydim	0	46	46
Synthetic auxins	Synthetic auxins (action like indoleacetic acid)	2,4-D	23	8	31
Bipyridyl	Photosystem-I-electron diversion	Paraquat	22	9	31
Amino acid	Inhibition of EPSP synthase	Glyphosate	15	14	29
Urea and Amide	Inhibition of photosynthesis at photosystem II	Chlorotoluron	8	16	24

Heap, I. The international survey of herbicide resistant weeds. Online. Internet. Monday, August 25, 2014. Available www.weedscience.org

diversifying the available herbicide option. Therefore, it is essential to develop efficient herbicides with novel modes of action or target-site to overcome this chemical resistant problem.

Most leading herbicides on the market were launched 10–60 years ago. For example, glyphosate was the first amino acid herbicide being introduced to the market by Monsanto in 1974. Currently, glyphosate is widely used in more than 20 crops such as maize, soybean, rice, rape, sugar beet, cotton, and sugarcane. Because glyphosate-resistant GM crop seeds were successfully commercialized in the recent years, the usage of glyphosate was increased year after year. Glyphosate was off limit to several cereals. That creates an opportunity to develop novel herbicides for cereals. The predominant cultivated cereals are wheat and barley, followed by varieties of rye, oats, triticale, sorghum, and millet.

Discovery of new herbicides with new herbicidal targets is exciting and challenging. Compounds that work on the pyruvate dehydrogenase complex (PDHc) have shown promising herbicidally activity. Therefore, PDHc could be a potential herbicidal target. Several unique phosphorus-containing compounds have been considered a potential inhibitor against plant PDHc [2]. However, so far none of those PDHc inhibitors have been successfully developed as commercial herbicides. We further explored the possibility using PDHc site as a possible target of novel herbicide.

On the other hand, several phosphorus-containing herbicides including glyphosate, glufosinate, sulfosate, and bitanalos have been successfully developed as leading herbicides due to their high efficiency, and low cost. Therefore, it would be

interesting to explore phosphorus-containing novel herbicides as effective inhibitors of plant PDHc. Plant PDHc could be a possible effective site of action of herbicides, but we are not sure of its mode of action. Maybe it belongs to the inhibition for energy-metabolism, lipid or protein biosynthesis.

1.1.4 Basic Methodology for Discovery of Hit/Lead Compounds

Good chemical weed control depends to a great extent on the synthesis of new active compounds; this field is more dynamic today than ever before. A new herbicide will be developed by first finding a lead compound with a desired herbicide activity. The basic methodology for discovery of a new active compound or lead compound can be divided into four basic approaches namely; random screening (hit generating), analog chemistry (lead optimization), natural products, and biorational design.

The method of random screening relies upon a proper bioassay system to pick up the hits from an ocean of compounds. The discovery of glyphosate is good example of using this random screening approach. However the success of this approach depends on serendipity, massive synthetic efforts, and luck.

The method of analog chemistry starts with known active compounds. For example, a commercial herbicide can be used as a hit and then develop the lead into a novel and patent-free area, followed by structural optimization to generate a desirable product. This way is the most reliable approach to guarantee the new compounds have biological activity. Unfortunately, the derivative products from this approach will normally share the same mode of action as the parents.

The use of natural products as herbicides or as lead structures for herbicide discovery programs is another alternative. Spinosads are an example of outstanding success in this approach. However, natural products in general are more complex in structure and more difficult to synthesize. In most case, this approach is not cost-effective.

Biorational design is the most intellectually attractive concept for discovering new agrochemicals. However, this requires a detail understanding of a biochemistry mechanism in the target species. Advancing biochemistry and bioorganic chemistry technologies are powerful tools for this approach. In this approach, proper bioassay to guide the synthetic direction is very important.

Fully understanding the interactions between chemicals and target organism is also an essential aspect of this biorational design approach. It is now possible to produce sufficient enzyme by the application of molecular biology techniques. Current advanced technologies also allow us to do crystallization and subsequent X-ray analysis in a timely manner. This can lead to construction of a molecular

model by computer-aided technology to design inhibitors. Therefore biorational design is the best way to design and discover compounds with novel modes of action or special targets.

Although biorational design has enjoyed limited success to date, this approach is advancing fast and promising in terms of finding potential to create effective crop protection compounds with novel modes of action. An excellent example was designing PDHc inhibitors as herbicides [2]. Details can be found in the following sections.

1.2 Pyruvate Dehydrogenase Complex (PDHc)

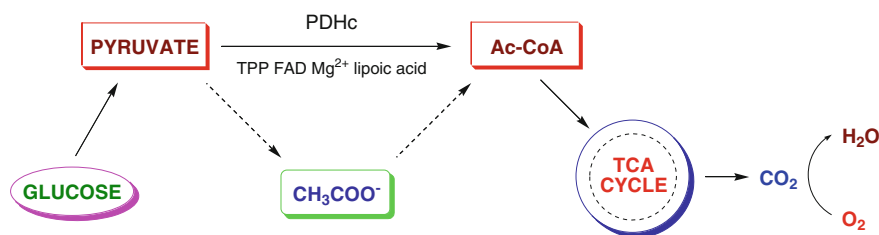
1.2.1 Function of PDHc

The PDHc is one of the most important oxidoreductases in living organisms. It catalyzes the oxidative decarboxylation of pyruvate to acetyl CoA which is a pivotal process in cellular metabolism that in turn has been studied extensively. Glucose, a major source of energy is first converted by glycolysis into pyruvate. Under aerobic conditions, pyruvate then can be converted by pyruvate dehydrogenase complex to acetyl coenzyme A which enters the citric acid cycle.

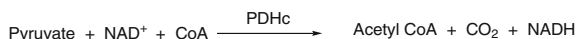
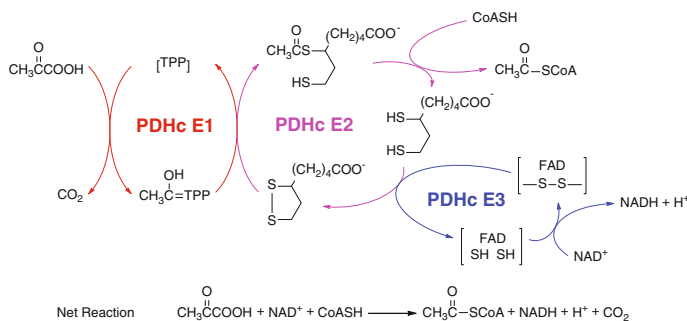
The conversion of pyruvate to acetyl CoA catalyzed by pyruvate dehydrogenase complex serves as a link between glycolysis and the tricarboxylic acid (Krebs or citric acid) metabolic cycle [3–5]. The pivotal role of the PDHc is shown in Scheme 1.1 [6].

PDHc oxidizes pyruvate (using NAD^+ which is reduced to NADH) to form acetyl CoA and CO_2 . Since the reaction involves both an oxidation and a loss of CO_2 , the process is called oxidative decarboxylation. This PDHc reaction can be simply shown in Scheme 1.2.

PDHc comprises three enzymes and five coenzymes. The three primary enzymes include pyruvate dehydrogenase E1 component or pyruvate decarboxylase (E1, EC 1.2.4.1), dihydrolipoamide acetyltransferase (E2, EC 2.3.1.12) and lipoamide dehydrogenase (E3, EC 1.8.1.4). E1 utilizes thiamin diphosphate (TPP) and Mg^{2+} as cofactors [7]. E2 contains covalently bound lipoyl groups [8], and E3 contains



Scheme 1.1 Pivotal role of pyruvate dehydrogenase complex (PDHc)

**Scheme 1.2** Oxidative decarboxylation catalyzed by PDHc**Scheme 1.3** Conversion of pyruvate to acetyl CoA catalyzed by PDHc

tightly bound FAD [9]. The sequential steps for conversion of pyruvate to acetyl coenzyme A catalyzed by PDHc are shown in Scheme 1.3 [10, 11].

In the process of conversion of pyruvate to acetyl CoA, the PDHc E1 catalyzes both the oxidative decarboxylation of pyruvate and the reductive transfer of the acetyl product onto the lipoyl group at E2 lipoyl domain. E2 catalyzes the transfer of the acetyl group from the lipoyl domain to CoA creating acetyl CoA. E3 regenerates the disulphide bond in the dithiolane ring of the lipoyl group [11].

1.2.2 Distribution of PDHc

Although PDHc can be found in microorganisms [12–15], plants [16–18], and mammals [19–21], the three-dimensional form and homology of the mammal's PDHc are different from their counterparts found in microorganisms and plants. Because of that, an effective herbicide that targets on plant PDHc should have no effect on animal PDHc and be safe for animals, including humans by biorational design.

In the structure of pyruvate dehydrogenase complex, the E2 component forms the central core of the complex. PDHc from Gram-negative bacteria possesses an octahedral E2 core while the Gram-positive and eukaryotic PDHc are based on an icosahedral core [22]. The E1 and E3 components are attached noncovalently to the E2 core. The E1 component occurs in two forms depending on the symmetry of the complex. In octahedral complexes, E1 component is an (α_2) homodimer with a subunit mass of approximately 100 kDa, while in icosahedral complexes, it exists as an ($\alpha_2\beta_2$) heterotetramer with subunits of approximately 41 kDa and 36 kDa [23, 24].

Because of these differences, we choose plant PDHc as target enzymes for new herbicides.

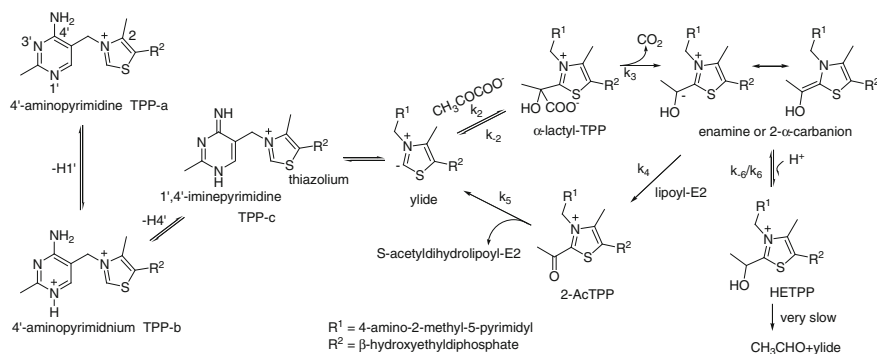
1.2.3 Plant PDHc E1 as Site of Action of Herbicide

In plants, the step of conversion from pyruvate to acetyl coenzyme A, which is catalyzed by the E1 component, is the only irreversible step in the overall PDHc catalytic reaction. Once the E1 activity is inhibited, the overall enzymatic reaction and production of acetyl coenzyme A will be blocked [2]. In the absence of acetyl coenzyme A which is necessary for the tricarboxylic acid cycle, the production of ATP will be reduced, which can lead to the difficulty in energy-metabolism and the injury of the cellular tissue, ultimately it can cause death of the plant. In view of its important role in metabolism, plant PDHc E1 should be an interesting site of action for herbicide R&D.

We tried to find a plant PDHc inhibitor by biorational design.

The detailed catalytic mechanism of E1 is shown in Scheme 1.4 [25–27].

Coenzyme TPP is in a fixed “V” conformation (TPP-a and TPP-b in Scheme 1.4) [28] Owing to the effect of nitrogen atom (N4') of the aminopyrimidine ring in its imino tautomer TPP-c, the C2 proton of the thiazolium ring is extracted by the N4' in the imino tautomer to generate a highly reactive carbanion or ylide. Ylide (C2 carbanion) attacks the keto carbon of pyruvate in a nucleophilic manner to yield a tetrahedral intermediate α -lactyl-TPP. The next step is releasing carbon dioxide then completes the formation of a metastable enamine-TPP or 2- α -carbanion, which also is known as hydroxyethylidene-TPP. The intermediate hydroxyethylidene-TPP reductively acylates the lipoyl group to produce an acetyl dihydrolipoyl moiety (2-AcTPP) and an acetyl-lipoyl adduct. Eventually, the S-acetyl dihydrolipoamide shuttles to the E2 subunit. This reaction continues to produce acetyl CoA, which is indicated in Scheme 1.3.



Scheme 1.4 Normal catalytic mechanism of PDHc E1 subunit

We speculate that the inhibition of plant PDHc and its function in acetyl coenzyme A is a key site of action that would interrupt the energy-metabolism, lipid, or protein biosynthesis in plants.

1.3 Progress in the Research of PDHc Inhibitors

There are a number of reports on the inhibition of PDHc, especially on its first enzyme, PDHc-E1. Different chemical structures have been designed and synthesized in several laboratories for PDHc inhibitors research. Although PDHc-E1 can be extracted from different biological origins such as yeast, bacteria, plant, animal (beef heart or pig heart), and human, most of the PDHc-E1 inhibitor studies were carried out with PDHc E1 from *Escherichia coli* (*E. coli*).

Arsenic- or copper-carrying pesticides and *sec*-butylamine fungicide have been known as rather strong PDHc inhibitors [29–32]. However, these pesticides were not ideal inhibitors, as they also affected related enzymes (e.g., 1-oxoglutarate dehydrogenase), and led to an undesirable side effect to mammals. Several copper-carrying reagents [32], organic mercurials [33], and acetaldehyde [34], have been reported as weak inhibitors against the *E. coli* PDHc.

Halo analogs of pyruvate, such as bromopyruvate and fluoropyruvate [35–39], as direct analogs of substrate pyruvate have been investigated.

Results indicated that bromopyruvate behaved as an active-site-directed inhibitor of *E. coli* PDHc-E1; it could inactivate the intact PDHc rapidly in a TPP-dependent process. Fluoropyruvate was also demonstrated as an inhibitor of PDHc in bacteria. The *E. coli* PDHc E1 could be rapidly inactivated using low concentrations of fluoropyruvate in a thiamin pyrophosphate (TPP)-dependent process.

However, fluoropyruvate was nonselective; as it also inhibited PDHc in mammals [38]. Compared with other inhibitors, halopyruvates were rather weak and slow. 2-Oxo-3-butenic acid as a substrate-analog also showed significant inhibitory effect against *E. coli* PDHc and their inhibitory effects were significantly better than that of bromopyruvate and fluoropyruvate. Further studies showed that 2-oxo-3-butenic acid targeted on the PDHc E1 but not E2 or E3.

Among other inhibitors for PDHc, phosphorus-containing inhibitors are one of the strongest ones. Selected organophosphorus (OP) inhibitors also have shown desirable selectivity against PDHc from different biological origins. The OP inhibitors including structures and their inhibition abilities are summarized as follows.

1.3.1 OP Compounds as Inhibitors of *E. coli* PDHc

Reviewing literatures on OP PDHc inhibitors, we noticed that most OP compounds acted as inhibitors of *E. coli* PDHc E1. Those OP inhibitors against *E. coli* PDHc E1 could be chemically classified into three types: (1) The analogs of substrate

pyruvate; (2) The analogs of cofactor—thiamin diphosphate (TPP); (3) The analogs of transition state.

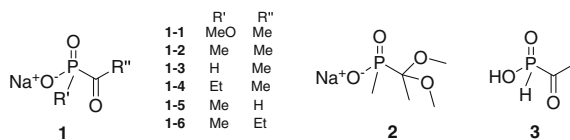
1.3.1.1 Pyruvate Analog as Inhibitors

Phosphonate analog of pyruvate as a potent inhibitor of *E. coli* PDHc was reported by Kluger and Pike in 1977 [40], which was a very interesting finding and paved the way for current PDHc inhibitor research. A series of sodium salts of acetylphosphinic acid or acetylphosphonic acid **1** as analogs of pyruvate was designed and synthesized (Scheme 1.5). Their inhibition on E1 component of *E. coli* PDHc was examined in detail. Sodium *O*-methyl acetylphosphonate **1-1** was found to be a powerful competitive inhibitor against *E. coli* PDHc E1 ($K_i = 5 \times 10^{-8}$ M). It also turned out to be a stable analog of pyruvate. Therefore, it was selected as the compound for the study of enzyme catalytic mechanism.

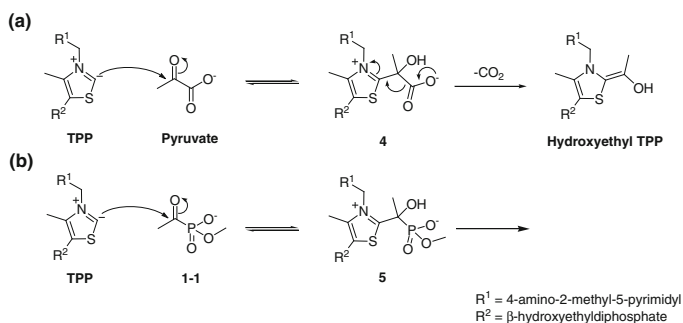
It has been well known that PDHc are multienzyme complexes responsible for the conversion of pyruvate into acetyl coenzyme A [41, 42]. The initial steps are catalyzed by PDHc E1 which promotes decarboxylation of pyruvate in the presence of a coenzyme, TPP [43–45]. When TPP is involved in this overall PDHc catalytic reaction, new reacted products can be expected [40]. It was believed that a covalent adduct of TPP was immediately formed in the initial conversion of pyruvate to a bound enzyme [46].

Hydrogen atom attached to the C atom between the N and S atom at the thiazole ring of TPP, was released to form a highly reactive carbanion. When pyruvate reacted with TPP, the carbanion could nucleophilically attack carbonyl carbon atoms of pyruvate to form adducts **4** (α -lactyl-TPP), and then **4** was further converted to an isolable product, hydroxyethyl TPP, by decarboxylation. In order to demonstrate the existence of reactive intermediate **4** (α -lactyl-TPP) in this reaction, a stable analog of pyruvate, sodium *O*-methyl acetylphosphonate **1-1** was selected to react with TPP. According to Kluger et al.'s report, **1-1** would compete with pyruvate for the active site of PDHc E1 and held the position of pyruvate, then bound to TPP.

This inhibition suggested a common type of covalent adduct existed and the inhibition was structurally specific for the 2-keto acid anion. The remarkable stability of the (**1-1**)-TPP-PDH complex (as indicated by strong K_i) showed the characteristic of covalent-activated intermediate analogs. This result suggested that α -lactyl-TPP (compound **4**) was a reactive intermediate in the reaction catalyzed by PDHc E1 [40].



Scheme 1.5 Phosphorus-containing analogs of pyruvate



Scheme 1.6 Comparison of the reactions of pyruvate and sodium *O*-methyl acetylphosphonate **1-1** with TPP

The proposed reactions of pyruvate and sodium *O*-methyl acetylphosphonate **1-1** with TPP are shown in Scheme 1.6. As described in Scheme 1.6, the normal catalytic process involves addition of TPP to pyruvate and the subsequent loss of carbon dioxide (equation a in Scheme 1.6). Sodium *O*-methyl acetylphosphonate **1-1** was thought to be structurally and functionally similar to pyruvate, it could also bind with TPP to form a phosphonic adduct **5**, which resembled the reactive intermediate α -lactyl-TPP **4**, and was assumed to form during the normal catalytic cycle of the enzyme (equation b in Scheme 1.6). However, phosphonic adduct **5** would not undergo a reaction analogous to the decarboxylation in equation a.

The study on inhibition against *E. coli* PDHc E1 by **1-1** suggested that **1-1** could bind at the pyruvate site and then reacted with TPP cofactor to give an analog **5** of the usual reaction intermediate. However, **5** could not carry out decarboxylation, the overall reaction was interrupted. Therefore, **1-1** is a powerful inhibitor against *E. coli* PDHc E1.

The inhibition mechanism of acetylphosphinic acid analog of pyruvate **3** against *E. coli* PDHc was further studied by Laber et al. in 1990 [47]. The results showed that **3** was a time-dependent inhibitor. At initial reaction, a reversible enzyme-inhibitor complex E1 was rapidly formed and then closely integrated into the complex E1. All of the experiments showed that the product formed by the interaction of **3** with PDHc E1 was similar to these intermediates formed by a normal reaction of substrate pyruvate and TPP.

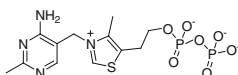
This work on the inhibition against *E. coli* PDHc by sodium *O*-methyl acetylphosphonate **1-1** exemplified a more modern approach to the design of specific enzyme (PDHc E1) inhibitors. Kluger et al. had established a new standard to promote the design and study on PDHc inhibitors using a biochemical theory.

1.3.1.2 TPP Analogs as Inhibitors

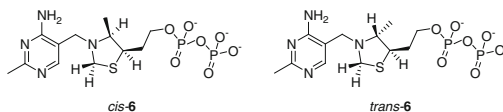
Analogs of coenzyme TPP could be a PHDc inhibitors. TPP is a coenzyme (Scheme 1.7), which participates in reactions involving formation and breaking of carbon–carbon bonds immediately adjacent to a carbonyl group. TPP is required in several catalytic reactions as an electron cave of many different TPP-dependent enzymes such as PDC (EC 4.1.1.1), PDHc E1 (EC 1.2.4.1), which can stabilize the carbon of carbonyl in form of an enamine intermediate. Study on the design and synthesis of analogs of cofactor TPP as PDHc inhibitors is therefore interesting and could be rewarding.

Considering the importance of TPP in the metabolic process of pyruvate, it is not a surprise to see many researches focused their effects on designing novel TPP analogs as inhibitors of *E. coli* PDHc E1. Tetrahydrothiamin pyrophosphate (tetrahydro-TPP) **6** (Scheme 1.8) as an analog of thiamin pyrophosphate (TPP) was reported in 1983 by Perham et al. [48]. Structure **6**, the thiazolium ring of TPP was changed to a thiazolidine ring and **6** turned out to be a potent inhibitor of *E. coli* PDHc E1. *Cis* isomer of tetrahydro-TPP (*cis*-**6**) bound to PDHc more tightly than TPP and *trans* isomer (*trans*-**6**) did.

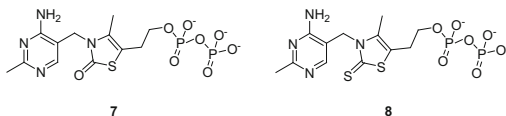
Thiamin 2-thiazolone diphosphate **7** and thiamin 2-thiazolethione diphosphate **8** (Scheme 1.9) were another analogs of TPP reported by Nemeria et al. in 2001 [42]. These compounds have a similar structure to TPP, therefore, they could compete with TPP to the substrate (pyruvate) consequently broke the normal metabolic pathway. Biochemical tests indicated that **7** and **8** had ever stronger binding ability to substrate than that of TPP. In 2004, Arjunan et al. reported the crystal structure of the complex of inhibitor **7** and *E. coli* PDHc [49]. Their finding validated the



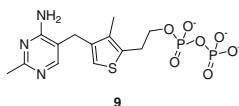
Scheme 1.7 The structure of coenzyme TPP



Scheme 1.8 *cis*-Tetrahydrothiamin pyrophosphate (*cis*-**6**) and *trans*-tetrahydrothiamin pyrophosphate (*trans*-**6**)

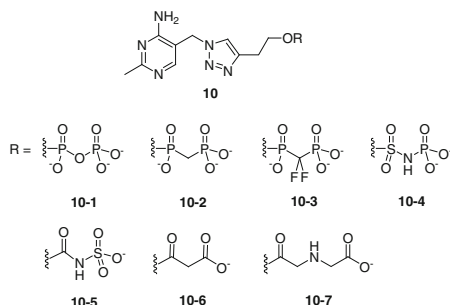


Scheme 1.9 Structures of 2-thiazolone TPP **7** and 2-thiazolthione TPP **8**



Scheme 1.10 The structure of deaza TPP **9**

Scheme 1.11 Triazole TPP analog **10**

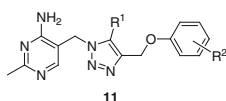


speculation that **7** could favorably compete with TPP to bind to PDHc enzyme, and stopped the normal metabolic process.

In 2005, Leeper et al. reported a new TPP analog, deaza TPP **9** as inhibitor which showed high selectivity to PDHc (Scheme 1.10) [50]. They speculated that nitrogen in the thiazole ring of TPP could be changed to carbon to form **9** as a new TPP analog. Deaza TPP **9** that is essentially identical in shape and size with TPP, but showed stronger binding ability to PDHc than that of TPP. Leeper et al.'s report showed the time required for **9** to bind to the PDHc-E1 was almost 7-fold faster than does its TPP counterpart. It was speculated that **9**'s strong binding ability was attributable to the changing charge state from +1 valence to 0 valence, consequently that should help to enhance the hydrophobic effect between **9** and amino acid in the active site of enzyme. The X-ray crystal structure of enzyme-**9** complex has been obtained by using **9** reacting with PDHc E1 subunit. Crystal structure strongly suggested that **9** bound to the identical position of the active site, as normally TPP will do. It was rather difficult to synthesis the inhibitor **9** due to that so many steps were involved. However another triazole TPP analogs **10**, could be synthesized using only 4 steps by Leeper et al. [51].

The pyrophosphoric acid moiety in TPP can form a coordination bond with Mg^{2+} resulting in the strongest affinity binding to the enzyme. Leeper et al. investigated different triazole TPP analogs **10-1-10-7** which contain different structures in the part of pyrophosphate (Scheme 1.11) [51]. Analog, **10-1** that showed slightly weaker inhibitory activity than compound **9**, but could be synthesized in only 4 steps. In activity, among TPP analogs **10-1-10-7**, the K_i value of analogs **10-2** and **10-3** were 30–40 times higher than that of analogs **10-1**. Analog **10-2** and **10-3** contain methylene in the part of pyrophosphate acid. From analogs **10-2** to **10-7**, their affinity for enzyme was in decreasing order. Especially, compounds **10-7** showed almost no affinity for enzyme at all.

Although several TPP analogs have showed potent inhibition against *E. coli* PDHc E1, there was no mention about their antibacterial or fungicidal activities. We speculate that those TPP analogs would have weak bactericidal or fungicidal activities due to their complex structure with highly charged pyrophosphate that leads to poor bioavailability. That may explain why there are no reports on their antibacterial or fungicidal activities. In order to overcome these problems, both pyrophosphate and thiazolium ring moiety in TPP were replaced by benzene ring and 1,2,3-triazole ring, respectively, to form novel TPP analogs **11** (Scheme 1.12). A series of novel 2-methylpyrimidine-4-ylamine derivatives **11** was designed and synthesized basing on the structure of the active site of PDHc E1 in our laboratory [52, 53]. Some of these compounds turned out to be not only an effective inhibitors of *E. coli* PDHc E1 but also exhibited antibacterial or antifungal activity. We are encouraged by these previous findings and decided to further explore in this area for novel herbicides, antibacterial, or fungicides.



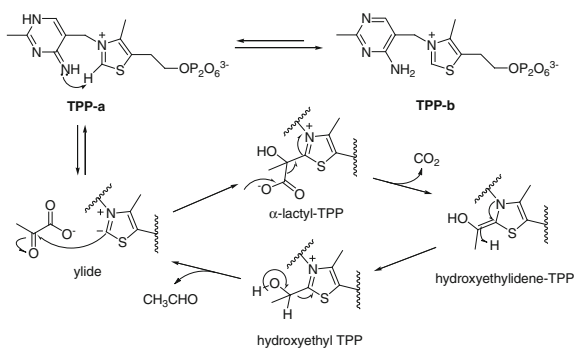
Scheme 1.12 TPP analog **11**

1.3.1.3 Transition State Analogs of TPP as Inhibitors

Since binding interaction between an enzyme and a substrate is more favorable ($>10^8$) at the transition state than at the ground state, a transition state analog was expected to be a much better inhibitor than a substrate analog. Therefore, design of analogs of transition-state in the enzyme catalytic reaction was another popular field of research on PDHc inhibitors [54]. The normal enzyme-catalyzed pyruvate metabolic process is described in Scheme 1.13 [42].

In the first step, the hydrogen atom on C-2 of thiazolium ring was removed to form ylide, and then the substrate carbonyl was attacked by the thiazolium C2

Scheme 1.13 Transition-state in the reaction of TPP and pyruvate



carbanion to yield a tetrahedral intermediate α -lactyl-TPP. The positive charge of thiazolium ring can accelerate the decarboxylation of α -lactyl-TPP, followed by the release of carbon dioxide, producing transition-state hydroxyethylidene-TPP (carbanion/enamine-T). Then hydroxyethylidene-TPP further formed hydroxyethyl-TPP. Finally ylide was re-formed when an acetaldehyde was removed from hydroxyethyl-TPP [50]. Analogs of transition-state including α -lactyl-TPP, hydroxyethylidene-TPP, and hydroxyethyl-TPP, could all act as inhibitors of PDHc.

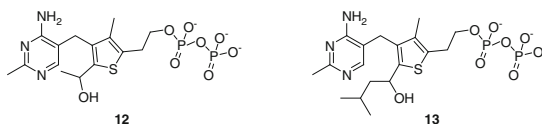
In order to get effective PDHc inhibitors, one approach was to replace those of transition-state in the reaction of TPP and pyruvate by a corresponding analog that resembles the key transition state. Unfortunately, the reported analog was incapable of catalysis [27]. Leeper et al. [50] followed up this idea and made compounds **12** and **13** (Scheme 1.14) as analogs of transition-state hydroxyethyl-TPP. It was observed that **12** and **13** did bind very tightly to *E. coli* PDHc E1. Their inhibitory activity was similar to deaza TPP **9** in terms of rate and affinity for binding with the active site of PDHc.

2-Thiazolone TPP **7** and 2-thiazoethione **8** (Scheme 1.9) also as analogs of transition state enamine-TPP were synthesized and studied by Gutowski and Lienhard [55, 56]. Exciting experimental results proved that **7** and **8** were potent inhibitors. They could bind to the sites of TPP at *E. coli* PDHc E1 and 20,000 times more strongly than TPP [54]. However, the result showed that **7** and **8** should be the analogs of thiamin pyrophosphate (TPP) [57].

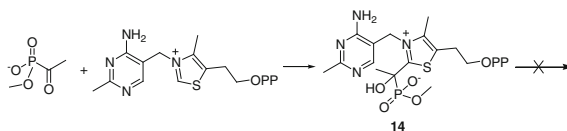
Another approach to get a PDHc inhibitor was to find a compound that could react with the transition-state of TPP to form an intermediate which could combine with a protein side chain and stop any further downstream reactions.

Sodium *O*-methyl acetylphosphonate **1-1** is an analog of pyruvate that appeared to bind and undergo partial reaction with the PDHc. It was proposed that it would be a powerful inhibitor because **1-1** could add to enzyme-bound thiamin diphosphate TPP. Studies showed that this type of compound could form an adduct structure with thiamin diphosphate TPP at the active site of the enzyme during the normal catalytic cycle of PDHc.

A synthetic adduct of thiamin diphosphate-methyl acetylphosphonate had been prepared by Kluger and Pike [58]. They confirmed this proposed mechanism of inhibition and provided detail information about the enzyme's active site. Sodium *O*-methyl acetylphosphonate **1-1** added to thiamin to form methyl 2-hydroxy-2-(2-thiamin)ethylphosphonate **14** (Scheme 1.15), which in turn served as a structural and electrostatic analog of reactive intermediate α -lactyl-TPP in which the planar carboxylate was replaced by a tetrahedral phosphonate.



Scheme 1.14 Analogs of transition-state hydroxyethyl-TPP



Scheme 1.15 Synthesis of **14**

The normal catalytic process involves addition of TPP to pyruvate and subsequent loss of carbon dioxide. It was proposed that **14** would not undergo a reaction analogous to the decarboxylation in the normal catalytic process because the necessary leaving species would be methyl metaphosphate. This process certainly involved a large energy barrier [58]. This analysis suggested the enzyme was responsible for catalyzing the formation of α -lactyl-TPP as a reactive intermediate.

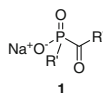
Therefore, **14** could be an analog of α -lactyl-TPP. An analog of a reactive intermediate in an enzymic reaction should bind tightly with the enzyme. The crystal structure of **14** was further reported by Turano et al. [59]. Furey and Jordan have also confirmed a similar phosphonolactyl-TPP structure by a high resolution crystal structure and spectroscopic analysis. It was observed that this type of compound was bound in the pyruvate dehydrogenase E1-subunit [60, 61].

1.3.2 OP Compounds as Inhibitors of Plant PDHc

Although a lot of PDHc E1 inhibitors were reported, most inhibitors were focused on the inhibition against *E. coli* PDHc E1. Studies on inhibitors against plant PDHc E1 were carried out only by a few researchers.

A series of sodium salts of acetylphosphonic acid as potent inhibitors of *E. coli* PDHc was reported by Kluger and Pike in 1977 [40]. Ten years later, on the basis of work of Kluger and Pike, further research on PDHc inhibitor was conducted by Baillie et al. in 1988 [2]. Plant PDHc E1 (EC 1.2.4.1) was used as the target to design a herbicide based on the understanding of key metabolic processes. In these metabolic processes, oxidative decarboxylation of pyruvate into acetyl coenzyme was catalyzed by PDHc E1. More than 50 alkyl acylphosphonates, acylphosphinates, and their salts as mechanism-based inhibitors of PDHc were synthesized. Their inhibition against pea PDHc was evaluated. Some of them were found to be very powerful inhibitors (Table 1.5) [2].

Previously, Kluger et al.'s work showed that **1-1** was a good inhibitor against *E. coli* PDHc. **1-1** was also found to be a good competitive inhibitor of pea PDHc by Baillie et al. later [2]. According to Baillie et al.'s work, **1-2** caused time-dependent inhibition with a half-life of inactivation ($t_{1/2}$) of approximately 12 min at 10 μM . **1-3** was an exceptional good time-dependent inhibitor with $t_{1/2}$ in the region of 3 min at 0.3 μM . **1-6** was much less active, whereas **1-5** with Me as R' and H as R'' were inactive at all.

Table 1.5 Structures of several inhibitors against PDHc from pea

Compound	R'	R''	Inhibition data
1-1	MeO	Me	IC ₅₀ = 70 μM ^a
1-2	Me	Me	t _{1/2} = 12 min at 10 μM ^b
1-3	H	Me	t _{1/2} = 3 min at 0.3 μM ^b
1-4	Et	Me	IC ₅₀ = 165 μM ^a
1-5	Me	H	Inactive
1-6	Me	Et	t _{1/2} = 12 min at 1mM ^b

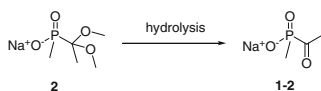
^a Reversible^b Time-dependent

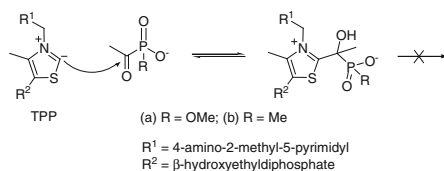
The above results suggested that substituents R' and R'' on the skeleton of the monosodium of acetylphosphonic acid or acetylphosphonic acid **1** would greatly affect the enzyme inhibitory ability. It is worth noting that when Me as R'' stayed the same, a smaller, weaker electronegativity R' on the phosphorus, there are noticeable increasing inhibition activity. Baillie et al.'s work showed that both **1-2** and **1-3**, which resemble pyruvate in structure, were good PDHc inhibitors. Compared with **1-2** (R' = R'' = Me), **1-3** (R' = H, R'' = Me) is a much better time-dependent inhibitor [2].

Post-emergence herbicidal activity of selected compounds including compounds in Table 1.5 and sodium 1,1-dimethoxyethyl(methyl)phosphinate **2** (Sect. 1.3.1) were evaluated at 2.8 kg ai/ha in a greenhouse against pea (*Pisum sativum*), white mustard (*Sinapis alba*), linseed (*Linum usitatissimum*), ryegrass (*Lolium perenne*), wild oat (*Avena sativa*), sugarbeet (*Beta vulgaris*).

Test results (2 weeks after treatment) showed that **1-2** and **2** had a significant better post-emergence activity than **1-1**, **1-3**, and **1-4** while **1-5** and **1-6** showed no activity at all. Sodium 1,1-dimethoxyethyl(methyl)phosphinate **2** was the most effective compound with 80–100 % control against tested weeds. It was speculated that **2** would hydrolyze to **1-2** in vivo (Scheme 1.16).

It was recognized that an acylphosphonate or acylphosphinate might act as an effective inhibitor against plant PDHc. Both compounds could compete with pyruvate for the active site of plant PDHc E1 by binding with TPP resulting a TPP complex. It was speculate that, a highly reactive carbanion of TPP should nucleophilically attack carbonyl carbon atoms of **1-2** to readily form a phosphinic adduct which resembled normal reactive intermediate α-lactyl-TPP. Once it was bond, the normal decarboxylation process in plant was shut off and plant die as their

**Scheme 1.16** **2** was presumably hydrolyzed to **1-2** in vivo



Scheme 1.17 Inhibition of the PDHc-catalyzed decarboxylation

aerobic metabolism was no longer functional. This explains why PDHc E1 is a possible target of herbicide research.

The mechanism of herbicidal activity of these inhibitors was further validated in a barley plant tissue study by measuring the release of radiolabelled carbon dioxide over a period of time. Sodium 1,1-dimethoxyethyl(methyl)phosphinate **2** and radiolabelled pyruvate were used in this study. It was found that the release of carbon dioxide from treated plant tissue was reduced by 35–40 % after treatment and stayed at such level until the plants began to die. The rise in the concentrations of pyruvate + alanine was also observed to be fast and increasing in volume in treated tissue. On the other hand, the declining levels of aspartate and glutamate were also entirely consistent with the inhibition of PDHc. The above observations suggested that **1-2** was mainly targeting the PDHc. The mechanism of herbicidal activity of inhibitors is presented in Scheme 1.17. Susceptible plants died as a direct result of PDHc inhibition [2]. A similar mechanism of inhibition against *E.coli* PDHc by sodium *O*-methyl acetylphosphonate **1-1** (Scheme 1.6), and sodium acetyl(methyl)phosphinate **1-2** has been mentioned in Sect. 1.3.1.

The most promising compound **2** was chosen as a candidate herbicide and extensively evaluated in several field trials. It turned out required relatively high application rate to achieve acceptable weeds control. Unfortunately, such high rate caused unacceptable phytotoxicity on a number of crops, such as cotton. With its inefficiency and phototoxicity problem, the development of **2** was terminated. Although the result was disappoint, the concept of using PDHc as a target for new herbicide is sound. Baillie et al.'s work has set a good example in designing agrochemicals using biochemical reasoning.

1.3.3 Enzyme-Selective Inhibition of OP Compounds

While inhibition of *E. coli* PDHc E1 by sodium salt of acetylphosphinic acid or sodium salt of acetylphosphonic acid were widely studied, the first paper on inhibition against human PDHc E1 by acetylphosphinate or acetylphosphonate was reported by Nemeria et al. in [62]. In order to achieve enzyme-selective inhibition by designing and testing inhibitors for TPP—dependent enzymes, they compared the inhibition of PDHc E1 from bacteria and human by using the identical substrate analog-type inhibitor. Jordan et al. studied the kinetics of binding and inactivation of *E. coli* PDHc E1 (homodimer) and the human PDHc E1 ($\alpha 2\beta 2$ heterotetramer) at

the presence of **1-2** and **1-3**. Both inhibitors were found to be competitive tight-binding reversible inhibitors.

Kinetic parameters (K_i) for the inhibition of *E. coli* PDHc E1 by substrate analogs **1-2** and **1-3** were 3.33 μM and 0.76 μM respectively. **1-3** turned out to be a tight slower binding but stronger inhibitor than **1-2** against human PDHc E1. ($K_i = 0.014 \mu\text{M}$ for **1-3** and $K_i = 1.46 \mu\text{M}$ for **1-2**) Kinetic analysis by measuring the reaction rate through the decarboxylation step revealed that both PDHc E1 either from *E. coli* or from human have the similar inhibition patterns. The result also showed that sodium acetylphosphinate **1-3** was a stronger inhibitor against both enzymes than sodium acetyl(methyl)phosphinate **1-2**.

A comparison of the second-order rate constants for the human and bacterial PDHc E1 enzyme indicated that sodium acetylphosphinate **1-3** was the most potent mechanism-based inhibitor, among several classes of inhibitors for both the human and *E. coli* PDHc E1 in Jordan et al.'s report. It was found that both sodium acetyl(methyl)phosphinate **1-2** and sodium acetylphosphinate **1-3** against human PDHc E1 were much stronger than sodium *O*-methyl acetylphosphonate **1-1**. **1-1** was so weak that the reduction for activity of human PDHc E1 was 20 % or less even at 500-fold molar excess [62]. It is interesting to see that **1-1** was a good inhibitor against *E. coli* PDHc [40] and plant PDHc [2]. These reports suggested that acetylphosphonate **1-1** had a selective inhibition against PDHc E1 on plant or bacteria but not for human PDHc E1.

Several OP compounds have been demonstrated to be one of the most potent PDHc inhibitors. Arming with this newly found favorable selectivity in acetylphosphonate **1-1** we believe that further studies in this biorational design approach for finding powerful and selective inhibitors is possible.

1.4 Design of Novel PDHc E1 Inhibitors as Herbicides

At present, herbicides even with different structures target on only a few active sites. In another words, many classes of herbicides are actually in the same "risk cup". This led to widespread cross-resistance to many classes of herbicides. This situation creates an urgent need for herbicides with novel modes of action. Hopefully, the new mechanisms of action could put the resistant weeds under control. Hunting for herbicides with new mode of action is more dynamic today than ever before.

1.4.1 Selecting Plant PDHc E1 as Target of New Herbicide

We know that PDHc E1 plays a pivotal role in cellular metabolism to convert the product of glycolysis (pyruvate) to acetyl-CoA [63]. Decarboxylation of pyruvate as the first step of a multistep process is a rate-limiting step which is catalyzed by PDHc E1 using thiamine pyrophosphate (TPP) and Mg^{2+} as cofactors [44, 45, 64].

Once PDHc E1 activity is inhibited, overall enzymatic reaction will be blocked in plant [22]. Our results about theoretical study toward understanding for catalytic mechanism of PDHc E1 also indicated that it would be more effective to inhibit the conversion of pyruvate to acetyl coenzyme by designing a PDHc E1 inhibitor to block decarboxylation of pyruvate.

It has been demonstrated that susceptible plants died as a direct result of inhibition on plant PDHc E1 [2, 65], which was concerned only with the first step of a series of the reaction from pyruvate to acetyl CoA [2, 66]. So far several PDHc inhibitors have showed promising activities in the greenhouse, but none of them was successfully developed as a commercial herbicide. As PDHc is an exciting new target for weeds control, further optimization studies on the PDHc inhibitors are needed. This situation provides us with an opportunity to explore plant PDHc as a novel target of commercial herbicide.

Organic phosphorus compounds display a wide range of biological activities. Phosphonates are an important class of heteroatomic compounds possessing extremely rich biological activities. These play an important role in agricultural chemicals, especially the phosphorus-containing herbicides that have been developed and are most widely used all over the world because of their affordability, high efficacy, and low persistency in the natural environment [67].

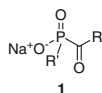
OP compounds have been reported to be the most effective inhibitors against plant PDHc E1 among other PDHc inhibitors. Optimal OP compounds therefore could be an effective, environmental friendly, and selective herbicides targeting on a novel mode of action site (plant PDHc E1), which is different from the target of commercial herbicide.

1.4.2 PDHc E1 Inhibitor Acylphosphonate as Hit Compound

An attempt to design inhibitors of PDHc E1 as herbicides using biochemical reasoning was carried out by Baillie et al. As stated in Sect.1.3.2, several acylphosphinates and acylphosphonates with modest herbicidal activity acting as potent inhibitors against plant PDHc E1 were found in 1988. The current understanding is that, this kind of compound is the most potent and specific inhibitor to plant PDHc E1. However, none of those PDHc inhibitors, including acylphosphinates, acylphosphonates, and relative compounds have been commercially developed. That is because of the following reasons:

- Failed to show sufficient effectiveness as herbicides in the field.
- Damage to crops due to phytotoxicity.
- Poor enzyme-selective inhibition between mammals and plant, with unfavorable mammal toxicity.

Although the most active sodium 1,1-dimethoxyethyl(methyl)phosphinate **2** exhibited 80–100 % inhibition against weeds at the rate of 2.8 kg ai/ha, it showed unacceptable phytotoxicity to the crops at such rates [2, 63]. Sodium salt of

Table 1.6 Inhibition of compounds against PDHc from different origins

Compound	R'	R''	Inhibition against <i>Pisum sativum</i> (Pea) PDHc E1	Inhibition against <i>E. coli</i> PDHc E1	Inhibition against human PDHc E1
1-1	MeO	Me	IC ₅₀ = 70 μM ^a	K _i = 0.05 μM ^c	Not result in more than 20 % reduction of activity of human PDHc E1 even at 500-fold molar excess. ^d
1-2	Me	Me	t _{1/2} = 12 min at 10 μM ^b	K _i = 3.33 μM ^d	K _i = 1.46 μM ^d
1-3	H	Me	t _{1/2} = 3 min at 0.3 μM ^b	K _i = 0.76 μM ^d	K _i = 0.014 μM ^d

^a Reversible^b Time-dependent^c Ref [40]^d Ref [62]

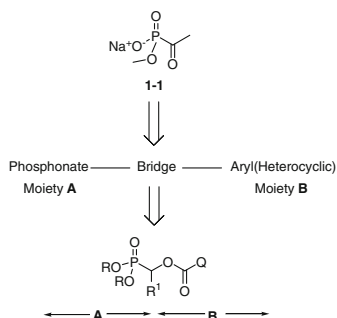
acetylmethyl phosphinic acid **1-2** and **1-3** exhibited a powerful inhibition against PDHc E1 in plant (*Pisum sativum*) and bacteria (*E. coli*), but also against human PDHc E1 (Table 1.6). Therefore, further improvement in the efficiency and selectivity of such PHDc inhibitors are needed. Sodium *O*-methyl acetylphosphonate **1-1**, as an analog of pyruvate was demonstrated to bind with TPP to form a phosphonic adduct **5** (Scheme 1.6), but it did not undergo a decarboxylation. These findings provided us a good foundation for further study on OP PDHc E1 inhibitors as herbicide.

Although these acylphosphinates and acylphosphonates were not active enough to be considered as herbicides, the SAR analysis provided a clue in designing better OP PDHc E1 inhibitors with better herbicidal activities. Data suggested that the phosphonate molecule played a very important role in plant PDHc E1 inhibition. We also noticed that acylphosphonates had better selectivity for plant PDHc E1 between mammals and plant than its acylphosphinates counterpart. For example the sodium *O*-methyl acetylphosphonate **1-1** was a much weaker inhibitor against human PDHc E1 compared to that of sodium acetyl(methyl)phosphinate **1-2** and sodium acetylphosphinate **1-3** (Table 1.6). Therefore, **1-1** that happens to be the best inhibitor in this group, deserves further modification and optimization.

1.4.3 Finding Lead Structure IA

On the basis of Baillie et al.'s work, sodium *O*-methyl acetylphosphonate **1-1** as a hit compound was optimized. Considering its ability in inhibition against plant

Scheme 1.18 1-Oxophosphonic acid derivatives



PDHc E1, phosphonate structural unit as moiety A was linked with an aryl or a heterocycle group as moiety B by a carboxylate ester bond to form 1-oxophosphonic acid derivatives (Scheme 1.18). In order to find a lead compound with desired herbicidal activity, different structural unit Q was introduced into this phosphonate scaffold resulting a series of 1-oxophosphonic acid derivatives [68].

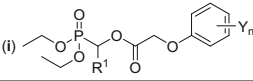
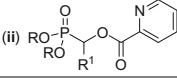
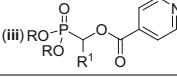
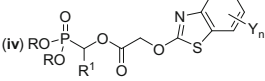
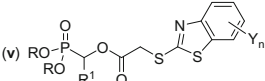
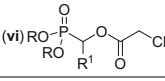
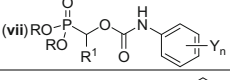
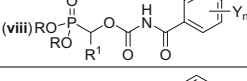
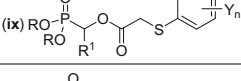
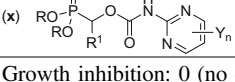
About 150 compounds including ten series of 1-oxophosphonic acid derivatives (i)–(x) were synthesized to examine their herbicidal activity at an early stage of our work. Their synthetic methods have been reported in the corresponding literatures [69–78].

The herbicidal activity of ten series of compounds at 2.25 kg ai/ha rate was evaluated in the greenhouse. The general structure and herbicidal activity of compounds (i)–(x) are listed in Table 1.7. Most series of compounds showed poor herbicidal activity, except some *O,O*-diethyl 1-(substituted phenoxyacetoxy)alkylphosphonate (i) (Table 1.7), such as **IA-1** (R = H, $Y_n = 4\text{-Cl}$) that exhibited significant herbicidal activity against dicotyledonous plants. It also showed **IA-1** had better herbicidal activity than that of these acylphosphinates and acylphosphonates counterparts. Because of their interesting herbicidal activities and promising selectivities, *O,O*-diethyl 1-(4-chlorophenoxyacetoxy)methylphosphonate **IA-1** was considered a new lead.

The reason for weak herbicidal activity of acylphosphinates or acylphosphonate **1** (such as **1-1**, **1-2** and **2**) was speculated stemming from the limited modifications in parent structure **1**. We first modified **1** to create a general structure of **I** for further modifications (Scheme 1.19).

In general structure **I**, there were five or even more substituents which could be changed by chemical modifications. Comparing to acylphosphinates or acylphosphonate **1**, structure **I** would have a much broader structure-range. The SAR analysis suggested structure **I** could be remarkably affected by variable combinations of R^1 , R^2 , R^3 , R^4 and Y_n . Thus, it is possible to come up with highly active analogs by the right combination. Another feature in structure **I**, which got our attention, was its carboxylate ester bond which in turn, should made **I** less persistent in the environment.

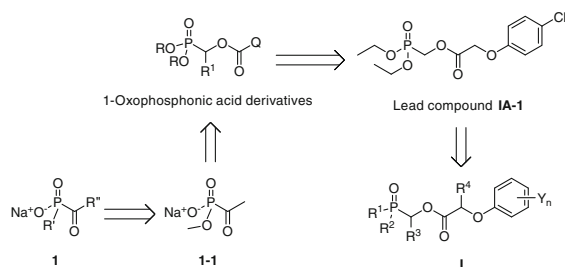
Table 1.7 Comparison of herbicidal activities in a series of structures (i)–(x)

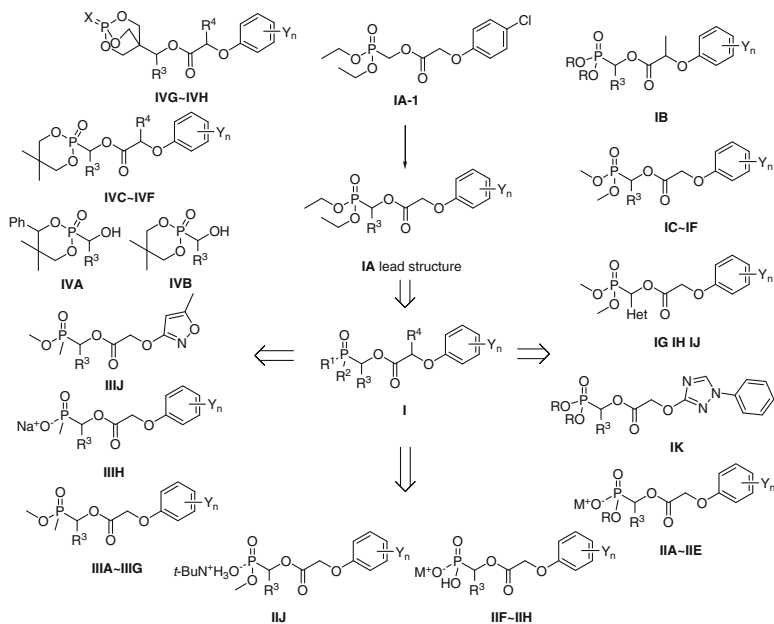
Structure	Herbicidal activities ^{a,b,c}
(i) 	≤100 % when R ¹ = H, Y _n = 4-Cl
(ii) 	≤48 %
(iii) 	≤48 %
(iv) 	≤32 %
(v) 	≤30 %
(vi) 	≤30 %
(vii) 	≤30 %
(viii) 	≤30 %
(ix) 	≤18 %
(x) 	0

^a Growth inhibition: 0 (no effect), 100 % (completely kill); at a rate of 2.25 kg ai/ha

^b Test plants: rape, common vetch, setose thistle, cucumber, common amaranth, barnyard grass, wheat, and Chinese sorghum

^c Compounds: (i) [75]; (ii) [72]; (iii) [73]; (iv) [71]; (v) [70]; (vi) [69]; (vii) [76]; (viii) [77]; (ix) [74]; (x) [78]

Scheme 1.19 Modification of lead structure



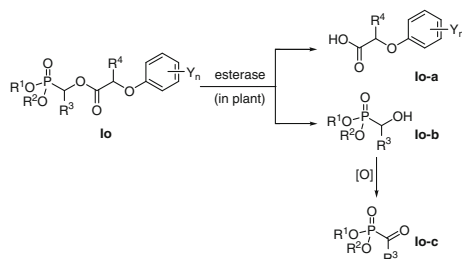
Scheme 1.20 Chemical modification of lead structure

In order to obtain more powerful PDHc E1 inhibitors with effective herbicidal activity, all substituents R^1 , R^2 , R^3 , R^4 , and Y_n in structure **I** were systemically modified. Through structural modification or optimization, more than thirty novel series of structure **I** including alkylphosphonates, monosalts of alkylphosphonic acids, alkylphosphinates, monosalts of alkylphosphinic acid, cyclic phosphate, and caged bicyclic phosphates were designed and synthesized (Scheme 1.20). Their herbicidal activities were evaluated. Structure-activity relationship was then established and analyzed. Enzyme inhibition, toxicities and usage of representative compounds in this group were also studied later.

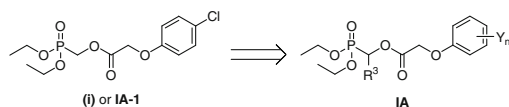
1.4.4 Optimization Strategy

Considering the ability and better selectivity of acylphosphonate **1-1** in inhibition against plant PDHc E1, the study on structure **I** was firstly focused on the phosphonate scaffold **Io**.

We proposed a metabolic pathway of phosphonates with structure **Io** in plants when these compounds **Io** were initially designed. **Io** might be metabolized to substituted phenoxyacetic acids (**Io-a**) as auxin-type herbicide and acylphosphonates (**Io-c**) as PDHc E1 inhibitors after the hydrolysis and oxidation by esterases and oxidases took place in plants (Scheme 1.21).



Scheme 1.21 Possible metabolic pathway of **Io** in plant



Scheme 1.22 **IA-1** as lead compound was further modified

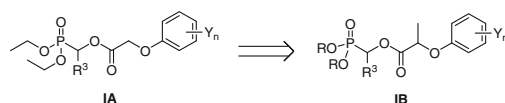
Acylphosphonates (**Io-c**) were considered to act as inhibitors of PDHc E1 to show herbicidal activity according to the work of Baillie et al. It was speculated that the herbicidal activity of **Io** might come from the effects of both possible metabolic products **Io-a** and **Io-c**. Therefore we expected **Io** would have better herbicide activity than **Io-a** or **Io-c**. We also expected **Io** would act as inhibitors of PDHc E1.

It would be interesting to examine this hypothesis in our continued work. It turned out that **Io** itself was responsible for both herbicidal activity and inhibitory potency against PDHc E1 through further study. These results are described in Chap.7. In the first stage of the modification of structure **I**, our synthesis effort was focused on the phosphonate scaffold **Io**. Different groups of R^1 , R^2 , R^3 , R^4 and Y_n were introduced into the general structure **Io** to form different series of alkylphosphonates **IA-IK**. On this phosphonate scaffold **Io**, the strategy for optimizing the lead compound **IA-1** is described step by step as follows.

The series of *O,O*-diethyl 1-(substituted phenoxyacetoxy)alkylphosphonates as **IA** was further designed and prepared by modification of *O,O*-diethyl 1-(4-chlorophenoxyacetoxy)methylphosphonate **IA-1** which showed significant herbicidal activity in our previous study. In **IA** series, the Et group as R^1 , R^2 and H as R^4 were kept, further optimization was focused on the modification of substituents R^3 and Y_n (Scheme 1.22). Herbicidal activity of **IA** including 24 compounds were evaluated at a rate of 2.25 kg ai/ha in the green house. Most **IA** exhibited excellent post-emergence herbicidal activity against dicotyledon. Structure **IA** that was a lead structure deserved further modification.

1.4.4.1 Design Strategy for Class IB

Knowing that the group R¹ which link to the phosphorus atom in the compounds **1** played an important role in inhibiting the plant PDHc E1 according to Baillie et al.'s report, the R¹ and R² of phosphorus-containing structural unit in structure **Io** were first modified. Resulting compounds were then evaluated for herbicidal activity. Me, Et, and Pr as R¹ and R² were introduced into structure **Io** to design a series of 1-(substituted phenoxyacetoxy)alkylphosphonates **IB** including 16 compounds, meanwhile substituents R³, R⁴ and Y_n in **IB** series were also modified (Scheme 1.23). SAR results for **IB** series suggested that smaller R¹ and R² (Me as R¹ and R²) would be beneficial to herbicidal activity.

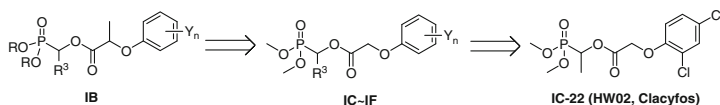


Scheme 1.23 Design of alkylphosphonates **IB** by extending structure **IA**

1.4.4.2 Design Strategy for Class IC–IF

According to the results of SAR for **IB** series, structure **IB** was further optimized to produce four series of novel *O,O*-dimethyl 1-(substituted phenoxyacetoxy)alkylphosphonates **IC–IF** (Scheme 1.24). In this **IC–IF** series, Me group as R¹, R² and H as R⁴ were kept in structure **Io**, further modification of substituents R³ and Y_n was carried out to validate our speculation that such modification would increase the herbicidal activity. When Me as R¹ and R² different substituents R³ and Y_n were introduced into parent structure **Io** to produce **IC–IF** series including 63 compounds. Pre-emergence and post-emergence herbicidal activity of compounds **IC–IF** were systematically evaluated at different rates in the greenhouse.

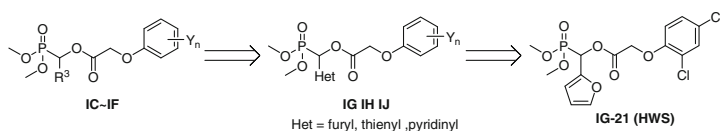
SAR analyses indicated that herbicidal activity could be increased greatly by optimizing R¹, R², R³, R⁴ and Y_n in phosphonate **Io**. *O,O*-dimethyl 1-(2,4-dichlorophenoxyacetoxy)ethylphosphonate **IC-22** (HW02, clacyfos) was found to be the most effective compound among **IA–IF** series against broadleaf in post-emergence application at the rate of 18.75–450 g ai/ha (see Chap. 2). **IC-22** also showed much higher and practical herbicidal activity than that of acylphosphinates or acylphosphonates **1**.



Scheme 1.24 Optimization of **IB** and finding active compound **IC-22**

1.4.4.3 Design Strategy for Class IG–IJ

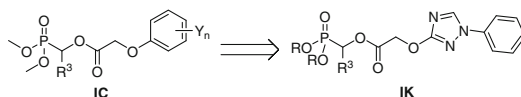
O,O-Dimethyl 1-(substituted phenoxyacetoxy)alkylphosphonates **IC** showed higher herbicidal activity than the first lead structure **IA**, happened to be a novel OP structure. It deserves further modifications. On the basis of the alkylphosphonates **IC**, furyl, thienyl and pyridyl groups as R³ were introduced to parent structure **Io**, separately, to form three series of novel alkylphosphonates **IG–IJ** (Scheme 1.25). We speculated that introduction of heterocyclic groups into the parent structure could result in better bioactivity. Results showed that the furyl or thienyl group as R³ were indeed beneficial to post-emergence herbicidal activity when compound with the Me group as R¹, R²; H as R⁴; and 2,4-Cl₂ as Y_n in structure **Io**. Data from this **IG–IJ** series including 57 compounds, showed that *O,O*-dimethyl 1-(2,4-dichlorophenoxyacetoxy)-1-(fur-2-yl)methylphosphonate **IG-21** (HWS) happened to be most effective compound. It demonstrated excellent herbicidal activity against broadleaf weeds at a rate of 37.5 g ai/ha. **IG-21** (HWS) also showed good selectivity. It worked effective against broadleaf and was rather safe for monocotyledonous crops. Later field trials confirmed that it showed very good crop safety on maize (see Chap. 8).



Scheme 1.25 Optimization of **IC** and finding active compound **IG-21**

1.4.4.4 Design Strategy for Class IK

When Me as R¹ and R²; H as R⁴; and 2,4-Cl₂ as Y_n; Me or furyl as R³ in structure **Io**, **IC-22** and **IG-21** exhibited the best activity against dicotyledons in post-emergence application among **IA–IJ** series. We wondered what and if that would affect the herbicidal activity when a heterocyclic ring was introduced into the phenoxyacetoxy moiety in parent structure **Io**. A novel series of 1-[(1-phenyl-1,2,4-triazol-3-yl)oxyacetoxy]alkylphosphonates **IK** including 7 compounds was then prepared by introducing a triazole ring into phenoxyacetoxy moiety in parent structure **Io**, where no substituent was on the benzene ring (Scheme 1.26). To our surprise, the post-emergence herbicidal activity of **IK** was almost completely gone.



Scheme 1.26 Modification of **IC**

These results indicated that phenoxyacetoxy moiety and proper substitution at phenoxyacetoxy moiety were very important for post-emergence activity. Acceptable post-emergence herbicidal activity of alkylphosphonates **1o** should have a reasonable combination of both phosphonate structural unit and proper substituted phenoxyacetate moieties. Detail study on alkylphosphonates **IA–IK** can be found in Chap. 2.

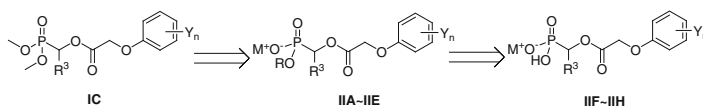
1.4.4.5 Design Strategy for Class **IIA–IIIE** and **IIIF–IIIH**

It has been speculated that the salts of 1-(substituted phenoxyacetoxy)alkylphosphonic acid could have good herbicidal activity because several salts of acetylphosphonic acid (such as sodium methylacetylphosphonate **1-1**) have been reported as a powerful PDHc E1 inhibitor. Because of that, five series of novel alkali metal salts of *O*-alkyl 1-(substituted phenoxyacetoxy)alkylphosphonic acids **IIA–IIIE** including 77 compounds were designed and synthesized (Scheme 1.27).

Compared with alkylphosphonates **1c** in Chap. 2, some of **IIA–IIIE** showed different degrees of herbicidal activity, when Me as R¹ was replaced with Li, Na or K in structure **1o**. Several alkali metal salts of *O*-alkyl 1-(substituted phenoxyacetoxy)alkylphosphonic acids showed much higher inhibitory activity against plant PDHc E1 as well as higher pre-emergence activity against dicotyledons than their corresponding phosphonates at 450 g ai/ha rate. Most of monosalts showed noticeable pre-emergence activities against both dicotyledon and monocotyledon at 1.5 kg ai/ha.

We assumed, 1-alkylphosphonic acid should have even better herbicidal activity, because it resembles to pyruvate which in turn is a natural substrate of PDHc E1. Therefore, three series of novel mono alkali metal salts of 1-(substituted phenoxyacetoxy)alkylphosphonic acids **IIIF**, **IIIG**, and **IIIH** including 36 compounds were designed and synthesized (Scheme 1.27).

Compared with alkylphosphonates **1c** and monosalts **IIA–IIIE**, several series of monosalts of alkylphosphonic acids **IIIF–IIIH** demonstrated higher inhibitory activity against monocotyledonous weeds in post-emergence application. **IIIF-1**, **IIIG-1**, and **IIIH-1** could provide 50–80 % control at 150 g ai/ha for the monocot weeds. However, their corresponding phosphonate **1c-22** and monosodium salt **IIIB-2** showed no activity under the same test conditions. We considered these alkali metal salts of alkylphosphonates or alkylphosphonic acids **IIA–IIIH** was a new OP herbicide lead which should be worth further optimization.

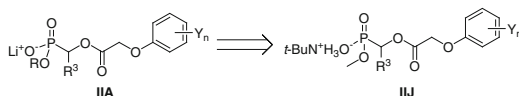


Scheme 1.27 Design of alkali metal salts of alkylphosphonates or alkylphosphonic acids **IIA–IIIH** by modification of **1c**

Detail study on monosalts of alkylphosphonic acid derivatives **IIA–IIH** is discussed in Chap. 3, while the inhibitory activity against plant PDHc E1 by sodium *O*-methyl 1-(2,4-dichlorophenoxyacetoxyl)alkylphosphonates **IIB** is discussed in Chap. 7

1.4.4.6 Design Strategy for Class IIJ

All monosalts of *O*-alkyl alkylphosphonic acids **IIA–IIE** (Na, K or Li as M in **IIA–IIE**) contain inorganic salts. Organic salts of alkylphosphonate are believed to have even more herbicidal activity than their inorganic salts counterparts. A novel series of *t*-butylammonium *O*-methyl 1-(substituted phenoxyacetoxyl)alkylphosphonates **IIJ** including 28 compounds was hence designed and synthesized (Scheme 1.28). Most of the aminium salts displayed noticeable herbicidal activity against broadleaves at 150 g ai/ha in post-emergence application. Among aminium salts **IIJ**, **IIJ-24** with Me as R³, 2,4-Cl₂ as Y_n turned out to be the most active compound. At 75 g ai/ha, it exhibited 70–95 % control of all tested broadleaves in post-emergence application. Compared with phosphonate **IC-22**, aminium salt **IIJ-24** showed different activity spectrum. For example, **IIJ-24** displayed significantly higher activity at 150 g ai/ha against barnyard grass than that of phosphonate **IC-22**. The results of study on aminium salts of alkylphosphonates **IIJ** are described in Chap. 3.

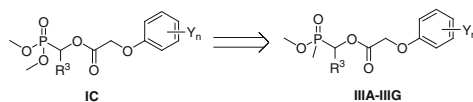


Scheme 1.28 Design of salts of alkylphosphonates **IIJ** by optimization of **IIA**

1.4.4.7 Design Strategy for Class IIIA–IIIG

Bioisosterism is an important aspect in designing bioactive compounds. For example, phosphinate unit is often used to replace the phosphonate unit to obtain a more active compound. Bailie et al.'s SAR analyses showed that the replacement of methoxyl in acylphosphonate (**1-1**) by methyl to produce acylphosphinate (**1-2**), would significantly improve the inhibitory potency and herbicidal activity. Therefore, we were interested in examining herbicidal activity of the alkylphosphinates. On the basis of *O,O*-dimethyl 1-(substituted phenoxyacetoxyl)alkylphosphonates **IC**, several novel series of *O*-methyl [1-(substituted phenoxyacetoxyl)alkyl]methylphosphinates **IIIA–IIIG** including 54 compounds were designed and synthesized (Scheme 1.29).

It was found that most alkylphosphinates **IIIC** showed higher inhibition activity against monocot species such as crab grass and barnyard grass than their corresponding alkylphosphonates **IC**, **IE**, or **IF**. Several alkylphosphinates however exhibited a higher selectivity between wheat and weeds than their corresponding



Scheme 1.29 Design of alkylphosphinates **IIIA–IIIG** by modification of **IC–IJ**

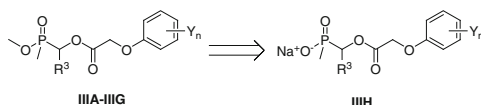
alkylphosphonates at 2.25 kg ai/ha. For example, alkylphosphinate **IIIC-1** displayed higher inhibition at both pre- and post-emergence studies against crab grass and barnyard grass than that of its corresponding alkylphosphonate **IC-22** (HW02, clacyfos). Compound **IIIC-1** also showed better safety for wheat than **IC-22** in pre-emergence application. The results of study on alkylphosphinates **IIIA–IIIG** are described in Chap. 4.

1.4.4.8 Design Strategy for Class IIIH

Through the study on monosalts of *O*-alkyl alkylphosphonic acids **IIA–IIIE**, several of them were found to possess higher inhibition activity against plant PDHc E1 and better water solubility than that of corresponding phosphonates. Baillie et al.'s work also showed sodium salt of acetyl(methyl)phosphinic acid **1-2** as the salt of phosphinate displayed higher enzyme inhibition and herbicidal activity than corresponding sodium *O*-methyl acetylphosphonate **1-1**. However, **1-2** was also much stronger inhibitor against human PDHc E1 than **1-1** [2].

These results encouraged us to design and prepare monosalts of alkylphosphinate to compare the herbicidal activity and enzymatic-selectivity between alkylphosphinate and their phosphonate counterparts. Therefore, a novel series of sodium [1-(substituted phenoxyacetoxy)alkyl]methylphosphinates **IIIH** was further designed through replacing the MeO group in **IIIA–IIIG** by NaO (Scheme 1.30).

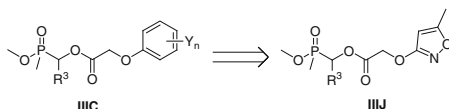
Comparing sodium salts of alkylphosphonic acids **IIIH** with their corresponding phosphinates **IIIG**, it was found that inhibitory activity against the growth of plant could be greatly enhanced when MeO attached to phosphorus in phosphinates **IIIG** was replaced by NaO. The results of study on **IIIH** are described in Chap. 4.



Scheme 1.30 Design of sodium salts of alkylphosphonic acids **IIIH** by modification of **IIIA–IIIG**

1.4.4.9 Design Strategy for Class IIIJ

There are several naturally occurring isoxazoles with interesting biological activity. For example, Muscimol and 4-hydroxy isoxazole, are seed-germination inhibitors



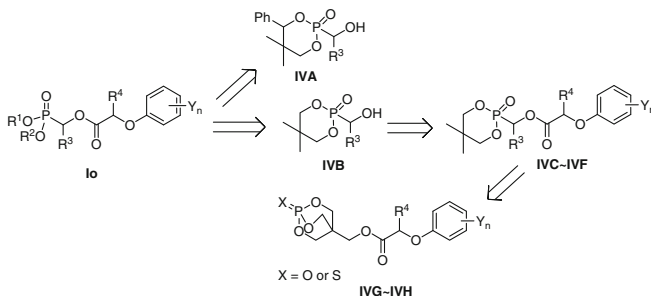
Scheme 1.31 Design of alkylphosphinates **IIIJ** by modification of **IIIC**

[79]. Their structures have been used as the basis for the design of a number of synthetic isoxazole derivatives. Some of those derivatives have been successfully launched as commercial agrochemicals [80]. In order to explore the herbicidal activity of compounds containing isoxazoles, the substituted phenoxyacetoxymethyl unit in **IIIC** was replaced by (5-methylisoxazol-3-yl)oxyacetoxymethyl unit; a novel series of *O*-methyl [1-(5-methylisoxazol-3-yl)oxyacetoxymethyl]methylphosphinates **IIIJ** including 7 compounds was designed and synthesized (Scheme 1.31). Unfortunately, bioassay results showed that alkylphosphinates containing isoxazoles **IIIJ** had much weaker herbicidal activity than that of alkylphosphinates **IIIC**. The results of study on alkylphosphinates **IIIJ** are described in Chap. 4.

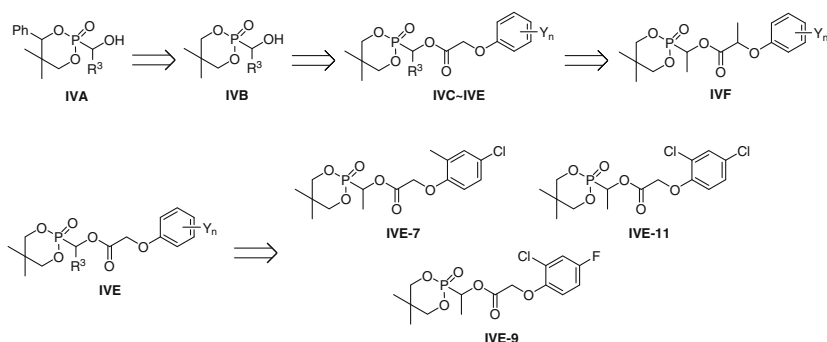
1.4.4.10 Design Strategy for Class IVA–IVH

A variety of studies have demonstrated that bioactivity and stability of phosphonates or phosphates could be increased by introducing a phosphorus-containing heterocyclic moiety to their parent structure. Considering possible contribution of cyclophosphonates to herbicidal activity, we extended our study to cyclic phosphonates.

Several different types of cyclic phosphonates **IVA–IVF** were designed on the basis of the alkylphosphonates **Io**. Moreover, the cyclic phosphonates **IVC–IVF** were further modified to the caged bicyclic phosphates **IVG–IVH** (Scheme 1.32). It was expected that herbicidal activity of compounds could be optimized by introducing a phosphorus-containing heterocyclic moiety. 82 of cyclic phosphonates **IVA–IVF** and 27 of caged bicyclic phosphates **IVG–IVH** hence were prepared.



Scheme 1.32 Design of cyclic phosphonates **IVA–IVF** and caged bicyclic phosphates **IVG–IVH**



Scheme 1.33 Finding new lead structure **IVE** and active compounds **IVE-7**, **IVE-9**, **IVE-11** by structural optimization

Using a systematic optimization approach for cyclic 1-hydroxyalkylphosphonates **IVA**, 2-[1-(substituted phenoxyacetoxy)alkyl]-5,5-dimethyl-1,3,2-dioxaphosphinane-2-one **IVE** turned out to be a new OP lead. By further optimization, **IVE-7**, **IVE-9**, and **IVE-11** (Scheme 1.33) were found to be the most effective compounds against broadleaves by post-emergence application at 18.5–75 g ai/ha in the greenhouse.

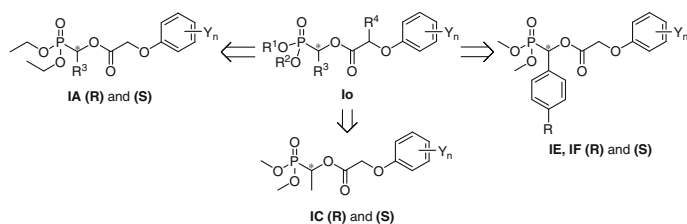
They exhibited noticeable post-emergence activity comparable to clacyfos (**IC-22**, HW02) and 2,4-D, and better than glyphosate at 18.5–75 g ai/ha against tested broadleaves. Cyclic phosphonates **IVE-7**, **IVE-9** and **IVE-11** showed good selectivity between dicotyledon and monocotyledon. At 150 g ai/ha, they were effective against tested dicotyledon weeds but non harmful to monocotyledonous crops such as wheat, rice and maize. Compound **IVE-11** showed good safety to wheat and rice at a rate up to 450 g ai/ha. Cyclic phosphonates **IVE-11** displayed potential as a selective post-emergence herbicide for weeds in wheat and rice fields. This warranted further investigation. The results of study on cyclic phosphonates and caged bicyclic phosphates **IVA–IVH** are described in Chap. 5.

1.5 Book Chapter Organization

This book consists of nine chapters. Chapter 1 is an overview.

Chapters 2–5 focus on the synthesis, spectroscopic analysis, and herbicidal activity of 30 series phosphorus-containing compounds including alkylphosphonates, monosalts of alkylphosphonic acids, alkylphosphinates, monosalts of alkylphosphinic acids, cyclic phosphonates, and caged bicyclic phosphates (Scheme 1.20). Their structure-activity relationships are discussed in detail in each chapter.

It is important to point out that all these substituted alkylphosphonates **IA–IJ** and **IVC–IVE** have a chiral carbon in their molecular skeletons, which contains different optically active isomers. It was well demonstrated that the absolute



Scheme 1.34 Several kinds of optically active 1-(substituted phenoxyacetoxy)alkylphosphonates

configuration of chiral herbicides could significantly affect their herbicidal activity [81, 82], enzymatic inhibition, [83] even the mode of action [84], crop safety [85], toxicity and environmental safety [86, 87]. Therefore, it is critically importance to sort out the preferred molecular chirality.

All substituted alkylphosphonates **IA–IJ** and **IVC–IVE** studied or reported previously were only based on their racemic forms. Considering the importance of chirality for herbicidal active, the synthesis and the biological activities of their optical counterparts would be very important. The methods of asymmetric synthesis of both chiral 1-hydroxyphosphonates and cyclic 1-hydroxy phosphonates, and several optically active 1-(substituted phenoxyacetoxy)alkylphosphonates were hence set up. So far, several series of optically active 1-(substituted phenoxyacetoxy)alkylphosphonates including **IA**, **IC**, **IE**, **IF** series were prepared (Scheme 1.34) and their biological activities were evaluated. Their asymmetric synthesis, enantiomeric selectivity in herbicidal activity, acute aquatic toxicity, and SAR discussion are summarized in Chap. 6.

In order to determine the probable binding conformations of title phosphonate derivatives, molecular docking and three-dimension quantitative structure-activity relationship (3D-QSAR) studies on the binding modes of alkylphosphonates to PDHcE1 were carried out. The methods and results of binding conformational analysis, CoMFA and CoMSIA analysis as well as validation of the 3D-QSAR models are described in Chap. 7. Both CoMFA and CoMSIA findings were in good agreement with the spatial and electronic structural characteristics of the binding groove of PDHc E1. Mapping 3D-QSAR models of the active site of PDHc E1 provided us a new insight into the protein-inhibitor interaction mechanism. Studies for both plant PDHc inhibition and herbicidal effects were carried out for several 1-(substituted phenoxyacetoxy)alkylphosphonates. Representative compounds, such as **IC-22** (HW02, clacyfos) and **IG-21** (HWS) showed promising herbicidal activity as well as strong inhibition activity against plant PDHc. SAR analyses indicated both inhibitory potency against plant PDHc and herbicidal activity of alkylphosphonates could be greatly increased by optimizing R^1 , R^2 , R^3 and Y_n in general structure **Io**. Effect of Y_n on both inhibitory potency against PDHc E1 and herbicidal activity of alkylphosphonates **Io** could be explained by molecular docking study showing the binding modes of these alkylphosphonates **Io** to PDHc E1.

Compound **IC-22** (HW02, clacyfos) was found to act as a competitive inhibitor of PDHc in plant and showed interesting selectivity among plants. It showed stronger inhibition against the PDHc from pea and mung bean than from rice. In the herbicide bioassay, it showed much higher herbicidal activity against broadleaf weeds than monocotyledonous weeds. These results indicated the PDHc inhibition ability is positively correlated with their herbicidal activities. The detailed about their selectivity are summarized in Chap. 7.

Potential lead compounds in both PDHc inhibition and herbicidal activity were obtained through systematic optimization approach. Several alkylphosphonate compounds that displayed promising herbicidal activity and desirable selectivity in the early stage were selected in our R/D program. Two representative compounds **IC-22** and **IG-21** showed good potential as post-emergence herbicides. However, to the best of our knowledge, so far none of the PDHc inhibitors has been successfully developed as a commercial herbicide due to some issues such as toxicity, poor selectivity and marginal herbicidal activity in the field.

Fortunately, *O,O*-dimethyl 1-(2,4-dichlorophenoxyacetoxy)ethylphosphonate **IC-22** acted as a competitive inhibitor of plant PDHc, showed low mammalian toxicity, low residue, good selectivity and promising herbicidal activities in the greenhouse. Therefore, **IC-22** was selected as candidate for further development. It had been evaluated extensively in the field. More than 40 field trials at different regions in China showed that **IC-22** (HW02, clacyfos) controlled a broad spectrum of broadleaf and sedge weeds at 150–450 g ai/ha for post-emergence applications in lawn, wheat and maize fields. HW02 (clacyfos) as a selective and environment-friendly herbicide that passed the pesticide standard procedure requirement and received a temporary registration in 2007 in China. It seems to be the first compound which shows practical herbicidal activity as a plant PDHc inhibitor.

Compound, *O,O*-dimethyl 1-(2,4-dichlorophenoxyacetoxy)-1-(fur-2-yl) methylphosphonate **IG-21** (HWS) is another plant PDHc inhibitor. Its low toxicity to rat, bees, birds, fish, and silkworm warranted further evaluation as well. **IG-21** was found to be an effective compound against broadleaf weeds at 50–300 g ai/ha rate and it was safe to maize and rice even at the rate as high as 0.9–1.2 kg ai/ha in the greenhouse. In maize field trials at different regions in China showed that **IG-21** could control a broad spectrum of broadleaf and sedge weeds at 135–270 g ai/ha for post-emergence applications. **IG-21** displayed good potential as a selective and environment-friendly herbicide. Detail discussion for **IC-22** and **IG-21** can be found in Chap. 8.

A systematic R&D work from basic research to field application to find an environment-friendly herbicide is our mission. We have been designing and synthesizing suitable alkylphosphonates as plant PDHc E1 inhibitors in our lab in the last 20 years. We have made great progress in creating phosphorus-containing PDHc inhibitors with effective herbicidal activity. For example alkylphosphonate **Io** was the result of optimization of acylphosphonates **1**. Alkylphosphonate **Io** is able to overcome some common problems associated with plant PHDc inhibitors such as low herbicidal activity, phytotoxicity and poor selectivity. Compared with other PDHc inhibitors, clacyfos (HW02), a good representative of alkylphosphonate **Io**,

showed much stronger herbicidal activity, better crop selectivity, and lower toxicity to bees, birds, fish, silkworm, and human. Field studies showed that clacyfos displayed much higher herbicidal effect than that of sodium 1,1-dimethoxyethyl (methyl)phosphinate **2** which was reported as a plant PDHc inhibitor with the most active post-emergence herbicidal activity at 2.8 kg ai/ha.

Our systematic optimization approach from a sound basic research idea to create field-test candidate herbicide provided valuable information on chemistry and biology of alkylphosphonates. Our research confirmed that plant PDHc E1 could be a new target for herbicide R/D. We hope that our biorational design in the synthesis of the alkylphosphonates as plant PDHc E1 inhibitors, paved the way for other biorational designs to find new pesticides with novel mode of action in the future.

References

1. Ohkawa H, Miyagawa H, Lee PW (eds) (2007) Pesticide chemistry: crop protection, public health, environmental safety. Wiley-VCH, Weinheim
2. Baillie AC, Wright K, Wright BJ et al (1988) Inhibitors of pyruvate dehydrogenase as herbicides. *Pestic Biochem Physiol* 30:103–112
3. Patel MS, Roche TE (1990) Molecular biology and biochemistry of pyruvate dehydrogenase complexes. *FASEB J* 4:3224–3233
4. Murarka A, Clomburg JM, Moran S et al (2010) Metabolic analysis of wild-type *Escherichia coli* and a pyruvate dehydrogenase complex (PDHC)-deficient derivative reveals the role of PDHC in the fermentative metabolism of glucose. *J Biol Chem* 285:31548–31558
5. Mattevi A, De Kok A, Perham RN (1992) The pyruvate dehydrogenase multienzyme complex. *Curr Opin Struct Biol* 2:877–887
6. Dugas H (1996) Bioorganic chemistry: a chemical approach to enzyme action. Springer, New York
7. Stephens PE, Darlison MG, Lewis HW et al (1983) The pyruvate dehydrogenase complex of *Escherichia coli* K12. Nucleotide sequence encoding the pyruvate dehydrogenase component. *Eur J Biochem* 133:155–162
8. Stephens PE, Darlison MG, Lewis HW et al (1983) The pyruvate dehydrogenase complex of *Escherichia coli* K12. Nucleotide sequence encoding the dihydrolipoamide acetyltransferase component. *Eur J Biochem* 133:481–489
9. Stephens PE, Lewis HM, Darlison MG et al (1983) Nucleotide sequence of the lipoamide dehydrogenase gene of *Escherichia coli* K12. *Eur J Biochem* 135:519–527
10. Reed LJ (1974) Multienzyme complexes. *Acc Chem Res* 7:40–46
11. Pei XY, Titman CM, Frank RAW et al (2008) Snapshots of catalysis in the E1 subunit of the pyruvate dehydrogenase multienzyme complex. *Structure* 16:1860–1872
12. Saumweber H, Binder R, Bisswanger H (1981) Pyruvate dehydrogenase component of the pyruvate dehydrogenase complex from *Escherichia coli* K12. Purification and characterization. *Eur J Biochem* 114:407–411
13. Henderson CE, Perham RN (1980) Purification of the pyruvate dehydrogenase multienzyme complex of *Bacillus stearothermophilus* and resolution of its four component polypeptides. *Biochem J* 189:161–172
14. Hengeveld AF, Westphal AH, De Kok A (1997) Expression and characterisation of the homodimeric E1 component of the *Azotobacter vinelandii* pyruvate dehydrogenase complex. *Eur J Biochem* 250:260–268

15. Schreiner ME, Fiur D, Holátko J et al (2005) E1 enzyme of the pyruvate dehydrogenase complex in *Corynebacterium glutamicum*: molecular analysis of the gene and phylogenetic aspects. *J Bacteriol* 187:6005–6018
16. Camp PJ, Randall DD (1985) Purification and characterization of the pea chloroplast pyruvate dehydrogenase complex. a source of acetyl-CoA and NADH for fatty acid biosynthesis. *Plant Physiol* 77:571–577
17. Szurmak B, Strokovskaya L, Mooney BP et al (2003) Expression and assembly of *Arabidopsis thaliana* pyruvate dehydrogenase in insect cell cytoplasm. *Prot Expr Puri* 28:357–361
18. Thelen JJ, Miernyk JA, Randall DD (1998) Partial purification and characterization of the maize mitochondrial pyruvate dehydrogenase complex. *Plant Physiol* 116:1443–1450
19. Dahl HM, Hunt SM, Hutchison WM et al (1987) The human pyruvate dehydrogenase complex. Isolation of cDNA clones for the E1 α subunit, sequence analysis, and characterization of the mRNA. *J Biol Chem* 262:7398–7403
20. Teague WM, Pettit FH, Wu TL et al (1982) Purification and properties of pyruvate dehydrogenase phosphatase from bovine heart and kidney. *Biochemistry* 21:5585–5592
21. Seifert F, Golbik R, Brauer J et al (2006) Direct kinetic evidence for half-of-the-sites reactivity in the E1 component of the human pyruvate dehydrogenase multienzyme complex through alternating sites cofactor activation. *Biochemistry* 45:12775–12785
22. De Kok A, Hengeveld AF, Martin A et al (1998) The pyruvate dehydrogenase multi-enzyme complex from Gram-negative bacteria. *Biochim Biophys Acta* 1385:353–366
23. Seifert F, Ciszak E, Korotchkina L et al (2007) Phosphorylation of serine 264 impedes active site accessibility in the E1 component of the human pyruvate dehydrogenase multienzyme complex. *Biochemistry* 46:6277–6287
24. Neveling U, Klasen R, Bringer-Meyer S et al (1998) Purification of the pyruvate dehydrogenase multienzyme complex of *Zymomonas mobilis* and identification and sequence analysis of the corresponding genes. *J Bacteriol* 180:1540–1548
25. Nemeria N, Baykal A, Joseph E et al (2004) Tetrahedral intermediates in thiamin diphosphate-dependent decarboxylations exist as a 1',4'-imino tautomeric form of the coenzyme, unlike the Michaelis complex or the free coenzyme. *Biochemistry* 43:6565–6575
26. Nemeria NS, Chakraborty S, Balakrishnan A et al (2009) Reaction mechanisms of thiamin diphosphate enzymes: defining states of ionization and tautomerization of the cofactor at individual steps. *FEBS J* 276:2432–2446
27. Kluger R, Tittmann K (2008) Thiamin diphosphate catalysis: enzymic and nonenzymic covalent intermediates. *Chem Rev* 108:1797–1833
28. Arjunan P, Nemeria N, Brunskill A et al (2002) Structure of the pyruvate dehydrogenase multienzyme complex E1 component from *Escherichia coli* at 1.85 Å resolution. *Biochemistry* 41:5213–5221
29. Stevenson KJ, Hale G, Perham RN (1978) Inhibition of pyruvate dehydrogenase multienzyme complex from *Escherichia coli* with mono- and bifunctional arsenoxides. *Biochemistry* 17:2189–2192
30. Adamson SR, Stevenson KJ (1981) Inhibition of pyruvate dehydrogenase multienzyme complex from *Escherichia coli* with a bifunctional arsenoxide: selective inactivation of lipoamide dehydrogenase. *Biochemistry* 20:3418–3424
31. Adamson SR, Robinson JA, Stevenson KJ (1984) Inhibition of pyruvate dehydrogenase multienzyme complex from *Escherichia coli* with a radiolabeled bifunctional arsenoxide: evidence for essential histidine residue at the active site of lipoamide dehydrogenase. *Biochemistry* 23:1269–1274
32. Corbett JR, Wright K, Baillie AC (1984) The biochemical mode of action of pesticides. Academic, London
33. Schwartz ER, Reed LJ (1970) α -Keto acid dehydrogenase complexes XIII. Reaction of sulfhydryl groups in pyruvate dehydrogenase with organic mercurials. *J Biol Chem* 245:183–187
34. Hard ML, Raha S, Spino M et al (2001) Impairment of pyruvate dehydrogenase activity by acetaldehyde. *Alcohol* 25:1–8

35. Apfel MA, Ikeda BH, Speckhard DC et al (1984) *Escherichia coli* pyruvate dehydrogenase complex. Thiamin pyrophosphate-dependent inactivation by 3-bromopyruvate. *J Biol Chem* 259:2905–2909
36. Maldonado ME, Oh KJ, Frey PA (1972) Studies on *Escherichia coli* pyruvate dehydrogenase complex I. Effect of bromopyruvate on the catalytic activities of the complex. *J Biol Chem* 247:2711–2716
37. Lowe PN, Perham RN (1984) Bromopyruvate as an active-site-directed inhibitor of the pyruvate dehydrogenase multienzyme complex from *Escherichia coli*. *Biochemistry* 23:91–97
38. Bisswanger H (1980) Fluoropyruvate: a potent inhibitor of the bacterial and the mammalian pyruvate dehydrogenase complex. *Biochem Biophys Res Commun* 95:513–519
39. Flournoy DS, Frey PA (1989) Inactivation of the pyruvate dehydrogenase complex of *Escherichia coli* by fluoropyruvate. *Biochemistry* 28:9594–9602
40. Kluger R, Pike DC (1977) Active site generated analogs of reactive intermediates in enzymic reactions. Potent inhibition of pyruvate dehydrogenase by a phosphonate analog of pyruvate. *J Am Chem Soc* 99:4504–4506
41. Krampitz LO (1969) Catalytic functions of thiamin diphosphate. *Annu Rev Biochem* 38:213–240
42. Nemeria N, Yan Y, Zhang Z et al (2001) Inhibition of the *Escherichia coli* pyruvate dehydrogenase complex E1 subunit and its tyrosine 177 variants by thiamin 2-thiazolone and thiamin 2-thiothiazolone diphosphates. Evidence for reversible tight-binding inhibition. *J Biol Chem* 276:45969–45978
43. Dobritzsch D, König S, Schneider G et al (1998) High resolution crystal structure of pyruvate decarboxylase from *Zymomonas mobilis*. Implications for substrate activation in pyruvate decarboxylases. *J Biol Chem* 273:20196–20204
44. Alvarez FJ, Ermer J, Hübner G et al (1991) Catalytic power of pyruvate decarboxylase. Rate-limiting events and microscopic rate constants from primary carbon and secondary hydrogen isotope effects. *J Am Chem Soc* 113:8402–8409
45. Kern D, Kern G, Neef H et al (1997) How thiamine diphosphate is activated in enzymes. *Science* 275:67–70
46. Linn TC, Pelley JW, Pettit FH et al (1972) α -Keto acid dehydrogenase complexes XV. Purification and properties of the component enzymes of the pyruvate dehydrogenase complexes from bovine kidney and heart. *Arch Biochem Biophys* 148:327–342
47. Schönbrunn-Hanebeck E, Laber B, Amrhein N (1990) Slow-binding inhibition of the *Escherichia coli* pyruvate dehydrogenase multienzyme complex by acetylphosphinate. *Biochemistry* 29:4880–4885
48. Lowe PN, Leeper FJ, Perham RN (1983) Stereoisomers of tetrahydrothiamin pyrophosphate, potent inhibitors of the pyruvate dehydrogenase multienzyme complex from *Escherichia coli*. *Biochemistry* 22:150–157
49. Arjunan P, Chandrasekhar K, Sax M et al (2004) Structural determinants of enzyme binding affinity. The E1 component of pyruvate dehydrogenase from *Escherichia coli* in complex with the inhibitor thiamin thiazolone diphosphate. *Biochemistry* 43:2405–2411
50. Leeper F, Hawksley D, Mann S et al (2005) Studies on thiamine diphosphate-dependent enzymes. *Biochem Soc Trans* 33:772–775
51. Erixon KM, Dabalos CL, Leeper FJ (2007) Inhibition of pyruvate decarboxylase from *Z. mobilis* by novel analogues of thiamine pyrophosphate: investigating pyrophosphate mimics. *Chem Commun* 43:960–962
52. Ren YL, He JB, Feng LL et al (2011) Structure-based rational design of novel hit compounds for pyruvate dehydrogenase multienzyme complex E1 components from *Escherichia coli*. *Bioorg Med Chem* 19:7501–7506
53. He JB, Feng LL, Li J et al (2012) Design, synthesis and biological evaluation of novel 2-methylpyrimidine-4-ylamine derivatives as inhibitors of *Escherichia coli* pyruvate dehydrogenase complex E1. *Bioorg Med Chem* 20:1665–1670
54. Wolfenden R (1972) Analog approaches to the structure of the transition state in enzyme reactions. *Acc Chem Res* 5:10–18

55. Gutowski JA, Lienhard GE (1976) Transition state analogs for thiamin pyrophosphate-dependent enzymes. *J Biol Chem* 251:2863–2866
56. Lienhard GE (1973) Enzymatic catalysis and transition-state theory. *Science* 180:149–154
57. Kluger R, Gish G, Kauffman G (1984) Interaction of thiamin diphosphate and thiamin thiazolone diphosphate with wheat germ pyruvate decarboxylase. *J Biol Chem* 259:8960–8965
58. Kluger R, Pike DC (1979) Chemical synthesis of a proposed enzyme-generated “reactive intermediate analogue” derived from thiamin diphosphate. Self-activation of pyruvate dehydrogenase by conversion of the analogue to its components. *J Am Chem Soc* 101:6425–6428
59. Turano A, Furey W, Pletcher J et al (1982) Synthesis and crystal structure of an analog of 2-(α -lactyl) thiamin, racemic methyl 2-hydroxy-2-(2-thiamin) ethylphosphonate chloride trihydrate. A conformation for a least-motion, maximum-overlap mechanism for thiamin catalysis. *J Am Chem Soc* 104:3089–3095
60. Arjunan P, Sax M, Brunskill A et al (2006) A thiamin-bound, pre-decarboxylation reaction intermediate analogue in the pyruvate dehydrogenase E1 subunit induces large scale disorder-to-order transformations in the enzyme and reveals novel structural features in the covalently bound adduct. *J Biol Chem* 281:15296–15303
61. Nemeria N, Baykal A, Joseph E et al (2004) Tetrahedral intermediates in thiamin diphosphate-dependent decarboxylations exist as a 1',4'-imino tautomeric form of the coenzyme, unlike the Michaelis complex or the free coenzyme. *Biochemistry* 43:6565–6575
62. Nemeria NS, Korotchkina LG, Chakraborty S et al (2006) Acetylphosphinate is the most potent mechanism-based substrate-like inhibitor of both the human and *Escherichia coli* pyruvate dehydrogenase components of the pyruvate dehydrogenase complex. *Bioorg Chem* 34:362–379
63. Evarsson A, Seger K, Turley S et al (1999) Crystal structure of 2-oxoisovalerate and dehydrogenase and the architecture of 2-oxo acid dehydrogenase multienzyme complexes. *Nat Struct Mol Biol* 6:785–792
64. Jordan F, Nemeria N, Guo F et al (1998) Regulation of thiamin diphosphate-dependent 2-oxo acid decarboxylases by substrate and thiamin diphosphate. Mg(II)–evidence for tertiary and quaternary interactions. *Biochim Biophys Acta* 1385:287–306
65. Baillie AC, Wright BJ, Wright K (1980) Pesticidally active salts and compositions containing them and process for their manufacture and use. EP 0,009,348, 2 Apr 1980
66. Evans D, Lawson K (1992) Crop protection chemicals-research and development perspectives and opportunities. *Pestic Outlook* 3:10–17
67. Eto M (1997) Functions of phosphorus moiety in agrochemical molecules. *Biosci Biotechnol Biochem* 61:1–11
68. He HW, Liu ZJ (2001) Progresses in research of alpha-oxophosphonic acid derivatives with herbicidal activity. *Chin J Org Chem* 21:878–883
69. Liu XF, He HW, Liu ZJ (1998) Studies on organophosphorus compounds with biological activity. *J Centr Chin Norm Univ (Nat Sci)* 32:52–55
70. Xu L, He HW, Liu ZJ (1996) Studies on organophosphorus compounds with biological activity. Synthesis and properties of α -(benzothiazolyl-2-thioacetoxy)alkyl phosphonates. *J Centr Chin Norm Univ Nat Sci* 30:53–57
71. Hu LM, He HW, Liu ZJ (1996) Studies on biological active organophosphorus compounds XII. Synthesis and property of α -(2-benzoxazolyl)oxyacetoxyalkyl phosphonates. *Chem J Chinese Univ* 17:1873–1986
72. He HW, Liu XF, Zhou QC et al (1999) plant growth regulation activity of α -(pyridine-4-carbonyloxy)alkyl phosphonates. *Chin J Pestic Sci* 1:90–92
73. Liu XF, He HW, Zhou QC et al (2001) Synthesis and plant growth regulation activity of α -(pyridine-2-carbonyloxy)alkylphosphonates. *Chin J Pestic Sci* 3:73–75
74. He HW, Zhang YM, Liu ZJ (1996) Synthesis of α -(o-tolylthio)acetoxy alkyl phosphonates. *Chin J Chem Reag* 18:70–72

75. He HW, Wang J, Liu ZJ (1994) Synthesis of α -(substituted phenoxyacetoxy)alkyl phosphonates. *Chin Chem Lett* 5:35–38
76. He HW, Wang SQ, Chen WB et al (1989) A facile synthesis of O, O-dialkyl α -(phenyl carbamoyloxy)alkyl phosphonates. *Chin Chem Lett* 9:415–416
77. Hu LM, Zhang YM, He HW et al (1997) Studies on biological active organophosphorus compounds XII. Synthesis of α -(2-substituted benzamidoformyloxy)hydrocarbyl phosphonate. *Chin J Synthesis Chem* 5:287–291
78. He HW, Xu L, Liu ZJ (1999) A convenient synthesis of 1-(dichloro-pyrimidinyl carbamoyloxy) alkyl phosphonates. *Phosphorus, Sulfur Silicon Relat Elem* 147:937–938
79. Gilchris TL (1997) *Heterocyclic Chemistry*. Addison Wesley Longman Limited, London
80. Worthing CR, Hance RJ (1991) *The pesticide manual*. British Crop Protection Council, Farnham
81. Gerwick BC, Jackson LA, Handly J et al (1988) Preemergence and postemergence activities of the (R) and (S) isomers of haloxyfop. *Weed Sci* 36:453–456
82. Grossmann K, Tresch S, Plath P (2001) Triaziflam and diaminotriazine derivatives affect enantioselectively multiple herbicide target sites. *Z Naturforsch* 56c: 559–569
83. Shaner DL, Singh BK (1997) Acetohydroxyacid synthase inhibitors. *Herbicide activity: toxicology, biochemistry and molecular biology*. IOS, Amsterdam, pp 69–110
84. Omokawa H, Konnai M (1990) PS II inhibitory activity of 2,4-diamino-6-chloro-s-triazine with a chiral sec-butyl and/or α -methylbenzyl group. *Agric Biolog Chem* 54:2373–2378
85. Omokawa H, Murata H, Kobayashi S et al (2004) Chiral response of oryzae and paniceae plants in α -methylbenzyl-3-*p*-tolyl urea agar medium. *Pest Manag Sci* 60:59–64
86. Fayez KA, Kristen U (1996) The influence of herbicides on the growth and proline content of primary roots and on the ultrastructure of root caps. *Environm Experim Botany* 36:71–81
87. Lin KD, Liu WP, Li L et al (2008) Single and joint acute toxicity of isocarbophos enantiomers to *Daphnia magna*. *J Agric Food Chem* 56:4273–4277

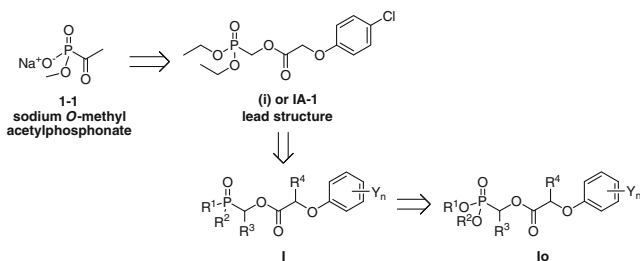
Chapter 2

Alkylphosphonates

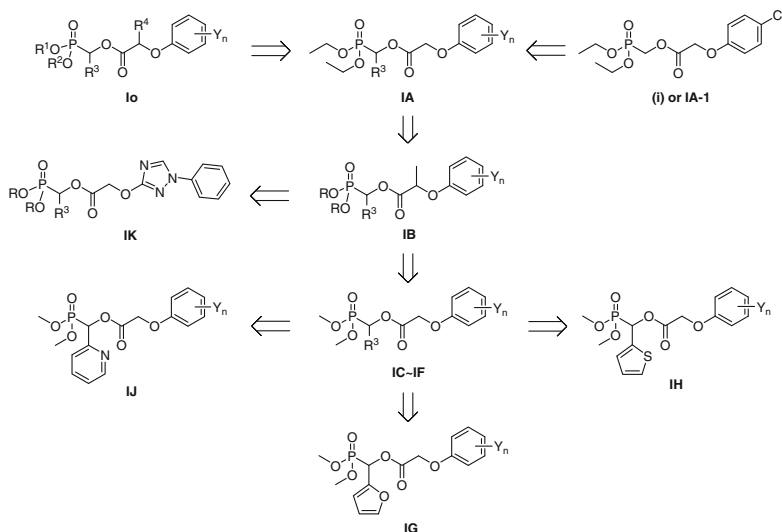
As stated in Chap. 1, through the modification of hit compound, sodium *O*-methylacetylphosphonate **1-1**, ten series of 1-oxophosphonic acid derivatives (**i**)–(**x**) (Table 1.7) were synthesized to examine their herbicidal activity at an early stage of our work. The results showed that only a few *O,O*-diethyl 1-(substituted phenoxyacetoxy)alkylphosphonates (**i**) (Scheme 2.1) exhibited significant herbicidal activity at 2.25 kg ai/ha in the greenhouse. In our continued work, the alkylphosphonates (**i**) were identified as the lead structure of a new class of herbicides. Therefore it was further extended to a general structure **I** which could be modified to form more than thirty series of compounds including alkylphosphonates, alkylphosphinates, cyclic phosphate, caged bicyclic phosphates and relative derivatives (Scheme 1.20).

According to the work of Baillie et al. [1] the structural unit of phosphonate was important for the inhibition against plant PDHc, therefore the study on structure **I** was firstly focused on the phosphonate scaffold **Io** by the modification of lead compound **IA-1** (Scheme 2.1). Different groups of R^1 , R^2 , R^3 , R^4 and Y_n were introduced into the general structure **Io** to form different series of alkylphosphonates **IA-1K** (Scheme 2.2), in an attempt to find compounds with better herbicidal activities.

In **IA** series, optimization was focused on the modification of substituents R^3 and Y_n . Most **IA** showed good herbicidal activity against dicotyledonous plants at 2.25 kg ai/ha. In order to examine the effect of R^1 , R^2 and R^4 in the



Scheme 2.1 Optimization of hit compound **1-1**



Scheme 2.2 Design of alkylphosphonates **IA–IK**

alkylphosphonates **Io** on herbicide activity, **IA** was modified to form **IB** (Scheme 2.2). Results of study on **IB** series suggested that R^1 , R^2 and R^4 with smaller groups in structure **Io** would show better herbicidal activity. Therefore, the structure **IB** was further optimized to produce *O,O*-dimethyl 1-(substituted phenoxyacetoxy)alkylphosphonates **IC–IF** (Scheme 2.2).

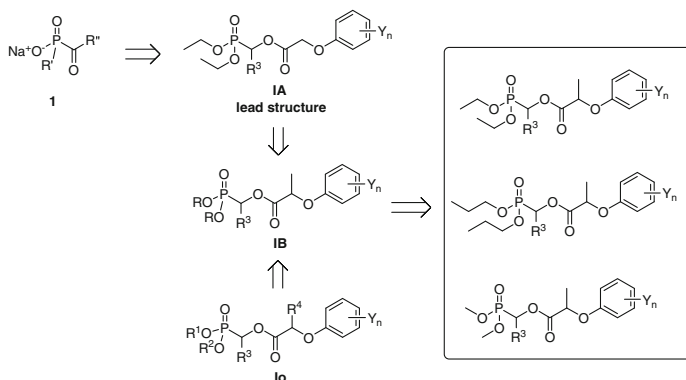
As shown in Scheme 2.2, the introduction of heterocyclic groups in R^3 of **IC–IF** led to the phosphonates **IG** (R^3 =fur-2-yl), **IH** (R^3 =pyrid-2-yl) and **IJ** (R^3 =thien-2-yl), respectively. The replacement of the substituted phenoxy moiety by the triazole ring in **IB** gave 1-(1-phenyl-1,2,4-triazol-3-yloxyacetoxy) alkylphosphonates **IK**. Several compounds in **IC** and **IG** series were found to be herbicidally active compounds against broadleaf weeds by systematic study of alkylphosphonates **IA–IK**.

In this chapter, we describe the synthesis, herbicidal activity and structure-activity relationship (SAR) of alkylphosphonates **IA–IK**. Herbicidal activity of **IC-22** and **IG-21** will be discussed in detail.

2.1 (Alkyl or Substituted Phenyl)Methylphosphonates IA–IF

2.1.1 Introduction

In order to systematically examine the herbicidal activity of lead structure (i), a series of *O,O*-diethyl 1-(substituted phenoxyacetoxy)alkylphosphonates as **IA** was further designed and prepared by the modification of lead compound **IA-1**.

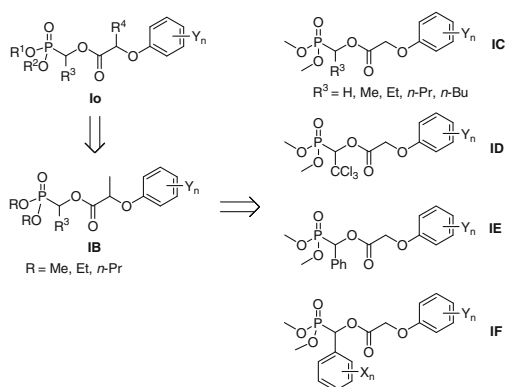


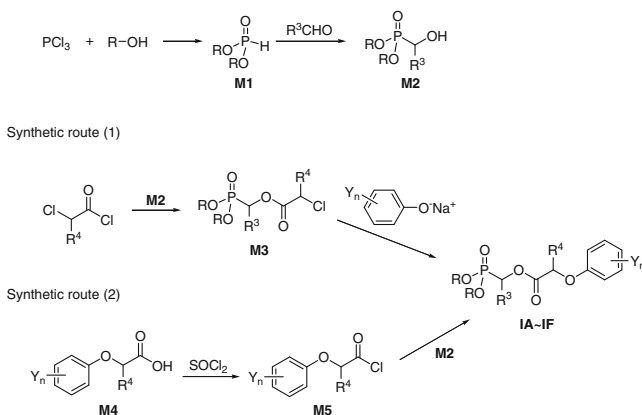
Scheme 2.3 Design of 1-(substituted phenoxyacetoxy)alkylphosphonates **IB**

According to the study on acylphosphonates by Baillie et al., substituent R^1 in monosodium acylphosphonates **1** (Scheme 2.3) greatly affected both enzyme inhibitory activity and herbicide activity of compounds. Therefore, R^1 and R^2 in structure **Io** were firstly modified to examine their effect on herbicidal activity. Me, Et or *n*-Pr as R^1 and R^2 was introduced into the structure **Io** to form **IB** (Scheme 2.3). In the **IB** series, where Me as R^4 was kept, further optimization was focused on the modification of R^3 and Y_n .

It was found that when smaller R (or Me as R^1 and R^2 in the structure **Io**) was introduced into the structure **IB**, the herbicidal activity of the compound could be significantly increased. Therefore, structure **IB** was further optimized to produce a series of *O,O*-dimethyl 1-(substituted phenoxyacetoxy)alkylphosphonates **IC–IF** (Scheme 2.4). In the **IC–IF** series, Me as R^1 and R^2 , H as R^4 in the structure **Io** were kept, optimization was focused on the modification of substituents R^3 . In the **IC** series, H, Me, Et, *n*-Pr, and *n*-Bu as R^3 ; In the **ID** series, CCl_3 as R^3 ; In the **IE** series, Ph as R^3 ; In the **IF** series, substituted Ph as R^3 . When R^3 was kept, further

Scheme 2.4 Design of *O,O*-dimethyl 1-(substituted phenoxyacetoxy)alkylphosphonates **IC–IF**





Scheme 2.5 Synthetic route of *O,O*-dialkyl 1-(substituted phenoxyacetoxy)alkylphosphonates **IA–IF**

optimization was focused on the modification of Y_n . It was expected that herbicidal activity would be improved by the chemical modifications of **IB**.

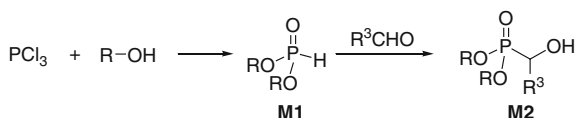
Based on the above consideration, six series of 1-(substituted phenoxyacetoxy) alkylphosphonate derivatives **IA–IF** were prepared. The synthesis and herbicidal activity of **IA–IF**, and their SAR are summarized in this Sect. 2.1.

We chose the following synthetic routes (1) or (2) to obtain *O,O*-dialkyl 1-(substituted phenoxyacetoxy)alkylphosphonates **IA–IF** (Scheme 2.5). In the synthetic route (1), the title compounds can be synthesized by the reaction of substituted phenol sodium with corresponding 1-(chloroacetoxy)alkylphosphonates **M3** in the presence of sodium iodide. In the synthetic route (2), the title compounds can be synthesized by the condensation of *O,O*-dialkyl 1-hydroxyalkylphosphonates **M2** and substituted phenoxyacetyl chlorides **M5** (Scheme 2.5).

The synthetic yields of **IA–IF** using the method of route (2) were better than that of route (1). Therefore, we mainly chose the synthetic route (2) to obtain **IA–IF**. *O,O*-Dialkyl 1-hydroxyalkylphosphonates **M2**, substituted phenoxyacetic acids **M4** and substituted phenoxyacetyl chlorides **M5** are the important intermediates for the synthesis of **IA–IF**. The preparation of **M2**, **M4** and **M5** is described in Sects. 2.1.2 and 2.1.3, respectively.

2.1.2 Synthesis of *O,O*-Dialkyl 1-Hydroxyalkylphosphonates **M2**

O,O-Dialkyl 1-hydroxyalkylphosphonates **M2** are key intermediates for the preparation of title compounds **IA–IF**. **M2** could be prepared by the nucleophilic addition of dialkyl phosphonates to several kinds of aldehydes (Scheme 2.6).

**Scheme 2.6** Synthesis of *O,O*-dialkyl 1-hydroxyalkylphosphonates **M2**

Some *O,O*-dialkyl 1-hydroxyalkylphosphonates have been prepared by the addition of dialkyl phosphonates to aldehydes under different reaction conditions [2], which can be summarized as follows: (1) non-catalytic thermal addition [3, 4], (2) base-catalysis addition [5], and (3) solvent-free catalytic process using potassium fluoride, calcium fluoride, aluminum oxide, or others, as a catalyst [6–8].

The method of base-catalyzed addition is a simple procedure, however, in this case the yield is not always good, and a mixture of products is sometimes obtained. In a strong alkaline medium, 1-hydroxyalkylphosphonates are easily cleaved to regenerate the starting carbonyl compounds [3]. Texier-Boullet reported a convenient solvent-free catalyzed addition using a mixture of potassium fluoride and alumina, or a mixture of potassium fluoride and aluminum oxide [6, 7]. This method had an advantage of higher yield, and the catalytic effect of the mixture of aluminum oxide and potassium fluoride was better than that of using only potassium fluoride or aluminum oxide.

In our work the methods (2) and (3) were chosen to prepare 1-hydroxyalkylphosphonates. *O,O*-Diethyl 1-hydroxyalkylphosphonates **M2-1–M2-16** and *O,O*-dimethyl 1-hydroxyalkylphosphonates **M2-17–M2-40** were prepared by the reaction of diethyl or dimethyl phosphonates **M1** with several kinds of aldehydes using triethylamine as a catalyst in the range of 58–93 % yields (method **M2-A**, Tables 2.1 and 2.2). If the above reaction was using a mixture of potassium fluoride and aluminum oxide (mass ratio 1:1) as a catalyst the yields were in the range of 68–98 % (method **M2-B**, Tables 2.1 and 2.2). The structures of compounds **M2-1–M2-40** are listed in Tables 2.1 and 2.2.

2.1.3 Synthesis of Substituted Phenoxyacetic Acids **M4** and Substituted Phenoxyacetyl Chlorides **M5**

According to the Ref. [9], substituted phenoxyacetic acids were prepared by the condensation of corresponding substituted phenols with chloroacetic acid in the presence of alkali, such as sodium hydroxide (method **M4-A**). The synthetic route is shown in Scheme 2.7. Substituted phenoxyacetic acids **M4-1–M4-16** prepared by this method **M4-A** are summarized in Table 2.3.

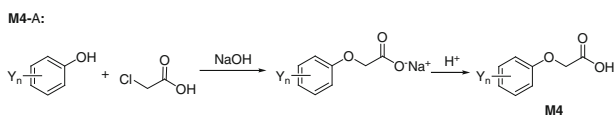
**Scheme 2.7** Synthesis of substituted phenoxyacetic acids **M4**

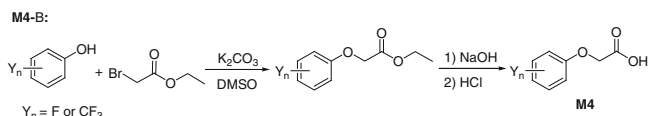
Table 2.1 Structure of *O,O*-diethyl 1-hydroxyalkylphosphonates **M2-1–M2-16**

Compound	R ³	Method	Compound	R ³	Method
M2-1	H	M2-A	M2-9	4-MeOPh	M2-A ^a M2-B ^b
M2-2	Me	M2-A	M2-10	4-FPh	M2-A M2-B
M2-3	Et	M2-A	M2-11	2-ClPh	M2-A M2-B
M2-4	<i>n</i> -Pr	M2-A	M2-12	3-ClPh	M2-A M2-B
M2-5	<i>i</i> -Pr	M2-A	M2-13	4-ClPh	M2-A M2-B
M2-6	Ph	M2-A M2-B	M2-14	2,4-Cl ₂ Ph	M2-A M2-B
M2-7	4-MePh	M2-A M2-B	M2-15	3,4-Cl ₂ Ph	M2-A M2-B
M2-8	3-NO ₂ Ph	M2-A M2-B	M2-16	3,4-OCH ₂ OPh	M2-A M2-B

^a Method **M2-A**: Et₃N as a catalyst

^b Method **M2-B**: KF/Al₂O₃ as a catalyst

In the reaction of chloroacetic acid with fluoro-substituted phenols or trifluoromethyl-substituted phenols in the presence of sodium hydroxide, products had low yields because of a strong electron-withdrawing nature of the substituent. However, by using the method of Brayer et al. [10], fluoro-substituted phenoxyacetic acids and trifluoromethyl-substituted phenoxyacetic acids **M4-17–M4-27** (Table 2.4) could be prepared in satisfactory yields by the reaction of fluoro-substituted phenols or trifluoromethyl-substituted phenols with ethyl bromoacetate in the presence of K₂CO₃ in DMSO followed by alkaline hydrolysis (Scheme 2.8, method **M4-B**). Thus, a series of substituted phenoxyacetic acids **M4-1–M4-27** was prepared by method **M4-A** or **M4-B**.



Scheme 2.8 Synthesis of fluoro and trifluoromethyl-substituted phenoxyacetic acids **M4**

In order to condense with 1-hydroxyalkylphosphonates in a highly effective way, substituted phenoxyacetic acids were converted to the corresponding substituted phenoxyacetyl chlorides **M5** by using thionyl chloride in high yields (>90 %).

Table 2.2 Structure of *O,O*-dimethyl 1-hydroxyalkylphosphonates **M2-17–M2-40**

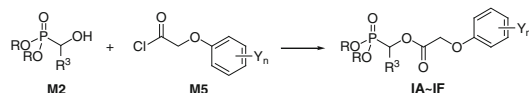
Compound	R ³	Method	Compound	R ³	Method
M2-17	H	M2-A	M2-29	4-MeOPh	M2-A ^a M2-B ^b
M2-18	Me	M2-A M2-B	M2-30	4-FPh	M2-A M2-B
M2-19	Et	M2-A	M2-31	2-ClPh	M2-A M2-B
M2-20	<i>n</i> -Pr	M2-A	M2-32	3-ClPh	M2-A M2-B
M2-21	<i>i</i> -Pr	M2-A	M2-33	4-ClPh	M2-A M2-B
M2-22	<i>n</i> -Bu	M2-A	M2-34	3-BrPh	M2-A
M2-23	CCl ₃	M2-A M2-B	M2-35	2,4-Cl ₂ Ph	M2-A M2-B
M2-24	Ph	M2-A M2-B	M2-36	3,4-Cl ₂ Ph	M2-A M2-B
M2-25	4-MePh	M2-A M2-B	M2-37	Fur-2-yl	M2-A M2-B
M2-26	3-NO ₂ Ph	M2-B	M2-38	Thien-2-yl	M2-39
M2-27	4-NO ₂ Ph	M2-A	M2-39	Pyrid-2-yl	M2-A M2-B
M2-28	2-HOPh	M2-A	M2-40	3,4-OCH ₂ OPh	M2-A M2-B

^a Method: **M2-A**: Et₃N as a catalyst

^b Method: **M2-B**: KF/Al₂O₃ as a catalyst

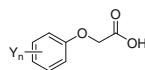
2.1.4 Synthesis of IA–IF

O,O-Dialkyl 1-(substituted phenoxyacetoxy)alkylphosphonates **IA–IF** could be conveniently synthesized by the condensation of 1-hydroxyalkylphosphonates **M2** with substituted phenoxyacetyl chlorides **M5** in the presence of pyridine as a base (Scheme 2.9).

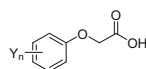


Scheme 2.9 Synthesis of *O,O*-dialkyl 1-(substituted phenoxyacetoxy)alkylphosphonates **IA–IF**

Considering that 1-hydroxyalkylphosphonates **M2** are easily regenerated to the starting carbonyl compounds in strong alkaline medium [3], pyridine, a weak base,

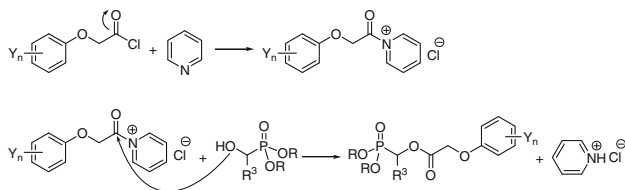
Table 2.3 Structure of substituted phenoxyacetic acids **M4-1–M4-16**

Compound	Y _n	Method	Compound	Y _n	Method
M4-1	H	M4-A	M4-9	2-Me,4-Cl	M4-A
M4-2	3-Me	M4-A	M4-10	3-Me,4-Cl	M4-A
M4-3	4-Me	M4-A	M4-11	2-Cl,5-Me	M4-A
M4-4	2-NO ₂	M4-A	M4-12	2,3-Cl ₂	M4-A
M4-5	4-NO ₂	M4-A	M4-13	2,4-Cl ₂	M4-A
M4-6	4-Cl	M4-A	M4-14	2,6-Cl ₂	M4-A
M4-7	4-Br	M4-A	M4-15	2,4-Br ₂	M4-A
M4-8	2,3-Me ₂	M4-A	M4-16	2-NO ₂ ,4-Cl	M4-A

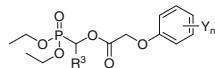
Table 2.4 Structure of substituted phenoxyacetic acids **M4-17–M4-27**

Compound	Y _n	Method	Compound	Y _n	Method
M4-17	3-CF ₃	M4-B	M4-23	3,5-F ₂	M4-B
M4-18	4-CF ₃	M4-B	M4-24	2-F,4-Cl	M4-B
M4-19	2-F	M4-B	M4-25	2-Cl,4-F	M4-B
M4-20	3-F	M4-B	M4-26	3-Cl,4-F	M4-B
M4-21	4-F	M4-B	M4-27	2-NO ₂ ,4-CF ₃	M4-B
M4-22	2,4-F ₂	M4-B			

was chosen for this reaction. It not only acted as an acid-binding agent but also was a catalyzer. The catalytic mechanism of pyridine is shown in Scheme 2.10.

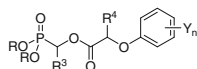
**Scheme 2.10** Catalytic mechanism of pyridine

Since 1-hydroxyalkylphosphonates are easy to decompose at high temperature [3] and **IA–IF** contain a carboxylic ester group which is sensitive to acid or base, the reaction required a temperature near room temperature in anhydrous solvents. We performed the reaction in two steps: first, the reaction was carried out at room temperature for several hours, and then at a higher temperature under mild reaction conditions. All **IA–IF** were conveniently synthesized in the presence of pyridine and anhydrous trichloromethane. The structures of **IA–IF** are listed in Tables 2.5, 2.6, 2.7, 2.8, 2.9, 2.10 and 2.11, respectively.

Table 2.5 Structure of *O,O*-diethyl 1-(substituted phenoxyacetoxy)alkylphosphonates **IA**^a

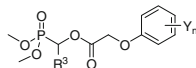
Compound	R ³	Y _n	Compound	R ³	Y _n
IA-1	H	4-Cl	IA-13	Ph	2,4-Cl ₂
IA-2	H	2,4-Cl ₂	IA-14	4-MePh	2,4-Cl ₂
IA-3	Me	4-Cl	IA-15	3-NO ₂ Ph	3-CF ₃
IA-4	Me	2,4-Cl ₂	IA-16	4-MeOPh	3-CF ₃
IA-5	CCl ₃	2-Me	IA-17	4-FPh	3-CF ₃
IA-6	CCl ₃	4-Cl	IA-18	2-ClPh	2,4-Cl ₂
IA-7	Et	4-Cl	IA-19	3-ClPh	3-CF ₃
IA-8	Et	2,4-Cl ₂	IA-20	4-ClPh	3-CF ₃
IA-9	<i>n</i> -Pr	4-Cl	IA-21	4-ClPh	2,4-Cl ₂
IA-10	<i>n</i> -Pr	2,4-Cl ₂	IA-22	2,4-Cl ₂ Ph	3-CF ₃
IA-11	Ph	3-CF ₃	IA-23	3,4-Cl ₂ Ph	3-CF ₃
IA-12	Ph	2-Cl	IA-24	3,4-OCH ₂ OPh	3-CF ₃

^a Synthesis of **IA-1–IA-4** and **IA-7–IA-10** [11, 12]; **IA-5, IA-6, IA-11** and **IA-12** [11, 13]; **IA-11, IA-17** and **IA-19** [14]; **IA-15, IA-22** and **IA-23** [15]; **IA-18** [16]; **IA-20** and **IA-24** [17]

Table 2.6 Structure of 1-(substituted phenoxyacetoxy)alkylphosphonates **IB**^a

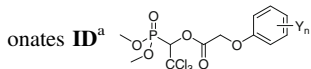
Compound	R	R ³	R ⁴	Y _n	Compound	R	R ³	R ⁴	Y _n
IB-1	Me	Me	Me	2-F	IB-9	Me	4-MePh	Me	2-Cl,4-F
IB-2	Me	Me	Me	2-Cl,4-F	IB-10	Me	4-FPh	Me	2-F
IB-3	Me	Me	Me	2,4-Cl ₂	IB-11	Me	4-FPh	Me	2-Cl,4-F
IB-4	Me	Pr	Me	2,4-Cl ₂	IB-12	Et	Me	Me	2,4-Cl ₂
IB-5	Me	CCl ₃	Me	2-F	IB-13	Et	Ph	Me	2,4-Cl ₂
IB-6	Me	CCl ₃	Me	2-Cl,4-F	IB-14	<i>n</i> -Pr	Me	Me	2,4-Cl ₂
IB-7	Me	Ph	Me	2,4-Cl ₂	IB-15	<i>n</i> -Pr	Ph	Me	2,4-Cl ₂
IB-8	Me	4-MePh	Me	2-F	IB-16	<i>n</i> -Pr	2-ClPh	Me	2,4-Cl ₂

^a Synthesis of for compounds: **IB-1, IB-2, IB-5, IB-6,** and **IB-8–IB-11** [18]; **IB-3, IB-4, IB-7, IB-12, IB-13** and **IB-14** [19]; **IB-15** [20]; **IB-16** [16]

Table 2.7 Structure of *O,O*-dimethyl 1-(substituted phenoxyacetoxy)alkylphosphonates **IC**^a

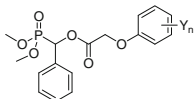
Compound	R ³	Y _n	Compound	R ³	Y _n
IC-1	H	2,4-Cl ₂	IC-18	Me	2-F,4-Cl
IC-2	Me	H	IC-19	Me	2-Cl,4-F
IC-3	Me	3-Me	IC-20	Me	3-Cl,4-F
IC-4	Me	4-Me	IC-21	Me	2,3-Cl ₂
IC-5	Me	3-CF ₃	IC-22	Me	2,4-Cl ₂
IC-6	Me	4-CF ₃	IC-23	Me	2,6-Cl ₂
IC-7	Me	2-F	IC-24	Me	2,4-Br ₂
IC-8	Me	3-F	IC-25	Me	2-NO ₂ ,4-Cl
IC-9	Me	4-F	IC-26	Et	3-CF ₃
IC-10	Me	4-Cl	IC-27	Et	2,4-Cl ₂
IC-11	Me	4-Br	IC-28	Et	2-NO ₂ ,4-CF ₃
IC-12	Me	2,3-Me ₂	IC-29	<i>n</i> -Pr	3-CF ₃
IC-13	Me	2-Me,4-Cl	IC-30	<i>n</i> -Pr	2-NO ₂
IC-14	Me	3-Me,4-Cl	IC-31	<i>n</i> -Pr	4-NO ₂
IC-15	Me	2-Cl,5-Me	IC-32	<i>n</i> -Pr	2,4-Cl ₂
IC-16	Me	2,4-F ₂	IC-33	<i>n</i> -Pr	2-NO ₂ ,4-CF ₃
IC-17	Me	3,5-F ₂	IC-34	<i>n</i> -Bu	2,4-Cl ₂

^a Synthesis of **IC-1** [21]; **IC-2** and **IC-5** [17]; **IC-4**, **IC-7**, **IC-11**, **IC-12**, **IC-20**, **IC-22**, **IC-24**, **IC-25**, **IC-27** and **IC-32** [21, 22]; **IC-6** and **IC-19** [15]; **IC-8**, **IC-9**, **IC-10**, **IC-13**, **IC-14**, **IC-15**, **IC-21** and **IC-23** [23]; **IC-16** and **IC-17** [14]; **IC-34** [16]

Table 2.8 Structure of *O,O*-dimethyl 1-(substituted phenoxyacetoxy)-2,2,2-trichloroethylphosphonates **ID**^a

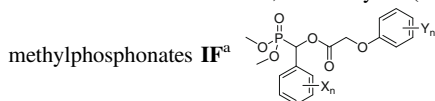
Compound	Y _n	Compound	Y _n
ID-1	4-CF ₃	ID-8	2,4-F ₂
ID-2	3-F	ID-9	3,5-F ₂
ID-3	4-F	ID-10	2-Cl,4-F
ID-4	4-Cl	ID-11	3-Cl,4-F
ID-5	2-Me,4-Cl	ID-12	2,3-Cl ₂
ID-6	3-Me,4-Cl	ID-13	2,4-Cl ₂
ID-7	2-Cl,5-Me	ID-14	2,6-Cl ₂

^a Synthesis of **ID-1** and **ID-10** [5]; **ID-2**–**ID-7**, **ID-12** and **ID-14** [23]; **ID-8** and **ID-9** [4]; **ID-11** and **ID-13** [22]

Table 2.9 Structure of *O,O*-dimethyl 1-(substituted phenoxyacetoxy)benzylphosphonates **IE**^a

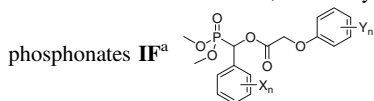
Compound	Y _n	Compound	Y _n	Compound	Y _n
IE-1	H	IE-9	3-F	IE-17	2,4-F ₂
IE-2	3-Me	IE-10	4-F	IE-18	2-F,4-Cl
IE-3	4-Me	IE-11	4-Cl	IE-19	2-Cl,4-F
IE-4	3-CF ₃	IE-12	4-Br	IE-20	3-Cl,4-F
IE-5	4-CF ₃	IE-13	2,3-Me ₂	IE-21	2,3-Cl ₂
IE-6	2-NO ₂	IE-14	2-Me,4-Cl	IE-22	2,4-Cl ₂
IE-7	4-NO ₂	IE-15	3-Me,4-Cl	IE-23	2,6-Cl ₂
IE-8	2-F	IE-16	2-Cl,5-Me	IE-24	2-NO ₂ ,4-CF ₃

^a Synthesis of compounds: **IE-1–IE-3**, **IE-5**, **IE-6**, **IE-13**, **IE-17**, **IE-19**, **IE-20** and **IE-24** [22]; **IE-8** [14]; **IE-9**, **IE-10**, **IE-14–IE-16**, **IE-21** and **IE-23** [23]; **IE-22** [21, 24]

Table 2.10 Structure of *O,O*-dimethyl 1-(substituted phenoxyacetoxy)-1-(substituted phenyl) methylphosphonates **IF**^a

Compound	X _n	Y _n	Compound	X _n	Y _n
IF-1	4-Me	3-CF ₃	IF-22	4-F	2,4-Cl ₂
IF-2	4-Me	4-F	IF-23	2-Cl	3-CF ₃
IF-3	4-Me	4-Cl	IF-24	2-Cl	2,4-Cl ₂
IF-4	4-Me	4-Br	IF-25	3-Cl	3-CF ₃
IF-5	4-Me	2-Me,4-Cl	IF-26	3-Cl	2,4-Cl ₂
IF-6	4-Me	2,4-F ₂	IF-27	4-Cl	3-CF ₃
IF-7	4-Me	2-F,4-Cl	IF-28	4-Cl	2-Me,4-Cl
IF-8	4-Me	2-Cl,4-F	IF-29	4-Cl	2-F,4-Cl
IF-9	4-Me	2,4-Cl ₂	IF-30	4-Cl	2-Cl,4-F
IF-10	2-OH	4-Cl	IF-31	4-Cl	2,4-Cl ₂
IF-11	2-OH	2-Cl,4-F	IF-32	3-Br	2,4-Cl ₂
IF-12	4-MeO	3-CF ₃	IF-33	2,3-Cl ₂	2,4-Cl ₂
IF-13	4-MeO	4-F	IF-34	2,4-Cl ₂	H
IF-14	4-MeO	4-Cl	IF-35	2,4-Cl ₂	3-CF ₃
IF-15	4-MeO	4-Br	IF-36	2,4-Cl ₂	2,4-Cl ₂
IF-16	4-MeO	2-Me,4-Cl	IF-37	3,4-Cl ₂	H
IF-17	4-MeO	2,4-F ₂	IF-38	3,4-Cl ₂	3-CF ₃
IF-18	4-MeO	2-F,4-Cl	IF-39	3,4-Cl ₂	2,4-Cl ₂
IF-19	4-MeO	2-Cl,4-F	IF-40	3,4-OCH ₂ O	3-CF ₃
IF-20	4-MeO	2,4-Cl ₂	IF-41	3,4-OCH ₂ O	2,4-Cl ₂
IF-21	4-F	3-CF ₃			

^a Synthesis of **IF-1**, **IF-23**, **IF-27** and **IF-40** [17]; **IF-5**, **IF-7** and **IF-8** [21]; **IF-24** [16]; **IF-9**, **IF-20**, **IF-22**, **IF-26**, **IF-33**, **IF-36**, **IF-39** and **IF-41** [24]; **IF-10**, **IF-11** and **IF-32** [22]; **IF-21** and **IF-25** [14]; **IF-35** and **IF-38** [15]

Table 2.11 Structure of *O,O*-dimethyl 1-(substituted phenoxyacetoxy)-1-(nitrophenyl)methyl-

Compound	X _n	Y _n	Compound	X _n	Y _n
IF-42	3-NO ₂	H	IF-53	3-NO ₂	2-Cl,5-Me
IF-43	3-NO ₂	3-CF ₃	IF-54	3-NO ₂	2,4-F ₂
IF-44	3-NO ₂	4-CF ₃	IF-55	3-NO ₂	2-Cl,4-F
IF-45	3-NO ₂	2-NO ₂	IF-56	3-NO ₂	3-Cl,4-F
IF-46	3-NO ₂	4-NO ₂	IF-57	3-NO ₂	2,3-Cl ₂
IF-47	3-NO ₂	2-F	IF-58	3-NO ₂	2,4-Cl ₂
IF-48	3-NO ₂	3-F	IF-59	3-NO ₂	2,6-Cl ₂
IF-49	3-NO ₂	4-F	IF-60	3-NO ₂	2-NO ₂ ,4-CF ₃
IF-50	3-NO ₂	4-Cl	IF-61	4-NO ₂	2-NO ₂
IF-51	3-NO ₂	2-Me,4-Cl	IF-62	4-NO ₂	2,4-F ₂
IF-52	3-NO ₂	3-Me,4-Cl	IF-63	4-NO ₂	2,4-Cl ₂

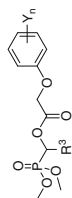
^a Synthesis of **IF-43**, **IF-44**, **IF-50–IF-54**, **IF-55**, **IF-56**, **IF-57**, **IF-59** and **IF-60** [22]; **IF-47** and **IF-48** [14]; **IF-45** and **IF-46** [25]; **IF-49** [15]; **IF-58**, and **IF-63** [21]

All of **IA–IF** could be prepared according to the general synthetic procedure of *O,O*-dialkyl 1-(substituted phenoxyacetoxy)alkylphosphonates **IA–IJ** in the Sect. 9.1.7. **IA–IF** are soluble in a variety of organic solvents such as benzene, diethyl ether, ethyl acetate, and so on. They are stable to light and air at room temperature but easily decompose under the acidic or basic conditions. The structures of **IA–IF** were characterized by ¹H NMR, IR, and confirmed by elementary analysis. Several compounds were also characterized by MS and ³¹P NMR spectra. Spectroscopic analysis of some representative **IA–IF** are given in the next section.

2.1.5 Spectroscopic Analysis of **IA–IF**

All main functional groups were characterized in IR spectra which showed normal stretching absorption bands indicating the existence of benzene ring (1,453–1,615 cm⁻¹), P–O–C (1,029–1,061 cm⁻¹), and P–C (705–833 cm⁻¹). A strong absorption near 1,760 cm⁻¹ (1,738–1,794 cm⁻¹) was identified for the absorption C=O. A sharp and weak band at 3,010–3,098 cm⁻¹ accounted for the C–H stretching of aromatic hydrocarbon. A strong peak at 1,213–1,261 cm⁻¹ accounted for P=O in phosphonates. Two strong peaks near 1,525 and 1,344 cm⁻¹ were the evidence for the NO₂ stretching in NO₂-containing compounds, such as **IC-28**, **IC-31**, **IE-24**, and **IF-45** (Table 2.12).

The IR spectrum of **IC-22** is shown in Fig. 2.1. A sharp and weak band 3,098–3,074 cm⁻¹ accounted for the C–H stretching of the aromatic hydrocarbon in

Table 2.12 IR spectra of **IC-28**, **IC-31**, **IE-24**, and **IF-45**

Compound	R ³	Y _n	ν _{Ar-H}	ν _{R-H}	ν _{C=O}	ν _{ArC-C}	ν _{P=O}	ν _{Ar-O-C}	ν _{C-O-C}	ν _{P-O-C}	ν _{P-C}	ν _{NO₂}	ν _{Ar-CF₃}
IC-28	Et	2-NO ₂ ,	3,061	2,952	1,767	1,629	1,261	1,233	1,193	1,054	824	1,544	1,330
		4-CF ₃		2,852		1,458							
IC-31	<i>n</i> -Pr	4-NO ₂	3,084	2,960	1,767	1,593	1,261		1,178	1,032	751	1,516	
				2,855		1,496							1,344
IE-24	Ph	2-NO ₂ ,	3,070	2,947	1,763	1,630	1,264	1,230	1,194	1,033	833	1,506	1,335
		4-CF ₃		2,857		1,483							
IF-45	3-NO ₂ Ph	2-NO ₂	3,046	2,951	1,787	1,590	1,253		1,178	1,037	745	1,528	
				2,856		1,497							1,350

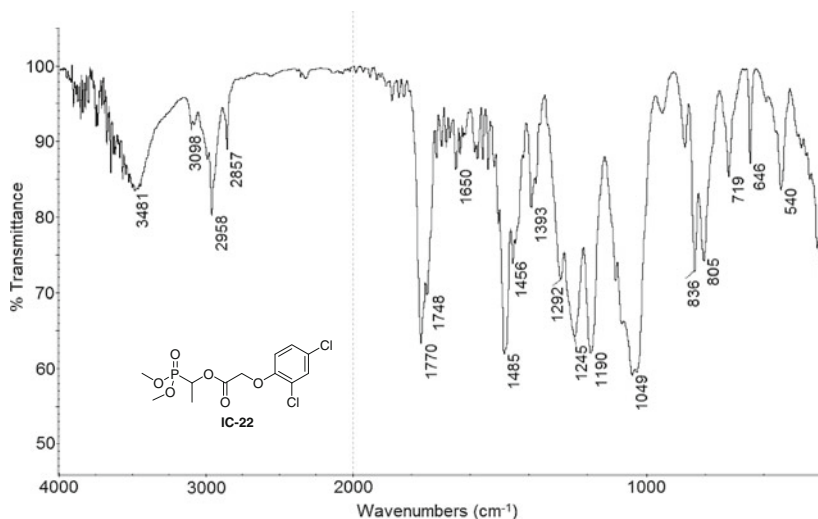


Fig. 2.1 IR spectrum of **IC-22**

IC-22. Peaks at 1,587, 1,485 cm^{-1} accounted for vibration of the skeleton of the benzene ring. Peaks at 866, 836, 719 cm^{-1} accounted for C–H flexural vibration of the benzene ring. Peaks at 2,993, 2,958, 2,857 cm^{-1} accounted for C–H stretching vibration of the saturated alkyl. Peaks at 1,456, 1,446, 1,393 cm^{-1} accounted for C–H flexural vibration of the saturated alkyl. A peak at 1,393 cm^{-1} also accounted for Me which existed in the molecule. A strong absorption at 1,770 cm^{-1} was identified for stretching vibration of C=O. A peak at 1,190 cm^{-1} accounted for stretching vibration of C–O–C and 1,292 cm^{-1} accounted for stretching vibration of Ar–O–C. A peak at 805 cm^{-1} accounted for the stretching vibration of C–Cl. A strong peak at 1,245 cm^{-1} accounted for P=O in phosphonates. Peaks at 1,049 and 646 cm^{-1} were identified for the stretching vibration of P–O–C and P–C, respectively.

The EI mass spectra of most **IC–IF** gave weak molecular ion peaks. The fragmentation ions of **IC–IF** were consistent with the structure. For example, **IC-22** ($\text{C}_{12}\text{H}_{15}\text{Cl}_2\text{O}_6\text{P}$) was characterized by MS spectra, EI-MS m/z (%): 356(M^+ , 11.4), 195(41.1), 175(40.3), 145(23.8), 138(83.9), 109(100), 93(83.3), 79(29.5). The MS spectrum of **IC-22** is shown in Fig. 2.2. In the EI mass spectra, **IC-22** gave weak molecular ion peak 356 with 11.4 % relative abundance. All fragmentation ions of **IC-22** were consistent with its structure.

In the ^1H NMR spectra of **IC**, **ID**, **IE**, and **IF**, the proton signals in both the P–C moiety and P–OMe moiety displayed as two doublets due to couplings to the phosphorus. In the *O,O*-dimethyl 1-(substituted phenoxyacetoxy)alkylphosphonates series, the proton signals corresponding to the two methoxy groups attached to phosphorus appeared as two doublets are caused by the phosphorus nucleus. ^1H NMR spectra of **IC-1**, **IC-8**, **ID-5**, **ID-12**, **IE-22**, **IF-24**, and **IF-32** are listed in Table 2.13. It was also noticed that the signals of methoxy protons attached to

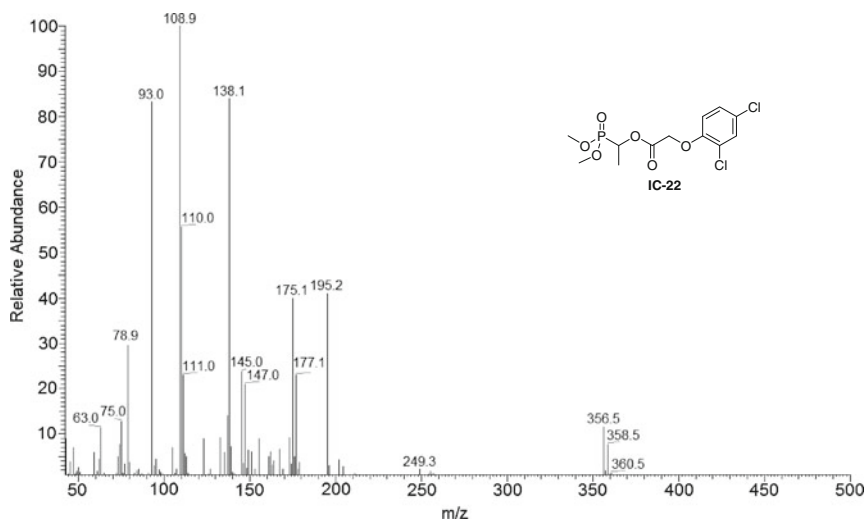
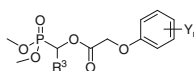


Fig. 2.2 EI-MS spectrum of IC-22

Table 2.13 ^1H NMR spectra of representative compounds

Compound	R ³	Y _n	δ /ppm
IC-1	H	2,4-Cl ₂	3.85 (d, 6H, $J = 10.8$ Hz, 2 × OMe), 4.30 (d, 2H, $J = 11.6$ Hz, CH ₂ P), 4.75 (s, 2H, OCH ₂ CO), 6.8–7.5 (m, 3H, C ₆ H ₃)
IC-5	Me	3-CF ₃	1.43–1.74 (d, 3H, Me), 3.50–3.55 (dd, 6H, 2 × OMe), 4.79 (s, 2H, OCH ₂ CO), 5.39 (m, 1H, OCHP), 7.04–7.39 (m, 4H, C ₆ H ₄)
IC-22	Me	2,4-Cl ₂	1.48–1.60 (t, 3H, Me), 3.76–3.85 (dd, 6H, 2 × OMe), 4.75 (s, 2H, OCH ₂ CO), 5.25–5.40 (m, 1H, CH), 6.80–7.50 (m, 3H, C ₆ H ₃)
IC-28	Et	2-NO ₂ ,4-CF ₃	0.95–1.13 (t, 3H, Me), 1.83–1.99 (m, 2H, CH ₂), 3.72–3.82 (dd, 6H, 2 × OMe), 4.96 (s, 2H, OCH ₂), 5.19–5.28 (m, 1H, CHP), 7.10–8.12 (m, 3H, C ₆ H ₃)
IC-33	<i>n</i> -Pr	2-NO ₂ ,4-CF ₃	0.88–0.95 (t, 3H, Me), 1.30–1.85 (m, 4H, 2 × CH ₂), 3.73–3.81 (dd, 6H, 2 × OMe), 4.84 (s, 2H, OCH ₂), 5.33–5.36 (m, 1H, CHP), 7.06–8.10 (m, 3H, C ₆ H ₃)
IC-34	<i>n</i> -Bu	2,4-Cl ₂	0.90 (t, 3H, Me), 1.25–1.85 (m, 6H, CH ₂ CH ₂ CH ₂), 3.80–3.90 (d, 6H, $J = 10.8$ Hz, 2 × OMe), 4.80 (s, 2H, OCH ₂ CO) (s, 2H, CH ₂), 5.25–5.45 (m, 1H, CHP), 6.80–7.40 (m, 3H, C ₆ H ₃)

(continued)

Table 2.13 (continued)

Compound	R ³	Y _n	δ/ppm
ID-5	CCl ₃	2-Me,4-Cl	2.28 (s, 3H, PhMe), 3.85–3.88 (d, 6H, <i>J</i> = 10.8 Hz, 2 × OMe), 4.86 (s, 2H, OCH ₂ CO), 5.97 (d, 1H, <i>J</i> = 11.6 Hz, OCHP), 6.65–7.27 (m, 3H, C ₆ H ₃)
ID-12	CCl ₃	2,3-Cl ₂	3.86–3.93 (d, 6H, <i>J</i> = 10.8 Hz, 2 × OMe), 4.95 (s, 2H, OCH ₂ CO), 5.97 (d, 1H, <i>J</i> = 11.6 Hz, OCHP), 6.79–7.16 (m, 3H, C ₆ H ₃)
IE-22	Ph	2,4-Cl ₂	3.70 (d, 6H, <i>J</i> = 10.8 Hz, 2 × OMe), 4.80 (s, 2H, OCH ₂ CO), 6.24 (d, 1H, <i>J</i> = 11.6 Hz, CHP), 6.72–7.42 (m, 8H, C ₆ H ₃ + C ₆ H ₅)
IF-24	2-ClPh	2,4-Cl ₂	3.85 (d, 6H, <i>J</i> = 10.8 Hz, 2 × OMe), 4.80 (s, 2H, OCH ₂ CO), 6.40 (d, 1H, <i>J</i> = 11.6 Hz, CHP), 6.80–7.40 (m, 7H, C ₆ H ₃ + 6H ₄)
IF-32	3-BrPh	2,4-Cl ₂	3.7–3.8 (d, 6H, <i>J</i> = 10.8 Hz, 2 × OMe), 4.75 (s, 2H, OCH ₂ CO), 6.20 (d, 6H, <i>J</i> = 12.0 Hz, CHP), 6.7–7.5 (m, 7H, C ₆ H ₃ + C ₆ H ₄)

phosphorus appeared as two doublets. For instance, the signals of both methyls (dd, 6H, 2 × CH₃O) in **IC-22** split into two doublets at δ 3.76 and 3.85, respectively, the difference in the chemical shifts of the two methyl groups was attributed to a stereogenic center of carbon in the molecule. When R³ in structure **ID**, **IE** or **IF** is Ph, substituted Ph or CCl₃, the proton signal corresponding to the moiety of OCHP attached to phosphorus appeared as a doublet split only by the phosphorus nucleus. ¹H NMR spectra of **ID-5**, **ID-12**, **IE-22**, **IF-24**, and **IF-32** are listed in Table 2.13. However, when R³ in structure **IB** or **IC** is Me, Et, *n*-Pr or *n*-Bu, the proton signal of the moiety of OCHP was split into a multiplet, which was caused

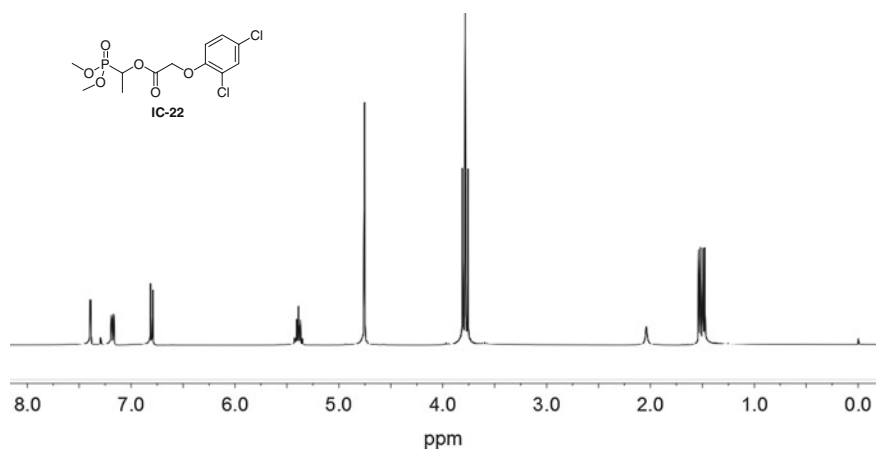
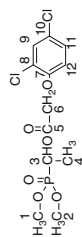
**Fig. 2.3** ¹H NMR spectrum of **IC-22** (CDCl₃, 400 MHz)

Table 2.14 ^{13}C NMR spectroscopic data of **IC-22** (DMSO- d_6 , 150 MHz)

No (C) ^a	1	2	3	4	5	6
δ (ppm)	53.29	53.37	65.17	14.92	166.95	66.10
	d	d	d	s	d	s
	$^2J_{\text{P-C}} = 7.7$	$^2J_{\text{P-C}} = 7.1$	$^1J_{\text{P-C}} = 170.0$		$^3J_{\text{P-C}} = 6.8$	
No (C) ^a	7	8	9	10	11	12
δ (ppm)	152.10	124.12	130.24	127.16	127.47	114.68
	s	s	s	s	s	s

^a Sequence number of C atom

by the effect of magnetic nucleus from both phosphorus and proton in R^3 . 1H NMR spectra of **IC-1**, **IC-5**, **IC-22**, **IC-28**, **IC-33**, and **IC-34** are also listed in Table 2.13.

In 1H NMR spectra of most compounds, the signal corresponding to the methylene group (OCH_2CO) between a phenoxy and a carbonyl group appeared as a singlet (see Table 2.13). As an example, 1H NMR spectrum of **IC-22** is shown in Fig. 2.3.

In 1H NMR spectrum of **IC-22**, the proton signal corresponding to the two methoxy groups attached to phosphorus appeared as two doublets was caused by the phosphorus nucleus. The signals of both methyls (dd, 6H, $2 \times CH_3O$) in **IC-22** were split into two doublets at δ 3.77 and 3.80, respectively. The proton signal of the moiety of OCHP in **IC-22** was split into a multiplet, which was caused by the effect of the magnetic nucleus from both phosphorus and proton in Me as R^3 . The signal corresponding to the methylene group (OCH_2CO) between a phenoxy and a carbonyl group in **IC-22** appeared at δ 4.75 as a singlet.

IC-22 was also characterized by ^{13}C NMR spectroscopic data (Table 2.14). The ^{13}C NMR spectrum of **IC-22** is shown in Fig. 2.4.

^{31}P NMR spectra of some **IC-IF** showed a singlet between δ 12 and 24 ppm. In the ^{31}P NMR spectrum of **IC-22**, its chemical shifts appeared as a singlet at δ 23.18 ppm which was consistent with the characterization of phosphonate. The ^{31}P NMR spectrum of **IC-22** is shown in Fig. 2.5.

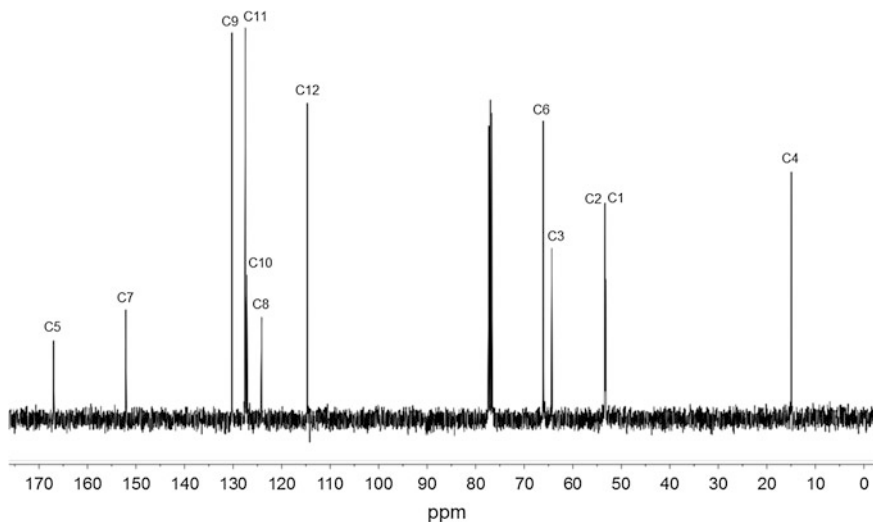


Fig. 2.4 ^{13}C NMR spectrum of **IC-22** ($DMSO-d_6$, 150 MHz)

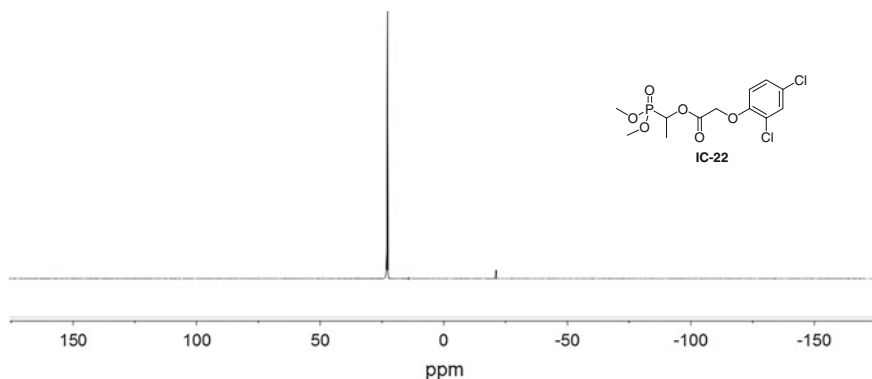


Fig. 2.5 ^{31}P NMR spectrum of IC-22 (CDCl_3 , 162 MHz)

2.1.6 Crystal Structure Analysis of IC-7

The molecular structure of IC-7 is shown in Fig. 2.6. The packing diagram of the unit cell of IC-7 is shown in Fig. 2.7. Selected bond lengths and angles are presented in Table 2.15. As can be seen from the X-ray single crystal structure of IC-7, all bond lengths and angles show normal values. The P(1)–O(5) bond length of 1.4649(11) Å is significantly shorter than the P(1)–O(4) and P(1)–O(6) distances of 1.553(4) and 1.5688(13) Å, respectively. The molecules are connected by

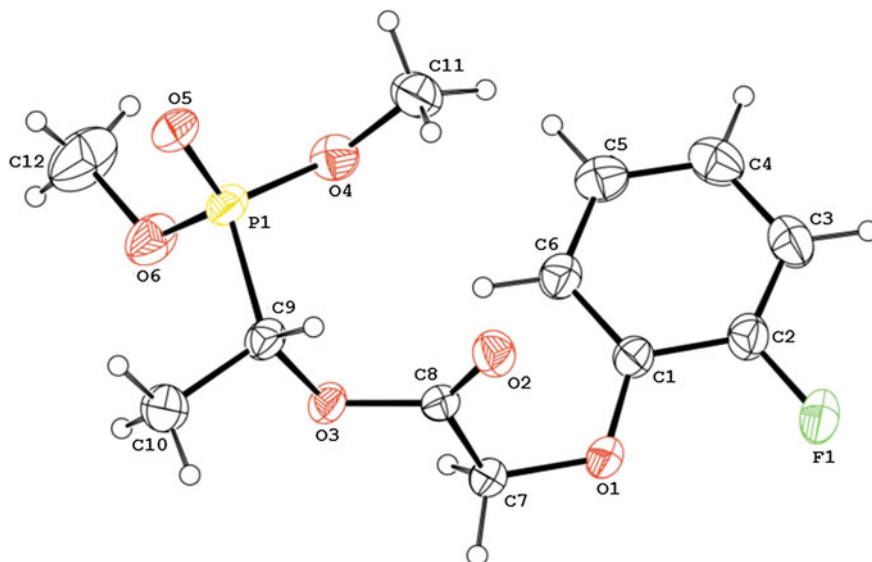
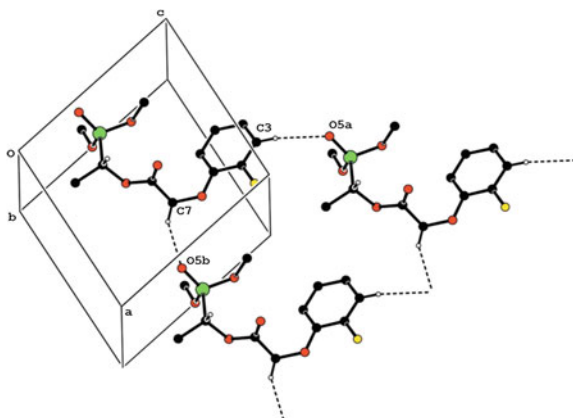


Fig. 2.6 Molecular structure of IC-7

Fig. 2.7 Packing diagram of **IC-7**



intermolecular C–H–O hydrogen bonds (Table 2.16), forming a layer parallel to (010) plane [26].

IC-7 was recrystallized from petroleum ether/dichloromethane (4/1, v/v) to give colorless crystals (0.30 mm × 0.30 mm × 0.20 mm) suitable for X-ray single-crystal diffraction. The crystal structure of **IC-7** was recorded on a Smart Apex CCD diffractometer using graphite monochromated MoK α radiation ($\lambda = 0.071073$ nm). In the range of $2.2^\circ \leq \theta \leq 28.2^\circ$, 9,060 independent reflections ($R_{\text{int}} = 0.018$), of which 3,314 contributing reflection had $I > 2\sigma(I)$, and all data were corrected using SADABS program. The structure was solved by direct methods using SHELXS-97, all other calculations were performed with the Bruker SAINT system and Bruker

Table 2.15 Selected bond distance (Å) and angles ($^\circ$) for **IC-7**

Bond	Distance	Bond	Angles deg.
C(1)–O(1)	1.3704(19)	O(5)–P(1)	1.4649(11)
C(7)–O(1)	1.4178(18)	O(6)–P(x1)	1.5688(13)
C(8)–O(2)	1.1927(17)	O(1)–C(1)–C(6)	126.52(14)
C(8)–O(3)	1.3454(17)	O(3)–C(8)–C(7)	108.99(12)
C(9)–O(3)	1.4573(16)	C(1)–O(1)–C(7)	116.99(12)
C(9)–P(1)	1.8110(15)	C(8)–O(3)–C(9)	117.31(11)
C(11)–O(4)	1.447(2)	O(5)–P(1)–O(6)	116.09(7)
O(4)–P(1)	1.5682(13)	O(4)–P(1)–O(6)	102.03(8)

Table 2.16 Hydrogen bond for **IC-7**

D–H...A	d(D–H)	d(H...A)	d(D...A)	\angle (DHA)
C(3)–H(3)...O(5) ^a	0.93	2.51	3.416(2)	165
C(7)–H(7A)...O(5) ^b	0.97	2.39	3.2793(19)	152
C(9)–H(9)...O(2)	0.98	2.33	2.7241(19)	103

Symmetry codes: ^a x + 1; y; z + 1; ^b x + 1; y; z

SMART programs. All non-hydrogen atoms were refined on F^2 anisotropically by full-matrix least squares method. Hydrogen atoms were observed and refined with a fixed isotropic displacement parameter. Full-matrix least-squares refinement gave final values of $R = 0.039$ and $R_w = 0.109$. The max and min difference between peaks and holes was 330 and -280 e nm^{-3} , respectively.

2.1.7 Herbicidal Activity of IA–IF

O,O-diethyl 1-(4-chlorophenoxyacetoxy)methylphosphonate **IA-1** with significant herbicidal activity was firstly found in our previous study. Further, a series of *O,O*-diethyl 1-(substituted phenoxyacetoxy) alkylphosphonates **IA** was prepared by the modification of **IA-1** and their herbicidal activity were examined systematically at 2.25 kg ai/ha in the green house.

The herbicidal activity data of **IA** are given in Table 2.17. Most **IA** exhibited significant herbicidal activity at 2.25 kg ai/ha against rape (*Brassica campestris*), pea (*Pisum sativum*), Chinese spinach (*Amaranthus tricolor*), and tomato (*Lycopersicon esculintum*) and had weaker activity against wheat (*Triticum aestivum*), barnyard grass (*Echinochloa crusgalli*), and wild oats (*Avena fatua*).

The data in Table 2.17 showed that most **IA** exhibited good post-emergence herbicidal activity against dicotyledon. Therefore structure **IA** was identified as the lead structure of a new herbicide and this lead structure was first extended to a phosphonate structure **Io** for further chemical modification (Scheme 2.11).

In order to examine the effect of size of R^1 , R^2 and R^4 on herbicidal activity, Me, Et and Pr as R^1 and R^2 , H as R^4 were introduced into structure **Io** to design a series of 1-(substituted phenoxyacetoxy)alkylphosphonates **IB**.

The IC_{50} values of some **IB** and **IA** against cucumber (*Cucumis sativa*) were tested to compare the effect of R^1 , R^2 , and R^4 on herbicidal activity. The results are listed in Table 2.18.

From the assay results in Table 2.18, it can be found that inhibitory potency against cucumber decreases with the increase in the size of R^1 , R^2 , and R^4 . When Et as R^1 and R^2 were replaced by *n*-Pr group in structure **Io**, the inhibitory potency of compounds were greatly decreased. For example, inhibitory potency against the root of cucumber: **IB-14** ($R^1 = R^2 = \text{Pr}$) < **IB-12** ($R^1 = R^2 = \text{Et}$); **IB-12** ($R^1 = R^2 = \text{Et}$, $R^4 = \text{Me}$) < **IA-4** ($R^1 = R^2 = \text{Et}$, $R^4 = \text{H}$).

The inhibitory potency against cucumber could be greatly improved when the *n*-Pr as R^1 and R^2 was replaced by the Me group in structure **Io**. Comparing the inhibitory activity of tested **IB** in Table 2.18, it can be found that when R^3 and R^4 are kept unchanged, compounds with Me as R^1 and R^2 group displayed higher inhibitory potency against cucumber than that of *n*-Pr as R^1 and R^2 group. For example, inhibitory potency against the stem of cucumber: **IB-3** ($R^1 = R^2 = \text{Me}$, $R^3 = R^4 = \text{Me}$) > **IB-14** ($R^1 = R^2 = \text{n-Pr}$, $R^3 = R^4 = \text{Me}$); **IB-7** ($R^1 = R^2 = \text{Me}$, $R^3 = \text{Ph}$, $R^4 = \text{Me}$) > **IB-15** ($R^1 = R^2 = \text{n-Pr}$, $R^3 = \text{Ph}$, $R^4 = \text{Me}$).

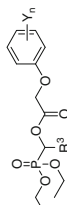
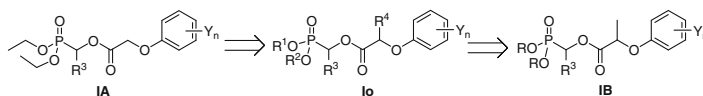


Table 2.17 Herbicidal activity of *O,O*-diethyl 1-(substituted phenoxyacetoxymethyl)alkylphosphonates **IA^a**

Compound	R ³	Y _n	Pre-emergence				Post-emergence						
			Monocotyledon		Dicotyledon		Monocotyledon		Dicotyledon				
			Tri ^b	Ave ^b	Bra ^b	Pis ^b	Lyc ^b	Ech ^b	Tri ^b	Ech ^b	Bra ^b	Pis ^b	Amt ^b
IA-1	H	4-Cl	51	0	91	100	90	42	40	42	100	51	60
IA-2	H	2,4-Cl ₂	45	0	99	100	100	42	9	42	100	100	80
IA-3	Me	4-Cl	60	0	91	94	100	41	36	41	100	100	0
IA-4	Me	2,4-Cl ₂	51	0	91	100	100	42	45	42	100	100	100
IA-5	CCl ₃	4-Me	0	0	100	41	0	42	30	42	0	66	60
IA-6	CCl ₃	4-Cl	0	0	100	100	100	42	38	42	79	77	60
IA-7	Et	4-Cl	52	0	91	100	100	42	49	42	27	73	100
IA-8	Et	2,4-Cl ₂	35	42	100	100	100	0	48	0	100	77	100
IA-9	<i>n</i> -Pr	4-Cl	45	3	91	100	100	71	30	71	100	22	100
IA-10	<i>n</i> -Pr	2,4-Cl ₂	60	0	91	100	100	42	62	42	100	51	100
IA-12	Ph	4-Cl	39	71	91	41	100	57	22	57	100	22	0
IA-13	Ph	2,4-Cl ₂	66	0	91	41	100	42	30	42	100	66	NT

^a Inhibitory potency (%) against the growth of plants at a rate of 2.25 kg ai/ha in the green house, 0 (no effect), 100 % (completely kill), NT (not tested)

^b Tri: wheat; Ave: wild oat; Bra: rape; Pis: pea; Lyc: tomato; Ech: barnyard grass; Amt: Chinese spinach

**Scheme 2.11** Design of 1-(substituted phenoxyacetoxy)alkylphosphonates **IB****Table 2.18** IC₅₀ values of some **IB** and **IA** against cucumber^a

Compound	R ¹ , R ²	R ³	R ⁴	Stem length IC ₅₀ (μM)	Compound	R ¹ , R ²	R ³	R ⁴	Root length IC ₅₀ (μM)
IB-3	Me	Me	Me	6.74	IA-4	Et	Me	H	0.300
IB-14	<i>n</i> -Pr	Me	Me	18.0	IB-12	Et	Me	Me	1.08
IB-7	Me	Ph	Me	30.1	IB-14	<i>n</i> -Pr	Me	Me	2.44
IB-15	<i>n</i> -Pr	Ph	Me	44.3	IB-15	<i>n</i> -Pr	Ph	Me	4.52

^a IC₅₀ is effective dose that provides 50% inhibition against the growth of cucumber (root or stem)

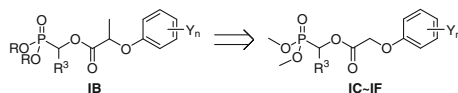
When H as R⁴ in structure **Io** was replaced by Me to form **IB**, the inhibitory potency of **IB** greatly decreased. For example, inhibitory potency against the root of cucumber: **IB-12** (R¹ = R² = Et, R³ = Me, R⁴ = Me) < **IA-4** (R¹ = R² = Et, R³ = Me, R⁴ = H).

Above bioassay results of **IB** showed that inhibitory potency could be greatly improved when the *n*-Pr or Et group as R¹ and R² was replaced by the Me group. Meanwhile, it showed that the compound with H as R⁴ had higher inhibitory potency than that of Me as R⁴. This suggested that smaller R¹, R², and R⁴ groups in the structure **Io** would be beneficial to herbicidal activity.

Therefore, the structure **IB** was further optimized to produce *O,O*-dimethyl 1-(substituted phenoxyacetoxy)alkylphosphonates **IC–IF** (Scheme 2.12).

Several series of *O,O*-dimethyl 1-(substituted phenoxyacetoxy)alkylphosphonates **IC–IF** were prepared to examine their herbicidal activity. It was expected that better herbicidal activities could be achieved by keeping a small methoxyl group which link with the phosphorus atom and H for R⁴ in the structure **Io**.

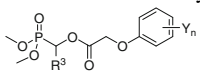
The herbicidal activity of **IC–IF** including **IA** and **IB** were evaluated at different rates in the greenhouse. Substituted phenoxyacetic acid as an structure unit of auxin-type herbicide was contained in the structure of **IA–IF**, therefore an auxin-type herbicide 2,4-D was used as a positive control for the test in the greenhouse. Considering 2,4-D against broadleaved weeds for post-emergence at a recommended rate of 0.2–2.0 kg ai/ha, a preliminary bioassay was first carried out at

**Scheme 2.12** Design of alkylphosphonates **IC–IF**

1.5 kg ai/ha. Pre-emergence and post-emergence inhibitory effect against rape (*Brassica campestris*), common amaranth (*Amaranthus retroflexus*), clover (*Medicago sativa*), barnyard grass (*Echinochloa crusgalli*), and crab grass (*Digitaria sanguinalis*) were examined in this preliminary bioassay.

Based on the preliminary bioassays, inhibition against some plants was further evaluated at a lower rate for pre-emergence and post-emergence herbicidal activity. The results are listed in Tables 2.19, 2.20, 2.21, 2.22, 2.23, 2.24, 2.25, 2.26, 2.27, 2.28, 2.29, 2.30 and 2.31. The herbicidal activity of IC–IF are reviewed as follows.

Table 2.19 Structure and pre-emergence herbicidal activity of *O,O*-dimethyl 1-(substituted phenoxyacetoxy)alkylphosphonates IC^a



Compound	R ³	Y _n	Pre-emergence				
			Dicotyledon			Monocotyledon	
			Bra ^b	Amr ^b	Med ^b	Ech ^b	Dig ^b
IC-1	H	2,4-Cl ₂	A	A	A	B	B
IC-2	Me	H	D	D	D	D	D
IC-4	Me	4-Me	B	B	B	C	D
IC-5	Me	3-CF ₃	A	B	A	B	A
IC-6	Me	4-CF ₃	D	D	D	D	D
IC-7	Me	2-F	D	D	D	D	D
IC-8	Me	3-F	D	D	D	D	D
IC-9	Me	4-F	B	C	B	C	A
IC-10	Me	4-Cl	A	A	A	A	A
IC-11	Me	4-Br	D	D	D	D	D
IC-12	Me	2,3-Me ₂	A	B	B	B	D
IC-13	Me	2-Me,4-Cl	A	A	A	A	A
IC-14	Me	3-Me,4-Cl	A	B	B	B	B
IC-15	Me	2-Cl,5-Me	D	D	D	D	D
IC-16	Me	2,4-F ₂	D	D	C	D	B
IC-17	Me	3,5-F ₂	D	D	D	D	D
IC-18	Me	2-F,4-Cl	D	D	D	D	D
IC-19	Me	2-Cl,4-F	A	A	A	A	A
IC-20	Me	3-Cl,4-F	D	D	B	C	C
IC-21	Me	2,3-Cl ₂	D	D	D	D	D
IC-22	Me	2,4-Cl ₂	A	A	A	B	B
IC-23	Me	2,6-Cl ₂	D	D	D	D	D
IC-24	Me	2,4-Br ₂	D	D	B	D	D
IC-25	Me	2-NO ₂ ,4-Cl	D	D	D	D	D
IC-27	Et	2,4-Cl ₂	A	A	A	D	A
IC-28	Et	2-NO ₂ ,4-CF ₃	D	D	D	D	D
IC-31	<i>n</i> -Pr	4-NO ₂	D	D	D	D	D
IC-32	<i>n</i> -Pr	2,4-Cl ₂	A	A	A	B	B

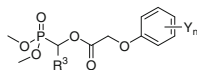
(continued)

Table 2.19 (continued)

Compound	R ³	Y _n	Pre-emergence				
			Dicotyledon			Monocotyledon	
			Bra ^b	Amr ^b	Med ^b	Ech ^b	Dig ^b
IC-33	<i>n</i> -Pr	2-NO ₂ ,4-CF ₃	D	D	D	D	D
IC-34	<i>n</i> -Bu	2,4-Cl ₂	A	A	A	D	B
2,4-D			A	A	A	B	A

^a Inhibitory potency (%) against the growth of plants at a rate of 1.5 kg ai/ha in the greenhouse was expressed as four scales—A: 90–100 %, B: 75–89 %, C: 50–74 %, D: <50 %

^b Bra: rape; Amr: common amaranth; Med: clover; Ech: barnyard grass; Dig: crab grass

Table 2.20 Structure and post-emergence herbicidal activity of *O,O*-dimethyl 1-(substituted phenoxyacetoxy)alkylphosphonates **IC**^a

Compound	R ³	Y _n	Post-emergence				
			Dicotyledon			Monocotyledon	
			Bra ^b	Amr ^b	Med ^b	Ech ^b	Dig ^b
IC-1	H	2,4-Cl ₂	A	A	A	C	C
IC-2	Me	H	D	D	D	D	D
IC-4	Me	4-Me	C	C	C	C	D
IC-5	Me	3-CF ₃	D	C	A	D	D
IC-6	Me	4-CF ₃	D	B	D	D	D
IC-7	Me	2-F	D	D	D	D	D
IC-8	Me	3-F	D	D	D	D	D
IC-9	Me	4-F	C	B	C	C	D
IC-10	Me	4-Cl	B	A	C	D	D
IC-11	Me	4-Br	B	C	C	D	D
IC-12	Me	2,3-Me ₂	B	C	C	C	D
IC-13	Me	2-Me,4-Cl	A	A	C	C	B
IC-14	Me	3-Me,4-Cl	C	C	C	D	D
IC-15	Me	2-Cl,5-Me	D	D	D	D	C
IC-16	Me	2,4-F ₂	B	B	C	D	C
IC-17	Me	3,5-F ₂	D	D	D	D	D
IC-18	Me	2-F,4-Cl	D	C	D	D	D
IC-19	Me	2-Cl,4-F	A	A	A	B	B
IC-20	Me	3-Cl,4-F	B	B	B	D	D
IC-21	Me	2,3-Cl ₂	D	C	D	D	D
IC-22	Me	2,4-Cl ₂	A	A	A	C	C
IC-23	Me	2,6-Cl ₂	D	C	D	D	D
IC-24	Me	2,4-Br ₂	A	A	A	D	D
IC-25	Me	2-NO ₂ ,4-Cl	D	D	D	D	D
IC-27	Et	2,4-Cl ₂	A	A	A	C	B
IC-28	Et	2-NO ₂ ,4-CF ₃	D	D	D	D	D

(continued)

Table 2.20 (continued)

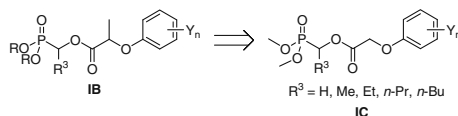
Compound	R ³	Y _n	Post-emergence				
			Dicotyledon			Monocotyledon	
			Bra ^b	Amr ^b	Med ^b	Ech ^b	Dig ^b
IC-31	<i>n</i> -Pr	4-NO ₂	D	D	D	D	D
IC-32	<i>n</i> -Pr	2,4-Cl ₂	A	A	A	C	C
IC-33	<i>n</i> -Pr	2-NO ₂ ,4-CF ₃	D	D	D	D	D
IC-34	<i>n</i> -Bu	2,4-Cl ₂	A	A	A	C	C
2,4-D			A	A	A	C	C

^a Inhibitory potency (%) against the growth of plants at a rate of 1.5 kg ai/ha in the greenhouse was expressed as four scales—A: 90–100 %, B: 75–89 %, C: 50–74 %, D: <50 %

^b Bra: rape; Amr: common amaranth; Med: clover; Ech: barnyard grass; Dig: crab grass

2.1.7.1 Herbicidal Activity of *O,O*-Dimethyl 1-(Substituted Phenoxyacetoxy)Alkylphosphonates **IC**

Thirty-four of **IC** were prepared to test their herbicidal activity. Further optimization was focused on the substituents Y_n (Scheme 2.13). The herbicidal activity of **IC** is listed in Tables 2.19 and 2.20.

**Scheme 2.13** Design of *O,O*-dimethyl 1-(substituted phenoxyacetoxy)alkylphosphonates **IC**

(A) Pre-emergence herbicidal activity of **IC**

As shown in Table 2.19, **IC-10** (R³ = Me, Y_n = 4-Cl), **IC-13** (R³ = Me, Y_n = 2-Me,4-Cl) and **IC-19** (R³ = Me, Y_n = 2-Cl,4-F) exhibited pre-emergence herbicidal activity against dicotyledons and crab grass comparable to that of 2,4-D, and they showed better activities than 2,4-D against barnyard grass at 1.5 kg ai/ha. Those compounds with 2,4-Cl₂ as Y_n, such as **IC-1**, **IC-22**, **IC-27**, **IC-32**, **IC-34** exhibited notable herbicidal activity against dicotyledons for pre-emergence application comparable to 2,4-D. Other compounds showed no significant pre-emergence herbicidal activity at 1.5 kg ai/ha.

(B) Post-emergence herbicidal activity of **IC**

As shown in Table 2.20, **IC-1**, **IC-22**, **IC-27**, **IC-32**, **IC-34** (Y_n = 2,4-Cl₂), **IC-19** (Y_n = 2-Cl,4-F), and **IC-24** (Y_n = 2,4-Br₂) exhibited notable herbicidal activity against dicotyledons for post-emergence application comparable to 2,4-D at 1.5 kg ai/ha. When 2,4-Cl₂; 2-Cl,4-F or 2,4-Br₂ as Y_n was on the phenoxy-benzene ring, all those compounds showed good herbicidal activity.

(C) SAR analyses for IC

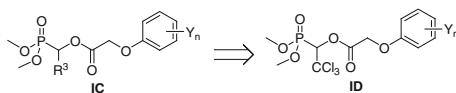
The substitutions of 4-Cl (**IC-10**), 2-Me,4-Cl (**IC-13**), and 2-Cl,4-F (**IC-19**) on the phenoxy-benzene ring were most promotive for pre-emergence herbicidal activity against dicotyledons and monocotyledons at 1.5 kg ai/ha. The substitutions of 2,4-Cl₂; 2-Cl,4-F and 2,4-Br₂ on the phenoxy-benzene ring were most promotive for post-emergence herbicidal activity against dicotyledons followed by 2-Me,4-Cl (**IC-13**). All compounds with 2,4-Cl₂ as Y_n (**IC-1**, **IC-22**, **IC-27**, **IC-32**, **IC-34**) or 2-Cl,4-F as Y_n (**IC-19**) exhibited notable herbicidal activity against dicotyledons for pre-emergence and post-emergence applications comparable to 2,4-D at 1.5 kg ai/ha, irrespective of H, Me, Et, *n*-Pr or *n*-Bu as R³, respectively. The introduction of 2,4-F₂ or 2-F,4-Cl as Y_n resulted in a sharp decrease in herbicidal activity. **IC-2** with no substituent on the phenoxy-benzene ring was completely inactive. Those compounds with 4-CF₃ (**IC-6**), 2-F (**IC-7**), 3-F (**IC-8**), 2-Cl,5-Me (**IC-15**), 3,5-F₂ (**IC-17**), 2,3-Cl₂ (**IC-21**), 2,6-Cl₂ (**IC-23**), 4-NO₂ (**IC-31**), 2-NO₂,4-Cl (**IC-25**), and 2-NO₂,4-CF₃ (**IC-28** and **IC-33**) as Y_n on the phenoxy-benzene ring, were almost inactive against both tested monocotyledons and dicotyledons.

2.1.7.2 Herbicidal Activity of *O,O*-Dimethyl 1-(Substituted Phenoxyacetoxy)-2,2,2-Trichloroethylphosphonates ID

The bioassays of **IC** showed that herbicidal activity could be greatly affected by different substituents Y_n on the phenoxy-benzene ring. However, the difference in the R³ moiety including H, Me, Et, *n*-Pr and *n*-Bu seems to have no significant change on herbicidal activity at 1.5 kg ai/ha. On the basis of structure **IC**, the structure of R³ was changed to CCl₃ to form a series of **ID** (Scheme 2.14), further modification was only focused on substituents Y_n. Fourteen of **ID** were prepared and their herbicidal activity was tested. The herbicidal activity of **ID** is listed in Tables 2.21 and 2.22.

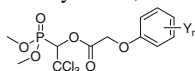
(A) Pre-emergence herbicidal activity of ID

As shown in Table 2.21, **ID-4** (Y_n = 4-Cl), **ID-5** (Y_n = 2-Me,4-Cl) and **ID-10** (Y_n = 2-Cl,4-F) exhibited pre-emergence herbicidal activity against dicotyledons and crab grass comparable to 2,4-D, and they showed better activity than 2,4-D against barnyard grass at 1.5 kg ai/ha. Compounds **ID-13** (Y_n = 2,4-Cl₂) also exhibited good herbicidal activity against dicotyledons and crab grass for pre-emergence application comparable to 2,4-D, while other compounds showed weak pre-emergence herbicidal activity at 1.5 kg ai/ha.



Scheme 2.14 Design of *O,O*-dimethyl 1-(substituted phenoxyacetoxy)-2,2,2-trichloroethylphosphonates **ID**

Table 2.21 Structure and pre-emergence herbicidal activity of *O,O*-dimethyl 1-(substituted phenoxyacetoxyl)-2,2,2-trichloroethylphosphonates **ID**^a

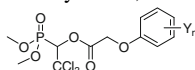


Compound	Y _n	Pre-emergence				
		Dicotyledon			Monocotyledon	
		Bra ^b	Amr ^b	Med ^b	Ech ^b	Dig ^b
ID-1	4-CF ₃	D	D	D	D	D
ID-2	3-F	D	D	D	D	D
ID-3	4-F	C	C	C	C	A
ID-4	4-Cl	A	A	A	A	A
ID-5	2-Me,4-Cl	A	A	A	A	A
ID-6	3-Me,4-Cl	C	C	C	C	C
ID-7	2-Cl,5-Me	D	D	D	D	D
ID-8	2,4-F ₂	D	D	B	D	B
ID-9	3,5-F ₂	D	D	D	D	D
ID-10	2-Cl,4-F	A	A	A	A	A
ID-11	3-Cl,4-F	D	C	C	C	B
ID-12	2,3-Cl ₂	D	D	D	D	D
ID-13	2,4-Cl ₂	A	A	A	C	A
ID-14	2,6-Cl ₂	D	D	D	D	D
2,4-D		A	A	A	B	A

^a Inhibitory potency (%) against the growth of plants at a rate of 1.5 kg ai/ha in the greenhouse was expressed as four scales—A: 90–100 %, B: 75–89 %, C: 50–74 %, D: <50 %

^b Bra: rape; Amr: common amaranth; Med: clover; Ech: barnyard grass; Dig: crab grass

Table 2.22 Structure and post-emergence herbicidal activity of *O,O*-dimethyl 1-(substituted phenoxyacetoxyl)-2,2,2-trichloroethylphosphonates **ID**^a



Compound	Y _n	Post-emergence				
		Dicotyledon			Monocotyledon	
		Bra ^b	Amr ^b	Med ^b	Ech ^b	Dig ^b
ID-1	4-CF ₃	D	B	D	D	D
ID-2	3-F	D	D	D	D	D
ID-3	4-F	C	B	C	C	D
ID-4	4-Cl	B	A	B	D	C
ID-5	2-Me,4-Cl	A	A	C	C	B
ID-6	3-Me,4-Cl	C	D	D	D	D
ID-7	2-Cl,5-Me	D	D	D	D	D
ID-8	2,4-F ₂	C	B	C	D	C
ID-9	3,5-F ₂	D	D	D	D	D
ID-10	2-Cl,4-F	B	A	A	B	B

(continued)

Table 2.22 (continued)

Compound	Y _n	Post-emergence				
		Dicotyledon			Monocotyledon	
		Bra ^b	Amr ^b	Med ^b	Ech ^b	Dig ^b
ID-11	3-Cl,4-F	B	A	C	C	D
ID-12	2,3-Cl ₂	D	D	D	D	D
ID-13	2,4-Cl ₂	A	A	A	D	D
ID-14	2,6-Cl ₂	D	B	D	D	D
2,4-D		A	A	A	C	C

^a Inhibitory potency (%) against the growth of plants at a rate of 1.5 kg ai/ha in the greenhouse was expressed as four scales—A: 90–100 %, B: 75–89 %, C: 50–74 %, D: <50 %

^b Bra: rape; Amr: common amaranth; Med: clover; Ech: barnyard grass; Dig: crab grass

(B) *Post-emergence herbicidal activity of ID*

As shown in Table 2.22, only **ID-13** (Y_n = 2,4-Cl₂) exhibited notable post-emergence herbicidal activity against dicotyledons comparable to 2,4-D followed by **ID-10** (Y_n = 2-Cl,4-F) and **ID-4** (Y_n = 4-Cl). Most **ID** had no significant herbicidal activity against monocotyledons for post-emergence application, except that **ID-10** (Y_n = 2-Cl,4-F) had medium activity against monocotyledons and it was better than 2,4-D.

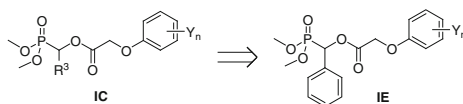
(C) *SAR analyses for ID*

Like SAR analyses for **IC**, the substitutions of 4-Cl (**ID-4**), 2-Me,4-Cl (**ID-5**) and 2-Cl,4-F (**ID-10**) on the phenoxy-benzene ring were most promotive for pre-emergence herbicidal activity against dicotyledons and monocotyledons. They were not only comparable to 2,4-D, but also were better than that of 2,4-D against barnyard grass at 1.5 kg ai/ha. The substitution of 2,4-Cl₂ (**ID-13**) on the phenoxy-benzene ring was very promotive for post-emergence herbicidal activity against dicotyledons comparable to 2,4-D. Noticed that 2-Cl,4-F substitution (**ID-10**) was most promotive for pre- and post-emergence herbicidal activity against both dicotyledons and monocotyledons at 1.5 kg ai/ha.

Herbicidal activity of compounds with 3-Cl,4-F (**ID-11**), 2,4-F₂ (**ID-8**), 3-Me, 4-Cl (**ID-6**), and 4-F (**ID-3**) substitutions was very weak. Compounds with 4-CF₃ (**ID-1**), 2-Cl,5-Me (**ID-7**), 2,3-Cl₂ (**ID-12**), 2,6-Cl₂ (**ID-14**), 3-F (**ID-2**), and 3,5-F₂ (**ID-9**) substitutions were almost inactive for pre- and post-emergence herbicidal activity against both dicotyledons and monocotyledons at 1.5 kg ai/ha.

2.1.7.3 Herbicidal Activity of *O,O*-Dimethyl 1-(Substituted Phenoxyacetoxy)Benzylphosphonates **IE**

On the basis of structure **IC**, Ph was introduced at R³ to form a series of **IE** (Scheme 2.15), further modification was only focused on substituents Y_n. Twenty-four **IE** were prepared to test their herbicidal activity. The herbicidal activity of **IE** is listed in Tables 2.23 and 2.24.



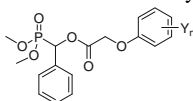
Scheme 2.15 Design of *O,O*-dimethyl 1-(substituted phenoxyacetoxy)benzylphosphonates **IE**

Table 2.23 Structure and pre-emergence herbicidal activity of *O,O*-dimethyl 1-(substituted phenoxyacetoxy)benzylphosphonates **IE**^a

Compound	Y _n	Pre-emergence				
		Dicotyledon			Monocotyledon	
		Bra ^b	Amr ^b	Med ^b	Ech ^b	Dig ^b
IE-1	H	D	D	D	D	D
IE-2	3-Me	B	B	B	D	D
IE-3	4-Me	B	B	B	D	D
IE-5	4-CF ₃	D	D	D	D	D
IE-6	2-NO ₂	D	D	D	D	D
IE-8	2-F	D	D	D	D	D
IE-9	3-F	D	D	D	D	D
IE-10	4-F	D	B	B	C	A
IE-11	4-Cl	A	A	A	A	A
IE-13	2,3-Me ₂	A	C	B	B	D
IE-14	2-Me,4-Cl	A	A	A	A	A
IE-15	3-Me,4-Cl	B	B	A	C	B
IE-16	2-Cl,5-Me	D	D	D	D	D
IE-17	2,4-F ₂	D	C	C	B	D
IE-19	2-Cl,4-F	A	A	A	A	A
IE-20	3-Cl,4-F	A	A	B	B	A
IE-21	2,3-Cl ₂	D	D	D	D	D
IE-22	2,4-Cl ₂	A	A	A	D	D
IE-23	2,6-Cl ₂	D	D	D	D	D
IE-24	2-NO ₂ ,4-CF ₃	D	D	D	D	D
2,4-D		A	A	A	B	A

^a Inhibitory potency (%) against the growth of plants at a rate of 1.5 kg ai/ha in the greenhouse was expressed as four scales—A: 90–100 %, B: 75–89 %, C: 50–74 %, D: <50 %

^b Bra: rape; Amr: common amaranth; Med: clover; Ech: barnyard grass; Dig: crab grass

Table 2.24 Structure and post-emergence herbicidal activity of *O,O*-dimethyl 1-(substituted phenoxyacetoxy)benzylphosphonates **IE**^a

Compound	Y _n	Post-emergence				
		Dicotyledon			Monocotyledon	
		Bra ^b	Amr ^b	Med ^b	Ech ^b	Dig ^b
IE-1	H	D	D	D	D	D
IE-2	3-Me	C	C	C	D	D
IE-3	4-Me	C	C	C	D	D
IE-5	4-CF ₃	D	D	D	D	D
IE-6	2-NO ₂	D	D	D	D	D
IE-8	2-F	D	D	D	D	D
IE-9	3-F	D	D	D	D	D
IE-10	4-F	C	B	C	C	C
IE-11	4-Cl	B	A	B	B	C
IE-13	2,3-Me ₂	B	D	C	C	D
IE-14	2-Me,4-Cl	A	A	A	B	C
IE-15	3-Me,4-Cl	B	B	C	D	D
IE-16	2-Cl,5-Me	D	D	D	D	D
IE-17	2,4-F ₂	D	A	D	D	D
IE-19	2-Cl,4-F	B	A	B	B	C
IE-20	3-Cl,4-F	B	B	C	C	D
IE-21	2,3-Cl ₂	D	D	D	D	D
IE-22	2,4-Cl ₂	A	A	A	D	D
IE-23	2,6-Cl ₂	D	B	D	D	D
IE-24	2-NO ₂ ,4-CF ₃	D	D	D	D	D
2,4-D		A	A	A	C	C

^a Inhibitory potency (%) against the growth of plants at a rate of 1.5 kg ai/ha in the greenhouse was expressed as four scales—A: 90–100 %, B: 75–89 %, C: 50–74 %, D: <50 %

^b Bra: rape; Amr: common amaranth; Med: clover; Ech: barnyard grass; Dig: crab grass

(A) Pre-emergence herbicidal activity of **IE**

The data in Table 2.23 showed that **IE-11** (Y_n = 4-Cl), **IE-14** (Y_n = 2-Me,4-Cl) and **IE-19** (Y_n = 2-Cl,4-F) exhibited pre-emergence herbicidal activity against dicotyledons and crab grass comparable to 2,4-D, and they showed better activity than 2,4-D against barnyard grass at 1.5 kg ai/ha. **IE-20** (Y_n = 3-Cl,4-F) and **IE-15** (Y_n = 3-Me,4-Cl) had medium activity. **IE-22** (Y_n = 2,4-Cl₂) exhibited good herbicidal activity against dicotyledons comparable to 2,4-D for pre-emergence, but it had no significant herbicidal activity against monocotyledons. **IE-10** (Y_n as 4-F) had significant herbicidal activity against crab grass. **IE-20** (Y_n = 3-Cl,4-F) exhibited pre-emergence herbicidal activity against monocotyledons comparable to

2,4-D. Other compounds showed weak herbicidal activity against dicotyledons and monocotyledons for pre-emergence at 1.5 kg ai/ha.

(B) *Post-emergence herbicidal activity of IE*

The data in Table 2.24 show that **IE-14** ($Y_n = 2\text{-Me}, 4\text{-Cl}$) and **IE-22** ($Y_n = 2, 4\text{-Cl}_2$) exhibited notable post-emergence herbicidal activity against dicotyledons comparable to 2,4-D followed by **IE-11** ($Y_n = 4\text{-Cl}$), **IE-19** ($Y_n = 2\text{-Cl}, 4\text{-F}$), **IE-15** ($Y_n = 3\text{-Me}, 4\text{-Cl}$), and **IE-20** ($Y_n = 3\text{-Cl}, 4\text{-F}$). Most **IE** had no significant herbicidal activity against monocotyledons for post-emergence application, but **IE-11** ($Y_n = 4\text{-Cl}$), **IE-14** ($Y_n = 2\text{-Me}, 4\text{-Cl}$), and **IE-19** ($Y_n = 2\text{-Cl}, 4\text{-F}$) showed better herbicidal activity against barnyard grass than 2,4-D at 1.5 kg ai/ha.

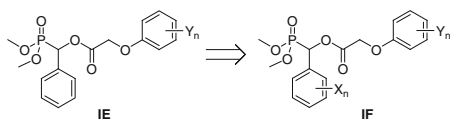
(C) *SAR analyses for IE*

Compounds with no substituent on the phenoxy-benzene ring (**IE-1**) had no herbicidal activity. When 4-Cl, 2-Me,4-Cl, 2-Cl,4-F and 2,4-Cl₂ were introduced as Y_n , respectively, **IE-11**, **IE-14**, **IE-19**, and **IE-22** showed good herbicidal activity against dicotyledons for pre-emergence and post-emergence applications at 1.5 kg ai/ha. Especially, compounds with 4-Cl (**IE-11**), 2-Me,4-Cl (**IE-14**) and 2-Cl,4-F (**IE-19**) substitutions on the phenoxy-benzene ring not only exhibited notable herbicidal activity against dicotyledons for pre-emergence and post-emergence applications, but also exhibited good herbicidal activity against monocotyledons for pre-emergence application. The herbicidal activity of compounds was almost lost when 4-CF₃; 2-NO₂; 2-F; 3-F; 2,4-F₂; 2-NO₂,4-CF₃; 2-Cl,5-Me; 2,3-Cl₂ or 2,6-Cl₂ as Y_n on the phenoxy-benzene ring, while 3-Me,4-Cl; 3-Cl,4-F; 3-Me; 4-Me; 4-F; 2,3-Me₂ as Y_n resulted in a decrease in herbicidal activity.

IC-IE with Y_n as 4-Cl, 2-Me,4-Cl and 2-Cl,4-F as Y_n exhibited good herbicidal activity against dicotyledons and monocotyledons for pre-emergence application, irrespective of H, Me, Et, *n*-Pr, *n*-Bu, CCl₃, or Ph as R³, respectively.

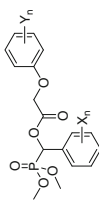
2.1.7.4 Herbicidal Activity of *O,O*-Dimethyl 1-(Substituted Phenoxyacetoxy)-1-(Substituted Phenyl)methylphosphonates **IF**

On the basis of structure **IE**, substituted phenyls were introduced to form a series of **IF**. Further modification was focused on substituents Y_n and X_n (Scheme 2.16). Sixty-three compounds of **IF** were prepared to test their herbicidal activity. The herbicidal activity of **IF** is listed in Tables 2.25 and 2.26.



Scheme 2.16 Design of *O,O*-dimethyl 1-(substituted phenoxyacetoxy)-1-(substituted phenyl)methylphosphonates **IF**

Table 2.25 Structure and pre-emergence herbicidal activity of *O,O*-dimethyl 1-(substituted phenoxyacetoxy)-1-(substituted phenyl)methylphosphonates **IF^a**



Compound	X _n	Y _n	Pre-emergence					
			Dicotyledon			Monocotyledon		
			Bra ^b	Amr ^b	Med ^b	Ech ^b	Dig ^b	
IF-1	4-Me	3-CF ₃	C	A	C	C	B	
IF-10	2-OH	4-Cl	D	D	A	D	C	
IF-11	2-OH	2-Cl,4-F	A	A	A	C	A	
IF-20	4-MeO	2,4-Cl ₂	D	D	D	A	A	
IF-21	4-F	3-CF ₃	B	A	A	C	A	
IF-22	4-F	2,4-Cl ₂	A	A	A	A	A	
IF-23	2-Cl	3-CF ₃	D	A	A	B	A	
IF-24	2-Cl	2,4-Cl ₂	A	A	A	A	A	
IF-25	3-Cl	3-CF ₃	A	A	A	C	D	
IF-26	3-Cl	2,4-Cl ₂	A	A	A	A	A	
IF-27	4-ClPh	3-CF ₃	C	D	A	C	C	
IF-31	4-Cl	2,4-Cl ₂	A	A	A	A	A	
IF-32	3-Br	2,4-Cl ₂	A	A	A	C	A	
IF-33	2,3-Cl	2,4-Cl ₂	A	A	A	A	A	
IF-35	2,4-Cl ₂	3-CF ₃	D	A	A	A	A	
IF-36	2,4-Cl ₂	2,4-Cl ₂	A	A	A	A	A	
IF-38	3,4-Cl ₂	3-CF ₃	B	A	A	B	A	
IF-39	3,4-Cl ₂	2,4-Cl ₂	B	B	B	A	A	
IF-40	3,4-OCH ₂ O	3-CF ₃	B	A	A	A	A	
IF-41	3,4-OCH ₂ O	2,4-Cl ₂	A	A	A	A	A	
IF-43	3-NO ₂	3-CF ₃	C	C	C	D	D	

(continued)

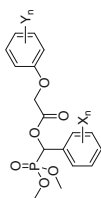
Table 2.25 (continued)

Compound	X _n	Y _n	Pre-emergence					
			Dicotyledon			Monocotyledon		
			Bra ^b	Amr ^b	Med ^b	Ech ^b	Dig ^b	
IF-44	3-NO ₂	4-CF ₃	D	D	D	D	D	D
IF-45	3-NO ₂	2-NO ₂	D	D	D	D	D	D
IF-46	3-NO ₂	4-NO ₂	D	D	D	D	D	D
IF-47	3-NO ₂	2-F	D	D	D	D	D	D
IF-48	3-NO ₂	3-F	D	D	D	D	D	D
IF-49	3-NO ₂	4-F	D	B	B	B	C	B
IF-50	3-NO ₂	4-Cl	A	A	A	A	A	A
IF-51	3-NO ₂	2-Me,4-Cl	C	B	B	B	A	A
IF-52	3-NO ₂	3-Me,4-Cl	C	B	B	B	D	C
IF-53	3-NO ₂	2-Cl,5-Me	D	D	D	D	D	D
IF-54	3-NO ₂	2,4-F ₂	D	D	D	C	D	C
IF-55	3-NO ₂	2-Cl,4-F	A	A	A	A	A	A
IF-56	3-NO ₂	3-Cl,4-F	D	C	C	C	C	B
IF-57	3-NO ₂	2,3-Cl ₂	D	D	D	D	D	D
IF-58	3-NO ₂	2,4-Cl ₂	A	A	A	A	C	D
IF-59	3-NO ₂	2,6-Cl ₂	D	D	D	D	D	D
IF-60	3-NO ₂	2-NO ₂ ,4-CF ₃	D	D	D	D	D	D
IF-62	4-NO ₂	2-NO ₂	D	D	D	D	D	D
IF-63	4-NO ₂	2,4-Cl ₂	A	A	A	A	C	D
2,4-D			A	A	A	A	B	A

^a Inhibitory potency(%) against the growth of plants at a rate of 1.5 kg ai/ha in the greenhouse was expressed as four scales: A—90–100 %, B: 75–89 %, C: 50–74 %, D: <50 %

^b Bra: rape; Amr:common amaranth; Med: clover; Ech: barnyard grass; Dig: crab grass

Table 2.26 Structure and post-emergence herbicidal activity of *O,O*-dimethyl 1-(substituted phenoxyacetoxy)-1-(substituted phenyl)methylphosphonates **IF^{aa}**



Compound	X _n	Y _n	Post-emergence					
			Dicotyledon			Monocotyledon		
			Bra ^b	Amr ^b	Med ^b	Ech ^b	Dig ^b	
IF-1	4-Me	3-CF ₃	A	D	B	D	D	
IF-10	2-OH	4-Cl	B	B	B	D	D	
IF-11	2-OH	2-Cl,4-F	A	A	A	C	D	
IF-20	4-MeO	2,4-Cl ₂	D	D	D	D	D	
IF-21	4-F	3-CF ₃	C	A	B	D	D	
IF-22	4-F	2,4-Cl ₂	B	B	B	D	D	
IF-23	2-Cl	3-CF ₃	C	A	B	D	D	
IF-24	2-Cl	2,4-Cl ₂	A	A	A	D	D	
IF-25	3-Cl	3-CF ₃	D	A	B	D	D	
IF-26	3-Cl	2,4-Cl ₂	A	A	A	D	D	
IF-27	4-Cl	3-CF ₃	B	A	D	C	D	
IF-31	4-Cl	2,4-Cl ₂	A	A	A	D	D	
IF-32	3-Br	2,4-Cl ₂	A	A	A	C	D	
IF-33	2,3-Cl ₂	2,4-Cl ₂	A	A	A	C	D	
IF-35	2,4-Cl ₂	3-CF ₃	C	A	B	D	D	
IF-36	2,4-Cl ₂	2,4-Cl ₂	A	A	A	D	D	
IF-38	3,4-Cl ₂	3-CF ₃	D	A	B	D	D	
IF-39	3,4-Cl ₂	2,4-Cl ₂	A	A	A	D	D	
IF-40	3,4-OCH ₂ O	3-CF ₃	D	B	B	D	D	
IF-41	3,4-OCH ₂ O	2,4-Cl ₂	B	B	B	D	D	

(continued)

Table 2.26 (continued)

Compound	X _n	Y _n	Post-emergence					
			Dicotyledon			Monocotyledon		
			Bra ^b	Amr ^b	Med ^b	Ech ^b	Dig ^b	
IF-43	3-NO ₂	3-CF ₃	C	D	D	C	D	
IF-44	3-NO ₂	4-CF ₃	D	C	D	D	D	
IF-45	3-NO ₂	2-NO ₂	D	D	D	D	D	
IF-46	3-NO ₂	4-NO ₂	D	D	D	D	D	
IF-47	3-NO ₂	2-F	D	D	D	A	D	
IF-48	3-NO ₂	3-F	D	D	D	D	D	
IF-49	3-NO ₂	4-F	C	B	C	D	C	
IF-50	3-NO ₂	4-Cl	B	B	B	B	C	
IF-51	3-NO ₂	2-Me,4-Cl	B	A	C	B	D	
IF-52	3-NO ₂	3-Me,4-Cl	D	B	B	D	D	
IF-53	3-NO ₂	2-Cl,5-Me	D	D	D	D	D	
IF-54	3-NO ₂	2,4-F ₂	B	B	C	D	C	
IF-55	3-NO ₂	2-Cl,4-F	B	A	C	B	C	
IF-56	3-NO ₂	3-Cl,4-F	C	B	C	C	D	
IF-57	3-NO ₂	2,3-Cl ₂	D	D	D	D	D	
IF-58	3-NO ₂	2,4-Cl ₂	A	A	A	D	D	
IF-59	3-NO ₂	2,6-Cl ₂	D	D	D	D	D	
IF-60	3-NO ₂	2-NO ₂ ,4-CF ₃	D	D	D	D	D	
IF-62	4-NO ₂	2-NO ₂	D	D	D	D	D	
IF-63	4-NO ₂	2,4-Cl ₂	A	A	A	D	D	
2,4-D			A	A	A	C	C	

^a Inhibitory potency (%) against the growth of plants at a rate of 1.5 kg ai/ha in the greenhouse was expressed as four scale—A: 90–100 %, B: 75–89 %, C: 50–74 %, D: <50 %

^b Bra: rape; Amr: common amaranth; Med: clover; Ech: barnyard grass; Dig: crab grass

(A) *Pre-emergence herbicidal activity of IF*

The data in Table 2.25 show **IF-22**, **IF-24**, **IF-26**, **IF-31**, **IF-33**, **IF-36**, **IF-41**, **IF-50** and **IF-55** exhibited pre-emergence herbicidal activity against dicotyledons and crab grass comparable to 2,4-D, and they showed better pre-emergence herbicidal activity against barnyard grass than that of 2,4-D at 1.5 kg ai/ha. **IF-32**, **IF-58** and **IF-63** only had pre-emergence herbicidal activity against dicotyledons comparable to 2,4-D. **IF-20**, **IF-35**, **IF-39**, **IF-40** and **IF-51** had significant pre-emergence herbicidal activity against monocotyledons. They showed activity against crab grass comparable to 2,4-D, against barnyard grass better than that of 2,4-D at 1.5 kg ai/ha. Other compounds showed weak herbicidal activity against dicotyledons and monocotyledons for pre-emergence application at 1.5 kg ai/ha.

(B) *Post-emergence herbicidal activity of IF*

As shown in Table 2.26, **IF-11**, **IF-24**, **IF-26**, **IF-31–IF-33**, **IF-36**, **IF-39**, **IF-58** and **IF-63** exhibited good herbicidal activity against dicotyledons for post-emergence application. Most **IF** had no significant herbicidal activity against monocotyledons for post-emergence application except **IF-47**, **IF-50**, **IF-51**, and **IF-55**, which had activity against barnyard grass.

(C) *SAR analyses for IF*

The data in Tables 2.25 and 2.26 showed that compounds with 2,4-Cl₂, 2-Cl,4-F or 4-Cl as Y_n on the phenoxy-benzene ring were most beneficial for pre-emergence herbicidal activity against dicotyledons and crab grass. While compounds with 2,4-Cl₂ or 2-Cl,4-F as Y_n were most beneficial for post-emergence herbicidal activity against dicotyledons. Compounds with 2-F,4-Cl; 2-Me,4-Cl; 4-Cl or 4-F as Y_n were beneficial for post-emergence herbicidal activity against barnyard grass at a rate of 1.5 kg ai/ha. Introduction of other substituents as Y_n led to a sharp decrease in herbicidal activity or loss of activity completely.

Herbicidal activity was also greatly affected by X_n even 2,4-Cl₂, 2-Cl,4-F or 4-Cl as Y_n were kept the same. Introduction of 4-MeO (**IF-20**), 4-F (**IF-22**), 3,4-OCH₂O (**IF-41**) or 3,4-Cl₂ (**IF-39**) as X_n into **IF** led to a decrease in herbicidal activity against dicotyledons for pre-emergence or post-emergence application. Particularly for **IF-20** (X_n = 4-MeO, Y_n = 2,4-Cl₂), its herbicidal activity against dicotyledons for both pre-emergence and post-emergence applications was completely lost.

All compounds with 2,4-Cl₂ as Y_n exhibited better pre-emergence herbicidal activity against barnyard grass than that of 2,4-D except compounds with NO₂ as X_n. Introduction of 3-NO₂ and 4-NO₂ as X_n led to a sharp decrease in pre-emergence herbicidal activity against monocotyledons, such as **IF-58** (X_n = 3-NO₂, Y_n = 2,4-Cl₂) and **IF-63** (X_n = 4-NO₂, Y_n = 2,4-Cl₂). However, compounds with 3-NO₂ as X_n, 2-Cl,4-F or 4-Cl as Y_n displayed good pre-emergence herbicidal activity against monocotyledons. **IF-10** (X_n = 2-OH, Y_n = 4-Cl) was almost inactive to monocotyledons and dicotyledons except clover for pre-emergence application at 1.5 kg ai/ha. Above SAR analyses indicated that improvement of herbicidal activity required a reasonable combination of both X_n and Y_n. Both the structure and position of Y_n, and the structure of X_n are critical for herbicidal activity.

2.1.7.5 Further Herbicide Activity Assay of Some 1-(Substituted Phenoxyacetoxy)Alkylphosphonates

Based on the preliminary bioassays, some 1-(substituted phenoxyacetoxy)-alkylphosphonates were further evaluated in greenhouse at a lower rate for pre-emergence and post-emergence herbicidal activity. Chingma abutilon (*Abutilon theophrasti*), spiny amaranth (*Amaranthus spinosus*), goosefoot (*Chenopodium album*), crab grass (*Digitaria Sanguinalis*), and green bristlegrass (*Setaria viridis*) were chosen as test species.

(A) Pre-emergence herbicide activity of some 1-(substituted phenoxyacetoxy)-alkylphosphonates

In order to confirm the pre-emergence herbicidal activity of 1-(substituted phenoxyacetoxy)alkylphosphonates, seven compounds were chosen for further herbicide activity assay at a lower rate for pre-emergence herbicidal activity. As shown in Table 2.27, they displayed very poor herbicidal activity against tested plants for pre-emergence application except **IA-4** and **IC-2** with 48–53 % inhibitory potency against dicotyledonous plants at 450 g ai/ha. All tested compounds had no pre-emergence herbicidal activity against tested plants at 150 or 75 g ai/ha, irrespective of difference in structure.

Table 2.27 Structure and pre-emergence herbicidal activity of some 1-(substituted phenoxyacetoxy)alkylphosphonates^a

Compound	R	R ³	Y _n	Rate (g ai/ha)	Abu ^b	Ams ^b	Che ^b	Dig ^b	Set ^b
IA-4	Et	Me	2,4-Cl ₂	75	0	0	0	0	0
				150	0	0	0	0	0
				450	48	50	53	10	6
IC-2	Me	Me	H	75	0	0	0	0	0
				150	0	0	0	0	0
				450	48	53	53	0	5
IC-5	Me	Me	3-CF ₃	75	0	0	0	0	0
				150	0	0	0	0	0
				450	0	0	0	36	36
IC-13	Me	Me	2-Me,4-Cl	150	0	0	0	0	0
				450	0	30	0	16	0
IC-22	Me	Me	2,4-Cl ₂	75	0	0	0	0	0
				150	0	0	0	0	0
				450	0	0	0	45	35
IE-22	Me	Ph	2,4-Cl ₂	75	0	0	0	0	0
				150	0	0	0	0	0
				450	0	0	0	45	30

(continued)

Table 2.27 (continued)

Compound	R	R ³	Y _n	Rate (g ai/ha)	Abu ^b	Ams ^b	Che ^b	Dig ^b	Set ^b
IF-58	Me	3-NO ₂ Ph	2,4-Cl ₂	75	0	0	0	0	0
				150	0	0	0	0	0
				450	0	0	0	0	0
2,4-D				75	0	0	0	0	0
				150	0	0	0	10	6
				450	0	0	0	65	65

^a Inhibitory potency (%) against the growth of plants in the greenhouse, 0 (no effect), 100 % (completely kill)

^b Abu: chingma abutilon; Ams: spiny amaranth; Che: goosefoot; Dig: crab grass; Set: green bristlegrass

(B) *Post-emergence herbicide activity of some 1-(substituted phenoxyacetoxy)-alkylphosphonates*

In order to confirm the post-emergence herbicide activity of 1-(substituted phenoxyacetoxy)alkylphosphonates, seven compounds were further evaluated at a lower rate for post-emergence herbicidal activity. The result showed that tested compounds displayed much higher herbicidal activity against dicotyledonous plants than monocotyledons for post-emergence application. All tested compounds exhibited excellent post-emergence herbicidal activity (with 90–100 % inhibitory potency) against tested dicotyledonous plants; however, they displayed very poor herbicidal activity (only with 0–37 % inhibitory potency) against monocotyledons, crab grass, and green bristlegrass at 450 g ai/ha.

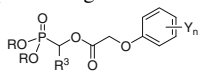
The data in Table 2.28 showed that compounds with 2,4-Cl₂ as Y_n had higher herbicidal activity than that of compounds with 2-Me,4-Cl or 3-CF₃ as Y_n. The compounds with 2,4-Cl₂ as Y_n exhibited potent herbicidal activity against dicotyledons for post-emergence application at 75 g ai/ha. It was found that **IC-22** with the *O,O*-dimethyl group exhibited better herbicidal activity than **IA-4** with the *O,O*-diethyl group at 75 g ai/ha. When 2,4-Cl₂ as Y_n stay the same, R³ as Me was much more beneficial than R³ as Ph or 3-NO₂Ph for post-emergence herbicidal activity. Among **IA–IF**, **IC-22** displayed the best post-emergence herbicide activity having >90 % inhibitory potency against dicotyledons better than or comparable to 2,4-D.

2.1.7.6 Inhibition on Growth of Cucumber

The IC₅₀ values of some **IC–IF** against cucumber (*Cucumis sativa*) were measured in order to further confirm the effect of substituent on herbicidal activity (Tables 2.29, 2.30 and 2.31).

Inhibitory potency shown by IC₅₀ values in Tables 2.29 and 2.30 corresponded well to the SAR analyses base on the herbicidal effect of those compounds in the greenhouse.

Table 2.28 Structure and post-emergence herbicidal activity of some 1-(substituted phenoxy-acetoxy)alkylphosphonates^a

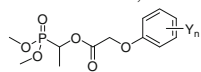


Compound	R	R ³	Y _n	Rate (g ai/ha)	Abu ^b	Ams ^b	Che ^b
IA-4	Et	Me	2,4-Cl ₂	75	98	53	63
				150	98	83	93
IC-2	Me	Me	H	75	83	63	83
				150	99	93	100
IC-5	Me	Me	3-CF ₃	75	28	0	33
				150	42	0	42
IC-13	Me	Me	2-Me,4-Cl	150	82	10	60
IC-22	Me	Me	2,4-Cl ₂	75	98	90	93
				150	100	100	96
IE-22	Me	Ph	2,4-Cl ₂	75	83	63	83
				150	93	70	93
IF-58	Me	3-NO ₂ Ph	2,4-Cl ₂	75	50	50	53
				150	90	100	83
2,4-D				75	73	60	73
				150	100	93	93

^a Inhibitory potency (%) against the growth of plants in the greenhouse, 0 (no effect), 100 % (completely kill)

^b Abu: chingma abutilon; Ams: spiny amaranth; Che: goosefoot

Table 2.29 IC₅₀ values of *O,O*-dimethyl 1-(substituted phenoxyacetoxy)alkylphosphonates against cucumber



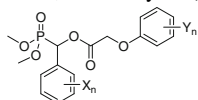
Compound	Y _n	Root length IC ₅₀ (μM) ^a	R
IC-22	2,4-Cl ₂	0.0025	0.9868
IC-19	2-Cl,4-F	0.2836	0.9902
IC-10	4-Cl	0.427	0.9903
IC-13	2-Me,4-Cl	0.4363	0.9543
IC-20	3-Cl,4-F	1.123	0.9936
IC-9	4-F	1.517	0.9908
IC-16	2,4-F ₂	1.838	0.9918
IC-14	3-Me,4-Cl	2.957	0.9961
IC-15	2-Cl,5-Me	48.59	0.9964
IC-2	H	89.10	0.9965
IC-23	2,6-Cl ₂	99.97	0.9975
IC-8	3-F	111.1	0.9934
IC-21	2,3-Cl ₂	207.5	0.9997
IC-6	4-CF ₃	246.9	0.9956

(continued)

Table 2.29 (continued)

Compound	Y _n	Root length IC ₅₀ (μM) ^a	R
IC-17	3,5-F ₂	287.0	0.9976
IC-7	2-F	376.5	0.9880
2,4-D		0.2280	0.9918

^a IC₅₀ is effective dose that provides 50 % inhibition against the growth of cucumber root

Table 2.30 IC₅₀ values of *O,O*-dimethyl 1-(substituted phenoxyacetoxy)-1-arylmethylphosphonates against cucumber

Compound	X _n	Y _n	Root length IC ₅₀ (μM) ^a	R
IE-22	H	2,4-Cl ₂	0.0142	0.9868
IE-19	H	2-Cl,4-F	0.3198	0.9905
IE-14	H	2-Me,4-Cl	0.3526	0.9916
IE-11	H	4-Cl	0.3964	0.9954
IE-20	H	3-Cl,4-F	0.5840	0.9989
IE-15	H	3-Me, 4-Cl	1.731	0.9970
IE-10	H	4-F	2.050	0.9868
IE-17	H	2,4-F ₂	3.246	0.9836
IE-9	H	3-F	64.23	0.9933
IE-16	H	2-Cl,5-Me	72.71	0.9982
IE-23	H	2,6-Cl ₂	85.11	0.9863
IE-6	H	2-NO ₂	223.0	0.9982
IE-21	H	2,3-Cl ₂	228.4	0.9951
IE-8	H	2-F	625.3	0.9963
IF-59	3-NO ₂	2,4-Cl ₂	0.0034	0.9868
IF-51	3-NO ₂	2-Me,4-Cl	0.3258	0.9836
IF-45	3-NO ₂	2-NO ₂	297.0	0.9982
IF-46	3-NO ₂	4-NO ₂	>11400	0.9863
2,4-D			0.2280	0.9918

^a IC₅₀ is effective dose that provides 50 % inhibition against the growth of cucumber root.

As shown in Table 2.29, substituent Y_n on the phenoxy-benzene ring had greater influence on inhibitory potency against the growth of the root of cucumber. Compared with **IC-2** which had no substituent on the phenoxy-benzene ring, inhibitory potency could be greatly enhanced by introducing 2,4-Cl₂; 2-Cl,4-F; 2-Me,4-Cl and 4-Cl on the phenoxy-benzene ring. Whereas the introduction of 2,3-Cl₂; 2,6-Cl₂; 2,3-F₂; 4-CF₃ or 3,5-F₂ as Y_n resulted in a sharp decrease in inhibitory potency against cucumber.

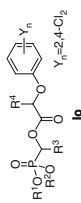


Table 2.31 IC₅₀ values of *O,O*-dialkyl 1-(substituted phenoxyacetoxy)alkylphosphonates against cucumber

Compound	R ¹ , R ²	R ³	R ⁴	Stem Length IC ₅₀ (μM) ^a	Compound	R ¹ , R ²	R ³	R ⁴	Root Length IC ₅₀ (μM) ^a
IF-58	Me	3-NO ₂ Ph	H	5.02	IC-22	Me	Me	H	0.0025
IB-3	Me	Me	Me	6.74	IF-58	Me	3-NO ₂ Ph	H	0.0034
IC-22	Me	Me	H	7.56	IC-32	Me	Pr	H	0.0075
IC-1	Me	H	H	7.79	IE-22	Me	Ph	H	0.0142
IE-22	Me	Ph	H	8.95	IA-13	Et	Ph	H	0.0488
IC-32	Me	<i>n</i> -Pr	H	9.34	IC-1	Me	H	H	0.0577
2,4-D				10.1	2,4-D				0.228
IA-2	Et	H	H	13.4	IA-4	Et	Me	H	0.300
IB-4	Me	<i>n</i> -Pr	Me	13.7	IA-8	Et	Et	H	0.310
IC-27	Me	Et	H	14.0	IC-27	Me	Et	H	0.327
IB-14	<i>n</i> -Pr	Me	Me	18.0	IB-12	Et	Me	Me	1.08
IA-18	Et	2-ClPh	H	21.1	IB-3	Me	Me	Me	1.42
IA-8	Et	Et	H	25.7	IA-18	Et	2-ClPh	H	1.49
IB-7	Me	Ph	Me	30.1	IB-14	<i>n</i> -Pr	Me	Me	2.44
IB-15	<i>n</i> -Pr	Ph	Me	44.3	IB-4	Me	<i>n</i> -Pr	Me	2.98
IA-13	Et	Ph	H	109	IB-15	<i>n</i> -Pr	Ph	Me	4.52
IB-16	<i>n</i> -Pr	2-ClPh	Me	164	IB-16	<i>n</i> -Pr	2-ClPh	Me	12.1

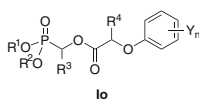
^a IC₅₀ is effective dose that provides 50 % inhibition against the growth of cucumber (root or stem)

As shown in Table 2.30, compounds with 2,4-Cl₂; 2-Cl,4-F; 2-Me,4-Cl and 4-Cl as Y_n on the phenoxy-benzene ring displayed higher inhibitory potency against the growth of the root of cucumber. Whereas the compounds with 2,3-Cl₂; 2,6-Cl₂; 2-Cl,5-Me; 2,3-F₂ or NO₂ on the phenoxy-benzene ring showed poor inhibitory potency. As a typical example, the introduction of a nitro group as Y_n on the phenoxy-benzene ring resulted in a sharp decrease in inhibitory potency, such as **IF-45** (IC₅₀ = 297 μM) and **IF-46** (IC₅₀ > 11,400 μM). However, the introduction of 3-NO₂ group into the benzene ring at X_n had a favorable effect on inhibitory potency when 2,4-Cl₂ was as Y_n, such as **IF-59** (IC₅₀ = 0.0034 μM).

The above results showed 2,4-Cl₂ as Y_n on the phenoxy-benzene ring to be most beneficial for herbicidal activity. In order to confirm the effect of R¹, R², R³, and R⁴ in structure **Io** on activity, the inhibitory potency of some compounds against cucumber was examined when 2,4-Cl₂ as Y_n was kept constant (Table 2.31).

As shown in Table 2.31, great differences for cucumber toxicity could be made due to a change of R¹, R², R³, and R⁴ in the phosphonate **Io** when 2,4-Cl₂ as Y_n were kept unchanged. Inhibitory activity decreased with the increase in the size of R¹, R², and R⁴. When *n*-Pr or Et was replaced by a smaller group (Me), inhibitory potency was greatly improved. Compounds with Me as R¹, R², and H as R⁴ displayed higher inhibitory potency, such as **IC-1**, **IC-22**, **IC-32**, **IE-22**, and **IF-58** displayed higher activity against the growth of root and stem of cucumber than that of 2,4-D. However several compounds with Et or *n*-Pr as R¹ and R², showed lower activity against the growth of cucumber than that of 2,4-D. These results indicated that the phosphonates **Io** themselves were responsible for the inhibitory potency against cucumber, not the possible metabolic product 2,4-D.

2.1.8 Structure-Herbicidal Activity Relationships



On the scaffold of the phosphonate **Io**, the effects of substituents R¹, R², R³, R⁴, and Y_n on herbicidal activity can be summarized as follows:

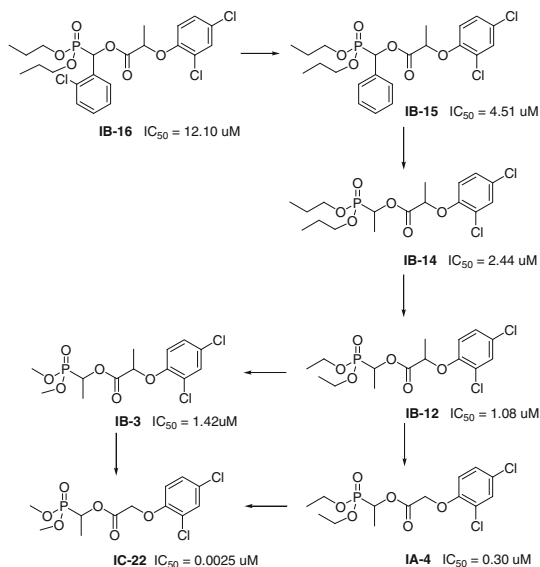
- (A) Herbicidal activity was highly dependent upon the structure and position of substituent Y_n on the phenoxy-benzene ring. Herbicidal activities of compounds against dicotyledons for post-emergence application could be greatly enhanced by introducing 2,4-Cl₂ or 2-Cl,4-F into the phenoxy-benzene ring compared with that of other substituents. Herbicidal activities of compounds would be weak or lost when 2-F, 3-F; 2,3-F₂; 3,5-F₂; 2-Cl,5-Me; 2,3-Cl₂; 2,6-Cl₂; 4-CF₃; 2-NO₂; 4-NO₂; 2-NO₂,4-Cl or 2-NO₂,4-CF₃ as Y_n were introduced into the phenoxy-benzene ring. Compounds with no substituent on the phenoxy-benzene ring were inactive.

- (B) Substituents R^1 , R^2 , and R^4 played a very important role in herbicidal activity. Herbicidal activity decreased with the increase in the size of R^1 , R^2 , and R^4 . Compounds with Me as R^1 and R^2 , H as R^4 displayed higher inhibitory potency than those of Et and *n*-Pr as R^1 and R^2 , and H or Me as R^4 even when 2,4-Cl₂ as Y_n was kept unchanged. This finding accorded with the SAR analyses for acylphosphonates by Baillie et al. They found that when a smaller substituent with weaker electronegativity was introduced to link with the phosphorus atom in the skeleton of acylphosphonates, herbicide activity of compound significantly increased.
- (C) When Y_n , R^1 , R^2 , and R^4 were kept unchanged in the phosphonate **Io**, the different substituent of R^3 also had great influence on the herbicidal activity. **IF-20** ($R^3 = 4\text{-MeOPh}$) exhibited low inhibitory potency (<50 %) against the tested plants, but **IF-31** ($R^3 = 4\text{-ClPh}$) exhibited 100 % post- or pre-emergence inhibitory potency against all tested dicotyledons in greenhouse (Tables 2.25 and 2.26). However, the effect of R^3 depends on structures of Y_n , R^1 , R^2 , and R^4 . As a typical example, the herbicidal activity of **IF-58** ($R^1 = R^2 = \text{Me}$, $R^3 = 3\text{-NO}_2\text{Ph}$, $R^4 = \text{H}$, $Y_n = 2,4\text{-Cl}_2$) was much higher than that of **IF-46** ($R^1 = R^2 = \text{Me}$, $R^3 = 3\text{-NO}_2\text{Ph}$, $R^4 = \text{H}$, $Y_n = 4\text{-NO}_2$).
- (D) There were remarkably different effects on herbicidal activity by introducing a nitro group as R^3 and/or Y_n . The introduction of a nitro group as Y_n on the phenoxy-benzene ring resulted in much lower herbicidal activity (such as compounds with 2-NO₂; 4-NO₂; 2-NO₂,4-Cl or 2-NO₂,4-CF₃ as Y_n). However, the introduction of a nitro group in R^3 had a favourable effect on herbicidal activity. Good herbicidal activity against dicotyledons was observed in the compounds **IF-58** ($R^1 = R^2 = \text{Me}$, $R^3 = 3\text{-NO}_2\text{Ph}$, $R^4 = \text{H}$, $Y_n = 2,4\text{-Cl}_2$) and **IF-63** ($R^1 = R^2 = \text{Me}$, $R^3 = 4\text{-NO}_2\text{Ph}$, $R^4 = \text{H}$, $Y_n = 2,4\text{-Cl}_2$). This indicated that introduction of a nitro group as Y_n on the phenoxy-benzene ring was not beneficial to herbicidal activity. Satisfactory herbicidal activity of the phosphonate **Io** could be achieved by introducing a nitro group in R^3 with a reasonable combination of Y_n , R^1 , R^2 , and R^4 .

The above SAR analyses indicated that improvement of herbicidal activity required a reasonable combination of both phosphorus-containing moiety and phenoxyacetate moiety. Herbicidal activity was remarkably variable by chemical modification of R^1 , R^2 , R^3 , R^4 , and Y_n . As shown in Scheme 2.17, when 2,4-Cl₂ were kept unchanged as Y_n , inhibitory potency against the growth of the root of cucumber was greatly enhanced by the chemical modification of substituents in the phosphorus-containing moiety.

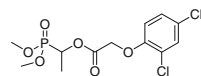
IC-22 with notable inhibitory potency was found by optimizing the structure of R^1 , R^2 , R^3 and R^4 in **Io** [22]. It also exhibited promising post-emergence herbicidal activity against dicotyledons better than or comparable to 2,4-D.

Scheme 2.17 Increase of inhibitory potency against the growth of the root of cucumber



2.1.9 Herbicidal Activity of IC-22

In order to confirm the practicality, **IC-22** (code number for development: HW02) was selected for further evaluation for its herbicidal activity and herbicidal spectrum at 18.75–450 g ai/ha in greenhouse. **IC-22** tested for post-emergence activity against a range of weed species including white eclipia (*Eclipta prostrata*), common amaranth (*Amaranthus retroflexus*), siberian cocklebur (*Xanthium strumarium*), hairy bittercress (*Cardamine hirsute*), purslane (*Portulaca oleracea*), clover (*Medicago sativa*) barnyard grass (*Echinochloa crusgalli*), and crab grass (*Digitaria sanguinalis*). As shown in Table 2.32, **IC-22** exhibited excellent herbicidal activity against broadleaf weeds by post-emergence application at 18.75–450 g ai/ha. However, no post emergence activity was seen against monocot weeds, barnyard grass, and crab grass at 450–18.75 g ai/ha. Crop selectivity of **IC-22** at 37.5–600 g ai/ha was further examined. Rape (*Brassica campestris*), carrot (*Daucus carota*), wheat (*Triticum aestivum*), maize (*Zea mays*), and rice (*Oryza sativa*) were chosen as representative crops to test **IC-22**'s selectivity (Table 2.32). Among tested crops, rape and carrot as dicotyledonous crop were very susceptible at a rate as low as 37.5 g ai/ha, whereas wheat, maize, and rice exhibited a higher tolerance to **IC-22** even at 600 g ai/ha. The data in Tables 2.32 and 2.33 further showed all tested broadleaf plants were highly sensitive to **IC-22** by post-emergence application at a lower rate. **IC-22** tested showed an indication of broad spectrum herbicide activity against broadleaf weeds and a higher level of selectivity between broadleaf weeds and wheat, maize, or rice.

Table 2.32 Herbicidal activity of **IC-22** for post-emergence application^a

Rate (g ai/ha)	Amr ^b	Car ^b	Ecl ^b	Por ^b	Med ^b	Xan ^b	Dig ^b	Ech ^b
18.75	65	75	56	50	60	50	0	0
37.5	83	84	72	65	72	60	0	0
75	90	88	82.5	75	84	72	0	0
150	96	90	90	85	90	90	15	0
225	96	95	96	90	95	95	23	10
300	100	100	100	95	97	100	32	20
450	100	100	100	100	100	100	37.5	35

^a Evaluation in greenhouse. Inhibitory potency (%) against the growth of plants, 0 (no effect), 100 % (completely kill)

^b Ecl: white eclipsta; Amr: common amaranth; Xan: siberian cocklebur; Car: hairy bittercress; Por: purslane; Med: clover; Ech: barnyard grass; Dig: crab grass

Table 2.33 Crop selectivity of **IC-22** for post-emergence application^a

Rate (g ai/ha)	Dau ^b	Bra ^b	Tri ^b	Ory ^b	Zea ^b
37.5	85	90	NT	NT	NT
75	90	93	NT	NT	NT
150	95	97	NT	NT	0
225	97	100	0	0	0
300	100	100	0	0	0
450	100	100	0	0	0
600	100	100	0	0	0

^a Inhibitory potency (%) against the growth of plants in the greenhouse, 0 (no effect), 100 % (completely kill), NT (not tested)

^b Dau: carrot; Bra: rape; Tri: wheat; Ory: rice; Zea: maize

2.1.10 Summary

O,O-Dialkyl 1-(substituted phenoxyacetoxy)alkylphosphonates **IA–IF** including 103 compounds as potential PDHc inhibitors were conveniently synthesized by the condensation of 1-hydroxyalkylphosphonates **M2** and substituted phenoxyacetyl chlorides **M5** in the presence of base under mild reaction conditions.

Some alkylphosphonates showed much higher herbicidal activity against dicotyledons than monocotyledons for post-emergence and pro-emergence applications in greenhouse. Their post-emergence herbicidal activity against dicotyledons was much better than pre-emergence herbicidal activity.

Bioassay results showed that satisfactory herbicidal activity of *O,O*-dialkyl 1-(substituted phenoxyacetoxy)alkylphosphonates could be achieved by a reasonable combination of both phosphorus-containing moiety and phenoxyacetate moiety. The herbicidal activity could be increased greatly by optimizing R, R³, R⁴, and Y_n in the parent structure **Io**. One requirement was *O*-methyl, rather than *O*-ethyl or *O*-*n*-propyl attached to phosphorus atom. The other was that two chlorine atoms or chlorine and fluorine atoms as Y_n should be substituted at the 2- and 4-positions on a phenoxy-benzene ring. Besides, smaller groups H as R⁴ and Me as R³ were beneficial to herbicidal activity. *O,O*-Dimethyl 1-(2,4-dichlorophenoxyacetoxy) ethylphosphonate **IC-22** was thus found to be the most effective against broadleaf weeds, better than or comparable to 2,4-D in post-emergence application at 18.75–450 g ai/ha.

IC-22 showed much higher herbicidal activity than that of those reported plant PDHc inhibitors, acylphosphinates and acylphosphonates [1, 27]. Those compounds exhibited 80–100 % inhibition against weeds at 2.8 kg/ha; but at this rate they had shown unacceptable phytotoxicity to the crops. Compared with acylphosphinates and acylphosphonates, **IC-22** exhibited promising herbicidal activity and selectivity for development as a selective post-emergence herbicide which may be used for broadleaf weed control in monocot crop fields.

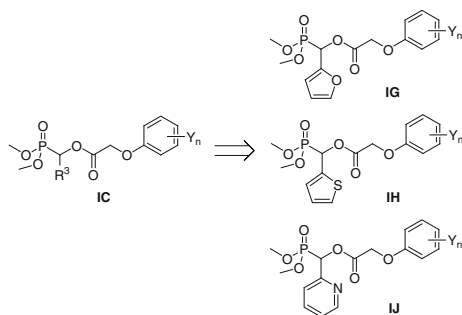
2.2 Heterocyclymethylphosphonates IG–IJ

2.2.1 Introduction

Through the optimization of lead structures **IA**, *O,O*-dimethyl 1-(2,4-dichlorophenoxyacetoxy)ethylphosphonate (**IC-22**) was found to be a potential herbicide [22], with an effective inhibition against plant PDHc E1 (see Chap. 7).

The further synthetic strategy was thus focused on the modifications of *O,O*-dimethyl 1-(substituted phenoxyacetoxy)alkylphosphonates scaffold. As many heterocyclic compounds had shown remarkable biological properties, we were interested in the design of heterocycle-containing 1-(substituted phenoxyacetoxy) alkylphosphonates. Different heterocyclic group such as furyl, thienyl, or pyridyl group as R³ was introduced to **IC** to form *O,O*-dimethyl 1-(substituted phenoxyacetoxy)-1-(fur-2-yl)methylphosphonates **IG**, *O,O*-dimethyl 1-(substituted phenoxyacetoxy)-1-(thien-2-yl)methylphosphonates **IH** and *O,O*-dimethyl 1-(substituted phenoxyacetoxy)-1-(pyrid-2-yl)methylphosphonates **IJ** (Scheme 2.18).

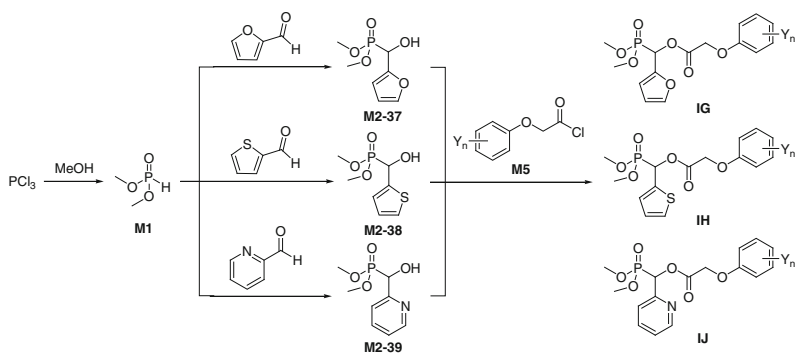
In this section we describe the synthesis, herbicidal activity, and SAR analyses of heterocyclymethylphosphonates **IG–IJ**. It has been found that **IG–21** and some of its analogs have shown potential utility as an herbicide against broadleaf weeds.



Scheme 2.18 Design of *O,O*-dimethyl 1-(substituted phenoxyacetoxy)-1-heterocyclymethylphosphonates **IG–IJ**

2.2.2 Synthesis of **IG–IJ**

Heterocyclymethylphosphonates **IG–IJ** were synthesized by the condensation of *O,O*-dimethyl 1-hydroxyl-1-heterocyclymethylphosphonates **M2** (**M2-37**, **M2-38** and **M2-39**) and substituted phenoxyacetyl chloride **M5**. The synthetic route in Scheme 2.19 was carried out for preparations of **IG–IJ**.



Scheme 2.19 Synthetic route of *O,O*-dimethyl 1-(substituted phenoxyacetoxy)-1-heterocyclymethylphosphonates **IG–IJ**

O,O-dimethyl 1-hydroxyl-1-heterocyclymethylphosphonates **M2-37**, **M2-38** and **M2-39** were prepared by a base-catalyzed nucleophilic addition of *O,O*-dimethyl phosphonate **M1** (or dimethyl phosphite) to corresponding heterocyclaldehydes using triethylamine as a catalyst in the range of 81–90 % yields. The method for the preparation of *O,O*-dimethyl 1-hydroxyl-1-heterocyclymethylphosphonates **M2** has

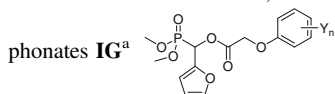
been discussed in Sect. 2.1.2. The yields and physicochemical data of **M2-37**, **M2-38** and **M2-39** are listed in Table 9.2.

The method for preparations of substituted phenoxyacetic acids **M4** and substituted phenoxyacetyl chlorides **M5** has been discussed in Sect. 2.1.3. **M5** were prepared from corresponding substituted phenoxyacetic acids **M4**. **M4-1–M4-3**, **M4-6–M4-8**, and **M4-9–M4-14** which were used to prepare **IG–IJ** are shown in Table 2.7. **M4** could be prepared according to the general synthesis procedure of **M4** in Sect. 9.1.5.

The synthetic reaction of **IG–IJ** required a temperature near room temperature using a weak base because **IG–IJ** contained a carboxylic ester group which was sensitive to acid or base. A large number of *O,O*-dimethyl 1-(substituted phenoxyacetoxy)alkylphosphonates have been prepared by the condensation of 1-hydroxyalkylphosphonates with substituted phenoxyacetyl chlorides in the presence of pyridine as an acid-binding agent. In the synthesis study of **IG–IJ**, triethylamine was also found to be a good acid-binding agent and as a catalyst for the condensation of **M2** and **M5**. In order to prevent hydrolysis of **M2** and **M5**, this condensation should be carried out in anhydrous solvent, such as anhydrous CH_2Cl_2 or CHCl_3 . The structures of **IG–IJ** are listed in Tables 2.34, 2.35 and 2.36.

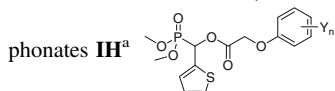
The general synthesis procedure of heterocyclymethylphosphonates **IG–IJ** is introduced in Sect. 9.1.7. **IG–IJ** were soluble in a variety of organic solvents such as benzene, diethyl ether, ethyl acetate, and so on. They were stable to light and air at room temperature but easily decomposed under the acidic or basic conditions. Their structures were characterized by ^1H NMR, ^{31}P NMR, IR and MS, and confirmed by elementary analysis. Spectroscopic analysis of some representative **IG–IJ** are given in the next section.

Table 2.34 Structure of *O,O*-dimethyl 1-(substituted phenoxyacetoxy)-1-(fur-2-yl)methylphosphonates **IG^a**



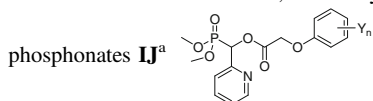
Compound	Y _n	Compound	Y _n	Compound	Y _n
IG-1	H	IG-9	2-Cl	IG-17	2,4-F ₂
IG-2	3-Me	IG-10	4-Cl	IG-18	2-F,4-Cl
IG-3	4-Me	IG-11	4-Br	IG-19	2-Cl,4-F
IG-4	3-CF ₃	IG-12	4-CN	IG-20	2,3-Cl ₂
IG-5	4-CF ₃	IG-13	2,3-Me ₂	IG-21	2,4-Cl ₂
IG-6	2-F	IG-14	2-Me,4-Cl	IG-22	2,6-Cl ₂
IG-7	3-F	IG-15	3-Me,4-Cl	IG-23	2,4,5-Cl ₃
IG-8	4-F	IG-16	2-Cl,5-Me		

^a Synthesis of **IG-1–IG-6**, **IG-9**, **IG-11–IG-13**, **IG-17–IG-19** and **IG-23** [28]; **IG-7**, **IG-8**, **IG-10**, **IG-14**, **IG-16**, **IG-20**, **IG-21** and **IG-22** [23]

Table 2.35 Structure of *O,O*-dimethyl 1-(substituted phenoxyacetoxy)-1-(thien-2-yl)methylphosphonates **IH**^a

Compound	Y _n	Compound	Y _n	Compound	Y _n
IH-1	3-CF ₃	IH-8	4-Br	IH-15	2-F,4-Cl
IH-2	4-CF ₃	IH-9	4-CN	IH-16	2-Cl,4-F
IH-3	2-F	IH-10	2,3-Me ₂	IH-17	2,3-Cl ₂
IH-4	3-F	IH-11	2-Me,4-Cl	IH-18	2,4-Cl ₂
IH-5	4-F	IH-12	3-Me,4-Cl	IH-19	2,6-Cl ₂
IH-6	2-Cl	IH-13	2-Cl,5-Me	IH-20	2,4,5-Cl ₃
IH-7	4-Cl	IH-14	2,4-F ₂		

^a Synthesis of **IH-4**, **IH-5**, **IH-7**, **IH-11**, **IH-13**, **IH-17**, **IH-18** and **IH-19** [23]; **IH-2**, **IH-6**, **IH-8**, **IH-9**, **IH-10**, **IH-14**, and **IH-15** [28]; **IH-1**, **IH-3**, **IH-12**, and **IH-16** [29]

Table 2.36 Structure of *O,O*-dimethyl 1-(substituted phenoxyacetoxy)-1-(pyrid-2-yl)methylphosphonates **IJ**^a

Compound	Y _n	Compound	Y _n	Compound	Y _n
IJ-1	3-CF ₃	IJ-6	4-Cl	IJ-11	2-Cl,4-F
IJ-2	4-CF ₃	IJ-7	2-Me,4-Cl	IJ-12	2,3-Cl ₂
IJ-3	2-F	IJ-8	3-Me,4-Cl	IJ-13	2,4-Cl ₂
IJ-4	3-F	IJ-9	2-Cl,5-Me	IJ-14	2,6-Cl ₂
IJ-5	4-F	IJ-10	2,4-F ₂		

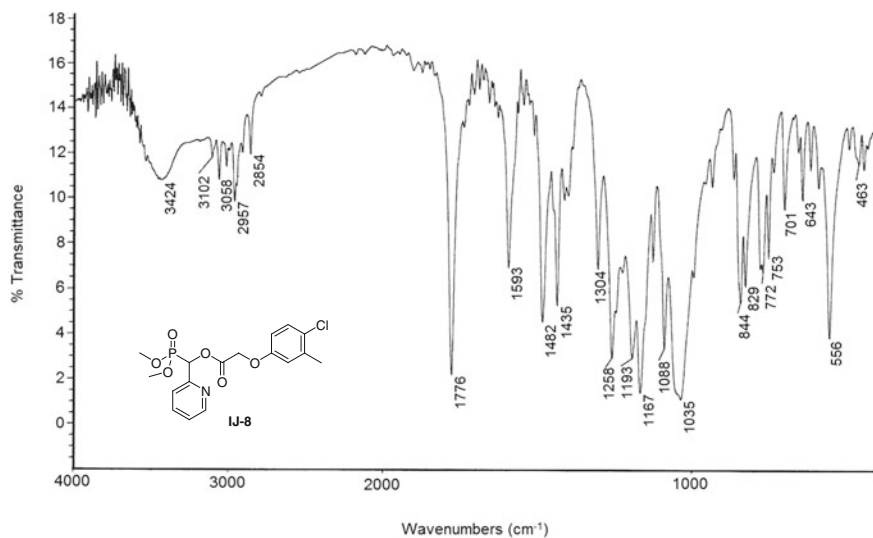
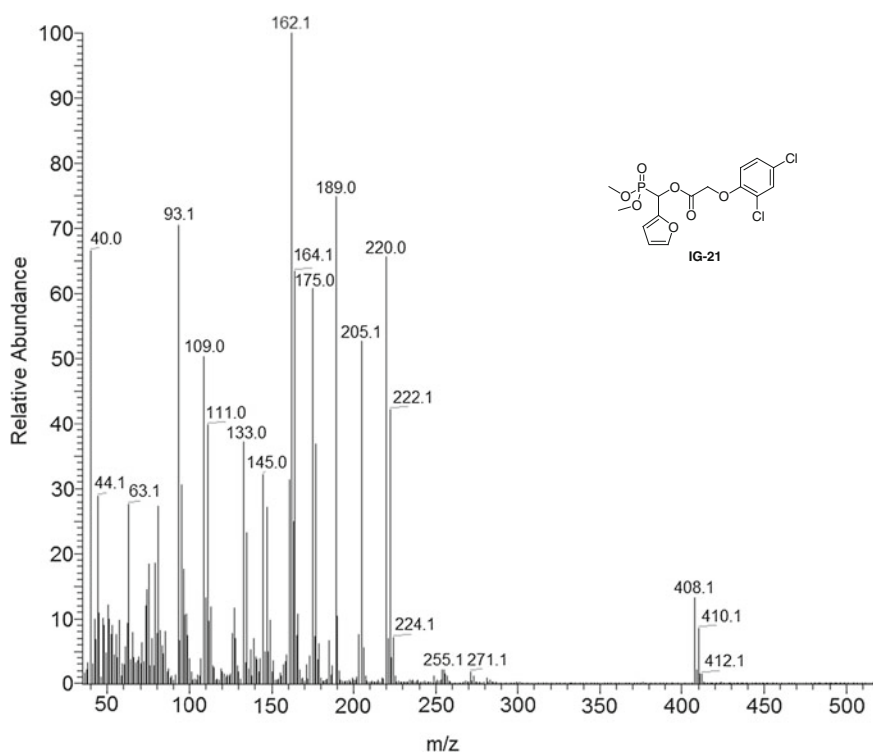
^a Synthesis of **IJ-1–IJ-14** [29]

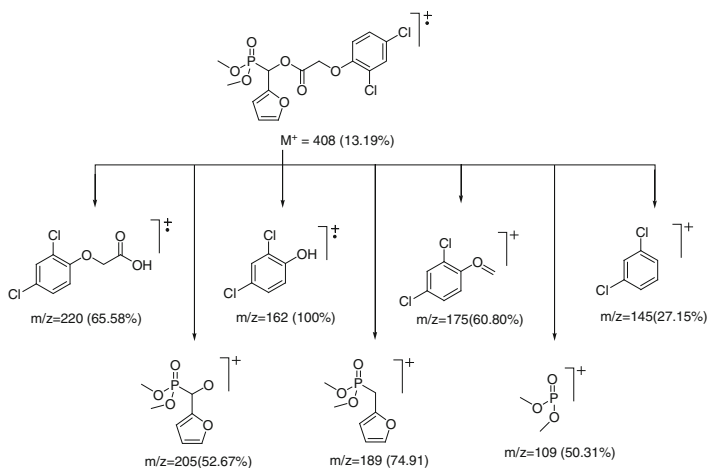
2.2.3 Spectroscopic Analysis of **IG–IJ**

All main functional groups in **IG–IJ** were characterized by IR which showed normal stretching absorption bands indicating the existence of benzene ring (1,450–1,615 cm⁻¹), P–O–C (1,026–1,054 cm⁻¹), P–C (730–750 cm⁻¹), and C–O–C (1,149–1,200 cm⁻¹). A strong absorption near 1,750–1,770 cm⁻¹ was identified for the absorption C=O. A sharp and weak band at 3,040–3,100 cm⁻¹ accounted for the C–H stretching of the benzene ring. A strong peak at 1,250–1,260 cm⁻¹ accounted for P=O in phosphonates. The IR spectrum of **IJ-8** is shown in Fig. 2.8.

The EI mass spectra of most **IG–IJ** gave molecular ion peaks. The fragment ions of **IG–IJ** were consistent with the structure and could be assigned. The primary fragmentations of most compounds **IG–IJ** were associated with the cleavages of C–O bond.

The MS spectrum of **IG-21** is shown in Fig. 2.9. The fragmentation of **IG-21** is shown in Scheme 2.20.

Fig. 2.8 IR spectrum of **IJ-8**Fig. 2.9 EI-MS spectrum of **IG-21**



Scheme 2.20 Fragmentation of **IG-21**

In the ^1H NMR spectra of **IG-IJ**, it could be observed that both the proton signals in the P–C–H moiety and P–OMe moiety displayed as two doublets due to couplings to the phosphorus. In the ^1H NMR spectra of **IG-IJ**, the proton signals corresponding to the two methoxyl groups attached to phosphorus appeared as two doublets at δ 3.65–3.85. The difference in the chemical shift of two methyl hydrogens due to the low rate of environmental exchange was caused by the slow rotation of P–C bond, and the magnetic nucleus phosphorus made the signals of both methyls split into two doublets. It was also noticed that the signal of methyl protons (MeO) attached to phosphorus in **IG-7**, **IG-8**, **IG-16**, **IH-4**, and **IH-5** appeared as two doublets. For instance, the signals of both methyls (dd, 6H, $2 \times \text{OCH}_3$) in **IG-16**, **IH-13**, and **IJ-13** split into two doublets at δ 3.73 and 3.84; δ 3.70 and 3.80; δ 3.73 and 3.79, respectively, the difference in chemical shift of the two methyl groups was attributed to a stereogenic center of α -carbon in the molecule.

In most of the compounds with alkyl as R^3 , the signal corresponding to the methylene group (OCH_2CO) between the phenoxy and carbonyl group appeared as a singlet. Noticeably the signal corresponding to the methylene group (CH_2) in some **IG** and **IH** flanked by the phenoxy group and carbonyl group appeared as a quartet. In this case, outside lines were smaller in size, which belonged to the AB system with a difference in chemical shift between the two mutually coupled protons A and B, at δ 4.72 ± 0.08 and 4.73 ± 0.08 in **IG-7** and **IG-8**, at δ 4.94 ± 0.06 and 4.98 ± 0.06 in **IH-4**, respectively. In **IG-7**, the methylene protons (OCH_2CO) were observed at δ 4.67 and 4.71 ppm, respectively, but in the extreme case, when A and B had exactly the same chemical shift, the outside lines disappeared, and the inside lines merged into a singlet. It can be exemplified by **IG-10**,

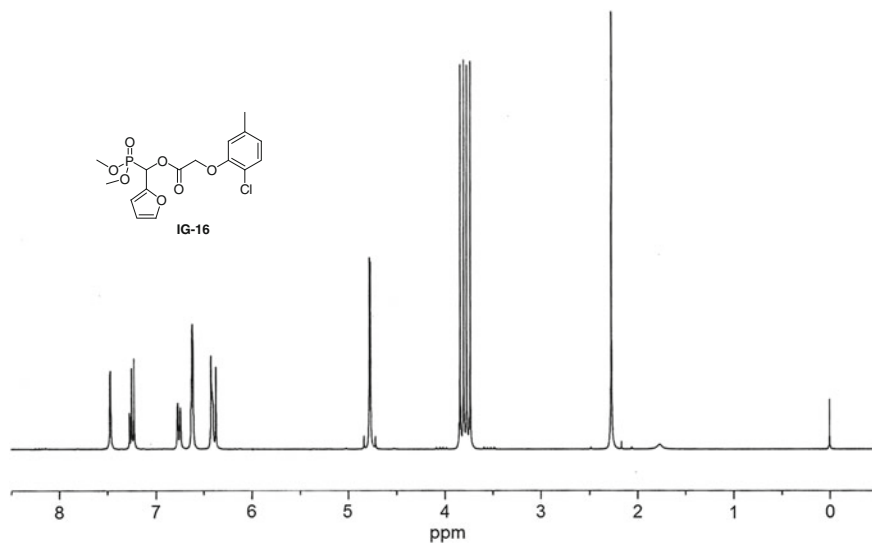


Fig. 2.10 ^1H NMR spectrum of **IG-16** (CDCl_3 , 300 MHz)

IG-16, **IG-22**, and **IH-4**. However, most of **IJ**, the signal of (OCH_2CO) between a phenoxy and carbonyl group appeared as a singlet. ^1H NMR spectra of **IG-16**, **IH-13** and **IJ-13** are shown in Figs. 2.10, 2.11 and 2.12, respectively.

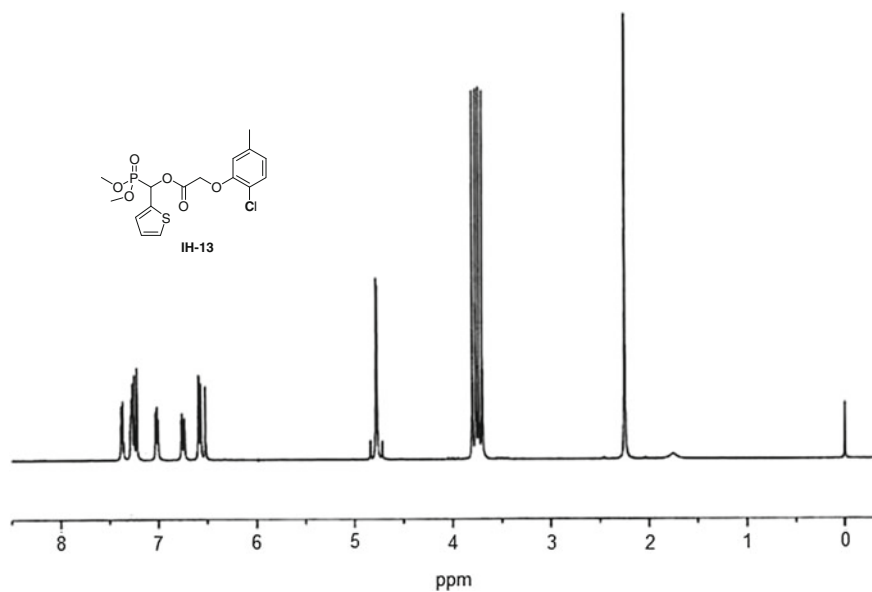


Fig. 2.11 ^1H NMR spectrum of **IH-13** (CDCl_3 , 300 MHz)

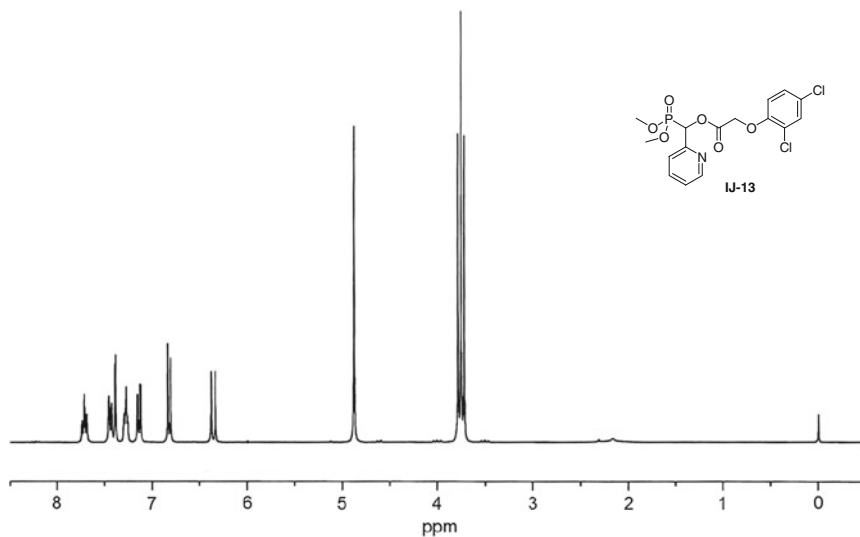


Fig. 2.12 ^1H NMR spectrum of **IJ-13** (CDCl_3 , 300 MHz)

2.2.4 Crystal Structure Analysis of **IH-18** and **IG-21**

2.2.4.1 Crystal Structure Analysis of **IH-18**

The molecular structure of **IH-18** is shown in Fig. 2.13. The packing diagram of the unit cell of **IH-18** is shown in Fig. 2.14. Selected bond lengths and angles are

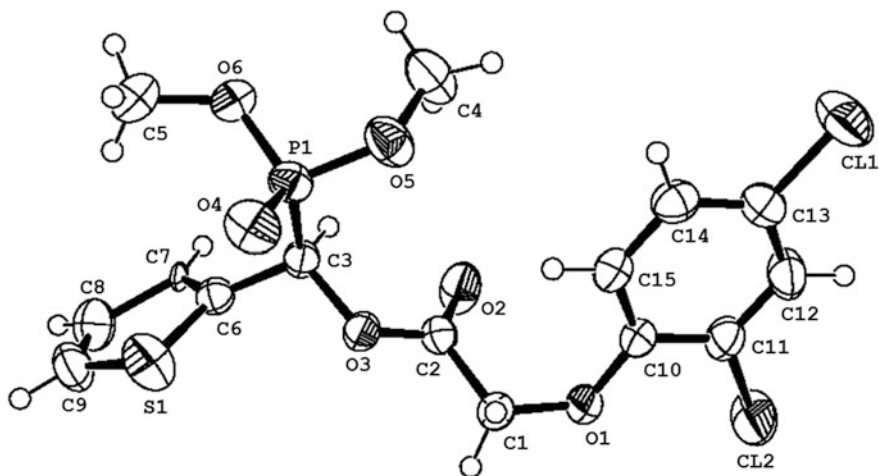


Fig. 2.13 Molecular structure of **IH-18**

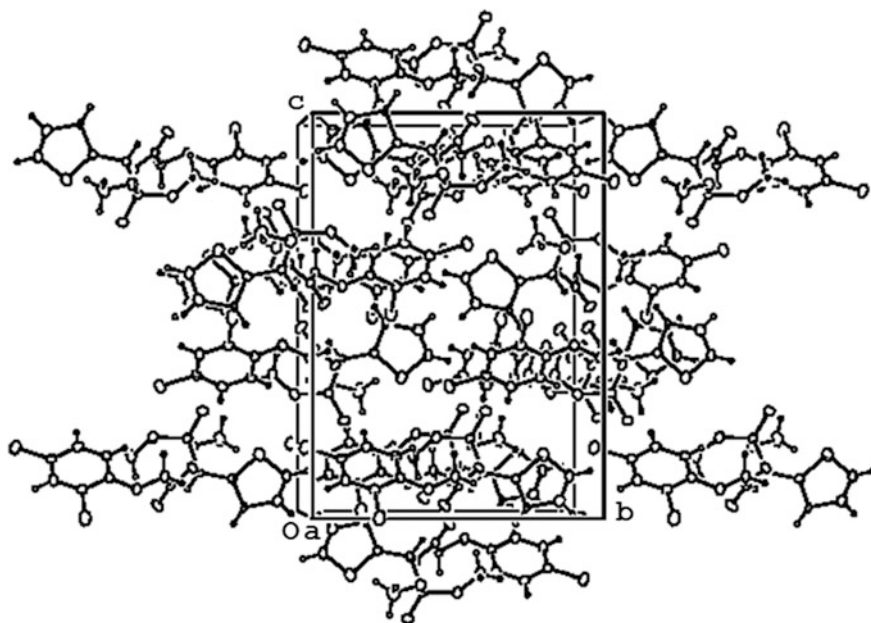


Fig. 2.14 Packing diagram of **IH-18**

presented in Table 2.37. As it can be seen from the X-ray single crystal structure of **IH-18**, all bond lengths and angles show normal values. The P(1)–O(4) bond length of 1.466(4) Å is significantly shorter than the P(1)–O(5) and P(1)–O(6) distances of 1.553(4) and 1.578(4) Å, respectively. O(4)–P(1)–O(5) and O(4)–P(1)–O(6) bond angles of **IH-18** are much larger than the O(5)–P(1)–O(6) bond angle, which indicates the phosphorus adopts a four-coordinate distorted-tetrahedral environment composed by three oxygen atoms and one carbon atom. The benzene and furan rings form a dihedral angle of 73.54°. The title molecule is mainly stabilized by van der Waals' force so that the construction of the single crystal is difficult.

IH-18 was recrystallized from trichloromethane and petroleum ether to give colorless crystals (0.10 mm × 0.25 mm × 0.30 mm) suitable for X-ray single-crystal

Table 2.37 Selected bond distance (Å) and angles (°) for **IH-18**

Bond	Dist.	Bond	Angles deg.
O(4)–P(1)	1.466(4)	C(6)–O(3)–C(3)	117.1(3)
O(5)–P(1)	1.553(4)	C(5)–O(6)–P(1)	121.6(4)
O(6)–C(5)	1.434(7)	O(4)–P(1)–O(5)	112.6(2)
O(6)–P(1)	1.578(4)	O(4)–P(1)–O(6)	116.2(2)
O(2)–C(6)	1.192(5)	O(5)–P(1)–O(6)	104.5(2)
P(1)–C(3)	1.821(4)	O(4)–P(1)–C(3)	113.6(2)

diffraction. The crystal structure of **IH-18** was recorded on a Smart Apex CCD diffractometer using graphite monochromated MoK α radiation ($\lambda = 0.071073$ nm). In the range of $2.32^\circ \leq \theta \leq 25.03^\circ$, 7,622 independent reflections ($R_{int} = 0.0282$), of which 3,294 contributing reflection had $I > 2\sigma(I)$, and all data were corrected using SADABS program. The structure was solved by direct methods using SHELXS-97; all other calculations were performed with Bruker SAINT system and Bruker SMART programs. All non-hydrogen atoms were refined on F^2 anisotropically using full-matrix least squares method. Hydrogen atoms were observed and refined with a fixed isotropic displacement parameter. Full-matrix least-squares refinement gave final values of $R = 0.0646$, $R_w = 0.1954$. The max and min difference between peaks and holes was 1,281 and -851 e nm $^{-3}$, respectively.

Crystallographic parameters of **IH-18**: $a = 0.8544(3)$, $b = 1.7536(5)$, $c = 1.2620(4)$ nm, $\alpha = 90.000$, $\beta = 98.963(5)$, $\gamma = 90.000(8)$, $V = 1.8678(9)$ nm 3 , $Mr = 425.22$, $Z = 7$, $D_c = 1.512$ mg/m 3 , $\mu = 0.573$ mm $^{-1}$, $F(000) = 872$. The summary of data collection statistics for the X-ray structure of **IH-18** was reported in literature [23].

2.2.4.2 Crystal Structure Analysis of IG-21

The molecular structure of **IG-21** is shown in Fig. 2.15. The packing diagram of the unit cell of **IG-21** is shown in Fig. 2.16. Hydrogen bonds are presented in Table 2.38. The crystal structure belongs to the monoclinic system with space group $P 2_1/c$, $a = 8.5380(7)$ Å, $b = 17.3111(14)$ Å, $c = 12.4003(10)$ Å, $\alpha = 90^\circ$, $\beta = 98.475(1)^\circ$, $\gamma = 90^\circ$, $V = 1812.8(3)$ Å 3 , $Z = 4$, $D_c = 1.499$ mg/m 3 , $\mu = 0.48$ mm $^{-1}$, $F(000) = 840$. It can be seen from the crystal structure, **IG-21** forms a racemate crystal with monoclinic ($P 2_1/c$) symmetry. The benzene and furan rings are non-planar, and the dihedral angle between two rings is $73.54(1)^\circ$. In the crystal structure, weak intermolecular C–H...O hydrogen bonds (Table 2.38) link the

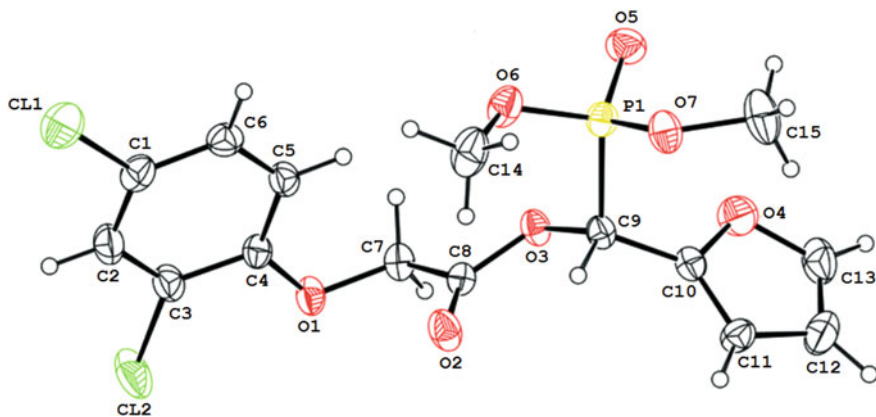


Fig. 2.15 Molecular structure of **IG-21**

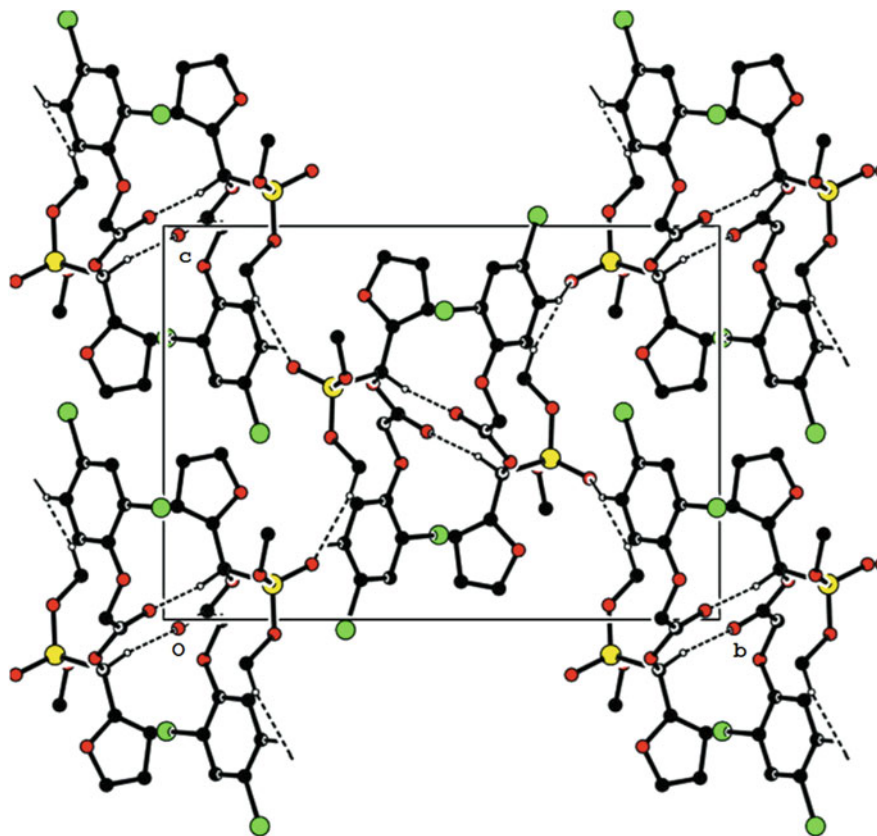


Fig. 2.16 Packing diagram of **IG-21**

Table 2.38 Hydrogen bonds of **IG-21**

<i>D</i> –H... <i>A</i>	<i>D</i> –H	H... <i>A</i>	<i>D</i> ... <i>A</i>	<i>D</i> –H... <i>A</i>
C(6)–H(6)...O(5) ^a	0.93	2.50	3.322(3)	148
C(9)–H(9)...O(2) ^b	0.98	2.35	3.270(2)	157
O(14)–H(14B)...O(5) ^a	0.96	2.44	3.379(3)	165

Symmetry code: ^a $x, -y + 1/2, z - 1/2$; ^b $-x + 2, -y + 1, -z + 1$

molecules into layers parallel to the (100) plane. Weak C–H... π interaction (C15... $Cg1 = 3.690(3)$ Å, C15–H15... $Cg1 = 137^\circ$, $Cg1$ is the centroid defined by atoms O4/C10–C13) is also observed in the crystal structure.

IG-21 was recrystallized from ethyl acetate to give colorless crystals (0.30 mm \times 0.20 mm \times 0.20 mm) suitable for X-ray single-crystal diffraction. The crystal structure of **IG-21** was recorded on a Smart Apex CCD diffractometer using graphite monochromated MoK α radiation ($\lambda = 0.071073$ nm). In the range of

$2.4^\circ \leq \theta \leq 28.2^\circ$, 4,135 independent reflections ($R_{\text{int}} = 0.048$), of which 3,158 contributing reflection had $I > 2\sigma(I)$, and all data were corrected using SADABS program. The structure was solved by direct methods using SHELXS-97, all other calculations were performed with Bruker SAINT system and Bruker SMART programs. All non-hydrogen atoms were refined on F^2 anisotropically using full-matrix least squares method. Hydrogen atoms were observed and refined with a fixed isotropic displacement parameter. Full-matrix least-squares refinement gave final values of $R = 0.049$, $R_w = 0.133$. The summary of data collection statistics for the X-ray structure of **IG-21** was reported in Ref. [30].

2.2.5 Herbicidal Activity of IG-IJ

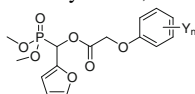
The herbicidal activities of heterocyclymethylphosphonates **IG-IJ** including **IC-22** were evaluated at a different rate in a set of experiments in the greenhouse. These compounds were first tested at 1.5 kg ai/ha for pre- and post-emergence activity against a range of weed species including rape (*Brassica campestris*), common amaranth (*Amaranthus retroflexus*), clover (*Medicago sativa*), barnyard grass (*Echinochloa Crusgalli*), and crab grass (*Digitaria Sanguinalis*). Post-emergence activity against rape (*Brassica campestris*), chingma abutilon (*Abutilon theophrasti*), common amaranth (*Amaranthus retroflexus*), white eclipta (*Eclipta prostrata*) and giant foxtail (*Setaria faberi*) was further evaluated at 450 or 150 g ai/ha in the greenhouse. The results are listed in Tables 2.39, 2.40, 2.41, 2.42, 2.43, 2.44, 2.45, 2.46 and 2.47. The herbicidal activity of **IG-IJ** including **IC-22** are reviewed as follows.

2.2.5.1 Herbicidal Activity of *O,O*-Dimethyl 1-(Substituted Phenoxyacetoxy)-1-(Fur-2-yl)methylphosphonates **IG**

Twenty-three of **IG** were prepared to test their herbicidal activity. The data of herbicidal activity of **IG** are listed in Tables 2.39, 2.40 and 2.41.

Table 2.39 Structure and pre-emergence herbicidal activity of *O,O*-dimethyl 1-(substituted

phenoxyacetoxy)-1-(fur-2-yl)methylphosphonates **IG**^a



Compound	Y _n	Pre-emergence				
		Dicotyledon			Monocotyledon	
		Bra ^b	Amr ^b	Med ^b	Ech ^b	Dig ^b
IG-4	3-CF ₃	D	D	D	D	D
IG-6	2-F	D	D	D	D	D
IG-7	3-F	C	D	D	D	D

(continued)

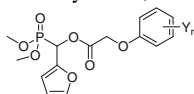
Table 2.39 (continued)

Compound	Y _n	Pre-emergence				
		Dicotyledon			Monocotyledon	
		Bra ^b	Amr ^b	Med ^b	Ech ^b	Dig ^b
IG-8	4-F	B	B	C	D	A
IG-10	4-Cl	A	B	B	B	A
IG-14	2-Me,4-Cl	D	D	C	D	C
IG-15	3-Me,4-Cl	A	C	B	B	B
IG-16	2-Cl,5-Me	D	D	D	D	D
IG-19	2-Cl,4-F	A	A	A	A	A
IG-20	2,3-Cl ₂	D	D	D	D	D
IG-21	2,4-Cl ₂	A	B	A	A	A
IG-22	2,6-Cl ₂	D	D	D	D	D
2,4-D		A	A	A	B	A

^a Inhibitory potency (%) against the growth of plants at a rate of 1.5 kg ai/ha in the greenhouse was expressed as four scales—A: 90–100 %, B: 75–89 %, C: 50–74 %, D: <50 %

^b Bra: rape; Amr: common amaranth; Med: clover; Ech: barnyard grass; Dig: crab grass

Table 2.40 Structure and post-emergence herbicidal activity of *O,O*-dimethyl 1-(substituted phenoxyacetoxy)-1-(fur-2-yl)methylphosphonates **IG^a**



Compound	Y _n	Post-emergence				
		Dicotyledon			Monocotyledon	
		Bra ^b	Amr ^b	Med ^b	Ech ^b	Dig ^b
IG-4	3-CF ₃	D	D	D	D	D
IG-6	2-F	D	D	D	D	D
IG-7	3-F	D	D	D	D	D
IG-8	4-F	D	C	C	D	C
IG-10	4-Cl	C	C	C	C	C
IG-14	2-Me,4-Cl	C	C	D	D	C
IG-15	3-Me,4-Cl	C	C	C	D	C
IG-16	2-Cl,5-Me	B	D	D	D	D
IG-19	2-Cl,4-F	A	A	A	C	B
IG-20	2,3-Cl ₂	D	D	D	D	D
IG-21	2,4-Cl ₂	A	A	A	D	C
IG-22	2,6-Cl ₂	D	D	D	D	D
2,4-D		A	A	A	C	C

^a Inhibitory potency (%) against the growth of plants at a rate of 1.5 kg ai/ha in the greenhouse was expressed as four scales—A: 90–100 %, B: 75–89 %, C: 50–74 %, D: <50 %

^b Bra: rape; Amr: common amaranth; Med: clover; Ech: barnyard grass; Dig: crab grass

(A) *Pre-emergence herbicidal activity of IG*

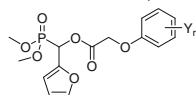
The data in Table 2.39 showed that **IG-19** ($Y_n = 2\text{-Cl}, 4\text{-F}$) and **IG-21** ($Y_n = 2, 4\text{-Cl}_2$) exhibited significant herbicidal activity against dicotyledons and monocotyledons for pre-emergence application comparable to 2,4-D at 1.5 kg ai/ha followed by **IG-10** ($Y_n = 4\text{-Cl}$) and **IG-15** ($Y_n = 3\text{-Me}, 4\text{-Cl}$). However all other compounds showed weak or no herbicidal activity against dicotyledons and monocotyledons for pre-emergence application at 1.5 kg ai/ha.

(B) *Post-emergence herbicidal activity of IG*

The data in Table 2.40 showed that only **IG-19** ($Y_n = 2\text{-Cl}, 4\text{-F}$) and **IG-21** ($Y_n = 2, 4\text{-Cl}_2$) exhibited significant herbicidal activity against dicotyledons for post-emergence application comparable to 2,4-D at 1.5 kg ai/ha. All tested **IG** had no significant herbicidal activity against monocotyledons for post-emergence application.

On the basis of the preliminary bioassay, post-emergence herbicidal activity of most **IG** was further examined at 150 g ai/ha in the greenhouse. The results of post-emergence herbicidal activity against rape, chingma abutilon, common amaranth, and white eclipta are listed in Table 2.41.

Table 2.41 Structure and post-emergence herbicidal activities of *O,O*-dimethyl 1-(substituted phenoxyacetoxy)-1-(fur-2-yl)methylphosphonates **IG**^a



Compound	Y_n	Post-emergence			
		Bra ^b	Abu ^b	Amr ^b	Ecl ^b
IG-1	H	28	22	6	31
IG-2	3-Me	37	39	36	30
IG-3	4-Me	36	32	23	30
IG-4	3-CF ₃	0	0	0	0
IG-5	4-CF ₃	0	0	0	0
IG-6	2-F	75	40	60	60
IG-9	2-Cl	40	0	40	30
IG-10	4-Cl	75	75	70	70
IG-11	4-Br	75	40	60	60
IG-12	4-CN	40	40	50	30
IG-13	2,3-Me ₂	40	50	50	30
IG-14	2-Me,4-Cl	85	80	80	60
IG-15	3-Me,4-Cl	80	80	80	75
IG-17	2,4-F ₂	60	40	50	40
IG-18	2-F,4-Cl	75	70	60	70
IG-19	2-Cl,4-F	85	75	90	75
IG-20	2,3-Cl ₂	30	20	25	35

(continued)

Table 2.41 (continued)

Compound	Y _n	Post-emergence			
		Bra ^b	Abu ^b	Amr ^b	Ecl ^b
IG-21	2,4-Cl ₂	95	95	95	90
IG-23	2,4,5-Cl ₃	85	75	75	80
IC-22 (Clacyfos)	2,4-Cl ₂	92	95	91	90
2,4-D		93	93	92	90

^a Inhibitory potency (%) against the plant growth at a rate of 150 g ai/ha in the greenhouse, 0 (no effect), 100 % (completely kill)

^b Bra: rape; Abu: chingma abutilon; Amr: common amaranth; Ecl: white eclipia

It was found that **IG-21** exhibited the best inhibition followed by **IG-19** at 150 g ai/ha. **IG-21** exhibited herbicidal activity comparable to **IC-22** and 2,4-D. **IG-10** (Y_n = 4-Cl), **IG-14** (Y_n = 2-Me,4-Cl), **IG-15** (Y_n = 3-Me,4-Cl), **IG-18** (Y_n = 2-F,4-Cl) and **IG-23** (Y_n = 2,4,5-Cl₃) had medium activity against tested dicotyledons with 60–85 % inhibition. However, other compounds had weak herbicidal activities or were almost inactive at 150 g ai/ha.

(C) SAR analyses for **IG**

IG-21 (Y_n = 2,4-Cl₂) exhibited the best herbicidal activity against dicotyledons for post-emergence application at 150 g ai/ha followed by **IG-19** (Y_n = 2-Cl,4-F).

Compounds **IG** with 2,4,5-Cl₃; 2-Me,4-Cl; 3-Me,4-Cl; 4-Cl and 2-F,4-Cl as Y_n showed modest herbicidal activity. However, **IG** with other groups as Y_n or no substituent on the phenoxy-benzene ring had weak herbicidal activity or almost inactive. Especially, **IG** with 3-CF₃ or 4-CF₃ as Y_n completely lost activity.

The results of SAR analysis for **IG** were similar to those for **IC-IF**, i.e., substituents Y_n on the phenoxy-benzene ring greatly affected the herbicidal activity, and 2- and 4-positions in the phenoxy-benzene ring were the most essential. It showed that the fur-2-yl group was beneficial to herbicidal activity when the compound had Y_n as 2,4-Cl₂ in structure **IG**.

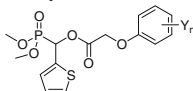
2.2.5.2 Herbicidal Activity of *O,O*-Dimethyl 1-(Substituted Phenoxyacetoxy)-1-(Thien-2-yl)methylphosphonates **IH**

Twenty of **IH** were prepared to test their herbicidal activity. The data of herbicidal activity of **IH** are listed in Tables 2.42, 2.43, 2.44 and 2.45.

(A) Pre-emergence herbicidal activity of **IH**

The data in Table 2.42 showed that **IH-7** (Y_n = 4-Cl), **IH-11** (Y_n = 2-Me,4-Cl), **IH-16** (Y_n = 2-Cl,4-F) and **IH-18** (Y_n = 2,4-Cl₂) exhibited significant herbicidal activities against dicotyledons and monocotyledons for pre-emergence application comparable to 2,4-D followed by **IH-9** (Y_n = 4-CN) and **IH-12** (Y_n = 3-Me,4-Cl)

Table 2.42 Structure and pre-emergence herbicidal activity of *O,O*-dimethyl 1-(substituted phenoxyacetoxy)-1-(thien-2-yl)methylphosphonates **IH^a**

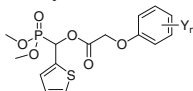


		Dicotyledon			Monocotyledon	
		Bra ^b	Amr ^b	Med ^b	Ech ^b	Dig ^b
IH-1	3-CF ₃	C	B	C	D	B
IH-2	4-CF ₃	D	D	D	D	B
IH-3	2-F	D	D	D	D	D
IH-4	3-F	D	D	D	A	D
IH-5	4-F	B	C	C	C	A
IH-6	2-Cl	D	D	C	D	D
IH-7	4-Cl	A	A	A	B	A
IH-8	4-Br	D	D	D	D	D
IH-9	4-CN	A	A	A	D	D
IH-10	2,3-Me ₂	D	D	D	D	D
IH-11	2-Me,4-Cl	A	A	A	A	A
IH-12	3-Me,4-Cl	B	B	A	C	B
IH-13	2-Cl,5-Me	D	D	D	D	D
IH-16	2-Cl,4-F	A	A	A	A	A
IH-17	2,3-Cl ₂	D	D	D	D	D
IH-18	2,4-Cl ₂	A	A	A	A	A
IH-19	2,6-Cl ₂	D	D	D	D	D
2,4-D		A	A	A	B	A

^a Inhibitory potency (%) against the growth of plants at a rate of 1.5 kg ai/ha in the greenhouse was expressed as four scales—A: 90–100 %, B: 75–89 %, C: 50–74 %, D: <50 %

^b Bra: rape; Amr: common amaranth; Med: clover; Ech: barnyard grass; Dig: crab grass

Table 2.43 Structure and post-emergence herbicidal activity of *O,O*-dimethyl 1-(substituted phenoxyacetoxy)-1-(thien-2-yl)methylphosphonates **IH^a**



Compound	Y _n	Post-emergence				
		Dicotyledon			Monocotyledon	
		Bra ^b	Amr ^b	Med ^b	Ech ^b	Dig ^b
IH-1	3-CF ₃	B	C	B	D	C
IH-2	4-CF ₃	D	D	D	D	C
IH-3	2-F	D	D	D	D	D
IH-4	3-F	D	D	D	D	D
IH-5	4-F	A	A	C	D	D
IH-6	2-Cl	C	C	D	D	D
IH-7	4-Cl	A	A	A	D	C

(continued)

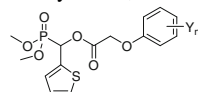
Table 2.43 (continued)

Compound	Y _n	Post-emergence				
		Dicotyledon			Monocotyledon	
		Bra ^b	Amr ^b	Med ^b	Ech ^b	Dig ^b
IH-8	4-Br	B	D	D	D	D
IH-9	4-CN	A	A	A	D	D
IH-10	2,3-Me ₂	D	D	D	D	C
IH-11	2-Me,4-Cl	A	A	A	C	D
IH-12	3-Me,4-Cl	C	C	D	D	D
IH-13	2-Cl,5-Me	D	D	D	D	C
IH-16	2-Cl,4-F	A	A	A	D	C
IH-17	2,3-Cl ₂	D	D	D	D	D
IH-18	2,4-Cl ₂	A	A	A	C	C
IH-19	2,6-Cl ₂	D	D	D	D	D
IH-20	2,4,5-Cl ₃	A	A	A	C	C
2,4-D		A	A	A	C	C

^a Inhibitory potency (%) against the growth of plants at a rate of 1.5 kg ai/ha in the greenhouse was expressed as four scales—A: 90–100 %, B: 75–89 %, C: 50–74 %, D: <50 %

^b Bra: rape; Amr: common amaranth; Med: clover; Ech: barnyard grass; Dig: crab grass

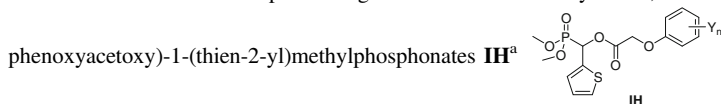
Table 2.44 Structure and post-emergence herbicidal activity of *O,O*-dimethyl 1-(substituted phenoxyacetoxy)-1-(thien-2-yl)methylphosphonates **IH^a**



Compound	Y _n	Rate (g ai/ha)	Post-emergence			
			Bra ^b	Abu ^b	Amr ^b	Ecl ^b
IH-6	2-Cl	450	30	40	50	60
IH-7	4-Cl	450	90	85	80	85
IH-8	4-Br	450	75	70	60	70
IH-9	4-CN	450	40	40	40	30
IH-10	2,3-Me ₂	450	0	0	40	0
IH-11	2-Me,4-Cl	450	95	90	100	85
IH-12	3-Me,4-Cl	450	60	60	60	70
IH-14	2,4-F ₂	450	80	75	70	60
IH-15	2-F,4-Cl	450	75	75	75	70
IH-16	2-Cl,4-F	450	95	90	100	90
IH-17	2,3-Cl ₂	450	40	40	60	50
IH-18	2,4-Cl ₂	450	100	100	100	100
IH-20	2,4,5-Cl ₃	450	95	85	90	85
IC-22 (Clacyfos)		450	100	100	100	100

^a Inhibitory potency (%) against the plant growth in the greenhouse, 0 (no effect), 100 % (completely kill)

^b Bra: rape; Abu: chingma abutilon; Amr: common amaranth; Ecl: white eclipia

Table 2.45 Structure and post-emergence herbicidal activity of *O,O*-dimethyl 1-(substituted

Compound	Y _n	Post-emergence			
		Bra ^b	Abu ^b	Amr ^b	Ecl ^b
IH-1	3-CF ₃	30	20	20	15
IH-2	4-CF ₃	20	15	20	30
IH-6	2-Cl	0	0	0	0
IH-7	4-Cl	70	70	70	70
IH-8	4-Br	70	50	50	60
IH-9	4-CN	30	30	40	0
IH-10	2,3-Me ₂	0	0	40	0
IH-11	2-Me,4-Cl	80	60	80	75
IH-12	3-Me,4-Cl	0	0	50	50
IH-14	2,4-F ₂	70	60	60	60
IH-15	2-F,4-Cl	70	70	70	70
IH-16	2-Cl,4-F	75	71	90	80
IH-17	2,3-Cl ₂	0	0	40	40
IH-18	2,4-Cl ₂	90	90	90	90
IH-20	2,4,5-Cl ₃	80	80	80	80
2,4-D		93	93	92	90
IC-22 (Clacyfos)		92	95	91	90

^a Inhibitory potency (%) against the plant growth at a rate of 150 g ai/ha in the greenhouse, 0 (no effect), 100 % (completely kill)

^b Bra: rape; Abu: chingma abutilon; Amr: common amaranth; Ecl: white eclipta

which only had herbicidal activity against dicotyledons for pre-emergence application at 1.5 kg ai/ha. **IH-11**, **IH-16**, and **IH-18** showed better pre-emergence herbicidal activity against barnyard grass than that of 2,4-D at 1.5 kg ai/ha. All other compounds showed weak or no herbicidal activity against dicotyledons and monocotyledons for pre-emergence application at 1.5 kg ai/ha.

(B) Post-emergence herbicidal activity of **IH**

The data in Table 2.43 showed that **IH-7** (Y_n = 4-Cl), **IH-11** (Y_n = 2-Me,4-Cl), **IH-16** (Y_n = 2-Cl,4-F), **IH-18** (Y_n = 2,4-Cl₂) and **IH-20** (Y_n = 2,4,6-Cl₃) exhibited significant herbicidal activity against dicotyledons for post-emergence application comparable to 2,4-D. All tested **IH** had no significant post-emergence herbicidal activity against monocotyledons at 1.5 kg ai/ha.

On the basis of preliminary bioassay, post-emergence herbicidal activity of most **IH** was further examined at 450 and 150 g ai/ha in the greenhouse. The results of post-emergence herbicidal activity against rape, chingma abutilon, common amaranth, and white eclipta are listed in Tables 2.44 and 2.45. The data in

Table 2.44 show that **IH-7**, **IH-11**, **IH-16**, **IH-18**, and **IH-20** still exhibited significant herbicidal activity against dicotyledons for post-emergence application at 450 g ai/ha.

Only **IH-16**, **IH-18**, and **IH-20** showed >70 % inhibition against dicotyledons for post-emergence at 150 g ai/ha (Table 2.45). **IH-18** had the best herbicidal activity at 150 g ai/ha comparable to **IC-22** and 2,4-D.

(C) SAR analyses for **IH**

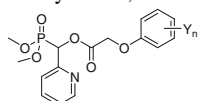
Like the results of SAR analyses for **IG**, substituents Y_n on the benzene ring of the phenoxy moiety greatly affected the activity as well. **IH-18** ($Y_n = 2,4\text{-Cl}_2$) exhibited the best herbicidal activity against dicotyledons for post-emergence at 150 g ai/ha followed by **IH-16** ($Y_n = 2,4,5\text{-Cl}_3$) and **IH-20** ($Y_n = 2\text{-Cl},4\text{-F}$). Compounds **IH** with 3-CF₃; 4-CF₃; 2-Cl,4-CN; 2,3-Me₂; 3-Me,4-Cl and 2,3-Cl₂ as Y_n had only 0–50 % inhibition against tested dicotyledons at 150 g ai/ha. It showed that 2,4-Cl₂ as Y_n was most beneficial to post-emergence herbicidal activity, and the thienyl group was also beneficial to herbicidal activity when the compounds had Y_n as 2,4-Cl₂ in the structure **IH**.

2.2.5.3 Herbicidal Activity of *O,O*-Dimethyl 1-(Substituted Phenoxyacetoxy)-1-(Pyrid-2-yl)methylphosphonates **IJ** in Greenhouse

It was also very interesting to examine the effect on herbicidal activity by the introduction of pyridyl group as R^3 into the structure **IC** to form a new series of **IJ**. In the series of **IJ**, further modification was only focused on substituents Y_n . The data of herbicidal activity of some **IJ** are listed in Tables 2.46 and 2.47.

Table 2.46 Structure and pre-emergence herbicidal activity of *O,O*-dimethyl 1-(substituted

phenoxyacetoxy)-1-(pyrid-2-yl)methylphosphonates **IJ**^a



Compound	Y_n	Pre-emergence					
		Dicotyledon			Monocotyledon		
		Bra ^b	Amr ^b	Med ^b	Ech ^b	Dig ^b	Sef ^b
IJ-1	3-CF ₃	B	C	C	C	C	C
IJ-3	2-F	B	C	B	A	D	A
IJ-5	4-F	A	A	A	B	B	B
IJ-6	4-Cl	A	C	A	C	C	C
IJ-8	3-Me,4-Cl	A	D	B	C	C	C
IJ-9	2-Cl,5-Me	D	D	D	C	D	D
IJ-10	2,4-F ₂	D	D	D	D	D	D
IJ-12	2,3-Cl ₂	D	D	D	D	D	D

(continued)

Table 2.46 (continued)

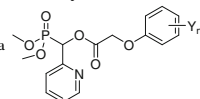
Compound	Y _n	Pre-emergence					
		Dicotyledon			Monocotyledon		
		Bra ^b	Amr ^b	Med ^b	Ech ^b	Dig ^b	Sef ^b
IJ-13	2,4-Cl ₂	A	B	B	C	B	B
IJ-14	2,6-Cl ₂	D	D	D	D	D	D
2,4-D		A	A	A	C	C	C

^a Inhibitory potency (%) against the growth of plants at a rate of 900 g ai/ha in the greenhouse was expressed as four scales—A: 90–100 %, B: 75–89 %, C: 50–74 %, D: <50 %

^b Bra: rape; Amr: common amaranth; Med: clover; Ech: barnyard grass; Dig: crab grass; Sef: giant foxtail

Table 2.47 Structure and post-emergence herbicidal activity of *O,O*-dimethyl 1-(substituted

phenoxyacetoxy)-1-(pyrid-2-yl)methylphosphonates **IJ**^a



Compound	Y _n	Post-emergence					
		Dicotyledon			Monocotyledon		
		Bra ^b	Amr ^b	Med ^b	Ech ^b	Dig ^b	Sef ^b
IJ-1	3-CF ₃	C	C	C	C	C	B
IJ-3	2-F	A	A	B	B	B	B
IJ-5	4-F	C	C	B	B	B	C
IJ-6	4-Cl	D	D	D	D	D	D
IJ-8	3-Me,4-Cl	C	C	C	D	D	D
IJ-9	2-Cl,5-Me	D	D	D	D	D	D
IJ-10	2,4-F ₂	D	D	D	D	D	D
IJ-12	2,3-Cl ₂	D	D	D	D	D	D
IJ-13	2,4-Cl ₂	A	B	B	C	B	B
IJ-14	2,6-Cl ₂	D	D	D	D	D	D
2,4-D		A	A	A	B	A	C

^a Inhibitory potency (%) against the growth of plants at a rate of 900 g ai/ha in the greenhouse was expressed as four scales—A: 90–100 %, B: 75–89 %, C: 50–74 %, D: <50 %

^b Bra: rape; Amr: common amaranth; Med: clover; Ech: barnyard grass; Dig: crab grass; Sef: giant foxtail

(A) Pre-emergence herbicidal activity of **IJ**

The data in Table 2.46 showed that **IJ-5** (Y_n = 4-F) exhibited pre-emergence activity against dicotyledons comparable to 2,4-D, and better pre-emergence activity against monocotyledons than that of 2,4-D at 900 g ai/ha. **IJ-3** (Y_n = 2-F) and **IJ-13** (Y_n = 2,4-Cl₂) also exhibited better pre-emergence activity against monocotyledons than that of 2,4-D, but weaker pre-emergence activity against dicotyledons than that of 2,4-D. All other compounds showed weak or no herbicidal activity against dicotyledons and monocotyledons for pre-emergence application at 900 g ai/ha.

(B) Post-emergence herbicidal activity of IJ

The data in Table 2.47 showed that **IJ-3** ($Y_n = 2\text{-F}$) and **IJ-13** ($Y_n = 2,4\text{-Cl}_2$) exhibited post-emergence herbicidal activity against dicotyledons and monocotyledons at 900 g ai/ha, but a little weaker than that of 2,4-D. Other tested **IJ** had no significant herbicidal activity against dicotyledons and monocotyledons at 900 g ai/ha.

(C) SAR analyses for IJ

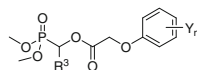
The introduction of apyridyl group as R^3 in **IC** resulted in a decrease in herbicidal activity against dicotyledons for pre-emergence and post-emergence applications even when 2,4- Cl_2 as Y_n . However, **IJ-5** ($Y_n = 4\text{-F}$) exhibited good pre-emergence herbicidal activity against dicotyledons comparable to 2,4-D. **IJ-3** ($Y_n = 2\text{-F}$), **IJ-5** ($Y_n = 4\text{-F}$) and **IJ-13** ($Y_n = 2,4\text{-Cl}_2$) showed better pre-emergence activity against monocotyledons than that of 2,4-D at 900 g ai/ha. These findings showed that **IJ** had a different SAR with **IG** and **IH**.

The results showed that pyridyl group as R^3 was beneficial to the pre-emergence herbicidal activity when 4-F as Y_n . Among the **IJ**, **IJ-5** exhibited the best pre-emergence herbicidal activity at 900 g ai/ha.

2.2.6 Structure-Herbicidal Activity Relationships

Structure-herbicidal activity relationships of **IG**, **IH**, and **IJ** can be summarized as follows: Similarly to the SAR analyses for **IA–IF**, herbicidal activity was highly dependent upon the structure and position of substituents Y_n in the phenoxyacetyl substructure and R^3 .

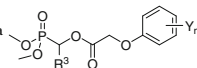
- (A) For post-emergence herbicidal activity: When fur-2-yl or thien-2-yl group as R^3 , 2,4- Cl_2 as Y_n were most beneficial to post-emergence herbicidal activity against dicotyledons, such as **IG-21** and **IH-13**. However when the pyrid-2-yl as R^3 , Compounds with 2-F as Y_n exhibited the best post-emergence herbicidal activity against dicotyledons, such as **IJ-3**, but it was not good as 2,4-D.
- (B) For pre-emergence herbicidal activity: When pyrid-2-yl group as R^3 compounds with 4-F as Y_n exhibited the best pre-emergence herbicidal activity against dicotyledons and monocotyledon, such as **IJ-5** was comparable to or better than 2,4-D at 900 g ai/ha. Whereas when fur-2-yl or thien-2-yl group as R^3 , compounds with 4-F as Y_n showed very weak or lower activity against dicotyledons and monocotyledon, such as **IG-8** and **IH-5**. However **IJ-13** with 2,4- Cl_2 as Y_n exhibited medium herbicidal activity for both pre- and post emergence application, it was not as good as 2,4-D.
- (C) Compounds with 2,3- Cl_2 or 2,6- Cl_2 as Y_n completely lost post-emergence herbicidal activity, irrespective of the fur-2-yl, thien-2-yl or pyrid-2-yl group as R^3 . Pre-emergence and post-emergence herbicidal activity of **IG-21**, **IH-13**,

Table 2.48 Pre-emergence herbicidal activity of **IG-21**, **IH-13**, and **IJ-13**^a

Compound	R ³	Y _n	Pre-emergence					
			Dicotyledon			Monocotyledon		
			Brj ^b	Amr ^b	Che ^b	Ech ^b	Dig ^b	Sef ^b
IG-21	Fur-2-yl	2,4-Cl ₂	60	60	10	0	50	0
IH-13	Thien-2-yl	2,4-Cl ₂	50	50	40	0	50	0
IJ-13	Pyrid-2-yl	2,4-Cl ₂	50	50	40	10	40	0
IC-22 (Clacyfos)	Me	2,4-Cl ₂	70	70	70	0	10	0

^a Inhibitory potency (%) against the growth of plants at a rate of 300 g ai/ha in the greenhouse, 0 (no effect), 100 % (completely kill)

^b Brj: leaf mustard; Amr: common amaranth; Che: goosefoot; Ech: barnyard grass; Dig: crab grass; Sef: giant foxtail

Table 2.49 Post-emergence herbicidal activity of **IG-21**, **IH-13**, and **IJ-13**^a

Compound	R ³	Y _n	Post-emergence					
			Dicotyledon			Monocotyledon		
			Brj ^b	Amr ^b	Che ^b	Ech ^b	Dig ^b	Sef ^b
IG-21	Fur-2-yl	2,4-Cl ₂	100	100	95	40	70	10
IH-13	Thien-2-yl	2,4-Cl ₂	100	100	80	50	50	0
IJ-13	Pyrid-2-yl	2,4-Cl ₂	100	100	85	20	30	0
IC-22 (Clacyfos)	Me	2,4-Cl ₂	100	100	95	20	50	10

^a Inhibitory potency (%) against the growth of plants at a rate of 300 g ai/ha in the greenhouse, 0 (no effect), 100 % (completely kill)

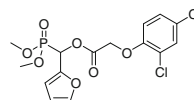
^b Brj: leaf mustard; Amr: common amaranth; Che: goosefoot; Ech: barnyard grass; Dig: crab grass; Sef: giant foxtail

IJ-13, and **IC-22** were further compared at 300 g ai/ha. The results of herbicidal activity against leaf mustard, common amaranth, goosefoot, barnyard grass, crab grass, and giant foxtail are listed in Tables 2.48 and 2.49.

As shown in Tables 2.48 and 2.49, **IG-21** exhibited notable post-emergence herbicidal activity comparable to **IC-22**. Its herbicidal activity seems better than that of **IH-13** and **IJ-13**. Both **IC-22** and **IG-21** would be promising for further development as post-emergence herbicides, and **IG-21** also displayed modest pre-emergence herbicidal activity against dicotyledons.

2.2.7 Herbicidal Activity of **IG-21**

The herbicidal activity and crop selectivity of **IG-21** (code number for development: HWS) were further examined at 1,200–50 g ai/ha. **IG-21** was tested for post-emergence activity against a range of plant species including purslane (*Portulaca oleracea*), slender amaranth (*Amaranthus ascendens*), goosefoot (*Chenopodium album*), spiny amaranth (*Amaranthus spinosus*), sugarbeet (*Beta vulgaris*), maize (*Zea mays*) and rice (*Oryza sativa*). Results are shown in Table 2.50.

Table 2.50 Post-emergence herbicidal activity of **IG-21**^a

Rate (g ai/ha)	Por ^b	Ama ^b	Che ^b	Ams ^b	Bet ^b	Zea ^b	Ory ^b
50	70	100	80	60	80	NT	NT
100	83	100	90	90	80	NT	NT
200	85	100	100	98	98	0	NT
300	91	100	100	98	98	0	0
450	100	100	100	100	100	0	0
900	100	100	100	100	100	0	0
1,200	100	100	100	100	100	10	20

^a Inhibitory potency (%) against the growth of plants in the greenhouse, 0 (no effect), 100 % (completely kill), NT (not tested)

^b Por: purslane; Ama: slender amaranth; Che: goosefoot; Ams: spiny amaranth; Bet: sugarbeet; Zea: maize; Ory: rice

IG-21 exhibited excellent herbicidal activity against broadleaf weeds by post-emergence application. Dicotyledonous crop sugarbeet was susceptible to **IG-21** at 50 or >50 g ai/ha, whereas the monocot crops maize and rice displayed high tolerance to **IG-21** even at the rates of 900–1200 g ai/ha. **IG-21** was safe for maize and rice and was selected for development as a useful selective herbicide for broadleaf weed control in monocot crop fields. Post-emergence herbicidal activity of **IG-21** and **IC-22** was further examined against common amaranth (*Amaranthus retroflexus*), goosefoot (*Chenopodium album*), leaf mustard (*Brassica juncea*), and morning glory (*Ipomoea nil*) compared with 2,4-D and glyphosate at 75–18.75 g ai/ha. Results are shown in Table 2.51.

Table 2.51 Post-emergence herbicidal activity of **IG-21** and **IC-22**^a

Compound	Rate (g ai/ha)	Post-emergence			
		Amr ^b	Che ^b	Brj ^b	Ipo ^b
IG-21	75	95	85	100	100
	37.5	95	80	100	90
	18.75	80	70	100	85
IC-22	75	100	85	100	100
	37.5	100	80	100	100
	18.75	90	70	100	100
2,4-D	75	95	95	100	100
	37.5	90	80	100	100
	18.75	70	75	80	90
glyphosate	75	75	80	80	75
	37.5	60	70	75	60
	18.75	60	50	70	50

^a Inhibitory potency (%) against the growth of plants in the greenhouse, 0 (no effect), 100 % (completely kill)

^b Ama: common amaranth; Che:goosefoot; Bra: leaf mustard; Ipo: morning glory

The effects of **IG-21** and **IC-22** including 30 % HW02 (**IC-22**) EC compared with 2,4-D and glyphosate against leaf mustard and morning glory for post-emergence application at 75 g ai/ha in the greenhouse were shown in Figs. 2.17, 2.18, 2.19 and 2.20.



Fig. 2.17 Effect against leaf mustard for post-emergence application at 75 g ai/ha (after 1 day)



Fig. 2.18 Effect against leaf mustard for post-emergence application at 75 g ai/ha (after 7 days)



Fig. 2.19 Effect against leaf mustard for post-emergence application at 75 g ai/ha (after 20 days)



Fig. 2.20 Effect against morning glory for post-emergence application at 75 g ai/ha (after 20 days)

As shown in Table 2.51 and Figs. 2.17, 2.18, 2.19 and 2.20, both **IG-21** and **IC-22** exhibited good effects against broadleaf weeds by post-emergence application at 75–18.75 g ai/ha. Both **IG-21** and **IC-22** exhibited notable post-emergence herbicidal activity comparable to 2,4-D and glyphosate and they exhibited better effects against tested broadleaf weeds than that of glyphosate at 18.75 g ai/ha.

2.2.8 Summary

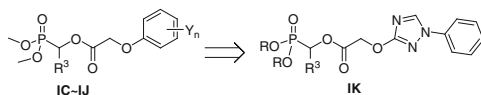
O,O-dialkyl 1-(substituted phenoxyacetoxy)-1-heterocyclylmethyl phosphonates **IG–IJ** including 57 compounds were synthesized by the condensation of *O,O*-dimethyl 1-hydroxy-1-heterocyclylmethylphosphonates **M2** and substituted phenoxyacetyl chlorides **M5** using a weak base.

The *O,O*-dimethyl heterocyclylmethylphosphonates **IG–IJ** with fur-2-yl or thien-2-yl group as R³ and 2,4-Cl₂ as Y_n as well as that with pyrid-2-yl group as R³ and 2-F or 4-F as Y_n were most beneficial to herbicidal activity. *O,O*-Dimethyl 1-(2,4-dichlorophenoxyacetoxy)-1-(fur-2-yl)methylphosphonate **IG-21** was found to be the most effective compound with excellent herbicidal activity against broadleaf weeds at 37.5 g ai/ha. **IG-21** showed a good selectivity and safe for monocotyledonous crops, such as maize and rice even at 0.9–1.2 kg ai/ha. **IG-21** is promising for development as a selective post-emergence herbicide.

2.3 (1-Phenyl-1,2,4-Triazol-3-yloxyacetoxy) Alkylphosphonates **IK**

2.3.1 Introduction

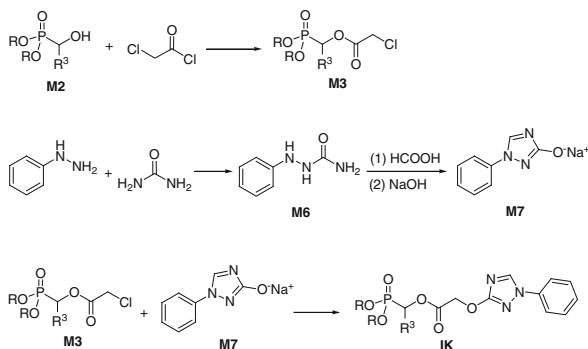
Compounds containing a triazole ring in the molecule are known to display diverse and useful biological properties [31, 32]. Some of them have been developed as fungicides, herbicides or plant growth regulators (PGRs) [33]. We were interested in the synthesis of a novel series of compounds which incorporated a triazole ring into the phenoxyacetoxy moiety in the molecule. A series of *O,O*-dialkyl 1-(1-phenyl-1,2,4-triazol-3-yloxyacetoxy)alkylphosphonates **IK** was thus prepared to examine biological effect by the introduction of a triazole ring into the phenoxyacetoxy moiety in **IC–IJ** (Scheme 2.21). In this section we describe the synthesis and the biological activity of **IK**.



Scheme 2.21 Design of 1-(1-phenyl-1,2,4-triazol-3-yloxyacetoxy)alkylphosphonates **IK**

2.3.2 Synthesis of **IK**

IK could be synthesized by the reaction of 1-(chloroacetoxy)alkylphosphonate **M3** with the sodium salt of 1-phenyl-3-hydroxy-1,2,4-triazole **M7** (Scheme 2.22).

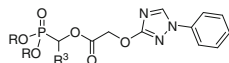


Scheme 2.22 Synthesis of 1-(1-phenyl-1,2,4-triazol-3-yloxyacetoxy)alkylphosphonates **IK**

As shown in Scheme 2.22, phenyl hydrazine reacted with urea to give phenylhydrazide **M6**. Condensation of **M6** with formic acid followed by addition of concentrated sulfuric acid gave 1-phenyl-3-hydroxy-1,2,4-triazole **M6** which was converted to the sodium salt of 1-phenyl-3-hydroxy-1,2,4-triazole **M7**. 1-(Chloroacetoxy)alkylphosphonates **M3** were prepared from *O,O*-dialkyl 1-hydroxyalkylphosphonate **M2** and chloroacetyl chloride in the presence of pyridine. **IK-1–IK-7** in Table 2.52 could be obtained by the reaction of **M7** with **M3** in acetonitrile using tetrabutylammonium bromide as a catalyst. The synthetic procedures of **M3** and **M7** are introduced in the Sects. 9.1.4 and 9.1.8, respectively.

The presence of catalytic tetrabutylammonium bromide was necessary for the reaction of sodium salt of 1-phenyl-3-hydroxy-1,2,4-triazole **M7** with 1-(chloroacetoxy)alkylphosphonates **M3** to get better yields. The experiment also showed that this reaction was affected by reaction temperature, base, and water. We observed that both the carboxylate ester bond and phosphonate ester bond in compounds **M3** or **IK** were easy to cleave by hydrolysis in the presence of base and water at a higher temperature. It was found that the carboxylate ester bond was easier to cleave than the phosphonate ester bond in diethyl phosphonate; however, the phosphonate ester bond was easier to cleave than the carboxylate ester bond in

Table 2.52 Structure of 1-(1-phenyl-1,2,4-triazol-3-yloxyacetoxy)alkylphosphonates **IK**^a



Compound	R	R ³	Compound	R	R ³
IK-1	Me	Ph	IK-5	Me	Et
IK-2	Me	3-NO ₂ Ph	IK-6	Me	<i>n</i> -Pr
IK-3	Me	2-ClPh	IK-7	Et	Ph
IK-4	Me	4-ClPh			

^a Synthesis of **IK-1–IK-7** [34]

dimethyl phosphonate under a harsh reaction condition. In this case the reaction of **M3** and **M7** was rationalized and carried out in dry acetonitrile at 40–50 °C using tetrabutylammonium bromide as a catalyst. Thus **IK-1–IK-7** could be obtained in 66–85 % yields.

The synthetic procedures of **IK-1–IK-7** are introduced in the Sect. 9.1.9. **IK-1–IK-7** were soluble in a variety of organic solvents such as CH₂Cl₂, CHCl₃, benzene, ethyl ether, acetonitrile, ethyl acetate, and so on. They were stable to light and air at room temperature but easy to decompose under the acidic or basic conditions. The structures of **IK-1–IK-7** were characterized by ¹H NMR, IR and confirmed by elementary analysis. The structures of some compounds were also confirmed by mass spectra.

2.3.3 Spectroscopic Analysis of *IK*

All main functional groups were characterized by IR spectra, which showed normal stretching absorption bands indicating the existence of benzen ring (1,460–1,640 cm⁻¹), P–O–C (1,030 and 950 cm⁻¹), and P–C (755–760 cm⁻¹). A strong absorption near 1,760–1,772 cm⁻¹ was identified for absorption C=O. A band near 3,050 cm⁻¹ accounted for C–H stretching of the benzene ring and the triazole ring. A strong band at 2,800–2,900 cm⁻¹ accounted for C–H stretching of the alkyl group. A strong peak near 1,250 cm⁻¹ accounted for P=O in phosphonates. A strong peak near 1,340 cm⁻¹ evidenced for C–N stretching in **IK-1–IK-7**.

EI mass spectra of **IK-1** gave stronger molecular ion peaks. Fragment ions of **IK-1** were consistent with the structure and could be assigned.

In the ¹H NMR spectra of **IK-1–IK-7**, the proton signals of the phenyl-triazol-3-yl group could be observed as follows: one proton in the triazol-3-yl moiety appeared as a multiplet at δ 7.2–7.6 ppm and five protons in the Ph moiety appeared as a multiplet near δ 8.2 ppm. The signal corresponding to the methylene group (OCH₂CO) flanked by the phenoxy group and the carbonyl group appeared as a singlet for **IK-1–IK-7**. Like **IA** and **IB**, the proton signals corresponding to the two methoxy groups attached to phosphorus appeared as two doublets split by the phosphorus nucleus. Two methyl groups in the CH₃CH₂O moiety of **IK-7** displayed as a multiplet, in fact it should be two triplets due to couplings to the CH₂ in the CH₃CH₂O moiety and couplings to the phosphorus. The proton signals corresponding to the group OCHP attached to phosphorus in compounds with Ph or substituted Ph as R³ appeared as a doublet split only by phosphorus nucleus.

However, protons (OCHP) in compounds with Et and *n*-Pr as R³ appeared as multiplets which were split by the effect of the magnetic nucleus from both phosphorus and proton in R³, such as **IK-5** and **IK-6**. The chemical shifts of proton signal in the OCHP could be affected by the structure of R³. For compounds with Et as R³, its signal in the OCHP appeared at δ 5.1–5.4 ppm, while for compounds with Ph or substituted Ph as R³, proton signals in the OCHP appear at 6.2–6.6 ppm. This

indicated that their chemical shifts moved to a lower field due to the effect of the attenuation on magnetic shielding caused by the electronegativity of Ph or substituted Ph.

2.3.4 *Herbicidal Activity of IK*

The herbicidal activity of *O,O*-dialkyl 1-(1-phenyl-1,2,4-triazol-3-yl oxyacetoxy) alkylphosphonates **IK** were evaluated at 2.25 kg ai/ha in the greenhouse. They were tested for pre- and post-emergence inhibitory effects against barnyard grass (*Echinochloa Crusgalli*), crab grass (*Digitaria Sanguinalis*), rape (*Brassica campestris*), setose thistle (*Cirsium japonicum*), cucumber (*Cucumis sativa*), and lettuce (*Lactuca sativa*). However, all of **IK** only showed less than 20 % inhibition against the above tested plants at 2.25 kg ai/ha, but they showed plant growth regulatory activity [34].

2.3.5 *Summary*

O,O-dialkyl 1-(1-phenyl-1,2,4-triazol-3-yloxyacetoxy)alkylphosphonates **IK** including 7 compounds were synthesized by the reaction of sodium salt of 1-phenyl-3-hydroxy-1,2,4-triazole **M7** with 1-(chloroacetoxy)alkylphosphonates **M3** using tetra-butylammonium bromide as a catalyst in acetonitrile.

All of **IK** showed very weak inhibitory activity (<20 % inhibition) against barnyard grass, crab grass, rape, setose thistle, cucumber, and lettuce for pre-emergence and post-emergence applications. It is noteworthy that there is no substituent on the benzene ring of 1-phenyl-3-hydroxy-1,2,4-triazole moiety in **IK**.

References

1. Baillie AC, Wright K, Wright BJ et al (1988) Inhibitors of pyruvate dehydrogenase as herbicides. *Pestic Biochem Physiol* 30:103–112
2. Brienne M, Jacques J, Brianso M et al (1978) Stereochemistry of rearrangement of 1-hydroxy-2,2,2-trichlorodialkyl ethylphosphonates in 2,2-dichlorovinyl phosphates and dialkyl phosphates. *Nouv J Chim* 2:19–20
3. Kharasch MS, Mosher RA, Bengelsdorf IS (1960) Organophosphorus chemistry addition reactions of diethyl phosphonate and the oxidation of triethyl phosphite. *J Org Chem* 25:1000–1006
4. Janzen A, Pollitt R (1970) Reaction of dialkyl phosphonates with hexafluoroacetone. *Can J Chem* 48:1987–1990
5. Ruveda MA, De Licastro SA (1972) Organophosphorus chemistry: Synthesis of dimethyl α -hydroxy phosphonates from dimethyl phosphite and phenacyl chloride and cyanide. *Tetrahedron* 28:6012–6018

6. Texier-Boullet F, Foucaud A (1982) A convenient synthesis of dialkyl 1-hydroxyalkane phosphonates using potassium or caesium fluoride without solvent. *Synthesis* 1982:165–166
7. Texier-Boullet F, Lequitte M (1986) An unexpected reactivity of simple heterogeneous mixture of γ -alumina and potassium fluoride: 1-hydroxyalkane phosphonic esters synthesis from non-activated ketones in “dry media”. *Tetrahedron Lett* 27:3515–3516
8. Li YF, Hammerschmidt F (1993) Enzymes in organic chemistry, part 1: Enantioselective hydrolysis of α -(acyloxy) phosphonates by esterolytic enzymes. *Tetrahedron Asymmetry* 4:109–120
9. Lv CX (2009) Preparation of organic intermediates. Beijing Chemical Industry, Beijing
10. Brayer JL, Talinani L, Tessier J (1990) Preparation of aryl and aryl oxyacetyl diaineoalkanes and analogs as agrochemical fungicides. EP 0,376,819, 4 July 1990
11. He HW, Wang J, Liu ZJ (1994) Synthesis of α -(substituted phenoxy acetoxy)alkyl phosphonates. *Chin Chem Lett* 5:35–38
12. He HW, Wang J, Liu ZJ et al (1994) Study on biologically active organophosphorus compounds V Synthesis and properties of α -(substituted phenoxyacetoxy)alkyl phosphonates. *Chin J Appl Chem* 11:21–24
13. He HW, Wang J, Liu ZJ et al (1994) Studies on biologically active organophosphorus compounds VI. Synthesis properties and biological activity of α -oxophosphonic acid derivatives. *J Centr Chin Norm Univ (Nat Sci)* 28:71–76
14. Chen T, Shen P, Li YJ et al (2006) Synthesis and herbicidal activity of O,O-dialkyl phenoxyacetoxyalkylphosphonates containing fluorine. *J Fluorine Chem* 127:291–295
15. Chen T, Shen P, Li YJ et al (2006) The synthesis and herbicidal evaluation of fluorine-containing phenoxyacetoxyalkylphosphonate derivatives. *Phosphorus Sulfur Silicon Relat Elem* 181:2135–2145
16. Wang J, Chen XY, Liu XF et al (1999) The synthesis and biological properties of α -halogenated phenoxy carbonyloxy alkylphosphonic acids and esters. *Chin J Chem Reag* 21:301–303
17. He HW, Chen T, Li YJ (2007) Synthesis and herbicidal activity of alkyl 1-(3-trifluoromethylphenoxyacetoxy)-1-substituted methylphosphonates. *J Pestic Sci* 32:42–44
18. Li YJ, He HW (2008) Synthesis and herbicidal activity of α -[2-(fluoro-substituted phenoxy) propionyloxy] alkyl phosphonates. *Phosphorus Sulfur Silicon Relat Elem* 183:712–713
19. He HW, Liu ZJ, Wang J (1998) Synthesis and biological activities of α -[2-(2,4-dichlorophenoxy)propionyloxy] alkyl phosphonates. *Chin J Appl Chem* 15:88–90
20. Wang J, He HW, Liu ZJ (1997) Synthesis of alpha-[2-(2,4-dichlorophenoxy) propionyloxy] alkyl phosphonates. *Chin Chem Lett* 8:943–944
21. Wang T, He HW (2004) Simple and improved preparation of α -oxophosphonate monolithium salts. *Phosphorus Sulfur Silicon Relat Elem* 179:2081–2089
22. He HW, Yuan JL, Peng H et al (2011) Studies of O,O-dimethyl α -(2,4-dichlorophenoxyacetoxy) ethylphosphonate (HW02) as a new herbicide. I. Synthesis and herbicidal activity of HW02 and analogues as novel inhibitors of pyruvate dehydrogenase complex. *J Agric Food Chem* 59:4801–4813
23. Peng H, Wang T, Xie P et al (2007) Molecular docking and three-dimensional quantitative structure-activity relationship studies on the binding modes of herbicidal 1-(substituted phenoxyacetoxy) alkylphosphonates to the E1 component of pyruvate dehydrogenase. *J Agric Food Chem* 55:1871–1880
24. Wang T, He HW, Miao FM (2009) Synthesis, crystal structure and herbicidal activity of 1-(2,4-dichlorophenoxyacetoxy)-1-arylmethylphosphonates. *Chin J Org Chem* 29:1152–1157
25. Meng LP, He HW, Liu ZJ (1998) Synthesis and biological activities of O,O-dimethyl α -(NO₂ substituted phenoxyacetoxy)alkylphosphonates. *Chin J HuBei Chem Ind (special issu):*40–41
26. Li YJ, He HW (2006) Dimethyl {1-[2-(2-fluorophenoxy)acetoxy]ethyl}phosphonate. *Acta Cryst E* 62:o1593–o1594
27. Evans D, Lawson K (1992) Crop protection chemicals-research and development perspectives and opportunities. *Pestic Outlook* 3

28. He HW, Peng H, Wang T et al (2013) α -(Substituted-phenoxyacetoxy)- α -heterocyclylmethyl phosphonates: synthesis, herbicidal activity, inhibition on pyruvate dehydrogenase complex (PDHc), and application as postemergent herbicide against broadleaf weeds. *J Agric Food Chem* 61:2479–2488
29. Wang T, Wang W, Peng H et al (2013) Synthesis and biological activity of 1-(substituted phenoxyacetoxy)-1-(pyridin-2-yl or thien-2-yl)methylphosphonates. *J Heterocycl Chem*. doi:10.1002/jhet.1944
30. Tan XS, Peng H, He HW (2010) (Dimethoxyphosphoryl)(furan-2-yl) methyl 2-(2,4-dichlorophenoxy) acetate. *Acta Cryst E* 66:o2962
31. Chaaban I, Ojioo J (1984) Synthesis and preliminary antibacterial activity of 3-(2-arylamino-1,3,4-thiodiazol-5-yl)-4-hydroxy-4'-substituted sulfamoylazobenzenes. *J Indian Chem Soc* 61:523–525
32. Miller FP, Kane JM (1988) Process for the preparation of 5-aryl-2,4-dialkyl-3H-1,2,4-triazole-3-thiones. EP 0,280,867, 7 Sept 1988
33. Beck JR (1987) Plant growth regulating triazoles. EP 0,227,284 A1, 1 July 1987
34. He HW, Meng LP, Hu LM et al (2002) Synthesis and plant growth regulatory activity of 1-(1-phenyl 1,2,4-triazole-3-oxycetoxy)alkyl phosphonates. *Chin J Pest Sci* 4:14–18

Chapter 3

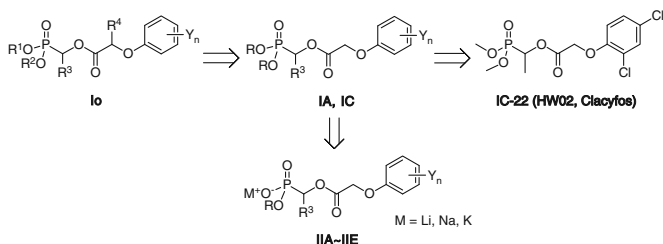
Salts of Alkylphosphonates

A detailed study of acylphosphinates and acylphosphonates showed that they were mechanism-based inhibitors of pyruvate dehydrogenase complex (PDHc) as analogues of pyruvate. However, these phosphinates and phosphonates were not active enough to be considered as herbicides [1–3]. As stated in Chap. 2, some 1-substituted alkylphosphonates **IC** and **IG** showed notable herbicidal activity. Furthermore, the substitution of R^1 , R^2 , R^3 , R^4 and Y_n in phosphonate **Io** could be directly relevant to their herbicidal activity. Among the 1-substituted alkylphosphonates **IA–IC**, **IC-22** (clacyfos) was found to be most effective against broadleaf weeds as a competitive inhibitor of PDHc (Scheme 3.1) [4]. This result prompted us to study continually on the design of novel PDHc inhibitors as potential herbicides.

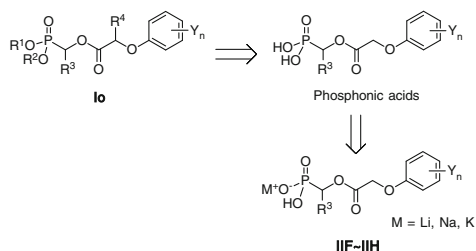
Based on the bioisosterism, the salts of alkylphosphonates **IA** or **IC** were assumed to have a more powerful inhibitory effect against plant PDHc E1 and better herbicidal activity than the corresponding alkylphosphonates, because sodium *O*-methyl acetylphosphonate **1-1** has been reported as a powerful PDHc E1 inhibitor [1]. Five series of novel alkali metal salts of *O*-alkyl 1-(substituted phenoxyacetoxy)alkylphosphonates **IIA–IIIE** were first designed as potential plant PDHc E1 inhibitors. **IIA–IIIE** could be easily synthesized from corresponding *O,O*-dialkyl 1-(substituted phenoxyacetoxy)alkylphosphonates **IA** or **IC** in one step. It was also expected that 1-(substituted phenoxyacetoxy)alkylphosphonic acids (Scheme 3.2) could have better herbicidal activity, because they were more analogous to pyruvic acid which acted as the substrate of PDHc. However, 1-(substituted phenoxyacetoxy)alkylphosphonic acids were not stable for long-time storage.

They often decomposed to afford substituted phenoxyacetic acids in three days. The reason was possibly that the carboxylic ester bond in the molecule cleaved easily in the acid environment supplied by phosphonic acid. Subsequently, alkali metal salts of 1-(substituted phenoxyacetoxy)alkylphosphonic acids **IIIF**, **IIIG** and **IIIH** (Scheme 3.2) were further synthesized as alternatives of 1-(substituted phenoxyacetoxy)phosphonic acids. These **IIIF**, **IIIG** and **IIIH**, unlike 1-(substituted phenoxyacetoxy)alkylphosphonic acids, are neutral salts with good stability.

Indeed, some mono sodium salts of 1-(substituted phenoxyacetoxy)alkylphosphonic acids showed much higher inhibitory activity against plant PDHc E1 and



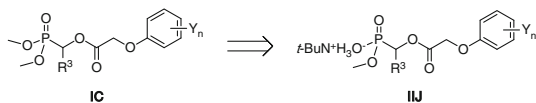
Scheme 3.1 Design of salts of alkylphosphonates **IIA–IIE**



Scheme 3.2 Chemical structure modification from **Io** to **IIF, IIG** and **IIH**

higher pre-emergence inhibitory potency against dicotyledons than their corresponding phosphonates at 450 g ai/ha.

The aminium salts of phosphonic acids or esters are well known as typical agrochemicals and good nitrogen sources for plant growth. Therefore, we extended the structure of *O,O*-dimethyl 1-(substituted phenoxyacetoxy)alkylphosphonates to their corresponding aminium salts. For this purpose, we synthesized *t*-butylaminium *O*-methyl 1-(substituted phenoxyacetoxy)alkylphosphonates **IIJ** (Scheme 3.3) by selective demethylation of the corresponding *O,O*-dimethyl 1-(substituted phenoxyacetoxy)alkylphosphonates **IC** with *t*-butylamine. Some of **IIJ** were indeed proven to be good herbicidal compounds by examining their herbicidal activity.



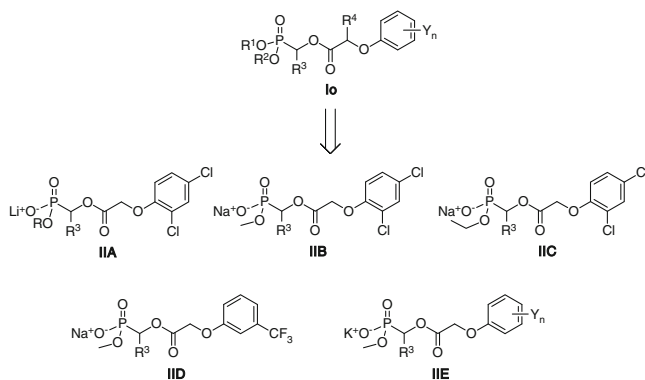
Scheme 3.3 Selective demethylation with *t*-butylamine giving *t*-butylaminium *O*-methyl 1-(substituted phenoxyacetoxy)alkylphosphonates **IIJ**

3.1 Alkali Metal Salts of *O*-Alkyl Alkylphosphonic Acids IIA–IIE

3.1.1 Introduction

Some of 1-(substituted phenoxyacetoxy)alkylphosphonates **IA–IF** stated in Chap. 2 displayed significant herbicidal activity against a wide range of broadleaf weeds. Considering sodium *O*-methyl acetylphosphonate **1-1** with powerful inhibitory effect against plant PDHc E1, we focused on the design of new alkali metal salts of *O*-alkyl 1-(substituted phenoxyacetoxy)alkylphosphonic acids **IIA–IIE**. As stated in Chap. 2, 1-(substituted phenoxyacetoxy)alkylphosphonates with 2,4-Cl₂ as Y_n were much more beneficial to post-emergence herbicidal activity against dicotyledons. Therefore, R⁴=H, Y_n=2,4-Cl₂ in **Io** were kept constant, Li or Na, and Me or Et as R¹ and R² were introduced to form **IIA–IIC** series, further modification was focused on substituent R³. Na and Me as R¹ and R², CF₃ as Y_n were introduced in **Io** to form **IID** series, further modification was also focused on substituent R³. K and Me as R¹ and R² were introduced in **Io** to form **IIE** series, further modification was focused on substituent R³ and Y_n (Scheme 3.4). **IIA–IIE** were expected to have a more powerful inhibitory effect against plant PDHc E1 and better herbicidal activity than corresponding alkylphosphonates. In order to examine the effect of salts on herbicidal activity, **IIA–IIE**, including lithium salts (**IIA-1–IIA-16**), sodium salts (**IIB-1–IIB-25**, **IIC-1–IIC-8** and **IID-1–IID-9**) and potassium salts (**IIE-1–IIE-19**) were synthesized.

In this section, we describe the synthesis, herbicidal activity and structure-activity relationships of alkali metal salts of *O*-alkyl 1-(substituted phenoxyacetoxy)alkylphosphonic acids **IIA–IIE**.



Scheme 3.4 Structure of alkali metal salts of *O*-alkyl 1-(substituted phenoxyacetoxy)alkylphosphonic acids **IIA–IIE**

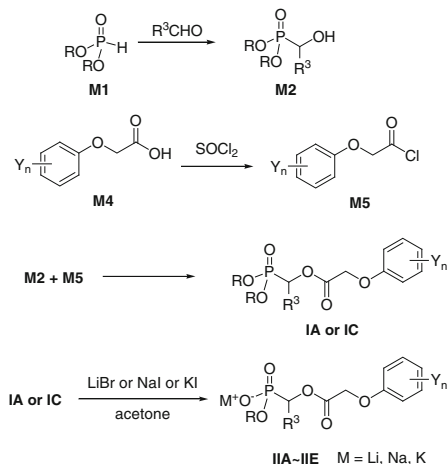
3.1.2 Synthesis of IIA–IIE

Alkali metal salts of *O*-alkyl 1-(substituted phenoxyacetoxy)alkylphosphonic acids **IIA–IIE** could be easily synthesized by the reaction of *O,O*-dialkyl 1-(substituted phenoxyacetoxy)alkylphosphonates **IA** or **IC** with corresponding lithium bromide, sodium iodide, or potassium iodide in refluxing acetone. The synthetic route of **IIA–IIE** is shown in Scheme 3.5. For the synthesis of **IIA–IIE**, 1-hydroxyalkylphosphonates **M2**, substituted phenoxyacetyl chloride **M5**, and *O,O*-dialkyl 1-(substituted phenoxyacetoxy)alkylphosphonates **IA** or **IC** could be prepared according to the known methods as stated in Chap. 2. *O,O*-Dialkyl phosphonate **M1** was used directly as obtained commercially or prepared by the reaction of phosphorus trichloride and methanol. **M1** reacted with different aldehydes to give *O,O*-dialkyl 1-hydroxyalkylphosphonates **M2**. The substituted phenoxyacetic acids **M4** were prepared in satisfactory yields by the reaction of corresponding substituted phenols with 2-chloroacetic acid or ethyl 2-bromoacetate followed by hydrolysis. The substituted phenoxyacetyl chlorides **M5** could be easily obtained by the treatment of **M4** with excess thionyl chloride. **M2** reacted with **M5** to provide **IA** or **IC** (Scheme 3.5).

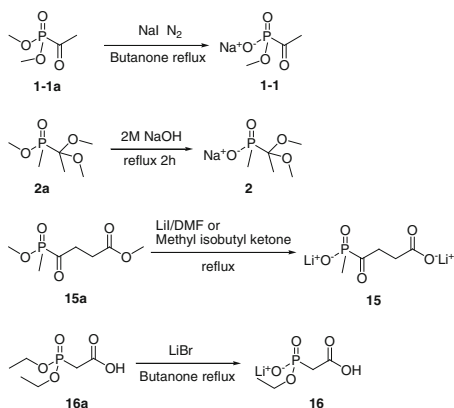
According to the literature [1], phosphonate or phosphinate salts could be generally synthesized by the reaction of the corresponding phosphonate or phosphinate esters with inorganic alkalis or salts. For example, as shown in Scheme 3.6, Baillie reported that sodium *O*-methyl acetylphosphonate **1-1** could be obtained by demethylation of *O,O*-dimethyl acetylphosphonate **1-1a** with sodium iodide in butanone [1, 5]. The phosphinate **2a** could be hydrolyzed to give the corresponding salts **2** in 2 M sodium hydroxide aqueous solution [1].

Krawczyk reported that *O*-methyl methylphosphinate **15a** could be demethylated into lithium methylphosphinate **15** in a 0.5 M solution of anhydrous lithium bromide in DMF or methyl isobutyl ketone, while *O,O*-diethyl phosphonate **16a** could be converted into lithium *O*-ethyl phosphonate **16** by using lithium bromide and butanone [6].

Scheme 3.5 Synthesis of alkali metal salts of *O*-alkyl 1-(substituted phenoxyacetoxy)alkylphosphonic acids **IIA–IIE**



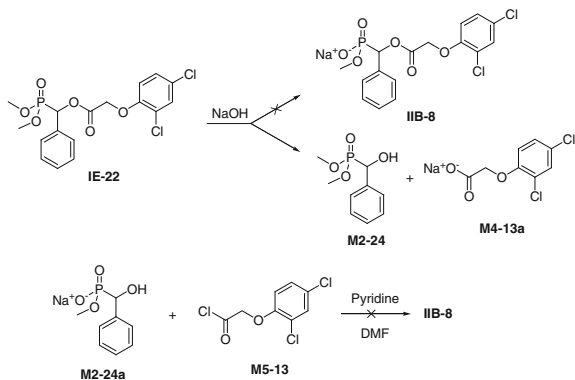
Scheme 3.6 Synthesis of some phosphinate or phosphonate salts reported in the literatures



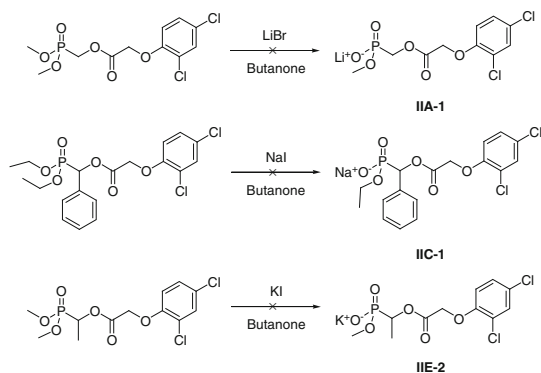
However, alkali metal salts of *O*-alkyl 1-(substituted phenoxyacetoxy)alkylphosphonates **IIA–IIE** could not be synthesized by using the method mentioned above. For instance, first attempted synthesis of **IIB-8** ($R^3=\text{Ph}$) using NaOH as the base was unsuccessful. In the presence of sodium hydroxide (pH = 9–10) at about 60 °C, **IE-22** ($R^1=R^2=\text{Me}$, $R^3=\text{Ph}$, and $R^4=\text{H}$) was easily hydrolyzed to yield *O,O*-dimethyl 1-hydroxybenzylphosphonate **M2-24** and sodium 2,4-dichlorophenoxyacetate **M4-13a**, not **IIB-8**, as shown in Scheme 3.7. Subsequently, a condensation of sodium *O*-methyl 1-hydroxybenzylphosphonate **M2-24a** with 2,4-dichlorophenoxyacetic chloride **M5-13** in the presence of pyridine, was also in vain (Scheme 3.7).

Then we attempted to synthesize alkali metal salts of *O*-alkyl 1-(substituted phenoxyacetoxy)alkylphosphonic acids **IIA–IIE** by using lithium bromide, sodium iodide or potassium iodide according to the literature [1, 5]. It was found that solvent and temperature were crucial to the reaction. For instance, it was not successful to prepare **IIA-1**, **IIC-1**, and **IIE-2** by using lithium bromide, sodium iodide or potassium iodide in refluxing methyl isobutyl ketone or butanone, but 2,4-dichlorophenoxyacetic acid and corresponding salts of 1-hydroxyphosphonic acids were obtained as by-products (Scheme 3.8). This was probably due to the cleavage of the carboxylic ester bond at high refluxing temperature.

Scheme 3.7 Attempted synthesis of **IIB-8**



Scheme 3.8 Reaction of phosphonates with LiBr, NaI, and KI in the butanone



When acetone was subsequently attempted as the solvent, five series of novel alkali metal salts of *O*-alkyl 1-(substituted phenoxyacetoxy)alkylphosphonic acids **IIA–IIIE** including 77 compounds were successfully synthesized. The *O,O*-dimethyl phosphonates are more easily dealkylated than the *O,O*-diethyl phosphonates under the optimized reaction conditions. As shown in Table 3.1, the dealkylation of the *O,O*-diethyl phosphonates required a longer reaction time than the *O,O*-dimethyl phosphonates did. For example, the reaction time of **IIA-8** (R=Me) was only 2 h, while that of **IIA-16** (R=Et) was 15 h. Moreover, the similar results were observed by comparing the reaction time in Table 3.2 with that in Table 3.3, implying that the reaction time might be prolonged with the increasing bulk of the R group. By comparing the reaction time in Tables 3.1, 3.2 with Table 3.5, lithium or sodium salts of the *O*-methyl phosphonic acids were more easily synthesized than potassium salts of the *O*-methyl phosphonic acids. The synthetic reaction time of lithium or sodium

Table 3.1 Structure and reaction time of lithium *O*-alkyl 1-(2,4-dichlorophenoxyacetoxy) alkylphosphonates **IIA**^a

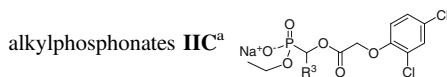
Compound	R	R ³	Time (h)	Compound	R	R ³	Time (h)
IIA-1	Me	H	3	IIA-9	Me	2-ClPh	4
IIA-2	Me	Me	3	IIA-10	Me	3-ClPh	3
IIA-3	Me	<i>n</i> -Pr	4	IIA-11	Me	2,4-Cl ₂ Ph	3
IIA-4	Me	Ph	4	IIA-12	Me	Fur-2-yl	2
IIA-5	Me	4-MePh	3	IIA-13	Me	Thien-2-yl	3
IIA-6	Me	3-NO ₂ Ph	3	IIA-14	Me	Pyrid-2-yl	2
IIA-7	Me	4-NO ₂ Ph	2	IIA-15	Me	3,4-OCH ₂ OPh	3
IIA-8	Me	4-FPh	2	IIA-16	Et	4-FPh	15

^a Synthesis of compounds: **IIA-1–IIA-15** [7]; **IIA-16** [8]

Table 3.2 Structure and reaction time of sodium *O*-methyl 1-(2,4-dichlorophenoxy)acetoxy

Compound	R ³	Time (h)	Compound	R ³	Time (h)
IIB-1	H	2	IIB-14	2-ClPh	3
IIB-2	Me	3	IIB-15	3-ClPh	3
IIB-3	Et	3	IIB-16	4-ClPh	2
IIB-4	<i>n</i> -Pr	4	IIB-17	2,3-Cl ₂ Ph	3
IIB-5	<i>i</i> -Pr	3	IIB-18	2,4-Cl ₂ Ph	3
IIB-6	<i>n</i> -Bu	4	IIB-19	3,4-Cl ₂ Ph	3
IIB-7	CCl ₃	3	IIB-20	Fur-2-yl	1
IIB-8	Ph	4	IIB-21	Thien-2-yl	2
IIB-9	4-MePh	2	IIB-22	Pyrid-2-yl	2
IIB-10	3-NO ₂ Ph	2	IIB-23	Pyrid-3-yl	2
IIB-11	4-NO ₂ Ph	3	IIB-24	Pyrid-4-yl	2
IIB-12	4-MeOPh	2	IIB-25	3,4-OCH ₂ Oph	3
IIB-13	4-FPh	2			

^a Synthesis of compounds: **IIB-1–IIB-4**, **IIB-7** [9]; **IIB-5**, **IIB-7**, **IIB-11**, **IIB-15**, **IIB-17**, **IIB-21**, **IIB-23**, **IIB-24** [8]; **IIB-8–IIB-10**, **IIB-12–IIB-14**, **IIB-16**, **IIB-18–IIB-20**, **IIB-22** [10]; **IIB-25** [11]

Table 3.3 Structure and reaction time of sodium *O*-ethyl 1-(2,4-dichlorophenoxy)acetoxy

Compound	R ³	Time (h)	Compound	R ³	Time (h)
IIIC-1	Ph	14	IIIC-5	4-FPh	22
IIIC-2	4-MePh	16	IIIC-6	2,4-Cl ₂ Ph	19
IIIC-3	3-NO ₂ Ph	10	IIIC-7	Pyrid-2-yl	12
IIIC-4	4-MeOPh	18	IIIC-8	3,4-OCH ₂ Oph	18

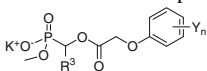
^a Synthesis of compounds: **IIIC-1–IIIC-3**, **IIIC-5–IIIC-6**, **IIIC-8** [11]; **IIIC-4**, **IIIC-7** [8]

Table 3.4 Structure and reaction time of sodium *O*-methyl 1-(3-trifluoromethylphenoxy)acetoxy

Compound	R ³	Time (h)	Compound	R ³	Time (h)
IID-1	Me	3	IID-6	2-ClPh	4
IID-2	Et	3	IID-7	4-ClPh	4
IID-3	4-MePh	4	IID-8	Pyrid-2-yl	3
IID-4	3-NO ₂ Ph	4	IID-9	3,4-OCH ₂ Oph	4
IID-5	4-NO ₂ Ph	4			

^a Synthesis of compounds: **IID-1–IID-9** [8]

Table 3.5 Structure and reaction time of potassium *O*-methyl 1-(substituted phenoxyacetoxy) alkylphosphonates **III**^a



Compound	R ³	Y _n	Time (h)	Compound	R ³	Y _n	Time (h)
III-1	H	2,4-Cl ₂	10	III-11	4-ClPh	2,4-Cl ₂	12
III-2	Me	2,4-Cl ₂	12	III-12	2,3-Cl ₂ Ph	2,4-Cl ₂	14
III-3	Et	2,4-Cl ₂	12	III-13	2,4-Cl ₂ Ph	3-CF ₃	13
III-4	<i>n</i> -Pr	2,4-Cl ₂	14	III-14	2,4-Cl ₂ Ph	2,4-Cl ₂	11
III-5	Ph	3-CF ₃	11	III-15	Fur-2-yl	2,4-Cl ₂	11
III-6	Ph	2,4-Cl ₂	12	III-16	Thien-2-yl	2,4-Cl ₂	13
III-7	4-MePh	2,4-Cl ₂	14	III-17	Pyrid-2-yl	3-CF ₃	12
III-8	3-NO ₂ Ph	2,4-Cl ₂	12	III-18	Pyrid-2-yl	2,4-Cl ₂	13
III-9	4-MeOPh	2,4-Cl ₂	15	III-19	3,4-OCH ₂ OPh	2,4-Cl ₂	13
III-10	2-ClPh	2,4-Cl ₂	11				

^a Synthesis of compounds: **III-1–III-4** [9]; **III-5–III-19** [12]

salts (1–4 h) was much shorter than that of potassium salts (10–15 h). Structure and reaction time of **IIA–III** are listed in Tables 3.1, 3.2, 3.3, 3.4 and 3.5. Detailed synthetic procedures for **IIA–III** are introduced in the Sect. 9.1.10 of Chap. 9.

The structure of alkali metal salts of *O*-alkyl 1-(substituted phenoxyacetoxy) alkylphosphonic acids **IIA–III** was confirmed by elemental analysis and characterized by IR, ¹H NMR. Some of them were further characterized by ³¹P NMR and mass spectrometry. The structure of sodium *O*-methyl 1-(2,4-dichlorophenoxyacetoxy)-1-(furan-2-yl)methylphosphonate **IIIB-20** was further analyzed by X-ray single-crystal diffraction.

IIA–III could be dissolved in water and polar organic solvents, such as DMF and DMSO. They are partially soluble in CHCl₃ and CH₂Cl₂, but not soluble in benzene and petroleum ether. They are easily decomposed under acidic or basic conditions.

3.1.3 Spectroscopic Analysis of **IIA–III**

The IR spectra of **IIA–III** showed normal stretching absorption bands indicating the existence of benzene ring (~1,650, ~1,480 cm⁻¹), C–O–C (1,050–1,250 cm⁻¹), and P–C (740–750 cm⁻¹). A sharp and weak band at 3,050–3,100 cm⁻¹ accounted for C–H stretching of the benzene ring. The C–H stretching of alkyl appeared at 2,860–2,950 cm⁻¹; strong absorption near 1,720–1,740 cm⁻¹ was identified for the absorption C=O. A strong peak near 1,260 cm⁻¹ accounted for P=O in phosphonates. An asymmetric stretching vibration for P–O–C appeared at 1,030–1,050 cm⁻¹. The IR spectrum of **III-8** (R³=3-NO₂Ph, Y_n=2,4-Cl₂) is shown in Fig. 3.1.

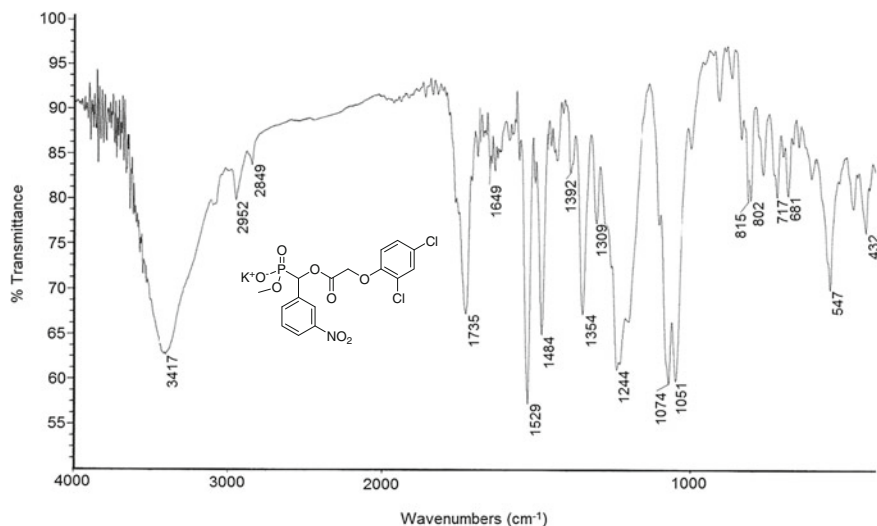


Fig. 3.1 IR spectrum of **III-8**

In the ^1H NMR spectra of **IIA–III**, the chemical shifts of aromatic protons appeared at 6.8–7.8 ppm. The proton signals corresponding to OCH_2P displayed as multiplets at 4.9–5.3 ppm for the compounds with aliphatic groups as R^3 . As for those compounds with aromatic groups as R^3 , the proton signal (OCH_2P) appeared at 5.7–6.5 ppm as a doublet due to the coupling with magnetic phosphorus. The signal corresponding to the methylene group flanked by the phenoxy group and carbonyl group appeared as a quartet with the two outside peaks smaller in size, which belongs to AB system with the difference in chemical shift between the two mutually coupled protons A and B. For example, methylene signal in **IIA-5** ($\text{R}=\text{Me}$, $\text{R}^3=4\text{-MePh}$) appeared at 5.06 and 5.01 ppm in A series and at 4.93 and 4.88 ppm in B series, respectively (Fig. 3.2). The proton signals of methoxy groups attached to phosphorus appeared as a doublet caused by the phosphorus nucleus, at ~ 3.4 ppm. As for **IIIC**, the proton signals of CH_3 and CH_2 groups in the $\text{P-OCH}_2\text{CH}_3$ appeared at ~ 1.0 and ~ 3.7 ppm, respectively. Compared with *O,O*-dialkyl phosphonates, the chemical shifts of alkali metal salts **IIA–III** moved upfield about 0.3–0.5 ppm due to the effect of the magnetic shielding by the oxygen anion.

^{31}P NMR chemical shifts of **IIA–III** appeared as a singlet at δ 8.2–8.7 ppm. Their chemical shifts moved upfield by approximately 15 ppm, compared with those of the corresponding *O,O*-dimethyl phosphonates. The ^{31}P NMR spectrum of **IIA-8** ($\text{R}=\text{Me}$, $\text{R}^3=4\text{-FPh}$) is shown in Fig. 3.3.

The ESI mass spectra in some **IIA–III** gave $[\text{M-Li}]^-$, or $[\text{M-Na}]^-$ or $[\text{M-K}]^-$ ion peaks in negative mode. For example, **IIB-20** ($\text{R}=\text{Me}$, $\text{R}^3=\text{fur-2-yl}$) was characterized by ESI-MS to give $393[\text{M-Na}]^-$ ion peak. The ESI-MS spectrum of **IIB-20** is shown in Fig. 3.4.

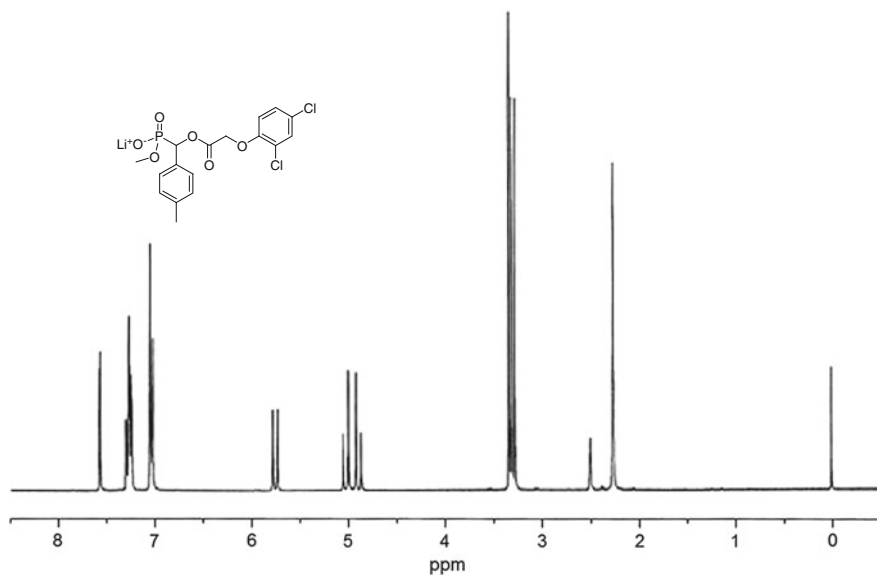


Fig. 3.2 ^1H NMR spectrum of **IIA-5** ($\text{DMSO-}d_6$, 300 MHz)

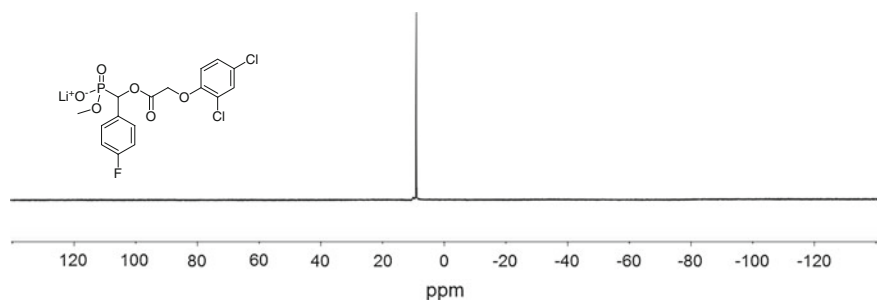


Fig. 3.3 ^{31}P NMR spectrum of **IIA-8** ($\text{DMSO-}d_6$, 162 MHz)

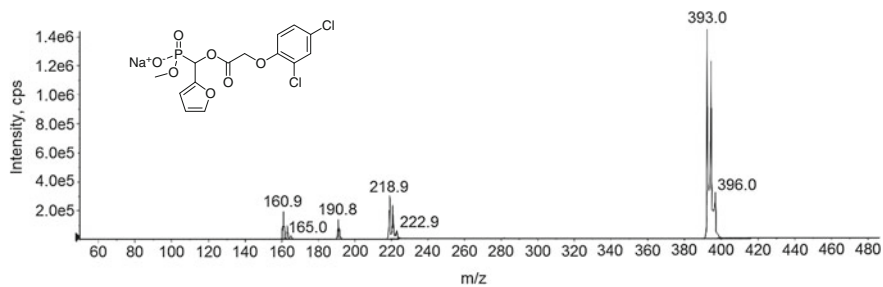


Fig. 3.4 ESI-MS spectrum of **IIB-20**

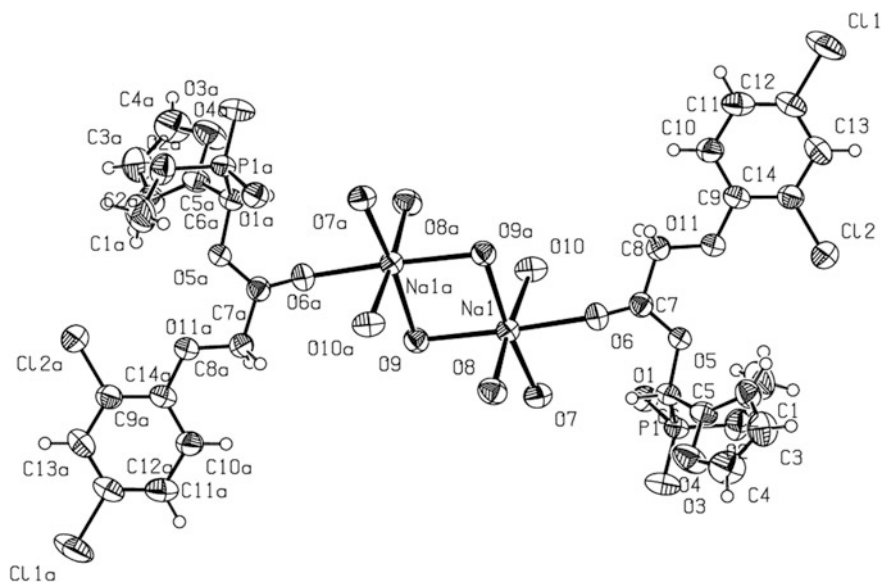


Fig. 3.5 Molecular structure of **IIB-20**

3.1.4 Crystal Structure Analysis of **IIB-20**

The molecular structure of **IIB-20** is shown in Fig. 3.5. The packing diagram of the unit cell of **IIB-20** is shown in Fig. 3.6. Selected bond lengths and angles are presented in Table 3.6. As can be seen from the X-ray single crystal structure of **IIB-20**, all bond lengths and angles show normal values. The P(1)-O(10) bond length of 1.5746(19) Å is significantly longer than the P(1)-O(9) and P(1)-O(8) distances of 1.4843(18) and 1.4937(18) Å, respectively. The O(9)-P(1)-O(10) and O(8)-P(1)-O(10) bond angles of **IIB-20** are much smaller than the O(9)-P(1)-O(8) bond angle. There are six oxygen atoms around every sodium atom to make two molecules with the same configuration to bind and form dimers. Eight O atoms from water and two O atoms from (C=O) participate in O–Na–O bonds, which plays a major role in stabilizing the molecules in the unit cell.

3.1.5 Herbicidal Activity of IIA–III

As a preliminary bioassay, some alkali metal salts of *O*-alkyl 1-(substituted phenoxyacetoxy)alkylphosphonic acids **IIA–III** were tested for herbicidal activity on barnyard grass (*Echinochloa crusgalli*) and cabbage type rape (*Brassica napus*) by the Petri dish method. For further herbicidal activity evaluation, most of

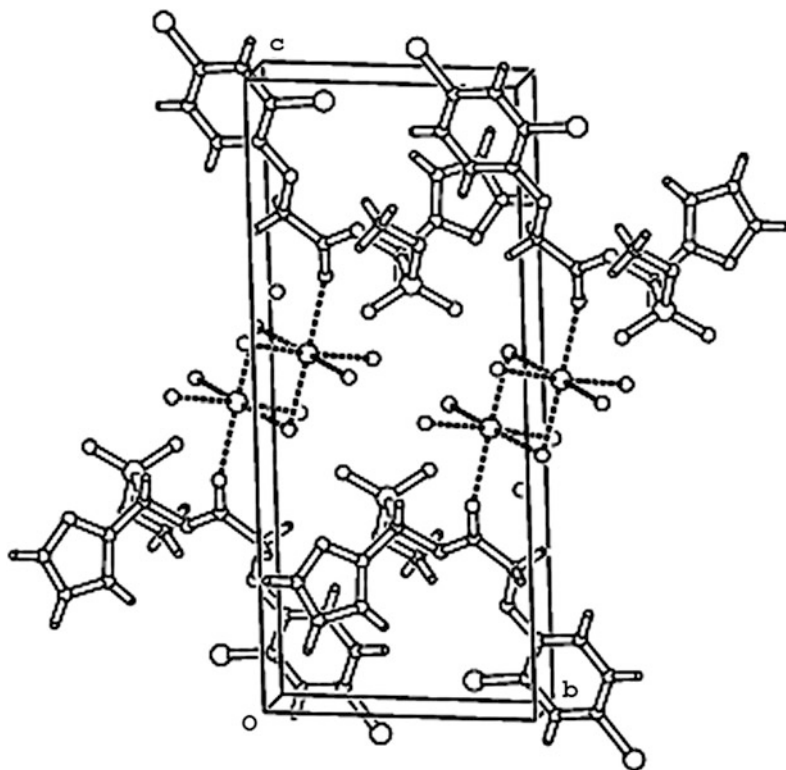


Fig. 3.6 Packing diagram of **IIB-20**

Table 3.6 Selected bond distance (Å) and angles (°) for **IIB-20**

Bond	Dist.	Bond	Angles deg.
P(1)-O(9)	1.4843(18)	O(9)-P(1)-O(8)	117.48(12)
P(1)-O(8)	1.4937(18)	O(9)-P(1)-O(10)	108.40(12)
P(1)-O(10)	1.5746(19)	O(8)-P(1)-O(10)	110.98(10)
P(1)-C(10)	1.838(3)	O(9)-P(1)-C(10)	105.73(11)
Cl(2)-C(26)	1.724(3)	O(8)-P(1)-C(10)	107.85(11)
Na(3)-O(2)	2.386(2)	O(10)-P(1)-C(10)	105.63(11)
Na(3)-O(5) ^a	2.390(2)	O(2)-Na(3)-O(5) ^a	96.35(7)
Na(3)-O(1)	2.401(2)	O(2)-Na(3)-O(1)	89.70(8)
Na(3)-O(5)	2.414(2)	O(5) ^a -Na(3)-O(1)	173.30(9)
Na(3)-O(3)	2.430(2)	O(2)-Na(3)-O(5)	170.17(8)
Na(3)-O(4)	2.473(2)	O(5) ^a -Na(3)-O(5)	86.08(7)
O(5)-Na(3) ^a	2.390(2)	O(1)-Na(3)-O(5)	88.43(7)
Na(3)-Na(3) ^a	3.5111(17)	O(2)-Na(3)-O(3)	94.95(8)

Symmetry transformations used to generate equivalent atoms: ^a $-x + 2, -y + 2, -z + 1$

IIA–III were evaluated at a rate of 1.5 kg ai/ha in the greenhouse. They were tested for pre-emergence and post-emergence inhibitory effects against barnyard grass, crab grass (*Digitaria sanguinalis*), rape (*Brassica campestris*), common amaranth (*Amaranthus retroflexus*) and clover (*Medicago sativa*). The results are listed in Tables 3.7, 3.8, 3.9, 3.10, 3.11, 3.12, 3.13, 3.14, 3.15, 3.16, 3.17, 3.18, 3.19, 3.20 and 3.21. The herbicidal activities of **IIA–III** are reviewed as follows.

3.1.5.1 Herbicidal Activity of Lithium *O*-Alkyl 1-(2,4-Dichlorophenoxyacetoxy)Alkylphosphonates **IIA**

Some of **IIA** were tested for herbicidal activity on barnyard grass and cabbage type rape by the Petri dish method. The results are listed in Table 3.7. All tested **IIA** in Table 3.7 displayed significant activity (>90 %) against the root of barnyard grass and cabbage type rape except **IIA-8** (R=Me, R³=4-FPh) at 10 mg/L. Only **IIA-12** (R=Me, R³=4-MePh) displayed inhibition (>90 %) against the stem of cabbage type rape at 10 mg/L. Although **IIA-12** exhibited good inhibitory activity against dicotyledons, it showed no significant inhibitory effect against monocotyledon. **IIA-3** (R=Me, R³=*n*-Pr), **IIA-7** (R=Me, R³=4-NO₂Ph) and **IIA-10** (R=Me, R³=3-ClPh) even showed stimulating activity for the stem of barnyard grass at 10 mg/L.

(A) Pre-emergence herbicidal activity of **IIA**

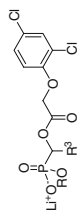
As shown in Table 3.8, all tested **IIA** displayed significant pre-emergence herbicidal activity (>90 %) against dicotyledonous rape, common amaranth and clover. Most of **IIA** also displayed significant pre-emergence herbicidal activity (>90 %) against monocotyledonous barnyard grass and crab grass at 1.5 kg ai/ha except **IIA-9** (R=Me, R³=2-ClPh), **IIA-15** (R=Me, R³=3,4-OCH₂OPh), and **IIA-16** (R=Et, R³=4-FPh). These three compounds showed moderate activity (75–89 %) against barnyard grass. In other words, all tested **IIA** exhibited good to moderate pre-emergence herbicidal activity against all the tested five plants at 1.5 kg ai/ha.

(B) Post-emergence herbicidal activity of **IIA**

As shown in Table 3.9, most **IIA** showed moderate-to-weak post-emergence herbicidal activity against dicotyledonous rape, common amaranth and clover. Among these compounds, **IIA-8** and **IIA-16** (R=Me or Et, R³=4-MePh) displayed significant post-emergence herbicidal activity (>90 %) against all tested dicotyledons, including rape, common amaranth and clover at 1.5 kg ai/ha.

However, all **IIA** displayed poor post-emergence inhibitory effect in C or D grade against monocotyledons. Although **IIA-16** exhibited good inhibitory activity against dicotyledons, it showed no significant herbicidal activity against monocotyledons.

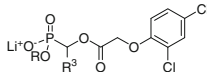
Table 3.7 Inhibitory activity of lithium *O*-alkyl 1-(2,4-dichlorophenoxyacetoxy)alkylphosphonates **IIA** against the growth of plants^a



Compound	R	R ³	Root		Stem	
			Brn ^b		Brn ^b	
			100 mg/L	10 mg/L	100 mg/L	10 mg/L
IIA-3	Me	<i>n</i> -Pr	100	99	100	89
IIA-7	Me	4-NO ₂ Ph	100	98	100	87
IIA-8	Me	4-FPh	100	79	100	37
IIA-10	Me	3-ClPh	99	99	97	89
IIA-12	Me	Fur-2-yl	100	99	100	93
IIA-13	Me	Thien-2-yl	99	99	97	89
IIA-14	Me	Pyrid-2-yl	100	99	97	89

^a Inhibitory potency (%) on the growth of plants in Petri dishes, 0 (no effect), 100 % (completely kill)

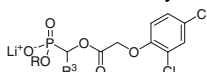
^b Brn: cabbage type rape; Ech: barnyard grass

Table 3.8 Structure and pre-emergence herbicidal activity of lithium *O*-alkyl 1-(2,4-dichlorophenoxy)alkylphosphonates **IIA**^a

Compound	R	R ³	Dicotyledon			Monocotyledon	
			Bra ^b	Amr ^b	Med ^b	Ech ^b	Dig ^b
IIA-1	Me	H	A	A	A	A	A
IIA-2	Me	Me	A	A	A	A	A
IIA-4	Me	Ph	A	A	A	A	A
IIA-5	Me	4-MePh	A	A	A	A	A
IIA-6	Me	3-NO ₂ Ph	A	A	A	A	A
IIA-9	Me	2-ClPh	A	A	A	B	A
IIA-11	Me	2,4-Cl ₂ Ph	A	A	A	A	A
IIA-15	Me	3,4-OCH ₂ OPh	A	A	A	B	A
IIA-8	Me	4-FPh	A	A	A	A	A
IIA-16	Et	4-FPh	A	A	A	B	A

^a Inhibitory potency (%) against the growth of plants at a rate of 1.5 kg ai/ha in the greenhouse was expressed as four scales—A: 90–100 %, B: 75–89 %, C: 50–74 %, D: <50 %

^b Bra: rape; Amr: common amaranth; Med: clover; Ech: barnyard grass; Dig: crab grass

Table 3.9 Structure and post-emergence herbicidal activity of lithium *O*-alkyl 1-(2,4-dichlorophenoxy)alkylphosphonates **IIA**^a

Compound	R	R ³	Dicotyledon			Monocotyledon	
			Bra ^b	Amr ^b	Med ^b	Ech ^b	Dig ^b
IIA-1	Me	H	C	C	C	D	D
IIA-2	Me	Me	B	C	B	C	C
IIA-4	Me	Ph	B	C	B	C	D
IIA-5	Me	4-MePh	B	B	C	C	D
IIA-6	Me	3-NO ₂ Ph	B	B	C	D	D
IIA-9	Me	2-ClPh	B	C	B	D	D
IIA-11	Me	2,4-Cl ₂ Ph	B	C	B	D	D
IIA-15	Me	3,4-OCH ₂ OPh	B	C	B	D	D
IIA-8	Me	4-FPh	A	A	A	B	D
IIA-16	Et	4-FPh	A	A	A	D	D

^a Inhibitory potency (%) against the growth of plants at a rate of 1.5 kg ai/ha in the greenhouse was expressed as four scales—A: 90–100 %, B: 75–89 %, C: 50–74 %, D: <50 %

^b Bra: rape; Amr: common amaranth; Med: clover; Ech: barnyard grass; Dig: crab grass

(C) SAR analysis for **IIA**

When the optimized substituent Me as R and 2,4-Cl₂ on the phenoxy-benzene ring were kept, almost all of the lithium salts of phosphonic acids **IIA** showed good inhibitory activity against dicotyledons and monocotyledons for pre-emergence at 1.5 kg ai/ha or against the root of cabbage type rape and barnyard grass at 10 mg/L as shown in Tables 3.7 and 3.8. The difference in the R (or R² in the structure **Io**) seemed to have no significant influence on pre-emergence herbicidal activity. As shown in Table 3.9, **IIA** showed moderate to weak post-emergence activity against dicotyledons and monocotyledons. **IIA-1** (R³=H) with no substituent on α-C of phosphorus showed poor inhibitory activity. By the modification of substituent R³, **IIA-8** (R³=4-FPh) and **IIA-16** (R³=4-FPh) displayed significant post-emergence herbicidal activity (>90 %) against dicotyledons. This implied that the structure of lithium salts of phosphonic acids with R=Me, Y_n=2,4-Cl₂ and R³=4-FPh was beneficial to the post-emergence herbicidal activity against dicotyledons.

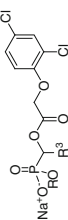
The above observations showed lithium salts of phosphonic acids **IIA** had much better pre-emergence herbicidal activity against dicotyledons and monocotyledons than their post-emergence herbicidal activity. Only a few **IIA** exhibited significant post-emergence activity against dicotyledons, but all **IIA** displayed poor post-emergence herbicidal activity against monocotyledons at 1.5 kg ai/ha.

3.1.5.2 Herbicidal Activity of Sodium *O*-Alkyl 1-(2,4-Dichlorophenoxyacetoxy)Alkylphosphonates **IIB** and **IIC**

The results of a preliminary bioassay by the Petri dish method are shown in Table 3.10. **IIB** displayed good activity (>90 %) against the root of barnyard grass and cabbage type rape at 10 mg/L. **IIC** displayed moderate to weak activity (<80 %) against the root of barnyard grass and cabbage type rape at 10 mg/L. All tested **IIB** in Table 3.10 displayed higher activity (>90 %) against the stem of cabbage type rape than that of barnyard grass at 10 mg/L, but only **IIC-4** (R=Et, R³=4-MeOPh) in **IIC** showed scale B activity (75–89 %) against the stem of cabbage type rape.

(A) Pre-emergence herbicidal activity of **IIB** and **IIC**

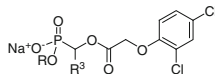
As shown in Table 3.11, most **IIB** displayed significant pre-emergence herbicidal activity (>90 %) against dicotyledons and monocotyledons at 1.5 kg ai/ha. Most **IIB** in Table 3.11 showed good inhibitory activity (>90 %) against all the tested five plants; however, **IIB-21** was almost inactive against all the tested plants and **IIB-3** showed weak herbicidal activity against clover and barnyard grass. Among **IIC** in Table 3.11, **IIC-7** showed the best pre-emergence activity (>90 %) against all the tested plants. Compared with **IIB**, most **IIC** showed relatively weaker pre-emergence activity than that of **IIB**.

Table 3.10 Inhibitory activity of sodium *O*-alkyl 1-(2,4-dichlorophenoxyacetoxy)alkylphosphonates **IIB** and **IIC** against the growth of plants^a

Compound	R	R ³	Root						Stem					
			Brn ^b			Ech ^b			Brn ^b			Ech ^b		
			100 mg/L	10 mg/L	10 mg/L	100 mg/L	10 mg/L	10 mg/L	100 mg/L	10 mg/L	10 mg/L	100 mg/L	10 mg/L	100 mg/L
IIB-5	Me	<i>i</i> -Pr	100	98	92	95	94	94	83	13	17			
IIB-15	Me	3-ClPh	99	99	97	97	94	89	17	17				
IIB-17	Me	2,3-Cl ₂ Ph	99	99	97	100	94	89	52	57				
IIB-23	Me	Pyrid-3-yl	100	99	97	100	100	91	83	0				
IIB-24	Me	Pyrid-4-yl	100	99	97	97	100	94	26	22				
IIC-1	Et	Ph	89	50	65	93	69	12	47	30				
IIC-4	Et	4-MeOPh	100	99	67	98	98	79	80	47				
IIC-6	Et	2,4-Cl ₂ Ph	100	49	65	100	100	19	93	60				
IIC-8	Et	3,4-OCH ₂ OPh	88	48	51	84	62	5	10	3				

^a Inhibitory potency (%) against the growth of plants in Petri dishes, 0 (no effect), 100 % (completely kill)^b Brn: cabbage type rape; Ech: barnyard grass

Table 3.11 Structure and pre-emergence herbicidal activity of sodium *O*-alkyl 1-(2,4-dichlorophenoxy)acetoxy)alkylphosphonates **IIB** and **IIC**^a



Compound	R	R ³	Dicotyledon			Monocotyledon	
			Bra ^b	Amr ^b	Med ^b	Ech ^b	Dig ^b
IIB-1	Me	H	A	A	A	A	A
IIB-2	Me	Me	A	A	A	A	A
IIB-3	Me	Et	B	A	D	D	A
IIB-4	Me	<i>n</i> -Pr	A	A	A	A	A
IIB-6	Me	<i>n</i> -Bu	A	A	A	A	A
IIB-7	Me	CCl ₃	A	A	A	A	A
IIB-8	Me	Ph	A	A	A	A	A
IIB-9	Me	4-MePh	A	A	A	A	A
IIB-10	Me	3-NO ₂ Ph	A	A	A	B	A
IIB-11	Me	4-NO ₂ Ph	A	B	A	A	A
IIB-12	Me	4-MeOPh	A	A	A	B	A
IIB-13	Me	4-FPh	A	A	A	A	A
IIB-14	Me	2-ClPh	A	A	A	A	A
IIB-16	Me	4-ClPh	A	A	A	A	A
IIB-18	Me	2,4-Cl ₂ Ph	A	A	A	A	A
IIB-19	Me	3,4-Cl ₂ Ph	A	A	A	A	A
IIB-20	Me	Fur-2-yl	A	A	A	A	A
IIB-21	Me	Thien-2-yl	D	D	D	D	D
IIB-22	Me	Pyrid-2-yl	A	A	A	A	A
IIB-25	Me	3,4-OCH ₂ OPh	A	A	A	A	A
IIC-2	Et	4-MePh	A	A	A	B	A
IIC-3	Et	3-NO ₂ Ph	A	A	A	C	B
IIC-5	Et	4-FPh	A	A	C	C	A
IIC-7	Et	Pyrid-2-yl	A	A	A	A	A

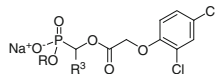
^a Inhibitory potency (%) against the growth of plants at a rate of 1.5 kg ai/ha in the greenhouse was expressed as four scales—A: 90–100 %, B: 75–89 %, C: 50–74 %, D: <50 %

^b Bra: rape; Amr: common amaranth; Med: clover; Ech: barnyard grass; Dig: crab grass

(B) Post-emergence herbicidal activity of **IIB** and **IIC**

All tested **IIB** in Table 3.12, showed higher post-emergence activity against dicotyledons than monocotyledons.

Especially for **IIB-1** (R=Me, R³=H), **IIB-2** (R=Me, R³=Me), **IIB-4** (R=Me, R³=*n*-Pr), **IIB-6** (R=Me, R³=*n*-Bu), **IIB-8** (R=Me, R³=Ph), **IIB-13** (R=Me, R³=4-FPh), **IIB-20** (R=Me, R³=fur-2-yl), and **IIB-25** (R=Me, R³=3,4-OCH₂OPh), they showed good inhibitory activity (>90 %) against three dicotyledonous plants, while showed weak inhibitory effect (<75 or <50 %) against monocotyledons. **IIC** showed weak inhibitory activity (<75 or <50 %) against all the tested dicotyledons and

Table 3.12 Structure and post-emergence herbicidal activity of sodium *O*-alkyl 1-(2,4-dichlorophenoxy)alkylphosphonates **IIB** and **IIC**^a

Compound	R	R ³	Dicotyledon			Monocotyledon	
			Bra ^b	Amr ^b	Med ^b	Ech ^b	Dig ^b
IIB-1	Me	H	A	A	A	D	D
IIB-2	Me	Me	A	A	A	D	D
IIB-3	Me	Et	D	A	A	D	D
IIB-4	Me	<i>n</i> -Pr	A	A	A	D	D
IIB-6	Me	<i>n</i> -Bu	A	A	A	C	C
IIB-7	Me	CCl ₃	B	A	A	D	D
IIB-8	Me	Ph	A	A	A	D	C
IIB-9	Me	4-MePh	A	B	A	C	D
IIB-10	Me	3-NO ₂ Ph	A	A	B	D	D
IIB-11	Me	4-NO ₂ Ph	C	A	C	D	C
IIB-12	Me	4-MeOPh	C	A	A	D	D
IIB-13	Me	4-FPh	A	A	A	C	D
IIB-14	Me	2-ClPh	C	B	B	D	D
IIB-16	Me	4-ClPh	B	A	A	D	D
IIB-18	Me	2,4-Cl ₂ Ph	A	A	B	D	D
IIB-19	Me	3,4-Cl ₂ Ph	A	A	B	D	D
IIB-20	Me	Fur-2-yl	A	A	A	C	C
IIB-21	Me	Thien-2-yl	D	D	D	D	D
IIB-22	Me	Pyrid-2-yl	C	A	A	D	D
IIB-25	Me	3,4-OCH ₂ OPh	A	A	A	D	C
IIC-2	Et	4-MePh	C	C	C	D	D
IIC-3	Et	3-NO ₂ Ph	C	D	C	D	D
IIC-5	Et	4-FPh	C	C	C	D	D
IIC-7	Et	Pyrid-2-yl	B	C	C	D	D

^a Inhibitory potency (%) against the growth of plants at a rate of 1.5 kg ai/ha in the greenhouse was expressed as four scales—A: 90–100 %, B: 75–89 %, C: 50–74 %, D: <50 %

^b Bra: rape; Amr: common amaranth; Med: clover; Ech: barnyard grass; Dig: crab grass

monocotyledons. Only **IIC-7** (R=Me, R³=pyrid-2-yl) showed scale B activity (75–89 %) against rape. **IIB-21** (R=Me, R³=thien-2-yl) was the worst herbicidal compound among **IIB** and **IIC**.

(C) SAR analysis for **IIB** and **IIC**

When the optimized substituent 2,4-Cl₂ on the phenoxy-benzene ring was kept, most of **IIB** and **IIC** showed moderate to good pre-emergence herbicidal activity against dicotyledons and monocotyledons, as shown in Tables 3.10 and 3.11. Different R³ groups had significant effect on pre-emergence herbicidal activity. Especially, Et and thien-2-yl as R³, **IIB-3** (R³=Et) showed a sharp decrease in pre-

emergence herbicidal activity against clover and barnyard grass, and **IIB-21** (R^3 =thien-2-yl) was almost inactive in pre-emergence applications.

For post-emergence application, shown in Table 3.12, when Me as R and 2,4-Cl₂ on the phenoxy-benzene ring were kept, **IIB-1** (R^3 =H), **IIB-2** (R^3 =Me), **IIB-4** (R^3 =*n*-Pr), **IIB-6** (R^3 =*n*-Bu), **IIB-8** (R^3 =Ph), **IIB-13** (R^3 =4-FPh), **IIB-20** (R^3 =fur-2-yl), and **IIB-25** (R^3 =3,4-OCH₂OPh) displayed good inhibitory activity against dicotyledons. However, compounds with other substituents as R^3 showed a decrease in post-emergence herbicidal activity. Especially, **IIB-21** (R^3 =thien-2-yl) showed the worst herbicidal activity to all the weed species for pre-emergence and post-emergence applications, implying the thien-2-yl group as R^3 is unfavorable to herbicidal activity.

As shown in Table 3.12, when R^3 was kept same, **IIB-9** (R=Me), **IIB-10** (R=Me), **IIB-13** (R=Me), and **IIB-22** (R=Me) showed higher post-emergence activity than corresponding **IIC-2** (R=Et), **IIC-3** (R=Et), **IIC-5** (R=Et), and **IIC-7** (R=Et). This result implied that Me as R (or R^2 in the structure **I**) in sodium salts of phosphonic acids is beneficial to post-emergence herbicidal activity.

The above observations indicated that herbicidal activity of sodium salts of phosphonic acids **IIB** and **IIC** could also be greatly affected by the modification of R (or R^2 in the structure **I**) and R^3 in the phosphonate moiety even if 2,4-Cl₂ on the phenoxy-benzene ring was kept.

Comparing the results shown in Tables 3.10, 3.11 and 3.12, sodium salts of phosphonic acids **IIB** and **IIC** inhibited the growth of tested dicotyledons and monocotyledons in pre-emergence application more strongly than in post-emergence application. Some of **IIB** exhibited significant post-emergence activity against dicotyledons, but all **IIB** and **IIC** displayed poor post-emergence inhibitory effect against monocotyledons.

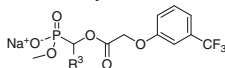
3.1.5.3 Herbicidal Activity of Sodium *O*-Methyl 1-(3-Trifluoromethylphenoxyacetoxy)Alkylphosphonates **IID**

(A) Pre-emergence herbicidal activity of **IID**

As shown in Table 3.13, most **IID** displayed weak pre-emergence herbicidal activity against dicotyledons and monocotyledons at 1.5 kg ai/ha. Most of them showed inhibitory activity in C or D grade (<75 or <50 %) against the tested plants. Only **IID-4** (R^3 =3-NO₂Ph) showed good inhibitory activity in A grade (>90 %) against crab grass and in B grade against common amaranth and clover. Moreover, **IID-7** (R^3 =4-ClPh), **IID-8** (R^3 =pyrid-2-yl), and **IID-9** (R^3 =3,4-OCH₂OPh) showed inhibitory activity in B grade against common amaranth.

(B) Post-emergence herbicidal activity of **IID**

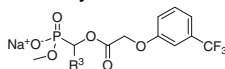
As shown in Table 3.14, most **IID** showed weak post-emergence herbicidal activity, the inhibitory activity of **IID** against dicotyledons was slightly higher than

Table 3.13 Structure and pre-emergence herbicidal activity of sodium *O*-methyl 1-(3-trifluoromethylphenoxy)alkylphosphonates **IID**^a

Compound	R ³	Dicotyledon			Monocotyledon	
		Bra ^b	Amr ^b	Med ^b	Ech ^b	Dig ^b
IID-1	Me	D	C	D	D	D
IID-2	Et	C	D	D	D	D
IID-3	4-MePh	D	C	C	D	D
IID-4	3-NO ₂ Ph	D	B	B	D	A
IID-5	4-NO ₂ Ph	D	C	D	D	D
IID-6	2-ClPh	D	D	D	D	D
IID-7	4-ClPh	B	B	D	D	D
IID-8	Pyrid-2-yl	D	B	D	D	C
IID-9	3,4-OCH ₂ OPh	C	B	D	D	C

^a Inhibitory potency (%) against the growth of plants at a rate of 1.5 kg ai/ha in the greenhouse was expressed as four scales—A: 90–100 %, B: 75–89 %, C: 50–74 %, D: <50 %

^b Bra: rape; Amr: common amaranth; Med: clover; Ech: barnyard grass; Dig: crab grass

Table 3.14 Structure and post-emergence herbicidal activity of sodium *O*-methyl 1-(3-trifluoromethylphenoxy)alkylphosphonates **IID**^a

Compound	R ³	Dicotyledon			Monocotyledon	
		Bra ^b	Amr ^b	Med ^b	Ech ^b	Dig ^b
IID-1	Me	C	C	B	D	D
IID-2	Et	D	D	B	D	D
IID-3	4-MePh	C	C	B	D	D
IID-4	3-NO ₂ Ph	C	C	B	D	D
IID-5	4-NO ₂ Ph	D	D	D	D	D
IID-6	2-ClPh	D	C	D	D	D
IID-7	4-ClPh	B	A	B	D	D
IID-8	Pyrid-2-yl	C	D	C	D	D
IID-9	3,4-OCH ₂ OPh	B	A	B	D	D

^a Inhibitory potency (%) against the growth of plants at a rate of 1.5 kg ai/ha in the greenhouse was expressed as four scales—A: 90–100 %, B: 75–89 %, C: 50–74 %, D: <50 %

^b Bra: rape; Amr: common amaranth; Med: clover; Ech: barnyard grass; Dig: crab grass

that against monocotyledons in post-emergence application. **IID-7** (R³=4-ClPh) and **IID-9** (R³=3,4-OCH₂OPh) showed post-emergence inhibitory activity in A and B grade against three dicotyledonous weeds. **IID-1** (R³=Me), **IID-2** (R³=Et), **IID-3** (R³=4-MePh), and **IID-4** (R³=3-NO₂Ph) showed inhibitory activity in B grade only against dicotyledonous clover. All tested **IID** displayed poor post-emergence inhibitory activity in D grade against monocotyledon at 1.5 kg ai/ha.

(C) *SAR analysis for IID*

As shown in Tables 3.13 and 3.14, most **IID** displayed weak pre-emergence herbicidal activity against tested weeds, especially for monocotyledons. Only **IID-4** ($R^3=3\text{-NO}_2\text{Ph}$) reached A grade against crab grass for pre-emergence application. **IID-7** ($R^3=4\text{-ClPh}$) and **IID-9** ($R^3=3,4\text{-OCH}_2\text{OPh}$) reached A grade against common amaranth for post-emergence application. The other compounds just showed post-emergence inhibitory activity in B to D grade. The herbicidal activity of **IID** with CF_3 on the phenoxy-benzene ring was apparently weaker than that of **IIA**, **IIb** and **IIc** that with $2,4\text{-Cl}_2$ on the phenoxy-benzene ring. It showed that $2,4\text{-Cl}_2$ on the phenoxy-benzene ring is still beneficial to the herbicidal activity of sodium salts of phosphonic acids.

3.1.5.4 Herbicidal Activity of Potassium *O*-Methyl 1-(Substituted Phenoxyacetoxy)Alkylphosphonates **IIe**

As a preliminary bioassay, some of **IIe** were tested for inhibitory activity against barnyard grass and cabbage type rape by the Petri dish method. The results are listed in Table 3.15.

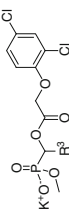
IIe-2 and **IIe-3** displayed good activity (>90 %) against the root of barnyard grass and cabbage type rape at 10 mg/L. **IIe-12** only had >90 % activity against the root of cabbage type rape. **IIe-2**, **IIe-3**, and **IIe-12** displayed much better activity (89–94 %) against the stem of cabbage type rape than that against barnyard grass (<35 %) at 10 mg/L.

(A) *Pre-emergence herbicidal activity of IIe*

As shown in Table 3.16, most **IIe** displayed moderate-to-good pre-emergence herbicidal activity against dicotyledons and monocotyledons at 1.5 kg ai/ha. **IIe-7** ($R^3=4\text{-MePh}$, $Y_n=2,4\text{-Cl}_2$) **IIe-10** ($R^3=2\text{-ClPh}$, $Y_n=2,4\text{-Cl}_2$), **IIe-16** ($R^3=\text{thien-2-yl}$, $Y_n=2,4\text{-Cl}_2$) and **IIe-19** ($R^3=3,4\text{-OCH}_2\text{OPh}$, $Y_n=2,4\text{-Cl}_2$) showed >90 % pre-emergence herbicidal activity against all the tested species. However, **IIe-4** ($R^3=n\text{-Pr}$, $Y_n=2,4\text{-Cl}_2$), **IIe-5** ($R^3=\text{Ph}$, $Y_n=3\text{-CF}_3$) and **IIe-13** ($R^3=2,4\text{-Cl}_2\text{Ph}$, $Y_n=3\text{-CF}_3$) showed much weaker inhibitory activity (<75 or <50 %). Other compounds displayed moderate pre-emergence herbicidal activity.

(B) *Post-emergence herbicidal activity of IIe*

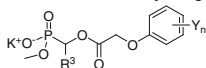
As shown in Table 3.17, post-emergence herbicidal activity of compounds **IIe** against dicotyledons was higher than that against monocotyledons. **IIe-6** ($R^3=\text{Ph}$) showed >90 % inhibitory activity against three dicotyledonous weeds; **IIe-1** ($R^3=\text{H}$), **IIe-8** ($R^3=3\text{-NO}_2\text{Ph}$), and **IIe-16** ($R^3=\text{thien-2-yl}$) showed >90 % inhibitory activity against rape and common amaranth; **IIe-11** ($R^3=4\text{-ClPh}$), and **IIe-14** ($R^3=2,4\text{-Cl}_2\text{Ph}$) showed >90 % inhibitory activity only against common amaranth. Most of **IIe** showed <75 or <50 % inhibitory activity against monocotyledons, except **IIe-6** ($R^3=\text{Ph}$) with >90 % inhibitory activity against monocotyledonous crab grass.

Table 3.15 Inhibitory activity of potassium *O*-methyl 1-(substituted phenoxyacetoxymethyl)alkylphosphonates **III** against the growth of plants^a

Compound	R ³	Root			Stem					
		Brm ^b			Brm ^b					
		100 mg/L	10 mg/L	Ech ^b	100 mg/L	10 mg/L	Ech ^b			
III-2	Me	100	99	100 mg/L	10 mg/L	97	100 mg/L	10 mg/L	100 mg/L	10 mg/L
III-3	Et	99	99	100	100	95	94	83	13	
III-12	2,3-Cl ₂ Ph	99	99	100	64	95	57	35		

^a Inhibitory potency (%) against the growth of plants in Petri dishes, 0 (no effect), 100 % (completely kill)^b Brm: cabbage type rape; Ech: barnyard grass

Table 3.16 Structure and pre-emergence herbicidal activity of potassium *O*-methyl 1-(substituted phenoxyacetoxy)alkylphosphonates **III**^a



Compound	R ³	Y _n	Dicotyledon			Monocotyledon	
			Bra ^b	Amr ^b	Med ^b	Ech ^b	Dig ^b
III-1	H	2,4-Cl ₂	A	A	A	B	A
III-4	<i>n</i> -Pr	2,4-Cl ₂	D	D	D	D	D
III-5	Ph	3-CF ₃	D	D	D	D	D
III-6	Ph	2,4-Cl ₂	A	A	A	B	A
III-7	4-MePh	2,4-Cl ₂	A	A	A	A	A
III-8	3-NO ₂ Ph	2,4-Cl ₂	A	B	A	A	A
III-9	4-MeOPh	2,4-Cl ₂	B	D	D	C	C
III-10	2-ClPh	2,4-Cl ₂	A	A	A	A	A
III-11	4-ClPh	2,4-Cl ₂	B	A	A	A	A
III-13	2,4-Cl ₂ Ph	3-CF ₃	C	D	D	D	D
III-14	2,4-Cl ₂ Ph	2,4-Cl ₂	B	A	A	B	A
III-15	Fur-2-yl	2,4-Cl ₂	D	C	A	B	A
III-16	Thien-2-yl	2,4-Cl ₂	A	A	A	A	A
III-17	Pyrid-2-yl	3-CF ₃	B	B	D	C	C
III-18	Pyrid-2-yl	2,4-Cl ₂	A	B	A	A	A
III-19	3,4-OCH ₂ Oph	2,4-Cl ₂	A	A	A	A	A

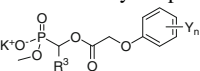
^a Inhibitory potency (%) against the growth of plants at a rate of 1.5 kg ai/ha in the greenhouse was expressed as four scales—A: 90–100 %, B: 75–89 %, C: 50–74 %, D: <50 %

^b Bra: rape; Amr: common amaranth; Med: clover; Ech: barnyard grass; Dig: crab grass

The above observations indicated that most of **III** influenced the growth of tested plants in pre-emergence application more strongly than they did in post-emergence application, but **III-4** (R³=*n*-Pr) and **III-9** (R³=4-MeOPh) exhibited the reverse responses against clover as well as **III-15** (R³=fur-2-yl) against rape and common amaranth.

(C) SAR analysis for **III**

As shown in Tables 3.15, 3.16, and 3.17, both R³ in the phosphonate moiety and Y_n on the phenoxy-benzene ring have an obvious impact on the herbicidal activity. All potassium salts of phosphonic acids **III** with Y_n=3-CF₃ exhibited weak inhibitory activity against dicotyledons and monocotyledons in pre-emergence and post-emergence applications at 1.5 kg ai/ha. Most **III** with Y_n=2,4-Cl₂ exhibited significant herbicidal activity against all tested dicotyledons and monocotyledons in pre-emergence application except **III-4** (R³=*n*-Pr), **III-9** (R³=4-MeOPh), and **III-15** (R³=fur-2-yl). Most potassium salts of phosphonates **III** with Y_n=2,4-Cl₂ showed weaker post-emergence herbicidal activity than their pre-emergence herbicidal activity against dicotyledons, and especially had no post-emergence herbicidal activity against monocotyledons at 1.5 kg ai/ha. Only **III-6** (R³=Ph, Y_n=2,4-Cl₂) was found to exhibit significant herbicidal activity against all tested dicotyledons and

Table 3.17 Structure and post-emergence herbicidal activity of potassium *O*-methyl 1-(substituted phenoxyacetoxy)alkylphosphonates **III**^a


Compound	R ³	Y _n	Dicotyledon			Monocotyledon	
			Bra ^b	Amr ^b	Med ^b	Ech ^b	Dig ^b
III-1	H	2,4-Cl ₂	A	A	C	C	B
III-4	<i>n</i> -Pr	2,4-Cl ₂	C	D	A	D	D
III-5	Ph	3-CF ₃	D	D	D	D	D
III-6	Ph	2,4-Cl ₂	A	A	A	C	A
III-7	4-MePh	2,4-Cl ₂	B	C	C	D	D
III-8	3-NO ₂ Ph	2,4-Cl ₂	A	A	C	C	C
III-9	4-MeOPh	2,4-Cl ₂	C	D	B	D	C
III-10	2-ClPh	2,4-Cl ₂	B	B	B	D	D
III-11	4-ClPh	2,4-Cl ₂	B	A	C	C	C
III-13	2,4-Cl ₂ Ph	3-CF ₃	D	D	D	D	D
III-14	2,4-Cl ₂ Ph	2,4-Cl ₂	B	A	C	D	D
III-15	Fur-2-yl	2,4-Cl ₂	B	A	A	D	C
III-16	Thien-2-yl	2,4-Cl ₂	A	A	B	C	C
III-17	Pyrid-2-yl	3-CF ₃	D	C	C	D	D
III-18	Pyrid-2-yl	2,4-Cl ₂	C	B	D	D	D
III-19	3,4-OCH ₂ OPh	2,4-Cl ₂	B	C	B	D	C

^a Inhibitory potency (%) against the growth of plants at a rate of 1.5 kg ai/ha in the greenhouse was expressed as four scales—A: 90–100 %, B: 75–89 %, C: 50–74 %, D: <50 %

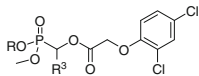
^b Bra: rape; Amr: common amaranth; Med: clover; Ech: barnyard grass; Dig: crab grass

monocotyledons except barnyard grass in post-emergence application. Apparently, the introduction of 2,4-Cl₂ on the phenoxy-benzene ring in potassium salts of phosphonic acids **III** is more beneficial to pre-emergence herbicidal activity.

3.1.5.5 Herbicidal Activity Analysis for IIA–III and IA

As shown in Table 3.18, herbicidal activity of **IIA–III** are compared with those of corresponding *O,O*-dimethyl phosphonates **IA**. Obviously, the introduction of Li, Na or K as R (or R¹ in the structure **Io**) resulted in a great change in herbicidal activity. Generally speaking, the pre-emergence herbicidal activity could be greatly enhanced by replacing Me with Li, Na or K as R¹ in the structure **Io**, but the same replacement had little effect on post-emergence herbicidal activity. For example, **IIA-1** (R=Li) and **IIIB-1** (R=Na) showed >90 % inhibitory activity against barnyard grass, while **IA-21** (R=Me) showed <50 % inhibitory activity for pre-emergence application. **IIA-4** (R=Li), **IIIB-8** (R=Na), and **III-6** (R=K) showed >90 % inhibitory activity against crab grass, while **IA-25** (R=Me) showed <50 % inhibitory activity for pre-emergence application. However, in some cases, the reverse response was also observed, that is **III-4** (R=K) showed <50 % inhibitory activity

Table 3.18 Structure and herbicidal activities of 1-(2,4-dichlorophenoxyacetoxymethyl)alkylphosphonates **IA** and **IIA–IIIE**^a



Compound	R	R ³	Pre-emergence			Post-emergence		
			Bra ^b	Ech ^b	Dig ^b	Bra ^b	Ech ^b	Dig ^b
IA-21	Me	H	A	D	A	A	D	D
IIA-1	Li	H	A	A	A	C	D	D
IIIB-1	Na	H	A	A	A	A	D	D
IIIE-1	K	H	A	B	A	A	C	B
IA-7	Me	Me	A	B	B	A	C	C
IIA-2	Li	Me	A	A	A	B	C	C
IIIB-2	Na	Me	A	A	A	A	D	D
IA-23	Me	<i>n</i> -Pr	A	B	B	A	C	C
IIA-4	Na	<i>n</i> -Pr	A	B	A	A	C	A
IIIE-4	K	<i>n</i> -Pr	D	A	A	C	C	D
IA-25	Me	Ph	A	D	D	A	D	D
IIA-4	Li	Ph	A	A	A	B	C	D
IIIB-8	Na	Ph	A	A	A	A	D	C
IIIE-6	K	Ph	A	B	A	A	C	A
IA-29	Me	2-ClPh	A	B	C	A	D	C
IIA-9	Li	2-ClPh	A	B	A	B	D	D
IIIB-14	Na	2-ClPh	A	A	A	C	D	D
IIIE-10	K	2-ClPh	A	A	A	B	D	D
IA-28	Me	4-ClPh	A	B	A	A	C	B
IIIB-16	Na	4-ClPh	A	A	A	B	D	D
IIIE-11	K	4-ClPh	B	A	A	B	C	C
IA-27	Me	4-MeOPh	D	D	D	D	D	D
IIIB-12	Na	4-MeOPh	A	B	A	C	D	D
IIIE-9	K	4-MeOPh	B	C	C	C	D	C
IA-26	Me	4-MePh	C	C	B	A	C	D
IIA-5	Li	4-MePh	A	A	A	B	C	D
IIIB-7	K	4-MePh	A	A	A	B	D	D
IA-33	Me	3-NO ₂ Ph	C	C	D	A	D	D
IIA-6	Li	3-NO ₂ Ph	A	A	A	B	D	D
IIIB-10	Na	3-NO ₂ Ph	A	B	A	A	D	D
IIIE-8	K	3-NO ₂ Ph	A	A	A	A	C	C

^a Inhibitory potency (%) against the growth of plants at a rate of 1.5 kg ai/ha in the greenhouse was expressed as four scales—A: 90–100 %, B: 75–89 %, C: 50–74 %, D: <50 %

^b Bra: rape; Ech: barnyard grass; Dig: crab grass

against rape, while compound **IA-23** (R=Me) showed >90 % inhibitory activity for pre-emergence application. The replacement of *O*-alkyl moiety by alkali metal salt in the 1-(2,4-dichlorophenoxyacetoxymethyl)alkylphosphonate **Io** is much beneficial to the pre-emergence herbicidal activity.

Comparing the herbicidal activity of salts of alkylphosphonic acids, in Table 3.18, the sodium salts of alkylphosphonic acids seem to have better activity than potassium and lithium salts of alkylphosphonic acids. Pre-emergence and post-emergence

herbicidal activity of some sodium salts of alkylphosphonic acids were further examined against common amaranth (*A. retroflexus*), chingma abutilon (*Abutilon theophrasti*), goosefoot (*Chenopodium album*), barnyard grass (*E. crusgalli*), and rice (*Oryza sativa*) at 450–75 g ai/ha in the greenhouse.

As shown in Table 3.19, sodium salts **IIA-1**, **IIA-2**, **IIA-3**, and **IIA-20** displayed moderate pre-emergence herbicidal activity (50–75 %) against common amaranth, chingma abutilon, and goosefoot, but very weak activity against monocotyledons (<35 %) at 450 g ai/ha. It was found that these sodium salts **IIA-1** (R=Na, R³=H), **IIA-2** (R=Na, R³=Me), **IIA-3** (R=Na, R³=Et), and **IIA-20** (R=Na, R³=fur-2-yl) displayed significant pre-emergence inhibitory potency against dicotyledons at 450 g ai/ha, but their corresponding *O,O*-dimethyl phosphonates **IC-1** (R=Me, R³=H), **IC-22** (R=Me, R³=Me), **IC-27** (R=Me, R³=Et) and **IG-21** (R=Me, R³=fur-2-yl) were no activity at 450 g ai/ha (Table 3.19). At 150–75g ai/ha, only **IIA-3** (R=Na, R³=Et) still showed pre-emergence herbicidal activity (50–65%) against tested dicotyledons, other sodium salts **IIA** lost activity.

As shown in Tables 3.20 and 3.21, **IIA-1** (R¹=Na, R³=H), **IIA-2** (R¹=Na, R³=Me), **IIA-3** (R¹=Na, R³=Et), **IIA-4** (R¹=Na, R³=*n*-Pr) and **IIA-20** (R¹=Na, R³=fur-2-yl) displayed good post-emergence herbicidal activity (>90 %) against common amaranth, chingma abutilon, and goosefoot comparable to their corresponding *O,O*-dimethyl phosphonates at 450 g ai/ha. The post-emergence herbicidal activity of these sodium salts decreased with the decrease of dose. They showed post-emergence herbicidal activity against tested dicotyledons comparable to or lower than their corresponding *O,O*-dimethyl phosphonates at 150–75 g ai/ha.

Among monosodium salts, **IIA-4** (R¹=Na, R³=*n*-Pr) showed best post-emergence herbicidal activity against tested dicotyledons at 150 g ai/ha. **IIA-1** (R¹=Na, R³=H), **IIA-2** (R¹=Na, R³=Me), **IIA-3** (R¹=Na, R³=Et), **IIA-4** (R¹=Na, R³=*n*-Pr) and **IIA-20** (R¹=Na, R³=fur-2-yl) displayed very weak post-emergence herbicidal activity against monocotyledons (0–50 %) at 450 g ai/ha and no post-emergence herbicidal activity against monocotyledons at 150–75 g ai/ha.

3.1.6 Summary

An efficient way to synthesize **IIA–III** containing a carboxylic ester group was devised by selective monodealkylation of *O,O*-dialkyl 1-(substituted phenoxy-acetoxy)alkylphosphonates with lithium bromide, sodium iodide or potassium iodide in refluxing acetone. 77 of the salts of *O*-alkyl 1-(substituted phenoxyacetoxy)alkylphosphonic acids **IIA–III** were synthesized by this way in considerable yields. Most of **IIA–III** showed notable pre-emergence herbicidal activity against tested dicotyledons and monocotyledons, and showed notable post-emergence herbicidal activity against dicotyledons at 1.5 kg ai/ha.

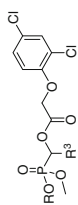


Table 3.19 Structure and pre-emergence herbicidal activity of 1-(2,4-dichlorophenoxyacetoxy)alkylphosphonates **IIB** and **IC**^a

Compound	R	R ³	Rate (g ai/ha)	Dicotyledon		Monocotyledon		
				Amr ^b	Abu ^b	Che ^b	Ech ^b	Ory ^b
IIB-1	Na	H	450	53	45	53	30	27
IC-1	Me	H	450	0	0	0	0	0
IIB-2	Na	Me	450	50	50	55	0	30
IC-22	Me	Me	450	0	0	10	45	35
IIB-3	Na	Et	450	70	70	75	0	30
IC-27	Me	Et	450	0	0	0	0	0
IIB-4	Na	<i>n</i> -Pr	450	0	0	0	0	25
IIB-20	Na	Fur-2-yl	450	55	50	50	0	35
IG-21	Me	Fur-2-yl	450	0	0	10	NT	NT
IIB-1	Na	H	150	0	0	0	0	10
IC-1	Me	H	150	0	0	0	0	0
IIB-2	Na	Me	150	0	0	0	0	25
IC-22	Me	Me	150	0	0	0	NT	NT
IIB-3	Na	Et	150	65	60	65	0	20
IIB-4	Na	<i>n</i> -Pr	150	0	0	0	0	10
IIB-20	Na	Fur-2-yl	150	0	0	0	0	10
IIB-1	Na	H	75	0	0	0	0	0
IC-1	Me	H	75	0	0	0	0	0

(continued)

Table 3.19 (continued)

Compound	R	R ³	Rate (g ai/ha)	Dicotyledon		Monocotyledon	
				Amr ^b	Abu ^b	Ech ^b	Ory ^b
IIB-2	Na	Me	75	0	0	0	10
IC-22	Me	Me	75	0	0	0	0
IIB-3	Na	Et	75	50	50	0	10
IIB-4	Na	<i>n</i> -Pr	75	0	0	0	0
IIB-20	Na	Fur-2-yl	75	0	0	0	0

^a Inhibitory potency (%) against the growth of plants in the greenhouse, 0 (no effect), 100 % (completely kill), NT (not tested)

^b Amr: common amaranth; Abu: chingma abutilon; Che: goosefoot; Ech: barnyard grass; Ory: rice

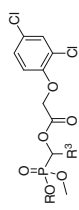


Table 3.20 Structure and post-emergence herbicidal activity of 1-(2,4-dichlorophenoxy)acetoxy/alkylphosphonates **IIB^a**

Compound	R	R ³	Rate (g ai/ha)	Dicotyledon		Monocotyledon		
				Amr ^b	Abu ^b	Che ^b	Ech ^b	Ory ^b
IIB-1	Na	H	450	91	93	93	10	12
IC-1	Me	H	450	100	100	100	0	0
IIB-2	Na	Me	450	99	98	97	50	27
IC-22	Me	Me	450	100	100	95	35	0
IIB-3	Na	Et	450	98	99	100	0	0
IIB-4	Na	<i>n</i> -Pr	450	100	100	100	0	0
IIB-20	Na	Fur-2-yl	450	93	100	100	50	45
IG-21	Me	Fur-2-yl	450	98	100	100	25	10
IIB-1	Na	H	150	83	93	93	0	0
IC-1	Me	H	150	95	98	100	0	0
IIB-2	Na	Me	150	73	93	88	0	0
IC-22	Me	Me	150	65	95	90	0	0
IIB-3	Na	Et	150	83	93	95	0	0
IIB-4	Na	<i>n</i> -Pr	150	98	100	100	0	0
IIB-20	Na	Fur-2-yl	150	63	88	93	0	0
IG-21	Me	Fur-2-yl	150	90	100	95	0	0
IIB-1	Na	H	75	63	78	83	0	0
IC-1	Me	H	75	55	85	85	0	0

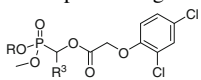
(continued)

Table 3.20 (continued)

Compound	R	R ³	Rate (g ai/ha)	Dicotyledon		Monocotyledon	
				Amr ^b	Abu ^b	Ech ^b	Ory ^b
IIB-2	Na	Me	75	83	78	83	0
IC-22	Me	Me	75	45	85	85	0
IIB-3	Na	Et	75	53	83	93	0
IIB-4	Na	<i>n</i> -Pr	75	61	53	100	0
IIB-20	Na	Fur-2-yl	75	53	78	83	0
IG-21	Me	Fur-2-yl	75	55	50	85	0

^a Inhibitory potency (%) against the growth of plants in the greenhouse, 0 (no effect), 100 % (completely kill)

^b Amr: common amaranth; Abu: chingma abutilon; Che: goosefoot; Ech: barnyard grass; Ory: rice

Table 3.21 Structure and post-emergence herbicidal activity of 1-(2,4-dichlorophenoxyacetoxy)alkylphosphonates^a


Compound	R	R ³	Y _n	Amr ^b	Bra ^b	Pis ^b
IC-22	Me	Me	2,4-Cl ₂	100	100	98
IIB-2	Na	Me	2,4-Cl ₂	100	98	72
IC-1	Me	H	2,4-Cl ₂	98	100	88
IIB-1	Na	H	2,4-Cl ₂	93	92	53
IG-21	Me	Fur-2-yl	2,4-Cl ₂	97	100	90
IID-10	Na	Fur-2-yl	2,4-Cl ₂	93	100	98

^a Inhibitory potency (%) against the growth of plants at a rate of 450 g ai/ha in the greenhouse, 0 (no effect), 100 % (completely kill)

^b Amr: common amaranth; Bra: rape; Pis: pea

The pre-emergence herbicidal activity could be enhanced by replacing Me by Li, Na, or K as R¹ in *O,O*-dimethyl 1-(substituted phenoxyacetoxy)alkylphosphonates, but the same replacement had little effect on post-emergence herbicidal activity. The 2,4-Cl₂ substituents on the phenoxy-benzene ring were beneficial to the herbicidal activity, while the 3-CF₃ substituent led the salts of *O*-alkyl 1-(substituted phenoxyacetoxy)alkylphosphonic acids to have weak inhibitory activity.

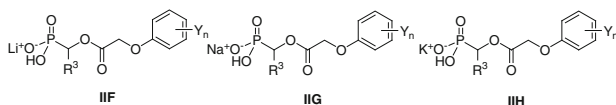
IIB-1 (R¹=Na, R³=H), **IIB-2** (R¹=Na, R³=Me), **IIB-3** (R¹=Na, R³=Et), **IIB-4** (R¹=Na, R³=*n*-Pr) and **IIB-20** (R¹=Na, R³=fur-2-yl) with 2,4-Cl₂ on the phenoxy-benzene displayed 50–75 % pre-emergence herbicidal activity against tested dicotyledons. However their corresponding *O,O*-dimethyl phosphonates had no pre-emergence activity at 450 g ai/ha. These **IIB** had >90 % post-emergence herbicidal activity comparable to their corresponding *O,O*-dimethyl phosphonates at the same dose. Some sodium salts of *O*-methyl 1-(2,4-dichlorophenoxyacetoxy)alkylphosphonic acids were further found to be potent PDHc inhibitors (see Chap. 7).

3.2 Alkali Metal Salts of Alkylphosphonic Acids IIF, IIG and IIH

3.2.1 Introduction

As stated in Sect. 3.1, alkali metal salts of *O*-alkyl 1-(substituted phenoxyacetoxy)alkylphosphonic acids showed notable herbicidal activity. Based on the bioisosterism, 1-alkylphosphonic acid was assumed to have better herbicidal activity, because it is more analogous to the pyruvic acid which acts as the substrate of PDHc.

However, the 1-(substituted phenoxyacetoxy)alkylphosphonic acids were not stable, because these compounds themselves were strong acids which would lead to the cleavage of carboxylate ester group. Alternatively, mono alkali metal salts of 1-(substituted phenoxyacetoxy)alkylphosphonic acids were designed including monolithium salts (**IIF-1–IIF-13**), monosodium salts (**IIG-1–IIG-13**), and monopotassium salts (**IIIH-1–IIIH-13**). These compounds were almost neutral salts with higher stability than the corresponding phosphonic acids (Scheme 3.9).



Scheme 3.9 Structure of mono alkali metal salts of 1-(substituted phenoxyacetoxy)alkylphosphonic acids **IIF**, **IIG** and **IIIH**

In this section, we describe the synthesis, herbicidal activity, and structure-activity relationships of mono alkali metal salts of 1-(substituted phenoxyacetoxy)alkylphosphonic acids **IIF**, **IIG** and **IIIH**.

3.2.2 Synthesis of **IIF**, **IIG** and **IIIH**

Mono alkali metal salts of phosphonic acids could be easily obtained from the corresponding phosphonic acids by the treatment with an equimolar inorganic base, such as lithium hydroxide, sodium hydroxide, and potassium carbonate. The phosphonic acids could be generally synthesized by the treatment with concentrated hydrochloric acid at high temperature. However, the method seems to be unfavorable to synthesize the compounds containing acid or base sensitive groups, i.e. carboxylate ester group in the molecule. As described in the literature [15–19], iodotrimethylsilane appears to be the best choice for the preparation of phosphonic acid from corresponding phosphonates via bis(trimethylsilyl)alkylphosphonates. In this reaction, two trimethylsilane groups were replaced by hydrogen with methanol. Iodotrimethylsilane could be easily obtained in situ by the treatment of chlorotrimethylsilane and sodium iodide in the solution of acetonitrile [15–19]. The synthetic route is shown in Scheme 3.10.

The prepared mono alkali metal salts of 1-(substituted phenoxyacetoxy)alkylphosphonic acids **IIF**, **IIG** and **IIIH** are listed in Tables 3.22, 3.23 and 3.24. A detailed synthetic procedure for mono alkali metal salts of 1-(substituted phenoxyacetoxy)alkylphosphonic acids **IIF**, **IIG** and **IIIH** is described in the Sect. 9.1.12 of Chap. 9.

The structure of mono alkali metal salts of 1-(substituted phenoxyacetoxy)alkylphosphonic acids **IIF**, **IIG** and **IIIH** was confirmed by elemental analysis and characterized by IR, ^1H NMR. Spectroscopic analysis of some of the representative **IIF**, **IIG** and **IIIH** is given in Sect. 3.2.3.

Scheme 3.10 Synthesis of mono alkali metal salts of 1-(substituted phenoxyacetoxy) alkylphosphonic acids **IIF**, **IIG** and **IIH**

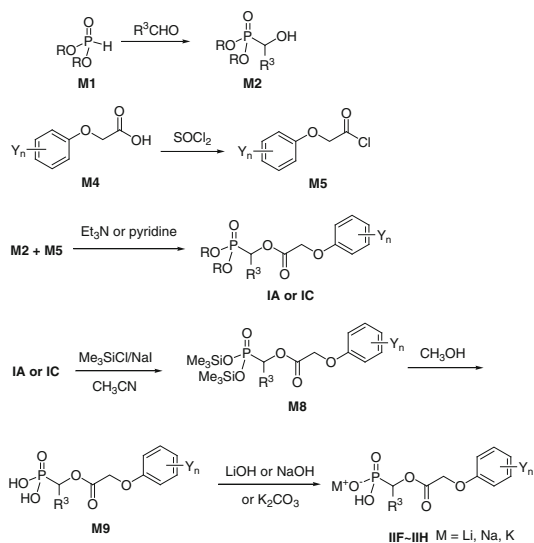
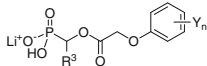


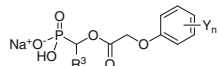
Table 3.22 Structure of mono lithium salts of 1-(substituted phenoxyacetoxy)alkylphosphonic acids **IIF**^a



Compound	R ³	Y _n	Compound	R ³	Y _n
IIF-1	Me	2,4-Cl ₂	IIF-8	Me	2-Me,4-Cl
IIF-2	Et	2,4-Cl ₂	IIF-9	Et	2-Me,4-Cl
IIF-3	<i>n</i> -Pr	2,4-Cl ₂	IIF-10	<i>n</i> -Pr	2-Me,4-Cl
IIF-4	<i>i</i> -Pr	2,4-Cl ₂	IIF-11	<i>i</i> -Pr	2-Me,4-Cl
IIF-5	<i>n</i> -Bu	2,4-Cl ₂	IIF-12	<i>n</i> -Bu	2-Me,4-Cl
IIF-6	Ph	2,4-Cl ₂	IIF-13	Ph	2-Me,4-Cl
IIF-7	Thien-2-yl	2,4-Cl ₂			

^a Synthesis for **IIF-1–IIF-13** [20]

Table 3.23 Structure of mono sodium salts of 1-(substituted phenoxyacetoxy)alkylphosphonic acids **IIG**^a



Compound	R ³	Y _n	Compound	R ³	Y _n
IIG-1	Me	2,4-Cl ₂	IIG-8	Me	2-Me,4-Cl
IIG-2	Et	2,4-Cl ₂	IIG-9	Et	2-Me,4-Cl
IIG-3	<i>n</i> -Pr	2,4-Cl ₂	IIG-10	<i>n</i> -Pr	2-Me,4-Cl
IIG-4	<i>i</i> -Pr	2,4-Cl ₂	IIG-11	<i>i</i> -Pr	2-Me,4-Cl
IIG-5	<i>n</i> -Bu	2,4-Cl ₂	IIG-12	<i>n</i> -Bu	2-Me,4-Cl
IIG-6	Ph	2,4-Cl ₂	IIG-13	Ph	2-Me,4-Cl
IIG-7	Thien-2-yl	2,4-Cl ₂			

^a Synthesis for **IIG-1–IIG-13** [21]

Table 3.24 Structure of mono potassium salts of 1-(substituted phenoxyacetoxy)alkylphosphonic acids **IIH**^a

$$\text{K}^+ \text{O}^- \text{P}(\text{OH})(\text{R}^3)\text{CH}_2\text{OCH}_2\text{C}_6\text{H}_4\text{Y}_n$$

Compound	R ³	Y _n	Compound	R ³	Y _n
IIH-1	Me	2,4-Cl ₂	IIH-8	Me	2-Me,4-Cl
IIH-2	Et	2,4-Cl ₂	IIH-9	Et	2-Me,4-Cl
IIH-3	<i>n</i> -Pr	2,4-Cl ₂	IIH-10	<i>n</i> -Pr	2-Me,4-Cl
IIH-4	<i>i</i> -Pr	2,4-Cl ₂	IIH-11	<i>i</i> -Pr	2-Me,4-Cl
IIH-5	<i>n</i> -Bu	2,4-Cl ₂	IIH-12	<i>n</i> -Bu	2-Me,4-Cl
IIH-6	Ph	2,4-Cl ₂	IIH-13	Ph	2-Me,4-Cl
IIH-7	Thien-2-yl	2,4-Cl ₂			

^a Synthesis for **IIH-1–IIH-13** [20]

3.2.3 Spectroscopic Analysis of IIF, IIG and IIH

The IR spectra of **IIF**, **IIG** and **IIH** showed normal stretching absorption bands indicating the existence of benzene ring ($\sim 1,620$, $\sim 1,450$ cm^{-1}), C–O–C ($1,080$ – $1,200$ cm^{-1}), and P–C (740 – 750 cm^{-1}). A sharp and weak band at $3,050$ – $3,100$ cm^{-1} accounted for the C–H stretching of the benzene ring. The C–H stretching of alkyl appeared at $2,860$ – $2,950$ cm^{-1} . A strong absorption near $1,720$ – $1,760$ cm^{-1} was identified for the absorption C=O. They also showed absorption bands at $3,300$ – $3,400$ cm^{-1} (OH) and the absorption at $\sim 1,200$ cm^{-1} was assigned to the P=O stretching absorption bands. The IR spectrum of **IIF-5** ($\text{R}^3 = n\text{-Bu}$, $\text{Y}_n = 2,4\text{-Cl}_2$) is shown in Fig. 3.7.

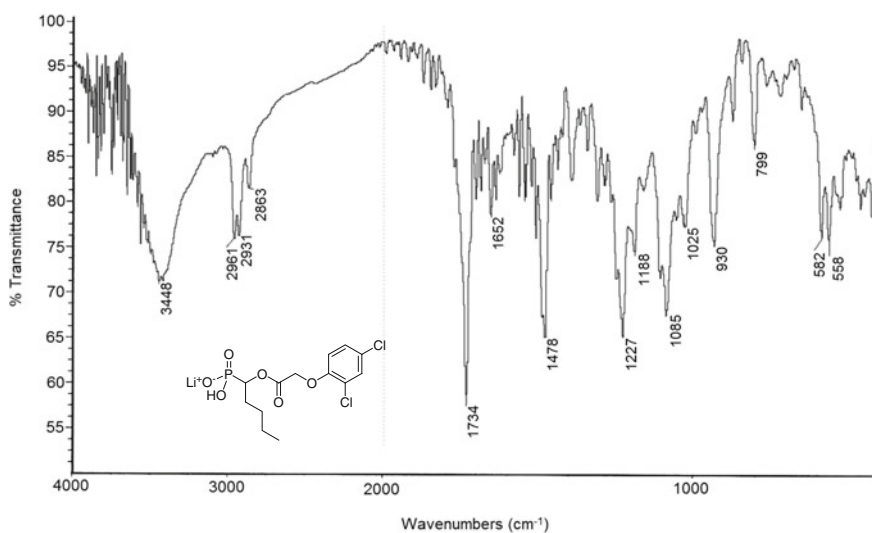


Fig. 3.7 IR spectrum of **IIF-5**

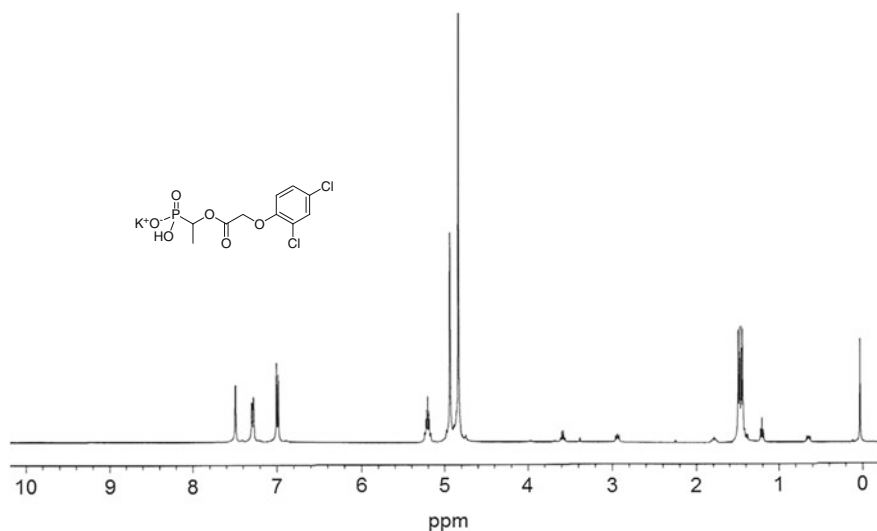


Fig. 3.8 ^1H NMR spectrum of **IIIH-1** (D_2O , 300 MHz)

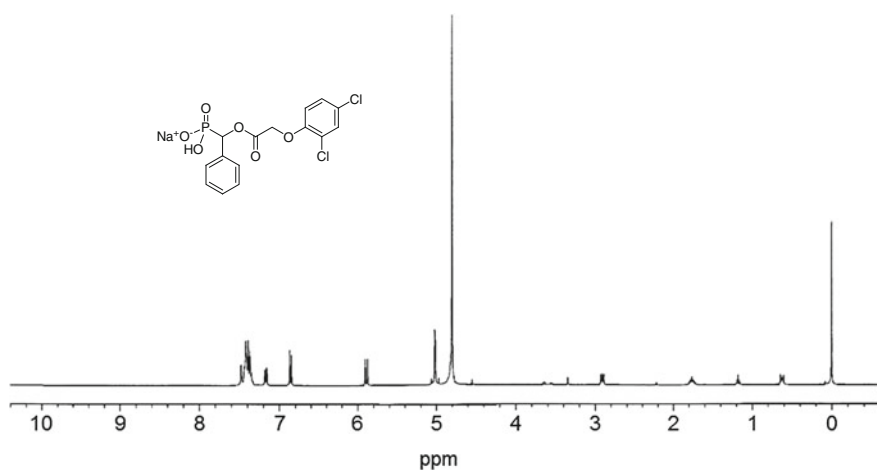


Fig. 3.9 ^1H NMR spectrum of **IIG-6** (D_2O , 300 MHz)

In the ^1H NMR spectra of **IIF**, **IIG** and **IIIH**, the chemical shifts of aromatic protons appeared at 6.8–7.8 ppm. As for the compounds with aliphatic groups as R^3 , the proton signal corresponding to OCHP displayed multiplets at 5.00–5.30 ppm, exemplified by **IIIH-1** ($\text{R}^3=\text{Me}$, $\text{Y}_n=2,4\text{-Cl}_2$) as shown in Fig. 3.8; as for the compounds with aromatic groups as R^3 , the proton signal appeared at

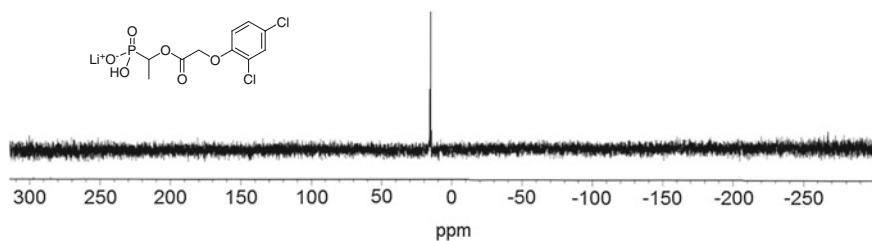


Fig. 3.10 ^{31}P NMR spectrum of **IIF-1** (D_2O , 162 MHz)

5.76–6.31 ppm as a doublet, due to the coupling with phosphorus. For example, ^1H NMR spectrum of **IIG-6** ($\text{R}^3=\text{Ph}$, $\text{Y}_n=2,4\text{-Cl}_2$) is shown in Fig. 3.9. ^{31}P NMR chemical shifts of **IIF**, **IIG** and **IIIH** appeared as a singlet at δ 15.5–16.2 ppm. Their chemical shifts moved upfield by approximately 7–8 ppm, compared with that of the corresponding *O,O*-dimethyl phosphonates at ~ 23 ppm. The ^{31}P NMR spectrum of **IIF-1** ($\text{R}^3=\text{Me}$, $\text{Y}_n=2,4\text{-Cl}_2$) is shown in Fig. 3.10.

3.2.4 Herbicidal Activity of **IIF**, **IIG** and **IIIH**

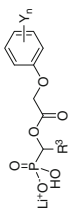
As a preliminary bioassay, all the mono salts of 1-substituted phosphonic acid **IIF**, **IIG** and **IIIH** were tested at 100–10 mg/L for inhibitory effect against barnyard grass (*E. crusgalli*) and cabbage type rape (*B. napus*) using the Petri dish method. The results are listed in Tables 3.25, 3.26 and 3.27.

As seen from Tables 3.25, 3.26 and 3.27, all **IIF**, **IIG** and **IIIH** showed >90 % of inhibition against the root of barnyard grass and cabbage type rape at 100–10 mg/L. All **IIF**, **IIG** and **IIIH** displayed higher inhibitory activity against the growth of the root than that of the stem of barnyard grass and cabbage type rape at 10 mg/L. All **IIF**, **IIG** and **IIIH** displayed higher post-emergence inhibition against the stem of cabbage type rape (80–89 %) than that of barnyard grass (<77 %) at 10 mg/L. For monocotyledons, **IIF**, **IIG** and **IIIH** against the root of barnyard grass reached 91–97 % inhibitory effect at 10 mg/L, while with much weaker inhibitory effect (<77 %) against the stem of barnyard grass.

(A) Post-emergence herbicidal activity of **IIF**, **IIG** and **IIIH**

Some of **IIF**, **IIG** and **IIIH** were selected for further examination in the greenhouse. They were evaluated at 150 g ai/ha for post-emergence herbicidal activity on barnyard grass, crab grass (*D. sanguinalis*), green bristlegrass (*Setaria viridis*), leaf mustard (*Brassica juncea*), common amaranth (*A. retroflexus*), and small goosefoot (*Chenopodium serotinum*). The results are shown in Tables 3.28, 3.29 and 3.30.

Table 3.25 Inhibitory activity of mono lithium salts of 1-(substituted phenoxyacetoxy)alkylphosphonic acids **III** against the growth of plants^a

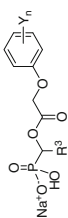


Compound	R ³	Y _n	Root			Stem			
			Brm ^b			Ech ^b			
			100 mg/L	10 mg/L	100 mg/L	100 mg/L	10 mg/L	100 mg/L	
III-1	Me	2,4-Cl ₂	99	99	96	92	83	64	61
III-2	Et	2,4-Cl ₂	99	99	97	92	88	57	53
III-3	<i>n</i> -Pr	2,4-Cl ₂	99	98	97	88	83	67	60
III-4	<i>i</i> -Pr	2,4-Cl ₂	99	99	97	88	83	57	50
III-5	<i>n</i> -Bu	2,4-Cl ₂	99	99	97	92	88	63	60
III-6	Ph	2,4-Cl ₂	99	99	95	89	85	72	52
III-7	Thien-2-yl	2,4-Cl ₂	98	98	97	84	80	58	45
III-8	Me	2-Me,4-Cl	98	96	97	84	80	65	29
III-9	Et	2-Me,4-Cl	99	99	95	92	89	64	60
III-10	<i>n</i> -Pr	2-Me,4-Cl	99	98	97	88	83	67	60
III-11	<i>i</i> -Pr	2-Me,4-Cl	99	99	95	92	89	76	76
III-12	<i>n</i> -Bu	2-Me,4-Cl	99	99	95	92	89	48	28
III-13	Ph	2-Me,4-Cl	99	99	97	92	88	63	60

^a Inhibitory potency (%) against the growth of plants in Petri dishes, 0 (no effect), 100 % (completely kill)

^b Brm: cabbage type rape; Ech: barnyard grass

Table 3.26 Inhibitory activity of mono sodium salts of 1-(substituted phenoxyacetoxy)alkylphosphonic acids **IIG** against the growth of plants^a

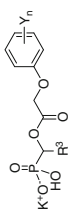


Compound	R ³	Y _n	Root			Stem			
			Brn ^b			Ech ^b			
			100 mg/L	10 mg/L	100 mg/L	100 mg/L	10 mg/L	100 mg/L	
IIG-1	Me	2,4-Cl ₂	99	99	96	92	88	75	68
IIG-2	Et	2,4-Cl ₂	99	98	97	92	88	57	7
IIG-3	<i>n</i> -Pr	2,4-Cl ₂	99	98	97	92	88	60	40
IIG-4	<i>i</i> -Pr	2,4-Cl ₂	99	99	97	92	83	80	13
IIG-5	<i>n</i> -Bu	2,4-Cl ₂	99	99	97	92	88	63	60
IIG-6	Ph	2,4-Cl ₂	99	98	97	92	87	83	70
IIG-7	Thien-2-yl	2,4-Cl ₂	99	98	97	88	83	80	57
IIG-8	Me	2-Me,4-Cl	98	98	97	84	80	61	29
IIG-9	Et	2-Me,4-Cl	99	99	95	92	89	80	64
IIG-10	<i>n</i> -Pr	2-Me,4-Cl	99	98	97	92	88	68	40
IIG-11	<i>i</i> -Pr	2-Me,4-Cl	99	99	95	92	89	80	36
IIG-12	<i>n</i> -Bu	2-Me,4-Cl	99	97	95	89	89	64	52
IIG-13	Ph	2-Me,4-Cl	99	98	97	92	88	83	50

^a Inhibitory potency (%) against the growth of plants in Petri dishes, 0 (no effect), 100 % (completely kill)

^b Brn: cabbage type rape; Ech: barnyard grass

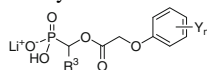
Table 3.27 Inhibitory activity of mono potassium salts of 1-(substituted phenoxyacetoxy)alkylphosphonic acids **IIIH** against the growth of plants^a



Compound	R ³	Y _n	Root			Stem			
			Brn ^b			Ech ^b			
			100 mg/L	10 mg/L	10 mg/L	100 mg/L	10 mg/L	10 mg/L	
IIIH-1	Me	2,4-Cl ₂	99	99	96	92	88	79	71
IIIH-2	Et	2,4-Cl ₂	99	99	97	92	88	67	30
IIIH-3	<i>n</i> -Pr	2,4-Cl ₂	99	98	97	92	88	53	43
IIIH-4	<i>i</i> -Pr	2,4-Cl ₂	99	99	97	92	83	57	47
IIIH-5	<i>n</i> -Bu	2,4-Cl ₂	99	98	97	92	88	67	60
IIIH-6	Ph	2,4-Cl ₂	99	99	97	92	87	68	40
IIIH-7	Thien-2-yl	2,4-Cl ₂	98	98	97	88	83	52	10
IIIH-8	Me	2-Me,4-Cl	98	98	97	84	80	52	32
IIIH-9	Et	2-Me,4-Cl	99	99	95	92	89	80	56
IIIH-10	<i>n</i> -Pr	2-Me,4-Cl	99	98	97	92	88	53	43
IIIH-11	<i>i</i> -Pr	2-Me,4-Cl	99	99	95	92	89	57	47
IIIH-12	<i>n</i> -Bu	2-Me,4-Cl	99	97	95	89	89	84	52
IIIH-13	Ph	2-Me,4-Cl	99	98	97	92	88	67	60

^a Inhibitory potency (%) against the growth of plants in Petri dishes, 0 (no effect), 100 % (completely kill)

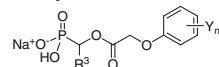
^b Brn: cabbage type rape; Ech: barnyard grass

Table 3.28 Structure and post-emergence herbicidal activity of mono lithium salts of 1-(substituted phenoxyacetoxy)alkylphosphonic acids **IIF^a**

Compound	R ³	Y _n	Monocotyledon			Dicotyledon		
			Ech ^b	Dig ^b	Set ^b	Brj ^b	Amr ^b	Chs ^b
IIF-1	Me	2,4-Cl ₂	80	65	60	85	90	85
IIF-2	Et	2,4-Cl ₂	40	40	30	95	75	60
IIF-3	<i>n</i> -Pr	2,4-Cl ₂	50	50	40	90	70	50
IIF-4	<i>i</i> -Pr	2,4-Cl ₂	40	40	50	90	70	60
IIF-5	<i>n</i> -Bu	2,4-Cl ₂	60	60	0	80	60	70
IIF-6	Ph	2,4-Cl ₂	50	50	0	85	80	70
IIF-7	Thien-2-yl	2,4-Cl ₂	50	0	0	80	60	40
IIF-9	Et	2-Me,4-Cl	40	0	0	85	70	60
IIF-11	<i>i</i> -Pr	2-Me,4-Cl	40	0	0	80	60	50
IIF-12	<i>n</i> -Bu	2-Me,4-Cl	0	40	0	80	50	60

^a Inhibitory potency (%) against the growth of plants at a rate of 150 g ai/ha in the greenhouse, 0 (no effect), 100 % (completely kill)

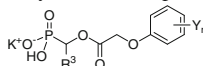
^b Ech: barnyard grass; Dig: crab grass; Set: green bristlegrass; Brj: leaf mustard; Amr: common amaranth; Chs: small goosefoots

Table 3.29 Structure and post-emergence herbicidal activity of mono sodium salts of 1-(substituted phenoxyacetoxy)alkylphosphonic acids **IIG^a**

Compound	R ³	Y _n	Monocotyledon			Dicotyledon		
			Ech ^b	Dig ^b	Set ^b	Brj ^b	Amr ^b	Chs ^b
IIG-1	Me	2,4-Cl ₂	60	50	50	80	80	80
IIG-2	Et	2,4-Cl ₂	0	40	50	90	80	60
IIG-3	<i>n</i> -Pr	2,4-Cl ₂	0	0	0	90	75	60
IIG-4	<i>i</i> -Pr	2,4-Cl ₂	0	0	0	90	40	60
IIG-5	<i>n</i> -Bu	2,4-Cl ₂	40	50	40	95	95	80
IIG-6	Ph	2,4-Cl ₂	0	0	40	100	95	90
IIG-7	Thien-2-yl	2,4-Cl ₂	50	60	60	90	80	80
IIG-9	Et	2-Me,4-Cl	40	0	40	85	70	50
IIG-11	<i>i</i> -Pr	2-Me,4-Cl	30	30	0	80	0	0
IIG-12	<i>n</i> -Bu	2-Me,4-Cl	0	0	0	80	70	70

^a Inhibitory potency (%) against the growth of plants at a rate of 150 g ai/ha in the greenhouse, 0 (no effect), 100 % (completely kill)

^b Ech: barnyard grass; Dig: crab grass; Set: green bristlegrass; Brj: leaf mustard; Amr: common amaranth; Chs: small goosefoots

Table 3.30 Structure and post-emergence herbicidal activity of mono potassium salts of1-(substituted phenoxyacetoxy)alkylphosphonic acids **III^a**

Compound	R ³	Y _n	Monocotyledon			Dicotyledon		
			Ech ^b	Dig ^b	Set ^b	Brj ^b	Amr ^b	Chs ^b
III-1	Me	2,4-Cl ₂	60	60	50	70	85	80
III-2	Et	2,4-Cl ₂	0	40	0	90	70	60
III-3	<i>n</i> -Pr	2,4-Cl ₂	0	0	0	80	75	60
III-4	<i>i</i> -Pr	2,4-Cl ₂	0	0	0	80	60	70
III-5	<i>n</i> -Bu	2,4-Cl ₂	0	0	0	90	75	70
III-6	Ph	2,4-Cl ₂	40	60	40	95	75	60
III-7	Thien-2-yl	2,4-Cl ₂	50	60	50	100	80	60
III-9	Et	2-Me,4-Cl	40	0	30	90	60	75
III-12	<i>n</i> -Bu	2-Me,4-Cl	40	60	40	85	50	50

^a Inhibitory potency (%) against the growth of plants at a rate of 150 g ai/ha in the greenhouse, 0 (no effect), 100 % (completely kill)

^b Ech: barnyard grass; Dig: crab grass; Set: green bristlegrass; Brj: leaf mustard; Amr: common amaranth; Chs: small goosefoots

The **IIF**, **IIG** and **III** displayed higher post-emergence herbicidal activity against dicotyledonous weeds than monocotyledons at 150 g ai/ha in the greenhouse. All **IIF**, **IIG** and **III** showed higher inhibition (79–100 %) against leaf mustard than common amaranth and small goosefoot. **IIF-1** (R³=Me, Y_n=2,4-Cl₂), **IIG-1** (R³=Me, Y_n=2,4-Cl₂), **IIG-5** (R³=*n*-Bu, Y_n=2,4-Cl₂), **IIG-6** (R³=Ph, Y_n=2,4-Cl₂), and **IIG-7** (R³=thien-2-yl, Y_n=2,4-Cl₂) could reach 80–100 % inhibitory effect against three tested dicotyledonous weeds. Especially, **IIG-6** (R³=Ph, Y_n=2,4-Cl₂) showed the best inhibitory effect (90–100 %) against three tested dicotyledonous weeds.

IIF-1 (R³=Me, Y_n=2,4-Cl₂), **IIG-1** (R³=Me, Y_n=2,4-Cl₂), **IIG-7** (R³=thien-2-yl, Y_n=2,4-Cl₂), **III-1** (R³=Me, Y_n=2,4-Cl₂), and **III-7** (R³=thien-2-yl, Y_n=2,4-Cl₂) displayed 50–80 % inhibitory effect against monocotyledons including barnyard grass, crab grass, and green bristlegrass, but other compounds were much weaker or inactive against barnyard grass, crab grass, and green bristlegrass at 150 g ai/ha in the greenhouse (Tables 3.28, 3.29 and 3.30).

(B) SAR analysis for **IIF**, **IIG** and **III**

Mono alkali metal salts of 1-(substituted phenoxyacetoxy)alkylphosphonic acids was beneficial to post-emergence herbicidal activity against monocot weeds. **IIG-1** (R³=Me, Y_n=2,4-Cl₂), **IIG-7** (R³=thien-2-yl, Y_n=2,4-Cl₂), **III-1** (R³=Me, Y_n=2,4-Cl₂), and **III-7** (R³=thien-2-yl, Y_n=2,4-Cl₂) display 50–60 % post-emergence herbicidal activity against monocot weeds. As shown in Table 3.31, **IIF-1** (R³=Me, Y_n=2,4-Cl₂) provided 60–80 % control at 150 g ai/ha for the monocot weeds. However their corresponding phosphonate **IC-22** (R³=Me, Y_n=2,4-Cl₂) and mono

Table 3.31 Comparing post-emergence herbicidal activity of 1-(substituted phenoxyacetoxy) alkylphosphonate derivatives^a

Compound	R ¹	R ²	R ³	Y _n	Monocotyledon			Dicotyledon		
					Ech ^b	Dig ^b	Set ^b	Brj ^b	Amr ^b	Chs ^b
IIF-1	Li	H	Me	2,4-Cl ₂	80	65	60	85	90	85
IIG-1	Na	H	Me	2,4-Cl ₂	60	50	50	80	80	80
IIIH-1	K	H	Me	2,4- Cl ₂	60	60	50	70	85	80
IIB-2	Na	Me	Me	2,4-Cl ₂	0	0	0	90	93	90
IC-22	Me	Me	Me	2,4-Cl ₂	0	0	0	100	100	98
IIF-5	Li	H	<i>n</i> -Bu	2,4-Cl ₂	60	60	0	80	60	70
IIG-5	Na	H	<i>n</i> -Bu	2,4-Cl ₂	40	50	40	95	95	80
IIG-12	Na	H	<i>n</i> -Bu	2-Me,4-Cl	0	0	0	80	70	70
IIIH-5	K	H	<i>n</i> -Bu	2,4-Cl ₂	0	0	0	90	75	70
IIF-6	Li	H	Ph	2,4-Cl ₂	50	50	0	85	80	70
IIG-6	Na	H	Ph	2,4-Cl ₂	0	0	40	100	95	90
IIIH-6	K	H	Ph	2,4-Cl ₂	40	60	40	95	75	60
IIF-7	Li	H	Thien-2-yl	2,4-Cl ₂	50	0	0	80	60	40
IIG-7	Na	H	Thien-2-yl	2,4-Cl ₂	50	60	60	90	80	80
IIIH-7	K	H	Thien-2-yl	2,4-Cl ₂	50	60	50	100	80	60
IIB-21	Na	Me	Thien-2-yl	2,4-Cl ₂	0	0	0	0	0	0

^a Inhibitory potency (%) against the growth of plants at a rate of 150 g ai/ha in the greenhouse, 0 (no effect), 100 % (completely kill)

^b Ech: barnyard grass; Dig: crab grass; Set: green bristlegrass; Brj: leaf mustard; Amr: common amaranth; Chs: small goosefoots

sodium salt of *O*-methyl alkylphosphonic acid **IIB-2** (R³=Me, Y_n=2,4-Cl₂) showed no activity under the same tested conditions.

The replacement of *O,O*-dialkyl phosphoryl group by mono alkali metal salt of phosphonic acid moiety could be enhanced on post-emergence herbicidal activity against monocot weeds, but it had little effect on post-emergence herbicidal activity against dicotyledons. In the structure **Io**, compounds with Na as R¹, H as R², Me, *n*-Bu, Ph or thien-2-yl as R³, 2,4-Cl₂ as Y_n on the phenoxy-benzene ring were beneficial to post-emergence herbicidal activity against dicotyledons, such as **IIF-1** (R³=Me, Y_n=2,4-Cl₂), **IIG-1** (R³=Me, Y_n=2,4-Cl₂), **IIG-5** (R³=*n*-Bu, Y_n=2,4-Cl₂), **IIG-6** (R³=Ph, Y_n=2,4-Cl₂), and **IIG-7** (R³=thien-2-yl, Y_n=2,4-Cl₂). Among compounds **IIF-IIIH**, **IIG-6** (R¹=Na, R²=H, R³=Ph, Y_n=2,4-Cl₂ in the structure **Io**) showed best post-emergence inhibitory effect (90–100 %) comparable to **IC-22** (clacyfos) against three tested dicotyledonous weeds.

3.2.5 Summary

In summary, we set up a practical and efficient procedure for the preparation of mono alkali metal salts of 1-(substituted phenoxyacetoxy)alkylphosphonic acids **IIF**, **IIG** and **IIH**. 36 of **IIF**, **IIG** and **IIH** were obtained from the *O,O*-dimethyl 1-(2,4-disubstituted phenoxyacetoxy)alkylphosphonates **IC** by the treatment of chlorotrimethylsilane and sodium iodide with acceptable yields.

Compared with *O,O*-dimethyl alkylphosphonates **IC** and the monosalts of *O*-alkyl alkylphosphonic acids **IIA–IIE**, these **IIF–IIH** showed higher inhibitory activity against monocotyledonous weeds in post-emergence application. Especial **IIF-1** ($R^1=Li$, $R^2=H$, $R^3=Me$, $Y_n=2,4-Cl_2$) provided 60–80 % control at 150 g ai/ha for the monocot weeds. However its corresponding *O,O*-dimethyl alkylphosphonate **IC-22** and the monosodium salt of *O*-methyl alkylphosphonic acid **IIB-2** ($R^3=Me$, $Y_n=2,4-Cl_2$) showed no activity under the same tested conditions. It showed that the introduction of HO was beneficial to post-emergence herbicidal activity against monocot weeds.

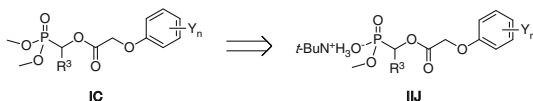
Some **IIF** or **IIG** had good herbicidal activity against dicotyledonous weeds just like those of alkali metal salts of *O*-alkyl 1-(substituted phenoxyacetoxy)alkylphosphonic acids and *O,O*-dialkyl 1-(substituted phenoxyacetoxy)alkylphosphonates. **IIG-6** ($R^1=Na$, $R^2=H$, $R^3=Ph$, $Y_n=2,4-Cl_2$ in the structure **Io**) showed best post-emergence inhibitory effect (90–100 %) comparable to **IC-22** (clacyfos) against three tested dicotyledonous weeds.

SAR analysis indicated that post-emergence herbicidal activity against monocot weeds could be enhanced by replacing both MeO with MO and HO in the structure of phosphonate **IC**, but the same replacement had little effect on post-emergence herbicidal activity against dicotyledons.

3.3 *t*-Butylamminium Salts of Alkylphosphonates **IIJ**

3.3.1 Introduction

As a part of our ongoing work, we have found the selective demethylation of *O,O*-dimethyl 1-(substituted phenoxyacetoxy)alkylphosphonates **IC** with *t*-butylamines giving *t*-butylamminium *O*-methyl 1-(substituted phenoxyacetoxy)alkylphosphonates **IIJ** (Scheme 3.11). It was expected that **IIJ** as organic salts might be more beneficial to herbicidal activity than that of those corresponding inorganic salts of alkylphosphonates **IIA–IIIE**.



Scheme 3.11 Design of *t*-butylamminium *O*-methyl 1-(substituted phenoxyacetoxy)alkylphosphonates **IIJ**

In this section we describe the synthesis, herbicidal activity, and structure-activity relationships of *t*-butylammonium *O*-methyl 1-(substituted phenoxyacetoxy) alkylphosphonates **IIJ**.

3.3.2 Synthesis of **IIJ**

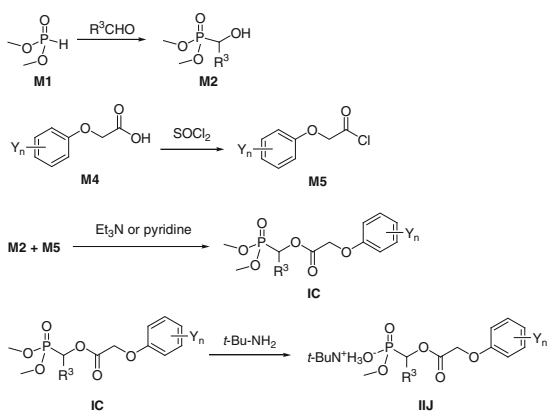
Some monosalts of alkylphosphonic acid derivatives like lithium, sodium, and potassium salts could be synthesized under harsh conditions by using metal iodides as catalysts under nitrogen atmosphere [7–12]. However the synthesis of *t*-butylammonium phosphonates could be performed under relatively mild conditions [22, 23].

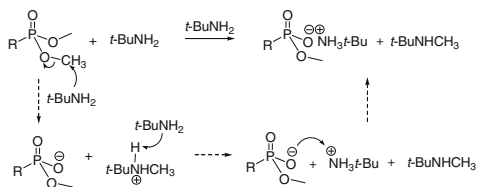
In our work, **IIJ** were obtained from corresponding *O,O*-dimethyl (1-substituted phenoxyacetoxy)alkylphosphonates **IC** directly. One of the MeO groups attached to phosphorus in **IC** could be replaced by ammonium ion in the synthesis. A detailed synthetic route of *t*-butylammonium *O*-methyl 1-(substituted phenoxyacetoxy)alkylphosphonates **IIJ** is outlined in Scheme 3.12.

The intermediates **M1**–**M5** were prepared according to the procedure described in Chap. 2. **IIJ** could be obtained by the treatment of *O,O*-dimethyl 1-(substituted phenoxyacetoxy)alkylphosphonates **IC** with an excess of *t*-butylamine. In this reaction, *t*-butylamine could selectively and quantitatively eliminate one methyl from two MeO groups which attached to phosphorus in **IC**. The possible reaction mechanism for forming *t*-butylammonium *O*-methyl phosphonate **IIJ** is outlined in Scheme 3.13. *t*-Butylamine first attacks the methyl carbon, forming intermediate *N-t*-butyl-*N*-methyl ammonium salt, which is then deprotonated by another *t*-butylamine to form *t*-butylammonium and *N*-methyl-*N-t*-butylamine. Finally, the cation of *t*-butylammonium binds with the anion of phosphonate to form the **IIJ**.

This synthetic method was moderate, simple, and clean. *t*-Butylammonium *O*-methyl phosphonates **IIJ** could be easily obtained by the evaporation of excessive *t*-butylamine and by-product, *N*-methyl-*N-t*-butylamine [24].

Scheme 3.12 Synthesis of *t*-butylammonium *O*-methyl 1-(substituted phenoxyacetoxy) alkylphosphonates **IIJ**





Scheme 3.13 Possible reaction mechanism for forming *t*-butylammonium *O*-methyl phosphonates

Table 3.32 Structure of *t*-butylammonium *O*-methyl 1-(substituted phenoxyacetoxy)alkylphosphonates **IIJ**^a

Compound	R ³	Y _n	Compound	R ³	Y _n
IIJ-1	Me	2-Me	IIJ-15	<i>n</i> -Bu	2-Me,4-Cl
IIJ-2	Et	2-Me	IIJ-16	Me	2-F,4-Cl
IIJ-3	<i>n</i> -Pr	2-Me	IIJ-17	Et	2-F,4-Cl
IIJ-4	<i>i</i> -Pr	2-Me	IIJ-18	<i>n</i> -Pr	2-F,4-Cl
IIJ-5	<i>n</i> -Bu	2-Me	IIJ-19	<i>i</i> -Pr	2-F,4-Cl
IIJ-6	Me	2-Cl	IIJ-20	<i>n</i> -Bu	2-F,4-Cl
IIJ-7	Et	2-Cl	IIJ-21	Me	2-Cl,4-F
IIJ-8	<i>n</i> -Pr	2-Cl	IIJ-22	Et	2-Cl,4-F
IIJ-9	<i>i</i> -Pr	2-Cl	IIJ-23	<i>i</i> -Pr	2-Cl,4-F
IIJ-10	<i>n</i> -Bu	2-Cl	IIJ-24	Me	2,4-Cl ₂
IIJ-11	Me	2-Me,4-Cl	IIJ-25	Et	2,4-Cl ₂
IIJ-12	Et	2-Me,4-Cl	IIJ-26	<i>n</i> -Pr	2,4-Cl ₂
IIJ-13	<i>n</i> -Pr	2-Me,4-Cl	IIJ-27	<i>i</i> -Pr	2,4-Cl ₂
IIJ-14	<i>i</i> -Pr	2-Me,4-Cl	IIJ-28	<i>n</i> -Bu	2,4-Cl ₂

^a Synthesis for compounds: **IIJ-1–IIJ-5**, **IIJ-11–IIJ-15**, **IIJ-24–IIJ-28** [13]; **IIA-6–IIA-10**, **IIJ-16–IIJ-23** [14]

Other tertiary amines, such as triethylamine and trimethylamine, couldn't react with **IC**. Furthermore, if R³ group attached to α -carbon of phosphorus in phosphonates **IC** was an aromatic group, such as phenyl or furanyl, **IIJ** could not be obtained by the reaction of **IC** with *t*-butylamine, but *t*-butylammonium phenoxyacetate was produced. The prepared **IIJ** are listed in Table 3.32. A detailed synthetic procedure for **IIJ** is described in the Sect. 9.1.13 of Chap. 9.

The structure of **IIJ** was confirmed by elemental analysis and characterized by IR, MS and ¹H NMR. The structure of **IIJ-24** (R³=Me, Y_n=2,4-Cl₂) was further established by X-ray crystallographic data. Spectroscopic analysis of some of **IIJ** is given in Sect. 3.3.3.

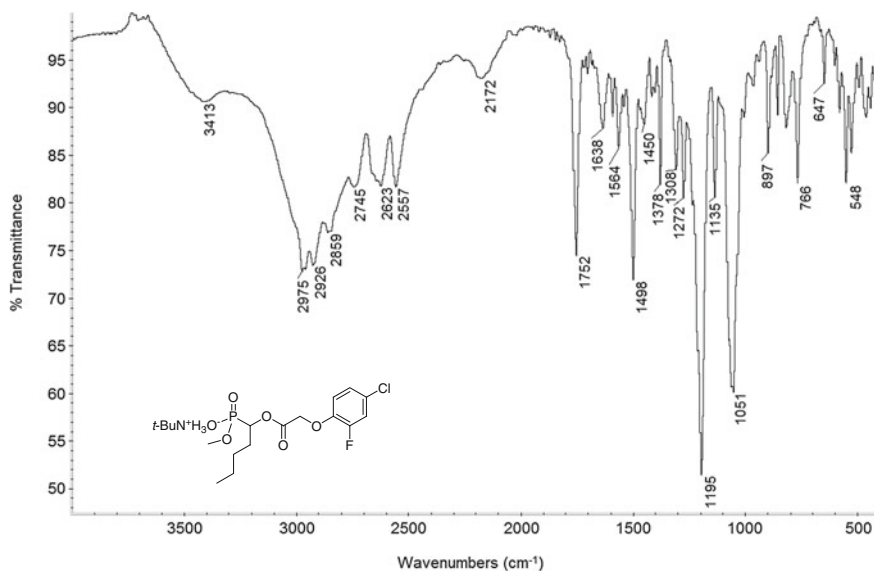


Fig. 3.11 IR spectrum of **IIJ-20**

3.3.3 Spectroscopic Analysis of **IIJ**

The IR spectra of **IIJ** indicated the existence of the O–H ($3,300\text{--}3,500\text{ cm}^{-1}$), C–H ($\sim 2,976, \sim 2,920\text{ cm}^{-1}$), C=O ($\sim 1,755\text{ cm}^{-1}$), P=O ($\sim 1,200\text{ cm}^{-1}$), and C–O–C ($\sim 1,060\text{ cm}^{-1}$). As an example, IR spectrum of **IIJ-20** ($R^3=n\text{-Bu}$, $Y_n=2\text{-F},4\text{-Cl}$) is shown in Fig. 3.11.

The ^1H NMR spectra of **IIJ** were similar to those of **IIA–IIH**. In general, the proton signal of the methoxy group attached to phosphorus appeared as a doublet at $\delta 3.58 \pm 0.02$. The magnetic nucleus of phosphorus made the signal of methyl splitting into a doublet. The proton signal of aminium (NH_3^+) appeared as a singlet at $\delta 1.37 \pm 0.01\text{ ppm}$. ^1H NMR spectrum of **IIJ-6** ($R^3=\text{Me}$, $Y_n=2\text{-Cl}$) is shown in Fig. 3.12.

The ^{31}P NMR chemical shifts of **IIJ** appeared as a singlet at $\delta 11.8\text{--}12.5\text{ ppm}$. Their chemical shifts moved upfield approximately 11–12 ppm compared with that of the corresponding *O,O*-dimethyl phosphonates (at $\sim 23\text{ ppm}$). The ^{31}P NMR spectrum of **IIJ-16** ($R^3=\text{Me}$, $Y_n=2\text{-F},4\text{-Cl}$) is shown in Fig. 3.13.

3.3.4 Crystal Structure Analysis of **IIJ-24**

An X-ray single-crystal structure of **IIJ-24** ($R^3=\text{Me}$, $Y_n=2,4\text{-Cl}_2$) is shown in Fig. 3.14. Packing diagrams of **IIJ-24** are shown in Fig. 3.15. Selected bond lengths and angles are presented in Table 3.33. Analysis of the crystal structure

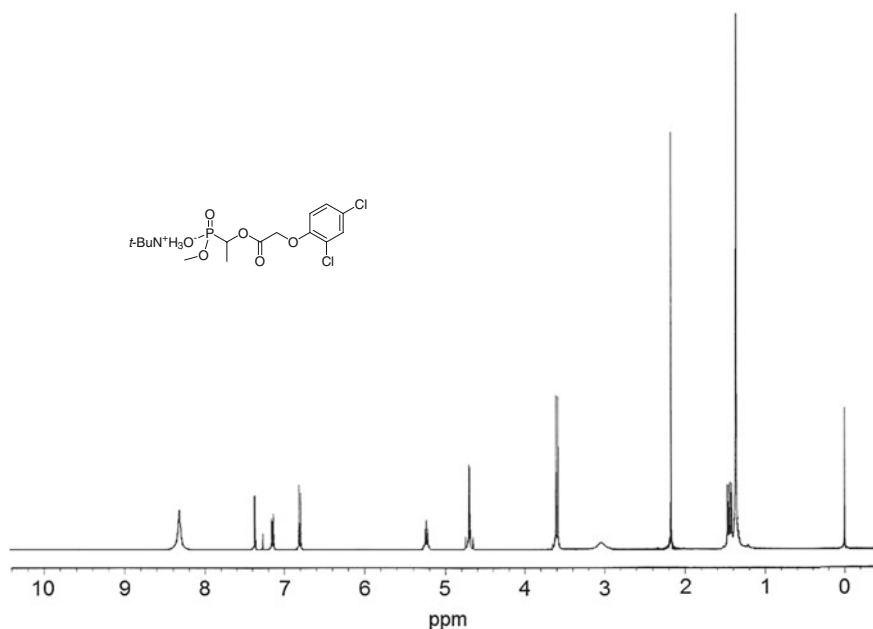


Fig. 3.12 ^1H NMR spectrum of **IIJ-6** (CDCl_3 , 400 MHz)

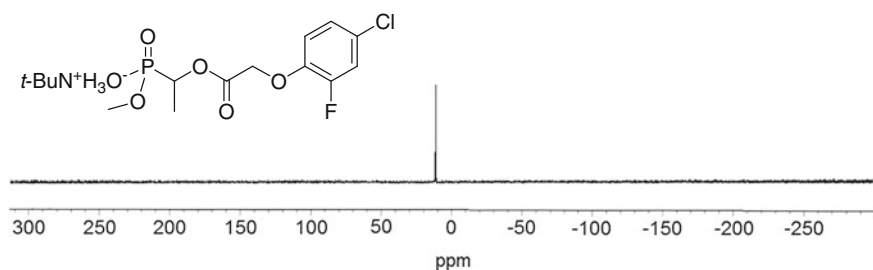


Fig. 3.13 ^{31}P NMR spectrum of **IIJ-16** (CDCl_3 , 162 MHz)

showed that the crystal of **IIJ-24** was a monoclinic system, and its space group was $\text{P}2(1)/c$. In **IIJ-24**, all bond lengths and angles showed normal values. The bond length of P1-O6 with $1.6005(15)$ Å was significantly longer than the bond length of P1-O4 and P1-O5 , with the distances of $1.4805(13)$ and $1.4964(13)$ Å, respectively.

There are many hydrogen bonds in the molecular, which make every two molecules with the same configuration to bind and form dimers. For example, three ammonium H atoms participate in $\text{N-H}\cdots\text{O}$ hydrogen bonds (Table 3.34), which stabilize the crystal packing (Fig. 3.15) along with weak intermolecular interactions of $\text{C-H}\cdots\text{O}$ (Table 3.34).

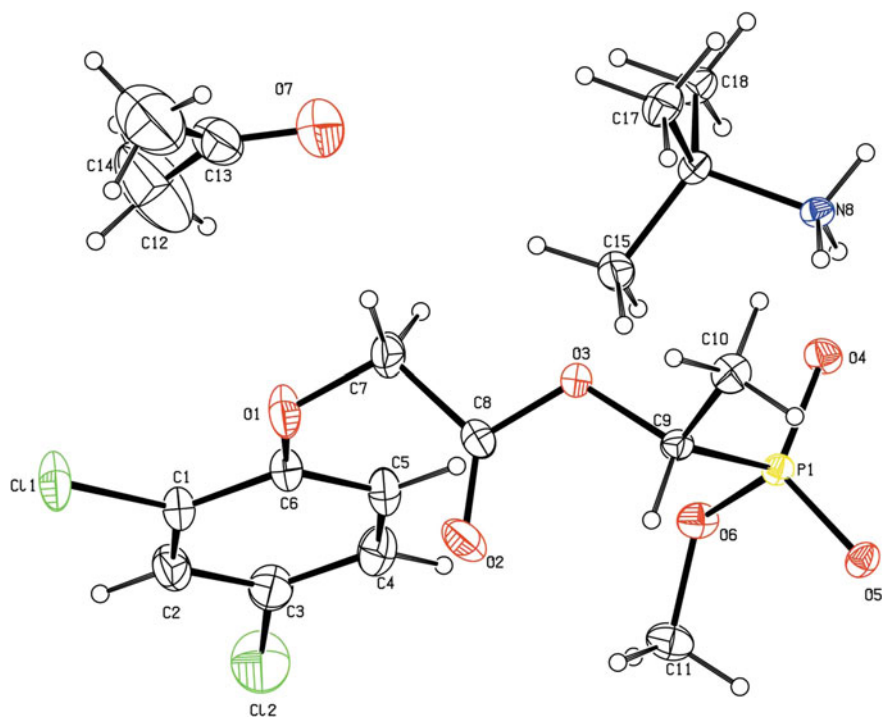


Fig. 3.14 Molecular structure of compound IIJ-24

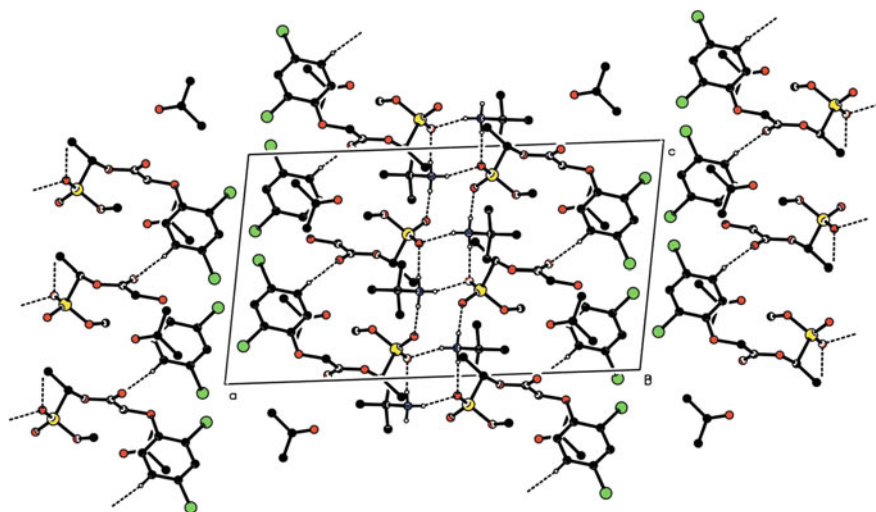


Fig. 3.15 Packing diagram of IIJ-24

Table 3.33 Selected bond distance (Å) and angles (°) for **IIJ-24**

Bond	Dist.	Bond	Angles Deg.
O(4)-P(1)	1.4805(13)	C(8)-O(3)-C(9)	118.33(16)
O(5)-P(1)	1.4964(13)	C(11)-O(6)-P(1)	122.20(13)
O(6)-C(11)	1.430(3)	O(4)-P(1)-O(5)	118.84(8)
O(6)-P(1)	1.6005(15)	O(4)-P(1)-O(6)	106.31(8)
O(7)-C(13)	1.189(4)	O(5)-P(1)-O(6)	110.45(8)
P(1)-C(9)	1.8279(19)	O(4)-P(1)-C(9)	109.69(8)

Table 3.34 Hydrogen bond for **IIJ-24**

D-H...A	d(D-H)	d(H...A)	d(D...A)	<(DHA)
N(8)-H(8B)...O(5) ^a	0.89	1.97	2.841(2)	164.0
N(8)-H(8C)...O(5) ^b	0.89	1.96	2.8419(19)	170.4
N(8)-H(8A)...O(4)	0.89	1.84	2.7290(19)	178.4

Symmetry transformations used to generate equivalent atoms: ^a $-x + 1, y + 1/2, -z + 1/2$; ^b $x, -y + 1/2, z - 1/2$

3.3.5 Herbicidal Activity of **IIJ**

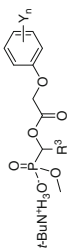
As a preliminary bioassay, all of *t*-butylammonium *O*-methyl 1-(substituted phenoxyacetoxy)alkylphosphonates **IIJ** were tested for herbicidal activity on barnyard grass and cabbage type rape with the Petri dish method. The results are listed in Table 3.35.

Most of the aminium salts **IIJ** in Table 3.35 showed >90 % inhibition against the root of cabbage type rape and 75–97 % inhibition against the root of barnyard grass at 10 mg/L, and displayed higher inhibition against the stem of cabbage type rape (67–90 %) than that of barnyard grass (22–80 %) at 10 mg/L. For example, **IIJ-26** ($R^3=n\text{-Pr}$, $Y_n=2,4\text{-Cl}_2$) showed 90 % inhibition against the stem of cabbage type rape while only 22 % inhibitory effect against the stem of barnyard grass at 10 mg/L. The aminium salts **IIJ** displayed higher inhibition against the growth of root than that of the stem. Most of **IIJ** showed >80 % inhibition against the root of barnyard grass, while 45–77 % inhibition against the stem of barnyard grass at 10 mg/L.

(A) Post-emergence herbicidal activity of **IIJ**

Some of **IIJ** with good herbicidal activity were evaluated at 150 g ai/ha for post-emergence herbicidal activity against barnyard grass (*E. crusgalli*), crab grass (*D. sanguinalis*), green bristlegass (*S. viridis*), leaf mustard (*B. juncea*), common amaranth (*Amaranthus retrofleris*), and small goosefoot (*Chenopodium serotinum*) in greenhouse. The results are shown in Table 3.36.

The aminium salts **IIJ** in Table 3.36 displayed higher post-emergence herbicidal activity against dicotyledonous weeds than monocotyledon at 150 g ai/ha in the greenhouse. Most of the aminium salt **IIJ** displayed herbicidal activity against

Table 3.35 Inhibitory activity of *t*-butylammonium *O*-methyl 1-(substituted phenoxyacetoxy)alkylphosphonates IIJ against the growth of plants^a

Compound	R ³	Y _n	Root		Brn ^b		Stem		
			Ech ^b	100 mg/L	10 mg/L	100 mg/L	10 mg/L	Ech ^b	100 mg/L
IIJ-1	Me	2-Me	97	88	97	98	67	94	77
IIJ-2	Et	2-Me	97	88	92	97	67	94	67
IIJ-3	<i>n</i> -Pr	2-Me	97	88	95	96	71	94	75
IIJ-4	<i>i</i> -Pr	2-Me	97	84	94	96	69	88	71
IIJ-5	<i>n</i> -Bu	2-Me	97	78	96	97	71	90	73
IIJ-6	Me	2-Cl	97	94	97	98	82	94	87
IIJ-7	Et	2-Cl	97	94	98	98	77	94	85
IIJ-8	<i>n</i> -Pr	2-Cl	97	97	98	98	75	94	88
IIJ-9	<i>i</i> -Pr	2-Cl	97	94	98	98	75	94	88
IIJ-10	<i>n</i> -Bu	2-Cl	97	97	98	98	75	94	85
IIJ-11	Me	2-Me,4-Cl	97	94	98	98	58	84	79
IIJ-12	Et	2-Me,4-Cl	100	95	97	99	68	92	89
IIJ-13	<i>n</i> -Pr	2-Me,4-Cl	97	94	98	98	55	84	84
IIJ-14	<i>i</i> -Pr	2-Me,4-Cl	95	95	99	99	68	92	89
IIJ-15	<i>n</i> -Bu	2-Me,4-Cl	95	94	97	99	58	89	84
IIJ-16	Me	2-F,4-Cl	91	84	95	98	71	88	69
IIJ-17	Et	2-F,4-Cl	94	75	96	98	70	94	81

(continued)

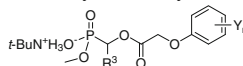
Table 3.35 (continued)

Compound	R ³	Y _n	Root				Stem			
			Ech ^b		Brn ^b		Ech ^b		Brn ^b	
			100 mg/L	10 mg/L	100 mg/L	10 mg/L	100 mg/L	10 mg/L	100 mg/L	10 mg/L
IIJ-18	<i>n</i> -Pr	2-F,4-Cl	88	81	97	96	72	59	90	85
IIJ-19	<i>i</i> -Pr	2-F,4-Cl	94	88	97	95	71	57	94	85
IIJ-20	<i>n</i> -Bu	2-F,4-Cl	91	81	97	95	75	59	94	71
IIJ-21	Me	2-Cl,4-F	97	97	98	97	84	64	94	92
IIJ-22	Et	2-Cl,4-F	97	94	97	95	78	77	96	79
IIJ-23	<i>i</i> -Pr	2-Cl,4-F	97	97	98	97	78	71	94	85
IIJ-24	Me	2,4-Cl ₂	96	92	99	99	79	57	93	88
IIJ-25	Et	2,4-Cl ₂	100	95	99	97	68	60	92	89
IIJ-26	<i>n</i> -Pr	2,4-Cl ₂	97	94	99	97	62	22	93	90
IIJ-27	<i>i</i> -Pr	2,4-Cl ₂	100	95	99	97	64	64	89	89
IIJ-28	<i>n</i> -Bu	2,4-Cl ₂	95	95	99	97	84	80	92	89

^a Inhibitory potency (%) against the growth of plants in Petri dishes, 0 (no effect), 100 % (completely kill)

^b Brn: cabbage type rape; Ech: barnyard grass

Table 3.36 Structure and post-emergence herbicidal activity of *t*-butylammonium *O*-methyl 1-(substituted phenoxyacetoxy)alkylphosphonates **IIJ**^a



Compound	R ³	Y _n	Monocotyledon			Dicotyledon		
			Ech ^b	Dig ^b	Set ^b	Brj ^b	Amr ^b	Chs ^b
IIJ-11	Me	2-Me,4-Cl	60	0	40	95	80	80
IIJ-12	Et	2-Me,4-Cl	30	40	0	90	70	70
IIJ-13	<i>n</i> -Pr	2-Me,4-Cl	40	0	40	100	100	90
IIJ-14	<i>i</i> -Pr	2-Me,4-Cl	40	30	40	85	50	70
IIJ-15	<i>n</i> -Bu	2-Me,4-Cl	0	0	0	90	70	70
IIJ-24	Me	2,4-Cl ₂	60	40	0	95	90	90
IIJ-25	Et	2,4-Cl ₂	0	0	0	80	90	70
IIJ-26	<i>n</i> -Pr	2,4-Cl ₂	40	40	30	80	90	80
IIJ-27	<i>i</i> -Pr	2,4-Cl ₂	50	40	0	95	80	85
IIJ-28	<i>n</i> -Bu	2,4-Cl ₂	40	50	0	85	75	70

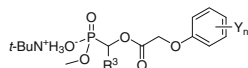
^a Inhibitory potency (%) against the growth of plants at a rate of 150 g ai/ha in the greenhouse, 0 (no effect), 100 % (completely kill)

^b Ech: barnyard grass; Dig: crab grass; Set: green bristlegrass; Brj: leaf mustard; Amr: common amaranth; Chs: small goosefoots

broadleaf weeds at 150 g ai/ha for post-emergence application. **IIJ-11** (R³=Me, Y_n=2-Me,4-Cl), **IIJ-13** (R³=*n*-Pr, Y_n=2-Me,4-Cl), **IIJ-24** (R³=Me, Y_n=2,4-Cl₂), **IIJ-26** (R³=*n*-Pr, Y_n=2,4-Cl₂), and **IIJ-27** (R³=*i*-Pr, Y_n=2,4-Cl₂) showed 80–100 % inhibitory effect against the three broadleaf weeds for post-emergence application. Especially, **IIJ-13** and **IIJ-24** showed >90 % control of the dicots leaf mustard, common amaranth, and small goosefoots at 150 g ai/ha in post-emergence application. Most of the aminium salt **IIJ** showed much weaker herbicidal activity against monocot weeds, such as barnyard grass, crab grass, and green bristlegrass. Only **IIJ-11** and **IIJ-24** showed 60 % control against barnyard grass at 150 g ai/ha.

IIJ-11 and **IIJ-24** were selected for further evaluation at 150–37.5 g ai/ha. They were tested for post-emergence activity against a range of weed species including leaf mustard (*Brassica juncea*), sickle senna (*Cassia tora*), white eclipta (*Eclipta prostrata*), common amaranth (*Amaranthus retroflexus*), field chickweed (*Cerastium arvense*), and common purslane (*Portulaca oleracea*). The results are shown in Table 3.37. **IIJ-24** showed higher activity than **IIJ-11**, exhibited >70 % control against all tested broadleaf weeds by post-emergence application at 75 g ai/ha.

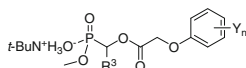
Crop safety of aminium salts **IIJ-11** and **IIJ-24** for rice (*Oryza sativa*), maize (*Zea mays*), cotton (*Gossypium hirsutum*), soybean (*Glycine max*), wheat (*Triticum aestivum*), and rape (*Brassica campestris*) was examined (Table 3.38). Both **IIJ-11** and **IIJ-24** were unsafe to rice, cotton and rape, but they showed good selectivity

Table 3.37 Structure and post-emergence herbicidal activity of **IIJ-11** and **IIJ-24**^a

Compound	R ³	Y _n	Rate (g ai/ha)	Brj ^b	Cas ^b	Ecl ^b	Amr ^b	Cer ^b	Por ^b
IIJ-11	Me	2-Me,4-Cl	150	85	80	85	90	80	90
			75	85	50	70	80	60	60
			37.5	85	0	70	70	50	50
IIJ-24	Me	2,4-Cl ₂	150	95	95	85	90	80	80
			75	95	85	80	85	70	80
			37.5	85	70	60	70	40	60

^a Inhibitory potency (%) against the growth of plants in the greenhouse, 0 (no effect), 100 % (completely kill)

^b Brj: leaf mustard; Cas: sickle senna; Ecl: white eclipta; Amr: common amaranth; Cer: field chickweed; Por: common purslane

Table 3.38 Growth inhibition of several crops by **IIJ-11** and **IIJ-24**

Compound	R ³	Y _n	Rate (g ai/ha)	Ory ^a	Zea ^a	Gos ^a	Gly ^a	Tri ^a	Bra ^a
IIJ-11	Me	2-Me,4-Cl	150	50	10	30	30	0	70
IIJ-24	Me	2,4-Cl ₂	150	30	0	40	0	0	70

^a Ory: rice; Zea: maize; Gos: cotton; Gly: soybean; Tri: wheat; Bra: rape

between some monocotyledonous crops and dicotyledonous weeds at 150 g ai/ha. **IIJ-11** was safe for maize and wheat. **IIJ-24** was very safe for maize, soybean, and wheat at 150 g ai/ha, which would be used on maize, wheat, and soybean fields for control of broadleaf weeds by post-emergence application. Soybean exhibited tolerance to **IIJ-24**, but was susceptible to **IC-22**, indicated that aminium salt **IIJ-24** displayed different biological characteristics from its corresponding phosphonate **IC-22**.

(B) SAR analysis for **IIJ**

When 2,4-Cl₂ or 2-Me,4-Cl as Y_n were kept invariant in **IIJ**, **IIJ** with Me or *n*-Pr as R³ showed higher activity against broadleaf weeds. For example, **IIJ-24** (R³=Me, Y_n=2,4-Cl₂), **IIJ-11** (R³=Me, Y_n=2-Me,4-Cl), and **IIJ-13** (R³=*n*-Pr, Y_n=2-Me,4-Cl) exhibited 80–100 % control against broadleaf weeds in post-emergence. Apparently, the di-substitution of 2- and 4-position on the phenoxy-benzene ring with 2,4-Cl₂ or 2-Me,4-Cl as Y_n was beneficial to the herbicidal activity. Aminium salt **IIJ-11** and **IIJ-24** were found to show 60 % control against barnyard grass at 150 g ai/ha.

3.3.6 Summary

A series of novel *t*-butylammonium *O*-methyl 1-(substituted phenoxyacetoxy)alkyl phosphonates **IIJ** including 28 compounds were selectively synthesized by the demethylation of dimethyl 1-(substituted phenoxyacetoxy)alkylphosphonates **IC** with *t*-butylamine. This reaction was mild, easy, clean, and good-yielding for the synthesis of *t*-butylammonium phosphonates.

Among ammonium salts **IIJ**, **IIJ-24** ($R^3=Me$, $Y_n=2,4-Cl_2$) was found to be the most active compound. It exhibited 70–95 % control of all tested broadleaf weeds by post-emergence application at 75 g ai/ha and was proved to be very safe for maize, soybean and wheat at 150 g ai/ha. Soybean exhibited tolerance to **IIJ-24**, but was susceptible to **IC-22**. Ammonium salt **IIJ-24** also showed 60 % control of barnyard grass at 150 g ai/ha, but its corresponding *O,O*-dimethyl alkylphosphonate **IC-22** (clacyfos) and the sodium salt of *O*-methyl alkylphosphonic acids **IIB-2** had no activity against barnyard grass. These observations indicated that ammonium salt **IIJ-24** displayed different biological characteristics from its corresponding phosphonate **IC-22** and sodium salt **IIB-2**.

References

1. Baillie AC, Wright K, Wright BJ et al (1988) Inhibitors of pyruvate dehydrogenase as herbicides. *Pestic Biochem Physiol* 30:103–112
2. Kluger R, Pike DC (1977) Active site generated analogues of reactive intermediates in enzymic reactions. Potent inhibition of pyruvate dehydrogenase by a phosphonate analogue of pyruvate. *J Am Chem Soc* 99:4504–4506
3. Kluger R, Gish G, Kauffman G (1984) Interaction of thiamin diphosphate and thiamin thiazolone diphosphate with wheat germ pyruvate decarboxylase. *J Biol Chem* 259:8960–8965
4. He HW, Yuan JL, Peng H et al (2011) Studies of *O,O*-dimethyl α -(2,4-dichlorophenoxyacetoxy) ethylphosphonate (HW02) as a new herbicide. 1. Synthesis and herbicidal activity of HW02 and analogues as novel inhibitors of pyruvate dehydrogenase complex. *J Agric Food Chem* 59:4801–4813
5. Turhanen PA, Ahlgren MJ, Järvinen T et al (2000) Bisphosphonate prodrugs. Selective synthesis of (1-hydroxyethylidene)-1,1-bisphosphonate partial esters. *Synthesis* 4:633–637
6. Krawczyk H (1997) A convenient route for monoalkylation of diethyl phosphonates. *Synth Commun* 27:3151–3161
7. Wang T, He HW (2004) Simple and improved preparation of α -oxophosphonate monolithium salts. *Phosphorus, Sulfur Silicon Relat Elem* 179:2081–2089
8. Wang T, Zou P, Peng H et al (2014) Synthesis, crystal structure and biological activity of lithium alkyl 1-(2-(substituted phenoxy)acetoxy)alkylphosphonate. *Chin J Org Chem* 34: 215–219
9. He HW, Wang T, Yuan JL (2005) Synthesis and herbicidal activities of methyl-1-(2,4-dichlorophenoxyacetoxy)alkylphosphonate monosalts. *J Organomet Chem* 690:2608–2613
10. Peng H, Wang T, Xie P et al (2007) Molecular docking and three-dimensional quantitative structure-activity relationship studies on the binding modes of herbicidal 1-(substituted phenoxyacetoxy)alkylphosphonate to the E1 component of pyruvate dehydrogenase. *J Agric Food Chem* 55:1871–1880

11. Wang T, He HW (2004) An efficient synthesis of α -(2,4-dichloro-phenoxyacetoxy)aryl methyl phosphonate monosodium salts. *Synth Commun* 34:1415–1423
12. Wang T, Wang W, Peng H et al (2013) Synthesis and herbicidal activities of potassium methyl 1-(substituted phenoxyacetoxy)alkylphosphonate. *Chem Res Chin U* 29:690–694
13. Peng H, Deng XY, Gao L et al (2014) Synthesis and herbicidal activities of 2-methylpropan-2-aminium *O*-methyl 1-(substituted phenoxyacetoxy)alkylphosphonates. *Chem Res Chin U* 30:82–86
14. Gao L, Deng XY, Tan XS et al (2013) Synthesis and herbicidal activities of 2-methylpropan-2-aminium methyl 1-(substituted phenoxyacetoxy)alkylphosphonates. *Phosphorus, Sulfur Silicon Relat Elem* 188:989–994
15. Zygmunt J, Kafarski P, Mastalerz P (1978) Preparation of oxoalkanephosphonic acids. *Synthesis* 1978(8):609–612
16. Kafarski P, Soroka M (1982) An improved synthesis of N-(phosphonoacetyl)amino acids. *Synthesis* 3:219–221
17. Vepsäläinen J, Nupponen H, Pohjala E (1993) Bisphosphonic compounds V. Selective preparation of (dichloromethylene)bisphosphonate partial esters. *Tetrahedron Lett* 34:4551–4554
18. Olah GA, Narang SC (1982) Iodotrimethylsilane—a versatile synthetic reagent. *Tetrahedron* 38:2225–2277
19. Olah GA, Narang SC, Gupta BGB et al (1979) Synthetic methods and reactions. 62. Transformations with chlorotrimethylsilane/sodium iodide, a convenient in situ iodotrimethylsilane reagent. *J Org Chem* 44:1247–1251
20. Peng H, Long QW, Deng XY et al (2013) Synthesis and herbicidal activities of lithium or potassium hydrogen 1-(substituted phenoxyacetoxy)alkylphosphonates. *Phosphorus, Sulfur Silicon Relat Elem* 188:1868–1874
21. Long QW, Deng XY, Peng H et al (2013) Synthesis and herbicidal activity of sodium hydrogen 1-(substituted phenoxyacetoxy)alkylphosphonates. *Phosphorus, Sulfur Silicon Relat Elem* 188:819–825
22. Smith DJH, Ogilvie KK, Gillen MF (1980) The methyl group as phosphate protecting group in nucleotide syntheses. *Tetrahedron Lett* 21:861–864
23. Gangjee A, Zhao Y, Hamel E et al (2011) Synthesis and biological activities of (R)- and (S)-N-(4-methoxyphenyl)-N,2,6-trimethyl-6,7-dihydro-5H-cyclopenta[d]pyrimidin-4-aminium chloride as potent cytotoxic antitubulin agents. *J Med Chem* 54:6151–6155
24. Moonen K, Laureyn I, Stevens CV (2004) Synthetic methods for azaheterocyclic phosphonates and their biological activity. *Chem Rev* 104:6177–6216

Chapter 4

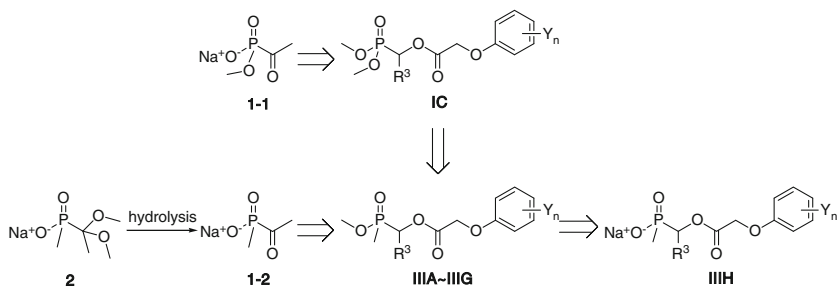
Alkylphosphinates

Sodium methylacetylphosphonate **1-1** with herbicidal activity was confirmed to be a good competitive inhibitor of plant PDHc E1. Sodium methylphosphinate **2** (Scheme 4.1) was further found to be a more effective compound than **1-1** by Baillie et al. [1]. These results showed that phosphinates had higher PDHc E1 enzyme inhibition and higher herbicidal activity than the corresponding acylphosphonate [2]. According to the aspect of bioisosterism in designing bioactive compounds [3, 4], phosphinate unit is also often used to replace the phosphonate unit to obtain a more active compound [5, 6]. Above reasons inspired us to replace the phosphonate moiety in the structure **Io** with phosphinate moiety.

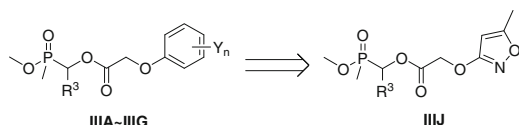
As stated in Chaps. 2 and 3, 1-substituted alkylphosphonates and salts of alkylphosphonates, such as **IC-22** (clacyfos, HW02), **IG-21** (HWS), and **IIJ-24** were found to display promising herbicidal activity and good selectivity for development as a potential herbicide. These results also encouraged us for further exploration on alkylphosphinates based on these alkylphosphonates. Therefore, we are very interested to design novel 1-(substituted phenoxyacetoxy) alkylphosphinates and examine their herbicidal activity.

One methoxyl group of *O,O*-dimethyl moiety in alkylphosphonates **IC** was replaced by methyl group to produce *O*-methyl [1-(substituted phenoxyacetoxy) alkyl]methylphosphinates **IIIA–IIIG** which hydrolyzed to give sodium [1-(substituted phenoxyacetoxy)alkyl]methylphosphinates **IIIH** (Scheme 4.1). Indeed, the preliminary bioassay results showed that most of the alkylphosphinates **IIIC–IIIH** exhibited different herbicidal activity from their corresponding alkylphosphonates.

The useful biological properties of compounds containing the isoxazole ring have received special attention. For the purpose of extending the structure type of phosphinates **III**, we attempted to replace the phenoxy-benzene ring in the structure of **IIIA–IIIG** by isoxazole ring, resulting in a new series of *O*-methyl [1-(5-methylisoxazol-3-yl)oxyacetoxy]alkyl]methylphosphinates **IIIJ** (Scheme 4.2). However, these **IIIJ** showed weak herbicidal activity in subsequent bioassay.



Scheme 4.1 Design of 1-(substituted phenoxyacetoxy)alkylphosphinates **IIIA-IIIH**



Scheme 4.2 Chemical structure modification from **IIIA-IIIH** to **IIIJ**

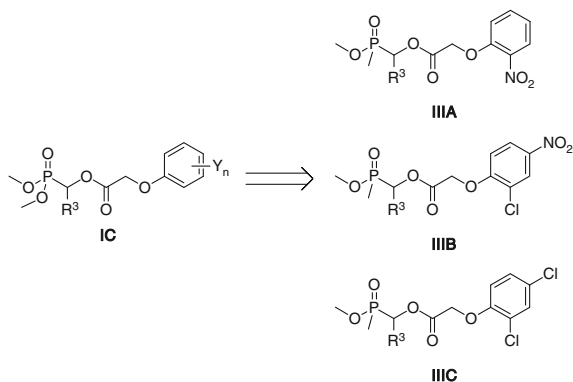
4.1 Alkylphosphinates **IIIA-IIIH**

4.1.1 Introduction

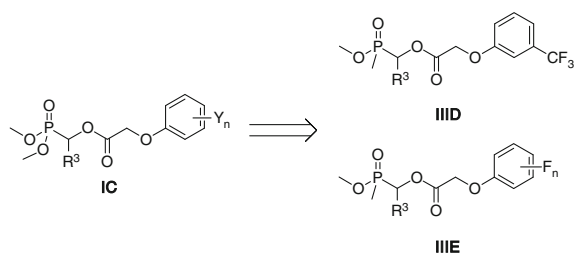
Baillie et al. found that sodium *O*-methyl acetylphosphonate **1-1** was a good competitive inhibitor of plant PDHc E1 and a weak inhibitor of human PDHc E1, but **1-1** was not effective as herbicide [1]. They reasoned that more powerful inhibitors could be produced if the methoxyl group attached to phosphorus was replaced by a smaller and less electronegative substituent. In fact sodium 1,1-dimethoxyethyl(methyl)phosphinate **2** was found to be the most effective herbicidal compound among acylphosphinates and acylphosphonates. The phosphinate **2**, which presumably hydrolyzed to sodium acetyl(methyl)phosphinate **1-2** in vivo (Scheme 4.1), exhibited 80–100 % inhibition against tested weeds at 2.8 kg ai/ha. However, field trials showed that **1-2** was not a candidate for commercial development due to the unacceptable phytotoxicity to the crops at rates that gave good weed control.

SAR analyzes of the relationship between enzyme inhibition and herbicidal activity conducted by Baillie et al. showed that the replacement of methoxyl in acylphosphonate **1-1** by methyl to produce acylphosphinate **1-2**, which indeed led to a great improvement in inhibitory potency and herbicidal activity. Considering that **1-2** had stronger enzyme inhibition and herbicidal activity than **1-1**, it was expected that alkylphosphinates **III** might have more powerful inhibition and herbicidal activity than the corresponding alkylphosphonates. The preliminary bioassay showed that most of **IIIC-IIIH** possessed moderate to good herbicidal activity.

First, three series of phosphinates including *O*-methyl [1-(2-nitrophenoxyacetoxy)alkyl]methylphosphinates **IIIA**, *O*-methyl [1-(2-chloro-4-nitrophenoxyacetoxy)



Scheme 4.3 Design of [1-(substituted phenoxyacetoxy)alkyl]methylphosphinates **IIIA–IIIC**

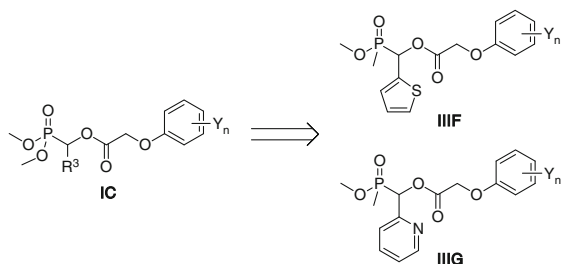


Scheme 4.4 Design of [1-(fluorine-substituted phenoxyacetoxy)alkyl]methylphosphinates **IIID–IIIE**

alkyl]methylphosphinates **IIIB** and *O*-methyl [1-(2,4-dichlorophenoxyacetoxy)alkyl]methylphosphinates **IIIC** were designed by the modification of **IC** (Scheme 4.3). In the **IIIA**, **IIIB** and **IIIC** series, the effect of Y_n as 2-NO₂, 2-Cl,4-NO₂ and 2,4-Cl₂ on herbicidal activity in the phosphinate structure was further examined.

On the other hand, fluorine-containing compounds drew much attention in the field of pesticides due to the unique properties of fluorine, such as osmotic effect, highest electronegativity, smallest atom size next to hydrogen, higher thermal stability, and lipophilicity. More and more attention has been paid to the design of fluorine-containing pesticides, because the introduction of fluorine may enhance the bioactivity and improve the environmental compatibility, as well as improve selectivity, produce high activity, and lower the application rate and toxicity [7–10]. Therefore, fluorine or fluorine-containing groups as Y_n were introduced into parent compound **IC**, which resulted in two series of *O*-methyl [1-(3-trifluoromethylphenoxyacetoxy)alkyl]methylphosphinates **IIID** and *O*-methyl [1-(fluorine-substituted phenoxyacetoxy)alkyl]methylphosphinates **IIIE** (Scheme 4.4).

Furthermore, the introduction of heterocycle groups, such as thienyl or pyridyl group into parent compounds usually to improve the biological activity of compounds [11–14]. Hence, thienyl or pyridyl group as R^3 was introduced into parent compound **IC**. Two series of *O*-methyl [1-(substituted phenoxyacetoxy)-1-(thien-2-yl)methyl]

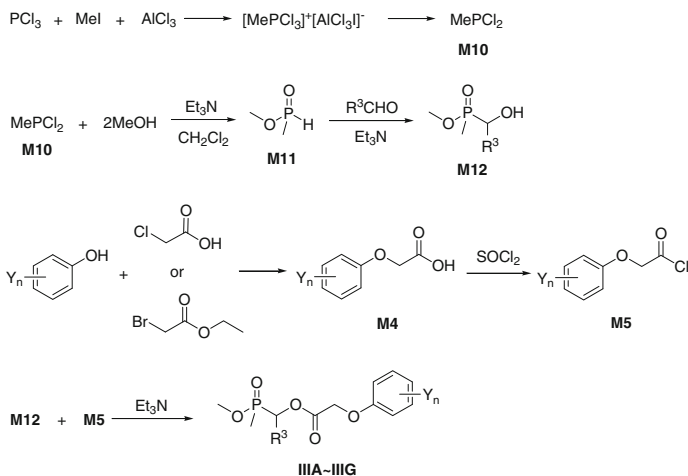


Scheme 4.5 Design of [1-(substituted phenoxyacetoxy)-1-(thien-2-yl or pyrid-2-yl)methyl] methylphosphinates **III F–III G**

methylphosphinates **III F** and *O*-methyl [1-(substituted phenoxyacetoxy)-1-(pyrid-2-yl)methyl]methylphosphinates **III G** were designed (Scheme 4.5).

O-methyl [1-(substituted phenoxyacetoxy)alkyl]methylphosphinates **III A–III G** were easily synthesized by the reaction of *O*-methyl (1-hydroxyalkyl)methylphosphinates with substituted phenoxyacetyl chlorides. The synthetic route of **III A–III G** is shown in Scheme 4.6. *O*-Methyl methylphosphate **M11** was prepared in a two-step sequence starting from phosphorus trichloride, methyl iodide, and aluminium trichloride. *O*-Methyl (1-hydroxyalkyl)methylphosphinates **M12** were prepared by the addition of **M11** and several kinds of aldehydes using triethylamine as the catalyst. Substituted phenoxyacetic acids **M4** and substituted phenoxyacetyl chlorides **M5** were prepared using the method which has been introduced in Chap. 2. **III A–III G** were obtained by the condensation of **M12** with different substituted phenoxyacetyl chlorides **M5**.

The synthetic methods of **III A–III G** and the intermediates are described as follows.

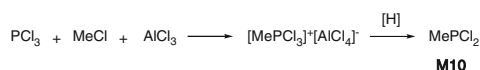


Scheme 4.6 Synthesis of *O*-methyl [1-(substituted phenoxyacetoxy)alkyl]methylphosphinates **III A–III G**

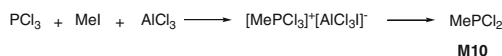
4.1.2 Synthesis of Dichloro(Methyl)Phosphine M10

M10 was prepared from phosphorus trichloride, chloromethane, and aluminum trichloride (Scheme 4.7) [15]. This process appeared to be the most popular methods to synthesize dichloro(methyl)phosphine on a small-scale.

According to the literature studies, aluminum chloride is a preferred reducing agent and chloromethane is replaced by iodomethane (Scheme 4.8) [16–18]. A complex containing methyltrichlorophosphonium ion was obtained in the reaction, which could be reduced to remove chlorine, then generated dichloro(methyl)phosphine **M10**. This reaction was highly exothermic and various by-products were formed.



Scheme 4.7 Synthesis of dichloro(methyl)phosphine **M10** using chloromethane

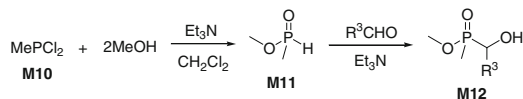


Scheme 4.8 Synthesis of dichloro(methyl)phosphine **M10** using iodomethane

4.1.3 Synthesis of *O*-Methyl (1-Hydroxyalkyl) Methylphosphinates M12

O-Methyl (1-hydroxyalkyl)methylphosphinates **M12** could be prepared by the nucleophilic addition of *O*-methyl methylphosphinate **M11** with several kinds of aldehydes (Scheme 4.9).

O-Methyl methylphosphinate **M11** could be prepared from the corresponding dichloro(methyl)phosphine **M10** by reacting with methanol under anhydrous condition. **M10** was very sensitive to water and easily oxidized, therefore, this reaction was protected from the atmosphere under anhydrous condition.



Scheme 4.9 Synthesis of *O*-methyl (1-hydroxyalkyl)methylphosphinates **M12**

There are several reports about the nucleophilic addition of *O*-methyl methylphosphinate with aldehydes. The synthetic methods of *O*-methyl (1-hydroxyalkyl)methylphosphinates **M12** with different reaction conditions are summarized as three kinds of methods:

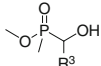
(1) Non-catalytic thermal addition [19, 20]. (2) Base-catalytic addition [21, 22]. (3) Na-catalytic addition [23]. Base-catalytic addition method was chosen to prepare **M12** in our work due to its advantage of being simple and clean. The nucleophilic addition of *O*-methyl methylphosphinate with aldehydes in the presence of a catalytic amount of Et₃N gave *O*-methyl (1-hydroxyalkyl)methylphosphinates **M12** in 53–69 % yields. However, **M12** could not be obtained, when KF/Al₂O₃ as a catalyst was used. The structures of **M12** are listed in Table 4.1.

4.1.4 Synthesis of IIIA–IIIG

The preparation of *O*-methyl [1-(substituted phenoxyacetoxy)alkyl]methylphosphinates **IIIA–IIIG** involved the condensation of substituted phenoxyacetyl chlorides **M5** and *O*-methyl (1-hydroxyalkyl)methylphosphinates **M12** (Scheme 4.6) [24].

Substituted phenoxyacetyl chlorides **M5** could be easily obtained by the reaction of substituted phenoxyacetic acids **M4** and thionyl chloride in high yields (>90 %). Substituted phenoxyacetic acid **M4** could be prepared starting from the substituted phenol and chloroacetic acid [24, 25]. It should be noticed that chloroacetic acid reacted with fluoro-substituted phenol or trifluoromethyl-substituted phenol producing **M4** in very low yield because of the electron withdrawing effect of the fluorine atom. Fluorine-substituted phenoxyacetic acids could be prepared in satisfactory yields by the reaction of fluorine-containing phenol and ethyl 2-bromoacetate followed by alkaline hydrolysis. This has been discussed in Chap. 2 in detail.

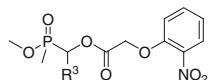
O-methyl [1-(substituted phenoxyacetoxy)alkyl]methylphosphinates **IIIA–IIIG** are similar to *O,O*-dimethyl 1-(substituted phenoxyacetoxy)alkylphosphonates.

Table 4.1 Structure of *O*-methyl (1-hydroxyalkyl)methylphosphinates **M12** 

Compound	R ³	Compound	R ³
M12-1	Me	M12-6	3-NO ₂ Ph
M12-2	Et	M12-7	4-MeOPh
M12-3	<i>n</i> -Pr	M12-8	2-ClPh
M12-4	Ph	M12-9	4-ClPh
M12-5	4-MePh		

They both contain carboxylic ester groups in the molecular structure, which is sensitive to acid, base, and high temperature. Therefore, **IIIA–IIIG** were synthesized at room temperature, and all related reagent and solvents needed to be dried and purified by standard techniques prior to use. On the basis of the above experiment, seven series of novel *O*-methyl [1-(substituted phenoxyacetoxy)alkyl]methylphosphinates **IIIA–IIIG** including 54 compounds were synthesized by condensation of *O*-methyl (1-hydroxyalkyl)methylphosphinates **M12** with substituted phenoxyacetyl chlorides **M5** in the presence of base under mild reaction conditions. Detailed synthetic procedures for **IIIA–IIIG** are introduced in Sect. 9.1.17. The structures of **IIIA–IIIG** are listed in Tables 4.2, 4.3, 4.4, 4.5, 4.6, 4.7 and 4.8, respectively.

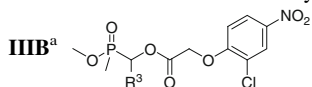
Table 4.2 Structure of *O*-methyl [1-(2-nitrophenoxyacetoxy)alkyl]methylphosphinates **IIIA**^a



Compound	R ³	Compound	R ³
IIIA-1	Me	IIIA-6	3-NO ₂ Ph
IIIA-2	Et	IIIA-7	4-MeOPh
IIIA-3	<i>n</i> -Pr	IIIA-8	2-ClPh
IIIA-4	Ph	IIIA-9	4-ClPh
IIIA-5	4-MePh		

^a Synthesis of **IIIA-1–IIIA-9** [24]

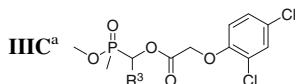
Table 4.3 Structure of *O*-methyl [1-(2-chloro-4-nitrophenoxyacetoxy)alkyl]methylphosphinates



Compound	R ³	Compound	R ³
IIIB-1	Me	IIIB-3	3-NO ₂ Ph
IIIB-2	Et	IIIB-4	4-ClPh

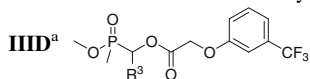
^a Synthesis of **IIIB-1–IIIB-4** [24]

Table 4.4 Structure of *O*-methyl [1-(2,4-dichlorophenoxyacetoxy)alkyl]methylphosphinates



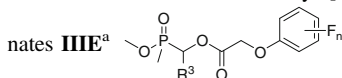
Compound	R ³	Compound	R ³
IIIC-1	Me	IIIC-6	3-NO ₂ Ph
IIIC-2	Et	IIIC-7	4-MeOPh
IIIC-3	<i>n</i> -Pr	IIIC-8	2-ClPh
IIIC-4	Ph	IIIC-9	4-ClPh
IIIC-5	4-MePh		

^a Synthesis of **IIIC-1–IIIC-9** [24]

Table 4.5 Structure of *O*-methyl [1-(3-trifluoromethylphenoxy)acetoxy]alkyl]methylphosphinates

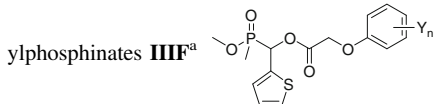
Compound	R ³	Compound	R ³
IIID-1	Me	IIID-4	2-ClPh
IIID-2	Et	IIID-5	4-ClPh
IIID-3	3-NO ₂ Ph	IIID-6	2,4-Cl ₂ Ph

^a Synthesis of **IIID-1–IIID-4** [24]; **IIID-5–IIID-6** [25]

Table 4.6 Structure of *O*-methyl [1-(fluorine-substituted phenoxy)acetoxy]alkyl]methylphosphinates **IIIE^a**

Compound	R ³	F _n	Compound	R ³	F _n
IIIE-1	Ph	2-F	IIIE-6	2-ClPh	2-F
IIIE-2	Ph	4-F	IIIE-7	2-ClPh	4-F
IIIE-3	4-MePh	2-F	IIIE-8	2-ClPh	2,4-F ₂
IIIE-4	4-MePh	2,4-F ₂	IIIE-9	2,4-Cl ₂ Ph	2-F
IIIE-5	4-FPh	2-F	IIIE-10	2,4-Cl ₂ Ph	4-F

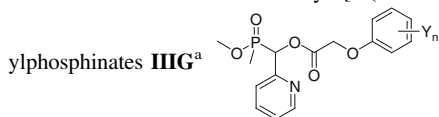
^a Synthesis of **IIIE-1–IIIE-10** [25]

Table 4.7 Structure of *O*-methyl [1-(substituted phenoxy)acetoxy]-1-(thien-2-yl)methyl]methylphosphinates **IIIF^a**

Compound	Y _n	Compound	Y _n
IIIF-1	3-CF ₃	IIIF-5	2-Cl,5-Me
IIIF-2	2-F	IIIF-6	2,3-Cl ₂
IIIF-3	4-Cl	IIIF-7	2,4-Cl ₂
IIIF-4	3-Me,4-Cl	IIIF-8	2,6-Cl ₂

^a Synthesis of **IIIF-1–8** [26]

The structures of *O*-methyl [1-(substituted phenoxy)acetoxy]alkyl]methylphosphinates **IIIA–IIIG** were established by IR, ¹H NMR and elemental analysis. Some of them were further characterized by ³¹P NMR, ¹³C NMR, and MS. **IIIE-9** was analyzed by X-ray single-crystal diffraction. Spectroscopic analyzes of some representative **IIIA–IIIG** are given in Sect. 4.1.5.

Table 4.8 Structure of *O*-methyl [1-(substituted phenoxyacetoxy)-1-(pyrid-2-yl)methyl]meth-

Compound	Y _n	Compound	Y _n
IIIG-1	3-CF ₃	IIIG-5	2-Cl,5-Me
IIIG-2	2-F	IIIG-6	2,3-Cl ₂
IIIG-3	4-Cl	IIIG-7	2,4-Cl ₂
IIIG-4	3-Me,4-Cl	IIIG-8	2,6-Cl ₂

^a Synthesis of **IIIG-1–8** [27]

4.1.5 Spectroscopic Analysis of IIIA–IIIG

The IR spectra of **IIIA–IIIG** showed normal stretching absorption bands, indicating the existence of the Ph–H (3,050 cm⁻¹), C=O (1,750–1,770 cm⁻¹), skeleton vibration of aromatic ring (1,620, 1,450 cm⁻¹), P=O (1,260 cm⁻¹), and P–O–C (1,025–1,045 cm⁻¹). The IR spectrum of **IID-4** is shown in Fig. 4.1.

The ¹H NMR spectra of **IIIA–IIIG** showed that the proton signals corresponding to methyl, methoxyl, and methylidyne attached to phosphorus appeared as two doublets, respectively. For example, the CH₃ signals of **IIIF-6** appeared at δ 1.49 (d) and 1.56 (d), the CH₃O signals at δ 3.69 (d) and 3.75 (d), and the CH signals at δ 6.50 (d) and 6.58 (d), respectively (Fig. 4.2). Proton signals of two pairs

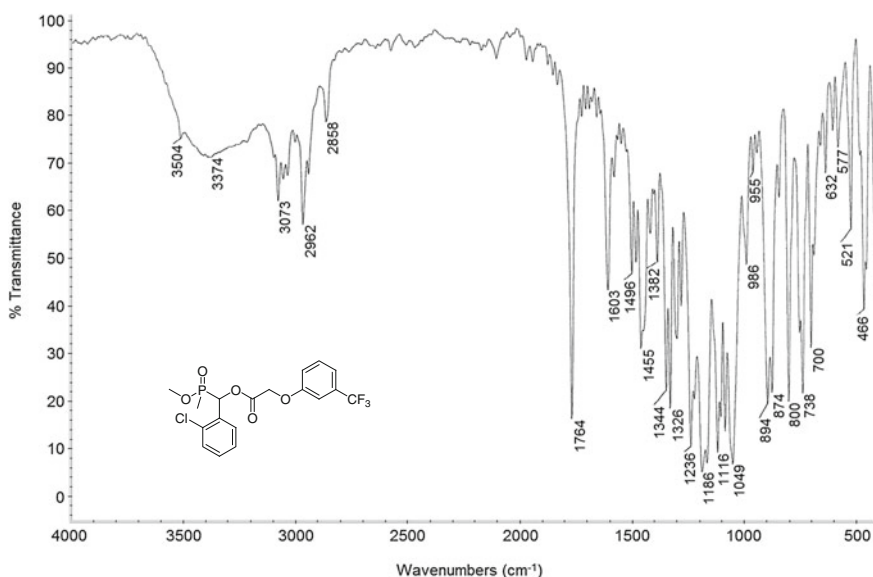


Fig. 4.1 IR spectrum of **IID-4**

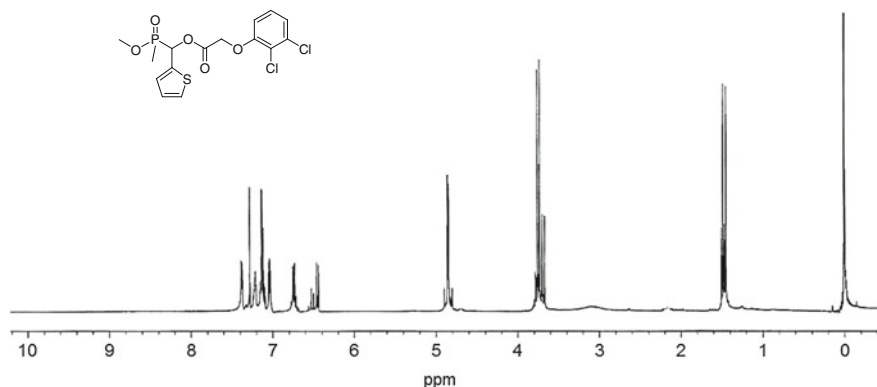


Fig. 4.2 ^1H NMR spectrum of **III F-6** (CDCl_3 , 400 MHz)

of diastereoisomers were split into two doublets signals by the magnetic nucleus phosphorus. The signal strength of these two doublets was different, which indicated the ratio of two conformations was different. However, in the extreme case, when two doublets were partly overlaid, they merged into an irregular triplet, exemplified by **III E-5** (Fig. 4.3). The CH_3 signals of **III E-5** appeared at δ 1.37 (t) and the CH_3O signals at δ 3.62 (t), respectively. The signal corresponding to the methylene group (CH_2) flanked by the phenoxy group and carbonyl group appeared as a quartet at δ 4.81, which belonged to the AB system with the difference in chemical shift between the two mutually coupled protons A and B.

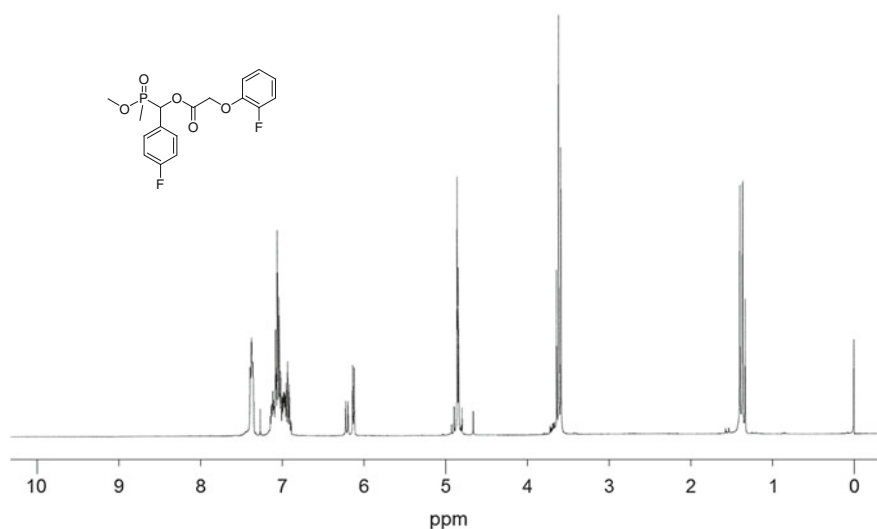


Fig. 4.3 ^1H NMR spectrum of **III E-5** (CDCl_3 , 400 MHz)

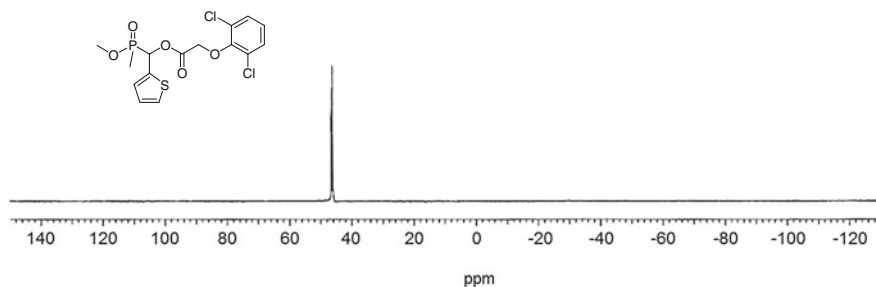


Fig. 4.4 ^{31}P NMR spectrum of **III F-8** (CDCl_3 , 162 MHz)

^{31}P NMR chemical shifts of **III** appeared as a doublet due to the two diastereoisomers. For example, chemical shifts of **III F-8** appeared at δ 46.13 and 46.59 ppm. The chemical shifts of phosphinates **IIIA–IIIG** moved upfield by approximately 20 ppm compared with that of the corresponding dimethyl alkyl phosphonates **IC**. The ^{31}P NMR spectrum of **III F-8** is shown in Fig. 4.4.

The EI mass spectra of phosphinates **IIIA–IIIG** gave weak molecular ion peaks. All the fragmentation ions of **IIIA–IIIG** were consistent with the structure and could be clearly assigned. For example, **III F-7** was characterized: MS m/z (%): 408 (M^+ , 11.68), 315 (4.96), 309 (6.61), 205 (7.96), 203 (2.51), 189 (9.07), 175 (31.71), 161 (6.46), 145 (32.14), 111 (79.22), 93 (100). MS spectra of **III F-7** and its fragmentation mechanism are shown in Figs. 4.5 and 4.6, respectively.

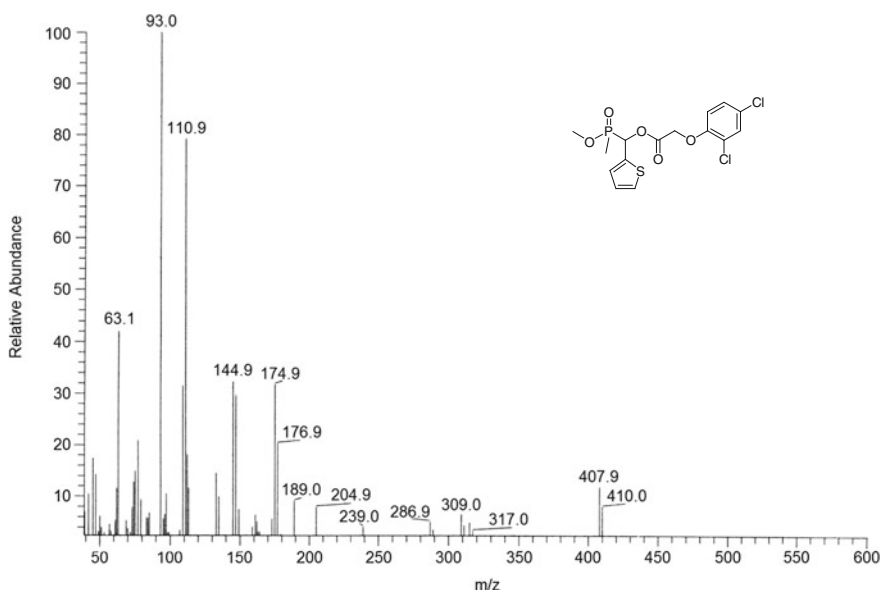


Fig. 4.5 EI-MS spectrum of **III F-7**

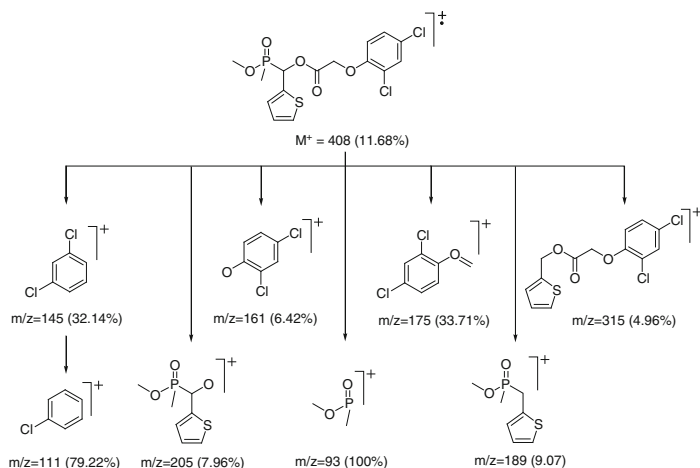


Fig. 4.6 Fragmentation mechanism of **III F-7**

4.1.6 Crystal Structure Analysis of **III E-9**

The molecular structure of **III E-9** is shown in Fig. 4.7. The packing diagram of the unit cell **III E-9** is shown in Fig. 4.8. Selected bond lengths and angles are presented in Table 4.9. It can be seen from the X-ray single crystal structure of **III E-9** that all

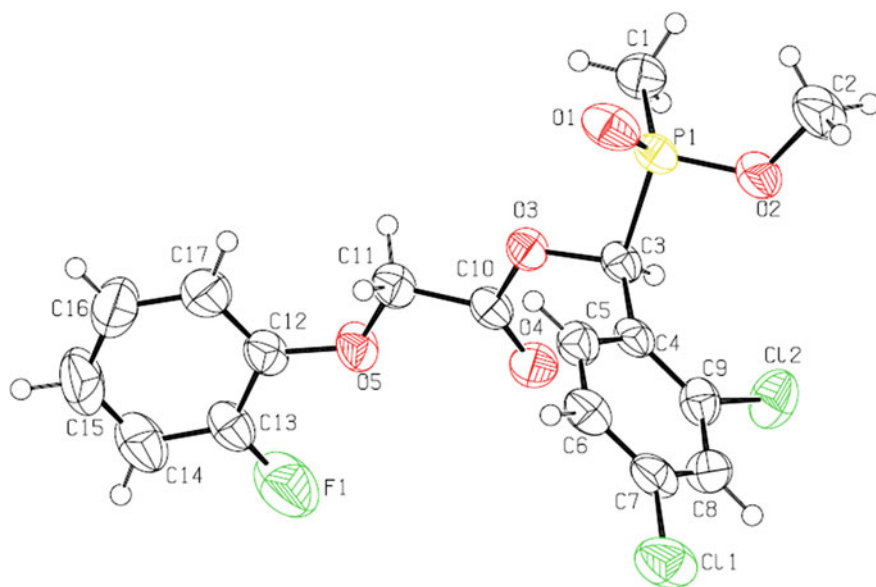


Fig. 4.7 Molecular structure of **III E-9**

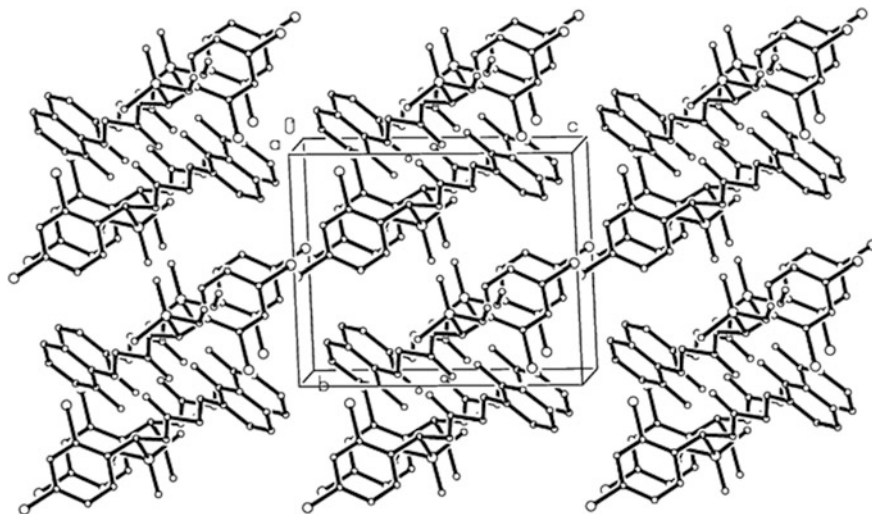


Fig. 4.8 Packing diagram of **III E-9**

Table 4.9 Selected bond distance (Å) and angles (°) for **III E-9**

Bond	Distance	Bond	Angles degree
P(1)–O(1)	1.476(4)	O(1)–P(1)–C(1)	113.5(2)
P(1)–O(2)	1.570(4)	O(2)–P(1)–C(1)	107.7(2)
P(1)–C(1)	1.769(5)	O(1)–P(1)–C(3)	114.9(2)
P(1)–C(3)	1.841(4)	O(2)–P(1)–C(3)	96.72(19)
O(2)–C(2)	1.433(6)	C(1)–P(1)–C(3)	105.5(2)
C(3)–O(3)	1.448(5)	C(2)–O(2)–P(1)	120.8(3)

bond lengths and angles show normal values. The tetrahedron of the phosphorus atom is greatly distorted. The O(2)–P(1)–C(3) and C(1)–P(1)–C(3) bond angles are 96.72° and 105.52° respectively, but the O(1)–P(1)–O(2) bond angle is 116.72°.

4.1.7 Herbicidal Activity of IIIA–IIIG

O-Methyl [1-(substituted phenoxyacetoxy)alkyl]methylphosphinates **IIIA–IIIC** and **IIID-1–IIID-4** were evaluated at 2.25 kg ai/ha for pre-emergence and post-emergence herbicidal activity in the greenhouse. These compounds were tested against a range of weed species including rape (*Brassica campestris*), cucumber (*Cucumis sativus*), lettuce (*Lactuca sativa*), setose thistle (*Cirsium japonicum*), wheat (*Triticum aestivum*), crab grass (*Digitaria sanguinalis*), and barnyard grass

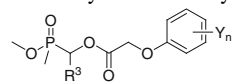
(*Echinochloa crusgalli*). The results are shown in Tables 4.10, 4.11, 4.12, 4.13, 4.14, 4.15 and 4.16. The herbicidal activity of **III D-5–III D-6** and **III E** were evaluated at 0.9 kg ai/ha in greenhouse. They were tested for pre-emergence and post-emergence inhibitory effect against leaf mustard (*Brassica juncea*), common amaranth (*Amaranthus retroflexus*), chingma abutilon (*Abutilon theophrasti*), barnyard grass (*E. crusgalli*), green bristlegrass (*Setaria viridis*), and crab grass (*D. sanguinalis*). The results are shown in Tables 4.17 and 4.18. The herbicidal activity of **III F–III G** against barnyard grass and cabbage type rape (*Brassica napus*) at 100 and 10 mg/L were evaluated by Petri dish method. The results are listed in Tables 4.19 and 4.20. The herbicidal activities of **III A–III G** are summarized as follows.

4.1.7.1 Herbicidal Activity of *O*-Methyl [1-(Substituted Phenoxyacetoxy) Alkyl]Methylphosphinates **III A** and **III B**

(A) Pre-emergence herbicidal activity of **III A** and **III B**

As shown in Table 4.10, most of *O*-methyl [1-(2-nitrophenoxyacetoxy)alkyl] methylphosphinates **III A** and *O*-methyl [1-(2-chloro-4-nitrophenoxyacetoxy)alkyl] methylphosphinates **III B** were almost inactive in pre-emergence application at 2.25 kg ai/ha except that **III A-8** ($R^3=2\text{-ClPh}$) and **III B-1** ($R^3=\text{Me}$) showed >90 % inhibitory activity against lettuce or crab grass, respectively.

Table 4.10 Structure and pre-emergence herbicidal activity of *O*-methyl [1-(substituted phenoxyacetoxy)alkyl]methylphosphinates **III A–III B**^a



Compound	R ³	Y _n	Dicotyledon				Monocotyledon		
			Bra ^b	Cuc ^b	Lac ^b	Cir ^b	Tri ^b	Dig ^b	Ech ^b
III A-1	Me	2-NO ₂	D	D	D	D	D	D	D
III A-2	Et	2-NO ₂	D	B	D	D	D	D	D
III A-3	<i>n</i> -Pr	2-NO ₂	D	D	D	D	D	D	D
III A-4	Ph	2-NO ₂	D	D	D	D	D	D	D
III A-5	4-MePh	2-NO ₂	D	D	D	D	D	D	D
III A-6	3-NO ₂ Ph	2-NO ₂	D	D	D	D	D	D	D
III A-7	4-MeOPh	2-NO ₂	D	D	D	D	D	D	D
III A-8	2-ClPh	2-NO ₂	D	D	A	D	D	D	D
III A-9	4-ClPh	2-NO ₂	D	D	D	D	D	D	D
III B-1	Me	2-Cl,4-NO ₂	D	NT	NT	D	D	A	C
III B-2	Et	2-Cl,4-NO ₂	D	D	D	D	D	D	D
III B-3	3-NO ₂ Ph	2-Cl,4-NO ₂	D	NT	D	D	D	D	D
III B-4	4-ClPh	2-Cl,4-NO ₂	D	D	D	D	D	D	D

^a Inhibitory potency (%) against the growth of plants at a rate of 2.25 kg ai/ha in the greenhouse was expressed as four scales—A: 90–100 %, B: 75–89 %, C: 50–74 %, D: <50 %, and NT: not tested

^b Bra: rape; Cuc: cucumber; Lac: lettuce; Cir: setose thistle; Tri: wheat; Dig: crab grass; Ech: barnyard grass

Table 4.11 Structure and post-emergence herbicidal activity of *O*-methyl [1-(substituted phenoxyacetoxy)alkyl]methylphosphinates **IIIA–IIIB**^a

Compound	R ³	Y _n	Dicotyledon				Monocotyledon		
			Bra ^b	Cuc ^b	Lac ^b	Cir ^b	Tri ^b	Dig ^b	Ech ^b
IIIA-1	Me	2-NO ₂	D	D	D	D	D	D	D
IIIA-2	Et	2-NO ₂	D	NT	D	D	D	D	D
IIIA-3	<i>n</i> -Pr	2-NO ₂	D	NT	NT	NT	D	D	D
IIIA-4	Ph	2-NO ₂	D	D	NT	D	D	D	D
IIIA-5	4-MePh	2-NO ₂	D	D	D	D	D	D	D
IIIA-6	3-NO ₂ Ph	2-NO ₂	D	D	D	D	D	D	D
IIIA-7	4-MeOPh	2-NO ₂	D	D	D	NT	D	D	D
IIIA-8	2-ClPh	2-NO ₂	D	D	D	D	D	D	D
IIIA-9	4-ClPh	2-NO ₂	D	D	D	D	D	NT	D
IIIB-1	Me	2-Cl,4-NO ₂	D	D	D	D	D	D	D
IIIB-2	Et	2-Cl,4-NO ₂	D	D	NT	C	D	C	D
IIIB-3	3-NO ₂ Ph	2-Cl,4-NO ₂	D	D	NT	D	D	D	D
IIIB-4	4-ClPh	2-Cl,4-NO ₂	D	D	D	C	D	D	D

^a Inhibitory potency (%) against the growth of plants at a rate of 2.25 kg ai/ha in the greenhouse was expressed as four scales—A: 90–100 %, B: 75–89 %, C: 50–74 %, D: <50 %, and NT: not tested

^b Bra: rape; Cuc: cucumber; Lac: lettuce; Cir: setose thistle; Tri: wheat; Dig: crab grass; Ech: barnyard grass

(B) Post-emergence herbicidal activity of **IIIA** and **IIIB**

As shown in Table 4.11, although a few compounds showed weak herbicidal activity, most of **IIIA** and **IIIB**, were almost inactive in post-emergence application at 2.25 kg ai/ha.

(C) SAR analysis for **IIIA** and **IIIB**

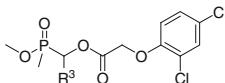
As shown in Tables 4.10 and 4.11, most of **IIIA** and **IIIB** were almost inactive in pre-emergence and post-emergence applications at 2.25 kg ai/ha. As shown in Tables 4.10 and 4.11 the introduction of 2-NO₂ or 2-Cl,4-NO₂ as Y_n on the phenoxy-benzene ring in the phosphinate structure was not beneficial to herbicidal activity.

4.1.7.2 Herbicidal Activity of *O*-Methyl [1-(2,4-Dichlorophenoxyacetoxy) Alkyl]Methylphosphinates **IIIC**

(A) Pre-emergence herbicidal activity of **IIIC**

As shown in Table 4.12, most of **IIIC** displayed significant pre-emergence herbicidal activity against dicotyledon and monocotyledon except wheat at 2.25 kg ai/ha. All of **IIIC** showed >90 % inhibitory activity against rape and cucumber. Most of **IIIC** displayed higher inhibitory activity against crab grass and barnyard grass, but were almost inactive against monocotyledonous crop, wheat at 2.25 kg ai/ha. It

Table 4.12 Structure and pre-emergence herbicidal activity of *O*-methyl [1-(2,4-dichlorophenoxyacetoxymethyl)alkyl]methylphosphinates **IIIc**^a



Compound	R ³	Dicotyledon				Monocotyledon		
		Bra ^b	Cuc ^b	Lac ^b	Cir ^b	Tri ^b	Dig ^b	Ech ^b
IIIc-1	Me	A	A	A	A	D	A	A
IIIc-2	Et	A	A	A	D	D	A	A
IIIc-3	<i>n</i> -Pr	A	A	A	C	D	A	A
IIIc-4	Ph	A	A	B	D	D	A	B
IIIc-5	4-MePh	A	A	A	C	D	A	B
IIIc-6	3-NO ₂ Ph	A	A	A	A	D	A	A
IIIc-7	4-MeOPh	A	A	C	D	D	A	A
IIIc-8	2-ClPh	A	A	NT	A	D	A	A
IIIc-9	4-ClPh	A	A	D	D	D	D	B

^a Inhibitory potency (%) against the growth of plants at a rate of 2.25 kg ai/ha in the greenhouse was expressed as four scales—A: 90–100 %, B: 75–89 %, C: 50–74 %, D: <50 %, and NT: not tested

^b Bra: rape; Cuc: cucumber; Lac: lettuce; Cir: setose thistle; Tri: wheat; Dig: crab grass; Ech: barnyard grass

showed that **IIIc** had a good selectivity between wheat and tested weeds species in pre-emergence application. Especially, **IIIc-1** (R³=Me) and **IIIc-6** (R³=3-NO₂Ph) showed >90 % inhibitory activity against all tested species except wheat at 2.25 kg ai/ha.

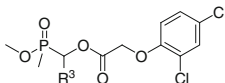
(B) Post-emergence herbicidal activity of **IIIc**

As shown in Table 4.13, most of **IIIc** displayed significant post-emergence herbicidal activity against the tested species at 2.25 kg ai/ha. Most of **IIIc** displayed higher inhibitory activity against dicotyledon than monocotyledon. All of **IIIc**, except **IIIc-2** (R³=Et), showed >90 % inhibitory activity against all the four tested dicotyledonous plants. As for monocotyledons, all of **IIIc** showed >90 % inhibitory activity against crab grass. Most of **IIIc** showed >75 % inhibitory activity against barnyard grass. However, they were almost inactive against wheat. It showed that **IIIc** had a good selectivity between wheat and tested weed species in post-emergence application. Especially, **IIIc-3** (R³=*n*-Pr) and **IIIc-6** (R³=3-NO₂Ph) showed >90 % inhibitory activity against all tested species except wheat at 2.25 kg ai/ha.

(C) SAR analysis for **IIIc**

The results in Tables 4.12 and 4.13 showed that most of [1-(2,4-dichlorophenoxyacetoxymethyl)alkyl]methylphosphinates **IIIc** displayed significant inhibitory activity against tested species except wheat in pre-emergence and post-emergence applications at 2.25 kg ai/ha. Compared with phosphinates **IIIa** (Y_n=2-NO₂) and **IIIb** (Y_n=2-Cl,4-NO₂), the herbicidal activity of phosphinates **IIIc** was greatly

Table 4.13 Structure and post-emergence herbicidal activity of *O*-methyl [1-(2,4-dichlorophenoxyacetoxy)alkyl]methylphosphinates **IIIC**^a



Compound	R ³	Dicotyledon				Monocotyledon		
		Bra ^b	Cuc ^b	Lac ^b	Cir ^b	Tri ^b	Dig ^b	Ech ^b
IIIC-1	Me	A	A	NT	A	D	A	A
IIIC-2	Et	A	A	NT	D	D	A	B
IIIC-3	<i>n</i> -Pr	A	A	A	A	D	A	B
IIIC-4	Ph	A	A	NT	A	D	A	B
IIIC-5	4-MePh	A	A	A	A	D	A	B
IIIC-6	3-NO ₂ Ph	A	A	NT	A	D	A	A
IIIC-7	4-MeOPh	A	NT	NT	A	D	A	D
IIIC-8	2-ClPh	A	A	A	A	D	A	B
IIIC-9	4-ClPh	A	A	A	A	D	A	C

^a Inhibitory potency (%) against the growth of plants at a rate of 2.25 kg ai/ha in the greenhouse was expressed as four scales—A: 90–100 %, B: 75–89 %, C: 50–74 %, D: <50 %, and NT: not tested

^b Bra: rape; Cuc: cucumber; Lac: lettuce; Cir: setose thistle; Tri: wheat; Dig: crab grass; Ech: barnyard grass

enhanced by introducing 2,4-Cl₂ as Y_n on the phenoxy-benzene ring in the phosphinate structure. It showed that the 2,4-dichlorophenoxy-benzene ring was a very important pharmacophore. When 2,4-Cl₂ as Y_n on the phenoxy-benzene ring were kept constant, the substituent R³ also had significant influence on the herbicidal activity of phosphinates **IIIC**. R³ as Me or 3-NO₂Ph was beneficial to pre-emergence and post-emergence activity, such as **IIIC-1** (R³=Me) and **IIIC-6** (R³=3-NO₂Ph) showed the best herbicidal activity against all tested species except wheat in pre-emergence and post-emergence application at 2.25 kg ai/ha. However, the introduction of other substituents as R³ resulted in a decrease in pre-emergence activity or post-emergence activity.

It was noted that when **IIIC** with 2,4-Cl₂ as Y_n were kept constant, irrespective of the difference of substituents in the R³ moiety, all of **IIIC** showed weak or no inhibitory activity against crop wheat (*T. aestivum*) for pre-emergence and post-emergence applications. The results suggested that **IIIC** would provide a high level of safety for wheat, one of China's main crops.

From the data in Table 4.14, we can see that alkylphosphinates **IIIC** displayed similar inhibitory activity against rape to their corresponding alkylphosphonates **IC**, **IE** and **IF**. It is noteworthy that most of the alkylphosphinates **IIIC** showed higher inhibition against monocot crab grass and barnyard grass than their corresponding alkylphosphonates **IC**, **IE** or **IF** in pre-emergence and post-emergence application at 2.25 kg ai/ha. Especially, several alkylphosphinates, such as **IIIC-1**, **IIIC-3**, and **IIIC-6** exhibited a higher selectivity between wheat and weeds than their corresponding alkylphosphonates.

Table 4.14 Herbicidal activity of phosphinates **III C** and phosphonates **IC**, **IE**, and **IF**^a

Compound	R ³	III C						IC, IE, IF					
		Pre-emergence			Post-emergence			Pre-emergence			Post-emergence		
		Dico ^b	Tri ^b	Ech ^b	Dico ^b	Tri ^b	Ech ^b	Dico ^b	Tri ^b	Ech ^b	Dico ^b	Tri ^b	Ech ^b
III C-1	Me	A	D	A	A	A	A	D	A	A	A	D	A
IC-22	Me	A	B	C	A	C	A	D	D	C	C	D	C
III C-2	Et	A	D	A	A	A	A	D	D	A	A	D	A
IC-27	Et	A	B	D	A	D	A	D	D	A	B	D	C
III C-3	<i>n</i> -Pr	A	D	A	A	A	A	D	D	A	A	D	A
IC-32	<i>n</i> -Pr	A	D	B	A	C	A	D	D	A	C	D	C
III C-4	Ph	A	D	A	A	A	A	D	D	A	A	D	B
IE-22	Ph	A	C	C	A	C	A	D	D	A	D	D	D
III C-5	4-MePh	A	D	A	A	B	A	D	D	A	A	D	B
IF-9	4-MePh	C	C	B	A	C	A	C	C	A	D	C	C
III C-6	3-NO ₂ Ph	A	D	A	A	A	A	D	D	A	A	D	A
IF-58	3-NO ₂ Ph	C	D	C	A	C	A	D	D	A	D	D	D
III C-7	4-MeOPh	A	D	A	A	A	A	D	D	A	D	D	D
IF-20	4-MeOPh	D	D	D	D	D	D	D	D	D	D	D	D
III C-8	2-ClPh	A	D	A	A	A	A	D	D	A	A	D	B
IF-24	2-ClPh	A	B	C	A	C	A	C	C	A	C	C	C
III C-9	4-ClPh	A	D	D	A	B	A	D	D	A	A	D	C
IF-31	4-ClPh	A	C	A	B	B	A	C	A	B	B	D	C

^a Inhibitory potency (%) against the growth of plants at a rate of 2.25 kg ai/ha in the greenhouse was expressed as four scales—A: 90–100 %, B: 75–89 %, C: 50–74 %, D: <50 %

^b Bra: rape; Tri: wheat; Dig: crab grass; Ech: barnyard grass

Alkylphosphinate **IIIC-1** displayed higher inhibition (>90 %) against crab grass and barnyard grass than that of its corresponding alkylphosphonate **IC-22** (HW02) in pre-emergence and post-emergence applications. **IIIC-1** also showed better safety for wheat than **IC-22** (HW02) in pre-emergence application.

The above results suggested that when 2,4-Cl₂ as Y_n on the phenoxy-benzene ring was kept constant, the replacement of the phosphonate moiety by the phosphinate moiety had a favorable effect on the inhibition against monocot and a higher selectivity between wheat and weeds.

4.1.7.3 Herbicidal Activity of *O*-Methyl [1-(3-Trifluoromethyl phenoxyacetoxy)Alkyl]Methylphosphinates IIID

(A) Pre-emergence herbicidal activity of IIID

As shown in Table 4.15, **IIID-1–IIID-4** displayed significant pre-emergence herbicidal activity against rape, setose thistle and crab grass at 2.25 kg ai/ha. All of **IIID-1–IIID-4** showed >90 % inhibitory activity against rape, setose thistle, and crab grass. **IIID-4** (R³=4-ClPh) may be the most active compound, which also showed >90 % inhibitory activity against monocotyledonous barnyard grass.

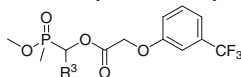
The herbicidal activity of **IIID-5** and **IIID-6** were evaluated at 0.9 kg ai/ha in the greenhouse. They were tested for pre-emergence activity against a range of weed species including barnyard grass (*E. crusgalli*), green bristlegrass (*S. viridis*), crab grass (*D. sanguinalis*), leaf mustard (*B. juncea*), common amaranth (*A. retroflexus*) and chingma abutilon (*A. theophrasti*). As shown in Table 4.17, **IIID-5** and **IIID-6** showed <50 % inhibitory activity against all the tested weeds for pre-emergence application at 0.9 kg ai/ha.

(B) Post-emergence herbicidal activity of IIID

As shown in Table 4.16, **IIID-1–IIID-4** displayed significant post-emergence herbicidal activity against dicotyledon and monocotyledon except wheat at a rate of 2.25 kg/ha. **IIID-1–IIID-4** with >90 % against most tested species including rape, cucumber, lettuce, setose thistle, crab grass, and barnyard grass at 2.25 kg/ha. It showed that these compounds had a good selectivity between wheat and tested weeds species. Furthermore, compared with pre-emergence herbicidal activity, the post-emergence herbicidal activity of **IIID-1–IIID-4** was slightly better.

The post-emergence herbicidal activity of **IIID-5** and **IIID-6** against barnyard grass, green bristlegrass, crab grass, leaf mustard, amaranth, and chingma abutilon,

Table 4.15 Structure and pre-emergence herbicidal activity of *O*-methyl [1-(3-trifluoromethylphenoxy)acetoxy]alkyl]methylphosphinates **IIID**^a

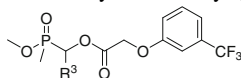


Compound	R ³	Dicotyledon		Monocotyledon		
		Bra ^b	Cir ^b	Tri ^b	Dig ^b	Ech ^b
IIID-1	Me	A	A	C	A	B
IIID-2	Et	A	A	C	A	C
IIID-3	3-NO ₂ Ph	A	A	D	A	C
IIID-4	4-ClPh	A	A	B	A	A

^a Inhibitory potency (%) against the growth of plants at a rate of 2.25 kg ai/ha in the greenhouse was expressed as four scales—A: 90–100 %, B: 75–89 %, C: 50–74 %, D: <50 %

^b Bra: rape; Cir: setose thistle; Tri: wheat; Dig: crab grass; Ech: barnyard grass

Table 4.16 Structure and post-emergence herbicidal activity of *O*-methyl [1-(3-trifluoromethylphenoxy)acetoxy]alkyl]methylphosphinates **IIID**^a



Compound	R ³	Dicotyledon				Monocotyledon		
		Bra ^b	Cuc ^b	Lac ^b	Cir ^b	Tri ^b	Dig ^b	Ech ^b
IIID-1	Me	A	A	A	A	D	A	B
IIID-2	Et	A	A	NT	A	D	A	A
IIID-3	3-NO ₂ Ph	A	A	A	A	D	A	C
IIID-4	4-ClPh	A	A	A	A	C	A	A

^a Inhibitory potency (%) against the growth of plants at a rate of 2.25 kg ai/ha in the greenhouse was expressed as four scales—A: 90–100 %, B: 75–89 %, C: 50–74 %, D: <50 %, and NT: not tested

^b Bra: rape; Cuc: cucumber; Lac: lettuce; Cir: setose thistle; Tri: wheat; Dig: crab grass; Ech: barnyard grass

were evaluated at 0.9 kg ai/ha in the greenhouse. As shown in Table 4.18, **IIID-5** and **IIID-6** showed higher post-emergence herbicidal activity than their pre-emergence herbicidal activity. **IIID-5** showed >75 % inhibitory activity against all tested plants except barnyard grass in post-emergence application.

(C) SAR analysis for **IIID**

The herbicidal activity of 1-(3-trifluoromethylphenoxy)acetoxy]alkyl]phosphinates **IIID** with 3-CF₃ substitution were higher than that of **IIIA** and **IIIB** with 2-NO₂ or 2-Cl,4-NO₂ substitution on the phenoxy-benzene ring which were almost inactive. Most of the compounds with 3-CF₃ on the phenoxybenzene ring showed >90 % inhibitory effect against dicotyledon and monocotyledon for post-emergence treatment at 2.25 kg ai/ha.

4.1.7.4 Herbicidal Activity of *O*-Methyl [1-(Fluorine-Substituted Phenoxyacetoxy)Alkyl]Methylphosphinates III E

The herbicidal activity of phosphinates **III E** were evaluated at a rate of 0.9 kg ai/ha in the greenhouse. They were tested for pre-emergence and post-emergence inhibitory effects against leaf mustard, common amaranth, chingma abutilon, barnyard grass, green bristlegrass, and crab grass. The results are listed in Tables 4.17 and 4.18.

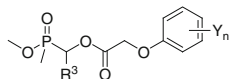
(A) Pre-emergence herbicidal activity of **III E**

As shown in Table 4.17, 1-(fluoro-substituted phenoxyacetoxy)alkylphosphinates **III E** showed weak inhibitory activity for pre-emergence application at 0.9 kg ai/ha. Most of **III E** showed <50 % inhibitory activity against all the tested weeds. Only **III E-2** showed >90 % inhibitory activity against leaf mustard, chingma abutilon, and green bristlegrass. Yet **III E-7** and **III E-10** showed >90 % inhibitory activity against leaf mustard chingma abutilon or barnyard grass, respectively.

(B) Post-emergence herbicidal activity of **III E**

As shown in Table 4.18, several 1-(fluoro-substituted phenoxyacetoxy)alkylphosphinates **III E** influenced the growth of tested plants in post-emergence application more

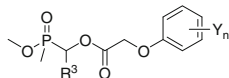
Table 4.17 Structure and pre-emergence herbicidal activity of **III D-5**, **III D-6** and **III E^a**



Compound	R ³	Y _n	Dicotyledon			Monocotyledon		
			Brj ^b	Amr ^b	Abu ^b	Ech ^b	Set ^b	Dig ^b
III D-5	2-ClPh	3-CF ₃	D	D	D	D	D	D
III D-6	2,4-Cl ₂ Ph	3-CF ₃	D	D	D	D	D	D
III E-1	Ph	2-F	D	D	D	D	D	D
III E-2	Ph	4-F	A	C	A	B	A	B
III E-3	4-MePh	2-F	D	D	D	D	D	D
III E-4	4-MePh	2,4-F ₂	D	C	D	D	D	C
III E-5	4-FPh	2-F	D	D	D	D	D	D
III E-6	2-ClPh	2-F	D	D	D	D	D	D
III E-7	2-ClPh	4-F	D	C	A	D	D	D
III E-8	2-ClPh	2,4-F ₂	D	D	D	D	D	D
III E-9	2,4-Cl ₂ Ph	2-F	D	D	D	D	D	D
III E-10	2,4-Cl ₂ Ph	4-F	C	C	B	A	B	B

^a Inhibitory potency (%) against the growth of plants at a rate of 0.9 kg ai/ha in the greenhouse was expressed as four scales—A: 90–100 %, B: 75–89 %, C: 50–74 %, D: <50 %

^b Brj: leaf mustard; Amr: common amaranth; Abu: chingma abutilon; Ech: barnyard grass; Set: green bristlegrass; Dig: crab grass

Table 4.18 Structure and post-emergence herbicidal activity of **IID-5**, **IID-6**, and **III-E**^a

Compound	R ³	Y _n	Dicotyledon			Monocotyledon		
			Brj ^b	Amr ^b	Abu ^b	Ech ^b	Set ^b	Dig ^b
IID-5	2-ClPh	3-CF ₃	B	B	A	C	B	B
IID-6	2,4-Cl ₂ Ph	3-CF ₃	A	D	A	C	D	B
III-E-1	Ph	2-F	D	D	D	D	D	D
III-E-2	Ph	4-F	A	B	A	A	A	A
III-E-3	4-MePh	2-F	D	D	D	D	D	D
III-E-4	4-MePh	2,4-F ₂	C	D	A	B	C	C
III-E-5	4-FPh	2-F	C	D	D	B	D	D
III-E-6	2-ClPh	2-F	D	D	D	D	D	D
III-E-7	2-ClPh	4-F	A	A	A	A	A	A
III-E-8	2-ClPh	2,4-F ₂	A	C	A	D	D	C
III-E-9	2,4-Cl ₂ Ph	2-F	D	D	D	D	D	D
III-E-10	2,4-Cl ₂ Ph	4-F	A	A	A	A	A	A

^a Inhibitory potency (%) against the growth of plants at a rate of 0.9 kg ai/ha in the greenhouse was expressed as four scales—A: 90–100 %, B: 75–89 %, C: 50–74 %, D: <50 %

^b Brj: leaf mustard; Amr: common amaranth; Abu: chingma abutilon; Ech: barnyard grass; Set: green bristlegrass; Dig: crab grass

strongly than they did in pre-emergence application. **III-E-7** and **III-E-10** displayed the best inhibitory activity (>90 %) against all tested plants followed by **III-E-2** for post-emergence application at 0.9 kg ai/ha.

(C) SAR analysis for **III-E**

The structure of substituent Y_n in alkylphosphinates still had a great influence on herbicidal activity according to the results in Tables 4.17 and 4.18. Substituent 4-F as Y_n on the phenoxy-benzene ring was beneficial to post-emergence herbicidal activity against dicotyledons and monocotyledons. Comparing with substituent 4-F, the substituent 2-F or 2,4-F₂ as Y_n resulted in a sharp decrease in herbicidal activity. All 1-(fluoro-substituted phenoxyacetoxy)alkylphosphinates with 2-F as Y_n (such as **III-E-1**, **III-E-3**, **III-E-5**, **III-E-6**, **III-E-9**) or 2,4-F₂ as Y_n (such as **III-E-4**, **III-E-8**) showed weak, or no inhibitory activity against tested plants for post-emergence application at 0.9 kg ai/ha.

SAR analysis showed that substituent 4-F as Y_n on the phenoxy-benzene ring was much beneficial to the post-emergence herbicidal activity of alkylphosphinates **III E**. However substituent 4-F as Y_n was not beneficial to the post-emergence herbicidal activity of alkylphosphonates **IC**. For both alkylphosphinates **III E** and alkylphosphonates **IC**, the introduction of 2-F or 2,4-F₂ as Y_n could result in a sharp decrease in post-emergence herbicidal activity.

4.1.7.5 Herbicidal Activity of *O*-Methyl [1-(Substituted Phenoxyacetoxy)-1-(Thien-2-yl or Pyridin-2-yl)Methyl] Methylphosphinates **IIIF** and **IIIG**

In the preliminary bioassay, **IIIF** and **IIIG** were tested for herbicidal activity against barnyard grass (*E. crusgalli*) and cabbage type rape (*Brassica napus*) by Petri dish method.

(A) *Inhibitory activity against the root of plant*

As seen from Tables 4.19 and 4.20, the inhibitory potencies of all compounds against tested weeds decreased with the decrease of concentration of compounds. **IIIF-3**, **IIIF-4**, **IIIF-7**, **IIIG-1**, **IIIG-3**, **IIIG-4**, and **IIIG-7** displayed >90 % inhibitory activity against the root of barnyard grass and cabbage type rape at 100 and 10 mg/L.

(B) *Inhibitory activity against the stem of plant*

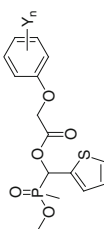
Most of **IIIF** and **IIIG** displayed much higher inhibitory effect on the growth of dicot rape than monocot barnyard grass, compounds **IIIF-3**, **IIIF-4**, **IIIF-7**, **IIIG-3**, **IIIG-4**, and **IIIG-7** showed good inhibitory activity against the stem of rape with more than 90 % inhibition at 100 and 10 mg/L. Although they had more than 90 % inhibition against the root of barnyard grass at 10 mg/L, all these compounds only had 33–68 % inhibition against the stem of barnyard grass at 10 mg/L.

(C) *SAR analysis for IIIF and IIIG*

Substituted methylphosphinates **IIIF** and **IIIG** displayed almost similar inhibitory potency at 100 and 10 mg/L, irrespective of thienyl or pyridyl as R³.

When the MeO and Me group as R¹, R², thienyl, or pyridyl as R³ and H as R⁴ were kept in the general structure **I**, substituent Y_n on the phenoxy-benzene ring had significant influence on the inhibitory activity of phosphinates **IIIF** or **IIIG**. In the **IIIF** or **IIIG** series, 4-Cl, 2,4-Cl₂ or 3-Me,4-Cl as Y_n on the phenoxy-benzene ring respectively, were beneficial to the inhibition against the growth of rape and the root of barnyard grass.

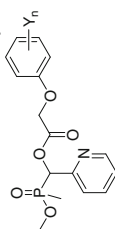
Table 4.19 Inhibitory activity of *O*-methyl [1-(substituted phenoxyacetoxy)-1-(thien-2-yl)methyl]methylphosphinates **IIIF** against the growth of plants^a



Compound	Y _n	Root		Stem					
		Ech ^b		Ech ^b					
		100 mg/L	10 mg/L	100 mg/L	10 mg/L				
IIIF-1	3-CF ₃	93	47	99	60	64	39	97	49
IIIF-2	2-F	80	71	72	4	61	57	31	-8
IIIF-3	4-Cl	98	96	100	99	64	46	97	92
IIIF-4	3-Me,4-Cl	98	96	100	100	54	36	97	95
IIIF-5	2-Cl,5-Me	82	58	94	40	61	57	56	8
IIIF-6	2,3-Cl ₂	96	60	93	26	82	68	54	3
IIIF-7	2,4-Cl ₂	98	98	100	100	89	39	100	97
IIIF-8	2,6-Cl ₂	87	76	97	47	68	68	92	21

^a Inhibitory potency (%) against the growth of plants in Petri dishes, 0 (no effect), 100 % (completely kill)

^b Ech: barnyard grass; Brm: cabbage type rape

Table 4.20 Inhibitory activity of *O*-methyl [1-(substituted phenoxyacetoxy)-1-(pyridin-2-yl)methyl]methylphosphinates **IIIG** against the growth of plants^a

Compound	Y _n	Root			Stem			
		Ech ^b			Ech ^b			
		100 mg/L	10 mg/L	Bm ^b 100 mg/L	100 mg/L	10 mg/L	Bm ^b 100 mg/L	
IIIG-1	3-CF ₃	95	90	98	46	37	94	83
IIIG-2	2-F	77	46	50	41	33	0	3
IIIG-3	4-Cl	97	92	99	52	41	94	92
IIIG-4	3-Me,4-Cl	98	98	99	79	61	95	95
IIIG-5	2-Cl,5-Me	80	49	97	28	35	89	67
IIIG-6	2,3-Cl ₂	91	62	94	68	68	85	5
IIIG-7	2,4-Cl ₂	97	95	99	67	56	94	92
IIIG-8	2,6-Cl ₂	82	42	90	57	57	72	21

^a Inhibitory potency (%) against the growth of plants in Petri dishes, 0 (no effect), 100 % (completely kill)^b Ech: barnyard grass; Bm: cabbage type rape

4.1.8 Summary

O-Methyl [1-(substituted phenoxyacetoxy)alkyl]methylphosphinates **IIIA–IIIG** including 54 compounds were easily synthesized by condensation of *O*-methyl (1-hydroxyalkyl)methylphosphinates **M12** with substituted phenoxyacetyl chlorides **M5** in the presence of base under mild reaction conditions.

The herbicidal activity of **IIIA–IIIG** was examined in Petri dishes or in the greenhouse. SAR analysis for **IIIA–IIIG** indicated that when the MeO and Me group as R¹, R², H as R⁴ were kept in general structure **I**, substituent R³ and Y_n on the phenoxy-benzene ring had significant influence on the inhibitory activity of alkylphosphinates. It showed that the 2,4-dichlorobenzene ring was a very important pharmacophore in the alkylphosphinates structure. The 2,4-Cl₂ substitution on the phenoxy-benzene ring in the alkylphosphinates was most promotive for herbicidal activity followed by 4-F; 4-Cl; 3-Me,4-Cl, and 3-CF₃. The introduction of 2-NO₂; 2-Cl,4-NO₂; 2-Cl,5-Me; 2,3-Cl₂; 2,6-Cl₂; 2-F or 2,4-F₂ as Y_n into the phenoxy-benzene ring, respectively, resulted in a sharp decrease in herbicidal activity. Alkylphosphinates with 2-NO₂ (**IIIA**) or 2-Cl,4-NO₂ (**IIIB**) as Y_n on the phenoxy-benzene ring were almost inactive in pre-emergence and post-emergence applications at 2.25 kg ai/ha. The substituent R³ also had significant influence on the herbicidal activity of alkylphosphinates, such as Me, 3-NO₂Ph, 2-ClPh, 2,4-Cl₂Ph, thienyl, or pyridyl as R³, respectively, were beneficial to the herbicidal activity of alkylphosphinates.

Most alkylphosphinates **IIIC** showed higher inhibition against monocot crab grass and barnyard grass than their corresponding alkylphosphonates **IC**, **IE** or **IF** in pre-emergence and post-emergence applications at 2.25 kg ai/ha. Especially, several alkylphosphinates such as **IIIC-1**, **IIIC-3**, and **IIIC-6** exhibited a higher selectivity between wheat and weeds than their corresponding alkylphosphonates. These results suggested that when 2,4-Cl₂ as Y_n on the phenoxy-benzene ring was kept constant, the replacement of the phosphonate moiety by the phosphinate moiety had a favorable effect on inhibition against monocot and a higher selectivity between wheat and weeds.

Several alkylphosphinates with notable inhibitory activity and selectivity were found by preliminary bioassay. Alkylphosphinates **IIIC** with 2,4-Cl₂ as Y_n exhibited significant inhibitory activity. Especially **IIIC-1** (R³=Me) and **IIIC-6** (R³=3-NO₂Ph) showed >90 % inhibitory activity against rape, cucumber, lettuce, setose thistle, crab grass, and barnyard grass except wheat for pre-emergence and post-emergence applications at 2.25 kg ai/ha. They showed >90 % inhibitory activity against monocot crab grass and barnyard grass, but were almost inactive against the monocot crop, wheat at 2.25 kg ai/ha. The alkylphosphinate **IIIC-1** displayed higher inhibition (>90 %) against crab grass and barnyard grass than that of its corresponding alkylphosphonate **IC-22** in pre-emergence and post-emergence applications. **IIIC-1** also showed better safety for wheat than **IC-22** in pre-emergence application. **IIIC-1** and **IIIC-6** displayed a high level of safety for wheat due to a good selectivity between wheat and tested weeds species.

Alkylphosphinates **IIIE** with 4-F as Y_n exhibited good inhibitory activity. **IIIE-7** (R³=2-ClPh) and **IIIE-10** (R³=2,4-Cl₂Ph) displayed >90 % inhibitory activity

against rape, common amaranth, chingma abutilon, barnyard grass, green bristle-grass, and crab grass in post-emergence application at 0.9 kg ai/ha. **III E-2** ($R^3=Ph$) was found to exhibit significant inhibitory activity against five or six tested species for pre-emergence and post-emergence applications at 0.9 kg ai/ha. Alkylphosphinates **IIIF-3**, **IIIF-4**, **IIIF-7** (thienyl as R^3 , 4-Cl; 3-Me,4-Cl; 2,4-Cl₂ as Y_n respectively), **IIIG-3**, **IIIG-4**, and **IIIG-7** (pyridyl as R^3 , 4-Cl; 3-Me,4-Cl; 2,4-Cl₂ as Y_n respectively) showed >90 % inhibitory activity against the root of barnyard grass and cabbage type rape, and the stem of cabbage type rape at 10 mg/L.

These alkylphosphinates **IIIC-1**, **IIIC-6**, **IIIE-2**, **IIIE-7**, **IIIE-10**, **IIIF-3**, **IIIF-4**, **IIIF-7**, **IIIG-3**, **IIIG-4**, and **IIIG-7** were selected for further evaluation at a lower rate to make sure of their herbicidal activity and potential usage.

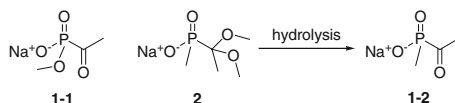
4.2 Sodium Salts of Alkylphosphinic Acids IIIH

4.2.1 Introduction

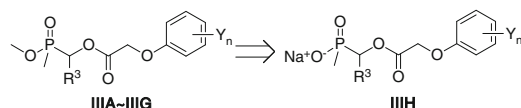
Sodium 1,1-dimethoxyethyl(methyl)phosphinate **2** was found to be the most effective herbicidal compound among plant PDHc E1 inhibitors by Baillie et al.'s work. **2** was presumably hydrolyzed to sodium salt of acetyl(methyl)phosphinic acid **1-2** in vivo to exhibit herbicidal activity (Scheme 4.10). **1-2** displayed higher enzyme inhibition and herbicidal activity than **1-1**. It has been found that **1-1** was a competitive inhibitor of PDHc, but **1-2** caused time-dependent inhibition. Baillie et al. gave a possible explanation for this result, the initial binding of inhibitors to the pyruvate site and subsequent reaction with thiamine pyrophosphate were rapid and reversible for both **1-1** and **1-2**. In the case of **1-2**, an enzyme-inhibitor complex was first formed and then underwent a time-dependent, essentially irreversible transformation to produce a more tightly bound form. In other words, **1-2** could act as a slow, tight binding inhibitor [1].

As stated in Chap. 7, salts of 1-(substituted phenoxyacetoxy)alkylphosphonate showed higher inhibitory activity against plant PDHc E1 than their corresponding phosphonic ester did, because these salts were more analogous to pyruvate which acted as the substrate of PDHc E1.

Therefore, sodium [1-(substituted phenoxyacetoxy)alkyl]methylphosphinates **IIIH** might have more powerful inhibition and herbicidal activity than the corresponding 1-alkylphosphinate. **IIIH** were designed through the replacement of the MeO group that attached to phosphorus by NaO in alkylphosphinates **IIIA–IIIG** (Scheme 4.11).



Scheme 4.10 Plant PDHc E1 inhibitors: sodium *O*-methyl acetylphosphonate **1-1**, sodium 1,1-dimethoxyethyl(methyl)phosphinate **2** and sodium acetyl(methyl)phosphinate **1-2**



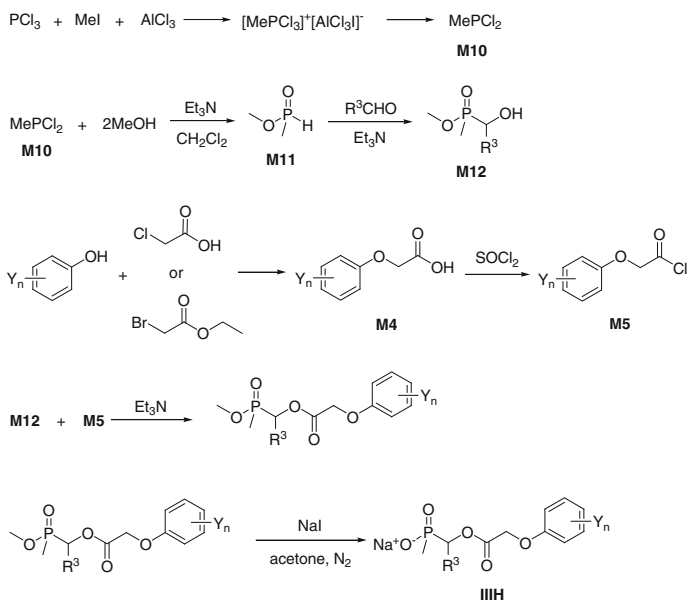
Scheme 4.11 Design of sodium [1-(substituted phenoxyacetoxy)alkyl]methylphosphinates **IIIH**

In the **IIIH** series, further modification was focused on substituent R^3 and Y_n . In this section, we introduce the synthesis, herbicidal activity, and structure-activity relationships of **IIIH**. As expected, **IIIH** possessed higher inhibitory activity against the growth of plant than their corresponding phosphinates **III G**.

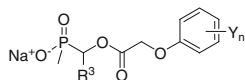
4.2.2 Synthesis of **IIIH**

Sodium [1-(substituted phenoxyacetoxy)alkyl]methylphosphinates **IIIH** could be easily prepared from the corresponding *O*-methyl [1-(substituted phenoxyacetoxy)alkyl]methylphosphinates which were prepared by the condensation of substituted phenoxyacetyl chlorides **M5** and *O*-methyl (1-hydroxyalkyl)methylphosphinates **M12**. The synthetic route is shown in Scheme 4.12. A detailed synthetic procedure for **IIIH** is introduced in the Sect. 9.1.18. The structures of **IIIH-1–IIIH-10** are listed in Table 4.21.

The structures of **IIIH** were confirmed by elemental analysis and characterized by IR, ^1H NMR, and MS. Spectroscopic analysis of some representative **IIIH** is given in Sect. 4.2.3.



Scheme 4.12 Synthesis of sodium [1-(substituted phenoxyacetoxy)alkyl]methylphosphinates **IIIH**

Table 4.21 Structure of sodium [1-(substituted phenoxyacetoxy)alkyl]methylphosphinates **IIIH**^a

Compound	R ³	Y _n	Compound	R ³	Y _n
IIIH-1	Ph	3-CF ₃	IIIH-6	Pyrid-2-yl	2-F
IIIH-2	Ph	2,4-Cl ₂	IIIH-7	Pyrid-2-yl	4-Cl
IIIH-3	2-ClPh	2,4-Cl ₂	IIIH-8	Pyrid-2-yl	2-Cl,5-Me
IIIH-4	2,4-Cl ₂ Ph	3-CF ₃	IIIH-9	Pyrid-2-yl	2,4-Cl ₂
IIIH-5	2,4-Cl ₂ Ph	2,4-Cl ₂	IIIH-10	Pyrid-2-yl	2,6-Cl ₂

^a Synthesis of **IIIH-1–IIIH-10** [28]

4.2.3 Spectroscopic Analysis of IIIH

The IR spectra of **IIIH** showed normal stretching absorption bands indicating the existence of benzene ring ($\sim 1,620$, $\sim 1,450$ cm^{-1}), C–O–C ($1,080$ – $1,200$ cm^{-1}), and P–C (740 – 750 cm^{-1}). A sharp and weak band at $3,030$ – $3,110$ cm^{-1} accounted for the C–H stretching of the benzene ring. The C–H stretching of alkyl appeared at $2,850$ – $2,970$ cm^{-1} . A strong absorption near $1,740$ – $1,770$ cm^{-1} was identified for the absorption C=O. A strong peak near $1,260$ cm^{-1} accounted for P=O in phosphonates. An asymmetric stretching vibration for P–O–C appeared at $1,030$ – $1,050$ cm^{-1} . The IR spectrum of **IIIH-9** is shown in Fig. 4.9.

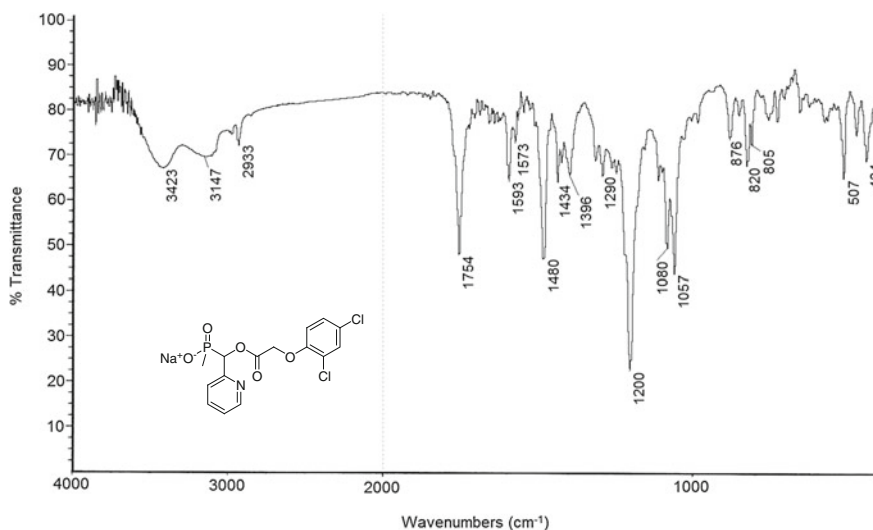


Fig. 4.9 IR spectrum of **IIIH-9**

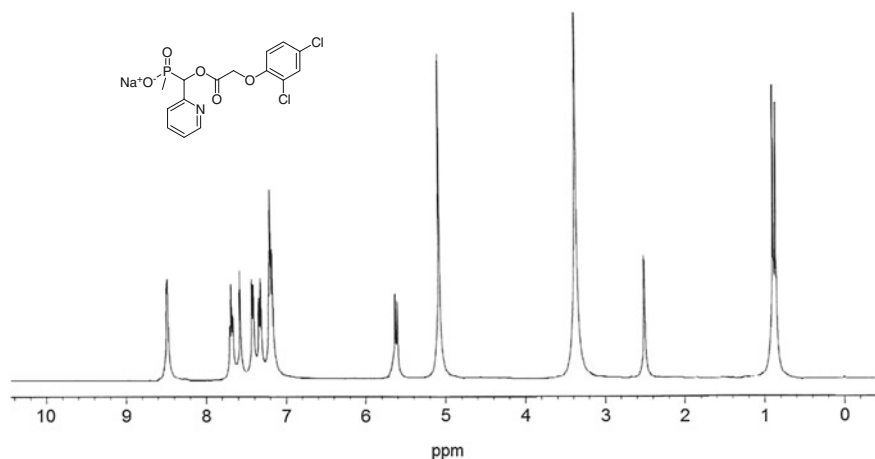


Fig. 4.10 ^1H NMR spectrum of **IIIH-9** ($\text{DMSO-}d_6$, 300 MHz)

In the ^1H NMR spectra of the salts of alkylphosphinic acids **IIIH**, the chemical shifts of aromatic protons appeared at 6.89–7.50 ppm. The proton signal in the OCHP moiety appeared at 5.56–5.96 ppm as a doublet due to the coupling with magnetic phosphorus. Comparing with *O*-methyl [1-(substituted phenoxyacetoxy) alkyl]methylphosphinates **IIIA–IIIG**, the chemical shifts (OCHP) of **IIIH** moved upfield about 0.4–0.5 ppm due to the effect of the magnetic shielding caused by the oxygen anion. In **IIIH-2**, the signal corresponding to the methylene group (CH_2) flanked by the phenoxy group and carbonyl group appeared as a quartet at 4.99 ppm, and the outside peaks were smaller in size. This signal belonged to the AB system with the difference in chemical shift between the two mutually coupled protons A and B. However, in the extreme case, when A and B had exactly the same chemical shift, the outside peaks disappeared, and the inside peaks merged into a singlet at 4.02–4.10 ppm, exemplified by **IIIH-1** and **IIIH-3–IIIH-10**. The ^1H NMR spectrum of **IIIH-9** is shown in Fig. 4.10.

The ESI mass spectra of some **IIIH** gave the ion peaks of molecular plus sodium and minus sodium. For example, **IIIH-5** was characterized by MS spectra using ESI negative and positive ionized mode, which displayed m/z 455 ($[\text{M}-23]^-$, negative) and 501 ($[\text{M}+23]^+$, positive) ion peak. ESI-MS spectra of **IIIH-5** is shown in Figs. 4.11 and 4.12.

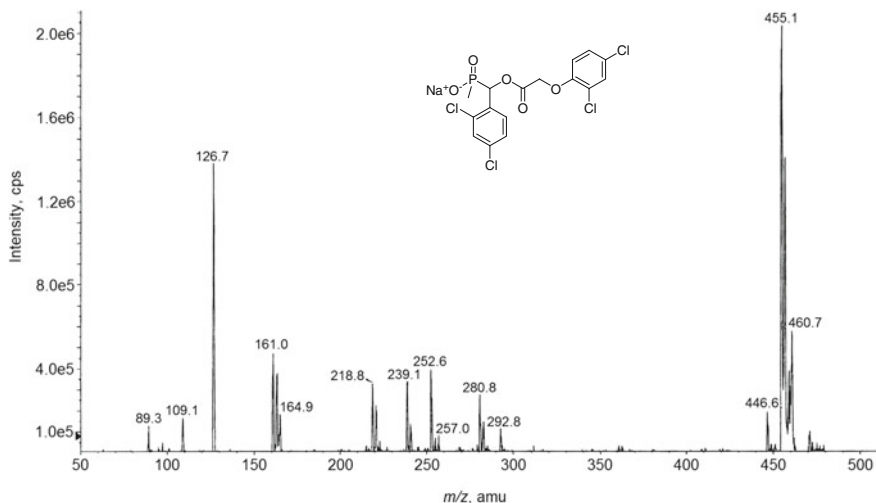


Fig. 4.11 ESI-MS spectrum of IIIH-5 (negative)

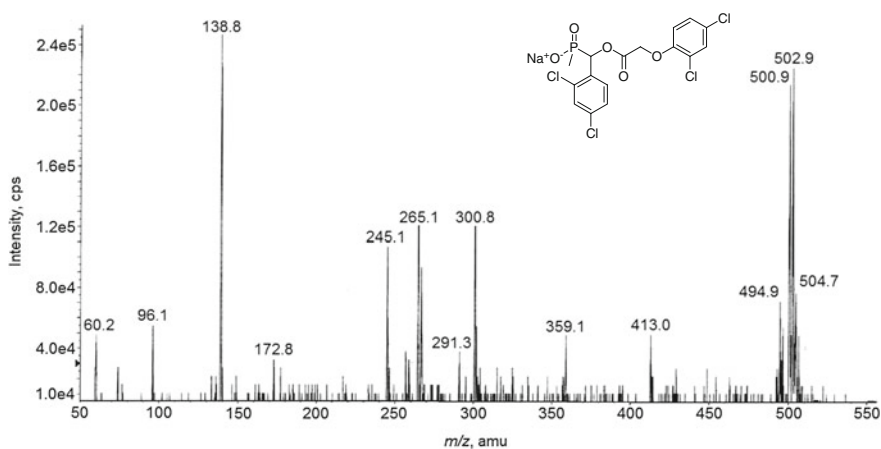
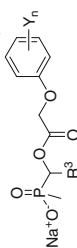


Fig. 4.12 ESI-MS spectrum of IIIH-5 (positive)

4.2.4 Herbicidal Activity of IIIH

In a preliminary bioassay, sodium [1-(substituted phenoxyacetoxy)alkyl]methylphosphinates IIIH, were tested for herbicidal activity against barnyard grass (*E. crusgalli*) and cabbage type rape (*B. napus*) by Petri dish method. The results are listed in Table 4.22.

Table 4.22 Inhibitory activity of sodium [1-(substituted phenoxyacetoxy)alkyl]methylphosphinates **IIIH** against the growth of plants^a



Compound	R ³	Y _n	Root		Stem			
			Ech ^b		Ech ^b			
			100 mg/L	10 mg/L	100 mg/L	10 mg/L		
IIIH-1	Ph	3-CF ₃	97	97	48	44	97	97
IIIH-2	Ph	2,4-Cl ₂	100	99	74	65	99	99
IIIH-3	2-ClPh	2,4-Cl ₂	87	64	61	61	100	95
IIIH-4	2,4-Cl ₂ Ph	3-CF ₃	92	73	44	26	86	67
IIIH-5	2,4-Cl ₂ Ph	2,4-Cl ₂	97	92	-9	-17	99	98
IIIH-6	Pyrid-2-yl	2-F	89	56	79	68	86	24
IIIH-7	Pyrid-2-yl	4-Cl	98	93	57	29	100	100
IIIH-8	Pyrid-2-yl	2-Cl,5-Me	89	64	64	64	99	76
IIIH-9	Pyrid-2-yl	2,4-Cl ₂	98	96	32	21	100	100
IIIH-10	Pyrid-2-yl	2,6-Cl ₂	98	98	25	7	100	99

^a Inhibitory potency (%) against the growth of plants in Petri dishes, 0 (no effect), 100 % (completely kill)

^b Ech: barnyard grass; Bm: cabbage type rape

(A) *Inhibitory activity against the root of plant*

As seen from Table 4.22, all of sodium salts of alkylphosphinic acids IIIH showed moderate to good herbicidal activity against the root of barnyard grass and rape at 100 and 10 mg/L. Especially, IIIH-1 ($Y_n=3\text{-CF}_3$, $R^3=\text{Ph}$), IIIH-2 ($Y_n=2,4\text{-Cl}_2$, $R^3=\text{Ph}$), IIIH-5 ($Y_n=2,4\text{-Cl}_2$, $R^3=2,4\text{-Cl}_2$), IIIH-7 ($Y_n=4\text{-Cl}$, $R^3=\text{pyrid-2-yl}$), IIIH-9 ($Y_n=2,4\text{-Cl}_2$, $R^3=\text{pyrid-2-yl}$), and IIIH-10 ($Y_n=2,6\text{-Cl}_2$, $R^3=\text{pyrid-2-yl}$) showed >90 % inhibitory activity against the growth of root of cabbage type rape and barnyard grass.

(B) *Inhibitory activity against the stem of plant*

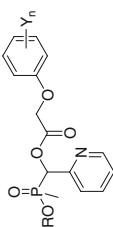
IIIH-1, IIIH-2 ($Y_n=2,4\text{-Cl}_2$, $R^3=\text{Ph}$), IIIH-3 ($Y_n=2,4\text{-Cl}_2$, $R^3=2\text{-ClPh}$), IIIH-5, IIIH-7, IIIH-9, and IIIH-10 displayed >90 % inhibitory activity against the growth of stem of rape at 100 and 10 mg/L but these compounds showed much weaker inhibitory activity against the growth of stem of barnyard grass. Only IIIH-2, IIIH-3, IIIH-6 ($Y_n=2\text{-F}$, $R^3=\text{pyrid-2-yl}$), and IIIH-8 ($Y_n=2\text{-Cl,5-Me}$, $R^3=\text{pyrid-2-yl}$) had 61–68 % inhibitory activity. All compounds displayed higher inhibitory activity against the growth of the root than that of the stem.

(C) *SAR analysis for IIIH*

In the IIIH series, further modification was focused on substituent R^3 and Y_n . Comparing the activity of IIIH in Table 4.22, both R^3 and Y_n had significant influence on the inhibitory activity. When R^3 groups were kept constant, sodium salts of alkylphosphinic acids with 2,4- Cl_2 as Y_n had better inhibitory activity against the growth of cabbage type rape and barnyard grass except the growth of stem of barnyard grass. When 2,4- Cl_2 as Y_n were kept constant, IIIH-2 ($R^3=\text{Ph}$) and IIIH-3 ($R^3=2\text{-ClPh}$) showed higher inhibitory activity against the growth of stem of barnyard grass than IIIH-5 ($R^3=2,4\text{-Cl}_2\text{Ph}$) and IIIH-9 ($R^3=\text{pyrid-2-yl}$). When 3- CF_3 as Y_n was kept constant, IIIH-1 ($R^3=\text{Ph}$) showed higher inhibitory activity against the growth of cabbage type rape and barnyard grass than IIIH-4 ($R^3=2\text{-ClPh}$).

As seen from Table 4.23, comparing the activity of IIIH with IIIG, it was found that inhibitory activity of some compounds could be greatly enhanced when MeO attached to the phosphorus atom was replaced by NaO (Y_n , R^3 and R^4 are kept constant). Especially, sodium salt IIIH-10 ($R=\text{Na}$, $Y_n=2,6\text{-Cl}_2$) displayed higher inhibitory activity (95–100 %) against the growth of root of cabbage type rape and barnyard grass, and stem of cabbage type rape than that of its corresponding phosphinates IIIG-8 ($R=\text{Me}$, $Y_n=2,6\text{-Cl}_2$) at 10 mg/L. IIIG-8 only had weak inhibitory activity (21–72 %). IIIH-6 ($R=\text{Na}$, $Y_n=2\text{-F}$) also had higher inhibitory activity against tested plant than that of its corresponding phosphinates IIIG-2 ($R=\text{Me}$, $Y_n=2\text{-F}$). Both sodium salts IIIH-6 and IIIH-8 showed 64–68 % inhibitory effect against the growth of stem of barnyard grass, but their corresponding phosphinates IIIG-2 and IIIG-5 only had 33–35 % inhibitory effect against the growth of stem of barnyard grass at 10 mg/L.

Table 4.23 Inhibitory activity of sodium [1-(substituted phenoxyacetoxy)alkyl]methylphosphinates **III**G and **III**H against the growth of plants^a



Compound	R	Y _n	Root		Stem				
			Ech ^b		Ech ^b				
			100 mg/L	10 mg/L	100 mg/L	10 mg/L			
III G-2	Me	2-F	46	8	50	20	33	0	3
III H-6	Na	2-F	89	56	86	24	79	68	3
III G-3	Me	4-Cl	97	92	99	97	52	41	92
III H-7	Na	4-Cl	98	93	100	100	57	29	92
III G-5	Me	2-Cl,5-Me	80	49	97	96	28	35	67
III H-8	Na	2-Cl,5-Me	89	64	99	76	64	64	36
III G-7	Me	2,4-Cl ₂	97	95	99	99	67	56	92
III H-9	Na	2,4-Cl ₂	98	96	100	100	32	21	95
III G-8	Me	2,6-Cl ₂	82	42	90	47	57	57	21
III H-10	Na	2,6-Cl ₂	98	98	100	99	25	7	95

^a Inhibitory potency (%) against the growth of plants in Petri dishes, 0 (no effect), 100 % (completely kill)

^b Ech: barnyard grass; Bm: cabbage type rape

4.2.5 Summary

A series of sodium [1-(substituted phenoxyacetoxy)alkyl]methylphosphinates **IIIH** including 10 compounds, was easily synthesized by the reaction of *O*-methyl [1-(substituted phenoxyacetoxy)alkyl]methylphosphinates with sodium iodide in refluxing acetone. The preliminary evaluation of the herbicidal activity showed that all of the compounds showed moderate-to-good inhibitory activity against barnyard grass and cabbage type rape at 100 and 10 mg/L. Most **IIIH** displayed higher inhibitory activity against the growth of root than that of stem of barnyard grass. Especially, **IIIH-1** ($R^3=\text{Ph}$, $Y_n=3\text{-CF}_3$), **IIIH-2** ($R^3=\text{Ph}$, $Y_n=2,4\text{-Cl}_2$), **IIIH-7** ($R^3=\text{pyrid-2-yl}$, $Y_n=4\text{-Cl}$), **IIIH-9** ($R^3=\text{pyrid-2-yl}$, $Y_n=2,4\text{-Cl}_2$) and **IIIH-10** ($R^3=\text{pyrid-2-yl}$, $Y_n=2,6\text{-Cl}_2$) displayed >90 % inhibitory activity against the growth of root and stem of cabbage type rape at 10 mg/L. **IIIH** also showed >90 % inhibitory activity against the growth of root of barnyard grass. Several sodium salts including **IIIH-2** ($R^3=\text{Ph}$, $Y_n=2,4\text{-Cl}_2$), **IIIH-3** ($R^3=2\text{-ClPh}$, $Y_n=2,4\text{-Cl}_2$), **IIIH-6** ($R^3=\text{pyrid-2-yl}$, $Y_n=2\text{-F}$) and **IIIH-8** ($R^3=\text{pyrid-2-yl}$, $Y_n=2\text{-Cl,5-Me}$) had 61–68 % inhibitory activity against the growth of stem of barnyard grass. The above results showed that both R^3 and Y_n had significant influence on the inhibitory activity of **IIIH**.

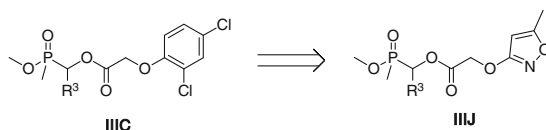
Comparing **IIIH** with **III G**, it was found that inhibitory activity against the growth of plant could be greatly enhanced when MeO attached to phosphorus in phosphinates **III G** was replaced by NaO (Scheme 4.11). It was similar to alkylphosphonic acid monosodium salts **IIA–II E** (Chap. 3), which also showed higher inhibitory potency against test plants and higher inhibitory potency against the stem of barnyard grass than their corresponding phosphonates and phosphinates.

Preliminary bioassay showed that substituent 2,6- Cl_2 as Y_n on the phenoxybenzene ring was beneficial to the inhibitory activity of the **IIIH**. For example, sodium salt of phosphinic acid **IIIH-10** ($Y_n=2,6\text{-Cl}_2$, $R^3=\text{pyrid-2-yl}$) displayed >90 % inhibitory activity against tested plant at 10 mg/L. However 2,6- Cl_2 as Y_n was not so beneficial to the herbicidal activity of it corresponding *O,O*-dimethyl 1-(pyrid-2-yl)methylphosphonate **IJ-14** and *O*-methyl 1-(pyrid-2-yl)methylphosphinate **III G-8**. **IIIH** need to be further tested at a lower rate to make sure of their herbicidal activity and potential usage. Their inhibition against plant PDHc E1 will be studied.

4.3 [(5-Methylisoxazol-3-yloxyacetoxy)Alkyl] Methylphosphinates IIIJ

4.3.1 Introduction

The useful biological properties of compounds containing isoxazole ring have received special attention. There are several naturally occurring isoxazoles with interesting biological activity, such as musimol and 4-hydroxy isoxazole, which is a seed-germination inhibitor [29]. Their structures had been used as the basis for the design of a number of synthetic isoxazole derivatives, some of those derivatives



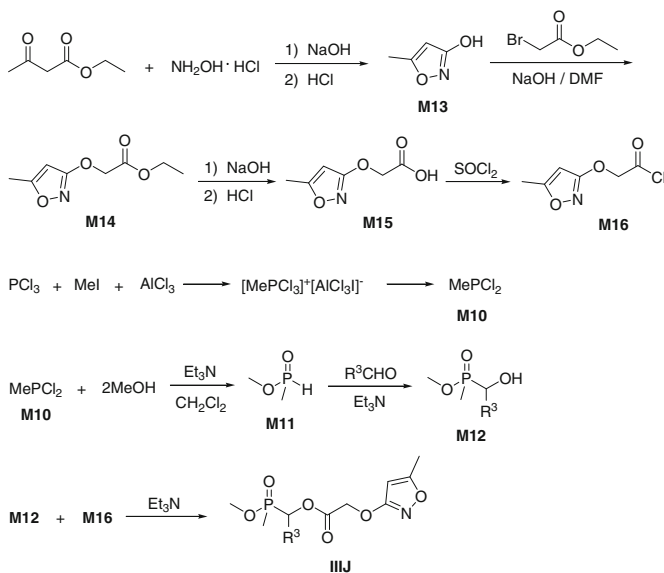
Scheme 4.13 Design of [(5-methylisoxazol-3-yloxyacetoxy)alkyl]methylphosphinates **IIIJ**

have been successfully launched as commercial agrochemicals [30]. As stated in the previous Sect. 4.1, a series of *O*-methyl [1-(substituted phenoxyacetoxy)alkyl]methylphosphinates **III C** displayed significant inhibitory activity against tested species except wheat in pre-emergence and post-emergence applications at 2.25 kg ai/ha. For the purpose of extending the structure type of phosphinates **III**, the isoxazole ring was introduced to replace the benzene ring in the structure of **III C** to produce a novel series of **III J** (Scheme 4.13).

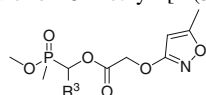
In this section, we describe the synthesis and herbicidal activity of *O*-methyl [1-(5-methylisoxazol-3-yloxyacetoxy)alkyl]methylphosphinates **III J**.

4.3.2 Synthesis of **III J**

O-Methyl [1-(5-methylisoxazol-3-yloxyacetoxy)alkyl]methylphosphinates **III J** could be conveniently synthesized by the reaction of *O*-methyl (1-hydroxyalkyl)methylphosphinates **M12** and 5-methylisoxazol-3-yloxyacetyl chloride **M16**. The synthetic route is shown in Scheme 4.14.



Scheme 4.14 Synthesis of *O*-methyl [1-(5-methylisoxazol-3-yloxyacetoxy)alkyl]methylphosphinates **IIIJ**

Table 4.24 Structure of *O*-methyl [1-(5-methylisoxazol-3-yloxyacetoxy)alkyl]methylphosphinates **IIIJ-1–IIIJ-8**

Compound	R ³	Compound	R ³
IIIJ-1	Me	IIIJ-5	4-MePh
IIIJ-2	Et	IIIJ-6	3-NO ₂ Ph
IIIJ-3	<i>n</i> -Pr	IIIJ-7	4-MeOPh
IIIJ-4	Ph	IIIJ-8	2-ClPh

^a Synthesis of **IIIJ-1–8** [31]

O-Methyl (1-hydroxyalkyl)methylphosphinates **M12** could be obtained by a four-step procedure starting from phosphorus trichloride, which has been discussed in Sect. 4.1.3. 5-Methylisoxazol-3-yloxyacetyl chloride **M16** was prepared by four steps using ethyl acetoacetate and hydroxylamine hydrochloride as starting materials. Hydroxylamine hydrochloride reacted with ethyl acetoacetate to give 3-hydroxy-5-methylisoxazole **M13**, which was converted to sodium salt of 3-hydroxy-5-methylisoxazole and reacted with ethyl bromoacetate to give ethyl (5-methylisoxazol-3-yl)oxyacetate **M14**. **M14** was further converted to 5-methylisoxazol-3-yloxyacetic acid **M15** by alkaline hydrolysis using sodium hydroxide followed by hydrochloric acid. 5-Methylisoxazol-3-yloxyacetyl chloride **M16** could be easily obtained in 80 % yield by treating **M15** with thionyl chloride. **IIIJ-1–IIIJ-8** could be obtained by the condensation of *O*-methyl (1-hydroxyalkyl)methylphosphinates **M12** with 5-methyl isoxazol-3-yloxyacetyl chloride **M16** in 33–65 % yields. Detailed synthetic procedure for intermediate **M13–M16** are introduced in the Sect. 9.1.19. All of **IIIJ** could be prepared according to the general synthetic procedure in Sect. 9.1.20. The structures of **IIIJ-1–IIIJ-8** are listed in Table 4.24.

The structures of **IIIJ** were confirmed by elemental analysis and characterized by IR, ¹H NMR. Several of them were further characterized by ³¹P NMR and mass spectrometry.

IIIJ-1–IIIJ-8 could be soluble in polar organic solvents such as CHCl₃, DMF, acetone, and so on. They were stable for light and air at room temperature, but easy to decompose under acidic or basic conditions. Spectroscopic analysis of some representative **IIIJ** is given in Sect. 4.3.3.

4.3.3 Spectroscopic Analysis of IIIJ

All the main functional groups were characterized in IR spectra which showed normal stretching absorption bands indicating the existence of aromatic ring (1,465–1,509 cm⁻¹), P–O–C (1,036–1,054 cm⁻¹) P–C (871–895 and 1,303 cm⁻¹), and C=O (1,765–1,775 cm⁻¹). A strong absorption at 1,146–1,149 cm⁻¹ was identified to be the absorption of N–O in the isoxazole ring. The absorption band at

3,060–3,140 cm^{-1} accounted for the C–H stretching of the aromatic ring and 2,850–2,980 cm^{-1} accounted for the C–H stretching of the CH_3 and methylene group. A peak at 1,175–1,197 cm^{-1} accounted for P=O in phosphinates. Two strong peaks near 1,529 and 1,352 cm^{-1} were the evidences of the NO_2 stretching in **IIIJ-6**.

The EI mass spectra of some compounds such as **IIIJ-8** gave very weak molecular ion peaks because of the facile cleavage of the C–Cl bond. Its fragmentation ions of the compound were consistent with the structure. In this series of compounds, the values of molecular ion peaks showed odd numbers except **IIIJ-6** containing a NO_2 group.

In the ^1H NMR spectra of **IIIJ**, three singlets near 2.3, 4.9, and 5.8 ppm could be observed. The three proton signals corresponded to the isoxazole-ring, the methyl group attached to isoxazole and the methylene group flanked by the carbonyl group, respectively. For compounds with Ph or substituted Ph as R^3 , the proton signals corresponding to the group OCHP appeared near 6.2 ppm as triplets or quartets. It may be caused by the two enantiomers due to asymmetric phosphorus in **IIIJ**. For compounds with alkyl as R^3 , the proton signal in OCHP also appeared near 5.4 ppm as a complex multiplet. Because of the asymmetric phosphorus in **IIIJ**, the proton signal corresponding to the methyl groups (CH_3) and the methoxyl groups (OCH_3) attached to phosphorus appeared at 1.4–1.6 and 3.6–3.8 ppm, respectively, as two quartets consisting of two doublets.

4.3.4 Herbicidal Activity of **IIIJ**

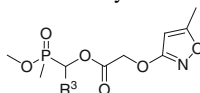
The herbicidal activity of **IIIJ** were evaluated at 2.25 kg ai/ha in a set of experiments in greenhouse. They were tested for pre-emergence and post-emergence inhibitory activity against wheat (*T. aestivum*), crab grass (*D. sanguinalis*), barnyard grass (*E. crusgalli*), rape (*B. campestris*), cucumber (*C. sativus*), lettuce (*L. sativa*), and setose thistle (*C. japonicum*). The bioassay data of **IIIJ** are listed in Table 4.25.

(A) Pre-emergence herbicidal activity of **IIIJ**

As shown in Table 4.25, all **IIIJ** had <50 % pre-emergence activity against wheat, crab grass, barnyard grass, and rape. **IIIJ-4** and **IIIJ-6** displayed >90 % inhibitory effect against cucumber, lettuce, or setose thistle, and **IIIJ-2** showed >90 % inhibitory effect against setose thistle in pre-emergence application at 2.25 kg ai/ha.

(B) Post-emergence herbicidal activity of **IIIJ**

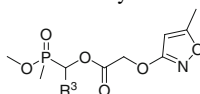
As shown in Table 4.26, all **IIIJ** showed weak post-emergence activity against wheat, crab grass, barnyard grass, and rape except **IIIJ-5** had >90 % inhibitory effect against crab grass. **IIIJ-4** displayed >90 % post-emergence herbicidal activity against cucumber, lettuce and setose thistle. **IIIJ-3**, **IIIJ-5**, and **IIIJ-6** exhibited >90 % post-emergence herbicidal activity against cucumber or setose thistle.

Table 4.25 Structure and pre-emergence herbicidal activity of *O*-methyl [1-(5-methylisoxazol-3-yloxyacetoxy)alkyl]methylphosphinates IIIJ^a

Compound	R ³	Tri ^b	Dig ^b	Ech ^b	Bra ^b	Cuc ^b	Lac ^b	Cir ^b
IIIJ-1	Me	D	D	D	D	NT	D	D
IIIJ-2	Et	D	C	D	D	NT	NT	A
IIIJ-3	<i>n</i> -Pr	D	D	D	D	D	NT	D
IIIJ-4	Ph	D	D	D	D	A	A	C
IIIJ-5	4-MePh	D	D	D	D	NT	D	D
IIIJ-6	3-NO ₂ Ph	D	D	D	D	A	NT	A
IIIJ-7	4-MeOPh	D	D	D	D	NT	NT	D
IIIJ-8	2-ClPh	D	D	D	D	NT	NT	D

^a Inhibitory potency (%) against the growth of plants at a rate of 2.25 kg ai/ha in the greenhouse was expressed as four scales—A: 90–100 %, B: 75–89 %, C: 50–74 %, D: <50 %, and NT: not tested

^b Tri: wheat; Dig: crab grass; Ech: barnyard grass; Bra: rape; Cuc: cucumber; Lac: lettuce; Cir: setose thistle

Table 4.26 Structure and post-emergence herbicidal activity of *O*-methyl [1-(5-methylisoxazol-3-yloxyacetoxy)alkyl]methylphosphinates IIIJ^a

Compound	R ³	Tri ^b	Dig ^b	Ech ^b	Bra ^b	Cuc ^b	Lac ^b	Cir ^b
IIIJ-1	Me	D	C	D	D	D	NT	D
IIIJ-2	Et	D	D	D	D	D	NT	D
IIIJ-3	<i>n</i> -Pr	D	D	D	D	D	D	A
IIIJ-4	Ph	D	D	D	D	A	A	A
IIIJ-5	4-MePh	D	A	D	D	D	D	A
IIIJ-6	3-NO ₂ Ph	D	D	C	D	A	NT	NT
IIIJ-7	4-MeOPh	D	C	D	D	NT	NT	NT
IIIJ-8	2-ClPh	D	D	D	D	NT	NT	B

^a Inhibitory potency (%) against the growth of plants at a rate of 2.25 kg ai/ha in the greenhouse was expressed as four scales—A: 90–100 %, B: 75–89 %, C: 50–74 %, D: <50 %, and NT: not tested

^b Tri: wheat; Dig: crab grass; Ech: barnyard grass; Bra: rape; Cuc: cucumber; Lac: lettuce; Cir: setose thistle

Among the tested IIIJ, IIIJ-4 seemed to have better pre- and post-emergence activity than other compounds at 2.25 kg ai/ha.

(C) SAR analysis for IIIJ

As shown in Tables 4.25 and 4.26, most IIIJ with 5-methylisoxazol-3-yloxy group showed much lower activity (<50 %) against all tested plants at 2.25 kg ai/ha. However most IIIJ with substituted phenoxy-benzene ring exhibited >90 % inhibitory effect against rape, cucumber, lettuce, setose thistle, crab grass and barnyard grass except wheat at 2.25 kg ai/ha. Above observations showed that

when substituted phenoxy-benzene ring in the structure of **III C** was replaced by 5-methylisoxazol-3-yloxy group, the herbicidal activity of compounds (**III J**) greatly decreased or lost.

4.3.5 Summary

A series of *O*-methyl [1-(5-methylisoxazol-3-yloxyacetoxy)alkyl]methyl phosphinates **III J** including eight compounds was synthesized by condensation of *O*-methyl (1-hydroxyalkyl)methylphosphinates **M12** with 5-methylisoxazol-3-yloxyacetyl chloride **M16** in 33–65 % yields.

The preliminary evaluation of the herbicidal activity showed that only several compounds displayed good herbicidal activity against some tested plants at 2.25 kg ai/ha. The best **III J-4** displayed >90 % inhibitory effect against cucumber, lettuce and/or setose thistle for pre and post-emergence applications at 2.25 kg ai/ha. Comparing with **III C**, most **III J** showed much lower activity (<50 %) against all tested plants. The replacement of the substituted phenoxy-benzene ring in **III A–III G** by 5-methylisoxazol-3-yloxy group like **III J** led to the reduction of herbicidal activity (Scheme 4.2). It showed that substituted phenoxy-benzene ring was an essential group for the herbicidal activity of phosphinates **III**.

References

1. Baillie AC, Wright K, Wright BJ et al (1988) Inhibitors of pyruvate dehydrogenase as herbicides. *Pest Biochem Physiol* 30:103–112
2. Evans DA, Lawson KR (1992) Crop protection chemicals-research and development perspectives and opportunities. *Pestic Outlook* 3:10–17
3. Kluger R, Pike DC (1977) Active site generated analogues of reactive intermediates in enzymic reactions. Potent inhibition of pyruvate dehydrogenase by a phosphonate analogue of pyruvate. *J Am Chem Soc* 99:4504–4506
4. Kluger R, Gish G, Kauffman G (1984) Interaction of thiamin diphosphate and thiamin thiazolone diphosphate with wheat germ pyruvate decarboxylase. *J Biol Chem* 259: 8960–8965
5. Burger A (1991) Isosterism and bioisosterism in drug design. *Prog Drug Res* 37:287–371
6. Meanwell NA (2011) Synopsis of some recent tactical application of bioisosteres in drug design. *J Med Chem* 54:2529–2591
7. Saeed A, Shaheen U, Hameed A et al (2009) Synthesis, characterization and antimicrobial activity of some new 1-(fluorobenzoyl)-3-(fluorophenyl)thioureas. *J Fluorine Chem* 130:1028–1034
8. Chen T, Shen P, Li YJ et al (2006) Synthesis and herbicidal activity of *O*, *O*-dialkyl phenoxyacetoxyalkylphosphonates containing fluorine. *J Fluorine Chem* 127:291–295
9. Liu YX, Zhao QQ, Wang QM et al (2005) Synthesis and herbicidal activity of 2-cyano-3-(2-fluoro-5-pyridyl)methylaminoacrylates. *J Fluorine Chem* 126:345–348
10. Zheng XM, Li Z, Wang YL et al (2003) Syntheses and insecticidal activities of novel 2,5-disubstituted 1,3,4-oxadiazoles. *J Fluorine Chem* 123:163–169

11. Jablonkai I (2003) Alkylating reactivity and herbicidal activity of chloroacetamides. *Pest Manag Sci* 59:443–450
12. Nizamuddin MG, Manoj KS (2001) Synthesis and fungicidal activity of substituted pyrazolo [5,4-b] pyridine/pyrid-6-ones and pyrazolo[5,4-d]thiazines. *Bull Chim Farm* 140:311–315
13. Wang QM, Sun HK, Huang RQ (2004) Synthesis and herbicidal activity of (Z)-ethoxyethyl 2-cyano-3-(2-methylthio-5-pyridylmethylamino) acrylates. *Heteroatom Chem* 15:67–70
14. Kuzmin VE, Lozitsky VP, Kamalov GL et al (2000) Analysis of the structure-anticancer activity relationship in a set of Schiff bases of macrocyclic 2,6-bis(2- and 4-formylaryloxy)methyl) pyridines. *Acta Biochim Pol* 47:867–875
15. Hoffmann FW, Moore TR (1958) Organic phosphorus compounds. II. Isomeric alkyl phosphoro- and phosphonothioates. *J Am Chem Soc* 80(5):1150–1154
16. Soroka M (1977) A simple preparation of methylphosphonous dichloride. *Synthesis* 1977 (7):450
17. Ferron JL, Perry BJ, Reesor JB (1960) A new synthetic route to alkylphosphonous dichlorides. *Nature* 188:227–228
18. Komkov JP, Karavanov KV, Ivin SZ (1958) New methods of preparing alkylchlorophosphines and dialkylchlorophosphines. *J Gen Chem USSR* 28:2992–2994
19. Barabanov VI, Abramov VS (1965) Esters of ethyl (methyl) α -hydroxy- β , β , β -trichloroethyl phosphinic acid analogs of chlorophos. *Zh Obsh Khim* 35:2225–2229
20. Baylis EK (1995) 1-Hydroxy-1-methyl ethylphosphinates intermediates for the synthesis of functional phosphorous acids. *Tetrahedron Lett* 36:9389–9392
21. Borisov G (1967) Attempts at adding dialkyl phosphites and monoalkyl phosphonites to aldehydes and ketones of the naphthalene series. *Izv Inst Org Khim Akad Nauk* 3:9–16
22. Morise X, Savignac P, Denis JM (1996) New synthesis of 1-chloroalkyl phosphinates. *J Chem Soc Pekin trans* 1:2179–2185
23. Yamashita M, Tsunekawa T, Sugiura M et al (1985) Direct deoxygenation of the hydroxyl group of methyl 1-hydroxy alkyl-(phenyl)-phosphinates using diphosphorous tetraiodide. *Synthesis* 6:896–897
24. Li MQ, You GY, Peng H et al (2013) Synthesis and herbicidal activities of *O*-methyl methyl [1-(substituted phenoxyacetoxy)alkyl]phosphinates. *J Pestic Sci* 38:78–84
25. Deng XY, Liao GH, Long QW et al (2013) Synthesis and herbicidal activity of [(substituted phenoxyacetoxy)(substituted phenyl)methyl](methyl)phosphinates containing fluorine. *Phosphorus, Sulfur Silicon Relat Elem* 188:663–671
26. Wang T, Peng H, He HW (2014) Synthesis and biological activity of *O*-methyl methyl 1-(substituted phenoxyacetoxy)-1-(thien-2-yl)methylphosphinates. *J Heterocycl Chem*. doi: [10.1002/jhet.2143](https://doi.org/10.1002/jhet.2143)
27. Wang T, He HW (2008) Synthesis and biological activity of α -oxo-2-pyridyl methyl phosphinates. *Phosphorus, Sulfur Silicon Relat Elem* 183:1884–1891
28. Wang T, He HW (2008) An efficient synthesis of sodium methyl α -(substituted phenoxy acetoxy)alkylphosphinates. *Phosphorus, Sulfur Silicon Relat Elem* 183:644–645
29. Gilchris TL (1997) *Heterocyclic chemistry*. Addison Wesley Longman, London
30. Worthing CR, Hance RJ (1991) *The pesticide manual*. British Crop Protection Council, Farnham
31. He HW, Li MQ, Lu AH et al (2002) Synthesis and biological activities of methyl 1-(5-methyl isoxazol-3-oxo acetoxy)alkyl methyl phosphinates. *Phosphorus, Sulfur Silicon Relat Elem* 177:1651–1655

Chapter 5

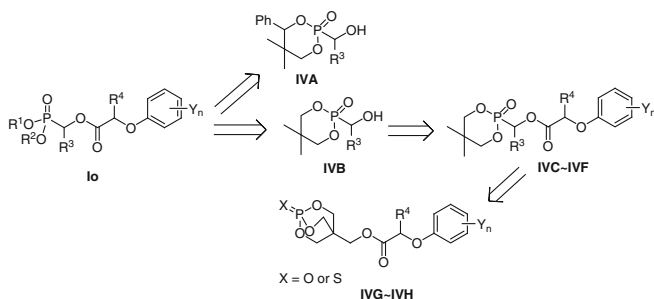
Cyclic Phosphonates and Caged Bicyclic Phosphates

Organic phosphorus compounds display a wide range of biological activities and have attracted considerable attention in the field of pesticides [1–4]. On the basis of acetylphosphonate **1-1** as a hit compound, several series of 1-substituted alkylphosphonates **IA–IK**, including more than 160 compounds, were designed and synthesized [5–21]. SAR analyses indicated that herbicidal activity and inhibition against plant PDHc E1 could be increased greatly by optimizing R¹, R², R³, R⁴, and Y_n in the general structure **Io**. Among the alkylphosphonates **IA–IK** series, *O,O*-dimethyl 1-(2,4-dichlorophenoxyacetoxy)ethylphosphonate **IC-22** (clacyfos, HW02) was found to be the most effective as a PDHc E1 inhibitor with good selectivity and excellent herbicidal activity against broad-leaved weeds by post-emergence application at 18.75–150 g ai/ha in the greenhouse. Furthermore, *O,O*-dimethyl 1-(2,4-dichlorophenoxyacetoxy)-1-(furan-2-yl)methylphosphonate **IG-21** (HWS) was also found to be a PDHc E1 inhibitor and excellent herbicidal activity against broad-leaved weeds at 37.5–150 g ai/ha in the greenhouse (Chap. 2). **IG-21** (HWS) had good selectivity between broad-leaved weeds and monocotyledonous crops (Chaps. 2 and 8). It showed better crop safety for maize than **IC-22** (clacyfos). These results encouraged us to make further modifications on the basis of the structure **Io**.

According to our study on the alkylphosphonates **IA–IK** series, in the structure **Io**, both R¹ and R² groups in the structural unit of phosphorus-containing played a very important role in both herbicidal activity and inhibition against plant PDHc E1. We noticed that a variety of studies had demonstrated that bioactivity and stability of phosphonates or phosphates could be increased by introducing a phosphorus-containing heterocyclic moiety to their parent structure [22, 23].

Therefore, several different types of cyclic phosphonates **IVA–IVF** were designed on the basis of the alkylphosphonates **Io**. Moreover, the cyclic phosphonates were modified to the caged bicyclic phosphates **IVG–IVH** (Scheme 5.1).

In this chapter, we focus on the synthesis, herbicidal activity, and structure-activity relationship of cyclic phosphonates **IVA–IVF**, and caged bicyclic phosphates **IVG–IVH**. Indeed, the bioassay results showed that several cyclic phosphonates exhibited promising herbicidal activity and potential utility as herbicides.



Scheme 5.1 Design of cyclic phosphonates **IVA–IVF** and caged bicyclic phosphates **IVG–IVH**

5.1 Cyclic 1-Hydroxyalkylphosphonates **IVA** and **IVB**

5.1.1 Introduction

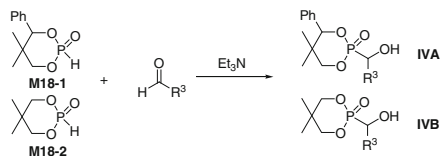
1-Hydroxyalkylphosphonates as a kind of active compound or important intermediate have received much attention [24–26]. Some of them were widely used as bio-phosphate mimics [27], enzyme inhibitors [28, 29] antibacterial agents [30, 31] antiviral agents [32], anti-cancer and antitumor agents [33, 34] anti-HIV agents [35, 36] and haptens for catalytic antibodies [37]. In addition, 1-hydroxyalkylphosphonates also served as an attractive precursor in the synthesis of various 1-substituted alkylphosphonates [38–40].

As stated in Chap. 2, several series of open-chain *O,O*-dialkyl 1-hydroxyalkylphosphonates **M2** have been prepared and studied. In order to examine the herbicidal activity of phosphorus-containing heterocyclic 1-hydroxyalkylphosphonate and their derivatives, firstly two series of cyclic 1-hydroxyalkylphosphonates including 2-(1-hydroxyalkyl)-5,5-dimethyl-4-phenyl-1,3,2-dioxaphosphinane-2-ones **IVA** and 2-(1-hydroxyalkyl)-5,5-dimethyl-1,3,2-dioxaphosphinane-2-ones **IVB** were synthesized.

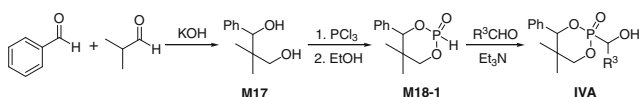
In the **IVA** and **IVB** series, further modification was focused on substituent R³. In this section, we describe the synthesis and herbicidal activity of cyclic 1-hydroxyalkylphosphonates, **IVA** and **IVB**. The results of preliminary bioassay indicated that **IVA** and **IVB** exhibited certain herbicidal activity.

5.1.2 Synthesis of **IVA** and **IVB**

Cyclic 1-hydroxyalkylphosphonates **IVA** and **IVB** could be synthesized by Pudovik reaction (Scheme 5.2) [41]. Cyclic 1-hydroxyalkylphosphonates **IVA** were prepared by hydrophosphonylation of various aldehydes with 5,5-dimethyl-4-phenyl-1,3,2-dioxaphosphinane-2-one **M18-1** in the presence of triethylamine as a basic catalyst. The cyclic phosphonate **M18-1** could be easily prepared by the reaction of



Scheme 5.2 Synthesis of cyclic 1-hydroxyalkylphosphonates **IVA** and **IVB**



Scheme 5.3 Synthesis of cyclic 1-hydroxyalkylphosphonates **IVA**

1-phenyl-2,2-dimethyl-1,3-propanediol **M17** with 1 equiv. of phosphorus trichloride in toluene and then by reacting with 1 equiv. of ethanol. **M17** could be obtained by the known aldol-Cannizzaro reaction, in which 2 equiv. of isobutyraldehyde, 1 equiv. of benzaldehyde, and 1 equiv. of KOH in ethanol were used to give **M17** in good yields (Scheme 5.3) [42].

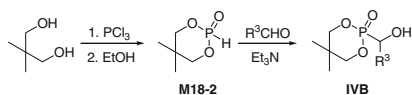
A series of cyclic 1-hydroxyalkylphosphonates **IVA** including 12 compounds was prepared. The structures of **IVA** are listed in Table 5.1.

The cyclic 1-hydroxyalkylphosphonates **IVB** were synthesized using a similar process to **IVA**. Neopentyl glycol reacted with 1 equiv. of phosphorus trichloride in 1,2-dichloroethane and then 1 equiv. of ethanol was added to form 5,5-dimethyl-1,3,2-dioxaphosphinane-2-one **M18-2** (Scheme 5.4) [43]. The addition of **M18-2** to various aldehydes gave cyclic 1-hydroxyalkylphosphonates **IVB**. A series of cyclic 1-hydroxyalkylphosphonates **IVB** including 13 compounds was prepared. The structures of **IVB** are listed in Table 5.2.

Detailed synthetic procedures for cyclic 1-hydroxyalkylphosphonates **IVA** and **IVB** are introduced in the Sect. 9.1.23 of Chap. 9. The structures of **IVA** and **IVB** were established by well-defined IR, ^1H NMR, and elemental analysis. **IVA-3** ($\text{R}^3 = 4\text{-ClPh}$) was further analyzed by X-ray single-crystal diffraction. Spectroscopic analyses of some representative **IVA** and **IVB** are given in Sect. 5.1.3.

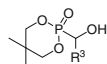
Table 5.1 Structure of cyclic 1-hydroxyalkylphosphonates **IVA**

Compound	R^3	Compound	R^3
IVA-1	Ph	IVA-7	4-MePh
IVA-2	2-ClPh	IVA-8	4-NO ₂ Ph
IVA-3	4-ClPh	IVA-9	Pyrid-2-yl
IVA-4	2,4-Cl ₂ Ph	IVA-10	Pyrid-3-yl
IVA-5	3,4-Cl ₂ Ph	IVA-11	Pyrid-4-yl
IVA-6	4-MeOPh	IVA-12	<i>n</i> -Bu



Scheme 5.4 Synthesis of cyclic 1-hydroxyalkylphosphonates **IVB**

Table 5.2 Structure of cyclic 1-hydroxyalkylphosphonates **IVB**



Compound	R ³	Compound	R ³
IVB-1	Ph	IVB-8	4-NO ₂ Ph
IVB-2	2-ClPh	IVB-9	Pyrid-2-yl
IVB-3	4-ClPh	IVB-10	Fur-2-yl
IVB-4	2,4-Cl ₂ Ph	IVB-11	Me
IVB-5	3,4-Cl ₂ Ph	IVB-12	<i>i</i> -Pr
IVB-6	4-MeOPh	IVB-13	<i>n</i> -Bu
IVB-7	4-MePh		

5.1.3 Spectroscopic Analysis of *IVA* and *IVB*

The IR spectra of *IVA* and *IVB* showed normal absorption bands indicating the existence of O–H ($\sim 3,450\text{ cm}^{-1}$), Ar–H ($\sim 3,050\text{ cm}^{-1}$), C–H ($2,850\text{--}2,960\text{ cm}^{-1}$), and aromatic systems ($1,490\text{--}1,640\text{ cm}^{-1}$). A strong peak near $1,240\text{ cm}^{-1}$ accounted for P=O in the phosphonates. A stretching vibration for P–O–C appeared at $1,020\text{--}1,050\text{ cm}^{-1}$. The IR spectrum of *IVA-3* is shown in Fig. 5.1.

In the ¹H NMR spectra of *IVA* and *IVB*, the chemical shifts of aromatic protons generally appeared at 6.9–8.2 ppm. When the phosphonates contained a pyridine moiety (as R³), the chemical shifts of aromatic protons moved to low field and appeared at 7.4–8.6 ppm. The proton signal at 6.5 ppm, which was accounted for the proton of hydroxyl, displayed as a double-doublet due to the coupling with a proton and phosphorus atom, and disappeared when a drop of heavy water was added. The proton signal corresponding to the P–CH appeared at 5.4 ppm also as a double-doublet due to the coupling with phosphorus and the proton of hydroxyl. The hydroxyl proton was replaced by deuterium when a drop of heavy water was added, which caused the signal change from a double-doublet to a doublet. The chemical shifts of the protons in two methyl groups on the 5-position of 1,3,2-dioxaphosphinane were not equivalent and appeared as two singlets between 0.7 and 1.0 ppm. The chemical shift of two protons of the methylene group at the 6-position of 1,3,2-dioxaphosphinane was also not equivalent. One appeared as a doublet at 4.7 ppm due to the geminal coupling with another proton, and the other displayed as a double-doublet at 4.05 ppm which was attributed to the proton geminal coupling and P–H coupling. From this fact we found that there was

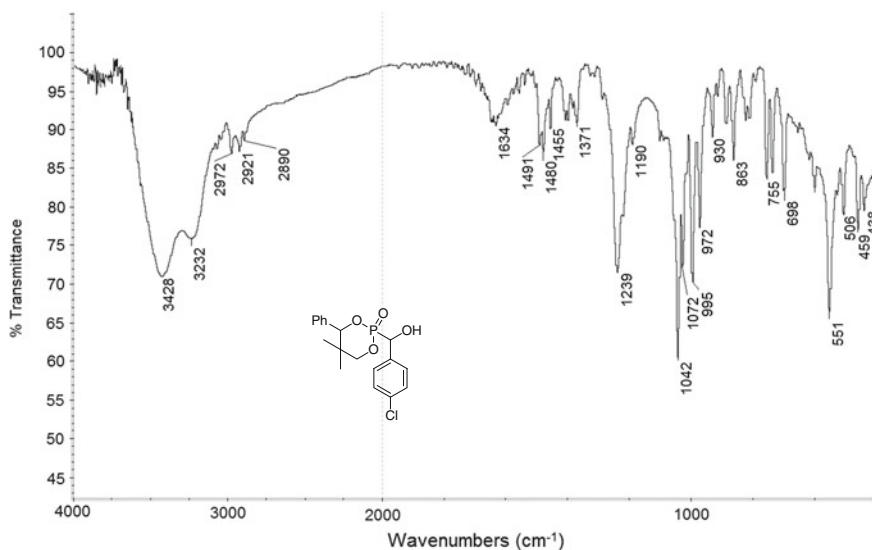


Fig. 5.1 IR spectrum of **IVA-3**

significant difference in the $^3J_{\text{P-H}}$ coupling constants of *trans* and *cis* structures in the phosphonates: $^3J_{\text{P-H}}(\textit{trans}) = 20$ Hz and $^3J_{\text{P-H}}(\textit{cis}) = 0$ Hz. The same situation was observed again in the ^1H NMR spectra, the signal of a proton on the 4-position of 1,3,2-dioxaphosphinane just appeared as a singlet at 5.7 ppm without splitting. It indicated that this proton located the *cis* position of phosphorus. The ^1H NMR spectra of compound **IVA-3** are shown in Figs. 5.2 and 5.3.

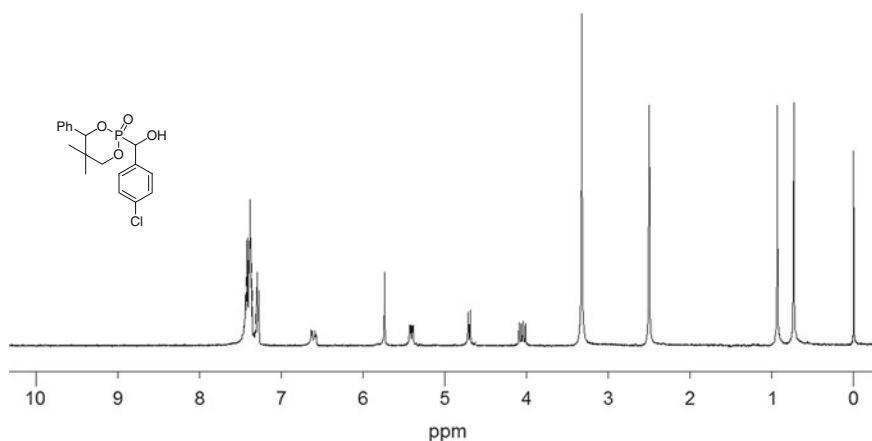


Fig. 5.2 ^1H NMR spectrum of **IVA-3** (DMSO-*d*₆, 400 MHz)

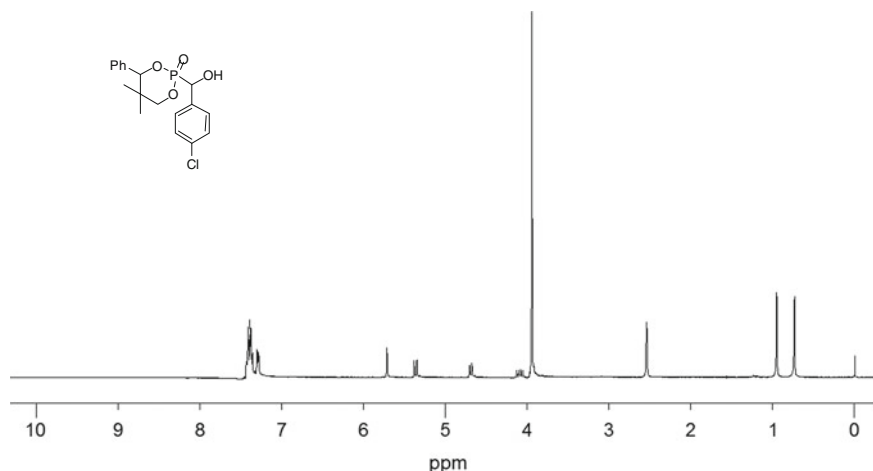


Fig. 5.3 ^1H NMR spectrum of **IVA-3** ($\text{DMSO-}d_6 + \text{D}_2\text{O}$, 400 MHz)

5.1.4 Crystal Structure Analysis of **IVA-3**

The molecular structure of 2-[1-hydroxy-1-(4-chlorophenyl)methyl]-5,5-dimethyl-4-phenyl-1,3,2-dioxaphosphinane-2-one **IVA-3** was further confirmed by the single crystal X-ray analysis [44].

The crystal belongs to the monoclinic system with space group $P 2(1)$, $a = 10.5609(14) \text{ \AA}$, $b = 6.4450(9) \text{ \AA}$, $c = 14.1161(19) \text{ \AA}$, $\alpha = 90^\circ$, $\beta = 110.475(2)^\circ$, $\gamma = 90^\circ$, $V = 900.1(2) \text{ \AA}^3$, $Z = 2$, $D_x = 1.353 \text{ mg/m}^3$, $\mu = 0.32 \text{ mm}^{-1}$, $F(000) = 384$. The molecular structure and cell packing of the compound are presented in Figs. 5.4 and 5.5, respectively. In the crystal, the dioxaphosphinane ring in the molecule adopts a chair conformation. Selected bond lengths and angles are listed in Table 5.3. The bond angles around P range from $106.1(1)$ to $112.3(1)^\circ$, indicating a

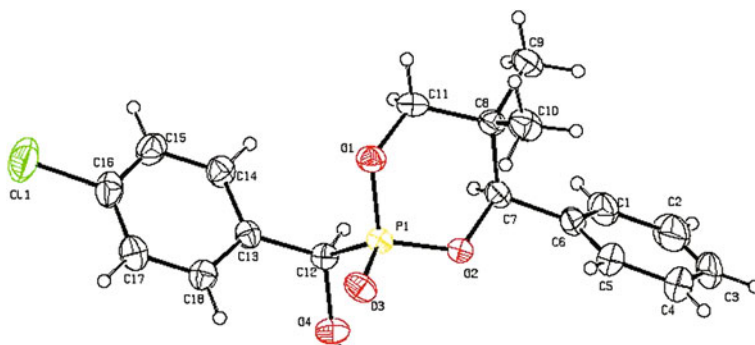


Fig. 5.4 Molecular structure of **IVA-3**

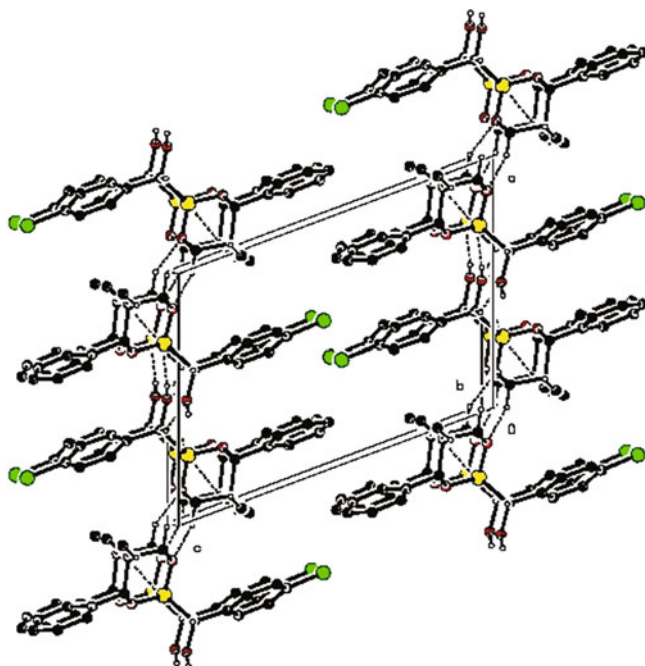


Fig. 5.5 Packing diagram of **IVA-3**

Table 5.3 Selected bond lengths (Å) and angles (°) for **IVA-3**

Bond	Dist.	Bond	Deg.
C12–P1	1.817(3)	O3–P1–O1	111.83(13)
O1–P1	1.564(2)	O3–P1–O2	111.64(13)
O2–P1	1.568(2)	O1–P1–O2	106.09(11)
O3–P1	1.466(2)	O3–P1–C12	112.29(14)
		O1–P1–C12	107.05(13)
		O2–P1–C12	107.60(13)

distorted tetrahedral configuration for the P atom. The crystal packing is stabilized by C–H···O and O–H···O hydrogen bonds (Table 5.4).

IVA-3 was recrystallized from chloroform to give colorless crystals (0.10 mm × 0.05 mm × 0.30 mm) suitable for X-ray single-crystal diffraction. The crystal structure of **IVA-3** was recorded on a Smart Apex CCD diffractometer using graphite monochromated MoK α radiation ($\lambda = 0.071073$ nm). In the range of $1.54^\circ \leq \theta \leq 26.99^\circ$, 3,837 independent reflections ($R_{int} = 0.032$), of which 2,940 contributing reflection had $I > 2\sigma(I)$, and all data were corrected using SADABS program. The structure was solved by direct methods using SHELXS-97, all other calculations were performed with Bruker SAINT system and Bruker SMART

Table 5.4 Hydrogen bonds for **IVA-3**

$D-H\cdots A$	$D-H$	$H\cdots A$	$D\cdots A$	$D-H\cdots A$
$C11-H11A\cdots O1^i$	0.97	2.57	3.290(4)	131
$C12-H12\cdots O4^{ii}$	0.98	2.29	3.126(4)	143
$C9-H9A\cdots O3^{iii}$	0.96	2.52	3.439(4)	159
$O4-H4A\cdots O3^{ii}$	0.814(10)	1.913(16)	2.696(3)	161(4)

Symmetry code (i) $-x + 2, y - 1/2, -z$; (ii) $-x + 1, y - 1/2, -z$; (iii) $x, y - 1, z$

programs. All non-hydrogen atoms were refined on F^2 anisotropically by full-matrix least squares method. Hydrogen atoms were observed and refined with a fixed isotropic displacement parameter. Full-matrix least-squares refinement gave final values of $R = 0.054$, $R_w = 0.112$. The max and min difference between peaks and holes was 295 and -229 e nm^{-3} , respectively. The summary of data collection statistics for the X-ray structure of **IVA-3** was reported in literature [44].

5.1.5 Herbicidal Activity of **IVA** and **IVB**

As a preliminary bioassay, the inhibitory activity of cyclic 1-hydroxyalkylphosphonates **IVA** and **IVB** against barnyard grass (*Echinochloa crusgalli*) and cabbage type rape (*Brassica napus*) were tested by using Petri dish methods. The inhibitory effect of **IVA** and **IVB** against the growth of roots and stems of tested plants were examined. The results are listed in Table 5.5.

(A) Inhibitory activity against the root of plant

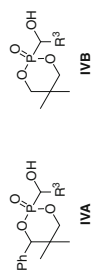
As seen from Table 5.5, **IVA-8**, **IVA-10**, and **IVA-11** displayed the best inhibitory activity ($>90\%$) against the root of barnyard grass, while **IVA-2**, **IVA-5** and **IVA-8** displayed the best inhibitory activity (84-87 %) against the root of cabbage type rape at 10 mg/L. Other cyclic 1-hydroxyalkylphosphonates showed weaker inhibitory activity at 10 mg/L.

(B) Inhibitory activity against the stem of plant

Only **IVA-8** had 86 % inhibitory activity against the stem of barnyard grass, but weak inhibitory activity against the stem of cabbage type rape at 10 mg/L. All other cyclic 1-hydroxyalkylphosphonates showed weaker inhibitory activity against the stem of barnyard grass and cabbage type rape at 10 mg/L.

As shown in Table 5.5, most of **IVA** and **IVB** displayed better inhibitory effects against the growth of cabbage type rape and barnyard grass at 100 mg/L than at 10 mg/L. They displayed a better inhibitory effect against the growth of the root than against the growth of the stem.

The IC_{50} of **IVB-1** and **IVB-10** against rape and barnyard grass were further tested. 2,4-D, a commercial herbicide, was used as a positive control for this

Table 5.5 Inhibitory activity of cyclic 1-hydroxyalkylphosphonates IVA and IVB against the growth of plants^a

Compound	R ³	Root		Stem		Bm ^b		Bm ^b	
		Ech ^b		Ech ^b		100 mg/L		100 mg/L	
		100 mg/L	10 mg/L	100 mg/L	10 mg/L	100 mg/L	10 mg/L	100 mg/L	10 mg/L
IVA-1	Ph	74	69	84	63	24	39	50	14
IVA-2	2-ClPh	90	87	96	84	47	39	57	51
IVA-3	4-ClPh	66	21	44	5	33	27	36	-7
IVA-4	2,4-Cl ₂ Ph	97	61	97	70	67	43	77	58
IVA-5	3,4-Cl ₂ Ph	74	74	99	87	17	11	89	74
IVA-6	4-MeOPh	91	57	94	31	49	9	50	27
IVA-7	4-MePh	79	56	87	48	89	44	50	46
IVA-8	4-NO ₂ Ph	100	97	97	84	92	86	86	46
IVA-9	Pyrid-2-yl	76	74	85	37	53	19	49	3
IVA-10	Pyrid-3-yl	95	92	99	57	72	56	86	49
IVA-11	Pyrid-4-yl	95	92	97	71	86	39	49	20
IVA-12	<i>n</i> -Bu	66	51	84	47	30	42	41	36
IVB-1	Ph	94	28	97	45	67	10	90	0
IVB-3	4-ClPh	97	39	90	59	28	37	67	26
IVB-4	2,4-Cl ₂ Ph	89	70	94	73	50	7	56	23
IVB-7	4-MePh	89	67	93	77	33	7	55	13
IVB-9	Pyrid-2-yl	84	25	96	66	74	22	88	29
IVB-10	Fur-2-yl	91	57	94	49	70	42	77	38
IVB-11	Me	37	33	56	21	64	51	52	16
IVB-13	<i>n</i> -Bu	94	72	89	68	52	47	58	16

^a Inhibitory potency (%) against the growth of plants in Petri dishes, 0 (no effect), 100 % (completely kill)

^b Ech: barnyard grass; Bm: cabbage type rape

Table 5.6 Inhibitory activities (IC_{50} , mg/L)^a of **IVB-1** and **IVB-10**

Compound	Brn ^b		Ech ^b	
	Root length IC_{50}	Stem length IC_{50}	Root length IC_{50}	Stem length IC_{50}
IVB-1	9.3385×10^{-1}	6.1726×10	8.2575×10^2	2.2024×10^2
IVB-10	4.6298×10^0	1.9352×10^2	3.1414×10^2	9.1593×10^2
2,4-D	7.4227×10^{-4}	1.3631×10^{-2}	2.1097×10^{-2}	2.9332×10

^a IC_{50} is effective dose that provides 50 % inhibition against the growth of plant (root or stem)

^b Ech: barnyard grass; Brn: cabbage type rape

experiments. Obviously, the inhibitory activity of **IVB-1** and **IVB-10** was lower than that of 2,4-D (Table 5.6).

(C) SAR analysis for **IVA** and **IVB**

IVA showed a little bit higher inhibition against the tested plants than that of **IVB**. A structural type of substituent R^3 had certain effect on inhibitory activity. Cyclic 1-hydroxyalkylphosphonates with pyrid-3-yl or pyrid-4-yl, 4- NO_2 Ph as R^3 exhibited better inhibitory activity. **IVA-8** ($R^3 = 4-NO_2Ph$) displayed the best inhibitory effect against barnyard grass and cabbage type rape. However, these cyclic 1-hydroxyalkylphosphonates did not show significant inhibitory activity at a lower rate.

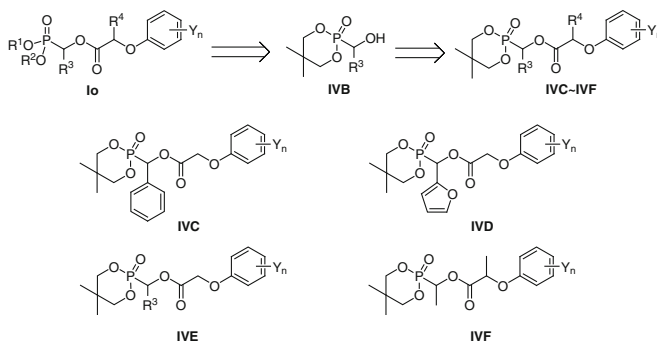
5.1.6 Summary

Two series of cyclic 1-hydroxyalkylphosphonates **IVA** and **IVB** were designed and synthesized by Pudovik reaction. The preliminary bioassay on inhibitory activity against plant showed that most of **IVA** and **IVB** exhibited good inhibitory activity against the root of barnyard grass and cabbage type rape at 100 mg/L. They displayed higher inhibitory activity against the growth of the root than that of the stem. Several cyclic 1-hydroxyalkylphosphonates **IVA-8**, **IVA-10**, and **IVA-11** were found to display inhibitory activity (>90 %) against the root of barnyard grass at 10 mg/L. Comparing **IVB-1** and **IVB-10** with 2,4-D by testing their IC_{50} data, the inhibitory activity of **IVB-1** and **IVB-10** against cabbage type rape and barnyard grass were lower than that of 2,4-D obviously. The above evaluation showed that cyclic 1-hydroxyalkylphosphonates **IVA** and **IVB** had no significant inhibitory activity at a lower rate.

5.2 Cyclic Alkylphosphonates **IVC–IVF**

5.2.1 Introduction

Through the study on the alkylphosphonates **IA–IK** series, it was found that higher herbicidal activity and inhibitory activity against plant PDHc E1 could be achieved by introducing small groups (Me) as R^1 and R^2 in the structure **Io**. This result



Scheme 5.5 Design of cyclic phosphonates **IVC–IVF**

indicated that the structural unit of phosphorus-containing played a very important role in herbicidal activity and the **IC** series could be used as a new lead structure. Considering the possible contribution of cyclophosphonates to herbicidal activity, an open-chain *O,O*-dimethyl phosphonate unit in the **IC** series was further modified by introducing a six-membered cyclic phosphonate unit. Four series of 2-[1-(substituted phenoxyacetoxy)alkyl]-5,5-dimethyl-1,3,2-dioxaphosphinane-2-one derivatives **IVC–IVF** were designed (Scheme 5.5).

As stated in Sect. 5.1, cyclic 1-hydroxyalkylphosphonates **IVB** exhibited certain herbicidal activity in the preliminary bioassay, and therefore it was expected that cyclic phosphonates **IVC–IVF** might be more active than the corresponding cyclic 1-hydroxyalkylphosphonates **IVB**.

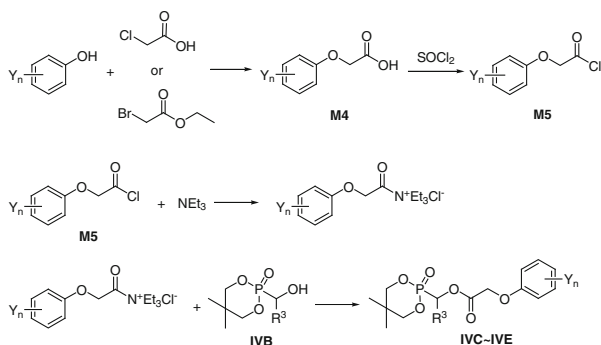
When H as R^4 remained the same, substituted phenyl, furyl or alkyl as R^3 was introduced into the parent structure of **IV** to form the **IVC**, **IVD**, and **IVE** series, respectively. In the **IVC**, **IVD**, and **IVE** series, substituted phenyl, furyl or alkyl as R^3 was kept constant, respectively; further modification was focused on substituent Y_n . In the **IVF** series, methyl as R^3 and R^4 was kept constant, further modification was also focused on substituent Y_n .

In this section, the synthesis and herbicidal activity of the **IVC–IVF** series are described, and their structure-activity relationships are discussed.

5.2.2 Synthesis of IVC–IVF

Cyclic phosphonates **IVC–IVE** could be conveniently prepared by the condensation of 2-(1-hydroxyalkyl)-5,5-dimethyl-1,3,2-dioxaphosphinane-2-one **IVB** with substituted phenoxyacetyl chlorides **M5** in the presence of a base (Scheme 5.6).

IVB could be prepared according to the description in Sect. 5.1.2. The substituted phenoxyacetyl chlorides **M5** could be easily synthesized starting from substituted phenols and chloroacetic acid or bromoacetic acid ester [45, 46], as



Scheme 5.6 Synthesis of cyclic phosphonates **IVC–IVE**

discussed in detail in Chap. 2. Considering that cyclic 1-hydroxyalkylphosphonates were easily regenerated to the starting carbonyl compounds in strong alkaline medium, triethylamine, a weak organic base, was chosen for this reaction. The structures of **IVC–IVE** are listed in Tables 5.7, 5.8, and 5.9.

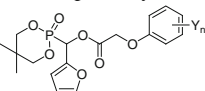
The preparation of **IVF** involved the condensation of substituted phenoxypropionyl chlorides **M20** and 2-(1-hydroxyethyl)-5,5-dimethyl-1,3,2-dioxaphosphinane-2-one **IVB-11** in the presence of triethylamine as a base. The substituted phenoxypropionyl chlorides **M20** could be easily obtained by the reaction of substituted phenoxypropionic acids **M19** and thionyl chloride in high yields. Substituted phenoxypropionic acids **M19** could be synthesized starting from

Table 5.7 Structure of 2-[1-(substituted phenoxyacetoxy)alkyl]-5,5-dimethyl-1,3,2-dioxaphosphinane-2-one **IVC**^a

Compound	R ³	Y _n	Compound	R ³	Y _n
IVC-1	Ph	H	IVC-13	Ph	2-Cl,4-F
IVC-2	Ph	2-Cl	IVC-14	Ph	2,4-F ₂
IVC-3	Ph	2-F	IVC-15	Ph	4-F
IVC-4	Ph	3-Me	IVC-16	Ph	2,4-Cl ₂
IVC-5	Ph	3-CF ₃	IVC-17	2-ClPh	2,4-Cl ₂
IVC-6	Ph	4- <i>t</i> -Bu	IVC-18	4-ClPh	2,4-Cl ₂
IVC-7	Ph	4-Cl	IVC-19	2,4-Cl ₂ Ph	2,4-Cl ₂
IVC-8	Ph	3-Me,4-Cl	IVC-20	3,4-Cl ₂ Ph	2,4-Cl ₂
IVC-9	Ph	2,3-Me ₂	IVC-21	4-MeOPh	2,4-Cl ₂
IVC-10	Ph	2,4,5-Cl ₃	IVC-22	4-MePh	2,4-Cl ₂
IVC-11	Ph	2-Me,4-Cl	IVC-23	4-NO ₂ Ph	2,4-Cl ₂
IVC-12	Ph	2-F,4-Cl			

^a Synthesis of **IVC-1**, **IVC-3**, **IVC-5**, **IVC-12**, **IVC-13**, and **IVC-15** [47]; **IVC-2**, **IVC-7**, **IVC-8**, **IVC-11**, **IVC-16**, **IVC-18**, and **IVC-19** [48]

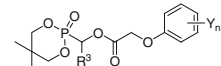
Table 5.8 Structure of 2-[1-(substituted phenoxyacetoxy)-1-(fur-2-yl)methyl]-5,5-dimethyl-1,3,2-dioxaphosphinane-2-one **IVD**^a



Compound	Y _n	Compound	Y _n
IVD-1	H	IVD-8	4-F
IVD-2	2-Cl	IVD-9	3-Me,4-Cl
IVD-3	2-F	IVD-10	2-Me,4-Cl
IVD-4	3-Me	IVD-11	2-F,4-Cl
IVD-5	3-CF ₃	IVD-12	2-Cl,4-F
IVD-6	4- <i>t</i> -Bu	IVD-13	2,4-Cl ₂
IVD-7	4-Cl		

^a Synthesis of **IVD-1**, **IVD-3**, **IVD-5**, **IVD-8**, **IVD-11**, and **IVC-12** [47]; **IVD-2**, **IVD-7**, **IVD-9**, **IVD-10**, and **IVD-13** [48]

Table 5.9 Structure of 2-[1-(substituted phenoxyacetoxy)alkyl]-5,5-dimethyl-1,3,2-dioxaphosphinane-2-one **IVE**^a



Compound	R ³	Y _n	Compound	R ³	Y _n
IVE-1	Me	H	IVE-8	Me	3-Me,4-Cl
IVE-2	Me	2-Cl	IVE-9	Me	2-Cl,4-F
IVE-3	Me	2-F	IVE-10	Me	2-F,4-Cl
IVE-4	Me	4-Cl	IVE-11	Me	2,4-Cl ₂
IVE-5	Me	4-F	IVE-12	<i>i</i> -Pr	2,4-Cl ₂
IVE-6	Me	3-CF ₃	IVE-13	<i>n</i> -Bu	2,4-Cl ₂
IVE-7	Me	2-Me,4-Cl			

^a Synthesis of **IVE-1**, **IVE-5**, **IVE-6**, **IVE-9**, and **IVE-10** [47]; **IVE-2**, **IVE-4**, **IVE-7**, **IVE-8**, **IVE-11**, **IVE-12**, and **IVE-13** [48]

substituted phenols and 2-bromopropionic acid ester (Scheme 5.7) [45–49]. The 2-(1-hydroxyethyl)-5,5-dimethyl-1,3,2-dioxaphosphinane-2-one **IVB-11** could be prepared according to the description in Sect. 5.1.2. The structures of **IVF** are listed in Table 5.10.

Since cyclic 1-hydroxyalkylphosphonates **IVB** were easily decomposed at a high temperature and phosphonates **IVC–IVF** containing carboxylic acid ester groups were also very sensitive to acid, base or water. Therefore the reaction required a moderate control of temperature. The reagents and solvents should be preprocessed in anhydrous state. The reaction was carried out in three stages: firstly, a solution of substituted phenoxyacetyl chloride was added dropwise to the solution of cyclic 1-hydroxyalkylphosphonate under 5 °C; secondly, the reaction solution was stirred at room temperature for several hours, and then at a higher temperature for further reaction in 1–2 h. By above synthetic method, 57 of cyclic phosphonates including **IVC** (23 compounds), **IVD** (13 compounds), **IVE** (13 compounds), and

Scheme 5.7 Synthesis of 2-[1-(substituted phenoxypropionyloxy)ethyl]-5,5-dimethyl-1,3,2-dioxaphosphinane-2-one **IVF**

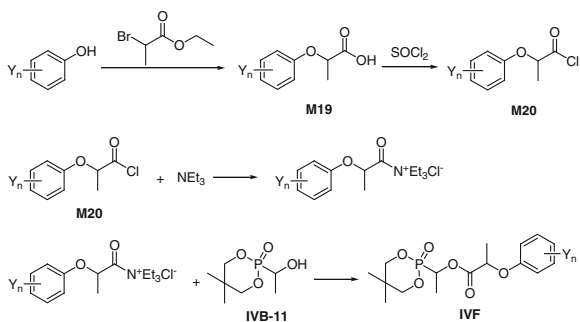
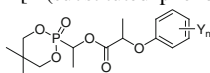


Table 5.10 Structure of 2-[1-(substituted phenoxypropionyloxy)ethyl]-5,5-dimethyl-1,3,2-dioxaphosphinane-2-one **IVF**



Compound	Y _n	Compound	Y _n
IVF-1	2-Cl	IVF-5	2-Me,4-Cl
IVF-2	4-Cl	IVF-6	3-Me,4-Cl
IVF-3	4-F	IVF-7	2-Cl,4-F
IVF-4	3-CF ₃	IVF-8	2,4-Cl ₂

IVF (8 compounds) series were conveniently synthesized in the presence of triethylamine and anhydrous trichloromethane. Detailed synthetic procedures for cyclic phosphonates **IVC–IVF** are introduced in the Sect. 9.1.26 of Chap. 9.

Cyclic phosphonates **IVC–IVF** were stable for light and air at room temperature but easily decomposed under acidic or basic conditions. The structures of **IVC–IVF** were confirmed by elementary analysis and were characterized by ¹H NMR, IR, and MS. Some of them were further characterized by ¹³C NMR and ³¹P NMR spectra. Spectroscopic analysis of some representative **IVC–IVF** are given in Sect. 5.2.3.

5.2.3 Spectroscopic Analysis of **IVC–IVF**

The IR spectra of **IVC–IVF** showed normal absorption bands of functional groups. The stretching frequency indicated the existence of Ar–H (3,050–3,100 cm⁻¹), C–H (2,850–2,960 cm⁻¹). The two or three bands in the 1,490–1,640 cm⁻¹ region were attributed to aromatic rings systems such as benzene or furan. A strong absorption band near 1,750–1,770 cm⁻¹ was identified for the stretching frequency of C=O. A strong peak near 1,280 cm⁻¹ accounted for P=O in phosphonates. A stretching vibration for P–O–C appeared at ~1,060 cm⁻¹. An asymmetric stretching vibration for C–O–C appeared near 1,180 cm⁻¹ and a symmetric stretching vibration for C–O–C was found near 1,090 cm⁻¹. The IR spectra of **IVC-17**, **IVD-13**, and **IVE-12** are shown in Figs. 5.6, 5.7 and 5.8.

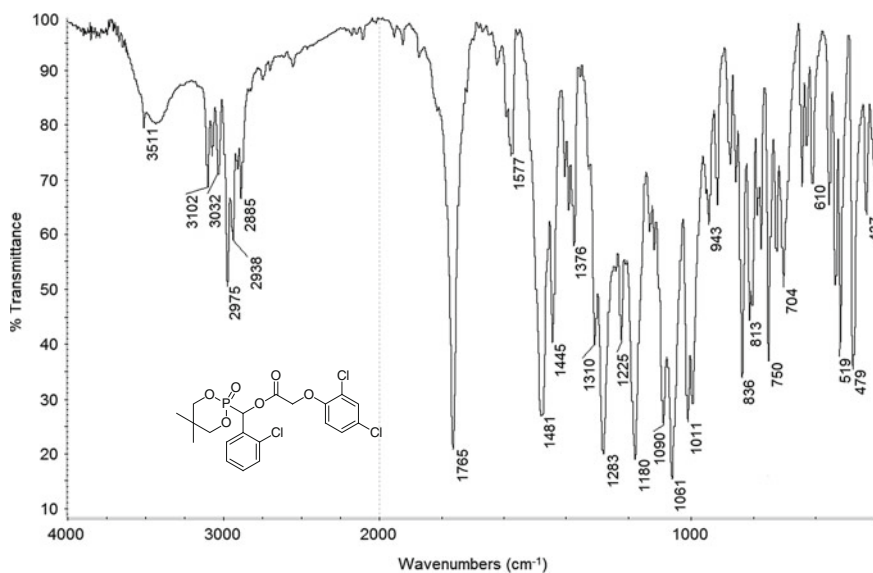


Fig. 5.6 IR spectrum of IVC-17

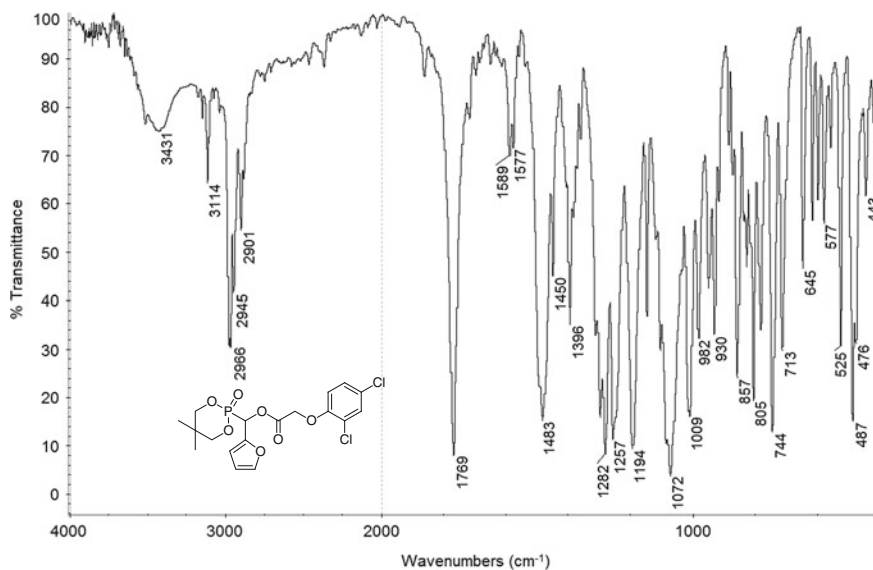


Fig. 5.7 IR spectrum of IVD-13

In ¹H NMR spectra of **IVC–IVE**, the chemical shifts of aromatic protons appeared at 6.5–7.7 ppm generally. The protons of two methyl groups on the 5-position of 1,3,2-dioxaphosphinane were not chemical-shift equivalent and

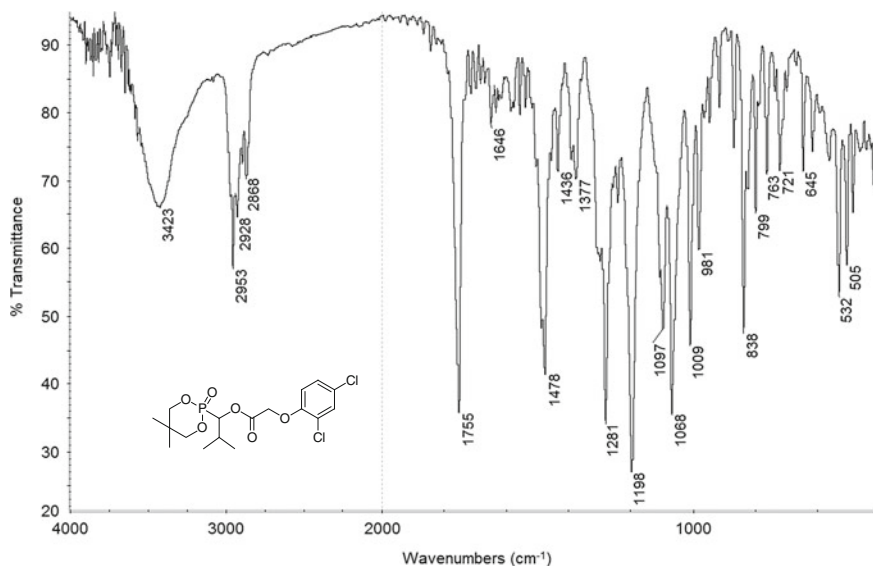


Fig. 5.8 IR spectrum of **IVE-12**

appeared as two singlets between 0.9 and 1.2 ppm. The protons of two methylene groups at the 4- and 6-position of 1,3,2-dioxaphosphinane were also not chemical-shift equivalent. Their signals appeared as a multiplet at 3.9–4.2 ppm due to the geminal coupling with another proton and P–H coupling. The protons of the methylene group (OCH₂CO) between the phenoxy and carbonyl group were not chemical-shift equivalent either and appeared as two doublets or AB system at 4.7–4.9 ppm. In ¹H NMR spectra of **IVC** and **IVD**, the proton signal corresponding to the P–CH–O appeared at 6.3–6.7 ppm as a doublet due to the coupling with phosphorus, whereas in ¹H NMR spectra of **IVE** and **IVF** the proton signal corresponding to the P–CH–O appeared at 5.4–5.6 ppm as a multiplet due to the coupling with phosphorus and hydrogen of alkyl.

For **IVF**, there are two chiral centers in their molecule structure which caused diastereoisomer mixtures. In ¹H NMR spectra of **IVF**, the chemical shift and coupling split of protons were similar to those of **IVE**, but we could observe signals divided into two groups very clearly. The ¹H NMR spectra of **IVC-19**, **IVE-7**, and **IVF-5** are shown in Figs. 5.9, 5.10, and 5.11.

In ¹³C NMR spectra of **IVC–IVF**, the chemical shifts of carbonyl carbon typically appeared at 165–168 ppm. The carbon signal corresponding to the P–CH–O appeared at 63–66 ppm as a doublet due to the coupling with phosphorus and the coupling constant ¹J_{P–C} was 160–170 Hz. The ¹³C NMR spectrum of **IVE-8** is shown in Fig. 5.12.

In ³¹P NMR spectra of **IVC–IVF**, chemical shifts of the phosphorus appeared very regularly according to the type of R³. **IVC** with substituted phenyl as R³, their phosphorus signals appeared at 8–10 ppm. **IVD** with furyl as R³, their phosphorus

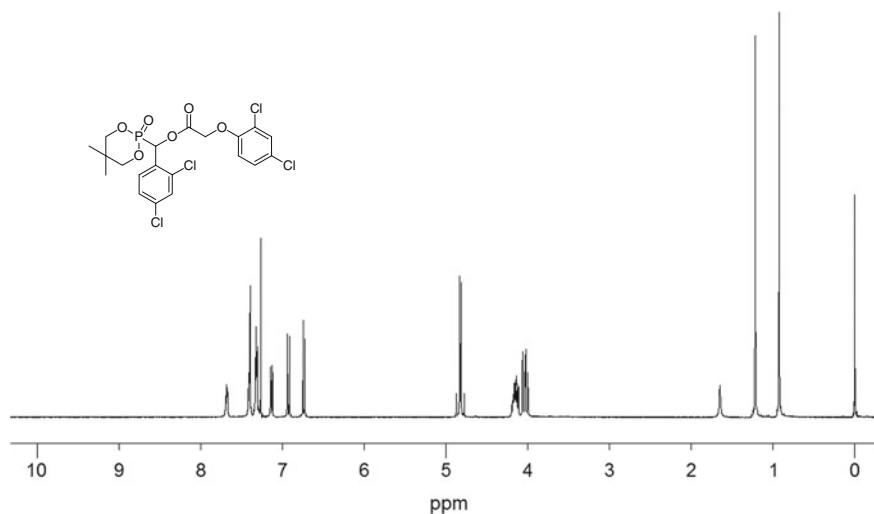


Fig. 5.9 ¹H NMR spectrum of **IVC-19** (CDCl₃, 600 MHz)

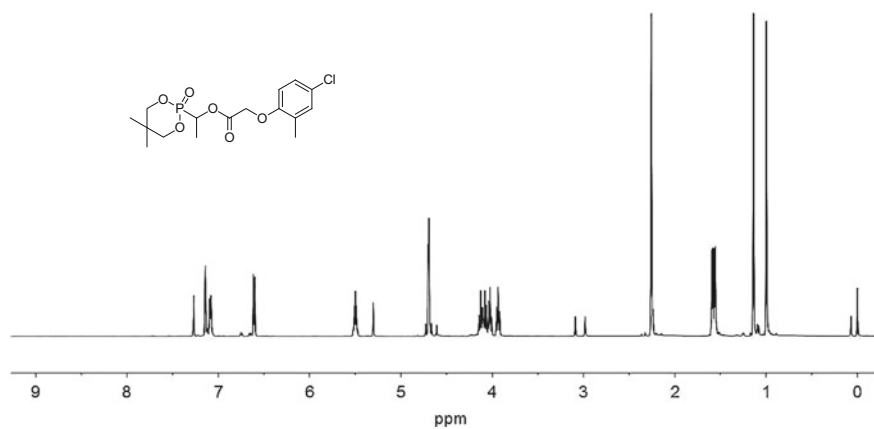


Fig. 5.10 ¹H NMR spectrum of **IVE-7** (CDCl₃, 600 MHz)

signals appeared at 6–7 ppm. **IVE** and **IVF** with alkyl as R³, their phosphorus signals appeared at 12–14 ppm. The ³¹P NMR spectrum of **IVE-9** is shown in Fig. 5.13.

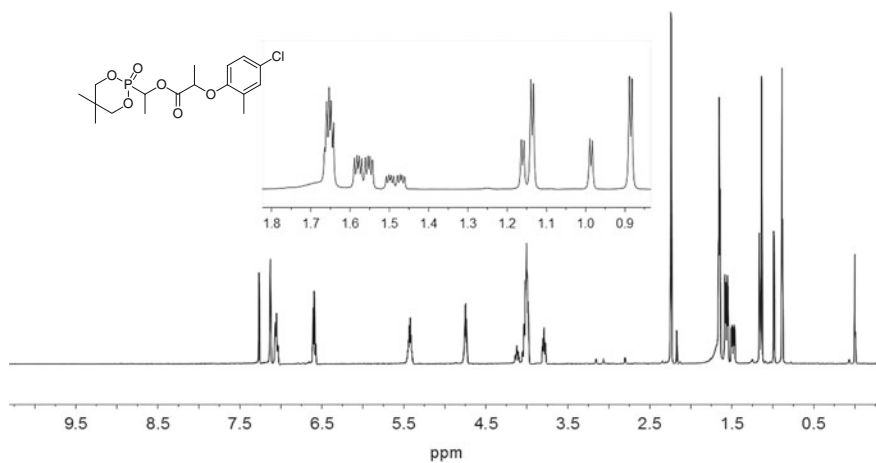


Fig. 5.11 ¹H NMR spectrum of IVF-5 (CDCl₃, 600 MHz)

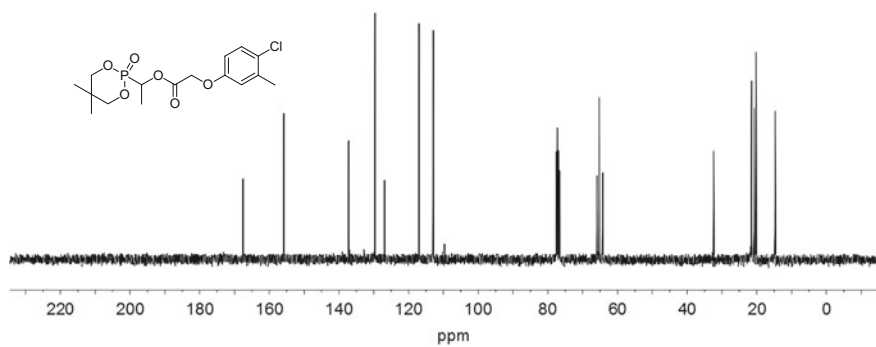


Fig. 5.12 ¹³C NMR spectrum of IVE-8 (CDCl₃, 150 MHz)

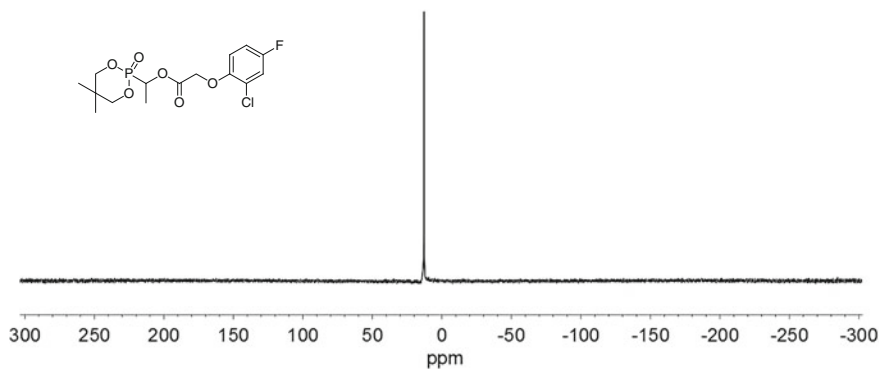


Fig. 5.13 ³¹P NMR spectrum of IVE-9 (CDCl₃, 243 MHz)

5.2.4 Crystal Structure Analysis of IVC-19

The molecular structure of 2-[1-(2,4-dichlorophenoxyacetoxy)-1-(2-chlorophenyl)methyl]-5,5-dimethyl-1,3,2-dioxaphosphinane-2-one **IVC-19**, was confirmed by the single-crystal X-ray analysis [50].

The crystal belongs to the triclinic system with space group $P-1$, $a = 8.8627(7)$ Å, $b = 10.4972(9)$ Å, $c = 13.3624(11)$ Å, $\alpha = 79.8340(10)^\circ$, $\beta = 83.7070(10)^\circ$, $\gamma = 69.9360(10)^\circ$, $V = 1147.75(16)$ Å³, $Z = 2$, $D_x = 1.428$ mg/m³, $\mu = 0.502$ mm⁻¹, $F(000) = 508$. The molecular structure and cell packing of **IVC-19** are presented in Figs. 5.14 and 5.15, respectively. Selected bond lengths and angles are listed in Table 5.11. All bond lengths and angles are normal. The bond angles around P range from 106.9 (1) to 113.8 (1), indicating a distorted tetrahedral configuration for the P atom. The crystal packing is stabilized by weak intermolecular C–H \cdots O and π – π interactions (Table 5.12 and Fig. 5.15).

IVC-19 was recrystallized from dichloromethane to give colorless crystals (0.30 mm \times 0.20 mm \times 0.20 mm) suitable for X-ray single-crystal diffraction. The crystal structure of **IVC-19** was recorded on a Smart Apex CCD diffractometer using graphite monochromated MoK α radiation ($\lambda = 0.071073$ nm). In the range of $2.09^\circ \leq \theta \leq 27^\circ$, 4,976 independent reflections ($R_{int} = 0.024$), of which 4,228 contributing reflection had $I > 2\sigma(I)$, and all data were corrected using SADABS program. The structure was solved by direct methods using SHELXS-97, all other calculations were performed with Bruker SAINT system and Bruker SMART programs. All non-hydrogen atoms were refined on F^2 anisotropically by full-matrix least squares method. Hydrogen atoms were observed and refined with a fixed value of their isotropic displacement parameter. Full-matrix least-squares refinement gave final values of $R = 0.051$, $R_w = 0.134$. The max and min difference

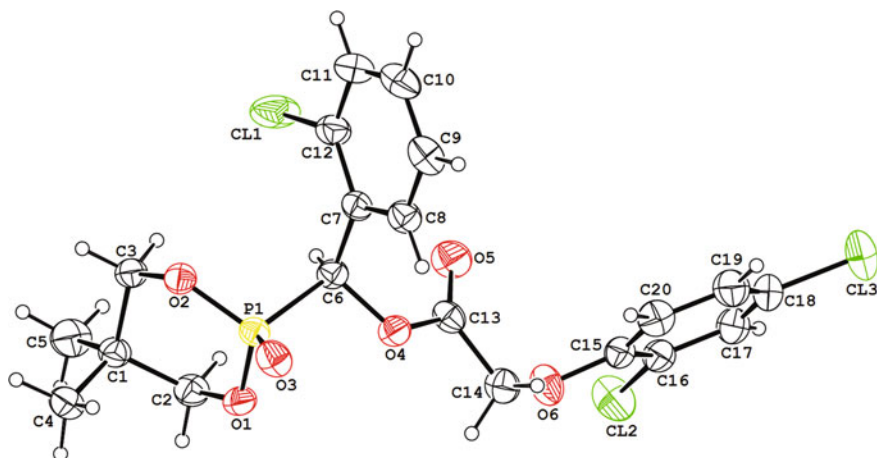


Fig. 5.14 Molecular structure of **IVC-19**

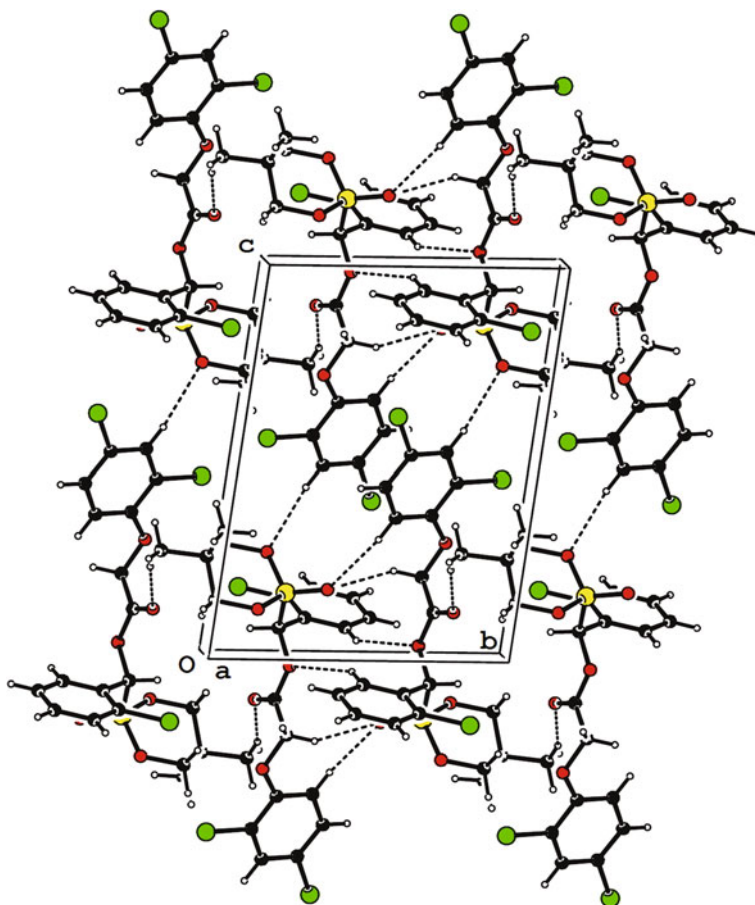


Fig. 5.15 Packing diagram of **IVC-19**

Table 5.11 Selected bond lengths (Å) and angles (°) for **IVC-19**

Bond	Dist.	Bond	Deg.
C6–P1	1.829(2)	O3–P1–O2	113.75(10)
O1–P1	1.5719(16)	O3–P1–O1	112.20(10)
O2–P1	1.5639(16)	O2–P1–O1	106.84(8)
O3–P1	1.4555(16)	O3–P3–C6	112.63(10)
		O2–P1–C6	105.53(9)
		O1–P1–C6	105.26(9)

between peaks and holes was 599 and -518 e nm^{-3} , respectively. The summary of data collection statistics for the X-ray structure of **IVC-19** was reported in the literature [50].

Table 5.12 Hydrogen bonds for **IVC-19**

$D-H\cdots A$	$D-H$	$H\cdots A$	$D\cdots A$	$D-H\cdots A$
$C17-H17\cdots O2^i$	0.93	2.60	3.463(3)	155
$C20-H20\cdots O3^{ii}$	0.93	2.50	3.417(3)	167
$C14-H14A\cdots O3^{ii}$	0.97	2.43	3.311(3)	150
$C8-H8\cdots O4^{ii}$	0.93	2.60	3.402(3)	145
$C5-H5A\cdots O5^{iii}$	0.96	2.59	3.488(4)	156

Symmetry code (i) $x, y, z - 1$; (ii) $-x + 1, -y + 1, -z + 2$; (iii) $-x + 1, -y, -z + 2$

5.2.5 Herbicidal Activity of IVC–IVF

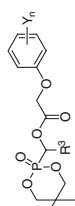
As mentioned in Chap. 2, several series of open-chain 1-(substituted phenoxy-acetoxy)alkylphosphonates were found to exhibit notable herbicidal activity against dicotyledons. In order to examine the effect of phosphorus-containing heterocyclic moiety on herbicidal activity, a phosphorus-containing six-member ring was introduced into different molecules to form cyclic phosphonates **IVC–IVF**. A set of experiments were performed to evaluate their herbicidal activity. The herbicidal activity of cyclic phosphonates **IVC–IVF** are reviewed as follows.

5.2.5.1 Herbicidal Activity of 2-[1-(Substituted Phenoxyacetoxy)Alkyl]-5,5-Dimethyl-1,3,2-Dioxaphosphinane-2-One **IVC**

Twenty-three cyclic phosphonates **IVC** were prepared to test their herbicidal activity. In series **IVC**, when phosphorus-containing heterocyclic moiety was kept; further examination was focused on the effect of substituents Y_n and R^3 including phenyl and substituted phenyl groups. As a preliminary bioassay, **IVC** were tested for the inhibitory effect on barnyard grass (*E. crusgalli*) and cabbage type rape (*B. napus*) using the Petri dish methods. The results are listed in Table 5.13. Based on the preliminary bioassays, the inhibition of some **IVC** against chingma abutilon (*Abutilon theophrasti*), leaf mustard (*B. juncea*), common amaranth (*Amaranthus retroflexus*), white eclipta (*Eclipta prostrate*), barnyard grass (*E. crusgalli*), crab grass (*Digitaria sanguinalis*), and green bristlegrass (*Setaira viridis*) was further evaluated for post-emergence herbicidal activity at 150, 75 and 37.5 g ai/ha, respectively. The data of the herbicidal activity of cyclic phosphonates **IVC** are listed in Tables 5.14 and 5.15.

(A) Inhibitory activity against the root of plant of **IVC**

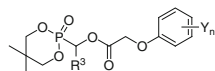
As shown in Table 5.13, **IVC-16–23** displayed good inhibitory effect (>90 %) on the growth of roots of cabbage type rape and barnyard grass at 100 and 10 mg/L. They will be further examined for their pre-emergence herbicidal activity in the greenhouse.

Table 5.13 Inhibitory activity of cyclic phosphonates IVC against the growth of plants^a

Compound	R ³	Y _n	Root			Stem				
			Ech ^b		Ech ^b		Brm ^b			
			100 mg/L	10 mg/L	100 mg/L	10 mg/L	100 mg/L	10 mg/L		
IVC-1	Ph	H	89	60	96	68	52	50	54	33
IVC-2	Ph	2-Cl	98	96	99	83	75	57	97	79
IVC-3	Ph	2-F	76	56	79	29	53	52	33	33
IVC-4	Ph	3-Me	89	64	97	88	62	50	83	46
IVC-5	Ph	3-CF ₃	96	93	93	75	57	50	88	54
IVC-6	Ph	4- <i>t</i> -Bu	67	60	31	8	55	43	15	-4
IVC-7	Ph	4-Cl	94	72	99	98	34	49	83	67
IVC-8	Ph	3-Me,4-Cl	96	89	99	97	59	55	83	79
IVC-9	Ph	2,3-Me ₂	93	69	97	79	64	50	94	67
IVC-16	Ph	2,4-Cl ₂	97	94	99	98	46	40	78	61
IVC-17	2-ClPh	2,4-Cl ₂	97	97	99	99	29	57	83	78
IVC-18	4-ClPh	2,4-Cl ₂	97	97	99	99	37	66	89	83
IVC-19	2,4-Cl ₂ Ph	2,4-Cl ₂	97	94	99	99	37	29	78	72
IVC-20	3,4-Cl ₂ Ph	2,4-Cl ₂	97	97	99	99	28	63	83	72
IVC-21	4-MeOPh	2,4-Cl ₂	100	97	99	99	43	54	84	83
IVC-22	4-MePh	2,4-Cl ₂	97	97	99	99	37	54	83	78
IVC-23	4-NO ₂ Ph	2,4-Cl ₂	99	99	99	99	34	52	83	78

^a Inhibitory potency (%) against the growth of plants in petri dishes, 0 (no effect), 100 % (completely kill)

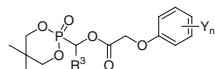
^b Ech: barnyard grass; Brm: cabbage type rape

Table 5.14 Structure and post-emergence herbicidal activity of cyclic phosphonates **IVC^a**

Compound	R ³	Y _n	Abu ^b	Brj ^b	Amr ^b	Ecl ^b	Ech ^b	Dig ^b	Set ^b
IVC-1	Ph	H	10	30	30	10	0	0	0
IVC-2	Ph	2-Cl	75	75	75	65	0	0	0
IVC-3	Ph	2-F	40	40	30	30	0	0	0
IVC-5	Ph	3-CF ₃	100	95	70	60	0	0	0
IVC-7	Ph	4-Cl	65	70	60	50	0	0	0
IVC-8	Ph	3-Me,4-Cl	65	65	65	60	0	0	0
IVC-10	Ph	2,4,5-Cl ₃	60	50	50	50	NT	NT	NT
IVC-11	Ph	2-Me,4-Cl	100	90	100	75	40	0	0
IVC-12	Ph	2-F,4-Cl	75	70	80	75	40	40	40
IVC-13	Ph	2-Cl,4-F	100	95	100	90	70	30	60
IVC-14	Ph	2,4-F ₂	50	50	50	50	NT	NT	NT
IVC-15	Ph	4-F	40	55	70	70	0	0	0
IVC-16	Ph	2,4-Cl ₂	98	100	90	80	0	0	0
IVC-18	4-ClPh	2,4-Cl ₂	90	98	80	70	0	0	0
IVC-19	2,4-Cl ₂ Ph	2,4-Cl ₂	95	100	80	70	0	0	0

^a Inhibitory potency (%) against the growth of plants at a rate of 150 g ai/ha in the greenhouse, 0 (no effect), 100 % (completely kill), NT (not tested)

^b Abu: chingma abutilon; Brj: leaf mustard; Amr: common amaranth; Ecl: white eclipta; Ech: barnyard grass; Dig: crab grass; Set: green bristlegrass

Table 5.15 Structure and post-emergence herbicidal activity of cyclic phosphonates **IVC^a**

Compound	R ³	Y _n	Brj ^b		Amr ^b		Ecl ^b	
			75 g/ha	37.5 g/ha	75 g/ha	37.5 g/ha	75 g/ha	37.5 g/ha
IVC-15	Ph	4-F	60	30	40	30	0	0
IVC-16	Ph	2,4-Cl ₂	95	90	80	50	55	50
IVC-18	4-ClPh	2,4-Cl ₂	90	80	50	30	0	0
IVC-19	2,4-Cl ₂ Ph	2,4-Cl ₂	55	50	20	20	34	30
Clacyfos (IC-22)			95	90	95	70	80	60

^a Inhibitory potency (%) against the growth of plants in the greenhouse, 0 (no effect), 100 % (completely kill)

^b Brj: leaf mustard; Amr: common amaranth; Ecl: white eclipta

(B) *Post-emergence herbicidal activity of IVC*

Cyclic phosphonates **IVC-2** and **IVC-7–23** exhibited 61–83 % inhibitory activity against the growth of the stem of cabbage type rape, but most cyclic phosphonates **IVC** showed <60 % inhibitory activity against the growth of the stem of barnyard grass except **IVC-18** and **IVC-20** with 66 and 60 inhibitory effect at 10 mg/L.

On the basis of preliminary bioassay, some of **IVC** was evaluated at 150 g ai/ha for their post-emergence herbicidal activity against chingma abutilon, leaf mustard, common common amaranth, white eclipta, barnyard grass, crab grass, and green bristlegrass in the greenhouse. The results are listed in Table 5.14.

As shown in Table 5.14, all test compounds displayed much higher herbicidal activity against dicotyledonous plants than monocotyledonous plants. **IVC-11**, **IVC-13**, **IVC-16**, **IVC-18**, and **IVC-19** exhibited significant herbicidal activity against chingma abutilon, leaf mustard, common amaranth, and white eclipta, especially **IVC-13** which displayed a notable 90–100 % inhibition effect against all tested broad-leaved weeds and 60–70 % inhibition effect against barnyard grass and green bristlegrass, but most **IVC** had no activity against monocot weeds.

(C) *SAR analysis for IVC*

Comparing the data of cyclic phosphonates **IVC** in Table 5.14, it could be found that substituent Y_n on the phenoxy-benzene ring greatly affected the herbicidal activity. The herbicidal activity of all compounds with substituents on the phenoxy-benzene ring were higher than that of compound **IVC-1** with no substituent on the phenoxy-benzene ring, which was almost inactive. Furthermore, the compounds with 2-Cl,4-F, 2,4-Cl₂ or 2-Me,4-Cl as Y_n , such as **IVC-13**, **IVC-11**, **IVC-16**, **IVC-18**, and **IVC-19**, exhibited significant herbicidal activity against tested dicotyledons for post-emergence application at 150 g ai/ha, irrespective of Ph, 2,4-Cl₂Ph or 4-CIPh as R^3 .

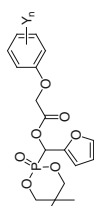
Cyclic phosphonates **IVC-15**, **IVC-16**, **IVC-18**, and **IVC-19** were selected for further bioassay at a lower rate for post-emergence herbicidal effect and clacyfos (**IC-22**, HW02) was used as a positive control. The results are listed in Table 5.15.

As seen from Table 5.15, **IVC-16** and **IVC-18** only had 80–90 % inhibition against leaf mustard, but weaker herbicidal effect against common amaranth and white eclipta at 37.5 g ai/ha. Other compounds **IVC-15** and **IVC-19** showed much weaker herbicidal effect against tested broad-leaved weeds at 37.5 g ai/ha. The herbicidal activity of cyclic phosphonates **IVC-15**, **IVC-16**, **IVC-18**, and **IVC-19** were not comparable to clacyfos (**IC-22**, HW02).

5.2.5.2 Herbicidal Activity of 2-[1-(Substituted Phenoxyacetoxy)-1-(Fur-2-yl)Methyl]-5,5-Dimethyl-1,3,2-Dioxaphosphinane-2-One **IVD**

Thirteen cyclic phosphonates **IVD** were prepared to test their herbicidal activity. In series **IVD**, when the phosphorus-containing six-member ring and furyl group as R^3 were kept, further examination was focused on the effect of substituent Y_n . As a preliminary bioassay, the cyclic phosphonates **IVD** were tested for inhibitory effect

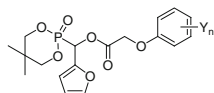
Table 5.16 Inhibitory activity of cyclic phosphonates **IVD** against the growth of plants^a



Compound	Y _n	Root			Stem			
		Ech ^b			Ech ^b			
		100 mg/L	10 mg/L	Brm ^b 100 mg/L	100 mg/L	10 mg/L	Brm ^b 100 mg/L	
IVD-1	H	91	62	91	63	59	48	21
IVD-2	2-Cl	96	93	99	97	66	57	83
IVD-3	2-F	64	68	40	18	42	34	0
IVD-4	3-Me	96	62	97	72	55	55	42
IVD-5	3-CF ₃	100	94	99	94	46	32	67
IVD-6	4- <i>t</i> -Bu	49	20	59	16	36	21	8
IVD-7	4-Cl	96	96	99	99	55	49	88
IVD-9	3-Me,4-Cl	98	93	99	97	71	62	79
IVD-13	2,4-Cl ₂	97	97	99	99	51	54	78

^a Inhibitory potency (%) against the growth of plants in Petri dishes, 0 (no effect), 100 % (completely kill)

^b Ech: barnyard grass; Brm: cabbage type rape

Table 5.17 Structure and post-emergence herbicidal activity of cyclic phosphonates **IVD**^a

Compound	Y _n	Abu ^b	Brj ^b	Amr ^b	Ecl ^b	Ech ^b	Dig ^b	Set ^b
IVD-1	H	10	40	30	10	0	0	0
IVD-2	2-Cl	70	90	85	70	0	0	0
IVD-3	2-F	45	45	40	30	0	0	0
IVD-5	3-CF ₃	85	90	70	50	0	0	0
IVD-7	4-Cl	70	70	55	50	0	0	0
IVD-8	4-F	80	70	30	40	50	70	30
IVD-9	3-Me,4-Cl	70	65	60	55	0	0	0
IVD-10	2-Me,4-Cl	100	90	100	70	60	0	0
IVD-11	2-F,4-Cl	70	70	70	70	30	40	0
IVD-12	2-Cl,4-F	100	95	100	90	75	70	50
IVD-13	2,4-Cl ₂	90	95	80	80	30	30	40
Clacyfos (IC-22)		100	85	96	90	0	0	0

^a Inhibitory potency (%) against the growth of plants at a rate of 150 g ai/ha in the greenhouse, 0 (no effect), 100 % (completely kill)

^b Abu: chingma abutilon; Brj: leaf mustard; Amr: common amaranth; Ecl: white eclipta; Ech: barnyard grass; Dig: crab grass; Set: green bristlegrass

on barnyard grass and cabbage type rape using the Petri dish methods. The results are listed in Table 5.16. Based on the preliminary bioassays, the inhibition of some of **IVD** against chingma abutilon, leaf mustard, common amaranth, white eclipta, barnyard grass, crab grass, and green bristlegrass was further evaluated at 150 g ai/ha for post-emergence herbicidal activity. The results are listed in Table 5.17.

(A) Inhibitory activity against the root of plant

As shown in Table 5.16, most of the tested compounds, except **IVD-1**, **IVD-3**, **IVD-4**, and **IVD-6**, displayed >90 % inhibitory effect against the growth of root of cabbage type rape and barnyard grass at 100 and 10 mg/L. They will be further examined for their pre-emergence herbicidal activity in the greenhouse.

(B) Post-emergence herbicidal activity of **IVD**

As shown in Table 5.16, some of the cyclic phosphonates including **IVD-2**, **IVD-7**, **IVD-9**, and **IVD-13** exhibited 78–88 % inhibitory activity against the growth of the stem of cabbage type rape, but only cyclic phosphonate **IVD-9** showed 62 % inhibitory activity against the growth of the stem of barnyard grass at 10 mg/L.

Some of **IVD** were further evaluated for post-emergence herbicidal activity in the greenhouse. All test compounds were applied at 150 g ai/ha for post-emergence herbicidal activity against chingma abutilon, leaf mustard, common amaranth, white eclipta, barnyard grass, crab grass, and green bristlegrass. clacyfos (**IC-22**, HW02) was used as a positive control. The results are listed in Table 5.17.

As shown in Table 5.17, all test compounds displayed much higher herbicidal activity against dicotyledons than monocotyledons. Cyclic phosphonates **IVD-10**, **IVD-12**, and **IVD-13** exhibited significant herbicidal activity against chingma abutilon, leaf mustard, common amaranth, and white eclipta. However most cyclic phosphonates **IVD** had no activity against monocot weeds except **IVD-8**, **IVD-10**, and **IVD-12** with 50–75 % inhibition effect against barnyard grass, crab grass or green bristlegrass. Especially **IVD-12** not only displayed 90-100% inhibition against all tested broad-leaved weeds, comparable to clacyfos (**IC-22**, HW02), but also exhibited 50-75% inhibition against barnyard grass, crab grass and green bristlegrass.

(C) SAR analysis for **IVD**

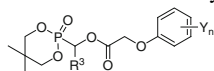
When the phosphorus-containing six-member ring and furyl group as R^3 were kept, substituent Y_n on the phenoxy-benzene ring in series **IVD** had significant influence on the herbicidal activity. Cyclic phosphonates **IVD** with two substituents on the 2- and 4-position of the phenoxy-benzene ring, such as **IVD-10** ($Y_n=2\text{-Me},4\text{-Cl}$), **IVD-12** ($Y_n=2\text{-Cl},4\text{-F}$) and (**IVD-13**, $Y_n=2,4\text{-Cl}_2$) exhibited significant herbicidal activity against tested dicotyledons for post-emergence application at 150 g ai/ha. It was very interesting that **IVD-12** ($Y_n=2\text{-Cl},4\text{-F}$) showed the best herbicidal activity, which could be comparable to clacyfos (**IC-22**, HW02); however, **IVD-11** ($Y_n=2\text{-F},4\text{-Cl}$) showed much weaker herbicidal activity. Other compounds with 3-Me,4-Cl or one substituent as Y_n on the phenoxy-benzene ring also had a weaker inhibition than that of **IVD-12** ($Y_n=2\text{-Cl},4\text{-F}$). Cyclic phosphonate **IVD-1** with no substituent on the phenoxy-benzene ring was almost inactive.

Compared with clacyfos (**IC-22**, HW02), **IVD-12** exhibited a slightly higher herbicidal effect against broad-leaved weeds, leaf mustard or common amaranth, and also showed much higher herbicidal activity against monocot weeds than that of clacyfos. However, cyclic 1-hydroxyalkylphosphonates **IVA** and **IVB** had no significant herbicidal activity (Sect. 5.1.5). All cyclic phosphonates **IVC** were also not comparable to clacyfos.

These results showed the replacement of the open-chain by the cyclic ring in the structure **Io** was favorable to herbicidal activity when 2-Cl,4-F, 2,4-Cl₂ or 2-Me,4-Cl as Y_n , furyl group as R^3 were kept.

5.2.5.3 Herbicidal Activity of 2-[1-(Substituted Phenoxyacetoxy)Alkyl]-5,5-Dimethyl-1,3,2-Dioxaphosphinane-2-One **IVE**

When phosphorus-containing heterocyclic moiety was kept, alkyl as R^3 was introduced into cyclic phosphonates **IV** to give series **IVE**; further modification was

Table 5.18 Inhibitory activity of cyclic phosphonates **IVE** against the growth of plants^a

Compound	R ³	Y _n	Root		Stem	
			Ech ^b	Brn ^b	Ech ^b	Brn ^b
			100 mg/L	100 mg/L	100 mg/L	100 mg/L
IVE-2	Me	2-Cl	0	100	0	90
IVE-3	Me	2-F	0	100	0	80
IVE-4	Me	4-Cl	0	100	0	100
IVE-5	Me	4-F	0	90	0	40
IVE-6	Me	3-CF ₃	0	85	0	30
IVE-7	Me	2-Me,4-Cl	70	100	80	100
IVE-8	Me	3-Me,4-Cl	0	90	0	90
IVE-9	Me	2-Cl,4-F	0	100	0	100
IVE-10	Me	2-F,4-Cl	0	95	0	95
IVE-11	Me	2,4-Cl ₂	100	99	57	92
IVE-12	<i>i</i> -Pr	2,4-Cl ₂	97	99	46	83
IVE-13	<i>n</i> -Bu	2,4-Cl ₂	97	99	29	83

^a Inhibitory potency (%) against the growth of plants in petri dishes, 0 (no effect), 100 % (completely kill)

^b Ech: barnyard grass; Brn: cabbage type rape

focused on the substituents Y_n. Thirteen cyclic phosphonates **IVE** were prepared to test their herbicidal activity.

As a preliminary bioassay, **IVE** were tested for inhibitory activity against barnyard grass as monocotyledon and cabbage type rape as dicotyledon by Petri dish methods. The inhibitory effect of **IVE** on the growth of roots and stems of plant was examined. The results are listed in Table 5.18.

(A) Inhibitory activity of **IVE** against the root of plant

As seen from Table 5.18, most of the cyclic phosphonates **IVE** displayed significant inhibitory effect (>90 %) against the growth of root of cabbage type rape, but showed much weaker inhibition against the growth of root of barnyard grass at 100 mg/L. Only **IVE-11**, **IVE-12**, and **IVE-13** displayed significant inhibitory effect (>90 %) against the growth of root of both cabbage type rape and barnyard grass at 100 mg/L. They will be further examined for their pre-emergence herbicidal activity in the greenhouse.

(B) Post-emergence herbicidal activity of **IVE**

As seen from Table 5.18, most of cyclic phosphonates **IVE** displayed significant inhibitory effect (>90 %) against the growth of stem of dicotyledonous cabbage type rape, but showed much weaker or no inhibition against the growth of stem of monocotyledonous barnyard grass except **IVE-7** with 80 % inhibitory activity at 100 mg/L. Based on the preliminary bioassays by Petri dish methods, the post-

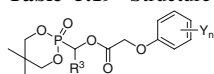
emergence herbicidal activity of **IVE** against chingma abutilon, leaf mustard, common amaranth, white eclipta, barnyard grass, crab grass, and green bristlegrass was evaluated at 150 g ai/ha. Clacyfos (**IC-22**, HW02) was used as a positive control.

The results are listed in Tables 5.19, 5.20, and 5.21.

As shown in Table 5.19, all cyclic phosphonates **IVE** displayed much higher post-emergence herbicidal activity against dicotyledons than monocotyledons. Cyclic phosphonates **IVE-7**, **IVE-9**, and **IVE-11**, exhibited notable post-emergence herbicidal activity (85–100 %) against all tested dicotyledons including chingma abutilon, leaf mustard, common amaranth, and white eclipta at 150 g ai/ha. Most cyclic phosphonates **IVE** had weak or no activity against monocot weeds except **IVE-9** with 70–85 % inhibition effect against barnyard grass, crab grass, and green bristlegrass.

Cyclic phosphonates **IVE-2**, **IVE-7**, **IVE-9**, **IVE-11**, **IVE-12**, and **IVE-13** were further examined for their post-emergence herbicidal activity against leaf mustard, common amaranth, and white eclipta at 75 and 37.5 g ai/ha, respectively (Table 5.20). The results showed cyclic phosphonates **IVE-2**, **IVE-7**, **IVE-9**, and **IVE-11** still exhibited significant post-emergence herbicidal activity against all

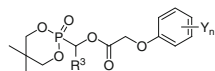
Table 5.19 Structure and post-emergence herbicidal activities of cyclic phosphonates **IVE**^a



Compound	R ³	Y _n	Abu ^b	Brj ^b	Amr ^b	Ecl ^b	Ech ^b	Dig ^b	Set ^b
IVE-1	Me	H	10	10	10	10	0	0	0
IVE-2	Me	2-Cl	70	90	90	75	20	0	0
IVE-3	Me	2-F	70	75	70	70	0	0	0
IVE-4	Me	4-Cl	70	75	70	60	10	0	0
IVE-5	Me	4-F	75	75	70	70	40	50	30
IVE-6	Me	3-CF ₃	100	85	50	50	60	0	0
IVE-7	Me	2-Me,4-Cl	100	100	100	90	30	0	0
IVE-8	Me	3-Me,4-Cl	70	70	60	60	0	0	0
IVE-9	Me	2-Cl,4-F	100	95	100	95	85	70	70
IVE-10	Me	2-F,4-Cl	75	75	60	60	0	0	0
IVE-11	Me	2,4-Cl ₂	95	95	95	85	30	30	30
IVE-12	<i>i</i> -Pr	2,4-Cl ₂	95	100	85	75	0	0	0
IVE-13	<i>n</i> -Bu	2,4-Cl ₂	90	100	85	75	0	0	0
Clacyfos (IC-22)			100	85	96	90	0	0	0

^a Inhibitory potency (%) against the growth of plants at a rate of 150 g ai/ha in the greenhouse, 0 (no effect), 100 % (completely kill)

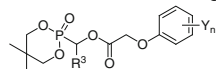
^b Abu: chingma abutilon; Brj: leaf mustard; Amr: common amaranth; Ecl: white eclipta; Ech: barnyard grass; Dig: crab grass; Set: green bristlegrass

Table 5.20 Structure and post-emergence herbicidal activities of cyclic phosphonates **IVE**^a

Compound	R ³	Y _n	Brj ^b		Amr ^b		Ecl ^b	
			75 g ai/ha	37.5 g ai/ha	75 g ai/ha	37.5 g ai/ha	75 g ai/ha	37.5 g ai/ha
IVE-2	Me	2-Cl	100	90	70	70	70	70
IVE-7	Me	2-Me,4-Cl	100	80	100	80	85	80
IVE-9	Me	2-Cl,4-F	100	70	100	60	85	60
IVE-11	Me	2,4-Cl ₂	95	90	75	70	70	50
IVE-12	<i>i</i> -Pr	2,4-Cl ₂	100	90	80	30	35	30
IVE-13	<i>n</i> -Bu	2,4-Cl ₂	100	90	70	50	40	30
Clacyfos (IC-22)			95	90	95	70	80	60

^a Inhibitory potency (%) against the growth of plants in the greenhouse, 0 (no effect), 100 % (completely kill)

^b Brj: leaf mustard; Amr: common amaranth; Ecl: white eclipa

Table 5.21 Post-emergence herbicidal activity of cyclic phosphonates **IVE**^a

Compound	R ³	Y _n	Rate (g ai/ha)	Amr ^b	Che ^b	Brj ^b	Ip ⁿ ^b
IVE-7	Me	2-Me,4-Cl	75	95	90	100	100
			37.5	80	80	95	80
			18.75	70	70	90	70
IVE-9	Me	2-Cl,4-F	75	100	90	100	100
			37.5	95	75	100	90
			18.75	90	70	95	90
IVE-11	Me	2,4-Cl ₂	75	100	90	100	100
			37.5	100	80	100	95
			18.75	100	70	95	85
2,4-D			75	95	95	100	100
			37.5	90	80	100	100
			18.75	70	75	80	90
Glyphosate			75	75	80	80	75
			37.5	60	70	75	60
			18.75	60	50	70	50
Clacyfos (IC-22)			75	100	95	100	100
			37.5	100	80	100	100
			18.75	90	70	100	100

^a Inhibitory potency (%) against the growth of plants in the greenhouse, 0 (no effect), 100 % (completely kill)

^b Amr: common amaranth; Che: goosefoot; Brj: leaf mustard; Ipⁿ: morning glory

tested plants at 37.5 g ai/ha, which seemed to be comparable to clacyfos (**IC-22**, HW02).

In order to make sure the practicality of **IVE** as an herbicide, cyclic phosphonates **IVE-7**, **IVE-9**, and **IVE-11** were selected for further bioassay at lower rate in the greenhouse. Post-emergence herbicidal activity of these compounds against common amaranth, goosefoot, leaf mustard, and morning glory were examined at 75, 37.5, and 18.75 g ai/ha, respectively. Glyphosate, 2,4-D, and clacyfos (**IC-22**, HW02) were used as positive controls. The results are listed in Table 5.21.

As shown in Table 5.21, **IVE-7**, **IVE-9**, and **IVE-11** displayed good post-emergence herbicidal activity against all tested broad-leaved weeds at 75 g ai/ha. Their herbicidal effect could be comparable to clacyfos and 2,4-D, and higher than that of glyphosate. For example, the effect of these compounds against leaf mustard or morning glory for post-emergence application could be comparable to 2,4-D, and higher than that of glyphosate at 75 g ai/ha, which was shown in Figs. 5.16 and 5.17.

Cyclic phosphonates **IVE-7**, **IVE-9**, and **IVE-11** still exhibited significant post-emergence herbicidal activity (70–100 %) against tested broad-leaved weeds even at 18.5 g ai/ha. Especially, **IVE-9** with 2-Cl,4-F as Y_n displayed the best inhibition against all tested broad-leaved weeds, which could be comparable to clacyfos (**IC-22**, HW02), and exhibited better herbicidal activity against tested broad-leaved weeds than that of 2,4-D and glyphosate at 18.5 g ai/ha.

The above observation showed that cyclic phosphonates **IVE-7**, **IVE-9**, and **IVE-11** exhibited promising post-emergence herbicidal activity against dicotyledon comparable to clacyfos, 2,4-D, and better than glyphosate. They had very good selectivity between dicotyledons and monocotyledons at 150 g ai/ha; they would be safe for monocotyledonous crops. Therefore cyclic phosphonates **IVE-7**, **IVE-9**,



Fig. 5.16 Effect against leaf mustard for post-emergence application at 75 g ai/ha (after 20 days)



Fig. 5.17 Effect against morning glory for post-emergence application at 75 g ai/ha (after 20 days)

and **IVE-11** displayed potential utility for further development as a selective post-emergence herbicide.

Cyclic phosphonate **IVE-11** was selected as a representative compound to determine its acute toxicity against rat according to the pesticide standard procedure. **IVE-11** exhibited low acute toxicity against rat (LD_{50} : percutaneous, 2,330 mg/kg; oral, >2,000 mg/kg).

(C) SAR analysis for **IVE**

In the series **IVE**, the phosphorus-containing six-member ring was kept, substituent R^3 and Y_n on the phenoxy-benzene ring had significant influence on the herbicidal activity of compounds. Cyclic phosphonates **IVE-7** ($Y_n=2\text{-Me},4\text{-Cl}$), **IVE-9** ($Y_n=2\text{-Cl},4\text{-F}$) and **IVE-11** ($Y_n=2,4\text{-Cl}_2$) on the phenoxy-benzene ring exhibited better post-emergence herbicidal activity against dicotyledons than other one or two substituents as Y_n . When there was no substituent on the phenoxy-benzene ring, the compound (**IVE-1**) was almost inactive. It was also found that **IVE-9** ($Y_n=2\text{-Cl},4\text{-F}$) showed much higher herbicidal activity than that of **IVE-10** ($Y_n=2\text{-F},4\text{-Cl}$). These results indicated that not only the position but also the type of substituents Y_n on the phenoxy-benzene ring was the decisive factor influencing the herbicidal activity.

Furthermore, the variety of R^3 also affected herbicidal activity obviously. Comparing **IVE-11**, **IVE-12**, and **IVE-13** in which $2,4\text{-Cl}_2$ as Y_n were kept the same, **IVE-11** with Me as R^3 exhibited the best herbicidal activity among **IVE-11**, **IVE-12**, and **IVE-13**. When Me as R^3 was replaced by *i*-Pr or *n*-Bu, the herbicidal activity against common amaranth and white eclipta decreased obviously at 150 and 37.5 g ai/ha, respectively. **IVE-11** had good herbicidal effect against common

amaranth (95 %) or white eclipta (85 %), but **IVE-12** ($R^3=i\text{-Pr}$) and **IVE-13** ($R^3=n\text{-Bu}$) showed much weaker herbicidal effect (50–85 %) at 150 g ai/ha.

5.2.5.4 Herbicidal Activity of 2-[1-(Substituted Phenoxypropionyloxy) Ethyl]-5,5-Dimethyl-1,3,2-Dioxaphosphinane-2-One **IVF**

Considering the possible contribution of cyclophosphonates to herbicidal activity, an open-chain dimethylphosphonate unit in the **IC** series was further modified by introducing a six-membered cyclic phosphonate unit. Three series of 2-[1-(substituted phenoxy-carboxy)alkyl]-5,5-dimethyl-1,3,2-dioxaphosphinane-2-one derivatives **IVC–IVE** were prepared. Through the study on cyclic phosphonates **IVC–IVE**, some **IVE** was found to be a very effective compound with post-emergence herbicidal activity against dicotyledons comparable to clacyfos, 2,4-D, and better than glyphosate. In order to examine the effect of R^4 on the herbicidal activity of cyclophosphonates **IV**, H as R^4 in the structure of **IVE** (see Scheme 5.1) was further modified to Me as R^4 . Therefore, the phosphorus-containing six-member ring was kept; methyl as R^3 and R^4 were introduced into cyclic phosphonates **IV** to give the series **IVF**. In other word, phenoxyacetyl moiety in the structure of **IVE** was modified to phenoxypropionyl moiety to give the series **IVF**. In the **IVF** series, further modification was focused on substituent Y_n . Eight cyclic phosphonates **IVF** were prepared to test their herbicidal activity.

As a preliminary bioassay, **IVF** were tested for inhibitory activity on barnyard grass and cabbage type rape using Petri dish methods. The inhibitory effect of **IVF** on the growth of roots and stems of plants was examined. The results are listed in Table 5.22.

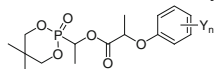
(A) *Inhibitory activity of IVF against the root of plant*

As seen from Table 5.22, except for **IVF-1**, all of the cyclic phosphonates **IVF** displayed 100 % inhibitory effect against the growth of root of cabbage type rape but they were inactive against monocotyledon barnyard grass at 100 mg/L. They will be further examined for their pre-emergence herbicidal activity against dicotyledons in the greenhouse.

(B) *Post-emergence herbicidal activity of IVF*

Except for **IVF-3** and **IVF-8**, most of the cyclic phosphonates **IVF** displayed 90–100 % inhibitory effect against the growth of stems of cabbage type rape, but they were inactive against the growth of stems of monocotyledon barnyard grass at 100 mg/L. It showed **IVF** had the selectivity between dicotyledons and monocotyledons.

Further bioassays were carried out in the greenhouse to confirm the post-emergence herbicidal activity of **IVF**. All of the compounds **IVF** were applied at 150 g ai/ha to evaluate their post-emergence herbicidal activity against chingma abutilon, leaf mustard, common amaranth, and white eclipta. The results are listed in Table 5.23.

Table 5.22 Inhibitory activity of cyclic phosphonates **IVF** against the growth of plants^a

Compound	Y _n	Root		Stem	
		Ech ^b	Brn ^b	Ech ^b	Brn ^b
IVF-1	2-Cl	0	80	0	100
IVF-2	4-Cl	0	100	0	100
IVF-3	4-F	0	100	0	30
IVF-4	3-CF ₃	30	100	30	100
IVF-5	2-Me,4-Cl	0	100	0	100
IVF-6	3-Me,4-Cl	0	100	0	100
IVF-7	2-Cl,4-F	0	100	0	90
IVF-8	2,4-Cl ₂	0	100	0	40

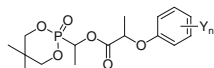
^a Inhibitory potency (%) against the growth of plants at 100 mg/L in Petri dishes, 0 (no effect), 100 % (completely kill)

^b Ech: barnyard grass; Brn: cabbage type rape

As shown in Table 5.23, most of the cyclic phosphonates **IVF** displayed 50–70 % inhibitory effect against dicotyledon, chingma abutilon, leaf mustard, common amaranth, and white eclipta at 150 g ai/ha. Compared cyclic phosphonates **IVF** with **IVE**, **IVF** exhibited much lower herbicidal effect against tested broad-leaved weeds than that of **IVE**.

(C) SAR analysis for **IVF**

In the structure of cyclic phosphonates **IVF**, substituent methyl as R³ and R⁴ was kept constant, Y_n on the phenoxy-benzene ring had no significant influence on the herbicidal activity of the compounds. Most of the cyclic phosphonates **IVF**

Table 5.23 Structure and post-emergence herbicidal activity of cyclic phosphonates **IVF**^a

Compound	Y _n	Abu ^b	Brj ^b	Amr ^b	Ecl ^b
IVF-1	2-Cl	70	70	60	60
IVF-2	4-Cl	60	70	50	60
IVF-3	4-F	60	70	50	60
IVF-4	3-CF ₃	75	75	60	50
IVF-5	2-Me,4-Cl	75	90	60	60
IVF-6	3-Me,4-Cl	70	70	60	70
IVF-7	2-Cl,4-F	70	90	60	60
IVF-8	2,4-Cl ₂	70	80	70	60

^a Inhibitory potency (%) against the growth of plants at 150 g ai/ha in the greenhouse, 0 (no effect), 100 % (completely kill)

^b Abu: chingma abutilon; Brj: leaf mustard; Amr: common amaranth; Ecl: white eclipta

displayed 50–70 % inhibitory effect against dicotyledons, even 2-Cl, 4-F, 2,4-Cl₂ or 2-Me,4-Cl as Y_n on the phenoxy-benzene ring. **IVF** exhibited much lower herbicidal effect against tested broad-leaved weeds than that of **IVE**. These results indicated herbicidal effects against broad-leaved weeds could be obviously decreased when the phenoxyacetoxyl moiety in cyclic phosphonates **IVE** was modified to the phenoxypropionyl moiety. In other word, H as R⁴ in the structure of cyclic phosphonates **IVE** was very important for herbicidal activity.

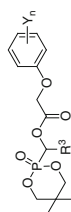
5.2.5.5 The Weed Spectrum of Cyclic Phosphonates IVC-IVE

Most of the cyclic phosphonates **IVC-IVE** displayed significant post-emergence herbicidal activity against dicotyledons, but weaker or no inhibition against monocotyledons.

In order to make sure the weed spectrum of cyclic phosphonates **IVC-IVE**, seven cyclic phosphonates were chosen to test at 150 and 75 g ai/ha for post-emergence herbicidal activity against twenty-one species of dicotyledonous plants including fourteen species of weeds and seven species of crops.

Seven species of crops included green vegetable (*B. chinensis*), tomato (*Lycopersicon esculentum*), radish (*Raphanus sativus*), soybean (*Glycine max*), cotton (*Gossypium hirsutum*), cucumber (*Cucumis sativus*), and rape (*B. campestris*). Fourteen species of weeds included common amaranth (*A. retroflexus*), goosefoot (*Chenopodium album*), leaf mustard (*B. juncea*), morning glory (*Ipomoea nil*), monarch redstem (*Ammannia baccifera*), pickerel weed (*Monochoria vaginalis*), ball cabbage (*B. oleracea*), wild vetch (*Vicia gigantea*), chili (*Capsicum annuum*), curled dock (*Rumex crispus*), chingma abutilon (*Abutilon theophrasti*), alligator-weed (*Alternanthera philoxeroides*), field chickweed (*Cerastium arvense*), white eclipta (*E. prostrata*); Glyphosate, 2,4-D, and clacyfos (**IC-22**, HW02) were used as positive controls. The results are listed in Tables 5.24 and 5.25.

All seven cyclic phosphonates in Tables 5.24 and 5.25 displayed significant post-emergence herbicidal activity and broad-spectrum activity against 21 broad-leaved plants at 150 and 75 g ai/ha. As shown in Table 5.24, chili, tomato, radish, soybean, cotton, cucumber, and rape as dicotyledonous crops were very susceptible to all seven cyclic phosphonates at ≤ 75 g ai/ha. Among seven cyclic phosphonates in Table 5.25, cyclic phosphonate **IVE-7** and **IVE-11** showed broad-spectrum activity to control broad-leaved weeds which is similar to glyphosate, 2,4-D, and clacyfos. They exhibited good inhibitory effect which was comparable to glyphosate and 2,4-D according to the average value of inhibitory effect. Especially, clacyfos (**IC-22**, HW02) with 90 % average inhibitory effect showed the highest herbicidal activity against fourteen species of weeds at 75 g ai/ha.

Table 5.24 Inhibitory activity of some cyclic phosphonates **IVC-IVE** against crops

Compound	R ³	Y _n	Rate (g ai/ha)	Inhibitory activity (%) ^a						
				Caa ^b	Lyc ^b	Rap ^b	Gly ^b	Gos ^b	Cuc ^b	Bra ^b
IVC-16	Ph	2,4-Cl ₂	150	70	80	80	80	60	50	80
			75	60	80	80	80	40	40	70
IVD-12	Fur-2-yl	2-Cl,4-F	150	70	80	80	60	50	20	70
			75	60	80	70	60	40	20	70
IVD-13	Fur-2-yl	2,4-Cl ₂	150	70	80	85	70	50	50	95
			75	60	80	80	60	30	30	80
IVE-7	Me	2-Me,4-Cl	150	80	70	80	70	70	70	85
			75	70	60	80	50	60	60	80
IVE-9	Me	2-Cl,4-F	150	75	100	80	70	70	70	75
			75	60	100	80	70	70	60	70
IVE-11	Me	2,4-Cl ₂	150	75	75	95	80	70	50	100
			75	70	70	90	60	30	40	90
IVE-12	i-Pr	2,4-Cl ₂	150	75	85	98	70	70	70	90
			75	75	80	80	50	60	50	80
Glyphosate			150	100	85	65	85	60	70	100
			75	100	85	60	85	40	50	100
2,4-D			150	80	100	85	80	90	85	50
			75	70	100	80	70	60	70	50
Clacyfos (IC-22)			150	80	90	100	100	90	70	100
			75	75	85	95	95	80	60	100

^a Inhibitory potency (%) against the growth of plants in the greenhouse for post-emergence application, 0 (no effect), 100 % (completely kill).

^b Caa: chili; Lyc: radish; Rap: soybean; Gos: cotton; Cuc: cucumber; Bra: rape

Table 5.25 Weed Spectrum of some cyclic phosphonates IVC-IVE

Compound	Rate (g ai/ ha)	Post-emergence herbicidal activity (Inhibitory potency % against the growth of weeds)												Average ^b value	
		Amm ^a	Che ^a	Brj ^a	Btc ^a	Ipn ^a	Amm ^a	Mon ^a	Bro ^a	Vig ^a	Rum ^a	Abu ^a	Alt ^a		Cer ^a
IVC-16	150	90	75	80	80	100	60	95	80	85	70	70	60	80	70
	75	80	70	70	70	100	50	30	70	70	70	60	60	80	50
IVD-12	150	80	80	70	70	100	100	100	50	100	70	60	60	75	40
	75	80	70	70	70	70	100	90	50	50	50	40	50	60	63
IVD-13	150	80	80	95	80	100	100	100	85	80	80	70	70	75	70
	75	70	70	90	70	100	100	100	80	70	75	60	60	70	50
IVE-7	150	100	75	90	80	100	100	100	70	80	75	70	70	80	65
	75	100	70	85	70	100	100	100	70	70	70	50	60	80	81
IVE-9	150	90	80	80	80	100	90	90	80	80	75	80	60	80	85
	75	90	80	80	80	100	60	50	70	70	70	70	60	80	60
IVE-11	150	95	85	95	85	100	100	100	90	100	80	75	60	90	90
	75	75	80	95	80	100	100	100	80	90	80	70	60	80	85
IVE-12	150	80	75	85	90	100	90	80	70	90	80	70	60	80	80
	75	80	75	70	70	100	80	70	70	70	70	60	60	70	73
Glyphosate	150	90	90	80	80	60	100	100	80	95	100	100	90	95	100
	75	90	70	30	70	60	100	100	70	95	100	80	90	90	81
2,4-D	150	100	100	98	98	100	100	100	60	100	90	80	70	90	90
	75	100	80	90	95	100	100	90	50	100	90	70	70	80	86
Clacifos (IC-22)	150	100	90	100	85	100	100	100	100	100	90	90	75	100	100
	75	100	85	100	80	100	100	100	80	100	85	85	70	80	90

^a Amr: common amaranth; Che: goosefoot; Brj: leaf mustard; Btc: field mustard; Ipn: morning glory; Amm: monarch redstem; Mon: pickernel weed; Bro: ball cabbage; Vig: wild vetch; Rum: curled dock; Abu: chingma abutilon; Alt: alligatorweed; Cer: field chickweed; Ecl: white eclipta

^b The average value of inhibitory potency % on the growth of all tested plants, 0 (no effect), 100 % (completely kill)

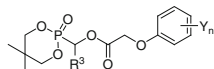
5.2.5.6 Crop Selectivity of Cyclic Phosphonates IVC-IVE

Crop selectivity and safety evaluations of some cyclic phosphonates **IVC-IVE** were carried out by post-emergence spray treatment. Above preliminary bioassay showed all tested cyclic phosphonates in Table 5.24 could result in injury to dicotyledonous crops, such as green vegetable, tomato, radish, chili, cotton, rape, and soybean even at 75 g ai/ha. Therefore, several cyclic phosphonates **IVC-IVE** were selected to evaluate their selectivity on monocotyledonous crops. The inhibition of these compounds against maize, rice, and wheat were tested at 150 g ai/ha. All compounds in Table 5.26 displayed weak or no inhibitory activity against maize and wheat at 150 g ai/ha. Most compounds would be safe to maize and wheat at 150 g ai/ha. Most of them also showed weak or no inhibitory activity against rice except **IVD-13**, **IVE-12**, and **IVE-13** with 20–40 % inhibition at 150 g ai/ha. We noticed that wheat, maize, and rice exhibited higher tolerance to **IVE-7**, **IVE-9** and **IVE-11**.

The crop selectivity and safety of **IVE-7** and **IVE-11** were further examined by post-emergence spray treatment at 450 g ai/ha. Maize, rice, wheat, cotton, rape, and soybean were selected as tested crops. 2,4-D was used as a control (Table 5.27).

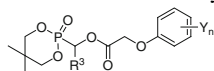
Among tested crops in Table 5.27, cotton, rape, and soybean as dicotyledonous crops were very susceptible to **IVE-7** and **IVE-11**, whereas wheat and rice exhibited a higher tolerance to **IVE-11** at 450 g ai/ha. From our observation, **IVE-11** still showed good safety to wheat and rice, but **IVE-7** showed 20–30 % inhibition against monocotyledonous crops, wheat, rice, and maize, at 450 g ai/ha. It showed **IVE-11** had a higher level of selectivity between monocotyledonous crops

Table 5.26 Inhibitory activity of some cyclic phosphonates **IVC-IVE** against crops^a



Compound	R ³	Y _n	Post-emergence inhibitory potency (%)		
			Maize	Rice	Wheat
IVC-5	Ph	3-CF ₃	0	0	0
IVC-16	Ph	2,4-Cl ₂	0	10	10
IVC-18	4-ClPh	2,4-Cl ₂	0	10	0
IVC-19	2,4-Cl ₂ Ph	2,4-Cl ₂	10	10	0
IVD-13	fur-2-yl	2,4-Cl ₂	0	40	10
IVE-7	Me	2-Me,4-Cl	0	10	0
IVE-9	Me	2-Cl,4-F	10	10	0
IVE-11	Me	2,4-Cl ₂	0	10	0
IVE-12	<i>i</i> -Pr	2,4-Cl ₂	0	20	10
IVE-13	<i>n</i> -Bu	2,4-Cl ₂	0	30	10

^a Inhibitory potency (%) against the growth of crops at a rate of 150 g ai/ha in the greenhouse, percent inhibition: 0–10 %, safe to crops; >10 %, not safe to crops

Table 5.27 Inhibitory activity of cyclic phosphonates **IVE-7** and **IVE-11** against crops^a

Compound	R ³	Y _n	Post-emergence inhibitory potency (%)					
			Maize	Rice	Wheat	Cotton	Rape	Soybean
IVE-7	Me	2-Me,4-Cl	30	20	20	60	100	90
IVE-11	Me	2,4-Cl ₂	20	10	0	85	100	100
2,4-D			30	30	20	60	100	100

^a Inhibitory potency (%) against the growth of crops at a rate of 450 g ai/ha in the greenhouse, percent inhibition: 0–10 %, safe to crops; >10 %, not safe to crops

and dicotyledonous weeds. Especially, **IVE-11** was found to exhibit promising post-emergence herbicidal activity against broad-spectrum broad-leaved weeds which was comparable to glyphosate and 2,4-D. Further development could be carried out for purposes of weed control in wheat and rice fields.

5.2.6 Summary

2-[1-(Substituted phenoxy-carboxy)alkyl]-5,5-dimethyl-1,3,2-dioxaphosphinane-2-one **IVC–IVF** were designed based on the modification of open-chain 1-substituted alkylphosphonates **Io**. Four series of cyclic phosphonates **IVC–IVF**, including 57 compounds, could be conveniently prepared by the condensation of cyclic 1-hydroxyalkylphosphonates **IVB** with substituted phenoxyacetyl chlorides **M5** in the presence of a base. The herbicidal activity of **IVC–IVF** was examined in Petri dishes and evaluated systematically in greenhouse. Cyclic phosphonates **IVC–IVF** displayed much higher herbicidal activity against dicotyledons than monocotyledons.

SAR analysis for **IVC–IVF** indicated the phosphorus-containing six-member ring were kept, R³, substituted phenoxyacetyl and Y_n on the phenoxy-benzene ring had significant influence on the herbicidal activity of the compounds. Both **IVA** and **IVB** with no substituted phenoxyacetyl moiety had no significant herbicidal activity (Sect. 5.1.5). However, cyclic phosphonates **IVC–IVF** with a substituted phenoxyacetyl moiety exhibited higher herbicidal activity against dicotyledons than that of cyclic 1-hydroxyalkylphosphonates **IVA** and **IVB**. Cyclic phosphonates with 2-Cl,4-F; 2,4-Cl₂ or 2-Me,4-Cl as Y_n on the phenoxy-benzene ring were found to be most promotive for herbicidal activity, while cyclic phosphonates with no substitution (H as Y_n) on the phenoxy-benzene ring was almost inactive. However, when substituted phenoxyacetyl moiety in cyclic phosphonates were replaced by substituted phenoxypropionyl moiety even 2-Me,4-Cl, 2-Cl,4-F or 2,4-Cl₂ as Y_n, Me as R³ were kept constant, compounds resulted in a sharp decrease in herbicidal activity. These compounds **IVF-5**, **IVF-7**, and **IVF-8** with substituted

phenoxypropionyl moiety (with Me as R⁴) displayed much weaker post-emergence herbicidal activity against dicotyledons than that of corresponding **IVE-7**, **IVE-9**, or **IVE-11** (with H as R⁴). It showed that substituted phenoxyacetyl moiety was a very important pharmacophore in the molecular skeletons of cyclic phosphonate. The substituent R³ also had significant influence on the herbicidal activity of cyclic phosphonate. When 2,4-Cl₂ as Y_n were kept the same, Me as R³ in **IVE** was replaced by *i*-Pr or *n*-Bu, respectively, the herbicidal activity against common amaranth and white eclipta decreased obviously at 150 and 37.5 g ai/ha. Furthermore, none of cyclic phosphonates **IVC** with phenyl or substituted phenyl as R³ were found to be comparable to clacyfos (**IC-22**, HW02). These results illustrated that *i*-Pr, *n*-Bu, phenyl or substituted phenyl as R³ in the cyclic phosphonates were not favorable to the enhancement of herbicidal activity. These findings suggested that 2-Cl, 4-F; 2,4-Cl₂ or 2-Me,4-Cl as Y_n on the phenoxy-benzene ring, and Me as R³ seemed to be most beneficial to the herbicidal activity of the cyclic phosphonates.

The above SAR analyses indicated that the improvement of herbicidal activity of cyclic phosphonates required a reasonable combination of both structure and position of Y_n, R³ and R⁴. The replacement of the phosphorus-containing open-chain moiety by the phosphorus-containing six-member ring was favorable to herbicidal activity when 2-Cl,4-F; 2,4-Cl₂ or 2-Me,4-Cl as Y_n, and Me or furyl group as R³ were kept in the parent structure **Io**.

Some cyclic phosphonates **IVC**, **IVD**, and **IVE** displayed good post-emergence herbicidal activity (>90 % inhibition) against dicotyledons at 150 g ai/ha in the greenhouse. Cyclic phosphonate **IVD-12** (R³=furyl, Y_n=2-Cl,4-F) showed excellent herbicidal activity comparable to clacyfos (**IC-22**, HW02) against dicotyledons at 150 g ai/ha in the greenhouse.

Cyclic phosphonates **IVE-7** (R³=Me, Y_n=2-Me,4-Cl), **IVE-9** (R³=Me, Y_n=2-Cl,4-F), and **IVE-11** (R³=Me, Y_n=2,4-Cl₂) exhibited promising post-emergence herbicidal activity against dicotyledons at 150-18.5 g ai/ha, which were comparable to 2,4-D and glyphosate. These compounds still exhibited significant post-emergence herbicidal activity (70–100 %) against tested broad-leaved weeds even at 18.5 g ai/ha. Cyclic phosphonate **IVE-11** was selected to test its acute toxicity and showed low acute toxicity against rat (LD₅₀: percutaneous, 2,330 mg/kg; oral, >2,000 mg/kg). **IVE-7**, **IVE-9**, and **IVE-11** had very good selectivity between dicotyledons and monocotyledons at 150 g ai/ha, and they were safe for monocotyledonous crops, wheat, rice, and maize, especially, **IVE-11** which still showed good safety to wheat and rice at 450 g ai/ha. Therefore, **IVE-11** displayed potential utility for further development as a selective post-emergence herbicide for weed control in wheat and rice fields.

5.3 Caged Bicyclic Phosphates IVG and IVH

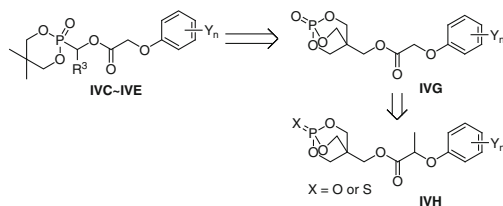
5.3.1 Introduction

Heterocyclic compounds containing a symmetric caged bicyclic phosphate have received much attention since they were first synthesized by Verkade and Reynolds in 1960 [51]. Several of these compounds with useful biological activity had been reported [52–64].

Through the study on cyclic phosphonates **IVA–IVF**, several cyclic phosphonates **IVD** and **IVE** were found to have notable post-emergence herbicidal activity. Considering the significant contribution of phosphorus-containing heterocyclic moiety to herbicidal activity, it would be interesting to evaluate the effect of caged bicyclic phosphates on herbicidal activity. Caged bicyclic phosphates **IVG** and **IVH** were further designed on the basis of cyclic phosphonates **IVC–IVF** (Scheme 5.8).

In the series of **IVG**, further modification was focused on substituent Y_n . On the basis of caged bicyclic phosphate **IVG**, substituted phenoxyacetyl moiety in **IVG** was modified into substituted phenoxypropionyl moiety to produce a series of **IVH**. In the series of **IVH**, O or S as X was kept constant respectively, further modification was focused on substituent Y_n .

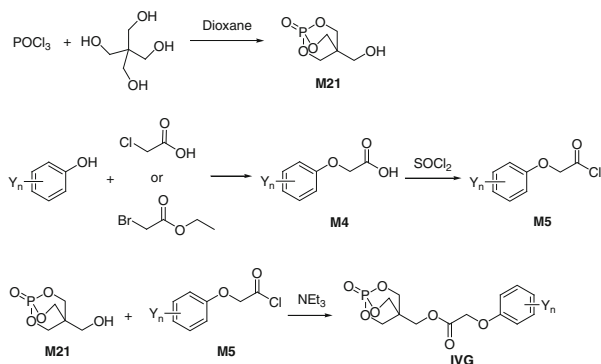
In this section, the synthesis and herbicidal activity of series **IVG** and **IVH** are described, and their structure-activity relationships are discussed.



Scheme 5.8 Design of caged bicyclic phosphates **IVG** and **IVH**

5.3.2 Synthesis of IVG and IVH

Caged bicyclic phosphates **IVG** were synthesized by the condensation of substituted phenoxyacetyl chlorides **M5** and 4-(hydroxymethyl)-2,6,7-trioxo-1-phosphabicyclo[2.2.2]octane-1-one **M21** in the presence of base (Scheme 5.9). Substituted phenoxyacetic acids **M4** and substituted phenoxyacetyl chlorides **M5** were prepared using the method which has been described in Chap. 2. The intermediate **M21** could be prepared by the treatment of the pentaerythritol with 1 equiv. of phosphorus oxychloride in dioxane according to the method reported in the literature [65]. Caged bicyclic phosphates **IVG** were found to be easily regenerated



Scheme 5.9 Synthesis of caged bicyclic phosphates **IVG**

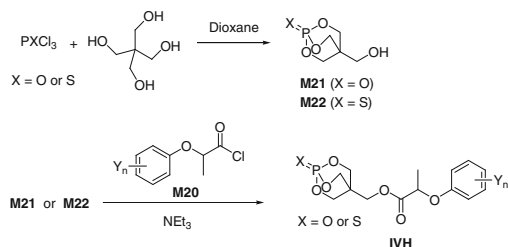
to the starting material in strong alkaline medium. In this case, triethylamine, a weak organic base, was chosen for this reaction.

A series of 4-[(substituted phenoxyacetoxy)methyl]-2,6,7-trioxa-1-phosphabicyclo[2.2.2]octane-1-one **IVG** including 15 compounds was prepared. Their structures are listed in Table 5.28.

Caged bicyclic phosphates **IVH** could be conveniently synthesized by the condensation of phosphabicyclo[2.2.2]octane-1-one **M21** or phosphabicyclo[2.2.2]octane-1-thione **M22** and substituted phenoxypropionyl chlorides **M20** in the presence of triethylamine as base (Scheme 5.10). The intermediates **M20** could be easily obtained by the reaction of substituted phenoxypropionic acids **M19** and thionyl chloride in high yields. The intermediates **M19** were synthesized starting from substituted phenols and 2-bromopropionic acid ester. 4-(Hydroxymethyl)-2,6,7-trioxa-1-phosphabicyclo[2.2.2]octane-1-thione **M22** could be prepared by treatment of the pentaerythritol with 1 equiv of phosphorus thiochloride in dioxane according to the method reported in the literature [65].

Table 5.28 Structure of caged bicyclic phosphates **IVG**

Compound	Y _n	Compound	Y _n
IVG-1	2,4-Cl ₂	IVG-9	2-Cl,4-F
IVG-2	2-Cl	IVG-10	2-Cl,5-Me
IVG-3	4-Cl	IVG-11	2,3-Me ₂
IVG-4	2-F	IVG-12	4-F
IVG-5	3-CF ₃	IVG-13	3-Me
IVG-6	4-Me	IVG-14	H
IVG-7	2-Me,4-Cl	IVG-15	4- <i>t</i> -Bu
IVG-8	3-Me,4-Cl		



Scheme 5.10 Synthesis of caged bicyclic phosphates **IVH**

A series of 4-[(substituted phenoxypropionyloxy)methyl]-2,6,7-trioxa-1-phosphabicyclo[2.2.2]octane-1-one (or thione) **IVH** including 12 compounds was prepared. Their structures are listed in Table 5.29.

Since a carboxylic acid ester bond which is sensitive to acid, base or water, is contained in caged bicyclic phosphate **IVG** and **IVH**, this synthetic reaction required moderate temperature and weak base. Reagents and solvents needed to be preprocessed in anhydrous state.

This synthetic reaction was carried out in the presence of triethylamine and anhydrous acetonitrile in three stages: Firstly, a solution of substituted phenoxyacetyl chloride **M20** was added dropwise to the solution of bicyclic phosphates **M21** or **M22** which cooled by ice water. Secondly, the reaction solution was stirred at room temperature for several hours, and then at a higher temperature further for 1–2 h under a mild reaction condition. In this way, 27 compounds **IVG** and **IVH** were conveniently synthesized. Detailed synthetic procedures for title compounds **IVG** and **IVH** are introduced in the Sect. 9.1.28 of Chap. 9.

The structures of **IVG** and **IVH** were confirmed by elemental analysis and characterized by IR, ^1H NMR. Several of them were further characterized by ^{31}P NMR. **IVG-10** was analyzed by X-ray single-crystal diffraction. Spectroscopic analysis of some of representative **IVG** and **IVH** are given in Sect. 5.3.3.

Table 5.29 Structure of caged bicyclic phosphates **IVH**

Compound	X	Y_n	Compound	X	Y_n
IVH-1	O	4-Cl	IVH-7	S	4-Cl
IVH-2	O	4-F	IVH-8	S	4-F
IVH-3	O	2,3- Cl_2	IVH-9	S	2,3- Cl_2
IVH-4	O	2,4- Cl_2	IVH-10	S	2,4- Cl_2
IVH-5	O	2-Cl,4-F	IVH-11	S	2-Cl,4-F
IVH-6	O	2-F,4-Cl	IVH-12	S	2-F,4-Cl

5.3.3 Spectroscopic Analysis of IVG and IVH

The IR spectra of **IVG** and **IVH** were similar. All functional groups showed normal absorption bands. The stretching frequency indicated the existence of Ar-H ($3,050\text{--}3,100\text{ cm}^{-1}$) and C-H ($2,850\text{--}2,960\text{ cm}^{-1}$). The two or three bands in the $1,490\text{--}1,640\text{ cm}^{-1}$ region were attributed to aromatic rings systems such as benzene. A strong absorption band near $1,750\text{--}1,760\text{ cm}^{-1}$ was identified for the stretching frequency of carbonyl in carboxylic ester. A strong peak near $1,300\text{--}1,320\text{ cm}^{-1}$ accounted for P=O in phosphonates. The stretching absorption bands of P=S in thiophosphonates could be observed at $580\text{--}750\text{ cm}^{-1}$. A stretching vibration for P-O-C appeared at $1,020\text{--}1,040\text{ cm}^{-1}$. An asymmetric stretching vibration for C-O-C appeared near $1,200\text{ cm}^{-1}$ and a symmetric stretching vibration for C-O-C was found near $1,100\text{ cm}^{-1}$. The IR spectrum of **IVH-5** is shown in Fig. 5.18.

In the ^1H NMR spectra of **IVG**, the chemical shifts of aromatic protons generally appeared at 6.8–7.6 ppm. The proton signal corresponding to three methylene groups on the bicyclic ring appeared at 4.6 ppm as a doublet due to the coupling with phosphorus. The protons of the methylene group between the bicyclic ring and oxygen appeared as a singlet at 4.0 ppm. The protons of the methylene group (OCH₂CO) between phenoxy group and carbonyl group also appeared as a singlet at 4.9 ppm. The ^1H NMR spectrum of **IVG-2** is shown in Fig. 5.19.

In the ^1H NMR spectra of caged bicyclic phosphates **IVH**, the chemical shifts of aromatic protons appeared at 6.8–7.5 ppm, generally. Six proton signals corresponding to three methylene groups on the bicyclic ring appeared at 4.5 ppm as a

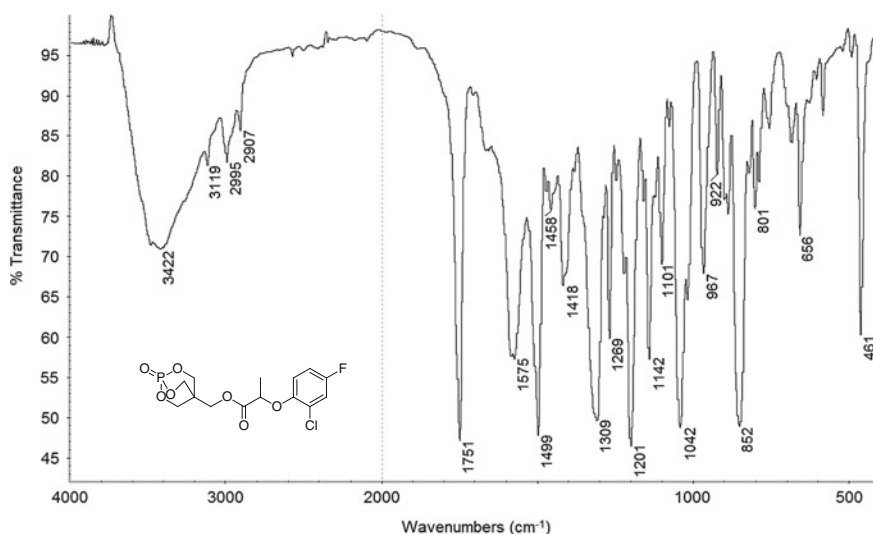


Fig. 5.18 IR spectrum of **IVH-5**

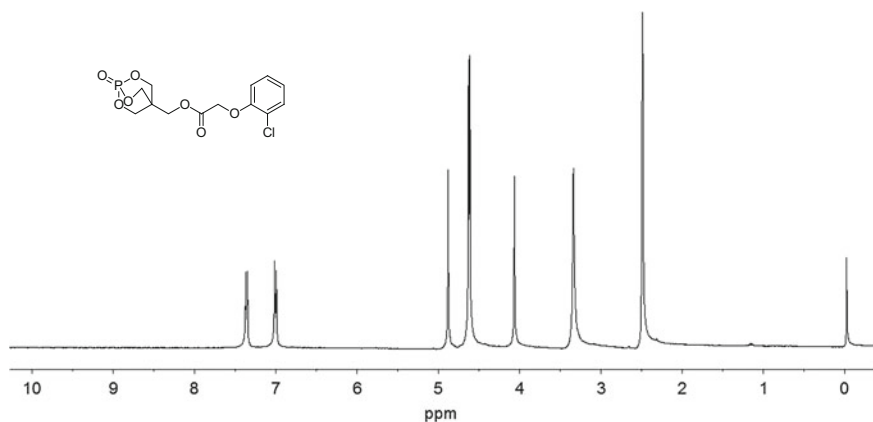


Fig. 5.19 ^1H NMR spectrum of **IVG-2** ($\text{DMSO-}d_6$, 400 MHz)

multiplet peak because of two methylene protons were not chemical-shift equivalent due to the coupling from phosphorus. Two protons of the methylene group between the bicyclic ring and oxygen were also not chemical-shift equivalent, and their signals appeared as two doublets or as an AB system at 4.0 ppm. The proton of the methine group ($\text{OCH}(\underline{\text{CH}}_3)\text{CO}$) between the phenoxy group and the carbonyl group appeared as quartet at 4.8 ppm due to the coupling from methyl, and the methyl ($\text{OCH}(\underline{\text{CH}}_3)\text{CO}$) displayed as a doublet. The $^3J_{\text{H-H}}$ was between 6.5 and 7.5 Hz. The ^1H NMR spectrum of **IVH-5** is shown in Fig. 5.20.

The ^{31}P chemical shift of **IVH-8** appeared at 56.7 ppm which was consistent with characterization of tetra-coordinate thiophosphate. The ^{31}P NMR spectrum of **IVH-8** is shown in Fig. 5.21.

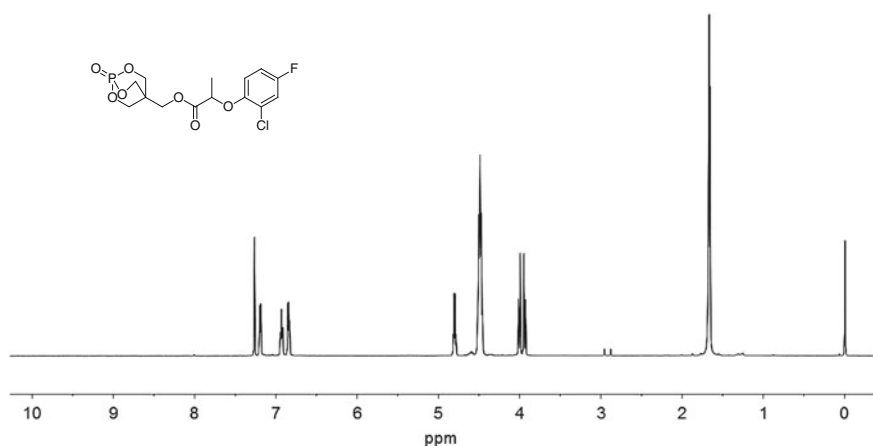


Fig. 5.20 ^1H NMR spectrum of **IVH-5** (CDCl_3 , 400 MHz)

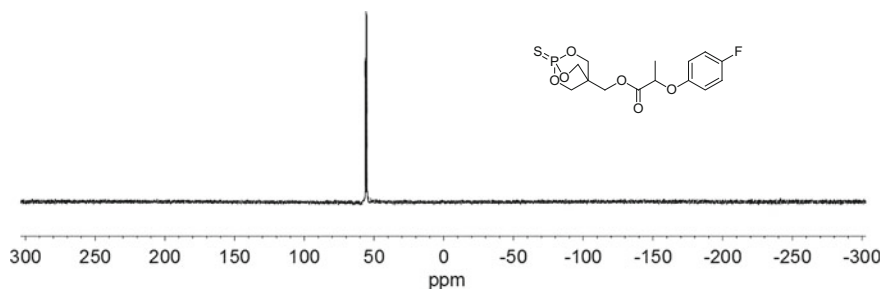


Fig. 5.21 ^{31}P NMR spectrum of **IVH-8** (CDCl_3 , 162 MHz)

5.3.4 Crystal Structure Analysis of **IVG-10**

The molecular structure of 4-[(2-chloro-5-methylphenoxy)acetoxy)methyl]-2,6,7-trioxa-1-phosphabicyclo[2.2.2]octane-1-one **IVG-10** was confirmed by the single crystal X-ray analysis [66].

The crystal belongs to the monoclinic system with space group $P2(1)/n$, $a = 12.4504(12)$ Å, $b = 6.3281(6)$ Å, $c = 0.201(2)$ Å, $\alpha = 90^\circ$, $\beta = 101.926(2)^\circ$, $\gamma = 90^\circ$, $V = 1557.2(3)$ Å³, $Z = 4$, $D_x = 1.547$ mg/m³, $\mu = 0.38$ mm⁻¹, $F(000) = 752$. The molecular structure and cell packing of the compound are presented in

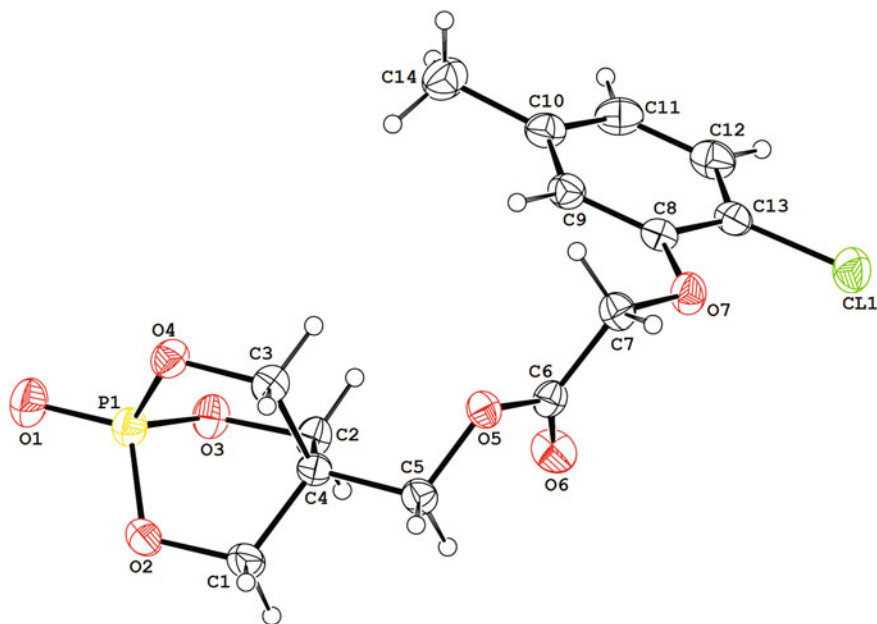


Fig. 5.22 Molecular structure of **IVG-10**

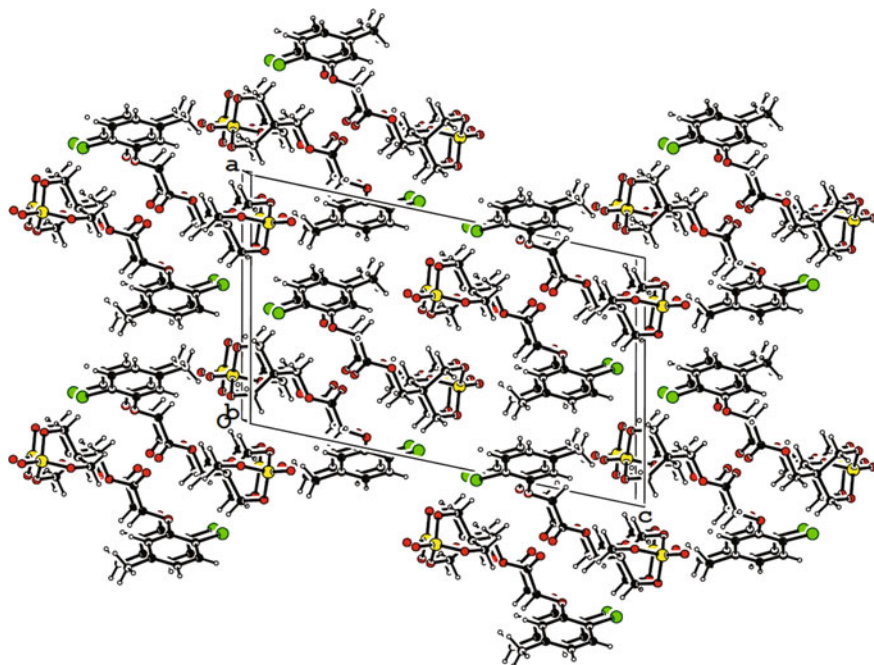


Fig. 5.23 Packing diagram of **IVG-10**

Table 5.30 Selected bond lengths (Å) and angles (°) for **IVG-10**

Bond	Dist./Deg.	Bond	Dist./Deg.
P1–O1	1.4426(16)	P1–O4	1.5724(14)
P1–O3	1.5696(14)	P1–O2	1.5766(15)
O1–P1–O3	114.01(9)	C5–C4–C3	110.94(15)
O1–P1–O4	114.03(9)	C5–C4–C2	111.51(15)
O3–P1–O4	104.15(7)	C3–C4–C2	109.37(16)
O1–P1–O2	115.02(9)	C5–C4–C1	108.72(15)
O3–P1–O2	103.99(8)	C3–C4–C1	107.48(16)
O4–P1–O2	104.39(8)	C2–C4–C1	108.70(16)
C4–C1–O2–P1	1.4(2)		

Figs. 5.22, 5.23, respectively. Selected bond lengths and angles are listed in Table 5.30. In the structure of **IVG-10**, the P atom is in a distorted tetrahedral configuration. The data reveal that some strain is probably existing in the bicyclic structure. The terminal O=P bond distance is 1.4426(16) Å, and the bridging P–O distances average 1.5728(14) Å. The average value of the O=P–O angles is 114.36 (2)°, while the average value of the O–P–O angles is 104.18(4)°.

IVG-10 was recrystallized from acetonitrile to give colorless crystals (0.20 mm × 0.20 mm × 0.10 mm) suitable for X-ray single-crystal diffraction. The crystal structure of **IVG-10** was recorded on a Smart Apex CCD diffractometer using graphite monochromated MoK α radiation ($\lambda = 0.071073$ nm). In the range of $1.77^\circ \leq \theta \leq 27.49^\circ$, 3,530 independent reflections ($R_{int} = 0.071$), of which 2,528 contributing reflections had $I > 2\sigma(I)$, and all data were corrected using SADABS program. The structure was solved by direct methods using SHELXS-97; all other calculations were performed with Bruker SAINT system and Bruker SMART programs. All non-hydrogen atoms were refined on F^2 anisotropically by full-matrix least squares method. Hydrogen atoms were observed and refined with a fixed value of their isotropic displacement parameter. Full-matrix least-squares refinement gave final values of $R = 0.047$, $R_w = 0.119$. The max and min difference between peaks and holes was 271 and -345 e nm $^{-3}$, respectively. The summary of data collection statistics for the X-ray structure of **IVG-10** was reported in the literature [66].

5.3.5 Herbicidal Activity of IVG and IVH

The herbicidal activity of **IVG** and **IVH** evaluated by Petri dish methods and in the greenhouse. The results are reviewed as follows.

5.3.5.1 Herbicidal Activity of 4-[(Substituted Phenoxyacetoxy)Methyl]-2,6,7-Trioxa-1-Phosphabicyclo[2.2.2]Octane-1-One IVG

As a preliminary bioassay, fifteen caged bicyclic phosphates **IVG** were tested for inhibitory activity against barnyard grass (*E. crusgalli*) and cabbage type rape (*B. napus*) using the Petri dish methods. The inhibitory effect of **IVG** on the growth of roots and stems of plant were examined. The results are listed in Table 5.31.

(A) Inhibitory activity against the root of plant

As seen from Table 5.31, most of the caged bicyclic phosphates **IVG** displayed good inhibitory effect on the growth of roots of dicotyledons and monocotyledons, especially **IVG-1**, **IVG-2**, **IVG-5**, **IVG-7**, **IVG-8**, and **IVG-9** with >90 % inhibitory effect against the growth of roots of both cabbage type rape and barnyard grass at 100 and 10 mg/L. **IVG-10** and **IVG-13** showed >90 % inhibitory effect only against roots of cabbage type rape. They will be further examined for their pre-emergence herbicidal activity in the greenhouse.

(B) Post-emergence herbicidal activity of IVG

Caged bicyclic phosphates **IVG** displayed higher herbicidal activity against the growth of stems of cabbage type rape than that of barnyard grass, especially **IVG-2**, **IVG-4**, **IVG-7**, **IVG-8**, and **IVG-9** with >90 % inhibitory effect against the growth

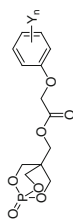


Table 5.31 Inhibitory activity of caged bicyclic phosphates **IVG** against the growth of plant^a

Compound	Y _n	Root			Stem			
		Ech ^b			Ech ^b			
		100 mg/L	10 mg/L	Bm ^b	100 mg/L	10 mg/L	Bm ^b	
IVG-1	2,4-Cl ₂	97	94	99	52	52	49	24
IVG-2	2-Cl	97	91	99	55	48	97	90
IVG-3	4-Cl	97	83	97	42	37	90	63
IVG-4	2-F	80	69	92	55	31	99	92
IVG-5	3-CF ₃	97	91	99	78	50	97	87
IVG-6	4-Me	94	51	97	22	4	88	34
IVG-7	2-Me,4-Cl	97	97	100	65	50	99	92
IVG-8	3-Me,4-Cl	97	91	100	63	55	97	90
IVG-9	2-Cl,4-F	95	95	100	54	43	99	93
IVG-10	2-Cl,5-Me	93	54	99	37	3	88	75
IVG-11	2,3-Me ₂	89	44	99	50	18	97	64
IVG-12	4-F	94	89	99	78	18	97	64
IVG-13	3-Me	94	83	99	39	0	77	37
IVG-14	H	94	89	99	82	0	83	23
IVG-15	4- <i>t</i> -Bu	72	67	79	43	25	49	5

^a Inhibitory potency (%) against the growth of plants in Petri dishes, 0 (no effect), 100 % (completely kill)

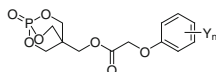
^b Ech: barnyard grass; Bm: rape

of stems of cabbage type rape at 100 and 10 mg/L, but all **IVG** showed <56 % inhibitory effect against the growth of stems of barnyard grass. It showed that caged bicyclic phosphates **IVG** had a much higher activity against dicotyledons than monocotyledons.

On the basis of the preliminary bioassay, further bioassays were carried out in the greenhouse to confirm the post-emergence herbicidal activity of **IVG**. As an initial evaluation, all test compounds were applied at 150 g ai/ha for post-emergence herbicidal activity against cabbage type rape (*B. napus*), leaf mustard (*B. juncea*), common amaranth (*A. retroflexus*), small goosefoot (*Chenopodium serotinum*), barnyard grass (*E. crusgalli*), and crab grass (*D. sanguinalis*). The results are listed in Table 5.32.

As shown in Table 5.32, **IVG-2**, **IVG-4**, and **IVG-6** exhibited good post-emergence herbicidal activity against tested dicotyledonous plants, especially **IVG-4** displayed a 100 % inhibition effect against all tested broad-leaved weeds at 150 g ai/ha. However, there was no activity against monocot weeds. **IVG-2**, **IVG-4**, and **IVG-6** will be further tested for their post-emergence herbicidal activity at a lower rate.

Table 5.32 Structure and post-emergence herbicidal activity of caged bicyclic phosphates **IVG**^a



Compound	Y _n	Ech ^b	Dig ^b	Brn ^b	Brj ^b	Amr ^b	Chs ^b
IVG-1	2,4-Cl ₂	0	0	NT	0	0	0
IVG-2	2-Cl	0	0	NT	90	70	80
IVG-3	4-Cl	0	0	NT	0	0	70
IVG-4	2-F	0	0	NT	100	100	100
IVG-5	3-CF ₃	0	0	NT	0	0	60
IVG-6	4-Me	0	0	NT	100	80	80
IVG-7	2-Me,4-Cl	0	0	NT	0	0	70
IVG-8	3-Me,4-Cl	0	0	NT	0	0	70
IVG-9	2-Cl,4-F	0	0	NT	60	40	70
IVG-10	2-Cl,5-Me	0	0	NT	0	40	0
IVG-11	2,3-Me ₂	22	0	12	40	33	0
IVG-12	4-F	20	0	41	NT	39	NT
IVG-13	3-Me	30	13	0	NT	21	NT
IVG-14	H	28	25	4	NT	26	NT
IVG-15	4- <i>t</i> -Bu	25	30	79	NT	85	NT

^a Inhibitory potency (%) against the growth of plants at a rate of 150 g ai/ha in the greenhouse, 0 (no effect), 100 % (completely kill), NT (not tested)

^b Ech: barnyard grass; Dig: crab grass; Bra: rape; Brj: leaf mustard; Amr: common amaranth; Chs: small goosefoot

(C) SAR analysis for **IVG**

As shown in Table 5.32, the 2-F substitution on the phenoxy-benzene ring was most promotive for post-emergence herbicidal activity followed by 2-Cl or 4-Me, but all compounds with two substitutions such as 2,4-Cl₂; 2-Me,4-Cl; 3-Me,4-Cl; 2-Cl,4-F; 2-Cl,5-Me; 2,3-Me₂ on the phenoxy-benzene ring showed much weaker or no herbicidal activity. It was noticed that compounds with one substitution on the phenoxy-benzene ring had much higher herbicidal activity than that of two substitutions on the phenoxy-benzene ring in the **IVG** series. Caged bicyclic phosphate **IVG** with mono-substituted phenoxy-benzene ring, such as **IVG-4** (Y_n=2-F), displayed the best activity against all tested broad-leaved weeds for post-emergence application. Among cyclic phosphonates **IVE**, the compounds with disubstituted phenoxy-benzene ring, such as 2,4-Cl₂; 2-Cl,4-F; 2-Me,4-Cl as Y_n were most promotive for post-emergence herbicidal activity. Whereas **IVG** with these disubstituted phenoxy-benzene ring displayed much lower herbicidal activity against tested plants. It showed that the structure-activity relationship (SAR) of **IVG** was much different from the SAR of **IVE**. The SAR was also significantly different between caged bicyclic phosphate **IVG** and open-chain alkylphosphonates **IA-IC**. In the structure of open-chain alkylphosphonates **IA-IC**, the herbicidal activity could be greatly enhanced by introducing 2,4-Cl₂ as Y_n on the phenoxy-benzene ring, but in the caged bicyclic phosphate **IVG**, **IVG-1** (Y_n=2,4-Cl₂), was almost inactive.

However, caged bicyclic phosphates **IVG** with 2,4-Cl₂; 2-Me,4-Cl; 3-Me,4-Cl; 2-Cl,4-F; 2-Cl; 3-CF₃ as Y_n on the phenoxy-benzene ring displayed better inhibitory effect at 100 and 10 mg/L against the growth of roots of tested plant than other substitutions. It showed the influence of Y_n on post-emergence herbicidal activity was different from the influence of Y_n on pre-emergence herbicidal activity.

5.3.5.2 Herbicidal Activity of 4-[(Substituted Phenoxypropionyloxy) Methyl]-2,6,7-Trioxa-1-Phosphabicyclo[2.2.2]Octane-1-One (or Thione) **IVH**

As a preliminary bioassay, the inhibitory activity of **IVH** was tested against barnyard grass and cabbage type rape using the Petri dish method. The inhibitory effect of **IVH** against the growth of roots and stems of plant were examined. The results are listed in Table 5.33.

(A) Inhibitory activity against the root of plant

As seen from Table 5.33, all caged bicyclic phosphates **IVH** displayed >90 % inhibitory activity against the root of cabbage type rape at 100 and 10 mg/L, but only **IVH-5**, **IVH-7**, and **IVH-10** exhibited >90 % inhibitory activity against the root of barnyard grass at 100 and 10 mg/L. The pre-emergence herbicidal activity of these compounds will be further examined in the greenhouse.

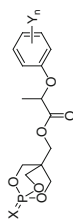


Table 5.33 Inhibitory activity of caged bicyclic phosphates **IVH** against the growth of plants^a

Compound	X	Y _n	Root			Stem				
			Ech ^b		Brm ^b	Ech ^b		Brm ^b		
			100 mg/L	10 mg/L	100 mg/L	100 mg/L	10 mg/L	10 mg/L		
IVH-1	O	4-Cl	93	86	97	97	44	39	92	73
IVH-2	O	4-F	96	88	99	96	50	25	93	79
IVH-3	O	2,3-Cl ₂	43	24	98	93	46	34	90	66
IVH-4	O	2,4-Cl ₂	91	85	97	94	43	30	93	71
IVH-5	O	2-Cl,4-F	97	94	99	98	59	28	94	90
IVH-6	O	2-F,4-Cl	92	86	98	98	49	40	94	74
IVH-7	S	4-Cl	97	93	99	97	43	36	96	91
IVH-8	S	4-F	97	87	99	94	64	35	93	67
IVH-9	S	2,3-Cl ₂	97	88	98	96	59	45	93	80
IVH-10	S	2,4-Cl ₂	97	91	99	97	54	37	93	89
IVH-11	S	2-Cl,4-F	97	79	98	96	47	40	93	62
IVH-12	S	2-F,4-Cl	93	77	98	96	46	42	90	84

^a Inhibitory potency (%) against the growth of plants in Petri dishes, 0 (no effect), 100 % (completely kill)

^b Ech: barnyard grass; Brm: cabbage type rape

(B) *Inhibitory activity against the stem of plant*

Only **IVH-5** and **IVH-7** exhibited >90 % inhibitory activity against the growth of stems of cabbage type rape at 100 and 10 mg/L, but all compounds **IVH** showed <50 % inhibitory effect against the growth of stems of barnyard grass at 10 mg/L. It showed that caged bicyclic phosphates **IVH-5** and **IVH-7** had selective inhibitory activity against dicotyledons.

(C) *SAR analysis for IVH*

In the **IVH** series, structural modification was focused on X and substituent Y_n on the phenoxy-benzene ring. The result showed that the change of X and Y_n in the **IVH** series had no significant influence on the inhibitory activity against the root of cabbage type rape, but had certain influence on the inhibitory activity against the growth of stems of cabbage type rape and root of barnyard grass at 10 mg/L.

Compared the inhibitory activity of **IVG** with that of **IVH**, they had similar inhibitory effects against the growth of plants. There was no significant influence on the inhibitory activity when substituted phenoxyacetyl moiety ($R^4=H$) was replaced by substituted phenoxypropionyl moiety ($R^4=Me$) in caged bicyclic phosphate structure (Table 5.34). However, herbicidal effects against broad-leaved weeds could be obviously decreased when phenoxyacetyl moiety in **IVE** was modified to phenoxypropionyl moiety to produce **IVF**. It showed the SAR of caged bicyclic phosphates was much different from the SAR of cyclic phosphonates.

5.3.6 Summary

Caged bicyclic phosphate **IVG** including 15 compounds were synthesized by the condensation of substituted phenoxyacetyl chloride **M5** and 4-(hydroxymethyl)-2,6,7-trioxa-1-phosphabicyclo[2.2.2]octane-1-one **M21** in the presence of base. On the basis of caged bicyclic phosphate **IVG**, a series of 4-[(substituted phenoxypropionyloxy)methyl]-2,6,7-trioxa-1-phosphabicyclo[2.2.2]octane-1-one (or thione) **IVH** was further designed by modifying substituted phenoxyacetyl moiety into substituted phenoxypropionyl moiety. Caged bicyclic phosphate **IVH** including 12 compounds were conveniently synthesized by the condensation of 4-(hydroxymethyl)-2,6,7-trioxa-1-phosphabicyclo[2.2.2]octane-1-one **M21** or corresponding thione **M22** and substituted phenoxypropionyl chlorides **M20** in the presence of base.

Caged bicyclic phosphate **IVG-1**, **IVG-2**, **IVG-5**, **IVG-7-9**, **IVH-5**, **IVH-7**, and **IVH-10** showed >90 % inhibitory effect against the growth of roots of both cabbage type rape and barnyard grass at 10 mg/L. The pre-emergence herbicidal activities of these compounds need to be further examined in the greenhouse. **IVG-2** ($Y_n=2-Cl$), **IVG-4** ($Y_n=2-F$), and **IVG-6** ($Y_n=4-Me$) were found to exhibit good herbicidal activity against tested dicotyledonous plants in the greenhouse, especially **IVG-4** displayed 100 % inhibition effect against all tested broad-leaved weeds at 150 g ai/ha. **IVG-2**, **IVG-4**, and **IVG-6** need to be further tested for their post-emergence herbicidal activity at a lower rate.

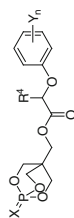


Table 5.34 Inhibitory activity of caged bicyclic phosphates **IVG** and **IVH** against the growth of plants^a

Compound	X	Y _n	R ⁴	Root			Stem			
				Ech ^b			Brn ^b			
				100 mg/L	10 mg/L	100 mg/L	100 mg/L	10 mg/L	100 mg/L	10 mg/L
IVG-1	O	2,4-Cl ₂	H	97	94	99	95	52	49	24
IVH-4	O	2,4-Cl ₂	Me	91	85	97	94	30	93	71
IVH-10	S	2,4-Cl ₂	Me	97	91	99	97	37	93	89
IVG-3	O	4-Cl	H	97	83	97	92	37	90	63
IVH-1	O	4-Cl	Me	93	86	97	97	39	92	73
IVH-7	S	4-Cl	Me	97	93	99	97	36	96	91
IVG-9	O	2-Cl,4-F	H	95	95	100	100	43	99	93
IVH-5	O	2-Cl,4-F	Me	97	94	99	98	28	94	90
IVH-11	S	2-Cl,4-F	Me	97	79	98	96	40	93	62
IVG-12	O	4-F	H	94	89	99	86	18	97	64
IVH-2	O	4-F	Me	96	88	99	96	25	93	79
IVH-8	S	4-F	Me	97	87	99	94	35	93	67

^a Inhibitory potency (%) against the growth of plants in Petri dishes, 0 (no effect), 100 % (completely kill).

^b Ech: barnyard grass; Brn: cabbage type rape.

SAR analysis for **IVG** and **IVH** indicated when caged bicyclic phosphate moiety were kept, R^4 had no significant influence on the herbicidal activity, but Y_n on the phenoxy-benzene ring had an obvious influence. It was worth noticing that compounds with one substitution had much higher post-emergence herbicidal activity than those with two substitutions in the **IVG** series. The 2-F substitution on the phenoxy-benzene ring was the most promotive for post-emergence herbicidal activity followed by 2-Cl or 4-Me, but all compounds with two substitutions such as 2,4-Cl₂; 2-Me,4-Cl; 2-Cl,4-F on the phenoxy-benzene ring showed much weaker or no post-emergence herbicidal activity. **IVG-4** with 2-F as Y_n displayed the best activity against all tested broad-leaved weeds for post-emergence. It showed the SAR of caged bicyclic phosphates **IVG** was much different from the SAR of cyclic phosphonates **IVE** or open-chain phosphonate **IA**, **IB**, and **IC**. In the **IVE** and **IA–IC** series, 2,4-Cl₂; 2-Cl,4-F; 2-Me,4-Cl as Y_n were very promotive for post-emergence herbicidal activity.

When substituted phenoxyacetyl moiety was modified to substituted phenoxy-propionyl moiety in the caged bicyclic phosphate, no significant influence on the herbicidal activity was found, but in the cyclic phosphonate **IVE**, herbicidal effect against broad-leaved weeds could be obviously decreased. It showed that the SAR of caged bicyclic phosphate was much different from the SAR of cyclic phosphonate.

References

1. Roy NK, Nidiry ES, Vasu K et al (1996) Quantitative structure-activity relationship studies of O, O-bisaryl alkylphosphonate fungicides by Hansch approach and principal component analysis. *J Agric Food Chem* 44:3971–3976
2. Forlani G, Giberti S, Berlicki L et al (2007) Plant P5C reductase as a new target for aminomethylenebisphosphonates. *J Agric Food Chem* 55:4340–4347
3. Forlani G, Occhipinti A, Berlicki L et al (2008) Tailoring the structure of aminobisphosphonates to target plant P5C reductase. *J Agric Food Chem* 56:3193–3199
4. Cox JM, Hawkes TR, Bellini P et al (1997) The design and synthesis of inhibitors of imidazoleglycerol phosphate dehydratase as potential herbicides. *Pestic Sci* 50:297–311
5. He HW, Wang J, Liu ZJ (1994) Synthesis of α -(substituted phenoxy acetoxy)alkyl phosphonates. *Chinese Chem Lett* 5:35–38
6. He HW, Wang J, Liu ZJ et al (1994) Study on biologically active organophosphorus compounds V, synthesis and properties of α -(substituted phenoxyacetoxy) alkyl phosphonates. *Chin J Appl Chem* 11:21–24
7. He HW, Wang J, Liu ZJ et al (1994) Studies on biologically active organophosphorus compounds. VI. Synthesis properties and biological activity of α -1-oxophosphonic acid derivatives. *J Centr Chin Norm Univ (Nat Sci)* 28:71–76
8. Chen T, Shen P, Li YJ et al (2006) Synthesis and herbicidal activity of O,O-dialkyl phenoxyacetoxyalkylphosphonates containing fluorine. *J Fluorine Chem* 127:291–295
9. Chen T, Shen P, Li Y et al (2006) The synthesis and herbicidal evaluation of fluorine-containing phenoxyacetoxyalkylphosphonate derivatives. *Phosphorus Sulfur Silicon Relat Elem* 181:2135–2145
10. Wang J, Chen XY, Liu XF et al (1999) The synthesis and biological properties of α -1-halogenated phenoxy carbonyloxy alkylphosphonic acids and esters. *Chin J Chem Reag* 21:301–303

11. He HW, Chen T, Li YJ (2007) Synthesis and herbicidal activity of alkyl 1-(3-trifluoromethylphenoxyacetoxy)-1-substituted methylphosphonates. *J Pest Sci* 32:42–44
12. Li YJ, He HW (2008) Synthesis and herbicidal activity of α -[2-(fluoro-substituted phenoxy)propionyloxy] alkyl phosphonates. *Phosphorus, Sulfur Silicon Relat Elem* 183:712–713
13. He HW, Liu ZJ, Wang J (1998) Synthesis and biological activities of α -1-[2-(2,4-dichlorophenoxy)propionyloxy] alkyl phosphonates. *Chin J Appl Chem* 15:88–90
14. Wang J, He HW, Liu ZJ (1997) Synthesis of α -[2-(2, 4-dichlorophenoxy) propionyloxy] alkyl phosphonates. *Chin Chem Lett* 8:943–944
15. Wang T, He HW (2004) Simple and improved preparation of α -oxophosphonate monolithium salts. *Phosphorus, Sulfur Silicon Relat Elem* 179:2081–2089
16. He HW, Yuan JL, Peng H et al (2011) Studies of O, O-dimethyl α -(2,4-dichlorophenoxyacetoxy) ethylphosphonate (HW02) as a new herbicide. 1. Synthesis and herbicidal activity of HW02 and analogues as novel inhibitors of pyruvate dehydrogenase complex. *J Agric Food Chem* 59:4801–4813
17. Peng H, Wang T, Xie P et al (2007) Molecular docking and three-dimensional quantitative structure-activity relationship studies on the binding modes of herbicidal 1-(substituted phenoxyacetoxy) alkylphosphonates to the E1 component of pyruvate dehydrogenase. *J Agric Food Chem* 55:1871–1880
18. Wang T, He HW, Miao FM (2009) Synthesis, crystal structure and herbicidal activity of α -(2,4-dichlorophenoxyacetoxy)- α -arylmethylphosphonates. *Chin J Org Chem* 29:1152–1157
19. Meng LP, He HW, Liu ZJ (1998) Synthesis and biological activities of O,O-dimethyl α -(NO₂ substituted phenoxyacetoxy)alkylphosphonates. *Chin J Hubei Chem Industry (special issue)*:40–41
20. He HW, Peng H, Wang T et al (2013) α -(Substituted-phenoxyacetoxy)- α -heterocyclymethylphosphonates: Synthesis, herbicidal activity, inhibition on pyruvate dehydrogenase complex (PDHc), and application as postemergent herbicide against broadleaf weeds. *J Agric Food Chem* 61:2479–2488
21. He HW, Meng LP, Hu LM et al (2002) Synthesis and plant growth regulatory activity of 1-(1-phenyl 1,2,4-triazole-3-oxoacetoxy)alkyl phosphonates. *Chin J Pest Sci* 4:14–18
22. Kiran YB, Reddy CD, Gunasekar D et al (2008) Synthesis and anticancer activity of new class of bisphosphonates/phosphanamidates. *Eur J Med Chem* 43:885–892
23. Sulsky R, Robl JA, Biller SA et al (2004) 5-Carboxamido-1,3,2-dioxaphosphanes, potent inhibitors of MTP. *Bioorg Med Chem Lett* 14:5067–5070
24. Patel DV, Rielly-Gauvin K, Ryono DE (1990) Peptidic α -hydroxy phosphinyls C-terminal modification methodology. *Tetrahedron Lett* 31:5591–5594
25. Stowasser B, Budt K-H, Jian-Qi L et al (1992) New hybrid transition state analog inhibitors of HIV protease with peripheral C₂-symmetry. *Tetrahedron Lett* 33:6625–6628
26. Sikorski JA, Miller MJ, Braccolino DS et al (1993) EPSP synthase: The design and synthesis of bisubstrate inhibitors incorporating novel 3-phosphate mimics. *Phosphorus, Sulfur Silicon Relat Elem* 76:115–118
27. Engel R (1977) Phosphonates as analogues of natural phosphates. *Chem Rev* 77:349–367
28. Allen MC, Fuhrer W, Tuck B et al (1989) Renin inhibitors. Synthesis of transition-state analog inhibitors containing phosphorus acid derivatives at the scissile bond. *J Med Chem* 32:1652–1661
29. Smith WW, Bartlett PA (1998) Macrocyclic inhibitors of penicillopepsin. 3. Design, synthesis, and evaluation of an inhibitor bridged between P2 and P1'. *J Am Chem Soc* 120:4622–4628
30. Allen J, Atherton F, Hall M et al (1978) Phosphonopeptides, a new class of synthetic antibacterial agents. *Nature* 272:56–58
31. Atherton FR, Hassall CH, Lambert RW (1986) Synthesis structure-activity relationships of antibacterial phosphonopeptides incorporating (1-aminoethyl) phosphonic acid and (aminomethyl) phosphonic acid. *J Med Chem* 29:29–40
32. Jennings LJ, Macchia M, Parkin A (1992) Synthesis of analogues of 5-iodo-2'-deoxyuridine-5'-diphosphate. *J Chem Soc Perkin Trans* 1:2197–2202

33. Patel DV, Rielly-Gauvin K, Ryono DE (1990) Preparation of peptidic α -hydroxy phosphonates a new class of transition state analog renin inhibitors. *Tetrahedron Lett* 31:5587–5590
34. Lavielle G, Hautefaye P, Schaeffer C et al (1991) New α -amino phosphonic acid derivatives of vinblastine: chemistry and antitumor activity. *J Med Chem* 34:1998–2003
35. Alonso E, Alonso E, Solís A et al (2000) Synthesis of *N*-alkyl-(α -aminoalkyl) phosphine oxides and phosphonic esters as potential HIV-protease inhibitors, starting from α -aminoacids. *Synlett* 2000:698–700
36. Camp NP, Hawkins PCD, Hitchcock PB et al (1992) Synthesis of stereochemically defined phosphoramidate-containing peptides: inhibitors for the HIV-1 proteinase. *Bioorg Med Chem Lett* 2:1047–1052
37. Hirschmann R, Smith AB, Taylor CM et al (1994) Peptide synthesis catalyzed by an antibody containing a binding site for variable amino acids. *Science* 265:234–237
38. Bischofberger N, Waldmann H, Saito T et al (1988) Synthesis of analogs of 1,3-dihydroxyacetone phosphate and glyceraldehyde 3-phosphate for use in studies of fructose-1,6-diphosphate aldolase. *J Org Chem* 53:3457–3465
39. Allen MC, Fuhrer W, Tuck B et al (1989) Renin inhibitors. Synthesis of transition-state analog inhibitors containing phosphorus acid derivatives at the scissile bond. *J Med Chem* 32:1652–1661
40. Palacios F, Alonso C, de los Santos JM (2005) Synthesis of β -aminophosphonates and-phosphinates. *Chem Rev* 105:899–932
41. Pudovik A, Konovalova I (1979) Addition reactions of esters of phosphorus (III) acids with unsaturated systems. *Synthesis* 1979:81–96
42. Ten Hoeve W, Wynberg H (1985) The design of resolving agents. Chiral cyclic phosphoric acids. *J Org Chem* 50:4508–4514
43. Kumaraswamy S, Selvi RS, Swamy KK (1997) Synthesis of new α -hydroxy-, α -halogeno- and vinylphosphonates derived from 5,5-dimethyl-1,3,2-dioxaphosphinane-2-one. *Synthesis* 1997:207–212
44. Zuo N, He HW (2006) 2-[(4-Chlorophenyl) hydroxymethyl]-5, 5-dimethyl-4-phenyl-1, 3, 2-dioxaphosphinane-2-one. *Acta Cryst E* 62:o4864–o4865
45. Chen T, Shen P, Li Y et al (2006) Synthesis and herbicidal activity of O, O-dialkyl s containing fluorine. *J Fluorine Chem* 127:291–295
46. Brayer JL, Talinani L (1990) Tessier J (1990) Preparation of aryl and aryl oxyacetyl diaineoalkanes and analogs as agrochemical fungicides. *EP* 376:819
47. Wang W, He HW, Zuo N et al (2012) Synthesis and herbicidal activity of 2-(substituted phenoxyacetoxy)alkyl-5,5-dimethyl-1,3,2-dioxaphosphinane-2-one containing fluorine. *J Fluorine Chem* 142:24–28
48. Wang W, He HW, Zuo N et al (2012) Synthesis and herbicidal activity of 2-(substituted phenoxyacetoxy)alkyl-5,5-dimethyl-1,3,2-dioxaphosphinane-2-one. *J Agric Food Chem* 60:7581–7587
49. Xie Q, Zheng J (1991) Synthesis and structure of tricyclohexylstannane aromatoxyacetates. *Chin J Org Chem* 11:82–87
50. Zuo N, He HW (2007) 2-[(2-Chlorophenyl)[(2,4-dichlorophenoxy) acetoxy] methyl]-5, 5-dimethyl-1,3,2-dioxaphosphinane-2-one. *Acta Cryst E* 63:o794–o795
51. Verkade J, Reynolds L (1960) The synthesis of a novel ester of phosphorus and of arsenic. *J Org Chem* 25:663–665
52. Rätz R, Sweeting OJ (1965) 4-Hydroxymethyl-1-phospha-2,6,7-trioxabicyclo[2.2.2]octane 1-sulfide and derived compounds. *J Org Chem* 30:438–442
53. Rätz R (1965) Bicyclic phosphorus-containing carbamates US patent 3,168,549, 2 Feb 1965
54. Rätz R (1966) US patent 3,287,448, 1966
55. Hechenbleikner I, Lanoue FC, Pause CW et al (1966) US patent 3,293,327, 20 Dec 1966
56. Bowery N, Collins J, Hill R (1976) Bicyclic phosphorus esters that are potent convulsants and GABA antagonists. *Nature* 261:601–603

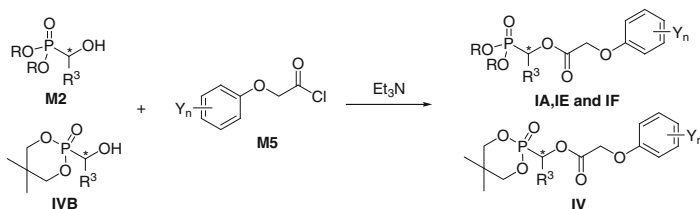
57. Toy DF, Walsh N (1987) Phosphorus chemistry in everyday living. American Chemical Society, Washington, DC, p 317
58. Ozoe Y, Mochida K, Eto M (1982) Reaction of toxic bicyclic phosphates with acetylcholinesterases and α -chymotrypsin. *Agric Biol Chem* 46:2527–2531
59. Li YG, Wang JJ, Han T (1988) Study of caged bicyclic phosphates I: 1-Oxo-4-substituted-2,6,7-trioxa-1-phosphabicyclo[2,2,2]octane and its reactions. *Acta Chim Sinica* 46:679–685
60. Li YG, Wang JJ, Liu YS (1989) Study of caged bicyclic phosphates (II)-synthesis of derivatives of 1-sulfo-1-phospha-4-methylene-2,6,7-trioxabicyclo[2,2,2]octane. *Chem J Chin Univ* 10:1002–1006
61. Shao RL, Wang SP, Wang DZ (1991) Studies on synthesis and biological activity of caged bicyclic phosphates compounds. *Chem J Chin Univ* 12:1063–1065
62. Li YG, Li JM, Ren HL et al (1992) Studies of caged bicyclic phosphates (V) Synthesis of 1-oxo-1-phospha-2,6,7-trioxabicyclo[2,2,2]-4-substituted carbonyl octane. *Chem J Chin Univ* 13:204–208
63. Li YG, Wang XL, Zhu XF et al (1995) Study on the synthesis of 1-sulfur-1-phospha-2,6,7-trioxabicyclo [2.2.2] octyl-4-methyl thioethers and its sulfoxides. *Chin J Org Chem* 15:57–60
64. Li YG, Zhu XF, Huang Q et al (1996) Studies on the Synthesis and Structure of N-(1-Oxo-1-phospha-2,6,7-trioxabicyclo[2.2.2]octane-4-carbonyl)-N'-aryl(alkyl)thioureas. *Chem J Chin Univ* 17:1394–1398
65. Vyverberg FJ, Chapman RW (2002) Process for the production of pentaerythritol phosphate alcohol US Patent 6,455,722, 24 Sep, 2002
66. Sheng XJ, He HW (2006) 4-[(2-Chloro-5-methylphenoxy)acetoxymethyl]-2,6,7-trioxa-1-phosphabicyclo[2.2.2]octane 1-oxide. *Acta Cryst E* 62:o4398–o4399

Chapter 6

Optically Active Alkylphosphonates

Chiral phosphonates are an important class of heteroatomic compounds possessing diverse biological activity, which have great significance in the research of pharmaceuticals, agricultural chemicals and natural bioactive compounds [1–15]. The biological activity of individual enantiomers of natural and synthetic chiral organophosphorous compounds have received much attention [16–20], especially their enantiomeric selectivity in toxicity, endocrine disruption and environmental fate were examined. Some studies have demonstrated that the biological activity of 1-substituted phosphonates depend largely on their absolute configuration.

So far, none of the pure chiral herbicide as inhibitor of pyruvate dehydrogenase complex (PDHc E1) has been reported. 1-(Substituted phenoxyacetoxy)alkylphosphonates **Io** have been found as inhibitors of PDHc E1 with good herbicidal activity in our previous work. As stated in Chaps. 2 and 5, a large number of 1-substituted alkylphosphonates **Io** based on plant PDHc E1 were designed and synthesized in our lab to discover novel herbicides. Herbicidal activity of these 1-substituted alkylphosphonates including open-chain phosphonates **IA–IK** [21–39] and cyclic phosphonates **IVA–IVF** [40, 41] were systemically examined at different rates. Some 1-substituted alkylphosphonates in the **IA–IJ** series and some cyclic phosphonates in the **IVC–IVE** series displayed good post-emergence herbicidal activity. Especially several active compounds such as open-chain phosphonates **IC-22** (HW02, clacyfos), **IG-21** (HWS), cyclic phosphonates **IVE-7**, **IVE-9** and **IVE-11** were found to be very effective compounds with potential utility for further development as selective post-emergence herbicides. It can be noticed that all of these 1-substituted alkylphosphonates **IA–IJ** and **IVC–IVE** have a chiral carbon in their molecular skeletons, which should contain two optical active isomers. It was well demonstrated that the absolute configuration of chiral herbicides could significantly affect their herbicidal activity [42, 43], enzyme inhibition [44], even the mode of action [45], crop safety [46], toxicity or environmental safety [47, 48]. Therefore, it is critically importance to sort out the preferred herbicidal molecular chirality, especially when they are applied in agriculture.



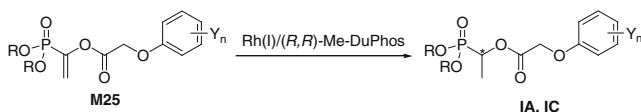
Scheme 6.1 Synthesis of optically active open-chain phosphonates **Ia** and cyclic phosphonates **IV**

Up to now, our study on all these chiral 1-substituted alkylphosphonates only limited to their racemic forms. Considering the importance of chirality for herbicidal active, it would be very interesting to examine the contribution of the optical counterparts to their biological activity. As our work aimed at the herbicidal effect of the optically active isomer of chiral 1-substituted alkylphosphonates, we first attempted to set up an efficient method to prepare the isomers of 1-substituted alkylphosphonates with optical activity.

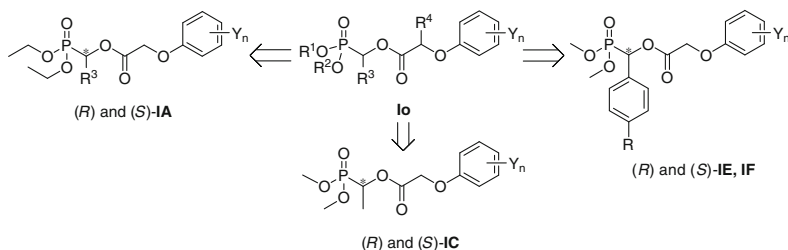
Two asymmetric synthesis strategies including synthetic routes 1 and 2 were considered to prepare the optically active 1-(substituted phenoxyacetoxy)alkylphosphonates including molecular skeletons of open-chain phosphonates **Ia** and cyclic phosphonates **IV**. In synthetic route 1, optically active 1-(substituted phenoxyacetoxy)alkylphosphonates **Ia** or **IV** could be prepared by the condensation of substituted phenoxyacetyl chlorides **M5** and optically pure 1-hydroxyalkylphosphonates **M2** or cyclic 1-hydroxyalkylphosphonates **IVB**, respectively (Scheme 6.1).

In synthetic route 2, optically active 1-(substituted phenoxyacetoxy)alkylphosphonates could be obtained via asymmetric hydrogenation of the corresponding prochiral 1,2-unsaturated phosphonates using Rh(I)/(*R,R*)-Me-DuPhos complex as the catalyst (Scheme 6.2) [49].

We made an effort to set up an efficient method with higher enantiomeric excess (*ee*) via above synthetic route 1 and 2 to prepare enantiomers of 1-substituted alkylphosphonates. In order to sort out the preferred optical active isomer, the herbicidal activity, crop safety, toxicity, and environmental safety of the optical counterparts of 1-substituted alkylphosphonates need to be examined. So far, several kinds of optically active 1-(substituted phenoxyacetoxy)alkyl phosphonates including **Ia**, **IC**, **IE**, and **IF** series were prepared (Scheme 6.3) and their biological activities evaluated. Their asymmetric synthesis, enantiomeric selectivity in herbicidal activity, acute aquatic toxicity and SAR discussion are introduced in this chapter.



Scheme 6.2 Asymmetric hydrogenation of 1,2-unsaturated phosphonates



Scheme 6.3 Optically active 1-(substituted phenoxyacetoxy)alkylphosphonates **IA**, **IC**, **IE** and **IF**

6.1 Optically Active 1-Hydroxyalkylphosphonates IVB and M2

6.1.1 Introduction

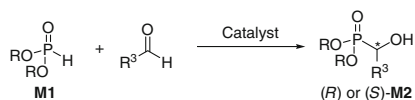
1-Hydroxyalkylphosphonates are an attractive class of biologically active compounds which have received a lot of attention in pharmaceutical chemistry, pesticide chemistry, and enzyme chemistry due to their intriguing biological activity. As one kind of important synthetic intermediates, they are also widely applied in the synthesis of enzyme inhibitors, medicine, and pesticides. The synthetic methods of chiral 1-hydroxyalkylphosphonates have received special attention because their biological activities usually depend on their absolute configuration. The research of the synthesis of chiral 1-hydroxyalkylphosphonates is usually focused on obtaining high enantioselectivity. Although the syntheses of a number of chiral 1-hydroxyalkylphosphonates have been reported, how to achieve high reactivity and enantioselectivity by a catalyst system is still challenging and interesting.

The 1-hydroxyalkylphosphonates and cyclic 1-hydroxyalkylphosphonates can be used as very useful synthetic intermediates of open-chain or cyclic alkylphosphonates. Therefore 1-hydroxyalkylphosphonates and cyclic 1-hydroxyalkylphosphonates as the key intermediates of our title compounds were first studied. According to the reports, two asymmetric synthetic methods could be considered to prepare 1-hydroxyalkylphosphonates.

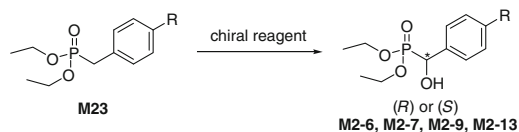
One approach is enantioselective hydrophosphonylation. Chiral 1-hydroxyalkylphosphonates **M2** could be prepared by the enantioselective hydrophosphonylation of dialkyl phosphonates **M1** and aldehydes (Scheme 6.4) [50–54].

Another approach is stereoselective hydroxylation. The stereoselective hydroxylation of dialkyl benzylphosphonates by using chiral reagent could yield enantiomerically pure 1-hydroxy(substituted phenyl)methylphosphonates **M2** including **M2-6**, **M2-7**, **M2-9**, and **M2-13** (Scheme 6.5) [55, 56].

Based on these two asymmetric synthetic approaches, a new route was designed and used to synthesize optically active 1-hydroxyalkylphosphonates in our laboratory [57]. A series of optically active 1-hydroxyalkylphosphonates was



Scheme 6.4 Asymmetric synthesis of 1-hydroxyalkylphosphonates **M2** by enantioselective hydrophosphonylation



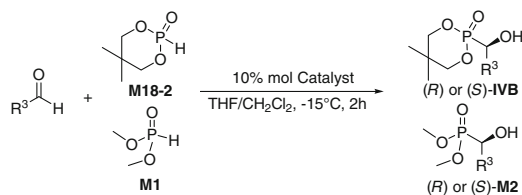
Scheme 6.5 Asymmetric synthesis of 1-hydroxy(substituted phenyl)methylphosphonates **M2** by stereoselective hydroxylation

successfully prepared in a higher enantiomeric excess (*ee*). These optically active 1-hydroxyalkylphosphonates could be further used to prepare optically active 1-(substituted phenoxyacetoxy)alkylphosphonates **10**. In this section, asymmetric synthesis of optically active 1-hydroxyalkylphosphonates is introduced and discussed.

6.1.2 Asymmetric Synthesis of 1-Hydroxyalkylphosphonates **IVB** and **M2** via Hydrophosphonylation

The base-catalysed hydrophosphonylation of aldehydes or imines (Pudovik reaction) [58] as a convenient method was widely used for the synthesis of 1-hydroxyalkylphosphonates. Since the pioneering work of Shibuya [50] and Spilling [51] was reported, much attention has been devoted to developing enantioselective catalysts for the synthesis of chiral 1-hydroxyalkylphosphonates. Chiral aluminium complexes were shown to be more effective chiral catalysts [59–62]. Based on the success of using Al(salen) and Al(salcyen) as asymmetric catalysts, Al-Schiff base complexes [63, 64] have been developed to catalyze the asymmetric addition reaction of dialkylphosphonates and aldehydes. Tridentate Schiff base metal complexes, such as vanadium, chromium, and iron [65], have been successfully applied in many asymmetric synthetic reactions. We noticed that Al(III) complexes could catalyse the asymmetric Pudovik reaction and these ligands could be easily synthesized [66–70].

In order to obtain 1-hydroxyalkylphosphonates **M2** and cyclic 1-hydroxyalkylphosphonates **IVB** in a higher enantiomeric excess (*ee*), we developed an efficient method [57] to asymmetrically synthesize **M2** and **IVB** via enantioselective hydrophosphonylation of aldehydes using tridentate Schiff base Al(III) complexes as catalysts (Scheme 6.6).

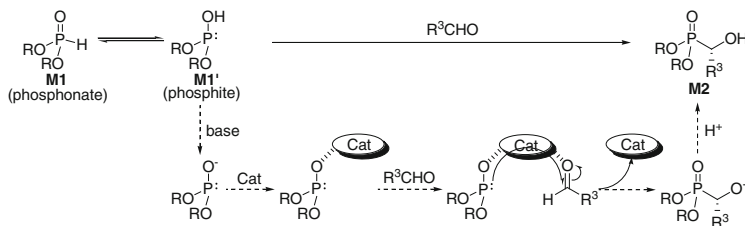


Scheme 6.6 Asymmetric synthesis of 1-hydroxyalkylphosphonates **M2** and cyclic 1-hydroxyalkylphosphonates **IVB** using Al(III) complexes as catalysts

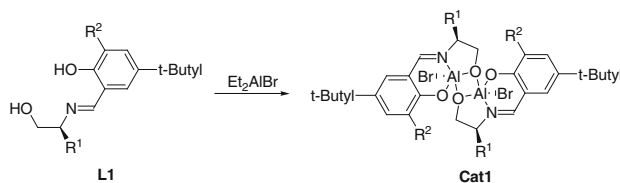
Dialkyl phosphonates undergo phosphite-phosphonate tautomerism and have two tautomeric forms: phosphonate and phosphite [71]. Here **M18-2** and **M1** are expressed as phosphonate form in Scheme 6.6.

The mechanism of the Pudovik reaction has been reported, it was thought that catalytically active dialkyl phosphite anion could be formed by the deprotonation of dialkyl phosphonate under the action of base, which is an agreement amongst chemists (Scheme 6.7) [54].

In our work, tridentate Schiff base ligands **L1** reacted in situ with Et_2AlBr to form catalyst **Cat1** (Scheme 6.8) which was used to catalyze asymmetric hydrophosphonylation of aldehydes and ketones. In order to improve the enantioselectivity of this reaction, the steric effects of ligands **L1** on enantioselectivity were examined. Different groups including *i*-Pr, *i*-Bu, Ph, benzyl or adamantyl as R^1 or R^2 were respectively introduced into ligands **L1** which were further used to prepare corresponding catalysts Al(III) complexes **Cat1**. As an example, these Al(III)



Scheme 6.7 Catalytic mechanism for the Pudovik reaction



Scheme 6.8 Synthesis of catalyst Al(III) complexes **Cat1**

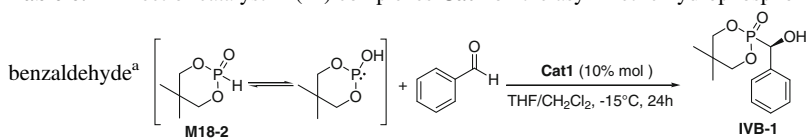
complexes **Cat1** as catalysts were applied in the asymmetric synthesis of cyclic 1-hydroxy(phenyl)methylphosphonates **IVB-1** (Table 6.1).

As shown in Table 6.1, the steric hindrance of substituent R^1 and R^2 , had a significant effect on enantioselectivity. When ligands possessed bulky groups, such as *t*-Bu as R^1 and adamantyl as R^2 , cyclic 1-hydroxy(phenyl)methylphosphonates **IVB-1** could achieve the highest enantioselectivity (99 % *ee*; Table 6.1, entries 6 and 8). It is noteworthy that both the size of substituent R^1 and the distance between the bulky group and the chiral center in the structure of **Cat1**, had a notable effect on the enantioselectivity. Although the size of phenyl is larger than that of isopropyl, the effect on enantioselectivity of both phenyl and isopropyl was almost the same (Table 6.1, entries 1 and 3). While R^1 was benzyl, there was a methylene inserted between the phenyl and the chiral carbon which made the phenyl far from the chiral center, the enantioselectivity significantly decreased (67 % *ee*, Table 6.1, entry 2).

However, the steric hindrance of substituent R^1 and R^2 had a minor effect on reactivity (81–84 % yield, Table 6.1, entries 1–8). Products **IVB-1** could retain the same absolute configuration with ligands **L1** in this reaction. The (*S*) or (*R*) **IVB-1** with the same *ee* value could be obtained in this reaction by using corresponding ligands with the same absolute configuration (*S*)-**L1** or (*R*)-**L1** (Table 6.1, entries 5–8).

The relationship between the enantiomeric excess of Schiff base ligand and the product was tested by Feng and co-workers [63]. The results indicated that there was a strong positive nonlinear effect, which implied that the reaction occurred due to the presence of a polymeric aluminium active species. The presence of dimeric

Table 6.1 Effect of catalyst Al(III) complexes **Cat1** on the asymmetric hydrophosphonylation of



Entry	Catalyst	Ligands L1		Yield ^b (%)	<i>ee</i> ^c (%)
		R^1	R^2		
1	(<i>S</i>)- Cat1-1	<i>i</i> -Pr	<i>i</i> -Bu	82	86 (<i>S</i>)
2	(<i>S</i>)- Cat1-2	Benzyl	<i>i</i> -Bu	84	67 (<i>S</i>)
3	(<i>S</i>)- Cat1-3	Ph	<i>i</i> -Bu	83	87 (<i>S</i>)
4	(<i>S</i>)- Cat1-4	<i>i</i> -Bu	<i>i</i> -Bu	83	91 (<i>S</i>)
5	(<i>S</i>)- Cat1-5	<i>i</i> -Pr	Adamantyl	81	94 (<i>S</i>)
6	(<i>S</i>)- Cat1-6	<i>i</i> -Bu	Adamantyl	82	99 (<i>S</i>)
7	(<i>R</i>)- Cat1-5	<i>i</i> -Pr	Adamantyl	80	94 (<i>R</i>)
8	(<i>R</i>)- Cat1-6	<i>i</i> -Bu	Adamantyl	82	99 (<i>R</i>)

^a Reactions were carried out under nitrogen: benzaldehyde (10 mmol), cyclic phosphite (12 mmol), a mixture of 4 mL CH_2Cl_2 and 6 mL THF

^b Isolated yield

^c Determined by HPLC analysis

aluminium species was further observed by HR-MS analysis, but the configuration of catalyst was still unclear. Fortunately, we got the single crystal of catalyst (*S*)-**Cat1-4**.

Crystal Structure Analysis of (S)-Cat1-4. The crystal belongs to the orthorhombic system with space group $C2(1)2(1)$, $a = 12.9848(17)$ Å, $b = 17.0304(17)$ Å, $c = 24.393(3)$ Å, $\alpha = 90^\circ$, $\beta = 90^\circ$, $\gamma = 90^\circ$, $V = 5394.2(11)$ Å³, $Z = 4$, $D_x = 1.289$ Mg/m³, $\mu = 1.77$ mm⁻¹, $F(000) = 2176$. The molecular structure and cell packing of the compound are presented in Figs. 6.1 and 6.2, respectively.

As shown in Fig. 6.1, the oxygen atom of the alcohol group acts as a bridge in the dimeric aluminum species. Though the exact transition state for the reaction is unclear, the crystal structure may provide us some valuable information to understand the catalysis mechanism of the reaction. The two Br ions of the dimer are substituted by the phosphite ions. Consequently, it is possible that the reaction proceeds via two pathways: monometallic catalysis or bimetallic catalysis. Perhaps the catalyst was capable of bringing both substrate and reagent together at a single metal center or one metal center might activate the phosphorus reagent whilst another metal center activated the carbonyl. The steric hindrance of substituent R² could force the carbonyl to get close to the chiral centre of the ligand, and the larger substituent R¹ would provide a more favorable chiral environment. Therefore, ligands with bulkier groups could achieve higher enantioselectivities.

Because dialkyl phosphonates undergo phosphite-phosphonate tautomerism, a simple strategy to accelerate the phosphite-phosphonate tautomerization is the deprotonation of phosphonates using a base. Inorganic bases, such as potassium carbonate, which have relatively weak basicity and low solubility in organic solvents, could make the dialkyl phosphonate to generate an active phosphite anion at

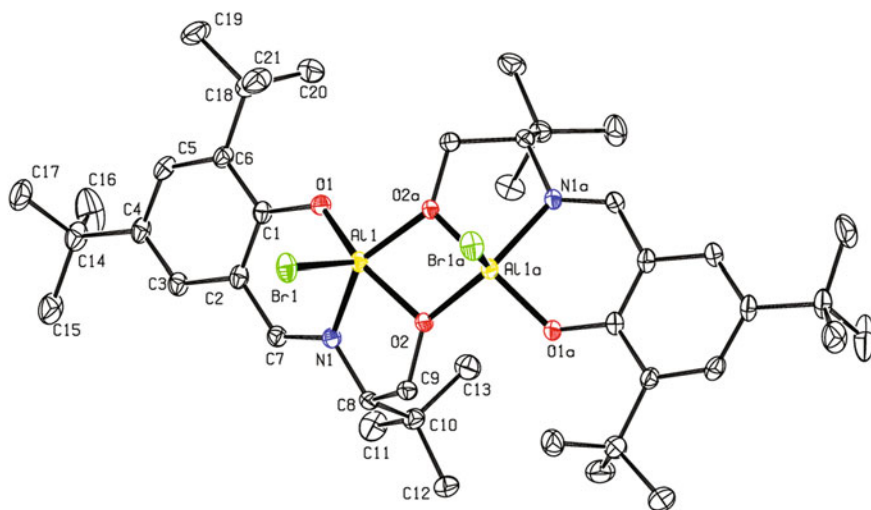


Fig. 6.1 Molecular structure of catalyst (*S*)-**Cat1-4**

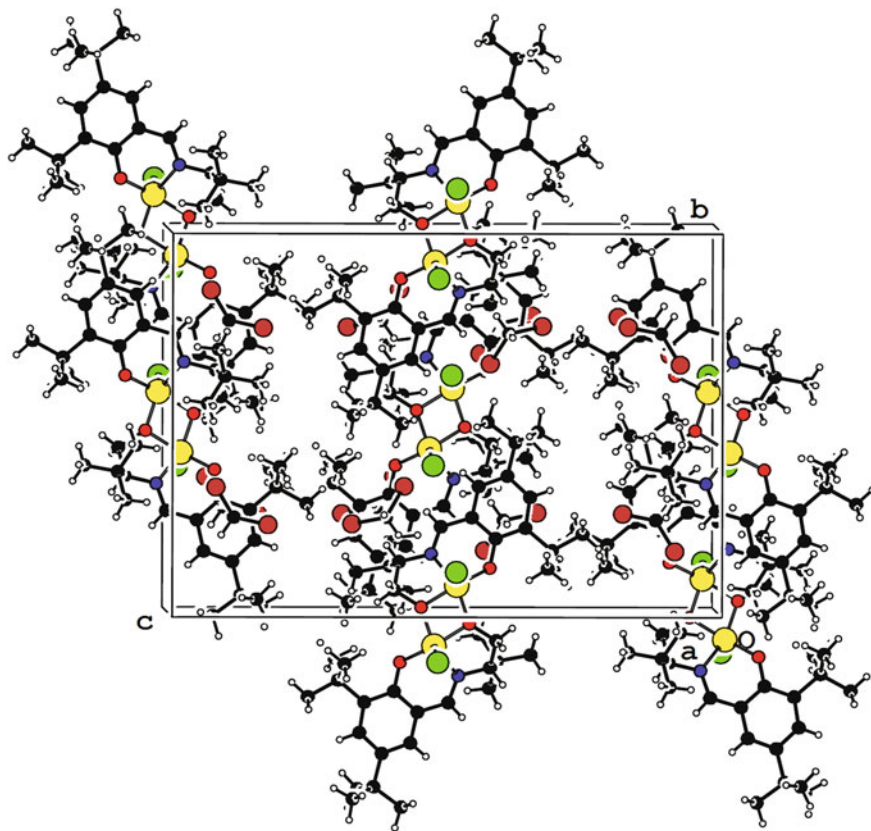
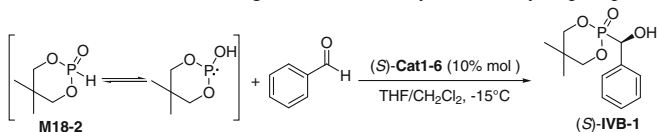


Fig. 6.2 Packing diagram of catalyst (*S*)-Cat1-4

an appropriate rate to enhance the hydrophosphonylation without reducing enantioselectivity.

The role of the inorganic salts in this reaction was also examined. Potassium carbonate, silver carbonate, or silver nitrate was respectively used in this experiment (Table 6.2). We found that the addition of 0.3–0.4 equivalent of potassium carbonate could effectively increase the reaction rate (Table 6.2, entries 3–4). It was surprising that the addition of 0.04 equivalent of silver carbonate could significantly accelerate this reaction. This reaction was completed in 2 h (Table 6.2, entries 8). Other silver-containing compounds such as silver nitrate (a weak acid), had a slight negative effect on this reaction (Table 6.2, entries 10–14). The results showed that basic reaction conditions favored the formation of phosphite anion, and the addition of these three inorganic salts did not affect enantioselectivity (Table 6.2).

Under optimized reaction conditions, the asymmetric hydrophosphonylation of aldehydes with corresponding cyclic phosphonates **M18-2** could be achieved in good yields with excellent enantioselectivities. On the basis of optimization, a series

Table 6.2 Effect of inorganic salts on asymmetric hydrophosphonylation of benzaldehyde^a

Entry	Salt	(mol%)	Time (h)	Yield ^b (%)	ee ^c (%)
1	K ₂ CO ₃	10	2/6/12	40/68/80	99
2	K ₂ CO ₃	20	2/6/12	45/76/82	99
3	K ₂ CO ₃	30	2/6/12	67/82/82	99
4	K ₂ CO ₃	40	2/6/12	75/81/83	99
5	Ag ₂ CO ₃	1	2/4/8	30/58/79	99
6	Ag ₂ CO ₃	2	2/4/8	44/60/78	99
7	Ag ₂ CO ₃	3	2/4	71/82	99
8	Ag ₂ CO ₃	4	2/4	82/82	99
9	Ag ₂ CO ₃	5	2/4	82/81	99
10	AgNO ₃	1	2/12/24	20/61/80	99
11	AgNO ₃	2	2/12/24	23/67/79	99
12	AgNO ₃	3	2/12/24	23/68/80	99
13	AgNO ₃	4	2/12/24	24/69/78	99
14	AgNO ₃	5	2/12/24	23/67/79	99

^a Reactions were carried out under nitrogen: benzaldehyde (10 mmol), cyclic phosphite (12 mmol), a mixture of 4 mL CH₂Cl₂ and 6 mL THF

^b Isolated yield

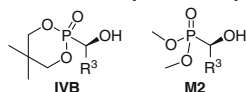
^c Determined by HPLC analysis

of optically active cyclic 1-hydroxyalkylphosphonates **IVB** including the configuration of (*S*) and (*R*) was synthesized in our laboratory.

Under the same conditions, optically active 1-hydroxyalkylphosphonates **M2** could be also synthesized by the asymmetric hydrophosphonylation of aldehydes with corresponding *O,O*-dimethylphosphonates **M1**. A series of optically active 1-hydroxyalkylphosphonates **M2** including the configuration of (*S*) and (*R*) was further obtained in good yields with excellent enantioselectivities in our laboratory.

The structures of all optically active **IVB** and **M2** were characterized by ¹H and ¹³C NMR, IR, MS and were confirmed by elementary analysis. Some of them are listed in Table 6.3. The absolute configuration of compound (*S*)-**IVB-4** was confirmed by the single-crystal X-ray analysis [72] and others were determined by comparison with (*S*)-**IVB-4** or comparison with literature data.

Crystal Structure Analysis of (S)-IVB-4. The crystal structure belongs to the monoclinic system with space group *P* 2(1), *a* = 7.0263(9) Å, *b* = 9.9443(13) Å, *c* = 10.6462(14) Å, $\alpha = 90^\circ$, $\beta = 93.975(2)^\circ$, $\gamma = 90^\circ$, *V* = 742.08(17) Å³, *Z* = 2, *D*_x = 1.455 mg/m³, $\mu = 0.55 \text{ mm}^{-1}$, *F*(000) = 336. The molecular structure and cell packing of this compound are presented in Figs. 6.3 and 6.4, respectively. In the

Table 6.3 Asymmetric synthesis of 1-hydroxyalkylphosphonates^a

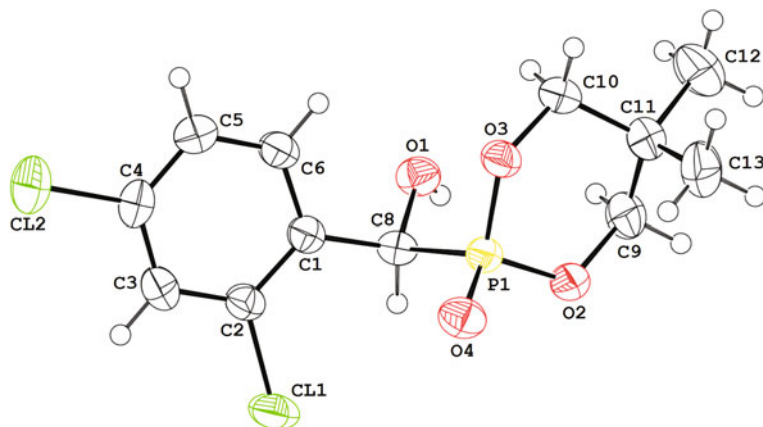
Compound	R ³	Yield ^b (%)	ee ^c (%)	Conf ^d
(<i>S</i>)-IVB-1	Ph	82	99	<i>S</i>
(<i>R</i>)-IVB-1	Ph	81	99	<i>R</i>
(<i>S</i>)-IVB-4	2,4-Cl ₂ Ph	77	99	<i>S</i>
(<i>S</i>)-M2-24	Ph	82	98	<i>S</i>
(<i>R</i>)-M2-24	Ph	85	96	<i>R</i>
(<i>S</i>)-M2-25	4-MePh	83	95	<i>S</i>
(<i>R</i>)-M2-25	4-MePh	80	98	<i>R</i>
(<i>S</i>)-M2-29	4-MeOPh	78	97	<i>S</i>
(<i>R</i>)-M2-29	4-MeOPh	79	98	<i>R</i>
(<i>S</i>)-M2-33	4-ClPh	80	98	<i>S</i>
(<i>R</i>)-M2-33	4-ClPh	67	97	<i>R</i>
(<i>S</i>)-M2-37	Fur-2-yl	75	98	<i>S</i>
(<i>R</i>)-M2-37	Fur-2-yl	75	98	<i>R</i>
(<i>S</i>)-M2-38	Thien-2-yl	76	98	<i>S</i>
(<i>R</i>)-M2-38	Thien-2-yl	76	98	<i>R</i>

^a Reactions were run under the conditions of entry 8 in Table 6.2, Synthesis of (*S*) and (*R*)-IVB-1 and (*S*)-IVB-4 [57]

^b Isolated yield

^c Determined by HPLC analysis

^d (*S*)-IVB-4 was confirmed by the crystal structure and others were determined by comparison with (*S*)-IVB-4 or comparison with literature data

**Fig. 6.3** Molecular structure of compound (*S*)-IVB-4

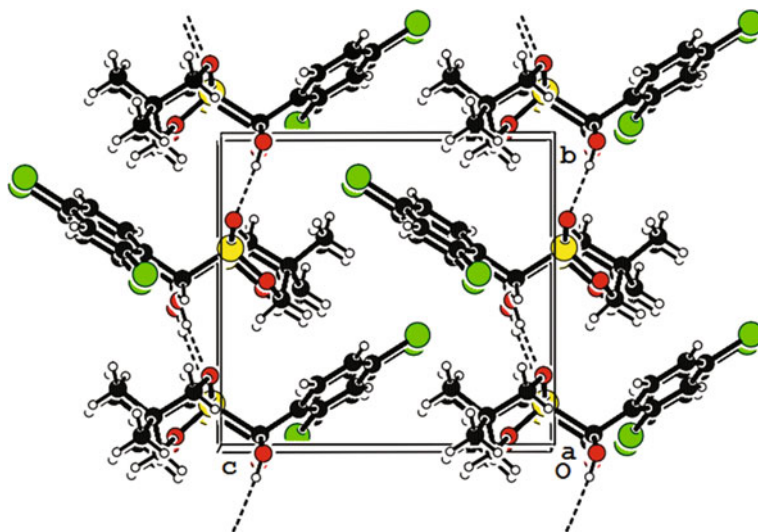


Fig. 6.4 Packing diagram of compound (*S*)-IVB-4

Table 6.4 Hydrogen bonds for compound (*S*)-IVB-4

<i>D</i> -H \cdots <i>A</i>	<i>D</i> -H	H \cdots <i>A</i>	<i>D</i> \cdots <i>A</i>	<i>D</i> -H \cdots <i>A</i>
O(1)-H(1) \cdots O(4) ⁱ	0.80(5)	1.89(5)	2.686(3)	173(4)

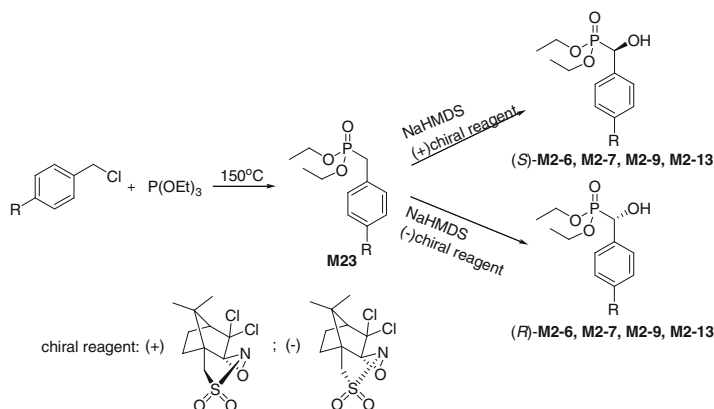
Symmetry code: (i) $-x + 2, y - 1/2, -z$

crystal, the cyclic dioxaphosphinane ring adopting a chair conformation and intermolecular O-H \cdots O hydrogen bonds (Table 6.4) links molecules into chains propagating along the *b* axis. The absolute configuration of (*S*)-IVB-4 was also confirmed as (*S*) [72].

6.1.3 Asymmetric Synthesis of 1-Hydroxyalkylphosphonates M2 via Hydroxylation

Oxaziridine-mediated hydroxylation of *O,O*-dialkyl benzylphosphonates was also reported to be applied to the synthesis of enantiomerically pure 1-hydroxy(phenyl)methylphosphonates, which is a stereoselective synthetic method with characteristics of simple operation and high efficiency [55, 56, 73].

Referring to the reported literatures [55, 56, 73], we attempted to prepare (*S*)-enantiomers of 1-hydroxy(substituted phenyl)methylphosphonates **M2** including **M2-6**, **M2-7**, **M2-9**, and **M2-13** by enantioselective hydroxylation. In this way, substituted benzyl chlorides and triethyl phosphite as starting materials via Arbuzov reaction[74] formed *O,O*-diethyl (substituted benzyl)phosphonates **M23**, which



Scheme 6.9 Asymmetric synthesis of 1-hydroxy(substituted phenyl)methylphosphonates **M2** via the enantioselective hydroxylation

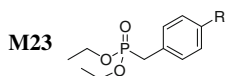
were further reacted with NaHMDS and chiral reagent, (+)-8,8-(dichlorocamphor) sulfonyloxaziridine, to give (*S*)-enantiomers of 1-hydroxy(substituted phenyl) methylphosphonates **M2** [55]. (*R*)-Enantiomers of 1-hydroxy(substituted phenyl) methylphosphonates **M2** could also be prepared under similar conditions by using chiral reagent (–)-8,8-(dichlorocamphor) sulfonyloxaziridine (Scheme 6.9).

Several *O,O*-diethyl (substituted benzyl)phosphonates **M23** as important intermediates were readily prepared from substituted benzyl chlorides and triethyl phosphite via Arbuzov reaction (Table 6.5) [74].

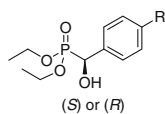
In order to improve the reaction rate and to increase the yield of compounds **M23**, an excess amount (two equivalents) of triethyl phosphite was used. The optimal reaction temperature was 150 °C and the reaction time should be extended to more than 3 h.

Several optically active 1-hydroxy(substituted benzyl)phosphonates **M2** including **M2-6**, **M2-7**, **M2-9**, and **M2-13** were prepared in high enantiomeric excess (*ee*) (Table 6.6). Enantiomeric purity was determined by the chiral HPLC analysis, and the absolute configuration of these products was established by comparing with literature data [75, 76].

Table 6.5 Structure and physicochemical data of *O,O*-diethyl (substituted benzyl)phosphonates



Compound	R	Appearance	Yield (%)
M23-1	H	Colorless oil	87
M23-2	4-Me	Colorless oil	85
M23-3	4-MeO	Colorless oil	80
M23-4	4-Cl	Colorless oil	80

Table 6.6 Structure and physicochemical data of 1-hydroxy(substituted phenyl)methylphosphonates **M2**

Compound	R	Appearance	Yield (%)	ee (%)
(S)- M2-6	H	Colorless oil	47	88
(R)- M2-6	H	Colorless oil	50	88
(S)- M2-7	4-Me	Colorless oil	49	90
(R)- M2-7	4-Me	Colorless oil	48	90
(S)- M2-9	4-OMe	Colorless oil	54	99
(R)- M2-9	4-OMe	Colorless oil	52	98
(S)- M2-13	4-Cl	Colorless oil	36	93
(R)- M2-13	4-Cl	Colorless oil	40	93

O,O-diethyl (substituted benzyl)phosphonates **M23** reacted with NaHMDS in THF at low temperature ($-78\text{ }^{\circ}\text{C}$) to generate phosphoryl-stabilized anions, which were further treated with (+) or (–)-8,8-(dichlorocamphor)sulfonyloxaziridine to produce (*S*) or (*R*) enantiomers of 1-hydroxy(substituted phenyl)methylphosphonates **M2** with yields of 36–54 %. However, (*S*) or (*R*) enantiomers of **M2** could be obtained in higher enantiomeric purity, with *ee* value of 88–99 % (Table 6.6).

The reactions were carried out at $-78\text{ }^{\circ}\text{C}$ under inert atmosphere with freshly distilled anhydrous solvents and avoided light. Two equivalents of oxaziridine were beneficial to yield of enantiomers of **M2**. Reaction time was a key factor affecting the stereoselective oxaziridine-mediated hydroxylation of *O,O*-dialkyl (substituted benzyl)phosphonates. Prolonging reaction time (>3 h) could result in the decrease of enantiomeric excess. Conversely, shortening reaction time (<3 h) might give a lower yield.

6.1.4 Summary

The base-catalyzed hydrophosphonylation of aldehydes as a convenient method is widely used for the synthesis of chiral 1-hydroxyalkylphosphonates. We have developed an efficient and stereoselective method for the synthesis of optically active 1-hydroxyalkylphosphonates and cyclic 1-hydroxyalkylphosphonates by asymmetric hydrophosphonylation using Al-Schiff base complexes as catalysts. The addition of silver carbonate was found to enhance this catalytic reaction rate significantly. Under optimized reaction conditions, several optically active cyclic 1-hydroxyalkylphosphonates **IVB** including (*S*) and (*R*) configuration could be prepared by the asymmetric hydrophosphonylation of aldehydes with corresponding cyclic phosphonates in 77–82 % yields with 99 % enantioselectivity. A series

of optically active 1-hydroxyalkylphosphonates **M2** including (*S*) and (*R*) configuration was further prepared by the asymmetric hydrophosphonylation of aldehydes with corresponding *O,O*-dimethylphosphonates in 67–83 % yields with 95–98 % enantioselectivity. Stereoselective oxaziridine-mediated hydroxylation of *O,O*-dialkyl benzylphosphonate was also applied to the synthesis of enantiomerically pure 1-hydroxybenzylphosphonates. Several optically active 1-hydroxy(substituted phenyl)methylphosphonates **M2** with 88–99 % enantioselectivity could be also prepared by the enantioselective hydroxylation of *O,O*-diethyl (substituted benzyl) phosphonates **M23**, using NaHMDS and chiral reagent (+) or (–)-8,8-(dichloro-camphor)sulfonyloxaziridine, but the yields of these optically active **M2** were in the range of 36–54 %, which were much lower than that of asymmetric hydrophosphonylation.

6.2 Optically Active (Substituted Phenyl) methylphosphonates **IA**, **IE** and **IF**

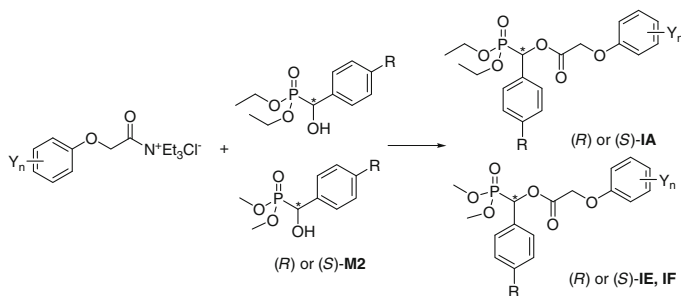
6.2.1 Introduction

As mentioned before, quite a few of *O,O*-dialkyl 1-(substituted phenoxyacetoxy) alkylphosphonates such as open-chain phosphonates **IA–IK** and cyclic phosphonates **IVA–IVF** as racemate have been synthesized in our laboratory. Some of these racemates in the **IA–IJ** and **IVC–IVE** series exhibited significant herbicidal activity. In order to examine the characteristics of two enantiomers of these racemates, we made an effort to set up an efficient synthetic method to prepare two enantiomers of these racemates including **IA–IJ** and **IVC–IVE** series.

At this stage, we made an effort to prepare two enantiomers of open-chain 1-(substituted phenoxyacetoxy)-1-(substituted phenyl)methylphosphonates **IA**, **IE** and **IF** series. The herbicidal activity of these optically active substituted benzyl phosphonates **IA**, **IE**, and **IF** were examined. In this section, the synthesis and herbicidal activity of optically active substituted benzylphosphonates **IA**, **IE** and **IF** are introduced. The structure-activity relationships of these optically active compounds together with their racemates are discussed.

6.2.2 Synthesis of Optically Active **IA**, **IE** and **IF**

Optically active substituted benzylphosphonates **IA**, **IE** and **IF** could be prepared by the condensation of substituted phenoxyacetyl chlorides **M5** and optically pure 1-hydroxy(substituted phenyl)methylphosphonates **M2** (Scheme 6.10). Substituted phenoxyacetyl chlorides **M5** could be easily synthesized starting from substituted phenols and bromoacetic acid ester [24, 77]. Optically active 1-hydroxy(substituted



Scheme 6.10 Synthesis of optically active 1-(substituted phenoxyacetoxy)alkylphosphonates **IA**, **IE** and **IF**

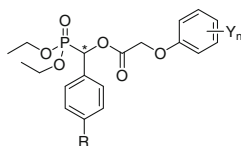
phenyl)methylphosphonates **M2** were prepared and confirmed according to the description in the Sect. 6.1.

It was found that optically active 1-hydroxyalkylphosphonates were easily racemized in strong base or acid medium. Therefore a Schotten-Baumann condition was chosen for the condensation of optically active 1-hydroxy (substituted phenyl)methylphosphonates and substituted phenoxyacetyl chlorides.

We also observed that target compounds **IA**, **IE** and **IF** containing carboxylic acid ester bonds were sensitive to acid, base or water, especially at higher temperatures. The preparation of optically active **IA**, **IE**, and **IF** required a control of moderate temperature, all reagents and solvents in this reaction needed to be pre-processed in anhydrous state. The preparation of optically active **IA**, **IE** and **IF** was carried out in three stages. First, a solution of substituted phenoxyacetyl chloride **M5** was added dropwise to the solution of optically active 1-hydroxy (substituted phenyl)methylphosphonates **M2** under 5 °C; Secondly, the reaction solution was stirred at room temperature for 2–4 h, and then for another 1–2 h at 40 °C under mild reaction conditions. In such a way, optically active **IA**, **IE** and **IF** could be conveniently obtained in good yield, and the *ee* value of enantiomers had no obvious decline compared with the *ee* value of **M2**.

Under this mild condition, the bond linked to chiral carbon in the molecular would not be cleaved, so the absolute configuration of the target compounds **IA**, **IE** and **IF** could remain the same configuration as intermediate 1-hydroxy(substituted phenyl)methylphosphonates **M2**.

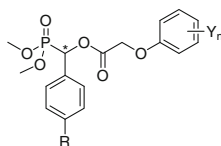
On the basis of the above experiment, three series of novel optically active *O,O*-dialkyl 1-(substituted phenoxyacetoxy)-1-(substituted phenyl)methylphosphonates **IA**, **IE** and **IF** including 78 (14 **IA**, 16 **IE** and 48 **IF**) optically active isomers were prepared successfully in high enantiomeric excess (*ee*) under the Schotten-Baumann

Table 6.7 Structure and enantiomeric purity of 1-(substituted phenoxyacetoxy)alkylphosphonates **IA**

Compound	R	Y _n	ee (%)
(<i>R</i>)- IA-13	H	2,4-Cl ₂	88
(<i>S</i>)- IA-13	H	2,4-Cl ₂	87
(<i>R</i>)- IA-14	Me	2,4-Cl ₂	87
(<i>S</i>)- IA-14	Me	2,4-Cl ₂	90
(<i>R</i>)- IA-21	Cl	2,4-Cl ₂	92
(<i>S</i>)- IA-21	Cl	2,4-Cl ₂	93
(<i>R</i>)- IA-25	MeO	2,4-Cl ₂	87
(<i>S</i>)- IA-25	MeO	2,4-Cl ₂	99
(<i>R</i>)- IA-26	Me	2-F,4-Cl	88
(<i>S</i>)- IA-26	Me	2-F,4-Cl	89
(<i>S</i>)- IA-27	Me	2-Cl,4-F	90
(<i>R</i>)- IA-28	Cl	2-Cl,4-F	90
(<i>S</i>)- IA-28	Cl	2-Cl,4-F	87
(<i>S</i>)- IA-29	MeO	2-Cl,4-F	99

conditions. The structures of optically active **IA**, **IE**, and **IF** are listed in Tables 6.7 and 6.8, respectively.

The enantiomeric purity of the products was determined by the chiral HPLC analysis on a chiral column. It should be noted that the enantiomeric excesses (*ee*) of **IA**, **IE**, and **IF** were reduced just a little compared with that of optically active 1-hydroxy(substituted phenyl)methylphosphonates **M2**. The absolute configurations of these optically active isomers originated from the configurations of optically active 1-hydroxy(substituted phenyl)methylphosphonates **M2**. The detailed synthetic procedure for the optically active isomers of **IA**, **IE**, and **IF** are introduced in Sect. 9.1.32 of Chap. 9.

Table 6.8 Structure and enantiomeric purity of 1-(substituted phenoxyacetoxy)alkylphosphonates **IE** and **IF**

Compound	R	Y _n	ee (%)	Compound	R	Y _n	ee (%)
(<i>R</i>)- IE-10	H	4-F	95	(<i>R</i>)- IF-13	MeO	4-F	96
(<i>S</i>)- IE-10	H	4-F	93	(<i>S</i>)- IF-13	MeO	4-F	99
(<i>R</i>)- IE-11	H	4-Cl	92	(<i>R</i>)- IF-14	MeO	4-Cl	96
(<i>S</i>)- IE-11	H	4-Cl	97	(<i>S</i>)- IF-14	MeO	4-Cl	99
(<i>R</i>)- IE-12	H	4-Br	95	(<i>R</i>)- IF-15	MeO	4-Br	95
(<i>S</i>)- IE-12	H	4-Br	92	(<i>S</i>)- IF-15	MeO	4-Br	99
(<i>R</i>)- IE-14	H	2-Me,4-Cl	97	(<i>R</i>)- IF-16	MeO	2-Me,4-Cl	96
(<i>S</i>)- IE-14	H	2-Me,4-Cl	96	(<i>S</i>)- IF-16	MeO	2-Me,4-Cl	96
(<i>R</i>)- IE-17	H	2,4-F ₂	92	(<i>R</i>)- IF-17	MeO	2,4-F ₂	95
(<i>S</i>)- IE-17	H	2,4-F ₂	92	(<i>S</i>)- IF-17	MeO	2,4-F ₂	93
(<i>R</i>)- IE-18	H	2-F,4-Cl	96	(<i>R</i>)- IF-18	MeO	2-F,4-Cl	96
(<i>S</i>)- IE-18	H	2-F,4-Cl	95	(<i>S</i>)- IF-18	MeO	2-F,4-Cl	96
(<i>R</i>)- IE-19	H	2-Cl,4-F	94	(<i>R</i>)- IF-19	MeO	2-Cl,4-F	96
(<i>S</i>)- IE-19	H	2-Cl,4-F	95	(<i>S</i>)- IF-19	MeO	2-Cl,4-F	96
(<i>R</i>)- IE-22	H	2,4-Cl ₂	96	(<i>R</i>)- IF-20	MeO	2,4-Cl ₂	96
(<i>S</i>)- IE-22	H	2,4-Cl ₂	96	(<i>S</i>)- IF-20	MeO	2,4-Cl ₂	95
(<i>R</i>)- IF-2	Me	4-F	96	(<i>R</i>)- IF-28	Cl	2-Me,4-Cl	96
(<i>S</i>)- IF-2	Me	4-F	95	(<i>S</i>)- IF-28	Cl	2-Me,4-Cl	96
(<i>R</i>)- IF-3	Me	4-Cl	95	(<i>R</i>)- IF-29	Cl	2-F,4-Cl	96
(<i>S</i>)- IF-3	Me	4-Cl	95	(<i>S</i>)- IF-29	Cl	2-F,4-Cl	96
(<i>R</i>)- IF-4	Me	4-Br	95	(<i>R</i>)- IF-30	Cl	2-Cl,4-F	95
(<i>S</i>)- IF-4	Me	4-Br	95	(<i>S</i>)- IF-30	Cl	2-Cl,4-F	96
(<i>R</i>)- IF-5	Me	2-Me,4-Cl	95	(<i>R</i>)- IF-31	Cl	2,4-Cl ₂	96
(<i>S</i>)- IF-5	Me	2-Me,4-Cl	96	(<i>S</i>)- IF-31	Cl	2,4-Cl ₂	95
(<i>R</i>)- IF-6	Me	2,4-F ₂	95	(<i>R</i>)- IF-62	NO ₂	2,4-F ₂	91
(<i>S</i>)- IF-6	Me	2,4-F ₂	99	(<i>S</i>)- IF-62	NO ₂	2,4-F ₂	90
(<i>R</i>)- IF-7	Me	2-F,4-Cl	95	(<i>R</i>)- IF-64	NO ₂	4-F	92
(<i>S</i>)- IF-7	Me	2-F,4-Cl	95	(<i>S</i>)- IF-64	NO ₂	4-F	92
(<i>R</i>)- IF-8	Me	2-Cl,4-F	95	(<i>R</i>)- IF-65	NO ₂	4-Cl	92
(<i>S</i>)- IF-8	Me	2-Cl,4-F	96	(<i>S</i>)- IF-65	NO ₂	4-Cl	94
(<i>R</i>)- IF-9	Me	2,4-Cl ₂	95	(<i>R</i>)- IF-66	NO ₂	4-Br	91
(<i>S</i>)- IF-9	Me	2,4-Cl ₂	96	(<i>S</i>)- IF-66	NO ₂	4-Br	92

6.2.3 Herbicidal Activity of Optically Active IA, IE and IF

As stated in Chap. 2, some chiral 1-(substituted phenoxyacetoxy)alkylphosphonates **IA**, **IE**, and **IF** exhibited significant post-emergence herbicidal activity against dicotyledons, but the examination of herbicidal activity was only limited their racemic forms. It would be very interesting to examine the contribution of optical active isomers in their herbicidal activity.

In order to explore the possible difference between two enantiomers in herbicidal activity, a set of experiments was performed to evaluate optically active 1-(substituted phenoxyacetoxy)alkylphosphonates **IA**, **IE**, and **IF**. The herbicidal bioassay was carried out according to the method mentioned in Chap. 9. The influences of molecular chirality on herbicidal activity are discussed as follows.

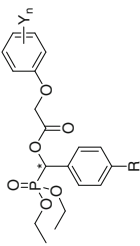
6.2.3.1 Herbicidal Activity of Optically Active 1-(Substituted Phenoxyacetoxy)alkylphosphonates IA

SAR analysis for racemic 1-(substituted phenoxyacetoxy)alkylphosphonates **IA**, **IE**, and **IF** showed the position, type, and number of substituents Y_n on the phenoxy-benzene ring had significant effect on herbicidal activity. These racemic compounds with 2-Cl,4-F, 2,4-Cl₂ or 2-Me,4-Cl as Y_n exhibited significant herbicidal activity against tested dicotyledons for post-emergence application. At this stage, 20 of *O,O*-diethyl 1-(substituted phenoxyacetoxy)-1-(substituted phenyl) methylphosphonates **IA** including their racemate, (*R*) and (*S*) isomers, were prepared to test their herbicidal activity. In their parent structure **Io**, Et as R^1 and R^2 , substituted benzyl as R^3 were kept, substituents Y_n on the phenoxy-benzene ring were limited to 2-Cl,4-F; 2-F,4-Cl; 2,4-Cl₂ or 2-Me,4-Cl, further examination was focused on the effect of (*R*) and (*S*) isomers on herbicidal activity.

The enantiomers of these **IA** including their racemate were evaluated for their herbicidal activity at different rates in the greenhouse. They were tested for pre-emergence and post-emergence herbicidal activity against chingma abutilon (*Abutilon theophrasti*), common amaranth (*Amaranthus retroflexus*), China ixeris (*Ixeris chinensis*), leaf mustard (*Brassica juncea*), and white eclipta (*Eclipta prostrate*) at different rates. In this bioassay, clacyfos (HW02, **IC-22**) was used as a positive control. The results are summarized in Tables 6.9, 6.10 and 6.11.

(A) Pre-emergence herbicidal activity of optically active compounds IA

The results for pre-emergence herbicidal activity of several 1-substituted benzylphosphonates **IA** are listed in Table 6.9. **IA-13**, **IA-14**, **IA-21**, and **IA-25** including their racemates, (*R*) and (*S*) optically active isomers, showed a certain pre-emergence inhibitory activity against common amaranth, China ixeris, and chingma abutilon at 450 g ai/ha, but almost no pre-emergence activity at 150 g ai/ha. The pre-emergence herbicidal activity of all optically active 1-substituted benzylphosphonates including **IA-13**, **IA-14**, **IA-21**, and **IA-25** and their racemates in Table 6.9

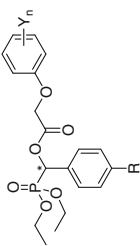
Table 6.9 Structure and pre-emergence herbicidal activity of 1-(substituted phenoxyacetoxy)alkylphosphonates IA^a

Compound	R	Y _n	Amr ^b		Abu ^b		Ixe ^b	
			450 g ai/ha	150 g ai/ha	450 g ai/ha	150 g ai/ha	450 g ai/ha	150 g ai/ha
<i>rac</i> -IA-13	H	2,4-Cl ₂	96	10	25	0	51	0
(<i>R</i>)-IA-13			88	71	55	0	65	0
(<i>S</i>)-IA-13			70	0	56	0	50	0
<i>rac</i> -IA-14	Me	2,4-Cl ₂	87	0	14	0	74	0
(<i>R</i>)-IA-14			77	53	28	0	67	0
(<i>S</i>)-IA-14			92	59	27	0	71	7
<i>rac</i> -IA-21	Cl	2,4-Cl ₂	84	0	61	48	78	0
(<i>R</i>)-IA-21			18	5	35	0	54	0
(<i>S</i>)-IA-21			29	0	30	23	30	0
<i>rac</i> -IA-25	MeO	2,4-Cl ₂	80	59	15	0	17	7
(<i>R</i>)-IA-25			49	0	16	0	66	0
(<i>S</i>)-IA-25			67	0	24	18	80	0
Clacyfos			90	81	69	8	100	95

^a Inhibitory potency (%) against the growth of plants in the greenhouse, 0 (no effect), 100 % (completely kill)

^b Amr: common amaranth; Abu: chingma abutilon; Ixe: China ixeris

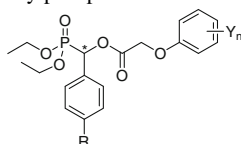
Table 6.10 Structure and post-emergence herbicidal activity of 1-(substituted phenoxyacetoxy)alkylphosphonates **IA**^a



Compound	R	Y _n	Amr ^b		Abu ^b		Ixe ^b	
			450 g ai/ha	150 g ai/ha	450 g ai/ha	150 g ai/ha	450 g ai/ha	150 g ai/ha
<i>rac</i> - IA-13	H	2,4-Cl ₂	100	96	100	50	89	79
(<i>R</i>)- IA-13			100	100	100	90	98	94
(<i>S</i>)- IA-13			100	96	100	54	92	88
<i>rac</i> - IA-14	Me	2,4-Cl ₂	100	96	100	39	96	96
(<i>R</i>)- IA-14			100	100	100	66	98	92
(<i>S</i>)- IA-14			100	100	99	53	93	86
<i>rac</i> - IA-21	Cl	2,4-Cl ₂	100	82	100	36	93	86
(<i>R</i>)- IA-21			100	90	68	35	92	74
(<i>S</i>)- IA-21			100	100	96	25	95	91
<i>rac</i> - IA-25	MeO	2,4-Cl ₂	100	100	90	53	89	86
(<i>R</i>)- IA-25			100	94	95	25	96	85
(<i>S</i>)- IA-25			100	88	91	36	96	84
Clacufos			100	100	100	100	100	95

^a Inhibitory potency (%) against the growth of plants in the greenhouse, 0 (no effect), 100 % (completely kill)

^b Amr: common amaranth; Abu: chingma abutilon; Ixe: China ixeris

Table 6.11 Structure and post-emergence herbicidal activity of 1-(substituted phenoxyacetoxy) alkylphosphonates **IA**^a

Compound	R	Y _n	Amr ^b	Abu ^b	Brj ^b	Ecl ^b
			150 g ai/ha	150 g ai/ha	150 g ai/ha	150 g ai/ha
<i>rac</i> - IA-26	Me	2-F, 4-Cl	90	75	85	70
(<i>R</i>)- IA-26			95	80	95	80
(<i>S</i>)- IA-26			95	95	95	85
<i>rac</i> - IA-28	Cl	2-Cl, 4-F	90	75	85	70
(<i>R</i>)- IA-28			90	95	95	80
(<i>S</i>)- IA-28			100	100	100	95
<i>rac</i> - IA-29	OMe	2-Cl, 4-F	100	75	80	80
(<i>S</i>)- IA-29			70	70	70	70
Clacyfos			85	90	85	85

^a Inhibitory potency (%) against the growth of plants in the greenhouse, 0 (no effect), 100 % (completely kill)

^b Amr: common amaranth; Abu: chingma abutilon; Brj: leaf mustard; Ecl: white eclipta

was much lower than that of racemic clacyfos (HW02, **IC-22**). It was found that (*R*)-**IA-13** exhibited 71 % pre-emergence activity against common amaranth, but (*S*)-**IA-13** had no pre-emergence activity at 150 g ai/ha. However, there was no significant difference in herbicidal activity between (*R*) and (*S*) isomers for other tested compounds.

(B) Post-emergence herbicidal activity of optically active compounds **IA**

The results for post-emergence herbicidal activity of several 1-substituted benzylphosphonates **IA** are listed in Tables 6.10 and 6.11. As seen from Table 6.10, **IA-13**, **IA-14**, **IA-21**, and **IA-25** including their racemate, (*R*) and (*S*) optically active isomers, exhibited excellent post-emergence herbicidal activity against common amaranth and China ixeris at the rates of 450 and 150 g ai/ha, respectively. These compounds also exhibited good post-emergence herbicidal activity against chingma abutilon at 450 g ai/ha. Several 1-substituted benzylphosphonates **IA-26**, **IA-28**, **IA-29** including their racemate, (*R*) and (*S*) optically active isomers in Table 6.11, exhibited significant post-emergence herbicidal activity against leaf mustard, chingma abutilon, common amaranth and white eclipta at 150 g ai/ha.

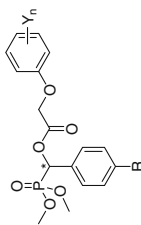
A certain difference in herbicidal effect among racemate, (*R*) and (*S*) optically active isomers, of some compounds **IA** could be observed. Between the two enantiomers of **IA-13**, (*R*) isomer showed higher post-emergence inhibitory potency against chingma abutilon than that of (*S*) isomer. (*R*)-**IA-14** showed little higher post-emergence inhibitory potency against China ixeris and chingma

abutilon than that of (*S*)-**IA-14**. However for compound **IA-21**, (*S*) isomer exhibited higher post-emergence inhibitory potency against common amaranth and China ixeris than that of (*R*) isomer (Table 6.10). It was noticed that the (*S*) isomer of **IA-28** exhibited little higher post-emergence inhibitory potency against four tested plants than that of (*R*) isomer and racemate (Table 6.11). Especially, the (*S*) isomer of **IA-28** displayed 95-100 % inhibitory potency for post-emergence application, it had higher post-emergence inhibitory potency than that of its racemate (70–90 %) and racemic clacyfos (85–90 %). The (*S*) isomer of **IA-26** also exhibited higher post-emergence inhibitory potency against four tested plants than that of its racemate (Table 6.11). Moreover, the (*R*) isomer of **IA-13** exhibited higher post-emergence inhibitory potency against chingma abutilon and China ixeris than that of its racemate and (*S*) isomer (Table 6.10). Through above study, optically active isomer (*S*)-**IA-28** with Et as R¹ and R², 4-CiPh as R³, 2-Cl,4-F as Y_n was found to be the most effective compound against broadleaf for post-emergence application among tested compounds **IA**.

6.2.3.2 Herbicidal Activity of Optically Active Compounds **IE** and **IF**

At this stage, 96 of *O,O*-dimethyl 1-(substituted phenoxyacetoxy)-1-substituted benzylphosphonates **IE** and **IF** including their racemates, (*R*) and (*S*) isomers were prepared to test their herbicidal activity. In their parent structure, Me as R¹ and R², substituted benzyl as R³ were kept, 2-Cl,4-F, 2,4-Cl₂, 2-Me,4-Cl or other substituents as Y_n on the phenoxy-benzene ring, further examination was focused on the effect of (*R*) and (*S*) isomers on herbicidal activity. The enantiomers of these compounds **IE** and **IF** including their racemate were divided into several groups to evaluate their herbicidal activity at different rates in the greenhouse. They were tested for post-emergence herbicidal activity against leaf mustard (*Brassica juncea*), chingma abutilon (*Abutilon theophrasti*), common amaranth (*Amaranthus retroflexus*) and white eclipta (*Eclipta prostrata*). The results are listed in Tables 6.12 and 6.13.

As seen from Tables 6.12 and 6.13, the change of substituents Y_n on the phenoxy-benzene ring in optically active 1-(substituted phenoxyacetoxy)alkylphosphonates **IE** and **IF** had significant effect on herbicidal activity. One or both enantiomers of most optically active 1-(substituted phenoxyacetoxy)alkylphosphonates **IE** and **IF** with 2-Cl,4-F; 2,4-Cl₂; 2-Me,4-Cl as Y_n exhibited >90 % post-emergence inhibitory potency against leaf mustard, chingma abutilon, common amaranth, and white eclipta at 450 g ai/ha. Most optically active 1-(substituted phenoxyacetoxy)alkylphosphonates **IE** and **IF** with 2-F,4-Cl as Y_n only had 50–80 % post-emergence inhibitory potency against tested plants at 450 g ai/ha (Table 6.12). When the rate decreased to 150 g ai/ha, the inhibitory potency of some optically active 1-(substituted phenoxyacetoxy)alkylphosphonates **IE** and **IF** also decreased. Several enantiomers still exhibited excellent post-emergence herbicidal activity at 150 g ai/ha, such as (*R*)-**IF-5** with 4-MePh as R³, 2-Me,4-Cl as Y_n, (*R*)-**IF-8** and (*S*)-**IF-8** with 4-MePh as R³, 2-Cl,4-F as Y_n. Especially (*R*)-**IF-8** showed

Table 6.12 Structure and post-emergence herbicidal activity of 1-(substituted phenoxyacetoxy)alkylphosphonates IE and IF^a

Compound	R	Y _n	Amr ^b		Abu ^b		Brj ^b		Ecl ^b	
			450 g ai/ha	150 g ai/ha	450 g ai/ha	150 g ai/ha	450 g ai/ha	150 g ai/ha	450 g ai/ha	150 g ai/ha
<i>rac</i> -IE-14	H	2-Me,4-Cl	90	75	90	80	90	80	85	70
(<i>R</i>)-IE-14			100	80	100	85	100	85	100	60
(<i>S</i>)-IE-14			90	75	100	85	100	85	90	60
<i>rac</i> -IE-18	H	2-F,4-Cl	75	70	75	70	75	75	75	70
(<i>R</i>)-IE-18			80	60	70	70	75	75	90	60
(<i>S</i>)-IE-18			80	60	70	60	75	60	75	60
<i>rac</i> -IF-7	Me	2-F,4-Cl	60	50	75	70	75	70	60	60
(<i>R</i>)-IF-7			70	50	70	50	70	50	70	70
(<i>S</i>)-IF-7			70	60	70	60	70	60	80	60
<i>rac</i> -IF-16	OMe	2-Me,4-Cl	90	80	75	60	100	90	90	80
(<i>R</i>)-IF-16			90	70	75	60	95	80	90	75
(<i>S</i>)-IF-16			95	75	75	70	100	90	90	70
<i>rac</i> -IF-18	OMe	2-F,4-Cl	70	50	60	50	100	100	75	60
(<i>R</i>)-IF-18			70	60	70	70	100	100	80	70
(<i>S</i>)-IF-18			70	60	75	50	95	85	80	60
<i>rac</i> -IF-19	OMe	2-Cl,4-F	100	75	95	85	85	80	95	80
(<i>R</i>)-IF-19			100	80	100	80	90	80	100	75
(<i>S</i>)-IF-19			80	75	95	80	90	75	90	75

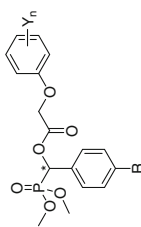
(continued)

Table 6.12 (continued)

Compound	R	Y _n	Amr ^b		Abu ^b		Brij ^b		Ecl ^b	
			450 g ai/ha	150 g ai/ha	450 g ai/ha	150 g ai/ha	450 g ai/ha	150 g ai/ha	450 g ai/ha	150 g ai/ha
<i>rac</i> - IF-28	Cl	2-Me,4-Cl	95	85	90	75	95	80	85	70
<i>(R)</i> - IF-28			100	90	90	75	95	90	90	85
<i>(S)</i> - IF-28			95	85	75	70	90	85	90	70
<i>rac</i> - IF-29	Cl	2-F,4-Cl	70	60	60	50	75	70	70	60
<i>(R)</i> - IF-29			75	60	60	60	75	70	70	60
<i>(S)</i> - IF-29			70	60	60	50	75	70	60	60

^a Inhibitory potency (%) against the growth of plants in the greenhouse, 0 (no effect), 100 % (completely kill)

^b Amr: common amaranth; Abu: chingma abutilon. Brij: leaf mustard; Ecl: white eclipta

Table 6.13 Structure and post-emergence herbicidal activity of 1-(substituted phenoxyacetoxy)alkylphosphonates IE and IF^a

Compound	R	Y _n	Amr ^b			Abu ^b			Brj ^b			Ecl ^b		
			450 g ai/ha	150 g ai/ha	85 g ai/ha	450 g ai/ha	150 g ai/ha	90 g ai/ha	450 g ai/ha	150 g ai/ha	90 g ai/ha	450 g ai/ha	150 g ai/ha	90 g ai/ha
<i>rac</i> -IE-19	H	2-Cl,4-F	80	85	90	90	90	100	100	90	90	90	80	
(<i>R</i>)-IE-19			95	90	80	75	100	100	100	80	95	70		
(<i>S</i>)-IE-19			100	80	100	100	100	100	100	90	100	75		
<i>rac</i> -IE-22	H	2,4-Cl ₂	100	80	90	80	100	100	100	90	100	80		
(<i>R</i>)-IE-22			90	80	90	85	100	100	100	80	95	75		
(<i>S</i>)-IE-22			75	70	75	60	90	90	90	85	80	60		
<i>rac</i> -IF-5	Me	2-Me,4-Cl	100	80	90	70	100	100	100	85	95	85		
(<i>R</i>)-IF-5			100	100	95	90	100	100	100	100	100	90		
(<i>S</i>)-IF-5			100	90	85	70	100	100	100	90	85	80		
<i>rac</i> -IF-8	Me	2-Cl,4-F	100	95	90	90	100	100	100	90	95	80		
(<i>R</i>)-IF-8			100	100	100	100	100	100	100	100	100	100		
(<i>S</i>)-IF-8			100	100	100	100	100	100	100	100	95	90		
<i>rac</i> -IF-9	Me	2,4-Cl ₂	90	80	90	75	100	100	100	90	85	80		
(<i>R</i>)-IF-9			100	90	85	75	100	100	100	100	85	75		
(<i>S</i>)-IF-9			100	90	90	70	100	100	100	95	100	90		
<i>rac</i> -IF-20	OMe	2,4-Cl ₂	95	85	95	95	100	100	100	95	70	80		
(<i>R</i>)-IF-20			100	100	100	95	100	100	100	100	100	80		
(<i>S</i>)-IF-20			95	85	95	80	100	100	100	95	85	80		

(continued)

Table 6.13 (continued)

Compound	R	Y _n	Amr ^b		Abu ^b		Brij ^b		Ecl ^b	
			450 g ai/ha	150 g ai/ha	450 g ai/ha	150 g ai/ha	450 g ai/ha	150 g ai/ha	450 g ai/ha	150 g ai/ha
<i>rac</i> - IF-30	Cl	2-Cl,4-F	90	95	90	90	100	90	85	75
(<i>R</i>)- IF-30			100	95	100	95	100	95	95	80
(<i>S</i>)- IF-30			95	80	100	80	100	95	80	70
<i>rac</i> - IF-31	Cl	2,4-Cl ₂	100	85	95	95	100	95	90	85
(<i>R</i>)- IF-31			100	85	100	100	100	100	90	75
(<i>S</i>)- IF-31			100	90	100	60	90	100	95	80

^a Inhibitory potency (%) against the growth of plants in the greenhouse, 0 (no effect), 100 % (completely kill)

^b Amr: common amaranth; Abu: chingma abutilon. Brij: leaf mustard; Ecl: white eclipta

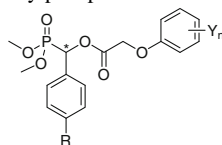
100 % inhibitory potency against all tested plants. Both (*R*) and (*S*) enantiomers of **IF-8** had similar high activity at 150 g ai/ha, and (*R*)-**IF-8** seems to had higher activity than that of its racemate and (*S*)-**IF-8** against white eclipta (Table 6.13).

There was no significant difference in herbicidal effect between (*R*) and (*S*) enantiomers for most 1-(substituted phenoxyacetoxy)alkylphosphonates **IE** and **IF** in Tables 6.12 and 6.13. However, a certain difference in herbicidal effect among racemate, (*R*) and (*S*) optically active isomers could be observed. A chiral selection in inhibitory potency against chingma abutilon between (*R*) and (*S*) enantiomers of **IE-19**, **IE-22**, **IF-5**, **IF-20**, **IF-30** and **IF-31** could be observed. Enantiomer (*R*)-**IF-5** had higher activity than that of its (*S*) enantiomer and racemate. (*R*)-**IF-31** exhibited 100 % inhibitory potency against chingma abutilon, but (*S*)-**IF-31** had only 60 % inhibitory potency at 150 g ai/ha. It was further observed at a rate of 75 g ai/ha that (*R*)-**IF-31** could achieve 100, 100, 90, and 80 % inhibitory potency against leaf mustard, chingma abutilon, common amaranth, and white eclipta, whereas (*S*)-**IF-31** only had 0, 30, 40, and 40 % inhibitory potency against four tested plants, respectively. It was one of the few compounds which were found to have a significant difference in herbicidal effect between its two enantiomers. Particularly, (*R*)-**IF-31** has outstanding herbicidal activity.

A series of optically active 1-(substituted phenoxyacetoxy)alkylphosphonates **IE** and **IF** with 4-F;4-Cl;4-Br and 2,4-F₂ as Y_n was also prepared to test their herbicidal activity. These optically active **IE** and **IF** including their racemate, (*R*) and (*S*) enantiomers, were tested for post-emergence herbicidal activity against Asia minor bluegrass (*Polypogon fugax*), American sloughgrass (*Beckmannia syzigachne*), annual bluegrass (*Poa annua*), small goosefoot (*Chenopodium serotinum*), leaf mustard (*Brassica juncea*), and chickweed (*Stellaria media*) at a rate of 150 g ai/ha. In this bioassay, 2,4-D was used as a positive control. The results are listed in Table 6.14.

As seen from Table 6.14, most of the tested compounds **IE** and **IF** had no activity against monocotyledons weeds, including Asia minor bluegrass, American sloughgrass, and annual bluegrass at 150 g ai/ha. Most optically active **IE** and **IF** in Table 6.14 showed 60–80 % inhibitory activity against dicotyledonous plants, including small goosefoot, leaf mustard, and chickweed at the same rate, only (*R*)-**IF-14** could exhibit 90 and 100 % inhibitory activity against leaf mustard and chickweed. The above observations showed the compounds **IE** and **IF** with 4-F; 4-Cl; 4-Br, and 2,4-F₂ as Y_n had lower inhibitory activity against dicotyledonous plants than that of these compounds **IE** and **IF** with 2-Cl,4-F; 2,4-Cl₂; 2-Me,4-Cl as Y_n.

No significant chiral selectivity was observed for most tested compounds **IE** and **IF** in Table 6.14, only (*R*) and (*S*) enantiomer of **IF-14** showed significant different inhibitory activity against leaf mustard and chickweed. (*R*)-**IF-14** exhibited 90–100 % inhibitory activity against leaf mustard and chickweed, but (*S*)-**IF-14** and its racemate only had 60–70 % inhibitory activity. **IE-10** and **IF-4** also seemed to have a certain chiral selectivity in inhibitory activity against chickweed. In order to make sure of their chiral selectivity in inhibitory activity, the (*R*) and

Table 6.14 Structure and post-emergence herbicidal activity of 1-(substituted phenoxyacetoxy) alkylphosphonates **IE** and **IF**^a

Compound	R	Y _n	150 g ai/ha					
			Pof ^b	Bec ^b	Poa ^b	Chs ^b	Brj ^b	Stm ^b
<i>rac</i> - IE-10	H	4-F	60	60	0	90	85	100
(<i>R</i>)- IE-10			70	30	0	70	70	90
(<i>S</i>)- IE-10			40	30	0	70	75	80
<i>rac</i> - IE-11	H	4-Cl	0	0	0	70	70	80
(<i>R</i>)- IE-11			0	0	0	75	70	75
(<i>S</i>)- IE-11			0	0	0	70	70	70
<i>rac</i> - IE-12	H	4-Br	0	0	0	75	75	80
(<i>R</i>)- IE-12			40	60	20	75	70	80
(<i>S</i>)- IE-12			0	20	0	70	70	70
<i>rac</i> - IE-17	H	2,4-F ₂	0	0	0	70	70	70
(<i>R</i>)- IE-17			30	30	0	70	75	80
(<i>S</i>)- IE-17			40	40	0	70	70	90
<i>rac</i> - IF-2	Me	4-F	30	0	0	75	75	70
(<i>R</i>)- IF-2			50	0	0	70	70	80
(<i>S</i>)- IF-2			40	0	0	70	70	70
<i>rac</i> - IF-3	Me	4-Cl	0	0	20	75	85	70
(<i>R</i>)- IF-3			0	0	0	80	75	80
(<i>S</i>)- IF-3			0	0	0	80	80	85
<i>rac</i> - IF-4	Me	4-Br	40	40	30	80	85	70
(<i>R</i>)- IF-4			0	0	0	80	75	85
(<i>S</i>)- IF-4			0	40	0	80	80	100
<i>rac</i> - IF-6	Me	2,4-F ₂	30	30	30	60	60	60
(<i>R</i>)- IF-6			50	40	0	75	75	80
(<i>S</i>)- IF-6			40	0	0	75	70	70
<i>rac</i> - IF-13	OMe	4-F	30	0	0	60	60	60
(<i>R</i>)- IF-13			30	20	0	65	70	75
(<i>S</i>)- IF-13			60	40	0	70	70	75
<i>rac</i> - IF-14	OMe	4-Cl	0	0	0	70	70	60
(<i>R</i>)- IF-14			0	0	0	70	90	100
(<i>S</i>)- IF-14			0	0	0	70	70	60
<i>rac</i> - IF-15	OMe	4-Br	40	0	0	70	70	70
(<i>R</i>)- IF-15			0	60	0	70	80	75
(<i>S</i>)- IF-15			0	0	0	70	70	70
<i>rac</i> - IF-17	OMe	2,4-F ₂	0	0	0	60	70	60

(continued)

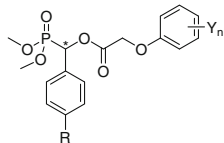
Table 6.14 (continued)

Compound	R	Y _n	150 g ai/ha					
			Pof ^b	Bec ^b	Poa ^b	Chs ^b	Brj ^b	Stm ^b
(<i>R</i>)- IF-17			0	0	0	75	75	70
(<i>S</i>)- IF-17			0	0	0	60	70	75
<i>rac</i> - IF-62	NO ₂	2,4-F ₂	0	0	0	60	60	60
(<i>R</i>)- IF-62			40	30	0	75	75	70
(<i>S</i>)- IF-62			0	0	0	60	60	60
<i>rac</i> - IF-64	NO ₂	4-F	50	40	0	70	60	70
(<i>R</i>)- IF-64			0	0	0	60	60	60
(<i>S</i>)- IF-64			0	0	0	50	60	60
<i>rac</i> - IF-65	NO ₂	4-Cl	0	0	0	60	60	70
(<i>R</i>)- IF-65			0	0	0	60	75	70
(<i>S</i>)- IF-65			0	0	0	70	75	70
<i>rac</i> - IF-66	NO ₂	4-Br	0	0	0	70	70	70
(<i>R</i>)- IF-66			0	0	0	70	70	70
(<i>S</i>)- IF-66			30	30	20	60	60	60
2,4-D			40	40	20	80	95	90

^a Inhibitory potency (%) against the growth of plants in the greenhouse, 0 (no effect), 100 % (completely kill)

^b Pof: Asia minor bluegrass; Bec: American sloughgrass; Poa: annual bluegrass; Chs: small goosefoot; Brj: leaf mustard; Stm: chickweed

(*S*) enantiomers of **IE-10**, **IF-4** and **IF-14** were selected for further bioassay to examine 50 % effective against chickweed (ED₅₀). The results are listed in Table 6.15.

Table 6.15 ED₅₀ of optically active **IE-10**, **IF-4** and **IF-14** against chickweed

Compound	R	Y _n	Regression equation	Related coefficient	ED ₅₀ (g ai/ha) ^a
(<i>R</i>)- IE-10	H	4-F	$Y = 41.95 + 17.14\ln X$	0.9487	24.0
(<i>S</i>)- IE-10			$Y = 29.62 + 26.02\ln X$	0.9600	32.9
(<i>R</i>)- IF-4	Me	4-Br	$Y = 28.39 + 8.38\ln X$	0.9516	197.7
(<i>S</i>)- IF-4			$Y = 41.13 + 21.04\ln X$	0.9407	22.8
(<i>R</i>)- IF-14	OMe	4-Cl	$Y = 35.43 + 12.68\ln X$	0.9214	47.4
(<i>S</i>)- IF-14			$Y = 26.76 + 12.07\ln X$	0.9345	102.9

^a ED₅₀ (g ai/ha) is effective dose that provides 50 % inhibition against the growth of chickweed

From the data of ED₅₀ in Table 6.15, we can see that **IE-10** showed different inhibitory activity between two enantiomers, the inhibitory activity of (*R*)-**IE-10** was 1.37 times higher than (*S*)-**IE-10**. We found **IF-4** and **IF-14** showed significant chiral selectivity in inhibitory activity against chickweed. The inhibitory activity of (*R*)-**IF-14** was 2.17 times higher than (*S*)-**IF-14**. (*S*)-**IF-4** with ED₅₀ of 22.8 g ai/ha, as a most effective enantiomer was found and its inhibitory activity was 8.17 times higher than (*R*)-**IF-4**. (*S*)-**IF-4** as a representative optically active isomer will be further examined. It could be noticed that the inhibitory activity of (*S*) configuration of **IF-4** was more effective than that of its (*R*) configuration, but the (*R*) configuration of **IE-10** and **IF-14** were more effective than their (*S*) configuration. These observations showed that different chiral 1-(substituted phenoxyacetoxy)alkylphosphonates **IE** and **IF** had a different relationship of absolute configuration and herbicidal activity.

6.2.4 Summary

We made an effort to set up a synthetic method for the preparation of two enantiomers of chiral 1-(substituted phenoxyacetoxy)alkylphosphonates by the condensation of substituted phenoxyacetyl chlorides **M5** and optically pure 1-hydroxy-1-(substituted benzyl)phosphonates **M2**. At this stage, three series of novel *O,O*-dialkyl 1-(substituted phenoxyacetoxy)-1-(substituted phenyl)methylphosphonates **IA**, **IE**, and **IF** including 78 (14 **IA**, 16 **IE** and 48 **IF**) optically active isomers were successfully prepared in higher enantiomeric excess (*ee*) under the Schotten-Baumann conditions. The structures of these optically active compounds were characterized by ¹H and ¹³C NMR, IR, and MS, and were confirmed by elementary analysis. The absolute configurations of these optically active products **IA**, **IE**, and **IF** originated from the configurations of optically active reactant, 1-hydroxy(substituted phenyl)methylphosphonates **M2**. The enantiomeric excesses (*ee*) of **IA**, **IE**, and **IF** were reduced just a little compared with those of chiral 1-hydroxy(substituted phenyl)methylphosphonates **M2**.

The herbicidal activity of optically active *O,O*-dialkyl 1-(substituted phenoxyacetoxy)-1-(substituted phenyl)methylphosphonates **IA**, **IE** and **IF** including 116 racemates, (*R*) and (*S*) enantiomers, were evaluated in greenhouse. The examination was focused on the effect of (*R*) and (*S*) isomers on herbicidal activity.

O,O-diethyl 1-(substituted phenoxyacetoxy)-1-(substituted phenyl)methylphosphonates **IA-13**, **IA-14**, **IA-21**, **IA-25**, **IA-26**, **IA-28**, and **IA-29** including their racemates, (*R*) and (*S*) enantiomers, were examined for pre- and post-emergence herbicidal activity. It was found that (*R*)-**IA-13** exhibited 71 % pre-emergence inhibitory activity, but (*S*)-**IA-13** exhibited no activity at 150 g ai/ha. These optically active enantiomers of **IA-13**, **IA-14**, **IA-21**, **IA-25** and their racemates showed much lower pre-emergence inhibitory activity than that of racemic clacyfos (HW02, **IC-22**). All these optically active enantiomers and their racemates exhibited significant post-emergence inhibitory effect against broadleaf plants at 150 g ai/ha.

A certain difference in post-emergence herbicidal effect could be observed among racemates, (*R*) and (*S*) enantiomers of **IA-13**, **IA-14**, **IA-21**, **IA-26**, and **IA-28**. It was found that (*S*) isomer of **IA-28** displayed 95–100 % post-emergence inhibitory potency against four tested plants, which was higher than that of its racemate (70–90 %) and racemic clacyfos (85–90 %). The (*S*) isomer of **IA-26** also exhibited higher post-emergence inhibitory potency against four tested plants than that of its racemate. The (*S*)-**IA-28** with Et as R¹ and R², 4-ClPh as R³, 2-Cl,4-F as Y_n was found to be the most effective compound against broadleaf for post-emergence application among tested compounds **IA**.

Ninety-six of *O,O*-dimethyl 1-(substituted phenoxyacetoxy)-1-(substituted phenyl)methylphosphonates **IE** and **IF** including their racemates, (*R*) and (*S*) enantiomers were tested for their post-emergence herbicidal activity. One or both enantiomers of optically active 1-(substituted phenoxyacetoxy)alkylphosphonates **IE** and **IF** with 2-Cl,4-F, 2,4-Cl₂, 2-Me,4-Cl as Y_n exhibited >90 % post-emergence inhibitory potency at 450 g ai/ha. However, most optically active **IE** and **IF** with 2-F,4-Cl as Y_n only had 50–80 % post-emergence inhibitory potency against tested plants. The substituent R in phenyl had almost no effect on their herbicidal activity. Several enantiomers such as (*R*)-**IF-5**, (*R*)-**IF-8**, and (*S*)-**IF-8** exhibited excellent herbicidal activity at 150 g ai/ha, especially (*R*)-**IF-8** showed 100 % inhibitory potency against all tested plants. Both (*R*) and (*S*) enantiomers of **IF-8** with Me as R¹ and R², 4-MePh as R³, 2-Cl,4-F as Y_n had similar high activity at 150 g ai/ha, but both had higher activity than that of its racemate.

No significant chiral selectivity was observed for most tested compounds **IE** and **IF**. A certain difference in herbicidal effect among racemate, (*R*) and (*S*) enantiomers could be observed. A chiral selection in inhibitory potency against plant could be observed between (*R*) and (*S*) enantiomers of **IF-4**, **IE-10**, **IE-19**, **IE-22**, **IF-5**, **IF-14**, **IF-20**, **IF-30** and **IF-31**. (*R*)-**IF-5** had higher activity (90 %) against chingma abutilon than that of its (*S*) enantiomer and racemate (70 %). **IF-4** and **IF-14** showed significant chiral selectivity in inhibitory activity against chickweed. The inhibitory activity of (*R*)-**IF-14** with ED₅₀ of 47.4 g ai/ha was 2.17 times higher than (*S*)-**IF-14**. (*S*)-**IF-4** with ED₅₀ of 22.8 g ai/ha was found to be the most effective enantiomer and its inhibitory activity against chickweed was 8.17 times higher than (*R*)-**IF-4**. Especially in **IF-31** was found to have significant differences in herbicidal effect between its two enantiomers. At 75 g ai/ha, (*R*)-**IF-31** could achieve 100, 100, 90, and 80 % inhibitory potency against leaf mustard, chingma abutilon, common amaranth, and white eclipta, whereas (*S*)-**IF-31** only had 0, 30, 40, and 40 % inhibitory potency against four tested plants, respectively. The above observations showed that the absolute configuration of different enantiomers in chiral 1-(substituted phenoxyacetoxy)alkylphosphonates **IE** and **IF** had different effects on herbicidal activity.

6.3 Optically Active Substituted Ethylphosphonates IA and IC

6.3.1 Introduction

The synthesis and herbicidal activity of the racemates **IA** and **IC** had been studied in our laboratory. As stated in Chap. 2, several 1-(substituted phenoxyacetoxy) ethylphosphonates **IA** and **IC** displayed good post-emergence herbicidal activity. Especially, *O,O*-dimethyl 1-(2,4-dichlorophenoxyacetoxy)ethylphosphonate **IC-22** (HW02, clacyfos) showed a potential utility for further development as a selective post-emergence herbicide. Considering the great significance of their possible enantiomeric selectivity in herbicidal activity, toxicity or environmental fate, it is necessary to obtain the enantiomers of these active compounds and examine their biological activity.

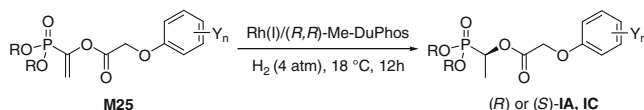
Asymmetric hydrogenation of 1,2-unsaturated phosphonates is a straightforward method for the asymmetric synthesis of some phosphonates [78–80], but this method is not suitable for the synthesis of substituted benzylphosphonates **IA**, **IE**, and **IF**. As stated in Sect. 6.2, three series of optically active *O,O*-dialkyl 1-(substituted phenoxyacetoxy)-1-(substituted phenyl)methylphosphonates **IA**, **IE**, and **IF** had been successfully prepared by the condensation of substituted phenoxyacetyl chlorides **M5** and optically active 1-hydroxy (substituted phenyl)methylphosphonate **M2**.

This method using 1,2-unsaturated phosphonates could be applied to synthesize some optically active 1-(substituted phenoxyacetoxy)alkylphosphonates, when an alkyl group as R^3 was attached to the chiral carbon in the parent structure **Io**. In this case, several optically active 1-(substituted phenoxyacetoxy)alkylphosphonates **IA** and **IC** with methyl or ethyl as R^3 could be synthesized by the asymmetric hydrogenation of the corresponding prochiral 1,2-unsaturated phosphonates.

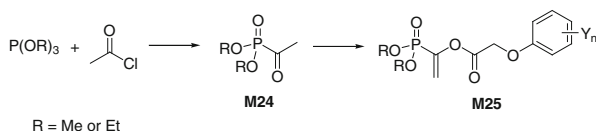
The characteristics and differences of enantiomers of these alkylphosphonates **IA** and **IC** will be examined on the basis of the study of herbicidal activity, crop safety, toxicity and environmental safety. At this stage, several optically active alkylphosphonates in the **IA** and **IC** series were tested for their enantiomeric selectivity in herbicidal activity and acute aquatic toxicity. In this section, the synthesis and herbicidal activity of optically active alkylphosphonates **IA** and **IC** are introduced. The differences of enantiomers of these alkylphosphonates **IA** and **IC** together with their racemates are discussed.

6.3.2 Synthesis of Optically Active IA and IC

At this stage, two enantiomers of several optically active 1-(substituted phenoxyacetoxy)alkylphosphonates **IA** and **IC** were synthesized by the asymmetric hydrogenation of the corresponding prochiral *O,O*-dialkyl 1-(substituted phenoxyacetoxy)vinylphosphonate **M25** (Scheme 6.11) [49].



Scheme 6.11 Syntheses of optically active 1-(substituted phenoxyacetoxy)alkylphosphonates **IA** and **IC**

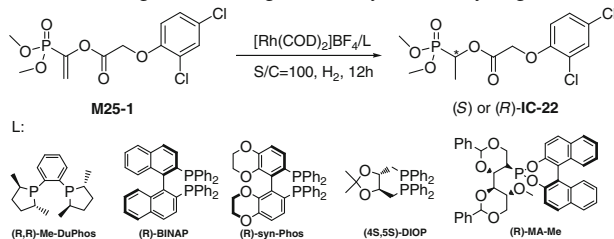


Scheme 6.12 Synthesis of *O,O*-dialkyl 1-(substituted phenoxy acetoxy)vinylphosphonates **M25**

In this reaction, 1-(substituted phenoxyacetoxy)vinylphosphonates **M25** are the key intermediates. **M25** were prepared by a two-step procedure as shown in Scheme 6.12. The Arbuzov reaction of trialkyl phosphates and acetyl chlorides gave 1-keto phosphonates **M24**, which were then treated with various substituted phenoxyacetyl chlorides in the presence of Et_3N from 0°C to room temperature to afford 1-(substituted phenoxy acetoxy)vinylphosphonates **M25** exclusively in 56–95 % isolated yields.

Vinylphosphonates **M25** were further asymmetrically hydrogenated by using chiral Rh(I)-complexes as catalysts to generate optically active products **IA** or **IC**. In the search for an efficient catalyst used in this asymmetric hydrogenation, a variety of chiral bisphosphine ligands and a monodentate phosphorus ligand were screened by using $[\text{Rh}(\text{COD})_2]\text{BF}_4$ as the catalyst precursor. The results are summarized in Table 6.16. Using *O,O*-dimethyl 1-(substituted phenoxy acetoxy) vinylphosphonate **M25-1** as a representative substrate, the asymmetric hydrogenation was carried out in methanol with a hydrogen pressure of 4 atm by using the in situ generated chiral Rh(I)-complexes (Table 6.16, entries 1–5). Ligands such as Me-DuPhos played an important role in this transformation, (*S*)-**IC-22** could be obtained using (*R,R*)-Me-DuPhos as ligand (Table 6.16, entry 1) and (*R*)-**IC-22** was obtained using (*S,S*)-Me-DuPhos as ligand (Table 6.16, entry 7). Under these reaction conditions, the asymmetric hydrogenation could be completed within 12 h at 18°C with excellent conversion (>95 %) and enantiomeric excess (94 %, *ee*). This method for generating the chiral catalyst had no obvious effects on reactivity nor enantioselectivity, and the reaction gave almost identical results, irrespective of the use of the in situ generated catalyst or commercially available one (Table 6.16, entries 1 vs. 7). Noticeably $[\text{Rh}(\text{COD})_2]\text{BF}_4/(\text{R,R})\text{-Me-DuPhos}$ and $[(\text{COD})\text{Rh}(\text{S,S})\text{-Me-DuPhos}]\text{OTf}$ constituted the same stereochemical environment, although the respective absolute configuration was different (Table 6.16, entries 1 and 7).

The effects on the asymmetric hydrogenation of **M25-1** by varying the reaction conditions were examined. The results are listed in Table 6.17. Using the $[\text{Rh}(\text{COD})_2]$

Table 6.16 Ligand screening for the asymmetric hydrogenation

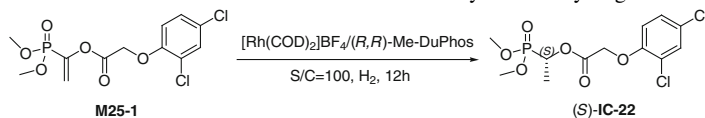
Entry	Pressure (atm)	Solvent	Ligand	Conv. ^a (%)	<i>ee</i> ^b (%)	Conf.
1	4	MeOH	(<i>R,R</i>)-Me-DuPhos	>95	94	<i>S</i>
2	4	MeOH	(<i>R</i>)-BINAP	<5	ND ^d	<i>S</i>
3	4	MeOH	(<i>R</i>)- <i>syn</i> -Phos	50	32	<i>S</i>
4	4	MeOH	(<i>4S,5S</i>)-DIOP	59	16	<i>S</i>
5	4	MeOH	(<i>R</i>)-MA-Me	<5	ND	<i>S</i>
6	10	CH ₂ Cl ₂	(<i>R</i>)-MA-Me	64	36	<i>S</i>
7	4	MeOH	(<i>S,S</i>)-Me-DuPhos ^c	>95	94	<i>R</i>

^a Conversions were determined by ¹H NMR

^b The values of *ee* were determined by chiral HPLC on a Daicel Chiralcel OJ-H column

^c Commercially available [(COD)Rh-(*S,S*)-Me-DuPhos]OTf as the catalyst

^d No data

Table 6.17 Effect of reaction conditions on the asymmetric hydrogenation

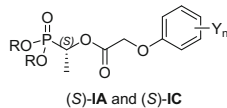
Entry	Pressure (atm)	Temp (°C)	Solvent	Conv. ^a (%)	<i>ee</i> ^b (%)
1	4	18	MeOH	>95	94
2	4	18	CH ₂ Cl ₂	>95	78
3	4	18	THF	>95	88
4	4	18	Toluene	<5	ND ^d
5	4	50	MeOH	>95	94
6	1.3	18	MeOH	>95	94
7	10	18	MeOH	>95	94
8 ^c	4	18	MeOH	15	93

^a Conversions were determined by ¹H NMR

^b The *ee* were determined by chiral HPLC on a Daicel Chiralcel OJ-H column

^c *S/C* = 500:1

^d No data

Table 6.18 Structure of (*S*)-**IA-8** and (*S*)-**IC**^a

Entry	Compound	R	Y _n	Conv. ^b (%)	ee ^c (%)
1	(<i>S</i>)- IA-8	Et	2,4-Cl ₂	>95	96
2	(<i>S</i>)- IC-2	Me	H	>95	93
3	(<i>S</i>)- IC-4	Me	4-Me	>95	91
4	(<i>S</i>)- IC-5	Me	3-CF ₃	>95	92
5	(<i>S</i>)- IC-9	Me	4-F	>95	94
6	(<i>S</i>)- IC-10	Me	4-Cl	>95	95
7	(<i>S</i>)- IC-22	Me	2,4-Cl ₂	>95	94
8	(<i>S</i>)- IC-35	Me	2-Cl	>95	93
9	(<i>S</i>)- IC-36	Me	4-MeO	91	95

^a Synthesis of (*S*)-**IA-8**, (*S*)-**IC-2**, (*S*)-**IC-4**, (*S*)-**IC-5**, (*S*)-**IC-9**, (*S*)-**IC-10**, (*S*)-**IC-22**, (*S*)-**IC-35**, (*S*)-**IC-36** [52]

^b Conversions were determined by ¹H NMR

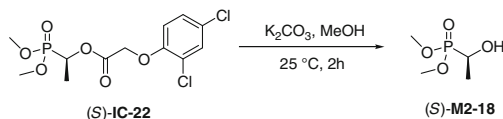
^c The values of *ee* were determined by chiral HPLC on a Daicel Chiralcel OJ-H column

BF₄/(*R,R*)-Me-DuPhos catalyst system, we observed that the enantioselectivity of the reaction depended on the solvents employed. Although the catalytic hydrogenation went to completion in both CH₂Cl₂ and THF, the reaction led to 78 and 88 % *ee*, respectively (Table 6.17, entries 2 and 3). Almost no product **IC-22** was observed in toluene probably due to the low solubility of the catalyst in toluene (Table 6.17, entry 4). Changing the hydrogen pressure to 1.3 or 10 atm resulted in identical results (Table 6.17, entries 6 and 7 vs. 1). Increasing the reaction temperature from 18 to 50 °C did not affect the reaction (Table 6.17, entries 1 and 5). Reducing the catalyst loading to *S/C* = 500:1 resulted in a much lower conversion, only 15 %. However, it did not decrease the *ee* value very much (Table 6.17, entry 8).

Based on the optimization for reaction conditions, some optically active (*S*)-1-(substituted phenoxyacetoxy)alkylphosphonates **IC** and **IA-8** were prepared by using 1 mol% of in situ generated [Rh(COD)₂]BF₄/(*R,R*)-Me-DuPhos catalyst in MeOH at 4 atm of H₂ for 12 h at 18 °C. The results are listed in Table 6.18.

This rhodium-catalyzed hydrogenation exhibited a broad substrate scope and excellent levels of enantioselectivity from 91 to 96 % *ee*. The (*R*)-1-(substituted phenoxyacetoxy)alkylphosphonates **IC** and **IA-8** were also achieved by using (*S,S*)-Me-DuPhos as a ligand. A detailed synthetic procedure for optically active **IC** and **IA-8** is introduced in the Sect. 9.1.34 of Chap. 9.

The structure of the target compounds were characterized by ¹H and ¹³C NMR, IR, MS and confirmed by elementary analysis. In order to determine the absolute configuration of optically active 1-(substituted phenoxyacetoxy)alkylphosphonates **IC**, (*S*)-**IC-22** was simply deprotected using K₂CO₃ in MeOH at room temperature for 2 h to afford the corresponding optically active 1-hydroxyalkylphosphonates **M2-18**, as shown in Scheme 6.13.



Scheme 6.13 Deprotection of optically active (*S*)-**IC-22**

The $[\alpha]_D$ value of (*S*)-**M2-18** was the same as the data reported in the literature [81], which indicated that the absolute configuration of these hydrogenation products was (*S*)-configuration.

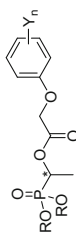
The above results showed that the rhodium-catalyzed hydrogenation of 1-substituted vinylphosphonates exhibited a broad substrate scope and excellent levels of enantioselectivity, therefore, this method could be applied to prepare other optically active 1-(substituted phenoxyacetoxy)alkylphosphonates, such as other optically active compounds in the **IA** and **IC** series.

6.3.3 Herbicidal Activity of Optically Active **IA** and **IC**

In order to investigate enantiomeric selectivity of chiral alkylphosphonates in the **IA** and **IC** series, the herbicidal activity of several optically active alkylphosphonates as typical compounds were evaluated by a preliminary bioassay.

At this stage, the inhibitory activity of several optically active compounds **IA-8**, **IC-5** and **IC-22** including their racemates, (*R*) and (*S*) enantiomers against rape (*Brassica napus*) and barnyard grass (*Echinochloa crusgalli*) were examined at 100 and 10 mg/L, respectively. Results are listed in Table 6.19.

As per the results listed in Table 6.19, the (*R*), (*S*) and racemic forms of **IA-8**, **IC-5**, and **IC-22** displayed high inhibition potency (>90 %) against the growth of root of rape and barnyard grass at 100 and 10 mg/L, respectively. All (*R*), (*S*), and racemic forms of **IA-8** and **IC-22** with 2,4-Cl₂ as Y_n also showed high inhibition potency (>90 %) against the stalk of rape, but all of them had weak activity against the stalk of barnyard grass at 100 and 10 mg/L, respectively. However, all (*R*), (*S*) configuration and racemic forms of these compounds exhibited almost the same herbicidal activity, no difference in herbicidal activity between the two enantiomers was observed at 100 and 10 mg/L. In order to make sure of the possible enantiomeric selectivity in herbicidal activity, the IC₅₀ of (*R*), (*S*) configuration of **IA-8** and **IC-22** against the growth of root of rape were further tested. According to their IC₅₀: IC₅₀ = 0.0361 M for (*R*)-**IA-8**; 0.0384 M for (*S*)-**IA-8**; IC₅₀ = 0.0342 M for (*S*)-**IC-22**; 0.0496 M for (*R*)-**IC-22**, there was no significant difference in IC₅₀ between the two enantiomers of compound **IA-8** or **IC-22**. The inhibition potency of both (*R*) and (*S*) enantiomers of **IA-8** or **IC-22** against rape was very similar. The results showed that **IA-8** and **IC-22** seemed to have no significant enantiomeric selectivity in inhibition against rape.

Table 6.19 Structure and inhibitory activity of IA-8, IC-5 and IC-22^a

Compound	R ³	Y _n	Root			Stem			
			Ech ^b			Ech ^b			
			100 mg/L	10 mg/L	Bra ^b 100 mg/L	100 mg/L	10 mg/L	Bra ^b 100 mg/L	
<i>rac</i> -IA-8	Et	2,4-Cl ₂	98	98	99	54	27	93	92
(<i>R</i>)-IA-8			98	98	99	26	24	95	91
(<i>S</i>)-IA-8			98	98	99	40	31	91	90
<i>rac</i> -IC-5	Me	3-CF ₃	93	93	99	37	30	87	77
(<i>R</i>)-IC-5			93	90	99	15	0	87	77
(<i>S</i>)-IC-5			97	90	98	48	0	87	73
<i>rac</i> -IC-22	Me	2,4-Cl ₂	98	95	99	26	26	93	93
(<i>R</i>)-IC-22			98	93	99	54	21	92	92
(<i>S</i>)-IC-22			98	95	99	33	23	93	91

^a Inhibitory potency (%) against the growth of plants in Petri dishes, 0 (no effect), 100 % (completely kill)

^b Ech: barnyard grass; Bra: rape

6.3.4 Aquatic Toxicity of Optically Active IA and IC

The aquatic toxicity of chiral organophosphorous (OP) compounds has received increasing attention. Lin et al. reported that the (+)-enantiomer of methamidophos was 7.0 times more toxic than its (–)-enantiomer against *Daphnia magna* in 48 h tests [82]. The acute aquatic toxicity of trichloronate against *Daphnia magna* was also found to be selective; the (–)-form was 8–11 times more toxic than its (+)-form, while the raceme showed intermediate toxicity [83].

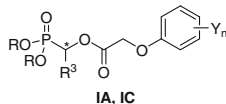
Considering significant enantiomeric selectivity in the aquatic toxicity of some chiral OP compounds and the possible effect of chiral OP compounds on environmental safety, the biological toxicity of chiral 1-(substituted phenoxyacetoxy) alkylphosphonates and their enantiomers should be also investigated.

At this stage, the acute aquatic toxicity against *Daphnia magna* of several chiral alkylphosphonates **IA** and **IC** and their enantiomers were examined by following method *in vivo* under static conditions [84]. These results would be helpful to evaluate their enantioselective behaviors and ecological risks in the environment.

Aquatic Toxicity Assay. Enantioselectivity in aquatic toxicity was evaluated through 48-h acute toxicity assays using *Daphnia magna* as the test species. The test organisms were obtained from a continuous culture maintained at 22 ± 1 °C in M4 culture medium [85] with a photoperiod of 12 h/day and a density of <50 animals per liter. The medium was renewed three times a week, and *Daphnia magna* were fed daily with the alga *Scenedesmus obliquus*, which were cultured in the laboratory using a nutrient medium. Stock organisms were originally obtained from the Chinese Academy of Protection and Medical Science (Beijing, China). Prior to testing, a sensitive test for *Daphnia magna* to potassium dichromate ($K_2Cr_2O_7$) was performed as a positive control, and the LC_{50} (24-h) value was in the range of 0.6–1.7 mg/L [82]. The overall testing procedures followed EPA guidelines [86]. Briefly, test solutions containing a given enantiomer or racemate with a range of concentrations were prepared (by dilution) from the resolved enantiomers using M4. The maximum content of acetone in the final test solutions was <0.2 % (by volume). Twenty mL of the prepared solutions were transferred to 50 mL glass beakers, and four replicates were prepared for each concentration level. Five active *Daphnia magna* aged 6–24 h were added into each beaker. The test organisms were fed with *Scenedesmus obliquus* 6 h prior to the exposure. All beakers were monitored at 24 h intervals until reaching 48 h of exposure. The concentration that caused 50 % mortality of the test population, or LC_{50} (mg/L), was determined by probit analysis (ToxCalc™ v5.0, Tidepool Scientific Software, McKinleyville, CA).

Acute aquatic toxicities were measured for the racemes and individual enantiomers of compound **IA-8**, **IC-9**, **IC-10**, **IC-27**, and **IC-35** using a 24 h and 48 h static test to *Daphnia magna*. The LC_{50} values are listed in Table 6.20.

According to the structure of compounds including their racemic form (*rac*) and two enantiomers (*R* and *S*) forms in Table 6.20, these compounds can be grouped

Table 6.20 Structure and acute aquatic toxicity to *Daphnia magna* of **IA** and **IC**

Compound	R	R ³	Y _n	LC ₅₀ (48 h mg/L) ^a	Average values LC ₅₀
<i>rac</i> - IA-8	Et	Me	2,4-Cl ₂	0.24	0.19
(<i>R</i>)- IA-8				0.14	
(<i>S</i>)- IA-8				0.18	
<i>rac</i> - IC-9	Me	Me	4-F	2.54	4.87
(<i>R</i>)- IC-9				2.30	
(<i>S</i>)- IC-9				9.77	
<i>rac</i> - IC-10	Me	Me	4-Cl	0.020	0.043
(<i>R</i>)- IC-10				0.097	
(<i>S</i>)- IC-10				0.012	
<i>rac</i> - IC-27	Me	Et	2,4-Cl ₂	1.14	1.47
(<i>R</i>)- IC-27				1.41	
(<i>S</i>)- IC-27				1.87	
<i>rac</i> - IC-35	Me	Me	2-Cl	2.97	2.56
(<i>R</i>)- IC-35				2.72	
(<i>S</i>)- IC-35				1.99	

^a LC₅₀ is effective concentration that caused 50 % mortality of the test population (*Daphnia magna*)

and categorized as **IA-8** to **IC-35**. Compounds from each category have been tested for their toxicities against *Daphnia magna*. The average LC₅₀ values of each group in increasing order are: **IC-10** < **IA-8** < **IC-27** < **IC-35** < **IC-9**. The results showed that, although they had similar chemical structures, **IA-8** and **IC-10** were highly toxic while **IC-27**, **IC-35**, and **IC-9** were moderate toxic to *Daphnia magna* according to the China official environmental safety test guidelines.

It is interesting to point out that significant differences were also observed among compounds in the same group. **IC-10** is the most toxic group against *Daphnia magna*. Within this group, the (*S*)-enantiomer of **IC-10** showed higher toxicity than its (*R*)-form and racemic form. The (*S*)-enantiomer is approximately 8.08 times more toxic than its (*R*)-form counterpart. Further calculation showed that the (*S*)-enantiomer of **IC-10** contributed about 91 % to its toxicity against *Daphnia magna*.

For **IC-27**, it was interesting to note that the toxicity of racemate was slightly higher than that of the individual enantiomer. By comparing the racemate of **IA-8** or **IC-35** with their corresponding enantiomers, we observed that both of the racemates showed the lowest toxicity, while the racemate of **IC-9** or **IC-10** showed intermediate toxicity compared with their corresponding enantiomers respectively. These findings indicate that the toxicological effects of racemate or equimolar mixtures of enantiomers cannot be predicted by the simple addition of the effect of the individual enantiomer.

The results in Table 6.20 also suggested that the toxicities of most chiral 1-(substituted phenoxyacetoxy)alkylphosphonates were enantiospecific. However, the

toxicity of the racemates is compound-dependant. The synergistic and antagonistic interactions between enantiomers may exist in biological processes and should be taken into consideration in pesticide risk assessment.

6.3.5 Summary

Several optically active (*S*)-1-(substituted phenoxyacetoxy)alkylphosphonates **IA** and **IC** were prepared by using $[\text{Rh}(\text{COD})_2]\text{BF}_4/(\text{R,R})\text{-Me-DuPhos}$ as catalyst. This rhodium-catalyzed hydrogenation exhibited broad substrate scope and excellent levels of enantioselectivity in the range from 91 to 96 % *ee*. The (*R*)-1-(substituted phenoxyacetoxy)alkylphosphonates **IA** and **IC** were also achieved by using (*S,S*)-Me-DuPhos as a ligand. This method could be further applied to prepare other optically active 1-(substituted phenoxyacetoxy)alkylphosphonates.

All racemic forms, (*R*) and (*S*) enantiomers of alkylphosphonates **IA-8**, **IC-5** and **IC-22** displayed high inhibition potency (>90 %) against the growth of root of rape and barnyard grass at 10 mg/L. The (*R*)-form, (*S*)-form and racemic forms of alkylphosphonates **IA-8** and **IC-22** with 2,4-Cl₂ as Y_n also showed high inhibition potency (>90 %) against the stalk of rape at 10 mg/L. There was no significant difference in inhibition potency against the growth of root and stalk of rape and barnyard grass between the two enantiomers of alkylphosphonates **IA-8**, **IC-5**, or **IC-22**.

Several chiral alkylphosphonates **IA-8**, **IC-9**, **IC-10**, **IC-27**, and **IC-35** including their enantiomers were assessed for their acute aquatic toxicity *in vivo* against *Daphnia magna*. Alkylphosphonate **IC-10** was found to be about 2–148.5 times more toxic against *Daphnia magna* than that of other four analogs. It was also found that there was a significant difference in acute aquatic toxicity against *Daphnia magna* among enantiomers and racemate. The (*S*)-**IC-10** showed 8.08 times higher toxicity than that of (*R*)-**IC-10**, revealed that the (*S*)-enantiomer of **IC-10** contributed about 91 % to the toxicity against *Daphnia magna* in the racemate. It was very interesting that there were different biological effects for different chiral alkylphosphonates. Comparing with the acute aquatic toxicity of enantiomers, the racemates of **IC-9** and **IC-10** showed intermediate toxicity, while racemates of **IC-27** or **IA-8** and **IC-35** showed synergistic or antagonistic effects, respectively.

The above observations showed that chiral 1-(substituted phenoxyacetoxy)alkylphosphonates had an enantiomeric selectivity against nontarget organisms. Therefore, more comprehensive study on their enantioselective in environmental behaviors is needed to evaluate their ecological risks.

References

1. Stawinski J, Kraszewski A (2002) How to get the most out of two phosphorus chemistries. Studies on H-phosphonates. *Acc Chem Res* 35:952–960
2. Stowasser B, Budt KH, Li JQ et al (1992) New hybrid transition state analog inhibitors of HIV protease with peripheric C₂-symmetry. *Tetrahedron Lett* 33:6625–6628
3. Sikorski JA, Miller MJ, Braccolino DS et al (1993) EPSP synthase: the design and synthesis of bisubstrate inhibitors incorporating novel 3-phosphate mimics. *Phosphorus Sulfur Silicon Relat Elem* 76:115–118
4. Hilderbrand RL (ed) (1983) The role of phosphonates in living systems. RCRC Press, Boca Raton
5. Szymańska A, Szymczak M, Boryski J et al (2006) Aryl nucleoside H-phosphonates. Part 15: synthesis, properties and, anti-HIV activity of aryl nucleoside 5'- α -hydroxyphosphonates. *Bioorg Med Chem* 14:1924–1934
6. Shi DQ, Sheng ZL, Liu XP et al (2003) Unsaturated cyclic α -hydroxyphosphonates. *Heteroatom Chem* 14:266–268
7. Ganzhorn AJ, Hoflack J, Pelton PD et al (1998) Inhibition of *myo*-inositol monophosphatase isoforms by aromatic phosphonates. *Bioorg Med Chem* 6:1865–1874
8. Allen JG, Atherton FR, Hall MJ et al (1978) Phosphonopeptides, a new class of synthetic antibacterial agents. *Nature* 272:56–58
9. Patel DV, Rielly-Gauvin K, Ryono DE et al (1995) α -Hydroxy phosphinyl-based inhibitors of human renin. *J Med Chem* 38:4557–4569
10. Engel R (1977) Phosphonates as analogues of natural phosphates. *Chem Rev* 77:349–367
11. Hammerschmidt F (1994) Incorporation of L-[methyl-²H₃]methionine and 2-[hydroxy-¹⁸O] hydroxyethylphosphonic acid into fosfomycin in *Streptomyces fradiae*-An unusual methyl-transfer. *Angew Chem Int Ed Engl* 33:341–342
12. Jennings LJ, Macchia M, Parkin A (1992) Synthesis of analogues of 5-iodo-2'-deoxyuridine-5'-diphosphate. *J Chem Soc Perkin Trans* 17:2197–2202
13. Lavielle G, Hautefaye P, Schaeffer C et al (1991) New α -amino phosphonic acid derivatives of vinblastine: chemistry and antitumor activity. *J Med Chem* 34:1998–2003
14. Allen MC, Fuhrer W, Tuck B et al (1989) Renin inhibitors. Synthesis of transition-state analogue inhibitors containing phosphorus acid derivatives at the scissile bond. *J Med Chem* 32:1652–1661
15. Smith WW, Bartlett PA (1998) Macrocyclic inhibitors of penicillopepsin. 3. Design, synthesis, and evaluation of an inhibitor bridged between P2 and P1'. *J Am Chem Soc* 120:4622–4628
16. Zhou SS, Lin KD, Yang HY et al (2007) Stereoisomeric separation and toxicity of a new organophosphorus insecticide chloramidophos. *Chem Res Toxicol* 20:400–405
17. Liu WP, Gan JY, Schlenk D et al (2005) Enantioselectivity in environmental safety of current chiral insecticides. *Proc Natl Acad Sci USA* 102:701–706
18. Castañeda OL, Kraak GVD, Canul RR (2007) Endocrine disruption mechanism of o, p'-DDT in mature male tilapia (*Oreochromis niloticus*). *Toxicol Appl Pharm* 221:158–167
19. Hoekstra PF, Burnison BK, Neheli T et al (2001) Enantiomer-specific activity of o, p'-DDT with the human estrogen receptor. *Toxicol Lett* 125:75–81
20. Atherton FR, Hall MJ, Hassall CH et al (1979) Phosphonopeptides as antibacterial agents: mechanism of action of alaphosphin. *Antimicrob Agents Chemother* 15:696–705
21. He HW, Wang J, Liu ZJ (1994) Synthesis of α -(substituted phenoxy acetoxy)alkyl phosphonates. *Chinese Chem Lett* 5:35–38
22. He HW, Wang J, Liu ZJ et al (1994) Study on biologically active organophosphorus compounds V, synthesis and properties of α -(substituted phenoxyacetoxy) alkyl phosphonates. *Chin J Appl Chem* 11:21–24
23. He HW, Wang J, Liu ZJ et al (1994) Studies on biologically active organophosphorus compounds VI, synthesis properties and biological activity of 1-oxophosphonic acid derivatives. *J Centr Chin Norm Univ (Nat Sci)* 28:71–76

24. Chen T, Shen P, Li YJ et al (2006) Synthesis and herbicidal activity of O, O-dialkyl phenoxyacetoxyalkylphosphonates containing fluorine. *J Fluorine Chem* 127:291–295
25. Chen T, Shen P, Li YJ et al (2006) The synthesis and herbicidal evaluation of fluorine-containing phenoxyacetoxyalkylphosphonate derivatives. *Phosphorus Sulfur Silicon Relat Elem* 181:2135–2145
26. Wang J, Chen XY, Liu XF et al (1999) The synthesis and biological properties of α -halogenated phenoxy carbonyloxy alkylphosphonic acids and esters. *Chin J Chem Reag* 21:301–303
27. He HW, Chen T, Li YJ (2007) Synthesis and herbicidal activity of alkyl 1-(3-trifluoromethylphenoxyacetoxy)-1-substituted methylphosphonates. *J Pestic Sci* 32:42–44
28. Li YJ, Duan JP, He HW (2007) Synthesis and herbicidal activity of α -[2-(fluoro-substituted phenoxy)propionyloxy]alkylphosphonates. *Chin J Appl Chem* 24:596–598
29. Li YJ, He HW (2008) Synthesis and herbicidal activity of α -[2-(fluoro-substituted phenoxy)propionyloxy] alkyl phosphonates. *Phosphorus Sulfur Silicon Relat Elem* 183:712–713
30. He HW, Liu ZJ, Wang J (1998) Synthesis and biological activities of 1-[2-(2,4-dichlorophenoxy)propionyloxy] alkyl phosphonates. *Chin J Appl Chem* 15:88–90
31. Wang J, He H, Liu Z (1997) Synthesis of α -[2-(2,4-dichlorophenoxy) propionyloxy] alkyl phosphonates. *Chin Chem Lett* 8:943–944
32. Wang T, He HW (2004) Simple and improved preparation of α -oxophosphonate monolithium salts. *Phosphorus Sulfur Silicon* 179:2081–2089
33. He HW, Yuan JL, Peng H et al (2011) Studies of O, O-dimethyl α -(2,4-dichlorophenoxyacetoxy) ethylphosphonate (HW02) as a new herbicide. 1. Synthesis and herbicidal activity of HW02 and analogues as novel inhibitors of pyruvate dehydrogenase complex. *J Agric Food Chem* 59:4801–4813
34. Peng H, Wang T, Xie P et al (2007) Molecular docking and three-dimensional quantitative structure-activity relationship studies on the binding modes of herbicidal 1-(substituted phenoxyacetoxy) alkylphosphonates to the E1 component of pyruvate dehydrogenase. *J Agric Food Chem* 55:1871–1880
35. Wang T, He HW, Miao FM (2009) Synthesis, crystal structure and herbicidal activity of 1-(2,4-dichlorophenoxyacetoxy)-1-arylmethylphosphonates. *Chin J Org Chem* 29:1152–1157
36. Meng LP, He HW, Liu ZJ (1998) Synthesis and biological activities of O, O-dimethyl α -(NO₂ substituted phenoxyacetoxy)alkylphosphonates. *Chin J HuBei Chem Industry (special issue)* 40–41
37. He HW, Peng H, Wang T et al (2013) α -(Substituted-phenoxyacetoxy)- α -heterocyclmethylphosphonates: synthesis, herbicidal activity, inhibition on pyruvate dehydrogenase complex (PDHc), and application as postemergent herbicide against broadleaf weeds. *J Agric Food Chem* 61:2479–2488
38. He HW, Meng LP, Hu LM et al (2002) Synthesis and plant growth regulatory activity of 1-(1-phenyl-1,2,4-triazole-3-oxoacetoxy)alkyl phosphonates. *Chin J Pest Sci* 4(3):14–18
39. He HW, Liu ZJ (2001) Progresses in research of alpha-oxophosphonic acid derivatives with herbicidal activity. *Chin J Org Chem* 21:878–883
40. Wang W, He HW, Zuo N et al (2012) Synthesis and herbicidal activity of 2-(substituted phenoxyacetoxy)alkyl-5,5-dimethyl-1,3,2-dioxaphosphinan-2-one containing fluorine. *J Fluorine Chem* 142:24–28
41. Wang W, He HW, Zuo N et al (2012) Synthesis and herbicidal activity of 2-(substituted phenoxyacetoxy)alkyl-5,5-dimethyl-1,3,2-dioxaphosphinan-2-one. *J Agric Food Chem* 60:7581–7587
42. Gerwick BC, Jackson LA, Handly J et al (1988) Preemergence and postemergence activities of the (R) and (S) enantiomers of haloxyfop. *Weed Sci* 36:453–456
43. Grossmann K, Tresch S, Plath P (2001) Triaziflam and diaminotriazine derivatives affect enantioselectively multiple herbicide target sites. *Z Naturforsch* 56c:559–569
44. Shaner DL, Singh BK (1997) Acetohydroxyacid synthase inhibitors. *Herbicide activity: toxicology, biochemistry and molecular biology*. IOS Press, Amsterdam, pp 69–110

45. Omokawa H, Konnai M (1990) PS II inhibitory activity of 2,4-diamino-6-chloro-s-triazine with a chiral sec-butyl and/or α -methylbenzyl group. *Agric Biolog Chem* 54(9):2373–2378
46. Omokawa H, Murata H, Kobayashi S (2004) Chiral response of *Oryzaeae* and *Panicaceae* plants in α -methylbenzyl-3-p-tolyl urea agar medium. *Pest Manag Sci* 60:59–64
47. Fayez KA, Kristen U (1996) The influence of herbicides on the growth and proline content of primary roots and on the ultrastructure of root caps. *Environm Experim Botany* 36:71–81
48. Lin KD, Liu WP, Li L et al (2008) Single and joint acute toxicity of isocarbophos enantiomers to *Daphnia magna*. *J Agric Food Chem* 56(11):4273–4277
49. Liu H, Zhou YG, Yu ZK et al (2006) Efficient catalytic asymmetric synthesis of α -substituted phenyloxyacetyloxy and aroyloxy phosphonates. *Tetrahedron* 62:11207–11217
50. Yokomatsu T, Yamgishi T, Shibuya S (1993) Enantioselective hydrophos-phonylation of aromatic aldehydes catalyzed by chiral titanium alkoxides. *Tetrahedron Asymmetry* 4:1779–1782
51. Groaning MD, Rowe BJ, Spilling CD (1998) New homochiral cyclic diol ligands for titanium alkoxide catalyzed phosphorylation of aldehydes. *Tetrahedron Lett* 39:5485–5488
52. Yokomatsu T, Yamgishi T, Shibuya S (1993) Enantioselectivity for hydrophosphonylation of aromatic aldehydes catalyzed by lanthanum binaphthol complex. Remarkable electronic effect of aromatic substituents. *Tetrahedron Asymmetry* 4:1783–1784
53. Arai T, Bougauchi M, Sasai H et al (1996) Catalytic asymmetric synthesis of α -hydroxy phosphonates using the Al-Li-BINOL complex. *J Org Chem* 61:2926–2927
54. Merino P, Marques E, Herrera RP et al (2008) Catalytic enantioselective hydrophosphonylation of aldehydes and imines. *Adv Synth Catal* 350:1195–1208
55. Pogatchnik DM, Wiemer DF (1997) Enantioselective synthesis of α -hydroxy phosphonates via oxidation with (camphorsulfonyl) oxaziridines. *Tetrahedron Lett* 38(20):3495–3498
56. Skropeta D, Schmidt RR (2003) Chiral, non-racemic α -hydroxyphosphonates and phosphonic stereoselective hydroxylation of diallyl benzylphosphonates. *Tetrahedron: Asymmetry* 14:265–273
57. Wang CB, Xu C, Tan XS et al (2012) The asymmetric synthesis of chiral cyclic α -hydroxy phosphonates and quaternary cyclic α -hydroxy phosphonates. *Org Biomol Chem* 10:1680–1685
58. Pudovik AN, Konovalova IV et al (1979) Addition reactions of esters of phosphorus (III) acids with unsaturated systems. *Synthesis* 2:81–96
59. Duxbury JP, Cawley A, Thornton-Pett M et al (1999) Chiral aluminium complexes as phospho-transfer catalysts. *Tetrahedron Lett* 40:4403–4406
60. Ward CV, Jiang M, Kee TP (2000) New chiral catalysts for phospho-transfer. *Tetrahedron Lett* 41:6181–6184
61. Saito B, Katsuki T (2005) Synthesis of an optically active C1-symmetric al(salalen) complex and its application to the catalytic hydrophosphonylation of aldehydes. *Angew Chem Int Ed* 44:4600–4602
62. Saito B, Egami H, Katsuki T (2007) Synthesis of an optically active al(salalen) complex and its application to catalytic hydrophosphonylation of aldehydes and aldimines. *J Am Chem Soc* 129:1978–1986
63. Zhou X, Liu XH, Yang X et al (2008) Highly enantioselective hydrophosphonylation of aldehydes catalyzed by tridentate schiff base aluminum(III) complexes. *Angew Chem Int Ed* 47:392–394
64. Zhou X, Zhang Q, Hui YH (2010) Catalytic asymmetric synthesis of quaternary α -hydroxy trifluoromethyl phosphonate via chiral aluminum (III) catalyzed hydrophosphonylation of trifluoromethyl ketones. *Org Lett* 12:4296–4299
65. Gupta KC, Sutar AK (2008) Catalytic activities of Schiff base transition metal complexes. *Coord Chem Rev* 252:1420–1450
66. Hayashi M, Inoue T, Miyamoto Y et al (1994) Asymmetric carbon carbon bond forming reactions catalyzed by chiral Schiff base-titanium alkoxide complexes. *Tetrahedron* 50:4385–4398

67. Cogan DA, Liu GC, Kim KJ et al (1998) Catalytic asymmetric oxidation of tert-butyl disulfide. Synthesis of tert-butanesulfinamides, tert-butyl sulfoxides, and tert-butanesulfinimines. *J Am Chem Soc* 120:8011–8019
68. Hartung J, Drees S, Greb M et al (2003) (Schiff-base) vanadium (V) complex-catalyzed oxidations of substituted bis (homoallylic) alcohols—stereoselective synthesis of functionalized tetrahydrofurans. *Eur J Org Chem* 13:2388–2408
69. Banphavichit V, Mansawat W, Bhanthumnavin W et al (2004) A highly enantioselective Strecker reaction catalyzed by titanium-*N*-salicyl- β -aminoalcohol complexes. *Tetrahedron* 60:10559–10568
70. Zeng QL, Wang HQ, Wang TJ et al (2005) Vanadium-catalyzed enantioselective sulfoxidation and concomitant, highly efficient kinetic resolution provide high enantioselectivity and acceptable yields of sulfoxides. *Adv Synth Catal* 347:1933–1936
71. Pietro WJ, Hehre WJ (1982) Tautomerization of dimethyl phosphonate. *J Am Chem Soc* 104:3594–3595
72. Wang CB, Peng H, Tan XS et al (2011) (*S*)-2-[(2,4-Dichlorophenyl)(hydroxy)methyl]-5,5-dimethyl-1,3,2-dioxaphosphinane 2-oxide. *Acta Crystallogr E* 67:920
73. Cermak DM, Yanming D, Wiemer DF (1999) Synthesis of nonracemic dimethyl α -(hydroxyfarnesyl) phosphonates via oxidation of dimethyl farnesylphosphonate with (camphorsulfonyl) oxaziridines. *J Org Chem* 64:388–393
74. Bhattacharya AK, Thyagarajan G (1981) Michaelis-arbuzov rearrangement. *Chem Rev* 81:415–430
75. Yokomatsu T, Yamagishi T, Shibuya S (1997) Enantioselective synthesis of α -hydroxyphosphonates through asymmetric Pudovik reactions with chiral lanthanoid and titanium alkoxides. *J Chem Soc Perkin Trans 1*(10):1527–1534
76. Qian C, Huang T, Zhu C et al (1998) Synthesis of 3,3', 6,6'- and 3,3', 6,6'-substituted binaphthols and their application in the asymmetric hydrophosphonylation of aldehydes—an obvious effect of substituents of BINOL on the enantioselectivity. *J Chem Soc Perkin Trans 1*:2097–2104
77. Brayer JL, Talinani L, Tessier J (1990) EP 376819
78. Rubio M, Suarez A, Alvarez E et al (2005) Highly enantioselective hydrogenation of enol ester phosphonates catalyzed by rhodium phosphine-phosphite complexes. *Chem Commun* 5:628–630
79. Gridnev ID, Yasutake M, Imamoto T et al (2004) Asymmetric hydrogenation of α , β -unsaturated phosphonates with Rh-BisP* and Rh-MiniPHOS catalysts: scope and mechanism of the reaction. *Proc Natl Acad Sci USA* 101:5385–5390
80. Burk MJ, Stammers TA, Straub JA (1999) Enantioselective synthesis of α -hydroxy and α -amino phosphonates via catalytic asymmetric hydrogenation. *Org Lett* 1:387–390
81. Sasaki M (1986) Optical resolution of 1-hydroxyethylphosphinic acid and its esters. *Agric Biol Chem* 50:741–745
82. Lin KD, Zhou SS, Xu C et al (2006) Enantiomeric resolution and biotoxicity of methamidophos. *J Agric Food Chem* 54:8134–8138
83. Liu WP, Lin KD, Gan JY (2006) Separation and aquatic toxicity of enantiomers of the organophosphorus insecticide trichloronate. *Chirality* 18:713–716
84. Li L, Zhou SS, Zhao MR et al (2008) Separation and aquatic toxicity of enantiomers of 1-(substituted phenoxyacetoxy) alkylphosphonate herbicides. *Chirality* 20:130–138
85. Organization for Economic Cooperation and development (OECD) (1995) Report of the Final Ring Test of the *Daphnia magna* Reproduction Study
86. Weber CI (1995) Methods for measuring the acute toxicity of effluents and receiving waters to freshwater and marine organisms. US Environmental Protection Agency, Cincinnati

Chapter 7

Biochemical Mechanism of Alkylphosphonates

In 1988, Baillie et al. demonstrated that susceptible plants died as a direct result of inhibition against plant PDHc E1 by pyruvate analog, sodium *O*-alkyl acylphosphonates **1**. As described in Chaps. 1 and 2, *O,O*-diethyl 1-(substituted phenoxyacetoxy) alkylphosphonates **1A** with significant herbicidal activity were found by the modification of sodium *O*-methyl acetylphosphonate **1-1**. *O,O*-Diethyl 1-(substituted phenoxyacetoxy)alkylphosphonates were identified as the lead structures for further chemical modification. Different series of 1-(substituted phenoxyacetoxy) alkylphosphonates **1o** as potential PDHc inhibitors were synthesized. The optimization of structure was carried out step by step on the basis of study on synthesis, herbicidal activity, and structure-activity relationship. Some alkylphosphonates **1o** were found to have much higher herbicidal activity against dicotyledons than monocotyledons for post-emergence application.

These alkylphosphonates **1o** were expected to be effective PDHc E1 inhibitors because they were obtained by the chemical modification of sodium *O*-methyl acetylphosphonate **1-1**, which is a potent PDHc E1 inhibitor. Therefore, it is interesting to examine inhibitory activity of these alkylphosphonates **1o** and explore the biochemical mechanism. The inhibition of several alkylphosphonates **1o** against PDHc was studied through two aspects:

- (1) In order to determine the probable binding conformations of the alkylphosphonates **1o**, molecular docking, three-dimensional quantitative structure-activity relationships (3D-QSAR) study on the binding modes of alkylphosphonates **1o** to PDHc E1 were performed by using the method of theoretical calculation.
- (2) The action mechanism of herbicidal activity of the alkylphosphonates **1o** was explored on the basis of biochemical experiments. Representative alkylphosphonates **1o** were selected to examine their inhibition against plant PDHc in vitro including enzyme activity assays, kinetic experiments, and enzyme selective inhibition. Correlation between the inhibitory potency against plant PDHc and the herbicidal activity of the alkylphosphonates **1o** was summarized on the basis of bioassay.

7.1 Molecular Docking and 3D-QSAR Studies

7.1.1 Introduction

Three-dimensional quantitative structure-activity relationships (3D-QSAR) have been applied for decades in the development of relationships between physico-chemical properties of chemical substances and their biological activities to obtain a reliable statistical model for prediction of the activities of new chemical entities. It has served as a valuable predictive tool in the design of pharmaceuticals and agrochemicals. Although the trial-and-error factor involved in the development of a new drug cannot be ignored completely, 3D-QSAR certainly decreases the number of compounds to be synthesized by facilitating the selection of the most promising candidates [1].

Pyruvate dehydrogenase complex (PDHc) is already known to be a site of pesticide action, because it plays a pivotal role in cellular metabolism by catalyzing the oxidative decarboxylation of pyruvate and the subsequent acetylation of coenzyme A (CoA) to produce acetyl-CoA [2–5]. The complex consists of three enzymes and a number of cofactors. Pyruvate dehydrogenase E1 component (PDHc E1, E.C. 1.2.4.1) is the initial member of PDHc, which catalyzes the first step of the multistep process, using thiamine pyrophosphate (TPP) and Mg^{2+} as cofactors [6–8], so PDHc E1 is of interest from the point of view of agrochemical design. As stated in previous chapters, we began a systematic study aiming to design new PDHc E1 inhibitors with phosphonate structure as potential herbicides. Several series of alkylphosphonates **1o** were synthesized as mechanism-based inhibitors of PDHc E1 and shown to be endowed with notable herbicidal activities [9–13]. Furthermore, it is interesting that herbicidal activities of the alkylphosphonates **1o** positively correlated with inhibition of PDHc E1 [14–16]. We carried out a three-dimensional quantitative structure-activity relationship (3D-QSAR) study on 1-(substituted phenoxyacetoxy) alkylphosphonates **1o** using comparative molecular field analysis (CoMFA) and comparative molecular similarity indices analysis (CoMSIA) models [17, 18].

The most important requirement for CoMFA and CoMSIA studies is that the 3D structures to be analyzed are aligned according to a suitable conformational template, which is assumed to be a ‘bioactive’ conformation. To make the 3D-QSAR predicting models more relevant to the real active site of the enzyme, a flexible molecular docking approach was carried out. The docking conformations were assumed to be the actual bioactive binding conformations.

Based on the binding conformations, highly predictive 3D-QSAR models were developed with q^2 values of 0.872 and 0.873 for CoMFA and CoMSIA, respectively. The predictabilities of these models were validated by using a set of compounds that were not included in the training set. Both the CoMFA and the CoMSIA field distributions are in good agreement with the spatial and electronic structural characteristics of the binding groove of PDHc E1. Mapping the 3D-QSAR models with the 3D topology of active site of PDHc E1 showed that the spatial and the electronic distributions of ligand-based models matched well with those of the active

site of the receptor, which provided further insight into the enzyme-inhibitor interaction mechanism. The binding model proposed herein is valuable and applicable in the further research and development of novel potent PDHc E1 targeted inhibitors.

7.1.2 Binding Conformational Analysis

Conventional CoMFA and CoMSIA are ligand-based modeling, but they cannot ensure the various field distributions of bioactivity predictable models. At present, there seems to be no report on X-ray structure of plant PDHc E1. We noticed X-ray structure of PDHc E1 from *E.coli* reported by Arjunan et al. [19, 20]. Therefore, the study on the binding mode of **1o** was explored on the basis of X-ray structure of *E.coli* PDHc E1. To explore a probable binding site in the PDHc E1, **IH-18** (see Table 7.2) with good herbicidal activity was chosen to dock into the active site of PDHc E1 [19, 20] by using the advanced docking program AutoDock 3.0 [21].

As stated in Chap. 2, we observed that the most important sites for enhancing the herbicidal activity were the 2-position and 4-position of the phenoxy-benzene ring. The simultaneous presence of electronegative groups (chlorine or fluorine) at the 2- and 4-positions was most favorable for herbicidal activity. The improvement of activity due to the presence of negative charge at these positions was assumed to be the results of electrostatic interactions between the electronegative chlorine or fluorine atoms, and positively charged counterparts of the receptor, such as protonated nitrogen atoms on Lys, Arg, Pro, and His side chains. Taking this essential electronic matching quality into account, the top 10 ranked conformations were selected, among which only one conformation could satisfy the electronic matching quality, with electropositive amino acid residues His106 and His640 around the 2-, 4-positions of phenoxy-benzene ring, respectively. Figure 7.1 depicts the probable binding conformations of 1-(substituted phenoxyacetoxy)alkylphosphonates **1o** in the binding pocket of the PDHc E1. Furthermore, the other molecules were aligned based on the assumption that they bound to the target site in the same manner. Apparently all the members of this series had similar binding characteristics. The main steric, electronic and hydrophobic interactions between the inhibitors and the residues such as His106, Met107, Ala108, Ser109, Tyr177, Leu264, Lys392, Ala399, Ala400, Glu522, Tyr599, Glu636, His640, and TDP887 in the binding pocket could be observed.

7.1.3 CoMFA and CoMSIA Analysis

The results of CoMFA and CoMSIA analysis are summarized in Table 7.1. The CoMFA PLS analysis yielded a high cross-validated correlation coefficient q^2 of 0.872 with standard error of prediction SEP of 0.383. The non-cross-validated PLS analysis gave a conventional r^2 of 0.974 with SE of 0.172. These values indicated a good statistical correlation and reasonable predictability of the CoMFA model.

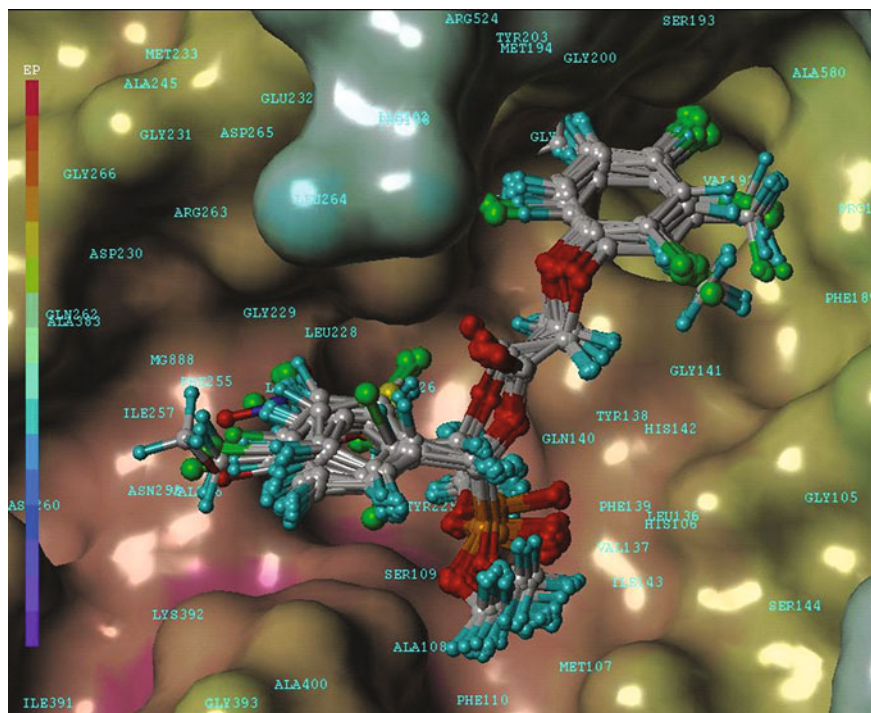


Fig. 7.1 The probable binding conformations of molecules used in training set displayed inside the active site of the PDHc E1. This image was generated with the MOLCAD program in SYBYL 7.0, with some residues removed for clear visualization. The enzyme surface was rendered with electrostatic potential

The steric field descriptors explained 42.7 % of the variance, while the electrostatic descriptors explained 57.3 %.

The CoMSIA analysis using steric, electrostatic, and lipophilic fields as descriptors gave a model with q^2 of 0.873 and r^2 of 0.954. The CoMSIA steric, electrostatic, and lipophilic fields explained the variance of 8.8, 40.9 and 50.2 %, respectively. This indicated that the hydrophobic interaction was a major factor to explain the field properties of the alkylphosphonates **10**. Further attempts to combine the hydrogen bond fields with the standard steric, electrostatic, and lipophilic fields did not lead to any significant improvement ($q^2 = 0.869$, $r^2 = 0.952$). Indeed, since hydrophobic and electrostatic interactions dominated the inhibitor binding in PDHc E1, correlation coefficients between the activity and the hydrogen bond field were expected to be low. All the results demonstrated that the CoMSIA model was also fairly predictive.

The steric contribution contour maps of CoMFA and CoMSIA are plotted in Figs. 7.2a and 7.3a, respectively. To aid visualization, the most herbicidally active compound **1H-18** is displayed in the maps. The CoMSIA approach provided more contiguous contour diagrams, which allowed physicochemical properties relevant

Table 7.1 CoMFA and CoMSIA results

	CoMFA	CoMSIA
<i>PLS statistics</i>		
q^2	0.872	0.873
N	6	6
SEP	0.383	0.383
r^2	0.974	0.954
SE	0.172	0.229
F	251.512	139.278
<i>Field distribution (%)</i>		
Steric	42.7	8.8
Electrostatic	57.3	40.9
Hydrophobic	/	50.2
<i>Testing set</i>		
r_{bs}^2 ^a	0.983	0.972
SD ^b	0.005	0.011
r_{pred}^2 ^c	0.883	0.908

^a Bootstrapped correlation coefficient^b Bootstrapped standard deviation^c $r_{pred}^2 = 1 - \frac{\sum (pI_{50}^{obsd} - pI_{50}^{pred})^2}{\sum (pI_{50}^{obsd} - pI_{50}^{mean})^2}$

for binding to be mapped back onto the molecular structures. Furthermore, CoMSIA isocontour diagrams lie within regions occupied by the ligands, whereas CoMFA contours highlight those areas where the ligand would interact with a possible environment. Yet, the combination of different approaches enabled one to verify the convergence of the results, or the obtained conclusions could complement each other. In this case, the combination of CoMFA and CoMSIA methods led to a better interpretation for QSAR at the 3D level.

The structures of all molecules used in the training and test sets are listed in Table 7.2. The CoMFA sterically favorable regions appeared around the 4-position of the phenoxy-benzene ring of **IH-18**, suggesting that bulky groups in this region were favored for higher activity. Comparing **IG-10**, **IH-7**, **IE-11**, **IC-10**, and **ID-4** ($Y_n = 4\text{-Cl}$) with **IG-8**, **IH-5**, **IE-10**, **IC-9**, and **ID-3** ($Y_n = 4\text{-F}$), a suitable increase in activity could also be seen by replacing 4-fluoro with 4-chloro as Y_n . No significant increase in activity could be found apparently for **IG-15**, **IH-12**, **IE-15**, **IC-14**, and **ID-6**, which bears an additional methyl group at the 3-position and the overlaps with the CoMSIA sterically disfavorable region. There is also a big region near the 2-position of phenoxy-benzene ring in Fig. 7.3a, indicating that more bulky substituents are needed in this position to improve the inhibitory activity. This was in agreement with the fact that the inhibitory activities of compounds **IG-21**, **IH-11**, **IE-14**, and **ID-5** with more bulky substituents were higher than those of compounds

IG-10, IH-7, IE-11, and ID-4. Since CoMFA analysis revealed a slight sterically disfavored area near the 2-position of phenoxy-benzene ring, it could be concluded that the size of the binding site was limited and there existed an optimal value for the steric effect. The prediction was confirmed by the alignment of inhibitor and receptor, which is shown in Fig. 7.2a; the residues Glu636, Tyr177, Tyr599, TDP887, Glu522, and Leu264 in the binding pocket of PDHc E1 are in the distance of less than 3.0 Å corresponding substructure of the inhibitors. Therefore, a substituent larger than chlorine may lead to collision with the corresponding residues in the pocket.

The electrostatic contour plots are shown in Figs. 7.2b and 7.3b. An important feature of the CoMFA model is that regions favorable to positive charges dominate the electrostatic contour map. It can be seen that a large positive potential favored region locates at the 3-position of the benzene ring of phenoxy-unit. When a fluoro or trifluoromethyl group bearing negative charges is introduced at the 3-position of the phenoxy-benzene ring, it results in the decrease of inhibitory activity. Therefore, the compounds with fluoro (**IG-7, IH-4, IE-9, IC-8, and ID-2**) or trifluoromethyl (**IF-1, IF-23, IF-25, IF-27, and IF-38**) at the 3-position of phenoxy-benzene ring showed much lower activity. As indicated in Fig. 7.2b, the key catalytic negative residues of Glu636 are rather near this region, favoring a strong electrostatic interaction with the positively charged substituent of the inhibitor. Several positive potential favored areas above the same side of the oxygen atom of both carbonyl and phosphoryl are representing the area where the positively charged sodium ions can move freely. A positive potential favored region around the thienyl ring accounts for the decrease in activities of compounds with electronegative substituents, like chloro, methoxy, fluoro and nitro groups, in this region. Electronegative groups (fluoro or chloro) at the 4-position of the phenoxy-benzene ring are essential for high activities, represented by the favorable isopleths near this area. This prediction is in agreement with the appearance of a positively charged residue of His640 at the corresponding position of the PDHc E1. As shown in Fig. 7.3b, the regions at the 2- and 4-position of phenoxy-benzene ring indicate that any electronegative group at these positions would enhance the activity. The region at the 3-position indicates that substituent of an electropositive group at this position would increase the activity, however simultaneously, the bulky substituent at 3-position is disfavored for enhancing the activity, while the bulky substituent at 2-position is favorable, which explains why **IH-11, IE-14, and ID-5** with 2-methyl have better herbicidal activity even than **IH-12, IE-15, and ID-6** with 3-methyl. Therefore the 2-position and 4-position are the most essential sites for substitution, and compounds even with the unfavorable electropositive methyl group at the 2-position still have higher activity, which suggests the contribution of the steric effect of the 2-position substituent for enhancing herbicidal activity is more significant than that of the electronic effect.

CoMSIA contour map in Fig. 7.3c indicates the areas where hydrophilic and hydrophobic properties are preferred, would be useful in selecting specific areas of the molecules, which could be utilized for adjusting the lipophilicity and hydrophilicity to improve the herbicidal activity. As shown in Fig. 7.3c, the area near the 4-position of the phenoxy-benzene ring is just in the space where the (green) region

appears in the steric contour of CoMFA, it could be reasonably assumed that there is a hydrophobic cavity in the receptor, producing hydrophobic interactions with the ligands. This can be seen from the activities of **IG-10**, **IH-7**, and **IE-11** that possess hydrophobic groups at the 4-position, which harbors the hydrophobic residues Tyr599, Thr525, and the counterpart of TDP887. A very distinct hydrophilic site is near the 3-position of the phenoxy-benzene ring, where the compounds contain a methyl group as the substituent (**IG-15**, **IH-12**, **IE-15**, **IC-14**, and **ID-6**) had lower herbicidal active. While the compounds with hydrophilic and electronegative substituents such as fluoro (**IG-7**, **IH-4**, **IE-9**, **IC-8**, and **ID-2**) and trifluoromethyl (**IF-1**, **IF-23**, **IF-25**, **IF-27**, and **IF-38**) showed lower inhibitory activities than that of compounds **IG-15**, **IH-12**, **IE-15**, **IC-14**, and **ID-6**. It can be reasonably assumed that both hydrophilic and electropositive substituents at 3-position of the phenoxy-benzene ring are favorable to inhibitory activity. The efficacy of electropositive substituents at 3-position are more important for enhancing activity than that of the hydrophilic substituents.

7.1.4 Validation of the 3D-QSAR Models

Eleven compounds that were not included in the training set were selected as a test data set to validate the QSAR models. All of the test compounds were well predicted. The mean and standard deviation of prediction errors were 0.28 and 0.005 for the CoMFA model, and only 0.33 and 0.011 for the CoMSIA model. The predictive r_{pred}^2 , which was analogous to the cross-validated correlation coefficient q^2 , was 0.883 for the CoMFA and 0.908 for the CoMSIA, suggesting a high reliability of these models.

The consistency between the CoMFA/CoMSIA field distributions and the 3D topology of the protein structure indicated the robustness of the 3D-QSAR models. Overall, the degree of predictability of the CoMSIA model appeared to be similar to that of the CoMFA model. The combined use of both the CoMFA and the CoMSIA model might be more suitable for the prediction of the activities of novel designed compounds [22].

7.1.5 Molecular Docking

All molecular modeling calculations were performed using SYBYL program [23], package version 7.0 on a bioinformatics grid computer system. To select initial conformations of compounds, we used the X-ray crystallographic coordinates of the higher herbicidal active compound **IH-18**. The structure of the PDHc E1 protein (PDB code 1L8A) [19] was obtained from the Protein Data Bank. The water molecules were removed and polar hydrogen was added. The geometries of these compounds were subsequently optimized using the Tripos force field [24]. The Powell

method [25] was used for energy minimization with an energy convergence gradient value of 0.001 kcal/mol. The Kollman unit-atom charges were assigned to protein atoms using SYBYL 7.0.

The automated molecular docking calculations were carried out using AutoDock 3.0. The AUTOTORS module of the AutoDock defined the active torsions for each docked compound. The active site of the protein was defined using AutoGrid. The grid map with $70 \times 70 \times 70$ points centered at the center of mass of TPP and a grid spacing of 0.375 Å was calculated using the AutoGrid program to evaluate the binding energies between the inhibitors and the protein. The Lamarckian Genetic Algorithm (LGA) [26] was used as the search method. Each LGA job consisted of 50 runs, and the number of generations in each run was 27,000 with an initial population of 100 individuals. The step size was set to 0.2 Å for translation and 5° for orientation and torsion. The maximum number of energy evaluations was set to 1,000,000. Operator weights for crossover, mutation, and elitism were 0.80, 0.02, and 1, respectively. The docked complexes of the inhibitor-enzyme were selected according to the criterion of interaction energy combined with geometrical and electronic matching quality.

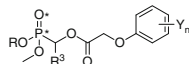
7.1.6 Molecular Alignment and 3D-QSAR Modeling

The complexes were energetically minimized with only the inhibitor and the side-chain atoms of the protein to be flexible. Energy minimizations were carried out using SYBYL 7.0. In each step, the MMFF94 force field was used with 0.01 kcal/Å convergence and 5,000 steps using the Powell method. The refined binding conformation of compound **IH-18** was used for the 3D-QSAR studies. A database of the energy-minimized structures was aligned using the 'align database' option of SYBYL with the compound **IH-18** as the template of the alignment. Asterisks in the molecular structure as shown in Table 7.2 indicate the atoms used for the alignments.

For 3D-QSAR analyses, 47 compounds were selected as the training set for model construction, and the remaining 11 compounds were selected as the test set for model validation.

7.1.7 CoMFA Analysis and CoMSIA Analysis Modeling

The steric and electrostatic potential fields for CoMFA were calculated at each lattice intersection of a regularly spaced grid of 2.0 Å. The lattice was defined automatically, and was extended 4 Å units past Van der Waals volume of all molecules in X, Y, and Z directions. An sp³ carbon atom with Van der Waals radius

Table 7.2 Structure and pIC₅₀ values of molecules used in training and test sets

Compound	R	R ³	Y _n	pIC ₅₀ ^a
IC-8	Me	Me	3-F	3.95
IC-9	Me	Me	4-F	5.82
IC-10^b	Me	Me	4-Cl	6.37
IC-13	Me	Me	2-Me,4-Cl	6.36
IC-14	Me	Me	3-Me,4-Cl	5.53
IC-15^b	Me	Me	2-Cl,5-Me	4.31
IC-21	Me	Me	2,3-Cl ₂	3.68
IC-23	Me	Me	2,6-Cl ₂	4.00
ID-2	Me	CCl ₃	3-F	4.08
ID-3	Me	CCl ₃	4-F	5.93
ID-4	Me	CCl ₃	4-Cl	6.14
ID-5	Me	CCl ₃	2-Me,4-Cl	6.40
ID-6	Me	CCl ₃	3-Me,4-Cl	5.46
ID-7	Me	CCl ₃	2-Cl,5-Me	4.12
ID-12^b	Me	CCl ₃	2,3-Cl ₂	4.15
ID-14	Me	CCl ₃	2,6-Cl ₂	3.94
IE-9	Me	Ph	3-F	3.95
IE-10^b	Me	Ph	4-F	5.82
IE-11	Me	Ph	4-Cl	6.37
IE-14	Me	Ph	2-Me,4-Cl	6.45
IE-15^b	Me	Ph	3-Me,4-Cl	5.59
IE-16	Me	Ph	2-Cl,5-Me	4.14
IE-21	Me	Ph	2,3-Cl ₂	3.64
IE-23	Me	Ph	2,6-Cl ₂	4.07
IF-1	Me	4-MePh	3-CF ₃	5.13
IF-23	Me	2-ClPh	3-CF ₃	5.10
IF-25	Me	3-ClPh	3-CF ₃	4.84
IF-27	Me	4-ClPh	3-CF ₃	5.16
IF-38^b	Me	3,4-Cl ₂ Ph	3-CF ₃	5.08
IG-7	Me	Fur-2-yl	3-F	4.17
IG-8	Me	Fur-2-yl	4-F	5.74
IG-10	Me	Fur-2-yl	4-Cl	6.19
IG-14	Me	Fur-2-yl	2-Me,4-Cl	5.42
IG-15	Me	Fur-2-yl	3-Me,4-Cl	5.44
IG-16	Me	Fur-2-yl	2-Cl,5-Me	4.06
IG-20	Me	Fur-2-yl	2,3-Cl ₂	3.35
IG-21	Me	Fur-2-yl	2,4-Cl ₂	6.47
IG-22^b	Me	Fur-2-yl	2,6-Cl ₂	3.49

(continued)

Table 7.2 (continued)

Compound	R	R ³	Y _n	pIC ₅₀ ^a
IH-4^b	Me	Thien-2-yl	3-F	3.90
IH-5	Me	Thien-2-yl	4-F	5.58
IH-7	Me	Thien-2-yl	4-Cl	6.24
IH-11	Me	Thien-2-yl	2-Me,4-Cl	6.33
IH-12	Me	Thien-2-yl	3-Me,4-Cl	5.63
IH-13	Me	Thien-2-yl	2-Cl,5-Me	4.29
IH-17^b	Me	Thien-2-yl	2,3-Cl ₂	3.23
IH-18	Me	Thien-2-yl	2,4-Cl ₂	6.55
IH-19	Me	Thien-2-yl	2,6-Cl ₂	3.75
IIB-8	Me	Ph	2,4-Cl ₂	6.02
IIB-9	Me	4-MePh	2,4-Cl ₂	5.87
IIB-10	Me	3-NO ₂ Ph	2,4-Cl ₂	5.91
IIB-12	Me	4-MeOPh	2,4-Cl ₂	6.02
IIB-13^b	Me	4-FPh	2,4-Cl ₂	6.11
IIB-14^b	Me	2-ClPh	2,4-Cl ₂	6.04
IIB-16	Me	4-ClPh	2,4-Cl ₂	5.88
IIB-18	Me	2,4-Cl ₂ Ph	2,4-Cl ₂	5.99
IIB-19	Me	3,4-Cl ₂ Ph	2,4-Cl ₂	6.05
IIB-20	Me	Fur-2-yl	2,4-Cl ₂	6.35
IIB-22	Me	Pyrid-2-yl	2,4-Cl ₂	6.24

^a pIC₅₀ = -log (IC₅₀)^b Selected as the test set for model validation.

of 1.52 Å and +1.0 charge was served as the probe atom to calculate steric (Lennard-Jones 6-12 potential) field energies and electrostatic (Columbic potential) fields with a distance-dependent dielectric at each lattice point. The steric and electrostatic contributions were truncated to 30.0 kcal/mol, and electrostatic contributions were ignored at lattice intersections with maximum steric interactions. The CoMFA steric and electrostatic fields generated were scaled by the CoMFA standard option given in SYBYL.

CoMSIA similarity indices descriptors were derived according to Klebe et al. [18] with the same lattice box used for the CoMFA. CoMSIA similarity indices (A_F) for a molecule j with atoms i at a grid point q are determined as follows:

$$A_{F,k}^q(j) = \sum_i \omega_{\text{probe},k} \omega_{ik} e^{-\alpha r_{iq}^2}$$

where ω_{ik} is the actual value of the physicochemical property k of atom i ; $\omega_{\text{probe},k}$ is the probe atom with a charge of +1, radius of 1 Å, hydrophobicity of +1, hydrogen bond donating of +1, and hydrogen bond accepting of +1; r_{iq} is the mutual distance

between the probe atom at grid point q and the atom i of the molecule. A Gaussian type distance dependence was considered between the grid point q and each atom i of the molecule, where r represents the distance. The default value of 0.3 was used as the attenuation factor (α). A lattice of 2 Å grid spacing was generated automatically.

7.1.8 PLS Calculations and Validations

Partial least-square (PLS) methodology was used for all 3D-QSAR analyses [27–29], in which the CoMFA and CoMSIA descriptors were used as independent variables, and pIC₅₀ values were used as dependent variables. The cross-validation with the leave-one-out option and the SAMPLS program [30], rather than column filtering, was carried out to obtain the optimum number of components to be used in the final analysis. The number of components used was not greater than 1/3 of the number (47) of rows in the training set. After the optimum number of components (N) was determined, a non-cross-validated analysis was performed without column filtering. The cross-validated correlation coefficient q^2 , standard error of prediction SEP, non-cross-validated correlation coefficient r^2 , and F values and standard error of estimate SE values were computed according to the definitions in SYBYL. To further assess the robustness and statistical confidence of the derived models, bootstrapping analyses (100 runs) were performed and the mean r^2 was given as bootstrap (r_{bs}^2).

7.1.9 Summary

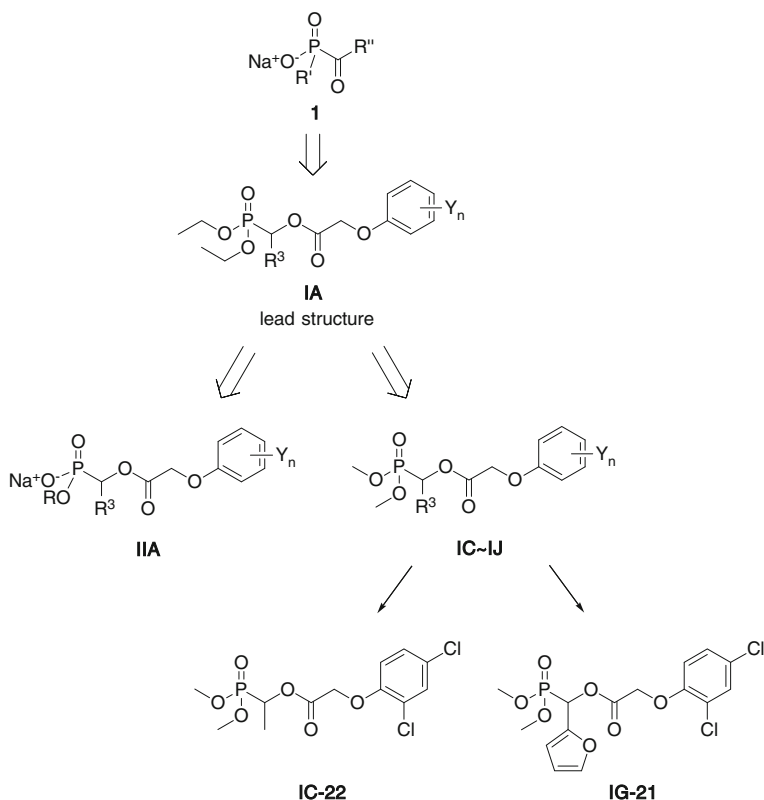
In summary, predictive CoMFA and CoMSIA models were developed for a series of 1-(aryloxyacetoxy)alkylphosphonates as potent PDHc E1 inhibitor with herbicidal activity by using the alignment scheme generated from the docking study. The models were validated with high reliability in the prediction of inhibitory activities. The consistency between the CoMFA/CoMSIA field distributions and the 3D topology of the protein structure indicates the robustness of the 3D-QSAR models. Overall, the degree of predictability of the CoMSIA model appeared to be similar to that of the CoMFA model. The combined use of both the CoMFA and the CoMSIA model may be most suitable for prediction of the activities of the novel designed compounds.

7.2 Enzyme Inhibition

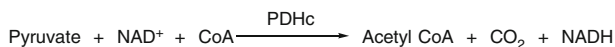
7.2.1 Introduction

Several series of 1-(substituted phenoxyacetoxy)alkylphosphonates such as **IC**, **IG**, and **IIA** were found to possess potent post-emergence herbicidal activity against dicotyledons through the optimization of the hit compound, sodium *O*-alkyl acylphosphonates **1** step-by-step (Scheme 7.1). Especially **IC-22** (HW02, clacyfos) and **IG-21**(HWS) exhibited promising practical herbicidal activity and good selectivity for broadleaf weeds control in monocot crop fields. Both compounds were expected to be developed as selective post-emergence herbicides.

These alkylphosphonates and the monosalts of corresponding phosphonic acid were expected to be effective inhibitors of plant PDHc E1. Some compounds



Scheme 7.1 Modification of lead structure



Scheme 7.2 Conversion of pyruvate to acetyl coenzyme A catalyzed by PDHc

including **IC-22**, **IG-21** and the corresponding sodium salts were chosen to examine their inhibition against plant PDHc.

7.2.2 Inhibitory Potency Against Plant PDHc

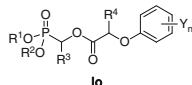
The overall reaction for PDHc catalyzing conversion of pyruvate to acetyl coenzyme A is shown in Scheme 7.2. In this reaction pyruvate is converted to acetyl-coenzyme A, while NAD^+ (oxidized nicotinamide adenine dinucleotide) is converted to NADH (reduced nicotinamide adenine dinucleotide).

The activity of PDHc can be determined by a sensitive spectrophotometric assay according to the literatures [31–34]. In this procedure, PDHc can be conveniently assayed by measuring the rate of appearance of product NADH, which absorbs the ultraviolet region at 340 nm [35]. Since absorbance is proportional to concentration, the rate of change in absorbance is proportional to enzyme activity. Thus, if NADH is produced during the course of the reaction, there will be the corresponding increase in absorbance at 340 nm. While if the reaction is prevented by an inhibitor, or enzyme PDHc E1 is inhibited by an inhibitor, NADH levels are expected to decrease, there will be the corresponding decrease in absorbance comparing with control. Thus the PDHc activity can be determined by measuring the formation of NADH.

As described in Chaps. 2–6, most of 1-(substituted phenoxyacetoxy)alkylphosphonates with 2,4- Cl_2 as Y_n on the phenoxy-benzene ring exhibited much better herbicidal activity against dicotyledons than monocotyledons. Therefore, some alkylphosphonates and the corresponding sodium salts with 2,4- Cl_2 as Y_n were chosen to examine their inhibition against PDHc from both dicotyledons and monocotyledons plants in vitro. Mung bean (*V. radiata*) and pea (*Pisum sativum*) as representative dicotyledonous plants, rice (*Oryza sativa*) as a representative monocotyledonous plant were used in enzyme assays. The IC_{50} values of the tested compounds against plant PDHc are listed in Table 7.3.

7.2.2.1 The Effect of Compounds Against PDHc from Dicotyledons

As shown in Table 7.3, all tested compounds except **IC-5** and **IJ-1** exhibited significant inhibition against PDHc from both mung bean and pea. **IA-4**, **IC-1**, **IC-22**, **IG-21**, and **IID-10** exhibited powerful inhibitory potency against PDHc from the tested dicotyledonous plants ($\text{IC}_{50} < 30 \mu\text{M}$). The most powerful inhibitor against

Table 7.3 IC₅₀ values of some alkylphosphonates **Io** against PDHc from three plants

Compound	R ¹	R ²	R ³	R ⁴	Y _n	IC ₅₀ (μM) ^a	Source
IC-22	Me	Me	Me	H	2,4-Cl ₂	12.75	Mung bean
IC-1	Me	Me	H	H	2,4-Cl ₂	19.70	Mung bean
IE-22	Me	Me	Ph	H	2,4-Cl ₂	95.38	Mung bean
IA-4	Et	Et	Me	H	2,4-Cl ₂	23.12	Mung bean
IC-22	Me	Me	Me	H	2,4-Cl ₂	18.19	Pea
IG-21	Me	Me	Fur-2-yl	H	2,4-Cl ₂	28.25	Pea
IID-10	Na	Me	Fur-2-yl	H	2,4-Cl ₂	6.96	Pea
IC-5	Me	Me	Me	H	3-CF ₃	442	Pea
IJ-1	Me	Me	Pyrid-2-yl	H	3-CF ₃	>2300	Pea
IIB-1	Na	Me	H	H	2,4-Cl ₂	29.14	Rice
IC-22	Me	Me	Me	H	2,4-Cl ₂	867.3	Rice
IIB-2	Na	Me	Me	H	2,4-Cl ₂	0.29	Rice
IIB-3	Na	Me	Et	H	2,4-Cl ₂	18.87	Rice
IIB-4	Na	Me	n-Pr	H	2,4-Cl ₂	3.26	Rice
IG-21	Me	Me	Fur-2-yl	H	2,4-Cl ₂	703.88	Rice
IID-10	Na	Me	Fur-2-yl	H	2,4-Cl ₂	41.14	Rice

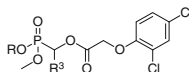
^a IC₅₀(μM) value is defined as the micromolar concentration required for 50 % inhibition against PDHc from plant

dicotyledons was **IID-10** (IC₅₀ = 6.96 μM). The inhibitory potencies of all tested compounds against PDHc from both mung bean and pea decreased with a decrease of concentration of inhibitors. The powerful inhibitory potency against plant PDHc should produce by inhibition against plant PDHc E1 according to the design idea of alkylphosphonates **Io**.

7.2.2.2 The Effect of Compounds Against PDHc from Monocotyledon Rice

Rice was chosen as a typical monocotyledonous plant for enzyme activity assays. There was much difference in inhibitory potency against rice PDHc among the tested compounds. As shown in Table 7.3, most of the tested compounds showed significant inhibitory potency against rice PDHc except **IC-22** and **IG-21**. Especially sodium salts **IIB-2**, **IIB-3**, and **IIB-4** exhibited very powerful inhibitory potency against rice PDHc (IC₅₀ < 20 μM). The higher the treated concentration, the greater the inhibitory potency against rice PDHc.

Table 7.4 Selective inhibition against plant PDHc



Compound	R	R ³	IC ₅₀ (μM) ^a		
			Rice	Pea	Mung bean
IC-22	Me	Me	867.3 (1) ^b	18.19 (47)	12.75 (68)
IG-21	Me	Fur-2-yl	703.88 (1)	28.25 (25)	
IID-10	Na	Fur-2-yl	41.14 (1)	6.96 (6)	

^a IC₅₀ (μM) value is defined as the micromolar concentration required for 50 % inhibition against PDHc from plant.

^b Figures in parentheses show relative activity based on IC₅₀ of rice.

7.2.2.3 Selective Inhibition Against PDHc from Different Plants

The tested compounds showed much higher inhibitory potency against dicotyledonous PDHc than that of monocotyledonous PDHc. As shown in Table 7.4, **IC-22**, **IG-21**, and **IID-10** exhibited powerful inhibitory potency against PDHc from both mung bean and/or pea, but they showed relatively lower inhibitory potency against PDHc from rice. The above observations showed that these compounds could selectively inhibit the PDHc from dicotyledonous plants. Especially **IC-22** and **IG-21** exhibited good selective inhibition against PDHc from dicotyledonous plants. Noticeably sodium salt **IID-10** showed much weaker selective inhibition between the monocotyledon and the dicotyledon than that of its corresponding phosphonate **IG-21**.

7.2.3 Kinetic Experiment of PDHc

In order to recognize the type of mechanism of the PDHc inhibitor, **IC-22** was chosen to study its inhibition against plant PDHc by kinetic experiment. The maximum velocity (V_{\max}) and Michaelis constant (K_m) were determined by measuring the enzyme catalytic effect at different concentrations of substrate (sodium pyruvate) in the presence or absence of the **IC-22** (Scheme 7.3).

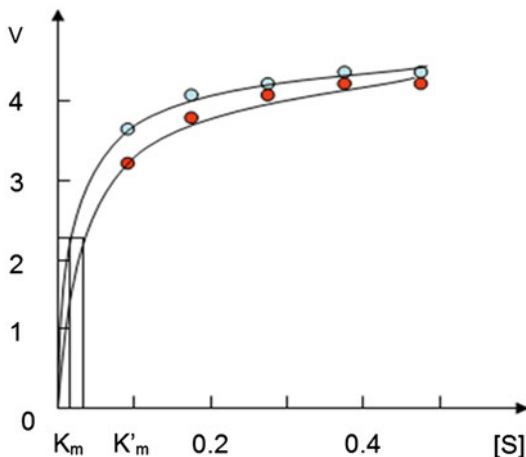
According to $V = \frac{V_{\max}[S]}{K_m + [S]}$, V_{\max} and K_m were obtained as follows.

According to the enzyme kinetic experiments of **IC-22** (Scheme 7.3), V_{\max} and K_m were obtained as:

In the presence of inhibitor **IC-22**: $K_m = 0.03262$ mM, $V_{\max} = 0.4349$ mM

In the absence of inhibitor **IC-22**: $K'_m = 0.01329$ mM, $V_{\max} = 0.4373$ mM

Scheme 7.3 Enzyme kinetic experiments of IC-22 as inhibitor. k_m no inhibitor, k_m' inhibitor present [S]: The concentration of substrate (sodium pyruvate)



The data showed that V_{\max} almost remained constant, and K_m increased in the presence of **IC-22**. The inhibition could be decreased with the increase in the concentration of sodium pyruvate as a substrate. When the concentration of substrate sodium pyruvate increased to 0.5 mM, the inhibition almost disappeared. This indicated that the inhibition of PDHc by **IC-22** could be overcome by increasing the concentration of substrate. K_m was increased in the presence of **IC-22**, which showed that the apparent affinity of enzyme for its substrate was decreased in the presence of **IC-22**. **IC-22** could diminish the rate of catalysis by reducing the proportion of enzyme molecules bound to the substrate. However, the V_{\max} were almost the same in the presence and absence of **IC-22**. **IC-22** was thus recognized to act as a competitive inhibitor of PDHc [16].

7.2.4 Selective Enzyme Inhibition

As stated in Sects. 1.3.3 and 1.4.2 in Chap. 1, sodium salts of acetyl(methyl) phosphinic acid **1-2** and **1-3** could exhibit powerful inhibition against PDHc E1 in plant (pea) and bacteria (*E. coli*). However, **1-2** and **1-3** had poor enzyme-selective inhibition between mammals and plant or bacteria, because they were also powerful inhibitors against human PDHc E1 [36].

In order to examine the inhibition against PDHc from different source and some other enzymes, **IC-22**, **IG-21**, and **IIB-2** were selected to test their selective enzyme inhibition. The effects against PDHc from plant, and animal were compared. The effects of **IC-22** on acetolactate synthase (ALS), peroxidase (POD) and superoxide dismutase (SOD) from plant were also examined.

As shown in Table 7.5, **IC-22** had very weak inhibition against pea ALS. It also showed very low inhibitory potency against POD and SOD from rice. Compared with the inhibitory potency against PDHc from different source, **IC-22** and **IG-21** exhibited much higher inhibitory potency against pea PDHc than against PDHc from animal (pig heart). Both compounds had almost no inhibition against PDHc from pig heart. **IIB-2** exhibited a powerful inhibition against rice PDHc but no inhibition against pig PDHc was observed. These findings showed that **IC-22**, **IG-21**, and **IIB-2** had very good selective inhibition against plant PDHc. The above observations also indicated that **IC-22** and **IG-21** could act as special inhibitor against dicotyledonous plant PDHc. Unlike PDHc inhibitors **1-2** and **1-3**, **IC-22**, **IG-21**, and **IIB-2** showed better enzyme-selective inhibition between plant and mammals, they as selective inhibitors of plant PDHc would be safe for animal or human. **IC-22** and **IG-21** were also confirmed to be very safe for mammals by later toxicity evaluation. Toxicity and eco-toxicity evaluation further showed that **IC-22** and **IG-21** exhibited low acute toxicity against rat and were not harmful to mammals, moreover, they were also less toxic and relatively harmless for bee, bird, zebra fish, and silkworm (see Chap. 8).

Table 7.5 Selective inhibition against enzymes in vitro of **IC-22**, **IG-21**, and **IIB-2**

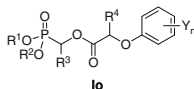
Compound	Enzyme	Enzyme source		IC ₅₀ ^a or Inhibitory potency % ^b
IC-22	PDHc	Plant	Pea	IC ₅₀ = 18 μM
			Rice	IC ₅₀ = 867 μM
		Animal	Pig heart	4 %
	ALS	Plant	Pea	IC ₅₀ = 280 μM
	POD		Rice	IC ₅₀ = 3,500 μM
SOD	Rice		IC ₅₀ = 1,760 μM	
IG-21	PDHc	Plant	Pea	IC ₅₀ = 28 μM
			Rice	IC ₅₀ = 704 μM
		Animal	Pig heart	5 %
IIB-2	PDHc	Plant	Rice	IC ₅₀ = 0.29 μM
		Animal	Pig heart	0 %

^a IC₅₀ (μM) value is defined as the micromolar concentration required for 50 % inhibition against PDHc from plant.

^b Inhibitory potency (%): Inhibitory potency of compounds against enzyme in vitro at 100 μM as average of triplicate.

7.2.5 Structure-Activity Relationships

7.2.5.1 Structure-Inhibitory Potency Relationships



The data in Table 7.3 suggest that substituents R^1 , R^2 , R^3 , and Y_n in the general structure of alkylphosphonate **10** had great influence on the inhibitory potency when H as R^4 was kept unchanged. On the scaffold of the alkylphosphonates **10** with H as R^4 , the effects of substituents R^1 , R^2 , R^3 , and Y_n on the inhibitory potency can be summarized as follows:

(A) Effect of Y_n on inhibitory potency

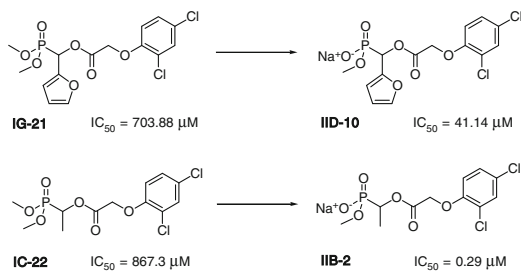
Inhibitory potency against plant PDHc was highly dependent on the structure and position of substituents Y_n on the phenoxy-benzene ring. All tested compounds with 2,4-dichloro as Y_n showed significant inhibition against plant PDHc. The inhibitory potency against pea PDHc could be greatly enhanced by introducing 2,4-Cl₂ into the phenoxy-benzene ring. When Me as R^1 , R^2 , and R^3 were kept constant, **IC-22** ($IC_{50} = 18.19 \mu\text{M}$) with 2,4-dichloro as Y_n exhibited much higher potency against pea PDHc than that of **IC-5** ($IC_{50} = 442 \mu\text{M}$) with 3-CF₃ as Y_n .

(B) Effect of R^1 and R^2 on inhibitory potency

R^1 and R^2 in the phosphonates were also essential for inhibitory potency against plant PDHc. When 2,4-dichloro as Y_n on the phenoxy-benzene ring was kept constant, inhibitory potency against plant PDHc could be greatly enhanced by the modifications of R^1 and R^2 .

It was found that inhibitory potency against plant PDHc increased with the decrease in the size of both R^1 and R^2 group in the phosphorus-containing moiety. **IC-22** ($IC_{50} = 12.75 \mu\text{M}$) with Me as R^1 and R^2 displayed higher inhibitory potency against mung bean PDHc than that of **IA-4** ($IC_{50} = 23.12 \mu\text{M}$) with Et as R^1 and R^2 .

All tested the monosodium salts displayed higher inhibitory potency against plant PDHc than that of their corresponding phosphonates. When one of Me as R^1 and R^2 was replaced by Na, the inhibitory potency against plant PDHc could be greatly improved (Table 7.3). For example, monosodium salt **IID-10** ($R^1 = \text{Na}$, $R^2 = \text{Me}$, $R^3 = \text{fur-2-yl}$, $IC_{50} = 6.96 \mu\text{M}$) exhibited higher inhibitory potency against pea PDHc than its corresponding phosphonate ester **IG-21** ($R^1 = R^2 = \text{Me}$, $R^3 = \text{fur-2-yl}$, $IC_{50} = 28.25 \mu\text{M}$). Monosodium salts **IID-10** ($IC_{50} = 41.14 \mu\text{M}$) and **IIB-2** ($R^1 = \text{Na}$, $R^2 = R^3 = \text{Me}$, $IC_{50} = 0.29 \mu\text{M}$) also displayed higher inhibitory potency against rice PDHc than their corresponding phosphonate esters **IG-21** ($IC_{50} = 703.88 \mu\text{M}$) and **IC-22** ($R^1 = R^2 = R^3 = \text{Me}$, $IC_{50} = 867 \mu\text{M}$).



Scheme 7.4 Inhibitory potency against rice PDHc in the conversion of phosphonate esters into their salts

(C) *Effect of R^3 on inhibitory potency*

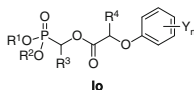
When Y_n , R^1 , R^2 , and R^4 were kept constant, R^3 bound to α -carbon also had great influence on the inhibitory potency. The introduction of Me as R^3 seems to have a favorable effect on inhibitory potency.

- Compounds with Me as R^1 and R^2 , H as R^4 , and 3-CF₃ as Y_n
Inhibitory potency: **IC-5** ($R^3 = \text{Me}$) > **IJ-1** ($R^3 = \text{pyrid-2-yl}$)
- Compounds with Me as R^1 and R^2 , H as R^4 , and 2,4-Cl₂ as Y_n
Inhibitory potency: **IC-22** ($R^3 = \text{Me}$) > **IC-1** ($R^3 = \text{H}$) > **IE-22** ($R^3 = \text{Ph}$)
- Compounds with Na as R^1 , Me as R^2 , H as R^4 , and 2,4-Cl₂ as Y_n
Inhibitory potency: **IIB-2** ($R^3 = \text{Me}$) > **IIB-4** ($R^3 = \text{n-Pr}$) > **IIB-3** ($R^3 = \text{Et}$) > **IIB-1** ($R^3 = \text{H}$) > **IID-10** ($R^3 = \text{fur-2-yl}$)

IIB-2 with Me as R^3 , as the monosodium salt of **IC-22** exhibited the best inhibitory potency against rice PDHc among compounds in Table 7.3. However, monosodium salt **IID-10** with fur-2-yl as R^3 showed weaker activity against rice PDHc than those of compounds with H or alkyl groups as R^3 , such as **IIB-1**, **IIB-2**, **IIB-3**, and **IIB-4**.

The analyses for structure-inhibitory potency relationships indicated that the improvement of inhibitory potency against plant PDHc required an optimal combination of R^1 , R^2 , R^3 , and Y_n . As shown in Scheme 7.4, when 2,4-Cl₂ as Y_n are kept constant, inhibitory potency of the compound could be greatly enhanced by the chemical modification of R^1 , R^2 , and R^3 in the phosphorus-containing moiety. Especially the conversion of phosphonate esters to their salts could make great improvement in inhibitory potency against plant PDHc. Thus **IIB-2** was found to exhibit the best inhibitory potency against rice PDHc.

7.2.5.2 Relationships between Inhibitory Potency Against Plant PDHc and Herbicidal Activity



Comparing the inhibitory potency against plant PDHc with the herbicidal activity of tested compounds, it could be found that their herbicidal activity correlated well with their enzyme inhibition including selectivity and SAR. Based on the general structure of phosphonates **10**, the relationship between enzyme inhibition and herbicidal activity is summarized as follows:

(A) *Selective inhibition*

All tested compounds, such as **IC-22**, **IG-21**, and **IID-10** showed much higher inhibitory potency against PDHc from dicotyledons (pea or mung bean) than their inhibitory potency against PDHc from monocotyledon (rice). They also exhibited higher herbicidal activity against dicotyledonous plants (such as pea, common amaranth, rape) than monocotyledonous plants (such as barnyard grass and rice). The data are listed in Table 7.6.

It is worth noting that both **IC-22** and **IG-21** showed higher inhibitory potency against PDHc from pea than rice *in vitro*; both compounds also showed higher herbicidal activity against pea than rice in the greenhouse. **IC-22** and **IG-21** showed much higher herbicidal activity against dicotyledonous plants than monocotyledonous plants. They also had weak activity against the monocot weed, such as barnyard grass and were safe for wheat and rice. **IC-22** and **IG-21** exhibited much better selectivity between pea and rice than **IID-10**. The above observations indicated that **IC-22** and **IG-21** could selectively inhibit the growth of dicotyledonous plants due to their selective inhibition against PDHc from dicotyledonous plants. Both **IC-22** and **IG-21** exhibited weak post-emergence activity against wheat, maize, and rice because they were weak against PDHc from monocotyledons. Therefore they could be useful as a selective herbicide for dicotyledonous weeds control in monocotyledonous crop fields. The inhibitory potency of **IC-22** against PDHc from pea, mung bean, and rice increased with the increase of concentration of **IC-22**. Its herbicidal activity against dicotyledons and some monocotyledons also increased with the increase of used dosage. Assay of PDHc showed that **IC-22** and **IG-21** had weak activity against *E. coli* PDHc E1, both compounds also showed very weak bactericidal or fungicidal activities.

(B) *Effect of Y_n on enzyme inhibition and herbicidal activity*

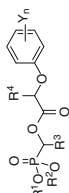
According to data in Table 7.3, both inhibitory potency against plant PDHc and herbicidal activity were highly dependent upon the structure and position of substituents Y_n on the phenoxy-benzene ring. **IC-22** with 2,4-Cl₂ as Y_n showed higher inhibitory potency against PDHc from dicotyledon (pea) than **IC-5** with 3-CF₃ as Y_n. **IC-22** also showed higher herbicidal activity against dicotyledons than that of **IC-5**. It showed that 2- and 4-positions on the phenoxy-benzene ring were the most

Table 7.6 Herbicidal activity and inhibitory potency against plant PDHc of some alkylphosphonates

Compound	R ¹	R ²	R ³	Y _n	Herbicidal activity for post-emergence (%) ^a				Inhibition against PDHc, IC ₅₀ (μM) ^b			
					Barnyard grass	Rice	Common amaranth	Rape	Pea	Pea	Mung bean	Rice
IC-22	Me	Me	Me	2,4-Cl ₂	35	0	100	100	98	18.19	12.75	867.3
IC-1	Me	Me	H	2,4-Cl ₂	0	0	98	100	88	NT	19.70	NT
IE-22	Me	Me	Ph	2,4-Cl ₂	25	10	88	98	97	NT	95.38	NT
IA-4	Et	Et	Me	2,4-Cl ₂	5	38	100	98	83	NT	23.12	NT
IG-21	Me	Me	Fur-2-yl	2,4-Cl ₂	25	10	97	100	90	28.25	NT	703.88
IHD-10	Na	Me	Fur-2-yl	2,4-Cl ₂	50	45	93	100	98	6.96	NT	41.14
IC-5	Me	Me	Me	3-CF ₃	0	33	58	83	10	442	NT	NT
IJ-1	Me	Me	Pyrid-2-yl	3-CF ₃	0	0	60	78	0	>2,300	NT	NT
IIB-1	Na	Me	H	2,4-Cl ₂	10	12	93	92	53	NT	NT	29.14
IIB-2	Na	Me	Me	2,4-Cl ₂	50	27	100	98	72	NT	NT	0.29
IIB-3	Na	Me	Et	2,4-Cl ₂	30	27	95	97	90	NT	NT	18.87
IIB-4	Na	Me	<i>n</i> -Pr	2,4-Cl ₂	45	22	96	97	78	NT	NT	3.26
2,4-D					35	38	100	100	98	>4,530	NT	NT

^a Herbicidal activity (%) against the plant growth for post-emergence application at a rate of 450 g ai/ha in the greenhouse; 0 (no effect), 100 % (completely kill), NT (not tested)

^b IC₅₀ value is defined as the micromolar concentration required for 50 % inhibition against PDHc from plant



The SAR analyses for R¹ and R² in 1-(substituted phenoxyacetoxy)alkyl phosphonates **Io** are consistent with the SAR analyses for R¹ in the acylphosphonates **1** by Baillie et al. It is clear that the methyl group is favorable for efficient binding to the enzyme.

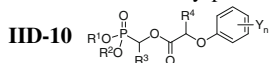
When the Me as one of R¹ and R² in phosphorus-containing moiety was replaced by Na, the inhibitory potency against plant PDHc (or PDHc E1) was greatly improved. Monosodium salts **IIB-2** and **IID-10** displayed higher inhibitory potency against rice PDHc and higher pre-emergence activity against monocotyledons than their corresponding, phosphonates **IC-22** and **IG-21** (Table 7.7). **IID-10** also exhibited higher inhibitory potency against pea PDHc than that of its corresponding phosphonates **IG-21**. However, phosphonate **IG-21** seemed to have a better selectivity between dicotyledons and monocotyledons than that of **IID-10**. The above results showed that R¹ and R² in the alkylphosphonates **Io** could significantly affect both inhibitory potency against plant PDHc (or PDHc E1) and herbicidal activity.

(D) *Effect of R³ on enzyme inhibition and herbicidal activity*

When Y_n, R¹, R² and R⁴ in the alkylphosphonates **Io** were kept constant. R³ bound to α-carbon also had influence on both inhibitory potency against PDHc and herbicidal activity. The introduction of Me as R³ seemed to have a favorable effect on both inhibitory potency against PDHc and herbicidal activity. When Me as R¹ and R², H as R⁴ and 2,4-Cl₂ as Y_n, **IC-22** with Me as R³ showed better inhibitory potency against both mung bean PDHc and cucumber than that of **IC-1** with H as R³ and **IE-22** with Ph as R³ (Table 7.8). **IC-22** also showed higher inhibitory potency against pea PDHc than that of **IG-21** with fur-2-yl as R³ (Table 7.3). It is shown that the methyl group as R³ is favorable for efficient binding to PDHc E1.

The above results indicate that the improvement of both inhibitory potency against plant PDHc and herbicidal activity requires a reasonable combination of R¹, R², R³, and Y_n.

Table 7.7 Inhibitory potency against PDHc and herbicidal activity of **IC-22**, **IG-21**, **IIB-2**, and

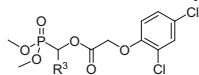


Compound	R ¹	R ²	R ³	IC ₅₀ (μM) ^a		
				Rice PDHc	Ech ^c	Dig ^c
IIB-2	Na	Me	Me	0.29	A	A
IC-22	Me	Me	Me	867.3	B	B
IID-10	Na	Me	Fur-2-yl	41.14	A	A
IG-21	Me	Me	Fur-2-yl	703.88	C	B

^a IC₅₀ (μM) value is defined as the micromolar concentration required for 50 % inhibition on PDHc from rice

^b Inhibitory potency (%) against the growth of plants at a rate of 900 g ai/ha in the greenhouse was expressed as four scales: A: 90–100 %, B: 75–89 %, C: 50–74 %, D: <50 %

^c Ech: barnyard grass; Dig: crab grass

Table 7.8 Inhibitory potency against PDHc and herbicidal activity of **IC-22**, **IC-1**, and **IE-22**

Compound	R ³	IC ₅₀ (μM) ^a	IC ₅₀ (μM) ^b , Cucumber	
			Root length	Stem length
		PDHc from mung bean		
IC-22	Me	12.75	0.0025	7.56
IC-1	H	19.70	0.058	7.79
IE-22	Ph	95.38	0.084	8.95

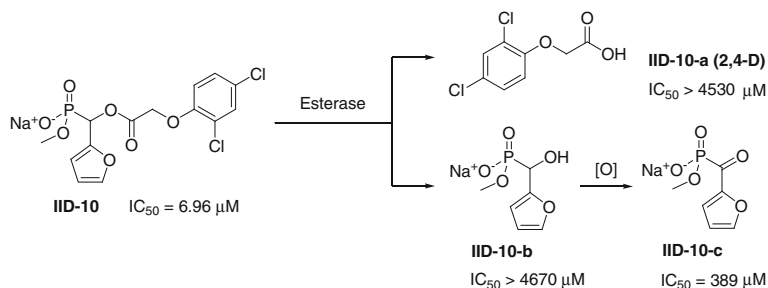
^a IC₅₀ (μM) value is defined as the micromolar concentration required for 50 % inhibition on PDHc from mung bean (in vitro)

^b IC₅₀ (μM) value is defined as the micromolar concentration required for 50 % inhibition against the growth of cucumber (root or stem)

7.2.5.3 Inhibitory Potency Against PDHc and Herbicidal Activity of Possible Metabolic Products

A presumption about a possible metabolic pathway of alkylphosphonates **Io** in plants is described in Chap. 1 (Scheme 1.21). We proposed a metabolic pathway of 1-(substituted phenoxyacetoxymethyl)alkylphosphonates **Io** in plants when **Io** were initially designed. These alkylphosphonates **Io** may be metabolized to substituted phenoxyacetic acids (**Io-a**) as an auxin-type herbicide and acylphosphonates (**Io-c**) as inhibitors of PDHc to show herbicidal activity after hydrolysis and oxidation by some esterases and oxidases in plants. For example, **IID-10** was presumably metabolized to **IID-10-a** (2,4-D), **IID-10-b**, and **IID-10-c** (Scheme 7.6). The herbicidal activity of **IID-10** might, therefore, come from the effects of both possible metabolic products **IID-10-a**, and **IID-10-c**. To examine this hypothesis, these possible metabolic products **IID-10-a** (2,4-D), **IID-10-b**, and **IID-10-c** were prepared and their inhibitory potency against pea PDHc in vitro was tested (Scheme 7.6). Greenhouse tests were also done for the inhibitory activity against the growth of barnyard grass (*Echinochloa crusgalli*), rice (*Oryza sativa*), common amaranth (*Amaranthus retroflexus*), leaf mustard (*Brassica juncea*) and pea (*Pisum sativum*) and rape (*Brassica campestris*) (Tables 7.9 and 7.10).

IID-10-b and **IID-10-c** had much lower inhibitions against pea PDHc in vitro than **IID-10**, and they were inactive against pea and other tested dicotyledonous plants in vivo in the greenhouse tests (Tables 7.9 and 7.10). Although **IID-10-a** (2,4-D) showed a high activity against pea and other tested dicotyledonous plants, it was almost inactive against pea PDHc. These findings indicated that **IID-10** itself was responsible for both inhibitory potency against pea PDHc enzyme and post-emergence herbicidal activity against pea. **IID-10** was also responsible for its



Scheme 7.6 Possible metabolic pathway of **IID-10** in plant and inhibitory potency against pea PDHc of possible metabolic products

Table 7.9 Herbicidal activity and inhibitory potency against pea PDHc of **IID-10** and its possible metabolic products^a

Compound	Barnyard grass	Rice	Common amaranth	Leaf mustard	Pea	IC_{50} (μM) ^b Pea PDHc
IID-10	50	45	95	100	98	6.96
IID-10-a (2,4-D)	35	38	100	100	98	>4,530
IID-10-b	18	NT	NT	0	0	>4,670
IID-10-c	25	NT	NT	25	35	389

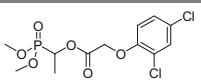
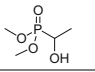
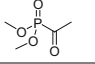
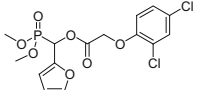
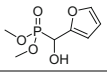
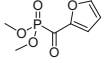
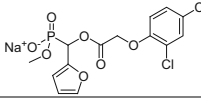
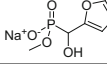
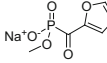
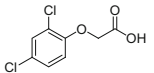
^a Herbicidal activity (%) against the growth of plants at 450 g ai/ha in the greenhouse for post-emergence applications. 0 (no effect), 100 % (completely kill), NT (not tested)

^b IC_{50} (μM) value is defined as the micromolar concentration required for 50 % inhibition on PDHc from pea (in vitro)

herbicidal activity against tested broadleaf plants by post-emergence applications. In order to further confirm the herbicidal effects of possible metabolic products of 1-(substituted phenoxyacetoxy)alkylphosphonates, **IC-22**, **IG-21** and its possible metabolic products, such as **IC-22-b**, **IC-22-c**, **IG-21-b**, and **IG-21-c** were also tested for their inhibitory activity against a set of plants. The data in Tables 7.9 and 7.10 showed that **IG-21**, **IID-10**, and **IC-22** displayed high activity against all tested dicotyledonous plants at 450 g ai/ha in the greenhouse, however, those possible metabolic products **IID-10-b** and **IID-10-c**, **IG-21-b** and **IG-21-c**, **IC-22-b** and **IC-22-c** exhibited very weak activity against all tested dicotyledonous plants in the same assay. These findings indicated that both enzyme inhibition and herbicidal activity of these compounds should come from the compounds themselves, not come from their possible metabolic products [38].

The above findings demonstrated that there was good correlation between enzyme inhibition and herbicidal activity, suggesting that PDHc could be a target for new herbicide design and development.

Table 7.10 Inhibitory potency against rape (*Brassica campestris*)^a

Compound	Structure	<i>Brassica campestris</i>		
		IC ₅₀ (μM) ^a	Post ^b	Pre ^b
IC-22		0.0344	98	96
IC-22-b		2,404.248	30	36
IC-22-c		1,875.671	45	34
IG-21		0.0418	92	94
IG-21-b		>4,672	20	25
IG-21-c		236.848	50	56
IID-10		0.0396	95	96
IID-10-b		>4,672	20	23
IID-10-c		3,245	30	20
IID-10-a (2,4-D)		0.0556	90	98

^a IC₅₀ (μM) value is defined as the micromolar concentration required for 50 % inhibition against the growth of rape root

^b Herbicidal activity (%) against the rape growth at 450 g ai/ha in the greenhouse for post-emergence and pre-emergence applications. 0 (no effect), 100 % (completely kill)

On the other hand, herbicide activity of **IG-21**, **IID-10** and some analogs were also observed on tested plants with symptoms of stunting, necrosis, and morphological effects. Some symptoms are similar to 2,4-D. Maybe **IG-21**, **IID-10** also has auxin-type herbicidal action as they are also the derivatives of 2,4-D acid.

SAR analyses indicated when 2,4-Cl₂ substituted phenoxyacetoxy units were kept constant, great difference in inhibitory potency could still be made by the change of R¹, R², R³, and R⁴ in alkylphosphonates **Io**. As stated in Chap. 2, we could obtain the compounds with higher activity than 2,4-D by optimizing R¹, R², and R⁴ (Me as R¹, R², and H as R⁴), but some compounds with Et or n-Pr as R¹, and

R² showed much lower activity than 2,4-D (Table 2.31). This finding also showed that these phosphonates themselves were responsible for their inhibitory activity, and not the possible metabolic product 2,4-D.

7.2.6 Assay of PDHc from Plant

7.2.6.1 Assay of PDHc from Pea (in Vitro)

(A) Preparation of pea (*P. sativum*) mitochondria

The preparation of pea mitochondria was carried out according to the procedure developed by Reid et al. [39] Pea (*P. sativum*) seeds were soaked in water overnight and grown at room temperature in the dark until the shoots were 20–30 cm in height. The shoots were cut into small pieces (about 10 mm) and frozen for 1 h in the refrigerator. Then the shoots were ground, using a mortar and pestle, in three times volume of 50 mM Tris-HCl buffer (pH 7.4) containing 0.25 M glucose, 3 mM EDTA, and 0.75 mM BSA. The homogenate was filtered through several layers of cheesecloth and centrifuged at 10,000 g for 15 min. The supernatant was centrifuged at 27,000 g for 45 min. The resulting pellet was resuspended in the grinding medium and centrifuged at 27,000 g for 45 min. The surface of the pellet was washed with ice water, then resuspended in acetone at $-20\text{ }^{\circ}\text{C}$, centrifuged at 27,000 g for 20 min. and resuspended and centrifuged an additional three times in cold acetone. The final pellet was dried with a stream of air and stored at $-20\text{ }^{\circ}\text{C}$.

(B) Preparation of enzyme sample

The powder of mitochondria in acetone was resuspended in 25 mM TES buffer (pH 7.4) containing 200 μM TPP (thiamine pyrophosphate), 5 mM DTT (dithiothreitol), and 2 mM MgSO_4 at a final concentration of 20 mg/mL, and undissolved material was removed at 27,000 g for 15 min.

(C) Inhibition of PDHc from pea (*P. sativum*)

Six samples of enzyme solution (0.5 mL) were taken. One of them was added to water as a control, and the rest were mixed with test compounds at a final concentration 10^{-3} , 10^{-4} , 10^{-5} , 10^{-6} and 10^{-7} g/mL respectively. The mixture was incubated at $25\text{ }^{\circ}\text{C}$ for 25 min and they were added to a 1 mL reaction mixture containing 25 mM TES (pH = 7.4), 1 mM MgCl_2 , 1 mM cysteine, 1 mM NAD^+ , 0.13 mM CoA (Na salt), 4 mM TPP, and then 0.3 mL (1 mM) sodium pyruvate as a substrate was added to start the reaction in a total volume of 3 mL. After 1 min at $25\text{ }^{\circ}\text{C}$ for temperature equilibration, the rate of formation of NADH was continuously monitored at 340 nm by a spectrophotometer. Three or five replications per concentration were performed and averaged, and the inhibitor concentration giving 50 % inhibition (IC_{50}) was calculated.

7.2.6.2 Assay of PDHc from Mung Bean (in Vitro)

(A) Preparation of mung bean (*V. radiata*) mitochondria

Mung bean (*V. radiata*) seeds were soaked in 0.9 % NaCl solution for 4 h and incubated at 28 °C in the dark until the shoots were grown to 10 cm in height. The shoots were harvested and ground, using a mortar and pestle, in three times volume of 50 mM Tris-HCl buffer (pH 7.4) containing 0.25 M glucose, 3 mM EDTA, and 0.75 mM BSA. The homogenate was filtered through several layers of cheesecloth and centrifuged at 10,000 g for 15 min. The supernatant was centrifuged at 27,000 g for 45 min. The resulting pellet was resuspended in the grinding medium and centrifuged at 27,000 g for 45 min. The surface of the pellet was washed with ice water, then resuspended in EtOH at -20 °C, centrifuged at 27,000 g for 20 min. and resuspended and centrifuged for additional three times in cold EtOH. The final pellet was dried with a stream of air and stored at -20 °C.

(B) Preparation of enzyme samples

The powder of mitochondria in EtOH was resuspended in 25 mM TES buffer (pH 7.4) containing 200 μM TPP (thiamine pyrophosphate), 5 mM DTT (dithiothreitol), and 2 mM MgSO₄ at a concentration of 20 mg/mL and undissolved material was removed at 27,000 g for 15 min.

(C) Inhibition of PDHc from mung bean (*V. radiata*)

The inhibition of enzyme from mung bean was tested according to the same method as that used for pea.

7.2.6.3 Assay of PDHc from Rice (in Vitro)

(A) Preparation of rice (*O. sativa*) mitochondria

Rice (*O. sativa*) seeds were soaked in water and incubated at 28 °C in the dark until the shoots were grown to 10 cm in height. The shoots were cut into small pieces (about 10 mm) and frozen for 1 h in the refrigerator. And then the shoots were ground, using a mortar and pestle, in three times volume of 50 mM Tris-HCl buffer (pH 7.4) containing 0.25 M glucose, 3 mM EDTA, and 0.75 mM BSA. The homogenate was filtered through several layers of cheesecloth and centrifuged at 10,000 g for 15 min. The supernatant was centrifuged at 27,000 g for 45 min. The resulting pellet was resuspended in the grinding medium and centrifuged at 27,000 g for 45 min. The surface of the pellet was washed with ice water, then resuspended in acetone at -20 °C, centrifuged at 27,000 g for 20 min and resuspended and centrifuged for additional three times in cold acetone. The final pellet was dried with a stream of air and stored at -20 °C.

(B) Preparation of enzyme solution

The powder of mitochondria in acetone was resuspended in 25 mM TES buffer (pH 7.4) containing 200 μ M TPP (thiamine pyrophosphate), 5 mM DTT (dithiothreitol), and 2 mM MgSO_4 at a final concentration of 20 mg/mL and ground thoroughly in glass homogenizer. The homogenate was centrifuged at 27,000 g for 20 min. The supernatant was used as an enzyme solution.

(C) Inhibition of PDHc from rice (*O. sativa*)

The solution (0.55 mL) containing various concentrations of test compounds was added to 0.5 mL of enzyme solution and then mixed thoroughly. Water was added to the controls. The mixture was incubated at 25 °C for 25 min and was added respectively at various times to obtain a 1 mL reaction mixture containing 25 mM TES (pH = 7.4), 1 mM MgCl_2 , 1 mM cysteine, 1 mM NAD^+ , 0.13 mM CoA (Na salt), 4 mM TPP and then 0.3 mL sodium pyruvate (1 mM) as a substrate was added to start the reaction in a total volume of 3 mL. After 1 min at 25 °C for temperature equilibration the rate of formation of NADH was continuously monitored at 340 nm using an ultraviolet-visible spectrophotometer. Three or five replications per concentration were performed and averaged. The reaction was measured and the inhibitor concentration giving 50 % inhibition (IC_{50}) was calculated.

7.2.6.4 Kinetic Experiment of PDHc from Mung Bean (*Vigna radiata*)

The maximum velocity V_{\max} and Michaelis constant K_m were determined by measuring the catalytic effect of enzyme in variable concentrations of sodium pyruvate as a substrate in the presence of a fixed concentration of inhibitors.

In this kinetic experiment, the concentration of **IC-22** was kept in 0.028 mM (10^{-5} g/mL); V_{\max} and K_m were determined experimentally by measuring V at different substrate concentrations in 0.1, 0.2, 0.3, 0.4, and 0.5 mM of sodium pyruvate separately. Under the same conditions, this set of experiments was also done in the absence of **IC-22**.

7.2.7 Assay of PDHc from *E. coli* and Pig Heart

7.2.7.1 Assay of PDHc from *E. coli* (in Vitro)

(A) Preparation of *E. coli* PDHc E1

The expressing plasmid pMal-C_{2X}-PDHc-E1 was transformed into *E. coli* stain TB1 and inoculated in Luria-Bertani (LB) broth containing 2 % glucose and 30 mg/ml ampicillin at 37 °C until reaching a cell density to A600 of 0.6–0.8. Then cells were

induced with a final concentration of 0.5 mM IPTG for 7 h at 25 °C before harvesting. Purification of the fusion protein was carried out using an MBP affinity column attached to an AKTA purifier 10 (UPC-F920, GE Healthcare Life Sciences). The concentrations of purified proteins were determined by the method of Bradford³ using bovine serum albumin (Tiangen) as standard. The final purify (>95 %) of the sample was verified by SDS-PAGE and then the purified protein was stored in 50 % (v/v) glycerol at -20 °C [40].

(B) *Inhibition of E. coli PDHc E1*

The inhibitory potencies of test compounds against PDHc E1 were measured at the *E. coli* PDHc E1 enzyme level in vitro. TTP and pyruvate were purchased from Sigma. *E. coli* PDHc-E1 activity was assayed by a modified methods of Nemeria [3] and measured by monitoring the reduction of 2,6-dichlorophenolindophenol (2,6-DCIP) at 600 nm using a microplate reader (BioTek Synergy2, USA). The total volume of 100 mL reaction mixture contained 50 mM K₃PO₄, pH 7.2, 2.0 mM sodium pyruvate as substrate, 0.8 mM 2,6-DCIP, 7.1 mM enzyme and different concentration of inhibitors. The reaction mixtures were incubated for 3 min at 37 °C, then added different concentration of TPP (ranging from 0 to 200 mM) to initiate the assay. The 50 % inhibition concentration (IC₅₀) of test compounds was estimated by non-linear least-squares fitting of the data using the logarithmic regression curves. One unit of activity is defined as the amount of 2,6-DCIP reduced (μmol/min/mg of PDHc-E1). All experiments were repeated for three times [40].

7.2.7.2 Assay of PDHc from Pig Heart (in vitro)

The inhibitory potencies of test compounds against PDHc E1 were measured with pig PDHc enzyme in vitro. TTP and pyruvate were purchased from Sigma. Pyruvate Dehydrogenase from porcine heart is purchased from Sigma (CAS: 9014-20-4).

The inhibitory activities of test compounds were measured by the enzymatic reaction. PDHc-E1 activity was measured by monitoring the absorbance at 566 nm wave length using a microplate reader (BioTek Synergy2, USA). The total final volume of 100 μL reaction mixture contained 50 mM K₃PO₄ (pH 7.0), 1.0 mM MgCl₂, 0.2 mM thiamine pyrophosphate (TPP), 0.5 mM thiazolyl blue (MTT), 6.5 mM Phenazine dimethyl sulfate (PMS), 2.0 mM sodium pyruvate (as substrate), 2.5 μL pyruvate dehydrogenase (PDHc enzyme), and buffered aqueous glycerol solution and different concentrations of inhibitor. The reaction mixtures were incubated for 3 min at 30 °C, then different concentrations of inhibitor was added to the initial reaction. The 50 % inhibition concentration (IC₅₀) of test compounds was estimated by nonlinear least-squares fitting of the data using the logarithmic regression curves. All experiments were repeated for three times.

7.2.8 Assay of Other Enzymes

7.2.8.1 Assay of Acetolactate Synthase from Pea (in Vitro)

The tested acetolactate synthase (ALS) was from pea (*Pisum sativum*). The ALS extraction, assay protocols, and the procedure of in vitro ALS assay followed the literature [41].

7.2.8.2 Assay of Peroxidase from Rice (in Vitro)

The tested peroxidase (POD) was from rice (*Oryza Sativa*). The POD assay in vitro was conducted according to the procedure reported in the literature [42, 43].

7.2.8.3 Assay of Superoxide Dismutase from Rice (in Vitro)

The tested superoxide dismutase (SOD) was from rice (*Oryza Sativa*). The SOD assay in vitro was conducted according to the procedure reported in the literature [44, 45].

7.2.9 Summary

The biochemical mechanism of herbicidal action of the alkylphosphonates was explored on the basis of biochemical experiments. Representative herbicidal active alkylphosphonates were selected to examine their inhibition against plant PDHc through enzyme activity assays, kinetic experiment, and enzyme-selective inhibition experiment. Based on the above study we can give the following conclusions:

- (1) **IC-22** (HW02, clacyfos), **IG-21** (HWS) and their sodium salts were demonstrated to be effective inhibitors against plant PDHc. **IC-22** and **IG-21** exhibited potent selective inhibition against dicot PDHc, but lower inhibitory potency against monocotyledonous rice PDHc. It showed that both compounds could selectively inhibit the growth of dicotyledonous plants due to their selective inhibition against dicot PDHc E1.
- (2) SAR analyses indicated that R^1 , R^2 , and Y_n in the alkylphosphonates **Io** were the most essential sites for both enzyme inhibition and herbicidal activity. Me or Na as R^1 and R^2 , and 2,4-Cl₂ as Y_n were most beneficial to activity. When 2,4-Cl₂ were kept constant as Y_n , enzyme inhibition could be greatly enhanced by the chemical modification of R^1 and R^2 . Sodium salts **IIB-2** and **IID-10** exhibited more powerful enzyme inhibition than the corresponding alkyl phosphonates **IC-22** and **IG-21**. However, good enzyme inhibition and herbicidal activity required an optimal combination of R^1 , R^2 , R^3 , R^4 , and Y_n in

alkylphosphonates **Io**. The degree of herbicidal activity of tested compounds positively correlated with that of their inhibition against plant PDHc.

- (3) In order to make sure enzyme inhibition and herbicidal activity of possible metabolic products, **IID-10** and its possible metabolic products were selected to examine and compare their activity. Possible metabolic products **IID-10-b** and **IID-10-c** had much lower inhibitions against pea PDHc than **IID-10**, and they were inactive against pea and other tested dicot plants. Although **IID-10-a** (2,4-D) showed a high activity against pea and other dicot plants, it was inactive against pea PDHc in vitro. It indicated that **IID-10** itself was responsible for both enzyme inhibitions against pea PDHc in vitro and inhibitory potency against pea in vivo. Therefore both enzyme inhibition and herbicidal activity of these alkylphosphonates **Io** should come from the compounds themselves, not come from their possible metabolic products.
- (4) **IC-22** exhibited excellent post-emergence herbicidal activity selectively against broadleaf weeds at 150–450 g ai/ha. **IC-22** showed good selective inhibition against dicot PDHc, but no significant inhibition against PDHc E1 from *E. coli* or pig heart. **IC-22** was recognized to act as a competitive inhibitor of PDHc by kinetic experiment. Therefore **IC-22** could be used as a selective herbicide in monocotyledonous crop fields due to its selective inhibition against dicot PDHc. **IC-22** exhibited more obvious advantages over those acylphosphonate or acylphosphinate, in enzyme-selective inhibition, crop safety, and effectiveness. These results show PDHc can be a target for the design and development of new herbicide.
- (5) The alkylphosphonates, such as **IG-21** and **IID-10** were also observed on tested plants with some symptoms like auxin-type herbicidal action. The present results turned out that the herbicidal action not come from the possible metabolic product 2,4-D, but come from these phosphonates themselves.

References

1. Verma J, Khedkar VM, Coutinho EC (2011) 3D-QSAR in drug design-a review. *Curr Top Med Chem* 10:95–115
2. Gutowski JA, Lienhard GE (1976) Transition state analogs for thiamin pyrophosphate-dependent. *J Biol Chem* 251:2863–2866
3. Nemeria N, Yan Y, Zhang Z et al (2001) Inhibition of the Escherichia coli pyruvate dehydrogenase complex E1 subunit and its tyrosine 177 variants by thiamin 2-thiazolone and thiamin 2-thiothiazolone diphosphates. *J Biol Chem* 276:45969–45978
4. Krampitz LO (1969) Catalytic functions of thiamine diphosphate. *Annu Rev Biochem* 38:213–240
5. Jordan F, Nemeria N, Guo FS et al (1998) Regulation of thiamin diphosphate-dependent 2-oxo acid decarboxylases by substrate and thiamin diphosphate. Mg (II) evidence for tertiary and quaternary interactions. *Biochem Biophys Acta* 1385:287–306
6. Dobritzsch D, König S, Schneider G et al (1998) High resolution crystal structure of pyruvate decarboxylase from *Zymomonas mobilis*. *J Biol Chem* 273:20196–20204

7. Alvarez FJ, Ermer J, Hübner G et al (1991) Catalytic power of pyruvate decarboxylase. Rate-limiting events and microscopic rate constants from primary carbon and secondary hydrogen isotope effects. *J Am Chem Soc* 113:8402–8409
8. Kern D, Kern G, Neef H et al (1997) How thiamin diphosphate is activated in enzymes. *Science* 275:67–70
9. He HW, Wang T, Yuan JL (2005) Synthesis and herbicidal activities of methyl-1-(2,4-dichlorophenoxyacetoxy)alkylphosphonate monosalts. *J Organomet Chem* 690:2608–2613
10. Wang T, He HW (2004) An efficient synthesis of α -(2,4-dichlorophenoxyacetoxy)aryl methyl phosphonate monosodium salts. *Synth Commun* 34:1415–1423
11. Wang T, He HW (2004) Simple and improved preparation of α -oxophosphonate monolithium salts. *Phosphorus Sulfur Silicon Relat Elem* 179:2081–2089
12. Chen T, Shen P, Li YJ et al (2006) Synthesis and herbicidal activity of O,O-dialkyl phenoxyacetoxyalkylphosphonates containing fluorine. *J Fluorine Chem* 127:291–295
13. He HW, Wang T, Li YJ et al (2007) Fungicidal and insecticide activity of (substituted phenoxyacetoxy)alkylphosphinates. CN Patent 1319449B:6
14. He HW, Liu ZJ (2001) Progresses in research of α -oxophosphonic acid derivatives with herbicidal activity. *Chin J Org Chem* 21:878–883
15. Tan HL, Yuan JL, He HW et al (2005) Effects of methylphosphonate monosodium on pyruvate dehydrogenase. *Chin J Chem Eng* 6:4–5
16. He HW, Yuan JL, Peng H et al (2011) Studies of O,O-dimethyl α -(2,4-dichlorophenoxyacetoxy) ethylphosphonate (HW02) as a new herbicide. 1. Synthesis and herbicidal activity of HW02 and analogues as novel inhibitors of pyruvate dehydrogenase complex. *J Agric Food Chem* 59:4801–4813
17. Cramer RD, Patterson DE, Bunce JD (1988) Comparative molecular field analysis (CoMFA). 1. Effect of shape on binding of steroids to carrier proteins. *J Am Chem Soc* 110:5959–5967
18. Klebe G, Abrahma U, Mietzner T (1994) Molecular similarity indices in a comparative analysis (CoMSIA) of drug molecules to correlate and predict their biological activity. *J Med Chem* 37:4130–4146
19. Arjunan P, Nemeria N, Brunskill A et al (2002) Structure of the pyruvate dehydrogenase multienzyme complex E1 component from *Escherichia coli* at 185 Å resolution. *Biochemistry* 41:5213–5221
20. Arjunan P, Chandrasekhar K, Sax M et al (2004) Structural determinants of enzyme binding affinity: the E1 component of pyruvate dehydrogenase from *Escherichia coli* in complex with the inhibitor thiamin thiazolone diphosphate. *Biochemistry* 43:2405–2411
21. Morris GM, Goodsell DS, Huey R et al (2001) Version 3.0.5 The Scripps Research Institute, Molecular Graphics Laboratory, Department of Molecular Biology
22. Boulamwini JK, Assefa H (2002) CoMFA and CoMSIA 3D QSAR and docking studies on conformationally-restrained cinnamoyl HIV-1 integrase inhibitors: exploration of a binding mode at the active site. *J Med Chem* 45:841–852
23. SYBYL, version 7.0 Tripos Inc, St Louis
24. Clark MC, Cramer RD, Van Opdenbosch N (1989) Validation of the general purpose tripos 52 force field. *J Comput Chem* 10:982–1012
25. Powell MJD (1977) Restart procedures for the conjugate gradient method. *Math Program* 12:241–254
26. Morris GM, Goodsell DS, Halliday RS et al (1998) Automated docking using a Lamarckian genetic algorithm and an empirical binding free energy function. *J Comput Chem* 19:1639–1662
27. Wold S, Rhue A, Wold H et al (1984) The covariance problem in linear regression The partial least squares (PLS) approach to generalized inverses. *SIAM J Sci Stat Comput* 5:735–743
28. Wold S, Albano C, Dunn WJ et al (1984) Multivariate data analysis in chemistry. NATO ASI Ser C 138:17–95
29. Clark M, Cramer RD (1993) The probability of chance correlation using partial least squares (PLS). *Quant Struct-Act Relat* 12:137–145

30. Bush BL, Nachbar RB (1993) Sample-distance partial least-squares PLS optimized for many variables, with application to CoMFA. *J Comput Aided Mol Des* 7:587–619
31. Baillie AC, Wright K, Wright BJ et al (1988) Inhibitors of pyruvate dehydrogenase as herbicides. *Pest Biochem Phys* 30:103–112
32. Schwartz ER, Reed LJ (1970) α -Keto acid dehydrogenase complexes. XIV. Regulation of the activity of the pyruvate dehydrogenase complex of *Escherichia coli*. *Biochemistry* 9:1434–1439
33. Gohil K, Jones DA (1983) A sensitive spectrophotometric assay for pyruvate dehydrogenase and oxoglutarate dehydrogenase complexes. *Biosci Rep* 3:1–9
34. Linn TC, Pelley JW, Pettit FH et al (1972) α -Keto acid dehydrogenase complexes XV. Purification and properties of the component enzymes of the pyruvate dehydrogenase complexes from bovine kidney and heart. *Arch Biochem Biophys* 148:327–342
35. Hames BD, Hooper NM, Houghton JD (1977) *Instant notes in biochemistry*. Bios scientific publishers, Oxford
36. Nemeria NS, Korotchkina LG, Chakraborty S et al (2006) Acetylphosphinate is the most potent mechanism-based substrate-like inhibitor of both the human and *Escherichia coli* pyruvate dehydrogenase components of the pyruvate dehydrogenase complex. *Bioorg Chem* 34:362–379
37. Peng H, Wang T, Xie P et al (2007) Molecular docking and three-dimensional structure-activity relationship studies on the binding modes of herbicidal 1-(substituted phenoxyacetoxy) alkylphosphonates to the E1 component of pyruvate dehydrogenase. *J Agric Food Chem* 55:1871–1880
38. He HW, Peng H, Wang T et al (2013) α -(Substituted-phenoxyacetoxy)- α -heterocyclymethylphosphonates: synthesis, herbicidal activity, inhibition on pyruvate dehydrogenase complex (PDHc), and application as postemergent herbicide against broadleaf weeds. *J Agric Food Chem* 61:2479–2488
39. Reid EE, Thompson P, Lyttle CR et al (1977) Pyruvate dehydrogenase complex from higher plant mitochondria and proplastids. *Plant Physiol* 59:842–848
40. He JB, Feng LL, Li J et al (2012) Design, synthesis and biological evaluation of novel 2-methylpyrimidine-4-ylamine derivatives as inhibitors of *Escherichia coli* pyruvate dehydrogenase complex E1. *Bioorg Med Chem* 20:1665–1670
41. Ray TB (1984) Site of action of chlorsulfuron. *Plant Physiol* 75:827–831
42. Evans JJ (1965) The distribution of peroxidases in extreme dwarf and normal tomato. *Phytochem* 4:499–503
43. Writtenbach VA, Bukavac MJ (1975) Cherry fruit abscission: peroxidase activity in the abscission zone in relation to separation. *J Amer Soc Hort Sci* 100:387–391
44. Giannopolitis CN, Ries SK (1977) Superoxide dismutases II. Purification and quantitative relationship with water-soluble protein in seedlings. *Plant Physiol* 59:315–318
45. Shan CB, Luo GH, Wang AG et al (1983) Comparison of several methods for evaluation of SOD activity. *Plant Physiol Comm* 5:46–49

Chapter 8

Evaluation and Application of Clacyfos and HWS

The R&D progresses of two alkylphosphonates, namely clacyfos and HWS, are introduced in this chapter. Clacyfos (**IC-22**, HW02), *O,O*-dimethyl 1-(2,4-dichlorophenoxyacetoxymethyl)phosphonate has received a temporary registration in ICAMA (Institute for the Control of Agrochemicals Ministry of Agriculture) in 2007 in China. Its herbicidal activity has been evaluated in more than forty field trials in different regions in China. Their field trials results as well as greenhouse data will be discussed in this chapter. Clacyfos provided adequate weeds control for post-emergence, for a broad spectrum of broad-leaved and sedge weeds at 270–450 g ai/ha in lawn, wheat, and maize fields. Clacyfos exhibited good systemic activity and a stronger rain stability. The toxicology, eco-toxicity, residues, and environmental fate of clacyfos are discussed in this chapter.

In addition to clacyfos, HWS (**IG-21**), *O,O*-dimethyl 1-(2,4-dichlorophenoxyacetoxymethyl)-1-(furan-2-yl)methylphosphonate, was considered as a candidate herbicide. Its biological activities will be included in this chapter as well. HWS was effective against broad-leaved weeds from 50 to 300 g ai/ha. It showed no phytotoxicity to maize and rice at a rate as high as 1.2 kg ai/ha. Field trials carried out in different regions in China showed that HWS controlled a broad spectrum of broad-leaved and sedge at 300–450 g ai/ha for post-emergence in maize fields. HWS provided adequate control against primary weeds in a maize field at 450 g ai/ha. It exhibited good systemic activity and stronger rain stability. The toxicology and, eco-toxicity of HWS are also discussed in this chapter.

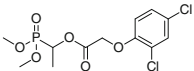
8.1 Evaluation of Clacyfos

8.1.1 Introduction

Clacyfos (HW02, **IC-22**), *O,O*-dimethyl 1-(2,4-dichlorophenoxyacetoxymethyl)phosphonate that was born by optimizing the lead structure **IA-1** (Chap. 2). Clacyfos was confirmed to be a competitive inhibitor of plant PDHc. It showed

much higher inhibitory potency against PDHc in pea and mung bean than in rice (Chap. 7). That is in perfect agreement with its higher herbicidal activity against pea than rice in a greenhouse test. Clacyfos as an effective inhibitor against dicotyledons PHDc exhibited excellent herbicidal activity against broad-leaved weeds, grass weeds, and sedges by post-emergence application at 450-20 g ai/ha in the greenhouse (Chap. 2) [1].

The breadth of spectrum and level of phytotoxicity of clacyfos are of further interest to us. Therefore, we decided to further evaluate its practical use.

Chemical Name	<i>O,O</i> -Dimethyl 1-(2,4-dichlorophenoxyacetoxy)ethylphosphonate
Chemical structure	
Empirical formula	C ₁₂ H ₁₅ O ₆ Cl ₂ P
Molecular weight	357.12
CAS registry number	215655-76-8
Common Name	Clacyfos
Experimental Name	HW02
Chemical class	Phosphonate
Pesticide Type	Herbicide
Site of action	PDHc

8.1.2 Physiochemical Properties

Physiochemical properties of clacyfos are shown in Table 8.1.

Table 8.1 Physiochemical properties of clacyfos

Parameter	Value
Appearance	Light yellow liquid
n_D^{25}	1.5172
Boiling point	195 °C/9 mmHg; >250 °C decomposed
Density (g/cm ³ , 25 °C)	1.371
Partition coefficient (1-octanol/water 25 °C)	1.55×10^2
Water solubility	0.97 g/L in water at 25 °C
Solvent solubility	4.31 g/L in n-hexane at 25 °C Miscible with acetone, ethanol, chloroform, toluene and xylene at 25 °C
Stability	Stable for light and air at room temperature, decompose under the acidic or basic conditions
Long-term storage	Keep in dark and dry place at low temperature (<15 °C)

8.1.3 Stability of Clacyfos

8.1.3.1 Hydrolysis of Clacyfos in Buffered Solutions

The hydrolytic kinetics and mechanisms of clacyfos were studied in buffered aqueous solutions under pH 5–9 at ambient temperature (Fig. 8.1) and under pH 7 at a range of temperature from 25–55 °C (Fig. 8.2). Clacyfos hydrolyzed very rapidly in the buffered solutions. Its hydrolysis rate was characterized by the first-order kinetics and accelerated with the increasing of pH and temperature [2].

The calculated half lives of clacyfos hydrolysis at 25 °C, in the solutions of pH 5, 7 and 9 were 191.3, 6.2, and 0.2 h respectively. Clacyfos hydrolyzed much faster in the basic solution than in acidic and neutral solution at the same temperature. We concluded that clacyfos was not stable in the aqueous environments.

The hydrolysis rate of clacyfos was increased as the temperature increased. Its half lives at pH 7 was 6.1, 4.2, 1.8, and 0.7 h when temperature was at 25, 35, 45

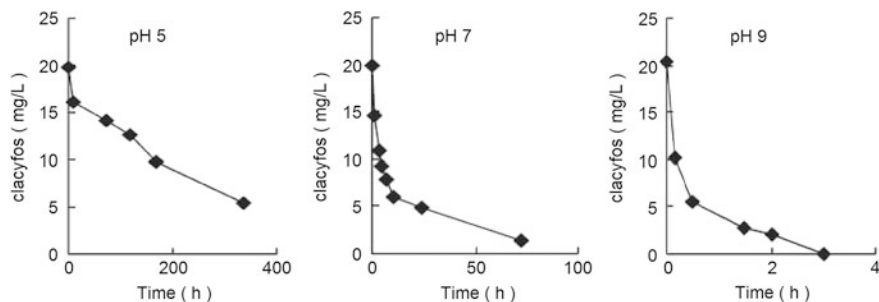
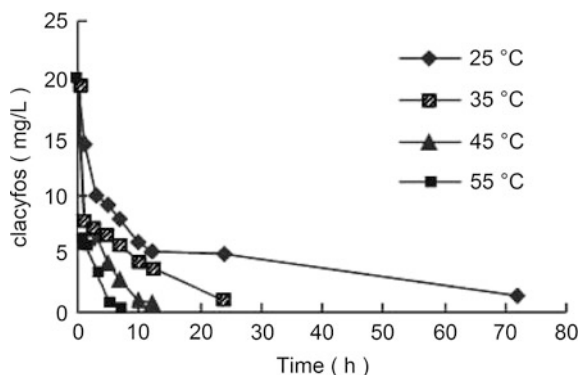


Fig. 8.1 The hydrolytic curve of clacyfos in the buffer solutions with different pH values (25 °C)

Fig. 8.2 The hydrolytic curve of clacyfos under different temperatures (pH 7 buffer solution)



and 55 °C, respectively. The temperature coefficient of hydrolysis for clacyfos was 1.46–2.64. There was no significant correlation between the activation enthalpy of hydrolysis and temperatures. Its average activation energy and activation enthalpy were 60.51 and 57.70 kJ/mol, respectively. The activation entropy absolute values of hydrolysis were increased with the increasing temperatures in the environment. The average value, -81.00 kJ (mol·K) suggested that hydrolysis of clacyfos in the aqueous solutions was driven by the activation entropy. Through isolation and identification of clacyfos's hydrolytic products using GC-MS detection, it was found that clacyfos was hydrolyzed through ester cleavage. The main hydrolyzate was 2,4-dichlorophenoxyacetic acid and methyl ester [2].

8.1.3.2 Photodegradation of Clacyfos in Organic Solvents

The photodegradation kinetics and mechanism of clacyfos (HW02) in the organic solvents were studied at 25 °C under the irradiation of ultraviolet light. Photochemical reaction of clacyfos in organic solvents such as *n*-hexane, methanol, xylene, and acetone under UV light could be well described by the first kinetic equation, and the photodegradation efficiency decreased with a order of *n*-hexane > methanol > xylene > acetone (Fig. 8.3).

The photodegradation efficiency constants (K , min^{-1}) of clacyfos in *n*-hexane, methanol, xylene, and acetone were 4.951×10^{-2} , 3.253×10^{-2} , 2.377×10^{-2} and $1.628 \times 10^{-2} \text{ min}^{-1}$, and the corresponding half-lives ($T_{1/2}$, min) were 13.99, 21.30, 29.15 and 42.56 min, respectively (Table 8.2). By separation and identification of photoproducts using GC-MS, it could be concluded that clacyfos photolyzed through ester cleavage, photo-dechlorination and photoisomerization of the molecule itself [3]. According to the identification of photodegradation products in the four organic solvents by Zhongbin Lu et al. [3], the possible mechanism of clacyfos (HW02) photodegradation was inferred as the follows. First, the cleavage of carbon-oxygen ester bond of clacyfos induced the production of *O,O*-dimethyl-1-hydroxyethyl phosphonate, 2,4-dichlorophenoxyacetic acid and *O,O*-dimethyl ethyl

Fig. 8.3 Photodegradation dynamics curves of clacyfos in different solvents under UV light

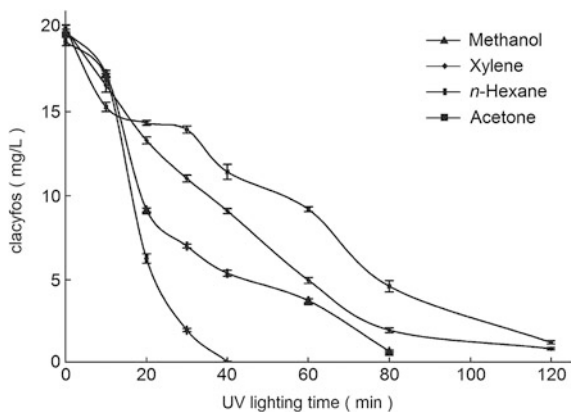


Table 8.2 Photodegradation of clacyfos in different organic solvents under UV light

Organic solvents	$T_{1/2}$ ^a , min	C_0 , mg/L	K^b , min ⁻¹	R	Fitness ^c , %	F value	Significant level P
<i>n</i> -Hexane	13.99	19.17	4.951×10^{-2}	0.9311	97.97	13.47	6.6×10^{-2}
Methanol	21.30	19.74	3.253×10^{-2}	0.9820	95.21	108.19	4.8×10^{-4}
Acetone	42.56	19.94	1.628×10^{-2}	0.9863	98.87	215.19	1.0×10^{-5}
Xylene	29.15	19.89	2.377×10^{-2}	0.9866	97.59	146.05	2.7×10^{-4}

^a $T_{1/2}$ half-lives^b K photodegradation efficiency constant^c Fitness means the identical degree between the observed data and kinetics equation

phosphonate. Second, dechlorination, and the carbon-chlorine bond scission produced *O,O*-dimethyl-1-(phenoxyacetoxy)ethyl phosphonate and 2,4-dihydroxy phenoxy acetic acid. Third, 2,4-dichlorophenoxyacetic acid methyl ester was formed by the photoisomerization of clacyfos. These intermediate products would continually undergo photodegradation, and final mineralize to the products of carbon dioxide, phosphoric acid and other non-toxic substances.

8.1.4 Herbicidal Activity in Greenhouse

Bioassay for clacyfos was carried out in the greenhouse for its pre- and post-emergence herbicidal activity, selectivity, crop safety and biological property at National Pesticide Discovery South Center (Zhejiang) or National Pesticide Engineering Research Center (Nankai University, Tianjin) in Chain. The results are summarized as follows.

8.1.4.1 Herbicidal Activity of Clacyfos in Different Growth Stages in Seedlings

As shown in Table 8.3, clacyfos exhibited high herbicidal activity against dicotyledonous plants, rape, and common amaranth, at all growing stages at 450 g ai/ha.

Table 8.3 Post-emergence herbicidal activity of Clacyfos in different growth stages

Seeding stage (450 g ai/ha)	Inhibition potency (%) ^a			
	Rape	Common amaranth	Barnyard grass	Crab grass
Before sprout	100	100	61	80
Cotyledon	100	100	49	57
1–2 leaves stage	100	100	28	27
3–4 leaves stage	100	100	22	17
5–6 leaves stage	100	100	24	13

^a Inhibitory potency (%) on the growth of plants in the greenhouse, 0 (no effect), 100 % (completely kill). Values are the average of triplicate

Table 8.4 Herbicidal activity of clacyfos for post-emergence application

Plant	Scientific name	Inhibitory potency (%) ^a	Sensitive degree
Rape	<i>Brassica campestris</i>	100	Active
Common amaranth	<i>Amaranthus retroflexus</i>	100	
Chinese cabbage	<i>Brassica pekinensis</i>	100	
Setose thistle	<i>Cirsium japonicum</i>	100	
Lobedleaf pharbitis	<i>Ipomoea heperacea</i>	100	
White eclipta	<i>Eclipta prostrata</i>	100	
Goosegrass	<i>Eleusine indica</i>	100	
Goosefoot	<i>Chenopodium album</i>	100	
Carrot	<i>Daucus carota</i>	100	
Sugar beet	<i>Beta Vulgaris</i>	95	
White mustard	<i>Sinapis alba</i>	95	
Clover	<i>Medicago sativa</i>	90	
Asian flatsedge	<i>Cyperus microiria</i>	90	
Chingma abutilon	<i>Abutilon theophrasti</i>	85	
Curly dock	<i>Rumex crispus</i>	80	
Bedstraw	<i>Galium aparine</i>	60	Minimal active
Green bristlegrass	<i>Setaria viridis</i>	50	
Annual bluegrass	<i>Poa annua</i>	50	
Crab grass	<i>Digitaria sanguinalis</i>	40	
Barnyard grass	<i>Echinochloa crusgalli</i>	30	
Shortawn foxtail	<i>Alopecurus aequalis</i>	0	

^a Inhibitory potency (%) of clacyfos against the growth of plants at a rate of 450 g ai/ha in the greenhouse, 0 (no effect), 100 % (completely kill). Values are the average of triplicate

However, the herbicidal activity against monocotyledonous plants such as barnyard grass and crab grass decreased with the growth of seedlings.

8.1.4.2 Selectivity of Clacyfos Against Weeds

Twenty-three species of test plants were examined for selectivity of clacyfos at 450 g ai/ha in the greenhouse (Table 8.4). Susceptibilities to clacyfos were different among the tested weed species. Clacyfos was active against dicotyledonous plants. Several monocotyledonous plants were also sensitive to clacyfos injury.

Table 8.5 Herbicidal activity of clacyfos for pre and post-emergence applications^a

Rate (g ai/ha)	Rape		Leaf mustard		Chingma abutilon		Curled dock		Carrot	
	Pre	Post	Pre	Post	Pre	Post	Pre	Post	Pre	Post
225	70	90	76	68	6	34	34	34	37	94
450	100	100	100	100	12	88	42	69	50	100
675	100	100	100	100	30	94	50	77	78	100
900	100	100	100	100	45	100	59	85	82	100
1,125	NT	NT	NT	NT	NT	NT	63	93	NT	NT

Rate (g ai/ha)	Clover		Barnyard grass		Crab grass		Giant foxtail		Annual bluegrass	
	Pre	Post	Pre	Post	Pre	Post	Pre	Post	Pre	Post
225	36	25	9	12	72	23	35	42	18	23
450	84	88	33	19	86	25	55	46	45	46
675	87	100	70	24	89	36	70	63	47	56
900	96	100	71	21	93	43	100	71	55	64
1,125	NT	NT	75	17	NT	75	100	80	66	69

^a Inhibitory potency (%) of clacyfos against the growth of plants in the greenhouse, 0 (no effect), 100 % (completely kill), NT (not tested). Values are the average of triplicate

8.1.4.3 Pre and Post-Emergence Herbicidal Activity of Clacyfos

The herbicidal activity of clacyfos was further evaluated at different rate for pre- and post-emergence activity in the greenhouse. Clacyfos was tested against a range of weed species including rape (*Brassica campestris*), leaf mustard (*Brassica juncea*), curled dock (*Rumex crispus*), carrot (*Daucus carota*), clover (*Medicago sativa*), barnyard grass (*Echinochloa crusgalli*), crab grass (*Digitaria sanguinalis*), giant foxtail (*Setaria faberi*), and annual bluegrass (*Poa annua*). The herbicidal activity of clacyfos against both dicotyledonous and monocotyledonous plants is linear with respect to the rate (Table 8.5).

8.1.4.4 Crop Selectivity and Safety

Crop safety of clacyfos for wheat, rice, maize, rape, cotton, and soybean was examined (Table 8.6). Clacyfos was safe for many monocotyledonous crops, such as wheat, rice, and maize at a rate as high as 1,350 g ai/ha, but showed phytotoxicity against certain dicotyledonous crops, such as cotton, soybean, and rape. Therefore, clacyfos can be a useful herbicide in monocotyledonous crop fields against dicotyledonous weeds.

Table 8.6 Growth inhibition (%) of several crops by clacyfos^a

Rate (g ai/ha)	Wheat	Rice	Maize	Rape		Cotton		Soybean	
	Post	Post	Post	Pre	Post	Pre	Post	Pre	Post
0	0	0	0	NT	NT	NT	NT	NT	NT
225	0	0	0	70	90	NT	NT	NT	NT
450	0	0	0	100	100	NT	NT	NT	NT
675	0	0	0	60	100	60	90	60	90
1,350	0	0	0	80	100	70	90	70	100
1,575	10	0	15	90	100	70	95	70	100
1,800	20	10	NT	95	100	80	98	70	100

^a Inhibitory potency (%) of clacyfos against the growth of plants in the greenhouse, 0 (no effect), 100 % (completely kill), NT (not tested). Values are the average of triplicate

Table 8.7 Inhibitory effect of clacyfos against common amaranth

Treatment	Inhibitory potency % ^a (12 DAT ^b)		
	Root length	Plant above ground	Plant fresh weight
Leaf-sprayed	100	100	100
Stem-sprayed	60	85	90
Root-poured	90	100	100

^a Inhibitory potency (%) of clacyfos against the growth of common amaranth in the greenhouse at the concentrations of 500 mg/L, 0 (no effect), 100 % (completely kill)

^b DAT is day after treatment. Values are the average of 3 replicates

8.1.5 Systemic Property of Clacyfos

The absorption and translocation properties of clacyfos were evaluated in the greenhouse at the National Pesticide Discovery South Center in (Zhejiang) in China. Common amaranth (*Amaranthus retroflexus*) was used as the target plant. The data in Table 8.7 showed that clacyfos would be absorbed through buds, roots, stems, and leaves and demonstrated its inhibitory effect against plant growth.

Clacyfos exhibited xylem mobility. It exhibited good inhibitory effect on plant growth through either foliar and stem spray or root application. The inhibitory effect was most significant through foliar application. Therefore, clacyfos is recommended as a post-emergence, foliage-applied herbicide.

8.1.6 Rainfast Characteristics of Clacyfos

To determine the influence of environmental factors and rainfast characteristics, 30 % clacyfos EC was used in a rainfast study. The inhibitory potency of clayfos was determined at different time of treatment under simulated rainy conditions against the common amaranth (*Amaranthus retroflexus*). 41 % MCPA (2-methyl-4-chloro) phenoxyacetic acid was included in this study as a positive control.

Table 8.8 The influence of rain water on the inhibitory activity of 30 % clacyfos EC and 41 % MCPA EC against common amaranth^a

Herbicides	Rate	Rain time ^b and corresponding inhibitory potency ^c (%)								No rain
		0 h	0.5 h	1 h	2 h	4 h	8 h	12 h	24 h	
30 % clacyfos EC	900	72	74	74	80	93	97	91	100	100
41 % MCPA EC	900	14	31	28	28	59	55	80	84	98

^a The experiment was done by using a rainfall simulator with 1,000 mL water (corresponding for 20 mm rainfall) at different times, respectively

^b The time after common amaranth was treated. For example, when the plant suffered rainfall at 0.5 h after being treated by clacyfos or MCPA, the inhibitory potency of clacyfos and MCPA against common amaranth is 74 and 31 %, respectively

^c Inhibitory potency against common amaranth was measured as percentage change in fresh weight compared to that of the control, 0 % (no effect), 100 % (completely kill); values are the average of 3 replicates

The data in Table 8.8 showed that the inhibitory potency of clacyfos was decreased 25 % or 10 % if the treated plants were scoured by rainwater 2 hours or 4 hours after treatment respectively. The inhibitory potency of MCPA was decreased more than 30 % in 2 hours after treatment and still decreased more than >10 % even 8 hours after treatment under the same simulant rainfall condition. This finding showed clacyfos had a stronger stability in rainfall than MCPA due to its rapid absorption and good osmosis. The data suggested that there is no effect on clacyfos's efficiency when the application was completed in 2 hrs before it rains.

8.1.7 Field Trials of Clacyfos

Clacyfos was further evaluated as a potential herbicide candidate in the field. A formulation of 18 and 30 % EC were used in the field testing.

Field trials were carried out on maize, lawn, wheat, rice, orchard, tea, and noncrop fields. More than 40 trials were performed in different regions such as Zhejiang, Jiangsu, Shandong, Hebei, Henan, Hubei, Shanxi, Jilin, and Heilongjiang province by the Institute of Plant Protection, Academy of Agricultural Science in corresponding province. Some results of clacyfos in field trials are summarized in Tables 8.9, 8.10, 8.11, 8.12, 8.13, 8.14.

8.1.7.1 Herbicidal Activity of Clacyfos (18 % EC) in No-Crop Fields

41 % ROUNDUP SL was used at a recommended rate (923 g ai/ha) as positive control. As shown in Table 8.9, clacyfos showed higher activity than that of ROUNDUP SL (glyphosate) at a lower rate (324 g ai/ha) against broad-leaved weeds, such as Japanese cayratia (*Cayratia japonica*), flaxleaved fleabane (*Erigeron*

Table 8.9 Post-emergence herbicidal activity of 18 % clacyfos EC and 41 % ROUNDUP SL in no-crop field^a

Weeds	Reduction in plant numbers, %			
	18 % Clacyfos EC 1800 mL/ha (324 g ai/ha)		41 % ROUNDUP SL ^b 2250 mL/ha (923 g ai/ha)	
	(7 DAT ^c)	(15 DAT)	(7 DAT)	(15 DAT)
Japanese cayratia	100	100	0	0
Flaxleaved fleabane	100	100	75	50
Pig's knee	100	100	50	75
Asian copperleaf	96	96	22	22
Leaf mustard	100	100	40	40
Nutgrass	100	100	100	100
Green bristlegrass	13	13	100	100
Bermudagrass	0	0	57	71
Creeping woodsorrel	52	57	100	100

^a The test was carried out in the middle of June, 2000, at Xiangfan, Hubei. Application method: spray one time by a shoulder sprayer

^b 41 % ROUNDUP SL = Glyphosate isopropyl amine salt 41 % SL

^c DAT is day after treatment. Weed numbers were counted at 7 and 15 DAT as percentage change compared to that of the untreated control

bonariensis), pig's knee (*Achyranthes bidentata*), Asian copperleaf (*Acalypha australis*), common amaranth (*Amaranthus retroflexus*), leaf mustard (*Brassica juncea*), and same effect against nutgrass (*Cyperus rotundus*), but clayfos showed lower activity than ROUNDUP SL against monocotyledonous weeds such as creeping woodsorrel (*Oxalis corniculata*), bermudagrass (*Cynodon dactylon*), and green bristlegrass (*Setaria viridis*).

8.1.7.2 Effects of Clacyfos (30 % EC) in Wheat Fields

China plants huge acreages of wheat (*Triticum aestivum*), mainly in the Yellow River basin and Huai River. The winter wheat is a major agronomic crop in China and its yield loss caused by weeds is very serious. Weed control in wheat fields has highly depended on herbicide in recent years in China. Tribenuron and 2,4-D or 2,4-D acid derivative are most commonly used herbicides for broadleaf weed control in wheat in China. However, applying 2,4-D type herbicides, such as 2,4-D butyl ester often results in injury to wheat due to improper use or to adjacent broadleaf crops, especially cotton, due to its volatilization and solution drifting [4, 5]. In China, repeatedly applying tribenuron has resulted in serious resistance of main weed, flixweed tansymustard (*Descurainia Sophia*) to this herbicide [6, 7]. Therefore the use area of these two herbicides is decreasing. At present, fluroxypyr and the co-formulation of mesosulfuron plus iodosulfuron are used in some wheat

areas in China. Fluroxypyr is very effective on some broadleaf weeds, but not effective against shepherd's purse (*Capsella bursa-pastoris*). Mesosulfuron plus iodosulfuron is also effective on the most weed species, but occasionally brings wheat injury [8]. There are urgently needs to develop new herbicides as an alternative measure to control broadleaf weeds in wheat.

Clacyfos can be a potentially useful herbicide for broadleaf weed control in wheat base on its selectivity and weed control spectrum. Hanwen Ni et al evaluated the efficacy of clacyfos against main broadleaf weeds in wheat field and compared its activity with 2,4-D in greenhouse and field conditions [8]. Injury symptoms twist and wilt of the treated weeds were observed 1 DAT for clacyfos and 2,4-D. Injures were getting severe with increasing dose. Clacyfos exhibited higher activity than 2,4-D against common amaranth (*Amaranthus retroflexus*), Water chickweed (*Malachium aquaticum*), Shepherd's purse (*Capsella bursa-pastoris*), and Flixweed tansymustard (*Descurainia Sophia*) base on their ED₅₀ values (Table 8.10).

For these four weed species, the ED₅₀ values of clacyfos ranged from 19.2 to 70.7 g ai/ha, the ED₅₀ values of 2,4-D ranged from 23.9 to 75.4 g ai/ha. Among these weed species, flixweed tansymustard was the most susceptible to clacyfos, its ED₅₀ values was only 19.2 g ai/ha and the ED₅₀ values of 2,4-D was 23.9 g ai/ha. Recently, flixweed tansymustard was found to result in serious resistance to tribenuron due to repeatedly applying this herbicide [6, 7]. Clacyfos as PDHc inhibitor, has different mode of action from ALS inhibitor, tribenuron . Therefore, clacyfos could be a good option for controlling resistant broadleaf weeds in wheat.

In order to evaluate the efficacy of clacyfos against weeds and safety to winter wheat in field conditions, the field trials were conducted in winter wheat at the experiment station of Hebei Academy of Agriculture and Forestry Sciences in Shijiazhuang, Hebei province, and a commercial wheat field in Haidian region, Beijing, China during 2010–2011. For example, clacyfos was tested in winter wheat

Table 8.10 Comparison of ED₅₀ between clacyfos and 2,4-D

Weed species	ED ₅₀ of herbicides (g ai/ha) ^{a,b,c}	
	Clacyfos (HW02)	2,4-D
Common amaranth	70.7	74.1
Flixweed tansymustard	19.2	23.9
Shepherd's purse	52.6	60.2
Water chickweed	52.2	75.4

^a ED₅₀ is effective dose that provides 50 % reduction of weed biomass

^b The test was carried out in the greenhouse. Each treatment had four replications. Fourteen days after treatment, weed plants were cut at ground level and immediately weighed for each pot

^c The herbicides were sprayed with an auto-spraying tower (Model PWT-510, manufactured by the Pesticide Machinery Group of China Agricultural University) at the pressure of 0.25 Mpa at the 4- to 5-leaf stage of the weeds

Table 8.11 Post-emergence herbicidal activity of Clacyfos (HW02) in winter wheat fields^{a,b,c}

Herbicides	Rate (g ai/ha)	Reduction in plant numbers % (45 DAT)	Reduction in biomass % (45 DAT)		Beijing
		Hebei	Beijing	Hebei	
Clacyfos (HW02)	75	89	77	98	92
	225	100	92	100	98
	375	100	100	100	100
	525	100	100	100	100
2,4-D butyl ester	525	100	100	100	100

^a DAT is day after treatment. Weed numbers were counted at 45 DAT and weed plants were cut from ground level and immediately weighed at 45 DAT at different rate as percentage change compared to that of the untreated control; Each treatment had four replications

^b The herbicides were sprayed at the 7- to 8-leaf stage of the weeds on March 29, 2011 at Hebei and at the 8- to 9-leaf stage of the weeds on April 12, 2011 at Beijing respectively, in China

^c Application method: spray with a knapsack sprayer (Model: AGROLEX HD 400) with flat fan nozzles at 30 PSI

at Hebei and Beijing respectively, in 2011. At both sites, clacyfos was applied at the rates of 75, 225, 375, and 525 g ai/ha. 2,4-D butyl ester as control herbicide was applied at the recommended rate of 525 g ai/ha. Clacyfos exhibited good performance in weed control when it was applied at the late tillering stage of winter wheat in spring. It provided 98 ~ 100 % reduction in weed biomass at 225 ~ 525 g ai/ha and 100 % reduction in weed numbers at 375 ~ 525 g ai/ha at 45 DAT after treatment. 2,4-D butyl ester as positive control was applied at 525 g ai/ha in both sites. Clacyfos could provide weed biomass reductions of 100 % in Hebei and 98 % in Beijing at 225 g ai/ha. It still made 92 ~ 98 % biomass reduction even at 75 g ai/ha (Table 8.11).

No evident injury of winter wheat was observed in all treatments by clacyfos during experimental period. However, some slightly abnormal ears were observed in 2,4-D treatment in Hebei, but not observed in Beijing. Grain yields of winter wheat were higher in all clacyfos treatments than in the untreated control in Beijing. However, there was no difference in grain yield among all treatments in Hebei, which might be due to the low density of weeds occurring in the experimental field (Weed densities were 14.4 plants m² in Hebei and 30.7 plants m² in Beijing). When clacyfos was applied in winter wheat at the tillering stage in spring even at the rate of up to 900 g ai/ha, no injury was observed and no grain reduction was measured [8]. The field trial in winter wheat at Yangling, Shanxi where is also a representative winter wheat-producing areas, as an example, is shown in Table 8.12. 30 % Clacyfos EC was tested in the wheat field at 600–3,600 mL/ha (180–1,080 g ai/ha) when weeds were at 3–5 leaves stage while wheat was at 3 leaves stage. 10 % Tribenuron methyl WP was used at a recommended rate 150 mL/ha (15 g ai/ha) as a positive control. After 90 days, clacyfos still exhibited good and lasting control

Table 8.12 Post-emergence herbicidal activity of 30 % clacyfos (HW02) EC against broad-leaved weeds in wheat field

Rate (g ai/ha)	Inhibitory potency, % (90 DAT) ^{a,b,c}				
	Leaf mustard	Gray field speedwell	Bedstraw	Henbit deadnettle	Flixweed tansymustard
180	94	82	90	96	95
360	95	99	96	97	99
540	99	90	96	90	97
720	99	98	94	94	98
1,080	97	97	96	98	99
10 % Tribenuron methyl WP 15	95	93	92	98	88

^a Inhibitory potency (%) of herbicides against weeds was measured as percentage change in each weed fresh weight compared to that of the untreated control. Values are the average of 4 replicates. DAT is day after treatment

^b The test was carried out in the middle of November, 2003 at Yangling, Shanxi

^c Application method: spray one time by a shoulder sprayer

against leaf mustard (*Brassica juncea*), gray field speedwell (*Veronica polita*), bedstraw (*Galium aparine*), henbit deadnettle (*Lamium amplexicaule*), and flixweed tansymustard (*Descurainia Sophia*) at a rate as low as 180 g ai/ha.

Many broad-leaved weeds in wheat fields were under control (>90 %) after 90 days by using clacyfos at a rate no more than 360 g ai/ha. 30 % Clacyfos EC showed comparable control to tribenuron methyl as a positive control. It is worth mentioning that clacyfos showed faster action than tribenuron methyl.

Results of the field trial in winter wheat at Yangling showed clacyfos was safe to wheat at as high as 1,080 g ai/ha, because the yield of production of wheat using clacyfos as weed control agent, increased remarkably comparing to the untreated controls.

Some field trials showed that when clacyfos was used in wheat field against weeds for post-emergence application at 300–450 g ai/ha, the yield of wheat could be increased 12–19 % comparing to the untreated controls. Henan province is also a representative winter wheat-producing area in China. The effects of clacyfos on yield of wheat in field trial at Henan, as an example, are shown in Table 8.13.

30 % Clacyfos EC was tested in wheat field at 990–3,750 mL/ha (300–1,125 g ai/ha) when weeds were at 2–8 leaves stage. 13 % MCPA (aqua) 3,750 mL/ha and 10 % tribenuron methyl WP 150 mL/ha, at the recommended rates, were used as the positive controls. A preponderance of weeds in this wheat field were flixweed tansymustard (*Descurainia Sophia*), shepherd's purse (*Capsella bursa-pastoris*), and chickweed (*Stellaria media*). There were also little wild oats (*Avena fatua*), cleavers (*Galium aparine*) and others. As shown in Table 8.13, after 50 days, clacyfos exhibited 91 % total control at 450 g ai/ha against weeds in this wheat field. The yield of wheat could rise to 6,495 kg/ha which is increased 19 % comparing to the negative untreated (5,430 kg/ha). However, the yield of wheat

Table 8.13 Effect of 30 % clacyfos (HW02) EC on the yield of wheat^{a,b,c}

Rate (g ai/ha)	Inhibitory potency % (total control)	Average yield (kg/ha)	Yield-increase rate %
300	86	6,225	14.6
450	91	6,495	19.6
600	91	6,465	19.1
750	94	6,510	19.9
1,125	97	6,465	19.1
13 % MCPA ^d (aqua) 488	89	5,730	5.5
10 % Tribenuron methyl WP ^e 15	89	6,405	18
Untreated control (only used water)		5,430	

^a Inhibitory potency (%) of clacyfos against weeds for post-emergence application in wheat field was measured after 50 days at different rate as percentage change in all weeds fresh weight compared to that of the untreated control, values are the average of 4 replicates

^b The test was carried out in the middle of March, 2003 at Zhengzhou, Henan province

^c Application method: spray one time by a mini type compressional sprayer

^d MCPA: 2-methyl-4-chlorophenoxyacetic acid

^e Tribenuron methyl:methyl 2-[4-methoxy-6-methyl-1,3,5-triazin-2-yl(methyl)carbamoylsulfamoyl]benzoate

could be only increased in 5.5 % by using 13 % MCPA due to its phytotoxicity against wheat.

At this 300–450 g/ha rate, clacyfos did better than MCPA. It was comparable to tribenuron methyl in the effect of both control weeds and increased the yield of wheat. Clacyfos was field tested in Henan, Shandong, Jiangsu, Shaanxi, Hubei, and other representative winter wheat-producing areas in China. For those areas, clacyfos was applied in November when weeds were at 3 to 5 leaves stage while wheat was at 3 leaves stage. Other trials were applied in March back to spring before the jointing stage of wheat in Hebei, Tianjin, Amur River, and other representative spring wheat-growing areas.

Clacyfos exhibited good effect against main weeds in wheat fields, especially for perennial broad-leaved weeds. It showed good and lasting control against the wide spectrum of weeds. Clacyfos could control many weeds such as common amaranth, knotgrass, henbit deadnettle, common vetch, common nipplewort, water dropwort, feather finger grass, cucumber-herb, shortawn foxtail, Japanese alopecurus, field bindweed, setose thistle, creeping thistle, flixweed tansymustard, shepherd's purse, and gray field speedwell. Therefore clacyfos could be applied in wheat field against weeds at 300–450 g ai/ha.

Table 8.14 Post-emergence herbicidal activity of 30 % clacyfos (HW02) EC in maize field^{a,b,c}

Rate (g ai/ha)	Inhibitory potency % (45 DAT)			
	Chingma abutilon	Slender amaranth	White eclipta	Purslane
270	97	90	92	100
360	98	99	97	100
450	98	97	100	100
720	100	99	100	100
20 % MCPA (aqua) 750	91	89	100	100

^a Inhibitory potency (%) was measured as percentage change in each weed fresh weight compared to that of the untreated control. Values are the average of 4 replicates. DAT is day after treatment

^b The test was carried out in late June, 2005 at Yangzhou (in Jiangsu Province)

^c Application method: Spray one time by a Jacto PJ-16 sprayer

8.1.7.3 Effects of Clacyfos (30 % EC) in Maize Fields

The data of greenhouse test demonstrated clacyfos exhibited excellent control against major broad-leaved weeds in maize fields. A number of field trials were carried out in different regions including Jiangsu, Shandong, Hebei and Heilongjiang provinces. 30 % Clacyfos EC was applied in maize fields when weeds were at 3–5 leaves stage and maize was at 3–6 leaves stage. The effects of clacyfos against major broad-leaved weeds in maize fields at Yangzhou in Jiangsu province, as an example, are shown in Table 8.14.

30 % Clacyfos EC was tested in the maize field at 900–2,400 mL/ha (270–720 g ai/ha) when weeds were at 3–5 leaves stage and maize was at 5 leaves stage. 20 % MCPA (aqua) was used at a recommended rate 3,750 mL/ha (750 g ai/ha) as a positive control. The results showed that 30 % Clacyfos EC at as low as 270 g ai/ha exhibited 90–100 % inhibitory effects against chingma abutilon (*Abutilon theophrasti*), slender amaranth (*Amaranthus blitum*), white eclipta (*Eclipta prostrate*), and purslane (*Portulaca oleracea*) in maize fields (Table 8.14).

The herbicidal activity of 30 % Clacyfos EC against primary broad-leaved weeds in the maize field in Jiangsu, Shandong, Hebei, and Heilongjiang provinces are shown in Table 8.15.

30 % Clacyfos EC was tested in the maize field against primary broad-leaved weeds in different regions at 900–4,050 mL/ha (270–1,215 g ai/ha) when weeds were at 3–5 leaves stage and maize was at 4–6 leaves stage. 4 % Nicosulfuron SC was used at a recommended rate 1,500 mL/ha (60 g ai/ha) as a positive control (Table 8.14). The results showed that 30 % Clacyfos EC exhibited 90–100 % inhibitory activity against Asian copperleaf (*Acalypha australis*), goosefoot (*Chenopodium album*), bunge's smartweed (*Polygonum bungeanum*), and Siberian cocklebur (*Xanthium strumarium*) at 360 g ai/ha in maize fields (Table 8.15). For the phytotoxicity measurement, clacyfos was safe to maize at a rate as high as 1.2 kg ai/ha. The production of maize with clacyfos as weed control agent was significantly increased comparing to the

Table 8.15 Post-emergence herbicidal activity of 30 % clacyfos (HW02) EC in maize fields in different regions^{a,b,c}

Rate (g ai/ha)	Inhibitory potency % (45 DAT)							
	Jiangsu		Shandong		Hebei	Heilongjiang		
	Ecl ^d	Aca ^d	Abu ^d	Che ^d	Che	PoJ ^d	Xan ^d	Sol ^d
270	91	76	98	89	NT ^f	NT	NT	NT
300	100	100	100	96	89	100	80	59
360	92	100	97	98	100	100	95	72
450	98	100	100	100	100	100	100	78
600	100	100	100	100	100	100	100	85
900	100	100	100	NT	100	100	100	100
1,215	100	100	100	NT	100	100	100	100
4 % Nicosulfuron SC ^e 60	52	100	94	NT	91	83	90	80

^a Inhibitory potency (%) was measured as percentage change in each weed fresh weight compared to that of the untreated control. Values are the average of 4 replicates. DAT is day after treatment

^b The test was carried out in late May or in late June, 2005

^c Application method: Spray one time by a Jacto PJ-16 or Matabi sprayer

^d Ecl: white eclipia, Aca: Asian copperleaf, Abu: chingma abutilon, Che: goosefoot, Pob: bunge's smartweed, Xan: Siberian cocklebur, Sol: black nightshade

^e Nicosulfuron:(1-(4,6-Dimethoxypyrimidin-2-yl)-3-(3-dimethylcarbamoyl-2-pyridyl sulfonyl)urea)

^f NT: not tested

untreated control. Field data showed that clacyfos at 300–450 g ai/ha provided acceptable broad-leaved weeds control. At this 300–450 g/ha, clacyfos did better than MCPA, at 750 g ai/ha (Table 8.14) the effect against weeds was comparable to nicosulfuron, at 60 g ai/ha (Table 8.15).

A number of fields' trials in different regions in China showed that clacyfos provided good control against a broad spectrum of broad-leaved and sedge weeds in wheat and maize fields. It exhibited potent activity against annual and perennial broad-leaved and sedge weeds at the recommended rates of 300–450 g ai/ha in wheat and maize fields. Clacyfos showed a lasting control against weeds and could be employed with a one-time treatment to control broad-leaved and sedge weeds by post-emergence application in the whole growth period of these crops.

8.1.7.4 Effects of Clacyfos (30 % EC) in Tall Fescue Lawn

Tall fescue (*Festuca arundinacea*) is an important cool-season perennial turf grass in the temperate region. Tall fescue is grown widely in China, Africa, and South America as turf and as a forage crop for grazing animals. With the development of city in China, tall fescue has been widely applied for all kinds of lawns because it has high resistance to disease and tolerance to extensive management. Tall fescue acreages has increased in China in recent years.

The results of greenhouse test showed clacyfos was safe for tall fescue. Therefore clacyfos was used as a selective herbicide in tall fescue lawn. A number of field trials were carried out in different regions including Shanghai, Beijing, and Hangzhou city, some areas in Shandong, Henan, Anhui, and Zhejiang provinces. The results of field trials at Beijing and Shanghai as representative planted regions of tall fescue are summarized in Tables 8.16 and 8.17.

Table 8.16 Post-emergence herbicidal activity of 30 % clacyfos (HW02) EC in tall fescue lawn^{a,b,c}

Rate (g ai/ha)	Inhibitory potency % (21 DAT)				
	Common amaranth	Morning glory	Common purslane	Other weeds	Total
270	94	100	62	79	92
405	97	100	72	100	96
540	100	100	69	100	98
810	100	100	83	100	99
72 % 2,4-D butyl ester EC 540	90	100	66	100	90

^a Inhibitory potency (%) was measured as percentage change in each weed fresh weight compared to that of the untreated control. Values are the average of 4 replicates. DAT is day after treatment

^b The test was carried out in July, 2005 at Beijing

^c Application method: Spray one time by a Jacto PJ-16 sprayer

Table 8.17 Post-emergence herbicidal activity of 30 % clacyfos (HW02) EC in tall fescue lawn^{a,b,c}

Rate (g ai/ha)	Inhibitory potency % (45 DAT)			
	Small goosefoot	Water chickweed	Slender amaranth	Total
300	90	48	34	60
450	98	85	100	95
610	98	97	100	100
900	100	100	100	100
20 % Starane ^d EC 180	0	100	78	56
32.5 % Flazasulfuron ^e EC 730	72	81	8	57

^a Inhibitory potency (%) was measured as percentage change in each weed numbers compared to that of the untreated control. Values are the average of 4 replicates. DAT is day after treatment

^b The test was carried out in Sep 11th, 2005 at Shanghai

^c Application method: Spray one time by a Jacto HD400 backpack sprayer

^d Starane: octan-2-yl 2-(4-amino-3,5-dichloro-6-fluoropyridin-2-yl)oxyacetate

^e Flazasulfuron: 1-(4,6-dimethoxypyrimidin-2-yl)-3-(3-trifluoromethyl-2-pyridylsulfonyl)urea

The herbicidal activity of clacyfos against major broad-leave weeds in the tall fescue lawn at Beijing, as an example, are shown in Table 8.16. 30 % Clacyfos EC was applied in the mature lawn at 900–2,700 mL/ha (270–810 g ai/ha) when weeds were at 3–5 leaves stage. 72 % 2, 4-D butyl ester EC was used at a recommended rate 750 mL/ha (540 g ai/ha) as a positive control. The results showed that 30 % Clacyfos EC was very safe at different rates for tall fescue and it exhibited good inhibitory activity against broad-leaved weeds with 92–96 % total control. Its herbicidal effect at 270–405 g ai/ha was comparable to that of 2,4-D butyl ester at 540 g ai/ha.

The herbicidal effect of clacyfos against major broad-leave weeds in the mature tall fescue lawn at Shanghai, as another example, are shown in Table 8.17. 30 % Clacyfos EC was applied in the mature lawn at 1,000–3,000 mL/ha (300–900 g ai/ha) when weeds were at 2–4 leaves stage. 20 % Starane EC 900 mL/ha and 32.5 % Flazasulfuron EC 2,250 mL/ha, at the recommended rates, were used as the positive controls.

The observation at lawn trial showed that clacyfos had no phytotoxicity to tall fescue at rate as high as 900 g ai/ha. Clacyfos exhibited 95 % total control against broad-leaved weeds at 450 g ai/ha. At 450 g/ha, clacyfos did better than flazasulfuron, one of the positive control, at 730 g ai/ha. At 300 g/ha, the total control of clacyfos against weeds comparable to starane, another positive control at 180 g ai/ha (Table 8.17)

Field trials showed that 30 % clacyfos EC could control a broader range of weed species in tall fescue lawn when weeds were at 2–8 leaves stage and had no phytotoxicity to tall fescue at 900–2,000 mL/ha (270–600 g ai/ha). 30 % clacyfos EC exhibited a broader spectrum and notable herbicidal activity against broad-leaves, such as common amaranth (*Amaranthus retroflexus*), common nipplewort (*Lapsanastrum apogonoides*), tall buttercup (*Ranunculus japonicus*), pinkhead smartweed (*Polygonum capitatum*), knotgrass (*Polygonum aviculare*), water pepper (*Polygonum flaccidum*), goosefoot (*Chenopodium album*), Chinese spinach (*Amaranthus tricolor*), common purslane (*Portulaca oleracea*), Asian copperleaf (*Acalypha australis*), wolf's milk (*Euphorbia humifusa*), chingma abutilon (*Abutilon theophrasti*), white eclipta (*Eclipta prostrata*), water chickweed (*Malachium aquaticum*), slender amaranth (*Amaranthus blitum*), dayflower (*Commelina communis*), creeping thistle (*Cirsium setosum*), and lobedleaf pharbitis (*Ipomoea hederacea*). It also exhibited good herbicidal activity against vigorous growth dayflower (*Commelina communis*), creeping thistle (*Cirsium setosum*), and lobedleaf pharbitis (*Ipomoea hederacea*) at higher rates.

On the basis of field trials in tall fescue, clacyfos (HW02) was registered to control broadleaf weeds in turf in 2007 in China.

More than 40 field trials in different regions in China showed that clacyfos exhibited potent activity against annual and perennial broad-leaved and sedge weeds in lawn, wheat and maize fields by post-emergence application. Clacyfos was safe for monocot crops or monocot turf grass at the recommended rates of

300–450 g ai/ha. Except field trials, clacyfos was further evaluated for its toxicity, eco-toxicity and residual effects on environment. Formulations were also developed and evaluated.

8.1.8 Toxicity Evaluation

Acute, chronic and other toxicity tests for clacyfos were carried out according to the standard operational procedures of pesticidal registration. The toxicity evaluation was performed by National Pesticide Engineering Research Center (Shenyang) in Chain. Test results suggested that clacyfos has low acute toxicity against rats and non-harmful to other tested animals.

8.1.8.1 Acute Toxicity

This procedure includes oral toxicity, dermal toxicity, inhalation toxicity, eye irritation, and dermal sensitization. The acute oral and acute dermal toxicity tests were performed in rates to determine the LD₅₀. The evaluation showed that both technical grade of clacyfos and 30 % clacyfos EC had low acute toxicity against rats. Neither significant eye irritation nor negative dermal sensitization of rabbit was observed.

Detailed information of the acute toxicity is listed in Tables 8.18 and 8.19.

Table 8.18 Acute toxicity of clacyfos

Study type	Results	Toxicity category
Acute oral (rat)	LD ₅₀ = 1,467 mg/kg ♀ 1711 mg/kg ♂	III or low toxicity
Acute dermal (rat)	LD ₅₀ > 2,000 mg/kg (♀,♂)	III or low toxicity
Primary eye irritation (rabbit)	Non-irritant	IV
Primary skin irritation (rabbit)	Non-irritant	IV

Table 8.19 Acute toxicity of 30 % clacyfos EC

Study type	Results	Toxicity category
Acute oral (rat)	LD ₅₀ = 2,000 mg/kg (♀, ♂)	III or low toxicity
Acute dermal (rat)	LD ₅₀ > 2,150 mg/kg (♀, ♂)	III or low toxicity
Primary eye irritation (rabbit)	Slight-irritant	IV
Primary skin irritation (rabbit)	Non-irritant	IV
Sensitization	Weak sensitization	

Table 8.20 Chronic and other toxicity of clacyfos

Study type	Results
Ames (rat liver S9 fraction)	Negative
Chromosome aberration of spermatocytes (rat)	Negative
Micronucleus test (rat)	Negative
one-year chronic (rat) and two-year carcinogenicity (rat)	No carcinogenicity observed
Two-generation-reproduction (rat)	No effect on development or reproduction observed
Neurotoxicity (hen)	No neurotoxicity observed

8.1.8.2 Chronic and Other Toxicity Tests

Chronic Ames, chromosome aberration of spermatocytes, and micronucleus tests were performed in rat. All tests results were negative.

Chronic toxicity including one-year chronic (rat) and two-year carcinogenicity (rat) was evaluated, no carcinogenicity was observed. The results of the two-generation-reproduction (rat) showed no effect on development or reproduction after ingestion and dermal exposure of clacyfos (Table 8.20). Because clacyfos is an organophosphorus compound, therefore, neurotoxicity test was additionally conducted, which was also negative (Table 8.20).

8.1.9 Environmental Fate

Environmental fate of clacyfos including hydrolysis, degradation, volatility and mobility in the soil was evaluated according to “Chemical pesticide environmental safety evaluation test guidelines”. These tests were performed by National Pesticide Engineering Research Center (Shenyang) in China. The hydrolysis of clacyfos was carried out at 25 and 50 °C under 3 different pH conditions (5, 7, 9). Clacyfos was very easy to hydrolyze in water. Residues of clacyfos in black soil (from Jilin), paddy soil (from Taihu), and red clay (from Jiangxi) were determined. Clacyfos could decompose in these soils. Little to no mobility of clacyfos was found in either black soil (Jilin), paddy soil (Taihu) or red clay (Jiangxi). It was also found that clacyfos was next to impossible to volatilize in air and water or from the surface of the soils (Table 8.21). Because clacyfos degrades so rapidly in soil or water, no clacyfos can be detected at the soil adsorption and bioaccumulation test.

Table 8.21 Environmental fate of clacyfos

Study type	Results	Grade
Hydrolysis	Ease to hydrolyze in water	Grade I
Degradation	Ease to degradation in soil	Grade I
Mobility in the soil	No mobility in the soil.	Grade V
Volatility	Difficult to volatilize in air, water, at the surface of soil	Grade IV

Analysis of environmental behaviors and characteristics of clacyfos showed that it had no negative impact on environment. Therefore, clacyfos would be an environmental-friendly herbicide.

8.1.10 Residues

Residual tests were carried out in maize fields at Agricultural Science Experimental Station of Jilin Agricultural University in 2005 and Hailun city in Heilongjiang in 2006. The residual tests were performed by College of Resource and Environmental Science, Jilin Agricultural University. During the growth season, maize was sprayed one time with 30 % clacyfos EC at 900 g ai/ha.

Clacyfos degraded very fast in soil and in fresh maize. The half-life of clacyfos in soil and in fresh maize was 0.2–0.4 day, and 0.1–0.4 day, respectively. Analysis of the final residual quantity confirmed that very low residues of clacyfos or no clacyfos at all could be found in soil and maize. The final residual quantity of clacyfos in maize grain was less than 0.005 mg/kg. MRL data of clacyfos in maize grain was suggested as 0.25 mg/kg which was reckoned according to no effect dosage (no effect dosage was determined by School of Public Health, Tongji Medical College of Huazhong University of Science & Technology in Wuhan, China).

8.1.11 Adsorption of Clacyfos on Soils

The adsorption behavior of clacyfos on five kinds of soils was investigated in the laboratory using batch equilibration technique by Zhongbin Lu et al. [9]. Clacyfos had a strong adsorption to the soils. Adsorption isotherms of clacyfos on the soils could be described well by the Freundlich equation. Adsorption coefficients (K_F) of clacyfos on chernozem soil, ablic soil, meadow soil, arenosols clay and clay were 332.65, 103.32, 672.97, 577.96, and 289.60, respectively. The adsorption coefficients of organic matter (K_{OM}) values ranged from 796.57 to 10197.18. This result suggests that clacyfos has very weak mobility in the soils according to McCall's classification scheme. Adsorption free energy (ΔG) of clacyfos on chernozem soil, ablic soil, meadow soil, arenosols clay and clay was -16.55 , -22.73 , -18.32 , -18.48 and -22.86 kJ/mol, respectively. This indicates that the clacyfos adsorption is dominated by physical adsorption. There were good correlations between adsorption coefficients (K_F) of clacyfos on the five different kinds of soils and the soil properties, such as organic matter, pH, and clay content. A poor correlation was found between K_F and cation exchange content of the soils. This indicates that organic matter, pH and clay content are the predominate factors influencing adsorption of clacyfos on the soils studied.

Table 8.22 Ecological effects of 30 % clacyfos EC

Study type	Results	Toxicity category
Bee	LD ₅₀ > 100.00 µg/bee	Low toxicity
Quail	LD ₅₀ ♂: 1999.9, ♀: 1790 mg/kg	Low toxicity
Zebra fish	LC ₅₀ (96 hr) : 21.79 mg/L	Low toxicity
Silkworm	LD ₅₀ > 10,000 mg/L	Low toxicity

8.1.12 Ecological Effects

Eco-toxicity evaluation of 30 % clacyfos EC on bee, birds, fishes and non-target organisms was carried out by National Pesticide Engineering Research Center (Shenyang) in China. The result showed that clacyfos had low toxicity to bees, birds, fishes, and the silkworm (Table 8.22).

8.1.13 Summary

The test results of more than forty field trials showed that clacyfos, (*O,O*-dimethyl 1-(2,4-dichlorophenoxyacetoxy)ethylphosphonate) had good selectivity between monocotyledonous crops and dicotyledonous weeds. It provided good control at 270–450 g ai/ha against broad spectrum of broad-leaved and sedge weeds by one time of post-emergence application in the whole season of lawn, wheat and maize. At 324 g ai/ha, clacyfos showed higher activity against broad-leaved weeds than glyphosate at 923 g ai/ha. At 300–450 g ai/ha, clacyfos exhibited the effect of weed control better than or comparable to MCPA (750 g ai/ha), 2,4-D (525 g ai/ha), or flazasulfuron (730 g ai/ha), it is also comparable to the effect of tribenuron methyl (15 g ai/ha), nicosulfuron (60 g ai/ha) or starane (180 g ai/ha). It was found that clacyfos could control some resistant weed which had serious resistance to tribenuron. These results showed clacyfos could be an alternative herbicide for resistant weed management because its mode of action is different from herbicides presently used. Clacyfos exhibited good xylem mobility and a stronger rain stability than MCPA due to its rapid absorption and good osmosis. It was very safe for the aftercrop crops due to its low residues in soil.

According to present reports, none of the PDHc inhibitors prepared was active enough to be commercialized as an herbicide. Although 1,1-dimethoxyethyl (methyl)phosphinate **2** as plant PDHc inhibitors were reported and evaluated in many field trials by Baillie et al. as early as 1988. Unfortunately, **2** had insufficient commercial potential due to high application rate (at 2.8 kg ai/ha), unacceptable phytotoxicity on crops. Our present work showed clacyfos was a selective inhibitor against dicot plant PDHc, but not against mammal PDHc (Chap. 7). Therefore, clacyfos could selectively control broadleaf weeds in monocotyledonous crop fields

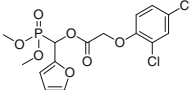
and it is not harmful to mammals, bees, birds, fishes and silkworm. Clacyfos is thus an effective and environment-friendly herbicide candidate with low toxicity.

Clacyfos exhibited an obvious advantage over those acylphosphinates or acylphosphonates in enzyme-selective inhibition, crop safety, and effectiveness. It seems to be the first compound which shows practical herbicidal activity as a plant PDHc inhibitor. These results proved the rationality and effectiveness of our study on the biorational design of plant PDHc E1 inhibitor.

8.2 Evaluation of HWS

8.2.1 Introduction

HWS (**IG-21**), *O,O*-dimethyl 1-(2,4-dichlorophenoxyacetoxy)-1-(furan-2-yl)methylphosphonate was found by modifying the structure of alkylphosphonates **IC** (Chap. 2). It could control a lot of broad-leaved weeds by post-emergence application at a rate as low as 18.75 g ai/ha in the greenhouse. It was also confirmed to be a potent inhibitor of plant PDHc. HWS showed much higher inhibitory potency against PDHc in pea than in rice *in vitro*. These findings indicated that HWS could selectively inhibit dicot plant PDHc, which is in agreement with its higher herbicidal activity against broad-leaved weeds in a greenhouse test [10]. HWS would be useful as a selective herbicide against broad-leaved weeds in monocot crop fields. These unique characters of HWS prompted us to further examine its potential as a selective herbicide.

Chemical name	<i>O,O</i> -Dimethyl 1-(2,4-dichlorophenoxyacetoxy)-1-(furan-2-yl)methylphosphonate
Chemical structure	
Empirical Formula	C ₁₅ H ₁₅ Cl ₂ O ₇ P
Molecular weight	409.16
CAS registry number	263722-89-0
Experimental Name	HWS
Chemical Class	Phosphonate
Pesticide Type	Herbicide
Site of action	PDHc

8.2.2 Physiochemical Properties

Physiochemical properties of HWS are shown in Table 8.23.

Table 8.23 Physiochemical properties of HWS

Parameter	Value
Appearance	Colorless crystal
m.p.	63–64 °C
Solubility	Miscible with acetone, ethanol, chloroform, toluene and xylene at 25 °C
Stability	Stable for air at room temperature But instable for light and easy to decompose under the acidic or basic conditions
Long-stem storage	Keep in dark and dry place at low temperature (<15 °C)

8.2.3 Herbicidal Activity in Greenhouse

Bioassay for HWS was carried out in the greenhouse for its post-emergence herbicidal activity, control spectrum, crop safety, and biological property at the National Pesticide Discovery South Center (Zhejiang or Hunan) in China. The results are summarized as follows.

8.2.3.1 Control Spectrum of HWS

Twenty-three different plants were chosen as targets. The bioassay was carried out at 300 g ai/ha in the greenhouse.

HWS exhibited 90–100 % control against a broad spectrum of dicotyledonous plants including bog chickweed (*Stellaria alsine*), common amaranth (*Amaranthus retroflexus*), leaf mustard (*Brassica juncea*), sickle senna (*Cassia tora*), small goosefoot (*Chenopodium serotinum*), chingma abutilon (*Abutilon theophrasti*), manyleaf bittercress (*Cardamine macrophylla*), knotgrass (*Polygonum aviculare*), and field chickweed (*Cerastium arvense*).

HWS showed medium activity against some plants was also observed at 300 g ai/ha. It displayed 60–89 % control against common vetch (*Vicia sativa*), white eclipta (*Eclipta prostrate*), ricefield flatsedge (*Cyperus iria*), caper spurge (*Euphorbia lathyris*), curled dock (*Rumex crispus*), and green bristlegrass (*Setaria viridis*), but <60 % control against southern crabgrass (*Digitaria ciliaris*), crab grass (*Digitaria sanguinalis*), shortawn foxtail (*Alopecurus aequalis*), green bristlegrass (*Setaria viridis*), American sloughgrass (*Beckmannia syzigachne*), Asia Minor bluegrass (*Polypogon fugax*), annual bluegrass (*Poa annua*), and Japanese alopecurus (*Alopecurus japonicus*).

The above observations showed that HWS had good herbicidal activity against dicotyledonous weeds, but relatively weak effects against monocotyledonous plants, indicating that HWS should be considered as an selective herbicide against dicotyledonous weeds.

Table 8.24 Post-emergence herbicidal activity of HWS^a

Rate (g ai/ha)	Por ^b	Ama ^b	Che ^b	Ams ^b	Bet ^b	Zea ^b	Ory ^b
1200	100	100	100	100	100	10	20
900	100	100	100	100	100	0	0
450	100	100	100	100	100	0	0
300	91	100	100	98	98	0	0
200	85	100	100	98	98	0	NT
100	83	100	100	90	80	NT	NT
50	70	100	80	60	80	NT	NT

^a Inhibitory potency (%) against the growth of plants in the greenhouse, 0 (no effect), 100 % (completely kill), NT (not tested)

^b Por: purslane; Ama: slender amaranth; Che: goosefoot; Ams: spiny amaranth; Bet: sugarbeet; Zea: maize; Ory: rice

8.2.3.2 Post-Emergence Herbicidal Activity of HWS

The herbicide activity and selectivity of HWS were further examined at 50–1,200 g ai/ha against common purslane (*Portulaca oleracea*), slender amaranth (*Amaranthus blitum*), goosefoot (*Chenopodium album*), spiny amaranth (*Amaranthus spinosus*), sugar beet (*beta vulgaris*), maize (*Zea mays*) and rice (*Oryza sativa*). The results are shown in Table 8.24.

As shown in Table 8.24, HWS exhibited excellent herbicidal activity against broad-leaved weeds by post-emergence application. Dicotyledonous crops such as sugar beet was susceptible to HWS at a rate as low as of 50 g ai/ha, whereas the monocot crops, maize, and rice displayed high tolerance to HWS even at 1.2 kg ai/ha. HWS was safe for maize and rice, and can be used as a broad-leaved weeds control agent in monocot crop fields.

Post-emergence herbicidal activity of HWS was further examined at 75–18.75 g ai/ha against common amaranth (*Amaranthus retroflexus*), goosefoot (*Chenopodium album*), leaf mustard (*Brassica juncea*), and morning glory (*Ipomoea nil*). 2,4-D and glyphosate at the same rates were used as positive controls (Table 8.25). HWS exhibited good effects against broad-leaved weeds at rate as low as 18.75 g ai/ha. Its herbicidal activity against broad-leaved weeds in general was comparable to 2,4-D and better than glyphosate.

8.2.3.3 Crop Safety

Maize, wheat, cotton, soybean, peanut, and rape were used to examine the crop safety of HWS. The data in Table 8.26 showed that HWS was relatively safe to monocotyledonous crops such as wheat and maize at 1.2 kg ai/ha or higher rate, but harmful to dicotyledonous crops, such as cotton, soybean, peanut, and rape at higher than 400 g ai/ha. HWS could be useful as a selective herbicide in monocotyledonous crop fields against dicotyledonous weeds.

Table 8.25 Post-emergence herbicidal activity of HWS^a

Herbicides	Rate (g ai/ha)	Post-emergence			
		Ama ^b	Che ^b	Brj ^b	Ipn ^b
HWS	75	95	85	100	100
	37.5	95	80	100	90
	18.75	80	70	100	85
2,4-D	75	95	95	100	100
	37.5	90	80	100	100
	18.75	70	75	80	90
glyphosate	75	75	80	80	75
	37.5	60	70	75	60
	18.75	60	50	70	50

^a Inhibitory potency (%) against the growth of plants in the greenhouse, 0 (no effect), 100 % (completely kill)

^b Ama: common amaranth; Che: goosefoot; Brj: leaf mustard; Ipn: morning glory

Table 8.26 Growth inhibition of several crops by HWS^{a,b}

Rate (g ai/ha)	Inhibitory potency %					
	Maize	Wheat	Cotton	Soybean	Peanut	Rape
400	-2	-4	21	18	18	100
600	3	-4	28	21	24	100
800	6	-5	34	29	27	100
1,200	10	8	39	34	36	100
1,600	12	9	45	39	41	100

^a Inhibitory potency (%) against the growth of plants in the greenhouse, 0 (no effect), 100 % (completely kill)

^b Values are the average of 3 replicates

Selectivity of HWS between maize and weeds was further examined. As shown in Table 8.27, HWS exhibited high herbicidal activity against dicotyledonous weeds, common amaranth (*Amaranthus retroflexus*), common purslane (*Portulaca oleracea*), and chingma abutilon (*Abutilon theophrasti*). However, Among these weed species, common amaranth, and common purslane were very susceptible to HWS, their ED₉₀ values was < 100 g ai/ha. Chingma abutilon was also susceptible to HWS, its ED₉₀ values was about 200 g ai/ha. Whereas crop maize had high tolerance to HWS even at 900 g ai/ha (ED₁₀ = 900 g ai/ha).

Above results indicated that HWS displayed high selectivity between maize and dicotyledonous weeds, such as common amaranth, common purslane, or chingma abutilon. Therefore, HWS can be a useful and safe herbicide in maize field against dicotyledonous weeds.

Table 8.27 Selectivity of HWS between maize and dicotyledonous weeds^{a,b}

Plant	Inhibitory potency %					
	150 (g ai/ha)	300 (g ai/ha)	450 (g ai/ha)	600 (g ai/ha)	750 (g ai/ha)	900 (g ai/ha)
Common amaranth	98	95	100	100	100	100
Common purslane	98	95	100	100	100	100
Chingma abutilon	80	100	100	100	100	100
Maize	0	0	0	0	0	10

^a Inhibitory potency (%) against the growth of plants by post-emergence application in the greenhouse, 0 (no effect), 100 % (completely kill)

^b Values are the average of 3 replicates

Table 8.28 Inhibitory activity of HWS against common amaranth

Treat method	Inhibitory potency ^a % (12 DAT) ^b		
	Root length	Plant above ground	Plant fresh weight
Leave-sprayed	100	100	100
Stem-sprayed	60	85	90
Root-poured	90	100	100

^a Inhibitory potency (%) against the growth of common amaranth in the greenhouse at the concentrations of 500 mg/L, 0 (no effect), 100 % (completely kill). Values are the average of 3 replicates

^b DAT is day after treatment

8.2.4 Systemic Property of HWS

The absorption and translocation of HWS were determined using a standard operational procedure developed by the National Pesticide Discovery South Center (Zhejiang). Common amaranth (*Amaranthus retroflexus*) was used as the target plant. Table 8.28 showed that HWS was absorbed through buds, roots, stems, and leaves and exhibited good inhibitory effect.

Data suggested that HWS exhibited xylem mobility. It could be translocated from leaf or stem to root, or from root to leaf or stem. HWS exhibited good inhibitory effect against the growth of plants by foliar and stem spray or root application. The inhibitory effect was produced mainly via foliar application. Therefore, HWS is recommended as a post-emergence herbicide.

8.2.5 Rainfast Characteristics of HWS

For the purpose of determining the influence of environmental factors and rainfall, herbicidal activity of 30 % HWS EC, was determined at different times of treatment under a simulant rainy condition. 41 % MCPA EC was included as a positive control. Common amaranth (*Amaranthus retroflexus*) was used as the tested plant.

Table 8.29 The influence of rain water on the inhibitory activity of 30 % HWS EC and 41 % MCPA EC at different time against common amaranth^{a,b,c}

Herbicides	Rate (g ai/ha)	Rain time and corresponding inhibitory activity (%)								No rain
		0 h	0.5 h	1 h	2 h	4 h	8 h	12 h	24 h	
30 % HWS EC	750	59	79	84	78	82	88	93	93	100
41 % MCPA EC	900	14	31	28	28	59	55	80	84	98

^a The experiment was done by using a rainfall simulator with 1,000 mL water (corresponding for 20 mm rainfall) at different time

^b The time after common amaranth was treated, for example the plant suffered rainfall at 0.5 h after being treated by HWS and MCPA, the inhibitory activity of HWS and MCPA against common amaranth are 79 and 31 %, respectively

^c Inhibitory potency against common amaranth was measured as percentage change in fresh weight compared to that of the untreated control. 0 % (no effect), 100 % (completely killed). Values are the average of 3 replicates

As seen from Table 8.29, the effect of HWS would decrease about 20 % if the plants were scoured by rainwater in 4 h, about 10 % in 8 h. Under the same treatment, MCPA would decrease more than 40 % in 8 h. HWS had stronger stability in rainfall than MCPA. This is due to the rapid absorption and good osmosis of HWS. Data showed that the herbicidal effect of HWS would be fully realized if the treatment is completed 8 h before it rains.

8.2.6 Field Trials of HWS

HWS was further evaluated as a potential herbicide candidate in maize field due to its safety to maize. A formulation of 30 % EC was used in the field testing. A series of field trials were carried out in different areas of China including Zhejiang, Shandong, Anhui, Tianjin, Heilongjiang, and Hainan. These trials were performed by the Institute of Plant Protection, Academy of Agricultural Science in corresponding province.

The results of field tests demonstrated that: 30 % HWS EC showed broad-spectrum and notable control on broad-leaved weeds in maize fields. When maize was at 2–5 leaves stage, many weeds were kept under control by post-emergence application. Common weeds in maize fields including common amaranth (*Amaranthus retroflexus*), common purslane (*Portulaca oleracea*), Asian copperleaf (*Acalypha australis*), chingma (*Abution theophrasti*), knotgrass (*Polygonum aviculare*), and goosefoot (*Chenopodium album*) could be effectively controlled by HWS at 300–450 g ai/ha. HWS was safe for maize and showed a significant yield increase. For examples, 30 % HWS EC was tested in maize fields in Shandong, Shaoxing and Jiaxing of Zhejiang respectively, during 2005–2008. HWS was applied at the rates of 225–900 g ai/ha, 4 % Nicosulfuron SC as positive control was applied at 48 g ai/ha in Shandong, 20 % Fluroxypyr as positive control was applied at 180 g ai/ha in Shaoxing and Jiaxing respectively. The results are shown in Tables 8.30, 8.31, 8.32.

Table 8.30 Post-emergence herbicidal activity of 30 % HWS EC in maize fields in Shandong

Herbicides	Rate (g ai/ha)	Inhibitory potency % (30 DAT) ^{a,b,c}					
		Reduction in weed numbers %			Reduction in biomass %		
		2005	2007	2008	2005	2007	2008
30 % HWS EC	225	/	85	96	/	86	99
	300	87	92	96	92	95	99
	375	93	98	99	94	99	100
	450	96	100	100	94	100	100
	900	99	100	99	98	100	100
4 % Nicosulfuron SC	48	98	98	100	95	97	100

^a Main weeds in maize field: purslane, common amaranth, Asian copperleaf, white eclipta

^b DAT is day after treatment. Weed numbers were counted at 30 DAT and weed plants were cut from ground level and immediately weighed at 30 DAT at different rate as percentage change compared to that of the untreated control. Each treatment had four replications, values are the average of four replicates

^c Application method: spray one time by a shoulder sprayer

Inhibitory potency against the growth of weeds in maize field was measured as percentage change in weeds numbers or in the fresh weight of weeds compared to that of the untreated control. As shown in Tables 8.30–8.32, HWS provided > 90 % weeds control in maize fields at 375 g ai/ha and comparable to the control effects of Nicosulfuron (48 g ai/ha) in Shandong. HWS provided adequate weeds control at 375–450 g ai/ha and comparable to the control effects of Fluroxypyr (180 g ai/ha) in Shaoxing, and Jiaxing respectively.

Table 8.31 Post-emergence herbicidal activity of 30 % HWS EC in maize fields in Shaoxing

Herbicides	Rate (g ai/ha)	Inhibitory potency % (30 DAT) ^{a,b,c}					
		Reduction in weed numbers %			Reduction in biomass %		
		2005	2007	2008	2005	2007	2008
30 % HWS EC	300	92	89	78	91	95	80
	375	93	93	83	92	96	85
	450	95	94	87	95	97	87
	900	96	95	90	97	98	91
20 % Fluroxypyr	180	96	95	94	96	97	95

^a Main weeds in maize field: Indian toothcup, prostrate false pimpernel, knotweed, spiny amaranth, small goosefoot and purslane in 2005; Asia minor bluegrass, goosefoot, and alligatorweed in 2007; white eclipta, common amaranth, and spotted spurge in 2008

^b DAT is day after treatment. Weed numbers were counted at 30 DAT and weed plants were cut from ground level and immediately weighed at 30 DAT at different rate as percentage change compared to that of the untreated control. Each treatment had four replications, values are the average of four replicates

^c Application method: spray one time by a shoulder sprayer

Table 8.32 Post-emergence herbicidal activity of 30 % HWS EC in maize fields in Jiaying

Herbicides	Rate (g ai/ha)	Inhibitory potency % (30 DAT) ^{a,b,c}			
		Reduction in weed numbers %		Reduction in biomass %	
		2007	2008	2007	2008
30 % HWS EC	300	66	70	68	77
	375	72	80	72	87
	450	83	88	84	93
	900	87	97	92	98
20 % Fluroxypyr	180	78	92	82	95

^a Main weeds in maize field: common amaranth, knotgrass, goosefoot, and alligatorweed in 2007; Asian copperleaf, common amaranth, goosefoot, and alligatorweed in 2008

^b DAT is day after treatment. Weed numbers were counted at 30 DAT and weed plants were cut from ground level and immediately weighed at 30 DAT at different rate as percentage change compared to that of the untreated control. Each treatment had four replications, values are the average of four replicates

^c Application method: spray one time by a shoulder sprayer

8.2.7 Toxicity Evaluation

The toxicity assessment of HWS was carried out at the School of Public Health, Tongji Medical College of Huazhong University of Science & Technology. The acute toxicities of HWS were determined by a serial of toxicity tests including acute oral and transdermal toxicity, skin and eye irritation, dermal allergic. The tests of bacterial reverse mutation, chromosome aberration of mouse primary spermatocyte, micro nucleated polychromatic erythrocytes in mice bone marrow, and subchronic toxicity were also performed. All toxicological parameters showed that HWS exhibited a low acute toxicity profile against rat and other animals.

8.2.7.1 Acute Toxicity

The acute toxicity includes oral toxicity, dermal toxicity, inhalation toxicity, eye irritation, and dermal sensitization. The acute oral and acute dermal toxicity were tested against rats. HWS was in toxicity category III and IV suggesting low acute toxicity (rat), neither significant eye irritation nor dermal sensitization (rabbit). The detailed information is shown in Table 8.33.

Table 8.33 Acute toxicity of HWS

Study type	Results	Toxicity category
Acute oral (rat)	LD ₅₀ = 3,162 mg/kg ♀ 2,712 mg/kg ♂	III or Low toxicity
Acute dermal (rat)	LD ₅₀ > 2,000 mg/kg (♀,♂)	III or Low toxicity
Primary eye irritation (rabbit)	Non-irritant	IV
Primary skin irritation (rabbit)	Non-irritant	IV

Table 8.34 Toxicity of HWS

Study type	Results
Ames (rat liver S9 fraction)	Negative
Chromosome aberration of spermatocytes (rat)	Negative
Micronucleus test (rat)	Negative

Table 8.35 Ecological effects of HWS

Study type	Results	Toxicity category
Bee	LD ₅₀ > 100.00 µg/bee	Low toxicity
Quail	LC ₅₀ > 1470 mg/kg	Low toxicity
Zebra fish	LC ₅₀ (96 h) > 21.77 mg/L	Low toxicity
Silkworm	LC ₅₀ (96 h) > 2000 mg/L	Low toxicity

8.2.7.2 Chronic and Other Toxicity

Chronic Ames, chromosome aberration of spermatocytes and micronucleus tests, were further performed in rat. All tests results were negative suggesting HWS was non harmful to rat after ingestion and dermal exposure. Therefore HWS was not harmful to any tested animals (Table 8.34).

8.2.8 Ecological Effects

Ecological impacts of HWS against representative non-target species were also evaluated. Studies for eco-acute toxicity of 30 % HWS against zebra fish, honey bee, quail, and silkworm representative non-target species were carried out at National Pesticide Engineering Research Center (Shenyang) in China.

The stomach toxicity LC₅₀ for HWS was >21.77 mg/L on Zebra fish (96 h), >100 µg/bee on honey bee, >1470 mg/kg•bw on quail, and >2000 mg/L on silkworm (96 h), respectively. HWS was relatively non-harmful to non-target species (Table 8.35).

8.2.9 Summary

HWS, *O,O*-dimethyl 1-(2,4-dichlorophenoxyacetoxy)-1-(furan-2-yl)methylphosphonate was an effective compound against broad-leaved weeds at as low as 50 g ai/ha in the greenhouse. It showed no phytotoxicity to monocot crops, such as wheat, maize, and rice even at as high as 1.2 kg ai/ha. Therefore, HWS could be a useful

herbicide used in monocot crop fields against dicotyledonous weeds. However several dicot crops, such as cotton, soybean, peanut, and rape are extremely sensitive to it.

Field trials in different regions in China confirmed that HWS could provide excellent weed control in the maize field against broad-leaved and sedge weeds at 300–450 g ai/ha for post-emergence application. HWS showed better weed control than that of the commercial herbicide 2-methyl-4-chlorophenoxyacetic acid (MCPA). At 450 g ai/ha, HWS was comparable to the effects of nicosulfuron (48 g ai/ha) and fluroxypyr (180 g ai/ha). HWS exhibited xylem mobility and a stronger rain stability than MCPA due to its rapid absorption and good osmosis.

HWS exhibited a potent inhibitory potency against dicot plant (pea) PDHc, which was consistent with its good selectivity against dicotyledonous weeds. HWS has a very weak inhibitory potency against PDHc from mammal (pig heart) (Chap. 7). HWS also has a low acute toxicity profile against rat and other tested animals. It is safe to non-target species, such as honey bee, quail, zebra fish, and silkworm.

References

1. He HW, Yuan JL, Peng H et al (2011) Studies of O,O-dimethyl α -(2,4-dichlorophenoxy acetoxy)ethylphosphonate (HW02) as a new herbicide. 1. Synthesis and herbicidal activity of HW02 and analogues as novel inhibitors of pyruvate dehydrogenase complex. *J Agric Food Chem* 59:4801–4813
2. Hou ZG, Zhang H, Wang Y et al (2012) Study on hydrolysis of novel herbicide O,O-dimethyl-1-(2,4-dichlorophenoxyacetoxy)ethylphosphonate in buffered solutions. *Chin J Pest Sci* 14:641–646
3. Lu ZB, Hou ZG, Wang XM et al (2010) Photodegradation of new herbicide HW-02 in organic solvents. *J Environ Sci* 22:1774–1778
4. Li XJ, Li BH, Su LJ et al (2002) Study on weed control efficacy and wheat injures of 2,4-D butylate. *J Hebei Agric Sci* 6(4):1–4
5. Zhang CX, He XG, Li HB (2005) Drift injury of 2,4-D butyl ester and remedial measures to cotton. *Hubei Plant Prot* 1:35–36
6. Cui HL, Zhang CX, Zhang HJ et al (2008) Confirmation of flixweed (*Descurainia sophia*) resistance to tribenuron in China. *Weed Sci* 56:775–779
7. Jiang RT, Zhang Y, Lu XT et al (2008) Weed resistance to tribenuron and safety to the next crop of pesticide residue. *Agrochemicals* 47:849–850
8. Cheng X, Ni HW (2013) Weed control efficacy and winter wheat safety of a novel herbicide HW02. *Crop Prot* 43:246–250
9. Lu ZB, Hou ZG, Wang XM (2009) Adsorption of novel herbicide HW-02 on soils. *Res Environ Sci* 22:851–855
10. He HW, Peng H, Wang T et al (2013) α -(Substituted-phenoxyacetoxy)- α - heterocyclylmethyl phosphonates: synthesis, herbicidal activity, inhibition on pyruvate dehydrogenase complex (PDHc), and application as postemergent herbicide against broadleaf weeds. *J Agric Food Chem* 61:2479–2488

Chapter 9

General Methodology

The synthesis, structural characterization, and biological activity of various compounds including alkylphosphonates, monosalts of alkylphosphonic acids, alkylphosphinates, monosalts of alkylphosphinic acid, cyclic phosphonates, and caged bicyclic phosphates are presented in Chaps. 2–8 respectively. The general synthetic procedure of important intermediates and the target compounds of various chemical classes are described in this chapter. Several special methods used for the synthesis of individual chemical class are discussed in corresponding sections respectively. The general information of structural characterization and the procedures of biological evaluation are also introduced.

9.1 General Synthetic Procedure

9.1.1 Chemicals, Reagents, and Solvents

Chemicals and reagents were obtained from commercial sources. Solvents were purified by standard techniques to give anhydrous solvents. Phosphorous trichloride, triethylamine, and thionyl chloride were distilled before use. Potassium fluoride, alumina, and sodium iodide were dried by oven before use. Thin layer chromatography (TLC) and column chromatography were performed on silica gel.

9.1.2 *O,O*-Dialkyl Phosphonates **M1**

O,O-Dialkyl phosphonates **M1** were prepared according to the literature (Scheme 9.1) [1, 2]. Dimethyl phosphonate was also obtained directly from commercial sources.

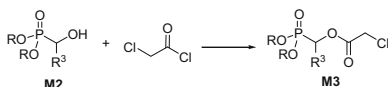
PCl_3 reacts rapidly with water to form phosphorous acid. In order to avoid the reaction of PCl_3 with the water in the air, we carried out the reaction under N_2 atmosphere. Moreover, PCl_3 reacts exothermically with alcohol to form the intermediate **M1**, so PCl_3 must be dropped slowly into the solution of alcohol.

small portions to the mixture of dialkyl phosphonates and aldehyde. The mixture was stirred for 0.5–2 h at room temperature. In the case of solid products, the mixture completely solidified after reaction. In all cases, the mixture was extracted with dichloromethane (2 × 25 mL) by shaking for 5 min. The solid catalyst was filtered off. Dichloromethane was evaporated under reduced pressure and the crude product was recrystallized from dichloromethane/petroleum ether (1/15, v/v) or purified by column chromatography on silica gel and eluted with petroleum ether/acetone (4/1, v/v) to give the corresponding pure 1-hydroxyalkylphosphonate.

The structures, physicochemical data, and yields of **M2** are listed in Table 9.2.

9.1.4 *O,O*-Dialkyl 1-(Chloroacetoxy)Alkylphosphonates **M3**

O,O-dialkyl 1-(chloroacetoxy)alkylphosphonates **M3** were prepared from corresponding *O,O*-dialkyl 1-hydroxyalkylphosphonate **M2** and chloroacetic chloride in the presence of pyridine (Scheme 9.3).

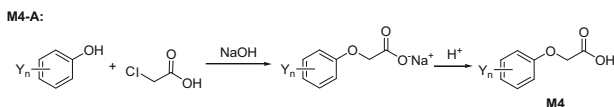


Scheme 9.3 Synthesis of *O,O*-dialkyl 1-(chloroacetoxy)alkylphosphonates **M3**

General procedure: A solution of 2-chloroacetyl chloride (0.022 mol) in dichloromethane (10 mL) was added to a stirred mixture of appropriate *O,O*-dialkyl 1-hydroxyalkylphosphonate **M2** (0.02 mol) and pyridine (0.022 mol) in dichloromethane (25 mL) at 0–5 °C. The resultant mixture was stirred for 3–5 h at room temperature. The dichloromethane layer was washed with 0.1 M hydrochloric acid, saturated sodium hydrogen carbonate solution and brine, dried and concentrated. The residue was purified by column chromatography on silica gel and eluted with petroleum ether/acetone (4/1, v/v) to give the corresponding pure *O,O*-dialkyl 1-(chloroacetoxy)alkylphosphonate **M3** as a yellowish liquid [6].

9.1.5 Substituted Phenoxyacetic Acids **M4**

Substituted phenoxyacetic acids **M4** were prepared by the condensation of corresponding substituted phenols with chloroacetic acid in the presence of alkali, such as sodium hydroxide (Scheme 9.4, method M4-A).



Scheme 9.4 Synthesis of substituted phenoxyacetic acids **M4** (Method M4-A)

Table 9.2 Structure and physicochemical data of *O,O*-dialkyl 1-hydroxyalkylphosphonates **M2**



Compound	R	R ³	Appearance	mp °C (bp °C/Pa)	Yield (%) ^a Method M2-A	Yield (%) ^b Method M2-B
M2-1	Et	H	Colorless liquid	(110/66.6)	58	ND ^c
M2-2	Et	Me	Colorless liquid	(116–119/199.9)	73	ND
M2-3	Et	Et	Colorless liquid	(110/133.3)	75	ND
M2-4	Et	<i>n</i> -Pr	Colorless liquid	(87/66.6)	78	ND
M2-5	Et	<i>i</i> -Pr	Colorless liquid	(96–97/40.0)	ND	68
M2-6	Et	Ph	Colorless crystal	82–83 ^c	60	98
M2-7	Et	4-MePh	Colorless crystal	80–81	82	88
M2-8	Et	3-NO ₂ Ph	Yellowish crystal	76–77	62	80
M2-9	Et	4-MeOPh	Colorless crystal	125–126	69	72
M2-10	Et	4-FPh	Colorless crystal	46	90	97
M2-11	Et	2-ClPh	Colorless crystal	64–65	86	91
M2-12	Et	3-ClPh	Colorless crystal	55–56	83	90
M2-13	Et	4-ClPh	Colorless crystal	65–66	84	89
M2-14	Et	2,4-Cl ₂ Ph	Colorless crystal	71–72	71	75
M2-15	Et	3,4-Cl ₂ Ph	Colorless crystal	61–63	77	75
M2-16	Et	3,4-OCH ₂ OPh	Colorless crystal	51–52	75	76
M2-24	Me	Ph	Colorless crystal	99–100 ^e	85	92
M2-25	Me	4-MePh	Colorless crystal	80–81	88	89
M2-26	Me	3-NO ₂ Ph	Yellowish solid	85–86	ND	86
M2-29	Me	4-MeOPh	Colorless crystal	75–76	81	82
M2-30	Me	4-FPh	Colorless crystal	41–42	93	95
M2-31	Me	2-ClPh	Colorless crystal	76–77	80	87

(continued)

Table 9.2 (continued)

Compound	R	R ³	Appearance	mp °C (bp °C/Pa)	Yield (%) ^a Method M2-A	Yield (%) ^b Method M2-B
M2-32	Me	3-CIPh	Colorless crystal	66–67	79	92
M2-33	Me	4-CIPh	Colorless crystal	85–86	86	92
M2-35	Me	2,4-Cl ₂ Ph	Colorless crystal	118–119	71	86
M2-36	Me	3,4-Cl ₂ Ph	Colorless crystal	71–73	70	88
M2-38	Me	Thien-2-yl	Colorless crystal	71–73	81	85
M2-39	Me	Pyrid-2-yl	Yellowish liquid	ND	89	70
M2-40	Me	3,4-OCH ₂ OPh	Colorless crystal	102–103	72	72

^a Method: M2-A; Et₃N as a catalyst

^b Method: M2-B; KF/Al₂O₃ as a catalyst

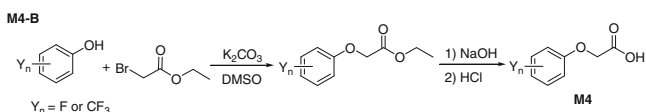
^c Reference [4]; mp 83 °C

^d Reference [5]; mp 102 °C

^e No data

Method M4-A: The typical procedure for the preparation of 2,4-dichlorophenoxyacetic acid as an example is described as follows [2]. 2,4-Dichlorophenol (40 mmol) and chloroacetic acid (42 mmol) were placed in a three-necked boiling flask and 40 % (w/w) potassium hydroxide solution was added until the solution became pH 10–11. The mixture was stirred and kept at 70–80 °C for 3 h and then neutralized with hydrochloric acid to pH 7. The precipitate was collected by filtration and the crude product was recrystallized from ethanol–water to give pure product in 90 % yield, mp 140–141 °C.

Fluoro-substituted phenoxyacetic acids and trifluoromethyl-substituted phenoxyacetic acids **M4** could be prepared by the reaction of fluoro-substituted phenols or trifluoromethyl-substituted phenols with ethyl bromoacetate in the presence of K_2CO_3 in DMSO followed by alkaline hydrolysis (Scheme 9.5, method M4-B).



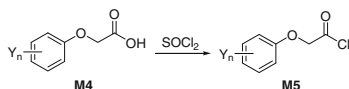
Scheme 9.5 Synthesis of substituted phenoxyacetic acids **M4** (Method M4-B)

Method M4-B: The following general procedure was used for the preparation of fluoro-substituted phenoxyacetic acids [7]. To a three-necked boiling flask, an appropriate fluoro-substituted phenol (40 mmol), ethyl bromoacetate (42 mmol), and potassium carbonate (43.5 mmol) were added in order, and then anhydrous DMSO (150 mL) was added. The mixture was stirred for 5 h at 70–80 °C, and poured into ice water. The precipitate was collected by filtration and dissolved in acetone (20 mL). To the solution was added sodium hydroxide solution (2 M, 30 mL) and the mixture was stirred for 2 h at room temperature. The solution was acidified with hydrochloric acid solution (2 M, 30 mL) and the precipitate was recrystallized to give the corresponding pure fluoro-substituted phenoxyacetic acid. A series of **M4** could be obtained by this way in the yields of 70–93 %.

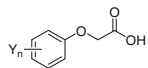
The structures, physicochemical data, and yields of **M4** are listed in Table 9.3.

9.1.6 Substituted Phenoxyacetyl Chlorides **M5**

Substituted phenoxyacetyl chlorides **M5** were converted from the corresponding substituted phenoxyacetic acids **M4** under the treatment of thionyl chloride (Scheme 9.6).



Scheme 9.6 Synthesis of substituted phenoxyacetyl chlorides **M5**

Table 9.3 Structure and physicochemical data of substituted phenoxyacetic acids **M4**

Compound	Y _n	Appearance	mp (°C)	Yield (%)	Method
M4-1	H	Colorless crystal	99–100	89	M4-A
M4-2	3-Me	Colorless crystal	102–103	86	M4-A
M4-3	4-Me	Colorless crystal	138–139	86	M4-A
M4-4	2-NO ₂	Yellow solid	186–188	58	M4-A
M4-5	4-NO ₂	Yellow solid	186–188	75	M4-A
M4-6	4-Cl	Colorless crystal	155–157	88	M4-A
M4-7	4-Br	ND ^a	153–154	ND	M4-A
M4-8	2,3-Me ₂	Colorless crystal	179–181	84	M4-A
M4-9	2-Me,4-Cl	Colorless crystal	116–117	90	M4-A
M4-10	3-Me,4-Cl	Colorless crystal	181–183	86	M4-A
M4-11	2-Cl,5-Me	Colorless crystal	136–137	79	M4-A
M4-12	2,3-Cl ₂	Colorless crystal	171–173	91	M4-A
M4-13	2,4-Cl ₂	Colorless crystal	140–141	90	M4-A
M4-14	2,6-Cl ₂	Colorless crystal	138–139	71	M4-A
M4-17	3-CF ₃	Colorless crystal	97–98	73	M4-B
M4-18	4-CF ₃	Colorless crystal	182–183	93	M4-B
M4-19	2-F	Colorless crystal	140–141	91	M4-B
M4-20	3-F	Colorless crystal	116–117	88	M4-B
M4-21	4-F	Colorless crystal	104–105	89	M4-B
M4-22	2,4-F ₂	Colorless crystal	126–128	93	M4-B
M4-23	3,5-F ₂	Colorless crystal	159–160	77	M4-B
M4-25	2-Cl,4-F	Colorless crystal	122–123	93	M4-B
M4-26	3-Cl,4-F	Colorless crystal	106–107	88	M4-B
M4-27	2-NO ₂ ,4-CF ₃	Colorless crystal	169–171	73	M4-B

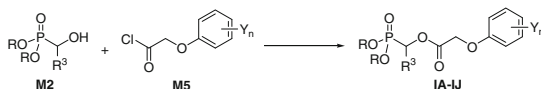
^a No data

General procedure: An appropriate substituted phenoxyacetic acid (0.1 mol) and thionyl chloride (50 mL) were refluxed for 2–4 h at 70 °C and then the unreacted thionyl chloride was removed under reduced pressure (50–52 °C/1.5 h/11.3 kPa) to give the residue as a yellow liquid. A series of **M5** could be obtained by this way in 85–96 % yields which could be used for the next reaction without purification [8, 9].

Thionyl chloride was used as both the reagent and solvent. Thionyl chloride and substituted phenoxyacetyl chloride are corrosive.

9.1.7 *O,O*-Dialkyl 1-(Substituted Phenoxyacetoxy) Alkylphosphonates **IA–IJ**

O,O-Dialkyl 1-(substituted phenoxyacetoxy)alkylphosphonates **IA–IJ** could be synthesized by the condensation of 1-hydroxyalkylphosphonates **M2** with substituted phenoxyacetyl chlorides **M5** in the presence of pyridine as a base (Scheme 9.7).



Scheme 9.7 Synthesis of *O,O*-dialkyl 1-(substituted phenoxyacetoxy)alkylphosphonates **IA–IJ**

General procedure: A solution of the appropriate substituted phenoxyacetyl chloride **M5** (0.022 mol) in trichloromethane (10 mL) was added to a stirred mixture of *O,O*-dialkyl 1-hydroxyalkylphosphonate **M2** (0.02 mol) and pyridine (0.022 mol) in trichloromethane (25 mL) at 10–25 °C. The resultant mixture was stirred for 3–5 h at room temperature, and then for 1–2 h at 40–42 °C. The trichloromethane layer was washed with 0.1 M hydrochloric acid, saturated sodium hydrogen carbonate solution and brine, dried and concentrated. The residue was purified by column chromatography on silica gel and eluted with petroleum ether/acetone (2/1, v/v) to give the corresponding pure title compound. The title compounds **IA–IJ** as a yellow liquid or colorless crystal could be obtained by this procedure [8–17].

The structures, physicochemical data, and yields of **IA–IJ** are listed in Tables 9.4, 9.5, 9.6, 9.7, 9.8, 9.9, 9.10, 9.11 and 9.12, respectively.

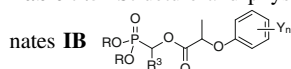
Table 9.4 Structure and physicochemical data of 1-(substituted phenoxyacetoxy)alkylphosphonates **IA**

Compound	R ³	Y _n	Appearance	n _D ²⁰ or mp (°C)	Yield (%) ^a
IA-1	H	4-Cl	Yellowish liquid	1.4931	75
IA-2	H	2,4-Cl ₂	Yellowish liquid	1.5100	77
IA-3	Me	4-Cl	Yellowish liquid	1.4912	70
IA-4	Me	2,4-Cl ₂	Yellowish liquid	1.5180	71
IA-5	CCl ₃	2-Me	White solid	37–38	68
IA-6	CCl ₃	4-Cl	White solid	41–42	75
IA-7	Et	4-Cl	Yellowish liquid	1.4902	68
IA-8	Et	2,4-Cl ₂	Yellowish liquid	1.5011	69
IA-9	<i>n</i> -Pr	4-Cl	Yellowish liquid	1.4919	64

(continued)

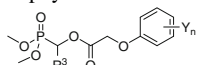
Table 9.4 (continued)

Compound	R ³	Y _n	Appearance	n _D ²⁰ or mp (°C)	Yield (%) ^a
IA-10	<i>n</i> -Pr	2,4-Cl ₂	Yellowish liquid	1.4982	65
IA-11	Ph	3-CF ₃	Colorless crystal	92–93	76
IA-12	Ph	2-Cl	Yellowish liquid	1.5103	62
IA-13	Ph	2,4-Cl ₂	Yellowish liquid	1.5398	64
IA-15	3-NO ₂ Ph	3-CF ₃	Yellowish solid	87–88	79
IA-16	4-MeOPh	3-CF ₃	Yellowish liquid	1.5069	57
IA-17	4-FPh	3-CF ₃	Yellowish liquid	1.4945	58
IA-18	2-ClPh	2,4-Cl ₂	Yellowish solid	69–70	55
IA-19	3-ClPh	3-CF ₃	Yellowish solid	36–37	64
IA-20	4-ClPh	3-CF ₃	Yellowish liquid	1.5121	63
IA-22	2,4-Cl ₂ Ph	3-CF ₃	Yellow liquid	1.5139	53
IA-23	3,4-Cl ₂ Ph	3-CF ₃	Yellow liquid	1.5159	79
IA-24	3,4-OCH ₂ OPh	3-CF ₃	Yellowish liquid	1.5102	80

^a Yields refer to purified compounds**Table 9.5** Structure and physicochemical data of 1-(substituted phenoxyacetoxy)alkylphosphonates **IB**

Compound	R	R ³	Y _n	Appearance	n _D ²⁰	Yield (%) ^a
IB-1	Me	Me	2-F	Yellow liquid	1.4795	66
IB-2	Me	Me	2-Cl,4-F	Yellow liquid	1.4879	55
IB-3	Me	Me	2,4-Cl ₂	Yellowish liquid	1.5050	65
IB-4	Me	Pr	2,4-Cl ₂	Yellowish liquid	1.4896	61
IB-5	Me	CCl ₃	2-F	Yellow liquid	1.5050	60
IB-6	Me	CCl ₃	2-Cl,4-F	Yellowish liquid	1.5072	20
IB-7	Me	Ph	2,4-Cl ₂	Yellowish liquid	1.5355	58
IB-8	Me	4-MePh	2-F	Yellow liquid	1.5215	70
IB-9	Me	4-MePh	2-Cl,4-F	Yellow liquid	1.5251	70
IB-10	Me	4-FPh	2-F	Yellowish liquid	1.5087	61
IB-11	Me	4-FPh	2-Cl,4-F	Yellow liquid	1.5180	49
IB-12	Et	Me	2,4-Cl ₂	Yellowish liquid	1.4849	64
IB-13	Et	Ph	2,4-Cl ₂	Yellowish liquid	1.5328	55
IB-14	Pr	Me	2,4-Cl ₂	Yellowish liquid	1.4728	51
IB-16	Pr	2-ClPh	2,4-Cl ₂	Yellowish liquid	1.5355	63

^a Yields refer to purified compounds

Table 9.6 Structure and physicochemical data of *O,O*-dimethyl 1-(substituted phenoxyacetoxy)alkylphosphonates **IC** 

Compound	R ³	Y _n	Appearance	n _D ²⁰ or mp (°C)	Yield (%) ^a
IC-1	H	2,4-Cl ₂	Yellowish liquid	1.5448	76
IC-2	Me	H	Yellowish liquid	1.4979	79
IC-3	Me	3-Me	Yellow liquid	1.5039	82
IC-4	Me	4-Me	Yellow liquid	1.4985	90
IC-5	Me	3-CF ₃	Yellowish liquid	1.4686	61
IC-6	Me	4-CF ₃	Yellow liquid	1.4609	69
IC-7	Me	2-F	Colorless crystal	62–63	59
IC-8	Me	3-F	Yellow liquid	1.4800	63
IC-9	Me	4-F	Yellow liquid	1.4831	67
IC-10	Me	4-Cl	Yellowish liquid	1.5049	89
IC-11	Me	4-Br	Yellow liquid	1.4920	84
IC-12	Me	2,3-Me ₂	Yellow liquid	1.5020	85
IC-13	Me	2-Me,4-Cl	Colorless liquid	1.5050	69
IC-14	Me	3-Me,4-Cl	Colorless liquid	1.5030	68
IC-15	Me	2-Cl,5-Me	Colorless liquid	1.5142	77
IC-16	Me	2,4-F ₂	Colorless crystal	38–40	68
IC-17	Me	3,5-F ₂	Yellow liquid	1.4721	57
IC-19	Me	2-Cl,4-F	Colorless crystal	118–120	86
IC-20	Me	3-Cl,4-F	Yellow liquid	1.4894	82
IC-21	Me	2,3-Cl ₂	Colorless liquid	1.5131	82
IC-22	Me	2,4-Cl ₂	Yellowish liquid	1.5172	92
IC-23	Me	2,6-Cl ₂	Yellowish liquid	1.5065	77
IC-24	Me	2,4-Br ₂	Yellow liquid	1.5032	84
IC-25	Me	2-NO ₂ ,4-Cl	Yellow liquid	1.5173	84
IC-26	Et	3-CF ₃	Yellowish liquid	1.4856	83.6
IC-27	Et	2,4-Cl ₂	Colorless crystal	58–60	68
IC-28	Et	2-NO ₂ ,4-CF ₃	Yellow liquid	1.5094	82
IC-29	<i>n</i> -Pr	3-CF ₃	Yellowish liquid	1.4630	83
IC-31	<i>n</i> -Pr	4-NO ₂	Light red solid	33–34	66
IC-32	<i>n</i> -Pr	2,4-Cl ₂	Yellow liquid	1.4859	66
IC-33	<i>n</i> -Pr	2-NO ₂ ,4-CF ₃	Yellow liquid	1.5036	74
IC-34	<i>n</i> -Bu	2,4-Cl ₂	Colorless crystal	53–55	61

^a Yields refer to purified compounds

Table 9.7 Structure and physicochemical data of *O,O*-dimethyl 1-(substituted phenoxyacetoxy)-2,2,2-trichloroethylphosphonates **ID**

Compound	Y _n	Appearance	n _D ²⁰ or mp (°C)	Yield (%) ^a
ID-1	4-CF ₃	Yellow liquid	1.4850	67
ID-2	3-F	Yellow liquid	1.5082	61
ID-3	4-F	Yellowish liquid	1.5097	63
ID-4	4-Cl	Yellowish liquid	1.5231	83
ID-5	2-Me,4-Cl	Colorless crystal	80–81	76
ID-6	3-Me,4-Cl	Yellowish liquid	1.5290	73
ID-7	2-Cl,5-Me	Brown liquid	1.5181	81
ID-8	2,4-F ₂	Colorless crystal	68–69	65
ID-9	3,5-F ₂	Yellow liquid	1.4892	60
ID-10	2-Cl,4-F	Colorless crystal	104–106	73
ID-11	3-Cl,4-F	Yellow liquid	1.5152	80
ID-12	2,3-Cl ₂	Yellow liquid	1.5392	80
ID-13	2,4-Cl ₂	Colorless crystal	77–78	62
ID-14	2,6-Cl ₂	Yellow liquid	1.5280	80

^a Yields refer to purified compounds**Table 9.8** Structure and physicochemical data of *O,O*-dimethyl 1-(substituted phenoxyacetoxy)benzylphosphonates **IE**

Compound	Y _n	Appearance	n _D ²⁰ or mp (°C)	Yield (%) ^a
IE-1	H	White solid	63–64	79
IE-2	3-Me	Yellow liquid	1.5273	88
IE-3	4-Me	White solid	80–81	84
IE-4	3-CF ₃	Yellowish liquid	1.5219	75
IE-5	4-CF ₃	Colorless crystal	104–105	76
IE-6	2-NO ₂	Yellowish solid	157–158	61
IE-8	2-F	Colorless crystal	66–68	64
IE-9	3-F	Yellow solid	48–50	66
IE-10	4-F	Yellow solid	131–132	71
IE-11	4-Cl	Colorless crystal	95–97	76
IE-13	2,3-Me ₂	Yellow liquid	1.5270	84
IE-14	2-Me,4-Cl	Yellowish liquid	1.5203	76
IE-15	3-Me,4-Cl	Colorless crystal	90–91	70
IE-16	2-Cl,5-Me	Colorless crystal	99–100	74
IE-17	2,4-F ₂	Colorless crystal	64–65	73
IE-18	2-F,4-Cl	Yellow solid	47–49	65

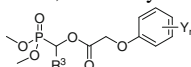
(continued)

Table 9.8 (continued)

Compound	Y _n	Appearance	n _D ²⁰ or mp (°C)	Yield (%) ^a
IE-19	2-Cl,4-F	Colorless crystal	86–87	69
IE-20	3-Cl,4-F	Colorless crystal	74–75	80
IE-21	2,3-Cl ₂	Colorless crystal	81–82	76
IE-22	2,4-Cl ₂	Yellow liquid	1.5069	59
IE-23	2,6-Cl ₂	Yellowish liquid	1.5145	74
IE-24	2–NO ₂ ,4–CF ₃	Yellowish solid	134–135	73

^a Yields refer to purified compounds

Table 9.9 Structure and physicochemical data of *O,O*-dimethyl 1-(substituted phenoxyacetoxy)-1-(substituted phenyl)methylphosphonates **IF**

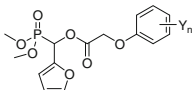


Compound	R ³	Y _n	Appearance	n _D ²⁰ or mp (°C)	Yield (%) ^a
IF-1	4-MePh	3-CF ₃	Colorless crystal	67–68	82
IF-5	4-MePh	2-Me,4-Cl	Yellow solid	45–46	63
IF-7	4-MePh	2-F,4-Cl	Yellow solid	61–63	68
IF-8	4-MePh	2-Cl,4-F	Yellow solid	61–63	68
IF-9	4-MePh	2,4-Cl ₂	Yellow liquid	1.5429	59
IF-10	2-HOPh	4-Cl	Yellow liquid	1.4955	78
IF-11	2-HOPh	2-Cl,4-F	Yellow liquid	1.4885	55
IF-12	4-MeOPh	3-CF ₃	Yellowish solid	48–49	67
IF-16	4-MeOPh	2-Me,4-Cl	Yellow solid	51–52	68
IF-18	4-MeOPh	2-F, 4-Cl	Yellow solid	65–66	65
IF-19	4-MeOPh	2-Cl,4-F	Yellow solid	69–70	68
IF-20	4-MeOPh	2,4-Cl ₂	Brown liquid	1.5517	57
IF-21	4-FPh	3-CF ₃	Yellowish solid	69–70	79
IF-22	4-FPh	2,4-Cl ₂	White solid	143–144	78
IF-23	2-ClPh	3-CF ₃	Colorless crystal	61–63	67
IF-24	2-ClPh	2,4-Cl ₂	Colorless crystal	60–62	57
IF-25	3-ClPh	3-CF ₃	Yellowish liquid	1.5138	70
IF-26	3-ClPh	2,4-Cl ₂	White solid	116–117	74
IF-27	4-ClPh	3-CF ₃	Yellowish solid	68–69	70
IF-28	4-ClPh	2-Me,4-Cl	Colorless crystal	67–68	63
IF-29	4-ClPh	2-F,4-Cl	Yellow solid	66.2–67.8	64
IF-30	4-ClPh	2-Cl,4-F	Colorless crystal	67–68	63
IF-31	4-ClPh	2,4-Cl ₂	Colorless crystal	50–51	64
IF-32	3-BrPh	2,4-Cl ₂	Yellow liquid	1.4529	53
IF-33	2,3-Cl ₂ Ph	2,4-Cl ₂	White solid	166–167	75
IF-35	2,4-Cl ₂ Ph	3-CF ₃	Yellowish liquid	1.5221	64
IF-36	2,4-Cl ₂ Ph	2,4-Cl ₂	White solid	140–142	69
IF-38	3,4-Cl ₂ Ph	3-CF ₃	Yellowish liquid	1.5320	73

(continued)

Table 9.9 (continued)

Compound	R ³	Y _n	Appearance	n _D ²⁰ or mp (°C)	Yield (%) ^a
IF-39	3,4-Cl ₂ Ph	2,4-Cl ₂	White solid	126–127	64
IF-40	3,4-OCH ₂ OPh	3-CF ₃	Colorless crystal	70–71	60
IF-41	3,4-OCH ₂ OPh	2,4-Cl ₂	White solid	120–120.5	78
IF-43	3-NO ₂ Ph	3-CF ₃	Yellow liquid	1.5233	71
IF-44	3-NO ₂ Ph	4-CF ₃	Yellowish liquid	1.4985	74
IF-45	3-NO ₂ Ph	2-NO ₂	Yellowish solid	86–87	61
IF-46	3-NO ₂ Ph	4-NO ₂	Colorless crystal	93–94	62
IF-47	3-NO ₂ Ph	2-F	Colorless crystal	83–84	73
IF-48	3-NO ₂ Ph	3-F	Yellow solid	83–84	62
IF-49	3-NO ₂ Ph	4-F	Yellowish liquid	1.5255	59.5
IF-50	3-NO ₂ Ph	4-Cl	Yellowish solid	80–83	80
IF-51	3-NO ₂ Ph	2-Me,4-Cl	Yellowish solid	132–133	61
IF-52	3-NO ₂ Ph	3-Me,4-Cl	Colorless crystal	72–73	71
IF-53	3-NO ₂ Ph	2-Cl,5-Me	Yellowish solid	109–110	69
IF-54	3-NO ₂ Ph	2,4-F ₂	Yellowish liquid	1.6010	75
IF-55	3-NO ₂ Ph	2-Cl,4-F	Colorless crystal	111–112	70
IF-56	3-NO ₂ Ph	3-Cl,4-F	Yellow solid	74–75	75
IF-57	3-NO ₂ Ph	2,3-Cl ₂	Colorless crystal	112–113	68
IF-58	3-NO ₂ Ph	2,4-Cl ₂	Yellowish solid	108–109	52
IF-59	3-NO ₂ Ph	2,6-Cl ₂	Colorless crystal	86–87	75
IF-60	3-NO ₂ Ph	2-NO ₂ ,4-CF ₃	Yellowish solid	107–108	70
IF-61	4-NO ₂ Ph	2-NO ₂	Yellow solid	162–163	55
IF-63	4-NO ₂ Ph	2,4-Cl ₂	Red brown solid	96–97	54

^a Yields refer to purified compounds**Table 9.10** Structure and physicochemical data of *O,O*-dimethyl 1-(substituted phenoxyacetoxy)-1-(fur-2-yl)methylphosphonates **IG**

Compound	Y _n	Appearance	n _D ²⁰ or mp (°C)	Yield (%) ^a
IG-1	H	White solid	70–71	81
IG-2	3-Me	White solid	52–53	82
IG-3	4-Me	White solid	56–57	85
IG-4	3-CF ₃	Yellowish solid	78–79	68
IG-5	4-CF ₃	Yellow oil	1.5182	67
IG-6	2-F	Yellowish solid	56–58	66
IG-7	3-F	Yellowish oil	1.5238	70
IG-8	4-F	White solid	69–71	65
IG-9	2-Cl	Yellow solid	51–52	66
IG-10	4-Cl	White solid	107–108	76

(continued)

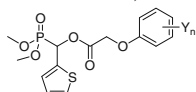
Table 9.10 (continued)

Compound	Y _n	Appearance	n _D ²⁰ or mp (°C)	Yield (%) ^a
IG-11	4-Br	Yellow solid	54–55	68
IG-12	4-CN	Yellow solid	57–59	64
IG-13	2,3-Me ₂	White solid	57–58	85
IG-14	2-Me,4-Cl	Yellow oil	1.5016	79
IG-15	3-Me,4-Cl	White solid	47–48	78
IG-16	2-Cl,5-Me	White solid	97–98	74
IG-17	2,4-F ₂	Yellowish solid	180–181	68
IG-18	2-F,4-Cl	Yellow oil	1.4387	70
IG-19	2-Cl,4-F	Yellow oil	1.5385	77
IG-20	2,3-Cl ₂	Yellowish solid	81–82	62
IG-21	2,4-Cl ₂	Yellowish solid	62–63	87
IG-22	2,6-Cl ₂	Yellowish solid	92–93	60
IG-23	2,4,5-Cl ₃	Yellow solid	57–59	69

^a Yields refer to purified compounds

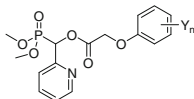
Table 9.11 Structure and physicochemical data of *O,O*-dimethyl 1-(substituted phenoxyacetoxy)-

1-(thien-2-yl)methylphosphonates **IH**



Compound	Y _n	Appearance	mp (°C)	Yield (%) ^a
IH-1	3-CF ₃	Yellowish solid	74–75	72
IH-2	4-CF ₃	Yellow solid	54–56	76
IH-3	2-F	White solid	73–74	72
IH-4	3-F	Yellowish solid	76–77	70
IH-5	4-F	White solid	55–56	74
IH-6	2-Cl	Yellow solid	54–56	66
IH-7	4-Cl	White solid	94–95	85
IH-8	4-Br	Yellow solid	53–54	70
IH-9	4-CN	Yellow solid	53–54	74
IH-10	2,3-Me ₂	Yellow solid	55–56	71
IH-11	2-Me,4-Cl	Yellowish solid	80–81	86
IH-12	3-Me,4-Cl	Yellowish solid	74–75	88
IH-13	2-Cl,5-Me	Yellowish solid	90–91	86
IH-14	2,4-F ₂	Yellowish solid	60–61	68
IH-15	2-F,4-Cl	Yellow solid	50–51	67
IH-16	2-Cl,4-F	Yellowish solid	68–70	78
IH-17	2,3-Cl ₂	Yellowish solid	108–110	72
IH-18	2,4-Cl ₂	White solid	92–93	91
IH-19	2,6-Cl ₂	White solid	78–79	74
IH-20	2,4,5-Cl ₃	Yellow solid	56–57	69

^a Yields refer to purified compounds

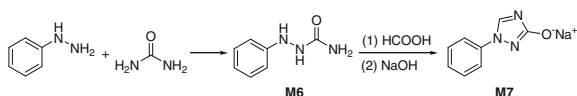
Table 9.12 Structure and physicochemical data of *O,O*-dimethyl 1-(substituted phenoxyacetoxy)-1-(pyrid-2-yl)methylphosphonates **IJ**

Compound	Y _n	Appearance	n _D ²⁰ or mp (°C)	Yield (%) ^a
IJ-1	3-CF ₃	White solid	79–80	71
IJ-2	4-CF ₃	White solid	73–74	68
IJ-3	2-F	Yellowish liquid	1.5062	63
IJ-4	3-F	Yellowish solid	79–80	66
IJ-5	4-F	Yellowish solid	68–70	67
IJ-6	4-Cl	White solid	124–125	76
IJ-7	2-Me,4-Cl	White solid	75–77	77
IJ-8	3-Me,4-Cl	White solid	83–85	74
IJ-9	2-Cl,5-Me	White solid	76–77	78
IJ-10	2,4-F ₂	Yellowish liquid	1.5183	67
IJ-11	2-Cl,4-F	White solid	124–126	74
IJ-12	2,3-Cl ₂	White solid	115–116	66
IJ-13	2,4-Cl ₂	White solid	105–106	88
IJ-14	2,6-Cl ₂	White solid	125–126	68

^a Yields refer to purified compounds

9.1.8 Phenylhydrazinecarboxamide **M6** and Sodium Triazol-3-olate **M7**

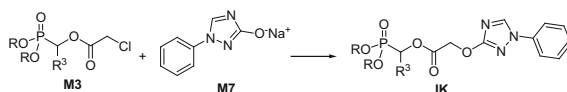
Phenylhydrazinecarboxamide **M6** and sodium triazol-3-olate **M7** were prepared according to the literature (Scheme 9.8) [18].

**Scheme 9.8** Synthesis of phenylhydrazinecarboxamide **M6** and sodium triazol-3-olate **M7**

To a stirred mixture of phenyl hydrazine (1 mol) and urea (1 mol) in dimethyl benzene (500 mL), concentrated hydrochloric acid was added. The mixture was stirred at 135 °C for 2.5 h with a water separator to remove water. When the mixture was cooled to 90 °C, 85 % formic acid (2.5 mol) followed by concentrated sulfuric acid (0.25 mol) were added. The mixture was kept at 90 °C for 6 h and then the mixture was cooled. The solid was collected by filtration and washed by water, and dried at 100 °C in vacuo to give phenylhydrazide **M6** as a white solid (mp 280–283 °C) in yield of 83 %. The hydrazide **M6** (0.5 mol) was dissolved in 0.6 M NaOH solution and stirred for 1–2 h. The mixture was filtered and the solid product was dried at 100 °C in vacuo to give the sodium salt of 1-phenyl-3-hydroxy-1,2,4-triazole **M7** [19].

9.1.9 (1-Phenyl-1,2,4-Triazol-3-yloxyacetoxy) Alkylphosphonates **IK**

(1-Phenyl-1,2,4-triazol-3-yloxyacetoxy)alkylphosphonates **IK** could be synthesized by the reaction of 1-(chloroacetoxy)alkylphosphonates **M3** with the sodium salt of 1-phenyl-3-hydroxy-1,2,4-triazole **M7** (Scheme 9.9).

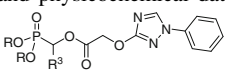


Scheme 9.9 Synthesis of (1-phenyl-1,2,4-triazol-3-yloxyacetoxy)alkylphosphonates **IK**

General procedure: To a stirred solution of the appropriate *O,O*-dialkyl 1-(chloroacetoxy)alkylphosphonates **M3** (0.01 mol) in 50 mL of dry acetonitrile, sodium salt of 1-phenyl-3-hydroxy-1,2,4-triazole **M7** (0.01 mol) and tetrabutylammonium bromide (0.4 mmol) were added at room temperature. The mixture was stirred at 40–50 °C for 4–5 h. The solid was filtered off and the filtrate was concentrated under reduced pressure. The residue was purified by column chromatography on silica gel and eluted with petroleum ether/acetone (2/1, *v/v*) to give the corresponding pure **IK** as yellow crystals or a sticky yellow liquid. A series of **IK** could be obtained by this procedure in yields of 66–85 % [19].

The structures, physicochemical data, and yields of **IK** are listed in Table 9.13.

Table 9.13 Structure and physicochemical data of 1-((1-phenyl-1,2,4-triazole-3-yl)oxyacetoxy) alkylphosphonates **IK**

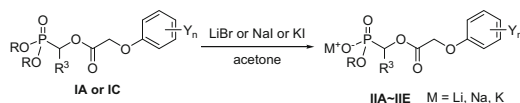


Compound	R	R ³	Appearance	n _D ²⁰ or mp (°C)	Yield (%) ^a	Corresponding M2 for preparation of IK
IK-1	Me	Ph	Yellow crystal	132–133	85	M2-24
IK-2	Me	3-NO ₂ Ph	Yellow crystal	166–167	66	M2-26
IK-3	Me	2-ClPh	Yellow crystal	68–69	69	M2-31
IK-4	Me	4-ClPh	Yellow crystal	87–88	73	M2-33
IK-5	Me	Et	Yellow liquid	1.4728	76	M2-19
IK-6	Me	<i>n</i> -Pr	Yellow liquid	1.4535	72	M2-21
IK-7	Et	Ph	Yellow liquid	1.5082	80	M2-6

^a Yields refer to purified compounds

9.1.10 Alkali Metal Salts of *O*-Alkyl Alkylphosphonic Acids IIA–IIE

Alkali metal *O*-alkyl 1-(substituted phenoxyacetoxy)alkylphosphonates **IIA–IIE** could be easily synthesized by the reaction of *O,O*-dialkyl 1-(substituted phenoxyacetoxy)alkylphosphonates **IA** or **IC** with lithium bromide, sodium iodide, and potassium iodide in refluxing acetone (Scheme 9.10).



Scheme 9.10 Synthesis of alkali metal salts of *O*-alkyl alkylphosphonic acids **IIA–IIE**

General procedure: A solution of the appropriate *O,O*-dialkyl 1-(substituted phenoxyacetoxy)alkylphosphonate (0.02 mol) and oven-dried lithium bromide, sodium iodide, or potassium iodide (0.02 mol) in dry acetone (molecular sieve 4 Å, 40 mL) was refluxed with stirring under nitrogen for 2–22 h. The solution was evaporated under reduced pressure. The residual solid was recrystallized from dichloromethane to afford corresponding pure product as a white solid or crystal. **IIA–IIE** could be obtained by this procedure in 43–88 % yields and these alkali metal salts were easily deliquescent in air [20–23].

The structures, physicochemical data, and yields of **IIA–IIE** are listed in Tables 9.14, 9.15, 9.16, 9.17 and 9.18, respectively.

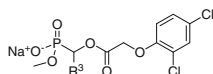
Table 9.14 Structure and physicochemical data of lithium *O*-alkyl 1-(2,4-dichlorophenoxyacetoxy)alkylphosphonates **IIA**

Compound	R	R ³	Appearance	mp (°C)	Yield (%) ^a
IIA-1	Me	H	White solid	138–139	78
IIA-2	Me	Me	White solid	103–105	74
IIA-3	Me	<i>n</i> -Pr	White solid	121–123	64
IIA-4	Me	Ph	White solid	244–245	79
IIA-5	Me	4-MePh	White solid	131–133	79
IIA-6	Me	3-NO ₂ Ph	White solid	227–228	80
IIA-7	Me	4-NO ₂ Ph	White solid	199–201	75
IIA-8	Me	4-FPh	White solid	237–238	76
IIA-9	Me	2-ClPh	White solid	176–178	71
IIA-10	Me	3-ClPh	White solid	169–171	65
IIA-11	Me	2,4-Cl ₂ Ph	White solid	259–262	81
IIA-12	Me	Fur-2-yl	White solid	132–134	82

(continued)

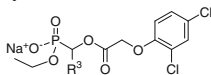
Table 9.14 (continued)

Compound	R	R ³	Appearance	mp (°C)	Yield (%) ^a
IIA-13	Me	Thien-2-yl	White solid	171–172	93
IIA-14	Me	Pyrid-2-yl	White solid	227–228	95
IIA-15	Me	3,4-OCH ₂ OPh	White solid	238–239	77
IIA-16	Et	4-FPh	White solid	164–166	72

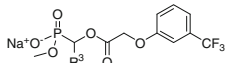
^a Yields refer to purified compounds**Table 9.15** Structure and physicochemical data of sodium *O*-methyl 1-(2,4-dichlorophenoxy-acetoxy)alkylphosphonates **IIB**

Compound	R ³	Appearance	mp (°C)	Yield (%) ^a
IIB-1	H	White solid	183–184	81
IIB-2	Me	White solid	46–47	84
IIB-3	Et	Yellowish solid	81–83	64
IIB-4	<i>n</i> -Pr	Yellowish solid	110–112	51
IIB-5	<i>i</i> -Pr	Yellowish solid	248–250	74
IIB-6	<i>n</i> -Bu	Yellowish solid	163–165	52
IIB-7	CCl ₃	White solid	121–123	65
IIB-8	Ph	White solid	164–165	78
IIB-9	4-MePh	White solid	108 (dec.)	78
IIB-10	3-NO ₂ Ph	Yellowish solid	98–99	85
IIB-11	4-NO ₂ Ph	Yellowish solid	242–243	78
IIB-12	4-MeOPh	Yellowish solid	109–110	88
IIB-13	4-FPh	White solid	143–144	79
IIB-14	2-ClPh	Yellowish solid	130–131	70
IIB-15	3-ClPh	White solid	155–157	68
IIB-16	4-ClPh	Yellowish solid	141–142	71
IIB-17	2,3-Cl ₂ Ph	Yellowish solid	278 (dec.) ^b	76
IIB-18	2,4-Cl ₂ Ph	Yellowish solid	151–152	82
IIB-19	3,4-Cl ₂ Ph	Yellowish solid	143–145	73
IIB-20	Fur-2-yl	White solid	99–100	95
IIB-21	Thien-2-yl	White solid	216	74
IIB-22	Pyrid-2-yl	White solid	238	88
IIB-23	Pyrid-3-yl	White solid	223	71
IIB-24	Pyrid-4-yl	White solid	156–158	79
IIB-25	3,4-OCH ₂ OPh	Yellowish solid	83–85	86

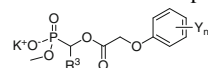
^a Yields refer to purified compounds^b dec.: decomposed

Table 9.16 Structure and physicochemical data of sodium *O*-ethyl 1-(2,4-dichlorophenoxyacetoxy)alkylphosphonates **IIC**

Compound	R ³	Appearance	mp (°C)	Yield (%) ^a
IIC-1	Ph	White solid	>261	72
IIC-2	4-MePh	White solid	>265	79
IIC-3	3-NO ₂ Ph	White solid	190–192	71
IIC-4	4-MeOPh	White solid	>278	68
IIC-5	4-FPh	White solid	>278	68
IIC-6	2,4-Cl ₂ Ph	White solid	>280	66
IIC-7	Pyrid-2-yl	White solid	>231	79
IIC-8	3,4-OCH ₂ OPh	White solid	195–197	72

^a Yields refer to purified compounds**Table 9.17** Structure and physicochemical data of sodium *O*-methyl 1-(3-trifluoromethylphenoxyacetoxy)alkylphosphonates **IID**

Compound	R ³	Appearance	mp (°C)	Yield (%) ^a
IID-1	Me	White solid	128–129	56
IID-2	Et	White solid	69–70	48
IID-3	4-MePh	White solid	69–70	63
IID-4	3-NO ₂ Ph	White solid	124–125	60
IID-5	4-NO ₂ Ph	White solid	206–208	62
IID-6	2-ClPh	White solid	68–69	68
IID-7	4-ClPh	White solid	138–140	62
IID-8	Pyrid-2-yl	White solid	>223	84
IID-9	3,4-OCH ₂ OPh	White solid	119–121	67

^a Yields refer to purified compounds**Table 9.18** Structure and physicochemical data of potassium *O*-methyl 1-(substituted phenoxyacetoxy)alkylphosphonates **IIE**

Compound	R ³	Y _n	Appearance	mp (°C)	Yield (%) ^a
IIE-1	H	2,4-Cl ₂	White solid	162–164	61
IIE-2	Me	2,4-Cl ₂	White solid	168–170	54
IIE-3	Et	2,4-Cl ₂	White solid	171–173	52
IIE-4	<i>n</i> -Pr	2,4-Cl ₂	White solid	146–149	43
IIE-5	Ph	3-CF ₃	White solid	>286	64
IIE-6	Ph	2,4-Cl ₂	White solid	138–140	67

(continued)

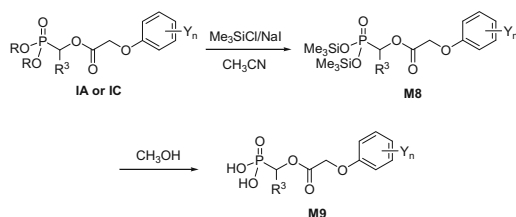
Table 9.18 (continued)

Compound	R ³	Y _n	Appearance	mp (°C)	Yield (%) ^a
IIE-7	4-MePh	2,4-Cl ₂	White solid	138–140	75
IIE-8	3-NO ₂ Ph	2,4-Cl ₂	White solid	220–223	68
IIE-9	4-MeOPh	2,4-Cl ₂	White solid	216–218	65
IIE-10	2-ClPh	2,4-Cl ₂	White solid	157–159	56
IIE-11	4-ClPh	2,4-Cl ₂	White solid	248–251	59
IIE-12	2,3-Cl ₂ Ph	2,4-Cl ₂	White solid	199–200	64
IIE-13	2,4-Cl ₂ Ph	3-CF ₃	White solid	>288	69
IIE-14	2,4-Cl ₂ Ph	2,4-Cl ₂	White solid	68–70	78
IIE-15	Fur-2-yl	2,4-Cl ₂	White solid	139–140	61
IIE-16	Thien-2-yl	2,4-Cl ₂	White solid	102–104	52
IIE-17	Pyrid-2-yl	3-CF ₃	White solid	100–102	64
IIE-18	Pyrid-2-yl	2,4-Cl ₂	White solid	>235	78
IIE-19	3,4-OCH ₂ OPh	2,4-Cl ₂	White solid	152–153	78

^a Yields refer to purified compounds

9.1.11 *O,O*-Bis(trimethylsilyl) Alkylphosphonates **M8** and Alkylphosphonic Acids **M9**

Alkylphosphonic acids **M9** were prepared from corresponding alkylphosphonates **IA** or **IC** which were treated by iodotrimethylsilane to form bis(trimethylsilyl)alkylphosphonates **M8**, and followed by the treatment with methanol (Scheme 9.11).



Scheme 9.11 Synthesis of *O,O*-bis(trimethylsilyl) alkylphosphonates **M8** and alkylphosphonic acids **M9**

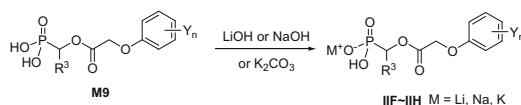
General procedure: Under a nitrogen atmosphere and in a dark environment, to a solution of appropriate *O,O*-dimethyl 1-(substituted phenoxyacetoxy)alkylphosphonate **IA** or **IC** (10 mmol) and sodium iodide (22 mmol) in acetonitrile (25 mL), trimethylchlorosilane (22 mmol) was added at 30 °C. Then the reaction mixture was stirred at 30 °C for 1–2 h. The mixture was filtered and washed with petroleum ether. The solution was evaporated at reduced pressure to afford corresponding

O,O-bis(trimethylsilyl) 1-substituted phenoxyacetoxy)alkylphosphonate **M8**, which could be used for the next reaction without purification.

A solution of appropriate *O,O*-bis(trimethylsilyl) 1-substituted phenoxyacetoxy)alkylphosphonate **M8** (10 mmol) in anhydrous methanol (25 mL), was stirred for 2–3 h at 30 °C, which was monitored by TLC. The solution was evaporated at reduced pressure. The residue was purified by column chromatography on silica gel and eluted with petroleum ether/*n*-propanol (*v/v*, 1/3) to give the corresponding pure 1-(substituted phenoxyacetoxy)alkylphosphonic acid **M9** as a colorless liquid. A series of **M9** could be obtained by this procedure in 80–90 % yields [24, 25].

9.1.12 Alkali Metal Salts of Alkylphosphonic Acids **IIF–IIH**

Alkali metal salts of alkylphosphonic acids **IIF–IIH** could be obtained from corresponding alkylphosphonic acids **M9** by the treatment with an equimolar inorganic base, such as hydrated lithium hydroxide, sodium hydroxide or potassium carbonate (Scheme 9.12).



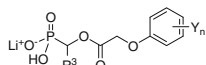
Scheme 9.12 Synthesis of alkali metal salts of alkylphosphonic acids **IIF–IIH**

General procedure: To a solution of 1-(substituted phenoxyacetoxy)alkylphosphonic acid **M9** (5.5 mmol) in methanol (20 mL) was added lithium hydroxide monohydrate (5 mmol), the mixture was stirred at room temperature 1–2 h and monitored by TLC analysis. The solution was evaporated at reduced pressure. The residual solid was recrystallized from acetonitrile to afford the pure product as a white solid, i.e., monolithium salt of 1-(substituted phenoxyacetoxy)alkylphosphonic acid **IIF**.

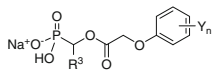
Monosodium salts of 1-(substituted phenoxyacetoxy)alkylphosphonic acids **IIG** and monopotassium salts of 1-(substituted phenoxyacetoxy)alkylphosphonic acids **IIH** could be synthesized using sodium hydroxide and potassium carbonate as bases, respectively, with the similar methods mentioned above [23, 24].

The structures, physicochemical data, and yields of **IIF–IIH** are listed in Tables 9.19, 9.20 and 9.21, respectively.

Table 9.19 Structure and physicochemical data of monolithium salts of 1-(substituted phenoxy-

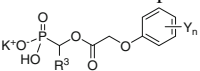
acetoxy)alkylphosphonic acids **IIF** 

Compound	R ³	Y _n	Appearance	mp (°C)	Yield (%) ^a
IIF-1	Me	2,4-Cl ₂	White solid	~ 224 (dec.) ^b	84
IIF-2	Et	2,4-Cl ₂	White solid	~ 228 (dec.)	77
IIF-3	<i>n</i> -Pr	2,4-Cl ₂	White solid	219–221	82
IIF-4	<i>i</i> -Pr	2,4-Cl ₂	White solid	207–209	83
IIF-5	<i>n</i> -Bu	2,4-Cl ₂	White solid	~ 190 (dec.)	84
IIF-6	Ph	2,4-Cl ₂	White solid	~ 150 (dec.)	85
IIF-7	Thien-2-yl	2,4-Cl ₂	White solid	>250	47
IIF-8	Me	2-Me,4-Cl	White solid	~ 176 (dec.)	90
IIF-9	Et	2-Me,4-Cl	White solid	~ 205 (dec.)	87
IIF-10	<i>n</i> -Pr	2-Me,4-Cl	White solid	~ 238 (dec.)	82
IIF-11	<i>i</i> -Pr	2-Me,4-Cl	White solid	203–205	92
IIF-12	<i>n</i> -Bu	2-Me,4-Cl	White solid	~ 210 (dec.)	89
IIF-13	Ph	2-Me,4-Cl	White solid	~ 153 (dec.)	85

^a Yields refer to purified compounds^b dec.: decomposed**Table 9.20** Structure and physicochemical data of monosodium salts of 1-(substituted phenoxyacetoxy)alkylphosphonic acids **IIG** 

Compound	R ³	Y _n	Appearance	mp (°C)	Yield (%) ^a
IIG-1	Me	2,4-Cl ₂	White solid	~ 150 (dec.) ^b	88
IIG-2	Et	2,4-Cl ₂	White solid	~ 133 (dec.)	92
IIG-3	<i>n</i> -Pr	2,4-Cl ₂	White solid	~ 173 (dec.)	86
IIG-4	<i>i</i> -Pr	2,4-Cl ₂	White solid	~ 157 (dec.)	84
IIG-5	<i>n</i> -Bu	2,4-Cl ₂	White solid	~ 179 (dec.)	91
IIG-6	Ph	2,4-Cl ₂	White solid	~ 145 (dec.)	87
IIG-7	Thien-2-yl	2,4-Cl ₂	White solid	~ 135 (dec.)	56
IIG-8	Me	2-Me,4-Cl	White solid	~ 140 (dec.)	89
IIG-9	Et	2-Me,4-Cl	White solid	~ 130 (dec.)	89
IIG-10	<i>n</i> -Pr	2-Me,4-Cl	White solid	~ 185 (dec.)	83
IIG-11	<i>i</i> -Pr	2-Me,4-Cl	White solid	~ 110 (dec.)	93
IIG-12	<i>n</i> -Bu	2-Me,4-Cl	White solid	~ 175 (dec.)	87
IIG-13	Ph	2-Me,4-Cl	White solid	~ 108 (dec.)	83

^a Yields refer to purified compounds^b dec.: decomposed

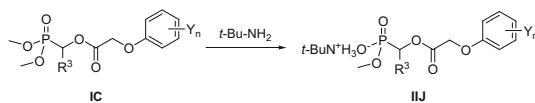
Table 9.21 Structure and physicochemical data of monopotassium salts of 1-(substituted phenoxyacetoxy)alkylphosphonic acids **IIIH**


Compound	R ³	Y _n	Appearance	mp (°C)	Yield (%) ^a
IIIH-1	Me	2,4-Cl ₂	White solid	~ 140 (dec.) ^b	93
IIIH-2	Et	2,4-Cl ₂	White solid	~ 100 (dec.)	93
IIIH-3	<i>n</i> -Pr	2,4-Cl ₂	White solid	~ 104 (dec.)	84
IIIH-4	<i>i</i> -Pr	2,4-Cl ₂	White solid	~ 108 (dec.)	87
IIIH-5	<i>n</i> -Bu	2,4-Cl ₂	White solid	~ 140 (dec.)	84
IIIH-6	Ph	2,4-Cl ₂	White solid	~ 142 (dec.)	86
IIIH-7	Thien-2-yl	2,4-Cl ₂	White solid	~ 145 (dec.)	65
IIIH-8	Me	2-Me,4-Cl	White solid	~ 155 (dec.)	91
IIIH-9	Et	2-Me,4-Cl	White solid	~ 105 (dec.)	85
IIIH-10	<i>n</i> -Pr	2-Me,4-Cl	White solid	~ 114 (dec.)	81
IIIH-11	<i>i</i> -Pr	2-Me,4-Cl	White solid	~ 103 (dec.)	95
IIIH-12	<i>n</i> -Bu	2-Me,4-Cl	White solid	~ 120 (dec.)	90
IIIH-13	Ph	2-Me,4-Cl	White solid	~ 110 (dec.)	82

^a Yields refer to purified compounds^b dec.: decomposed

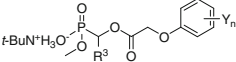
9.1.13 *t*-Butylamminium Salts of Alkylphosphonates **IIJ**

t-Butylamminium salts of alkylphosphonates **IIJ** could be obtained by the treatment of *O,O*-dimethyl 1-(substituted phenoxyacetoxy)alkylphosphonates **IC** with an excess of *t*-butylamine (Scheme 9.13).

**Scheme 9.13** Synthesis of *t*-butylamminium salts of alkylphosphonates **IIJ**

General procedure: An appropriate dimethyl 1-(substituted phenoxyacetoxy) alkylphosphonate (0.0025 mol) was added to 2-methylpropan-2-amine (5 mL). The resultant mixture was stirred at room temperature for 20–36 h or refluxed at 46 °C for 6–8 h. Then the excess 2-methylpropan-2-amine was removed under reduced pressure and washed with acetone to afford crude products as white solids or colorless oil. Further, recrystallization from acetonitrile or flash column chromatography on silica gel using a mixture of petroleum ether/ethanol (*v/v* 3/1) afforded corresponding **IIJ** as a white solid or colorless oil. A series of **IIJ** could be obtained by this procedure [26, 27].

The structures, physicochemical data, and yields of **IIJ** are listed in Table 9.22.

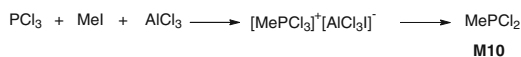
Table 9.22 Structure and physicochemical data of 2-methylpropan-2-amini-um of alkylphosphonates **IIJ**


Compound	R ³	Y _n	Appearance	mp (°C) or n _D ²⁰	Yield (%) ^a
IIJ-1	Me	Me	White solid	126–127	78
IIJ-2	Et	Me	White solid	116–118	78
IIJ-3	<i>n</i> -Pr	Me	White solid	105–107	80
IIJ-4	<i>i</i> -Pr	Me	White solid	109–111	65
IIJ-5	<i>n</i> -Bu	Me	White solid	91–92	55
IIJ-6	Me	Cl	White solid	133–135	71
IIJ-7	Et	Cl	White solid	112–114	73
IIJ-8	<i>n</i> -Pr	Cl	White solid	122–124	74
IIJ-9	<i>i</i> -Pr	Cl	White solid	128–130	66
IIJ-10	<i>n</i> -Bu	Cl	White solid	120–122	68
IIJ-11	Me	2-Me,4-Cl	White solid	110–111	93
IIJ-12	Et	2-Me,4-Cl	White solid	130–132	89
IIJ-13	<i>n</i> -Pr	2-Me,4-Cl	White solid	135–136	92
IIJ-14	<i>i</i> -Pr	2-Me,4-Cl	White solid	129–131	90
IIJ-15	<i>n</i> -Bu	2-Me,4-Cl	White solid	104–106	88
IIJ-16	Me	2-F,4-Cl	White solid	108–110	70
IIJ-17	Et	2-F,4-Cl	White solid	115–117	63
IIJ-18	<i>n</i> -Pr	2-F,4-Cl	White solid	132–134	65
IIJ-19	<i>i</i> -Pr	2-F,4-Cl	White solid	68–70	58
IIJ-20	<i>n</i> -Bu	2-F,4-Cl	White solid	111–112	63
IIJ-21	Me	2-Cl,4-F	White solid	115–117	73
IIJ-22	Et	2-Cl,4-F	White solid	119–121	66
IIJ-23	<i>i</i> -Pr	2-Cl,4-F	White solid	108–110	67
IIJ-24	Me	2,4-Cl ₂	White solid	110–112	86
IIJ-25	Et	2,4-Cl ₂	White liquid	1.4989	95
IIJ-26	<i>n</i> -Pr	2,4-Cl ₂	White solid	122–124	90
IIJ-27	<i>i</i> -Pr	2,4-Cl ₂	White solid	104–106	91
IIJ-28	<i>n</i> -Bu	2,4-Cl ₂	White liquid	1.5028	92

^a Yields refer to purified compounds

9.1.14 Dichloro(Methyl)Phosphine **M10**

Dichloro(methyl)phosphine **M10** was prepared from phosphorus trichloride, iodomethane, and aluminum trichloride (Scheme 9.14).

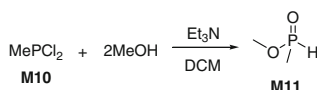


Scheme 9.14 Synthesis of dichloro(methyl)phosphine **M10**

Phosphorus trichloride (1 mol) and anhydrous aluminum chloride (1.14 mol) were added in the flask. The mixture is heated for 30 min at 60–70 °C, cooled in ice bath, and methyl iodide (1 mol) is added dropwise over 0.5 h with continuous stirring. After 1 h the complex solidifies and stirring is impossible. Then a mixture of dry potassium chloride (1.4 mol) and iron powder (60 g) were added to the solid complex. The reflux condenser was exchanged for a distillation condenser. The mixture was distilled to give 150 g of the fraction collected at 78–165 °C. Then the mixture was fractionated three times to give the pure dichloro(methyl)phosphine **M10** as a colorless liquid in 60 % yield.

9.1.15 *O*-Methyl Methylphosphinate **M11**

O-Methyl methylphosphinate **M11** was prepared from the corresponding dichloro(methyl)phosphine **M10** by reacting with methanol according to the literature (Scheme 9.15) [1, 2].

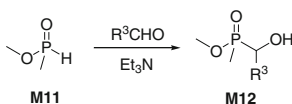


Scheme 9.15 Synthesis of *O*-methyl methyl phosphinate **M11**

In order to avoid the reaction of dichloro(methyl)phosphine **M10** with the water in the air, we carried out the reaction under N₂ atmosphere. Moreover, **M10** reacts exothermically with alcohol, so **M10** must be dropped slowly into the solution of alcohol. Be cautious! **M10** is very toxic and corrosive.

9.1.16 *O*-Methyl (1-Hydroxyalkyl)methylphosphinates **M12**

O-Methyl (1-hydroxyalkyl)methylphosphinates **M12** could be prepared by the nucleophilic addition of *O*-methyl methylphosphinates **M11** with several kinds of aldehydes (Scheme 9.16).

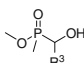


Scheme 9.16 Synthesis of *O*-Methyl (1-hydroxyalkyl)methylphosphinates **M12**

General procedure: *O*-Methyl methylphosphinate **M11** (0.02 mol) and an appropriate aldehyde (0.024 mol) were stirred at room temperature for 10 min. To this mixture cooled in an ice-water bath triethylamine (0.01 mol) was slowly added

Table 9.23 Structure and physicochemical data of *O*-Methyl (1-hydroxyalkyl)methylphosphinates **M12**

M12



Compound	R	Appearance	n_D^{20} or mp (°C)	Yield (%) ^a
M12-1	Me	Yellow liquid	1.4539	53
M12-2	Et	Yellow liquid	1.4551	56
M12-3	<i>n</i> -Pr	Yellow liquid	1.4598	57
M12-4	Ph	Colorless crystal	62–64	67
M12-5	4-MePh	Colorless crystal	50–52	60
M12-6	3-NO ₂ Ph	Yellow solid	79–81	69
M12-7	4-MeOPh	Yellow solid	46–48	62
M12-8	2-ClPh	Colorless crystal	66–67	67

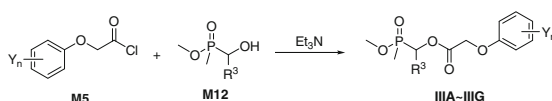
^a Yields refer to purified compounds

as a catalyst. The mixture was stirred for 4–6 h at room temperature. The components with a lower boiling point were evaporated in vacuo to give the crude compound **M12**. Purification by column chromatography on silica gel and elution with petroleum ether/acetone (4/1, *v/v*) gave the corresponding pure **M12**. A series of **M12** could be obtained by this procedure in 53–69 % yields [7, 28, 29].

The structures, physicochemical data, and yields of **M12** are listed in Table 9.23.

9.1.17 Alkylphosphinates **IIIA–IIIG**

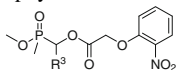
The preparation of *O*-methyl [1-(substituted phenoxyacetoxy)alkyl]methylphosphinates **IIIA–IIIG** involved the condensation of substituted phenoxyacetyl chlorides **M5** and *O*-methyl (1-hydroxyalkyl) methylphosphinates **M12** (Scheme 9.17).

**Scheme 9.17** Synthesis of alkylphosphinates **IIA–IIIG**

General procedure: A solution of an appropriate substituted phenoxyacetic chloride **M5** (0.022 mol) in trichloromethane (10 mL) was added to a stirred mixture of corresponding *O*-methyl (1-hydroxyalkyl)methylphosphinate (0.02 mol) and triethylamine (0.022 mol) in trichloromethane (25 mL) at 2–4 °C. The resultant mixture was stirred at ambient temperature for 3–5 h, and then at 40 °C for 1–2 h. The mixture was washed with 0.1 M hydrochloric acid, saturated sodium hydrogen carbonate solution and brine, dried and evaporated. The residue was purified by column chromatography on silica gel and eluted with petroleum ether/acetone (6/1, *v/v*) to give the corresponding title compound as a yellow liquid or white solid. **IIIA–IIIG** could be obtained by this procedure in 58–89 % yields [7, 28–30].

The structures, physicochemical data, and yields of **III A–III G** are listed in Tables 9.24, 9.25, 9.26, 9.27, 9.28, 9.29 and 9.30, respectively.

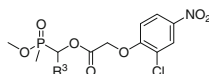
Table 9.24 Structure and physicochemical data of *O*-methyl [1-(2-nitrophenoxyacetoxy)alkyl]methylphosphinates **III A**



Compound	R ³	Appearance	n _D ²⁰	Yield (%) ^a
III A-1	Me	Brown liquid	1.5145	71
III A-2	Et	Yellow liquid	1.5096	80
III A-3	<i>n</i> -Pr	Brown liquid	1.5122	68
III A-4	Ph	Brown liquid	1.5388	77
III A-5	4-MePh	Brown liquid	1.5372	80
III A-6	3-NO ₂ Ph	Brown liquid	1.5403	80
III A-7	4-MeOPh	Yellow liquid	1.5349	81
III A-8	2-ClPh	Brown liquid	1.5538	84
III A-9	4-ClPh	Yellow liquid	1.5400	81

^a Yields refer to purified compounds

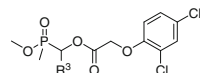
Table 9.25 Structure and physicochemical data of *O*-methyl [1-(2-chloro-4-nitrophenoxyacetoxy)alkyl]methylphosphinates **III B**



Compound	R ³	Appearance	n _D ²⁰ or mp (°C)	Yield (%) ^a
III B-1	Me	Yellow liquid	1.5300	55
III B-2	Et	Yellow liquid	1.5240	55
III B-3	3-NO ₂ Ph	Yellow solid	60–62	57
III B-4	4-ClPh	Yellow solid	68–70	67

^a Yields refer to purified compounds

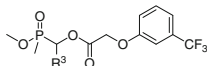
Table 9.26 Structure and physicochemical data of *O*-methyl [1-(2,4-dichlorophenoxyacetoxy)alkyl]methylphosphinates **III C**



Compound	R ³	Appearance	n _D ²⁰ or mp (°C)	Yield (%) ^a
III C-1	Me	Yellowish liquid	1.5138	51
III C-2	Et	Colorless liquid	1.5121	43
III C-3	<i>n</i> -Pr	White solid	97–99	84
III C-4	Ph	Colorless liquid	1.5418	78
III C-5	4-MePh	Colorless liquid	1.5430	76
III C-6	3-NO ₂ Ph	Yellowish liquid	1.5550	82
III C-7	4-MeOPh	Colorless liquid	1.5371	82
III C-8	2-ClPh	Colorless liquid	1.5452	80
III C-9	4-ClPh	Colorless liquid	1.5428	85

^a Yields refer to purified compounds

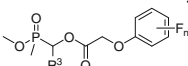
Table 9.27 Structure and physicochemical data of *O*-methyl [1-(3-trifluoromethylphenoxyacetoxymethyl)methylphosphinates **III D**



Compound	R ³	Appearance	n _D ²⁰ or mp (°C)	Yield (%) ^a
III D-1	Me	Yellow liquid	1.4670	69
III D-2	Et	Yellow liquid	1.4676	52
III D-3	3-NO ₂ Ph	Brown liquid	1.5130	48
III D-4	2-ClPh	White solid	88–90	72
III D-5	4-ClPh	Brown liquid	1.5119	34
III D-6	2,4-Cl ₂ Ph	White solid	92–93	81

^a Yields refer to purified compounds

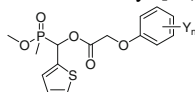
Table 9.28 Structure and physicochemical data of *O*-methyl [1-(fluorine-substituted phenoxyacetoxymethyl)methylphosphinates **III E**



Compound	R ³	F _n	Appearance	n _D ²⁰ or mp (°C)	Yield (%) ^a
III E-1	Ph	2-F	White solid	106–107	78
III E-2	Ph	4-F	White solid	88–89	66
III E-3	4-MePh	2-F	Yellow liquid	1.5239	57
III E-4	4-MePh	2,4-F ₂	Yellow liquid	1.5088	56
III E-5	4-FPh	2-F	White solid	89–91	54
III E-6	2-ClPh	2-F	Yellow liquid	1.5482	82
III E-7	2-ClPh	4-F	White solid	94–95	86
III E-8	2-ClPh	2,4-F ₂	Yellow liquid	1.5392	86
III E-9	2,4-Cl ₂ Ph	2-F	White solid	106–107	82
III E-10	2,4-Cl ₂ Ph	4-F	White solid	91–92	77

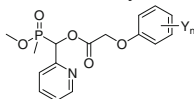
^a Yields refer to purified compounds

Table 9.29 Structure and physicochemical data of *O*-methyl [1-(substituted phenoxyacetoxymethyl)-1-(thien-2-yl)methyl]methylphosphinates **III F**



Compound	Y _n	Appearance	n _D ²⁰	Yield (%) ^a
III F-1	3-CF ₃	Yellowish liquid	1.5421	62
III F-2	2-F	Yellowish liquid	1.5240	66
III F-3	4-Cl	Yellowish liquid	1.4868	70
III F-4	3-Me,4-Cl	Yellowish liquid	1.5423	72
III F-5	2-Cl,5-Me	Yellowish liquid	1.5382	75
III F-6	2,3-Cl ₂	Yellowish liquid	1.5241	61
III F-7	2,4-Cl ₂	Yellowish liquid	1.5121	64
III F-8	2,6-Cl ₂	Yellowish liquid	1.5186	63

^a Yields refer to purified compounds

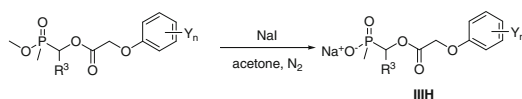
Table 9.30 Structure and physicochemical data of *O*-methyl [1-(substituted phenoxyacetoxy)-1-(pyrid-2-yl)methyl]methylphosphinates **III G**

Compound	Y _n	Appearance	n _D ²⁰	Yield (%) ^a
III G-1	3-CF ₃	Yellowish liquid	1.5248	62
III G-2	2-F	Yellowish liquid	1.5216	68
III G-3	4-Cl	Yellowish liquid	1.5198	76
III G-4	3-Me,4-Cl	Yellowish liquid	1.5275	70
III G-5	2-Cl,5-Me	Yellowish liquid	1.5131	70
III G-6	2,3-Cl ₂	Yellowish liquid	1.5162	61
III G-7	2,4-Cl ₂	Yellowish liquid	1.5412	73
III G-8	2,6-Cl ₂	Yellowish liquid	1.5026	64

^a Yields refer to purified compounds

9.1.18 Sodium Salts of Alkylphosphinic Acids **III H**

Sodium [1-(substituted phenoxyacetoxy)alkyl]methylphosphinates **III H** could be prepared from the corresponding *O*-methyl [1-(substituted phenoxyacetoxy)alkyl]methyl phosphinates reacted with sodium iodide (Scheme 9.18).

**Scheme 9.18** Synthesis of sodium salts of alkylphosphinic acids **III H**

General procedure: A solution of appropriate *O*-methyl [1-(substituted phenoxyacetoxy)alkyl]methyl phosphinate (0.02 mol) and oven-dried sodium iodide (0.02 mol) in dry acetone (molecular sieve 4 Å, 40 mL) was refluxed with stirring under nitrogen for 4–6 h. The solution was evaporated under reduced pressure. The residual solid was recrystallized from methanol to afford corresponding pure product **III H**. **III H** could be obtained by this procedure as white solids or crystals in 63–82 % yields and these sodium salts were easily deliquescent in air [31].

The structures, physicochemical data, and yields of **III H** are listed in Table 9.31.

Table 9.31 Structure and physicochemical data of sodium [1-(substituted phenoxyacetoxy)alkyl]

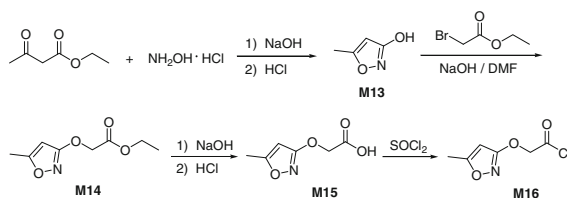
Compound	R ³	Y _n	Appearance	mp (°C)	Yield (%) ^a
IIIH-1	Ph	3-CF ₃	White solid	163–165	72
IIIH-2	Ph	2,4-Cl ₂	White solid	162–164	78
IIIH-3	2-ClPh	2,4-Cl ₂	White solid	>280	63
IIIH-4	2,4-Cl ₂ Ph	3-CF ₃	White solid	>282 (dec.) ^b	76
IIIH-5	2,4-Cl ₂ Ph	2,4-Cl ₂	White solid	225–227	82
IIIH-6	Pyrid-2-yl	2-F	White solid	>276 (dec.)	68
IIIH-7	Pyrid-2-yl	4-Cl	White solid	234–235	66
IIIH-8	Pyrid-2-yl	2-Cl,5-Me	White solid	>265 (dec.)	70
IIIH-9	Pyrid-2-yl	2,4-Cl ₂	White solid	229–230	76
IIIH-10	Pyrid-2-yl	2,6-Cl ₂	White solid	>257 (dec.)	64

^a Yields refer to purified compounds

^b dec.: decomposed

9.1.19 3-Hydroxy-5-Methylisoxazole Derivatives **M13–M16**

5-Methylisoxazol-3-yloxyacetyl chloride **M16** was prepared according to the literatures [32] by four steps using ethyl acetoacetate and hydroxylamine hydrochloride as starting materials (Scheme 9.19).

**Scheme 9.19** Synthesis of 3-hydroxy-5-methylisoxazole derivatives **M13–M16**

Ethyl acetoacetate (0.2 mol) was added to a solution of hydroxylamine hydrochloride (0.1 mol) in 100 mL of 2 N sodium hydroxide and reacted at -26 to -30 °C for 1 h, and the reaction mixture was kept in pH 10. The mixture was treated by adding an excess of concentrated hydrochloric acid at once at -20 °C and left overnight at room temperature. The product was extracted with dichloromethane several times. Dichloromethane was evaporated under reduced pressure and the residual solid product was recrystallized from cyclohexane/trichloromethane (4/1, *v/v*) to give 3-hydroxy-5-methyl-isoxazole **M13** in 70 % yield as colorless crystal, mp 86–87 °C.

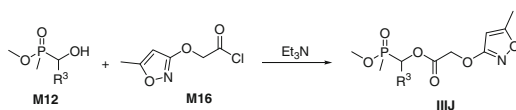
To a solution of **M13** (4.75 g) dissolved in 80 mL of DMF, NaOH (1.92 g) was added with stirring at room temperature for 3 h. Ethyl bromoacetate (8.02 g) was added dropwise to the mixture at 0–5 °C and then the mixture was left overnight at room temperature. After 320 mL of water were added to the mixture, the product was extracted with 640 mL of diethyl ether. The ether solution was washed with water and brine separately, dried and evaporated to give pure ethyl (5-methylisoxazol-3-yl)oxyacetate **M14**.

The intermediate **M14** was converted to (5-methylisoxazol-3-yl)oxyacetic acid **M15** by treating with 5 % sodium hydroxide (98 mL) at room temperature for 4 h, followed by acidification to pH 2 with 10 % HCl solution. The product was extracted with trichloromethane and the solvent was evaporated in vacuo. The residue was recrystallized from benzene to give pure **M15** as yellowish crystal in 48 % overall yield, mp 122–124 °C.

A mixture of **M15** (0.1 mol) and thionyl chloride (50 mL) was refluxed at 60 °C for 4 h and then unreacted thionyl chloride was removed under reduced pressure to give (5-methylisoxazol-3-yl)oxyacetyl chloride **M16** as a yellow liquid in 80 % yield. Crude **M16** was used for next reaction without purification.

9.1.20 *O*-Methyl [1-(5-Methylisoxazol-3-yloxyacetoxy)Alkyl] Methylphosphinates **IIIJ**

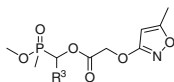
O-Methyl methyl 1-(5-methylisoxazol-3-yloxyacetoxy)alkylphosphinates **IIIJ** could be conveniently synthesized by the reaction of *O*-methyl methyl 1-hydroxyalkylphosphinate **M12** and 5-methylisoxazol-3-yloxyacetyl chloride **M16** (Scheme 9.20).



Scheme 9.20 Synthesis of *O*-methyl [1-(5-methylisoxazol-3-yloxyacetoxy)alkyl]methylphosphinates **IIIJ**

General procedure: To a stirred solution of appropriate *O*-methyl (1-hydroxyalkyl)methylphosphinates **M12** (0.005 mol) and triethylamine (0.0072 mol) in 5 mL of trichloromethane, (5-methylisoxazol-3-yl)oxyacetyl chloride **M16** (0.006 mol) in 5 mL of trichloromethane was added dropwise below 0 °C. The mixture was stirred at room temperature for 4–6 h. Normal workup and purification by column chromatography on silica gel and elution with petroleum ether/acetone (5/1, v/v) gave the corresponding pure title compound. **IIIJ-1–IIIJ-8** could be obtained by this procedure in 23–55 % yields [32].

Table 9.32 Structure and physicochemical data of *O*-Methyl methyl 1-((5-methyl isoxazol-3-yl)oxyacetoxymethyl)alkylphosphinates **IIIJ**



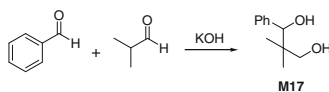
Compound	R ³	Appearance	n _D ²⁰	Yield (%) ^a
IIIJ-1	Me	Yellowish liquid	1.4682	39
IIIJ-2	Et	Brown liquid	1.4691	53
IIIJ-3	<i>n</i> -Pr	Brown liquid	1.4669	33
IIIJ-4	Ph	Brown liquid	1.5120	59
IIIJ-5	4-MePh	Brown liquid	1.5005	53
IIIJ-6	3-NO ₂ Ph	Yellow liquid	1.5192	39
IIIJ-7	4-MeOPh	Brown liquid	1.5102	65
IIIJ-8	2-ClPh	Brown liquid	1.5129	55

^a Yields refer to purified compounds

The structures, physicochemical data, and yields of **IIIJ-1–IIIJ-8** are listed in Table 9.32.

9.1.21 1-Phenyl-2,2-Dimethyl-1,3-Propanediol **M17**

1-Phenyl-2,2-dimethyl-1,3-propanediol **M17** could be obtained by the known aldol-Cannizzaro reaction, in which 2 equiv. of isobutyraldehyde, 1 equiv. of benzaldehyde, and 1 equiv. of KOH in ethanol were used to give the product **M17** (Scheme 9.21).

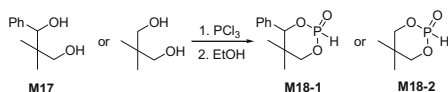


Scheme 9.21 Synthesis of 1-phenyl-2,2-dimethyl-1,3-propanediol **M17**

A mixture of benzaldehyde (0.1 mol) and isobutyraldehyde (0.2 mol) was added into a three-necked round-bottomed flask fitted with a condenser. An exothermic reaction started when a solution of KOH (0.1 mol) in absolute ethanol (90 mL) was added dropwise. When the temperature of the mixture had reached 50 °C, the flask was cooled by a water bath. The reaction mixture was heated at 50–60 °C for 5 h and then evaporated at aspirator vacuum. Water (100 mL) was added to the remaining residue and this mixture was filtered after it was put for 12 h. The crude product was obtained, which can be purified by crystallization from toluene. The purified product was white solid with 85 % yield, m.p. 80.2–81.0 °C.

9.1.22 Cyclic Phosponates **M18**

Cyclic phosphonates **M18** could be prepared by the reaction of 1-phenyl-2,2-dimethyl-1,3-propanediol **M17** or 2,2-dimethyl-1,3-propanediol with phosphorus trichloride and then by reacting with ethanol (Scheme 9.22).

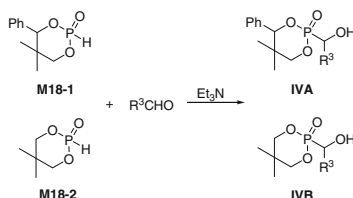


Scheme 9.22 Synthesis of cyclic phosphonates **M18**

Phosphorus trichloride (0.11 mol) was added slowly to a solution of 1-phenyl-2,2-dimethyl-1,3-propanediol **M17** or 2,2-dimethyl-1,3-propanediol (0.1 mol) in 1,2-dichloroethane (40 mL) and cooled by an ice-water bath. After stirring at 5–10 °C for 2 h, a solution of absolute ethanol in 1,2-dichloroethane (30 mL) was added dropwise and the reaction solution was heated under reflux for 1.5 h then evaporated. The residue was purified by crystallization from toluene to give 5,5-dimethyl-4-phenyl-1,3,2-dioxaphosphorinan-2-one **M18-1** or 5,5-dimethyl-1,3,2-dioxaphosphorinan-2-one **M18-2** with 90 % yield, as a white solid, m.p.: **M18-1**: 170–172 °C, **M18-2**: 56–58 °C.

9.1.23 Cyclic 1-Hydroxyalkylphosponates **IVA** and **IVB**

Cyclic 1-hydroxyalkylphosponates **IVA** and **IVB** could be synthesized by hydrophosphonylation of various aldehydes with cyclic phosphonates **M18** in the presence of triethylamine as a basic catalyst (Scheme 9.23).



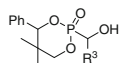
Scheme 9.23 Synthesis of cyclic 1-hydroxyalkylphosponates **IVA** and **IVB**

General procedure: A solution of cyclic phosphonate **M18-1** or **M18-2** (0.01 mol) and appropriate aldehyde (0.01 mol) in dichloromethane (10 mL) was added into a three-necked round-bottomed flask. Triethylamine (0.01 mol) was added dropwise to stirred mixture while cooling with an ice-water bath. The

reaction solution was stirred at room temperature for 2–3 h, and then evaporated. The residue was crystallized by absolute ethanol to give cyclic 1-hydroxyalkylphosphonate as a white solid. **IVA** or **IVB** could be obtained by this procedure in 49–90 % yields.

The structures, physicochemical data and yields of **IVA** and **IVB** are listed in Table 9.33 and 9.34.

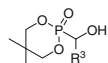
Table 9.33 Structure and physicochemical data of cyclic 1-hydroxyalkylphosphonates **IVA**



Compound	R ³	Appearance	mp (°C)	Yield (%) ^a
IVA-1	Ph	White solid	206–208	84
IVA-2	2-ClPh	White solid	220–221	81
IVA-3	4-ClPh	White solid	226–227	83
IVA-4	2,4-Cl ₂ Ph	White solid	225–226	75
IVA-5	3,4-Cl ₂ Ph	White solid	228–229	87
IVA-6	4-MeOPh	White solid	194–197	77
IVA-7	4-MePh	White solid	222–223	87
IVA-8	4-NO ₂ Ph	White solid	>280	89
IVA-9	Pyrid-2-yl	White solid	149–150	78
IVA-10	Pyrid-3-yl	White solid	169–171	74
IVA-11	Pyrid-4-yl	White solid	187–189	73
IVA-12	<i>n</i> -Bu	White solid	189–190	80

^a Yields refer to purified compounds

Table 9.34 Structure and physicochemical data of cyclic 1-hydroxyalkylphosphonates **IVB**

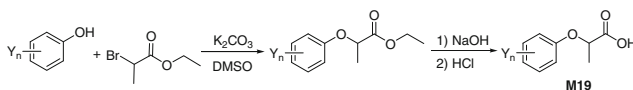


Compound	R ³	Appearance	mp (°C)	Yield (%) ^a
IVB-1	Ph	White solid	154–157	78
IVB-2	2-ClPh	White solid	174–175	85
IVB-3	4-ClPh	White solid	176–177	90
IVB-4	2,4-Cl ₂ Ph	White solid	210–212	89
IVB-5	3,4-Cl ₂ Ph	White solid	217–218	85
IVB-6	4-MeOPh	White solid	188–189	78
IVB-7	4-MePh	White solid	170–172	80
IVB-8	4-NO ₂ Ph	White solid	196–197	86
IVB-9	Pyrid-2-yl	White solid	155–156	53
IVB-10	Fur-2-yl	White solid	225–226	70
IVB-11	Me	White solid	94–96	50
IVB-12	<i>i</i> -Pr	White solid	142–144	52
IVB-13	<i>n</i> -Bu	White solid	120–122	49

^a Yields refer to purified compounds

9.1.24 Substituted Phenoxypropionic Acids M19

Substituted phenoxypropionic acids **M19** could be synthesized starting from substituted phenols and 2-bromopropionic acid ester (Scheme 9.24).

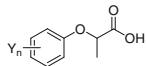


Scheme 9.24 Synthesis of substituted phenoxypropionic acids **M19**

General procedure: To a three-necked boiling flask, an appropriate substituted phenol (0.04 mol), ethyl 2-bromopropionate (0.042 mol), and potassium carbonate (5.8 g) were added by order, then DMSO (100 mL) was added as solvent. The mixture was stirred and kept at 70–80 °C for 5 h, then was treated with ice water immediately. After yellow solid was filtered off, and dissolved in acetone (20 mL), 2 mol/L NaOH were added, then stirred for another 2 h at room temperature. Then added 2 mol/L HCl, and the corresponding substituted phenoxypropionic acid **M19** was formed. The solid could be recrystallized as a white crystal. Several **M19** could be obtained by this procedure in 75–95 % yields.

The structures, physicochemical data, and yields of substituted phenoxypropionic acids **M19** are listed in Table 9.35.

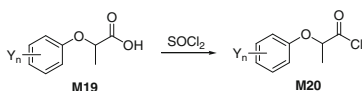
Table 9.35 Structure and physicochemical data of substituted phenoxypropionic acids **M19**



Compound	Y _n	Appearance	mp (°C)	Yield (%)
M19-1	4-Cl	White solid	111.0–113.0	75
M19-2	4-F	White solid	108.5–110.5	86
M19-3	2-Cl,4-F	White solid	79.0–81.5	90
M19-4	2-F,4-Cl	White solid	101.0–103.0	95
M19-5	2,3-Cl ₂	White solid	128.5–129.5	77
M19-6	2,4-Cl ₂	White solid	114.0–115.5	80

9.1.25 Substituted Phenoxypropionyl Chlorides M20

Substituted phenoxypropionyl chlorides **M20** could be obtained by the reaction of substituted phenoxypropionic acids **M19** and thionyl chloride (Scheme 9.25).

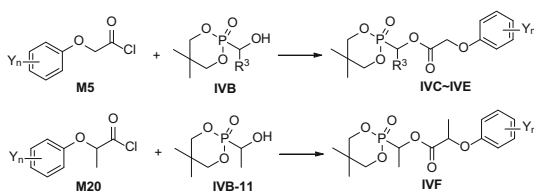


Scheme 9.25 Synthesis of substituted phenoxypropionyl chlorides **M20**

An appropriate substituted phenoxypropionic acid (0.1 mol) and thionyl chloride (50 mL) were refluxed for 2–4 h at 70 °C and then the unreacted thionyl chloride was removed under reduced pressure (50–52 °C/1.5 h/11.3 kPa) to give the corresponding substituted phenoxypropionyl chloride **M20** as a yellow liquid. Several **M20** were obtained by this procedure in 85–96 % yields, which could be used for the next reaction without purification.

9.1.26 Cyclic Alkylphosphonates **IVC–IVF**

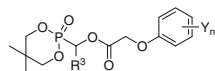
Cyclic alkylphosphonates **IVC–IVF** could be conveniently prepared by the condensation of cyclic 1-hydroxyalkylphosphonates **IVB** with substituted phenoxyacetyl chlorides **M5** or phenoxypropionyl chlorides **M20** in the presence of triethylamine as a base (Scheme 9.26).



Scheme 9.26 Synthesis of cyclic alkylphosphonates **IVC–IVF**

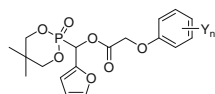
General procedure: A solution of substituted phenoxyacetyl chlorides **M5** or phenoxypropionyl chlorides **M20** (0.01 mol) in dichloromethane (15 mL) was added dropwise to the stirred mixture of appropriate 2-(hydroxy(substituted) methyl)-5,5-dimethyl-1,3,2-dioxaphosphinan-2-one **IVB** (0.01 mol) and triethylamine (0.011 mol) in dichloromethane (20 mL) under 5 °C, the reaction solution was stirred at room temperature for 2–4 h, and then at 40 °C for another 1–2 h. The resultant mixture was washed with 0.1 M hydrochloric acid solution, saturated sodium bicarbonate solution and brine separately, dried and evaporated. The residue was chromatographed on silica with ethyl acetate/petroleum ether (1/3) as eluent to give the corresponding cyclic alkylphosphonate as a white or yellowish solid. All **IVC–IVF** series could be obtained by this procedure.

The structures, physicochemical data, and yields of cyclic alkylphosphonates **IVC–IVF** are listed in Tables 9.36, 9.37, 9.38 and 9.39, respectively.

Table 9.36 Structure and physicochemical data of cyclic alkylphosphonates **IVC**

Compound	R ³	Y _n	Appearance	mp (°C) or n _D ²⁰	Yield (%) ^a
IVC-1	Ph	H	Yellow solid	80–81	80
IVC-2	Ph	2-Cl	Yellow solid	87–88	82
IVC-3	Ph	2-F	Yellow solid	70–71	77
IVC-4	Ph	3-Me	White solid	76–77	74
IVC-5	Ph	3-CF ₃	White solid	101–102	75
IVC-6	Ph	4- <i>t</i> -Bu	Yellow oil	1.5121	65
IVC-7	Ph	4-Cl	White solid	59–60	78
IVC-8	Ph	3-Me,4-Cl	Yellow solid	70–71	80
IVC-9	Ph	2,3-Me ₂	White solid	82–83	66
IVC-10	Ph	2,4,5-Cl ₃	Yellow solid	96–98	74
IVC-11	Ph	2-Me,4-Cl	White solid	98–100	79
IVC-12	Ph	2-F,4-Cl	White solid	117–119	76
IVC-13	Ph	2-Cl,4-F	White solid	110–112	77
IVC-14	Ph	2,4-F ₂	White solid	79.1–80.8	75
IVC-15	Ph	4-F	White solid	109.8–112.6	82
IVC-16	Ph	2,4-Cl ₂	White solid	149.8–151.2	67
IVC-17	2-ClPh	2,4-Cl ₂	White solid	118.0–120.3	70
IVC-18	4-ClPh	2,4-Cl ₂	White solid	120.1–120.5	71
IVC-19	2,4-Cl ₂ Ph	2,4-Cl ₂	White solid	169.8–170.1	65
IVC-20	3,4-Cl ₂ Ph	2,4-Cl ₂	White solid	107.0–108.0	72
IVC-21	4-MeOPh	2,4-Cl ₂	White solid	120.3–123.6	77
IVC-22	4-MePh	2,4-Cl ₂	White solid	106.2–108.1	87
IVC-23	4-NO ₂ Ph	2,4-Cl ₂	Yellow solid	123.9–125.5	73

^a Yields refer to purified compounds

Table 9.37 Structure and physicochemical data of cyclic alkylphosphonates **IVD**

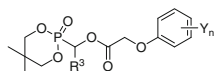
Compound	Y _n	Appearance	n _D ²⁰ or mp (°C)	Yield (%) ^a
IVD-1	H	Yellow oil	1.5169	78
IVD-2	2-Cl	Yellow oil	1.5211	82
IVD-3	2-F	Yellow oil	1.5051	75
IVD-4	3-Me	Yellow oil	1.5125	74
IVD-5	3-CF ₃	Yellow oil	1.5612	75
IVD-6	4- <i>t</i> -Bu	Yellow oil	1.4790	65
IVD-7	4-Cl	Yellow oil	1.5213	80
IVD-8	4-F	White solid	67–70	75

(continued)

Table 9.37 (continued)

Compound	Y _n	Appearance	n _D ²⁰ or mp (°C)	Yield (%) ^a
IVD-9	3-Me,4-Cl	Yellow oil	1.5213	82
IVD-10	2-Me,4-Cl	White solid	63–65	73
IVD-11	2-F,4-Cl	White solid	70–72	74
IVD-12	2-Cl,4-F	White solid	58–61	78
IVD-13	2,4-Cl ₂	White solid	110–113	72

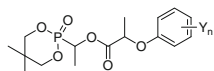
^a Yields refer to purified compounds

Table 9.38 Structure and physicochemical data of cyclic alkylphosphonates **IVE**

Compound	R ³	Y _n	Appearance	mp (°C)	Yield (%) ^a
IVE-1	Me	H	Colorless oil	ND ^b	81
IVE-2	Me	2-Cl	White solid	99–101	89
IVE-3	Me	2-F	White solid	63–65	87
IVE-4	Me	4-Cl	White solid	62–64	80
IVE-5	Me	4-F	White solid	68–69	74
IVE-6	Me	3-CF ₃	White solid	69–71	76
IVE-7	Me	2-Me,4-Cl	White solid	82–84	86
IVE-8	Me	3-Me,4-Cl	White solid	104–106	88
IVE-9	Me	2-Cl,4-F	White solid	82–84	85
IVE-10	Me	2-F,4-Cl	White solid	107–109	81
IVE-11	Me	2,4-Cl ₂	White solid	62–64	64
IVE-12	<i>i</i> -Pr	2,4-Cl ₂	White solid	120–121	86
IVE-13	<i>n</i> -Bu	2,4-Cl ₂	White solid	75–76	73

^a Yields refer to purified compounds

^b No data

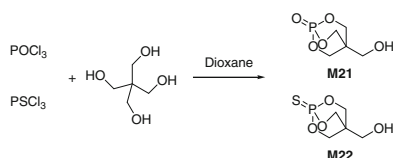
Table 9.39 Structure and physicochemical data of cyclic alkylphosphonates **IVF**

Compound	Y _n	Appearance	mp (°C)	Yield (%) ^a
IVF-1	2-Cl	White solid	91–93	80
IVF-2	4-Cl	White solid	94–96	82
IVF-3	4-F	White solid	62–64	80
IVF-4	3-CF ₃	White solid	65–67	84
IVF-5	2-Me,4-Cl	White solid	82–84	78
IVF-6	3-Me,4-Cl	White solid	66–68	87
IVF-7	2-Cl,4-F	White solid	72–74	83
IVF-8	2,4-Cl ₂	White solid	101–103	79

^a Yields refer to purified compounds

9.1.27 4-(Hydroxymethyl)-2,6,7-Trioxa-1-Phosphabicyclo[2.2.2]Octane-1-One/Thione **M21**/**M22**

4-(Hydroxymethyl)-2,6,7-trioxa-1-phosphabicyclo[2.2.2]octane-1-one/thione **M21**/**M22** could be prepared by the treatment of the pentaerythritol with 1 equiv. of phosphorus oxychloride/phosphorus thiochloride in dioxane (Scheme 9.27).

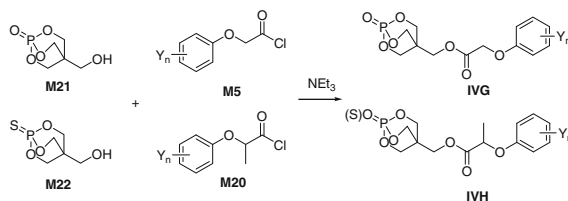


Scheme 9.27 Synthesis of 4-(hydroxymethyl)-2,6,7-trioxa-1-phosphabicyclo[2.2.2]octane-1-one/thione **M21**/**M22**

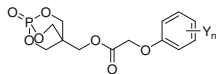
To a solution of pentaerythritol (6.8 g, 50 mmol) in 1,4-dioxane (30 mL), phosphorus oxychloride (7.8 g, 50 mmol) or phosphorus thiochloride (8.5 g, 50 mmol) was added dropwise under 90 °C. After stirring for 2 h, the reaction solution was heated under reflux for 6 h. A white solid was precipitated, filtered off, and subsequently washed with 1,4-dioxane. The crude product was recrystallized from absolute ethanol, giving 4-(hydroxymethyl)-2,6,7-trioxa-1-phosphabicyclo[2.2.2]octane-1-one **M21** in 92 % yield as a white solid, or 4-(hydroxymethyl)-2,6,7-trioxa-1-phosphabicyclo[2.2.2]octane-1-thione **M22** in 60 % yield as a white solid, m.p.: **M21**: 212.5–214.5 °C, **M22**: 160.0–163.0 °C.

9.1.28 Caged Bicyclic Phosphates **IVG** and **IVH**

Caged bicyclic phosphate **IVG** and **IVH** could be conveniently synthesized by the condensation of 4-(hydroxymethyl)-2,6,7-trioxa-1-phosphabicyclo[2.2.2]octane 1-oxide **M21** or 4-(hydroxymethyl)-2,6,7-trioxa-1-phosphabicyclo[2.2.2]octane 1-sulfide **M22** and substituted phenoxyacetyl chlorides **M5** or substituted phenoxypropionyl chlorides **M20** in the presence of triethylamine as a base (Scheme 9.28).



Scheme 9.28 Synthesis of caged bicyclic phosphate **IVG** and **IVH**

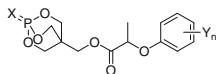
Table 9.40 Structure and physicochemical data of caged bicyclic phosphates **IVG**

Compound	Y _n	Appearance	mp (°C)	Yield (%) ^a
IVG-1	2,4-Cl ₂	White solid	164–165	78
IVG-2	2-Cl	White solid	140–142	68
IVG-3	4-Cl	White solid	182–183	67
IVG-4	2-F	White solid	148–149	73
IVG-5	3-CF ₃	White solid	137–139	69
IVG-6	4-Me	White solid	158–159	71
IVG-7	2-Me,4-Cl	White solid	143–145	71
IVG-8	3-Me,4-Cl	Yellow solid	122–123	65
IVG-9	2-Cl,4-F	Yellow solid	148–150	82
IVG-10	2-Cl,5-Me	White solid	170–173	58
IVG-11	2,3-Me ₂	White solid	183–184	54
IVG-12	4-F	White solid	139–141	82
IVG-13	3-Me	White solid	145–146	52
IVG-14	H	White solid	154–155	69
IVG-15	4- <i>t</i> -Bu	White solid	200–202	51

^a Yields refer to purified compounds

General procedure: A solution of substituted phenoxyacetyl chlorides **M5** or phenoxypropionyl chlorides **M20** (0.01 mol) in dichloromethane (15 mL) was added dropwise to the stirred mixture of a **M21** or **M22** (0.01 mol) and triethylamine (0.011 mol) in dichloromethane (20 mL) under 5 °C, the reaction solution was stirred at room temperature for 2–4 h, and then at 40 °C for another 1–2 h. The resultant mixture was washed with 0.1 M hydrochloric acid solution, saturated sodium bicarbonate solution and brine separately, dried and evaporated. The residue was chromatographed on silica with ethyl acetate/petroleum ether (1/3) as eluent to give corresponding caged bicyclic phosphate **IVG** or **IVH** as a white or yellow solid. All caged bicyclic phosphate **IVG** and **IVH** series could be obtained by this procedure.

The structures, physicochemical data and yields of caged bicyclic phosphates **IVG** and **IVH** are listed in Tables 9.40 and 9.41, respectively.

Table 9.41 Structure and physicochemical data of caged bicyclic phosphates **IVH**

Compound	X	Y _n	Appearance	mp (°C)	Yield (%) ^a
IVH-1	O	4-Cl	White solid	148–150	71
IVH-2	O	4-F	White solid	107–108	67
IVH-3	O	2,3-Cl ₂	White solid	185–188	73

(continued)

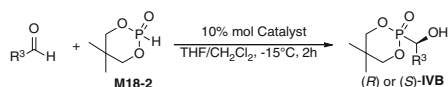
Table 9.41 (continued)

Compound	X	Y _n	Appearance	mp (°C)	Yield (%) ^a
IVH-4	O	2,4-Cl ₂	White solid	132–134	70
IVH-5	O	2-Cl,4-F	White solid	56–58	70
IVH-6	O	2-F,4-Cl	White solid	107–108	68
IVH-7	S	4-Cl	White solid	115–117	69
IVH-8	S	4-F	White solid	119–121	66
IVH-9	S	2,3-Cl ₂	White solid	102–104	69
IVH-10	S	2,4-Cl ₂	White solid	108–110	66
IVH-11	S	2-Cl,4-F	White solid	80–82	70
IVH-12	S	2-F,4-Cl	White solid	98–100	76

^a Yields refer to purified compounds

9.1.29 Optically Active Cyclic 1-Hydroxyalkylphosphonates **IVB**

Cyclic 1-hydroxyalkylphosphonates **IVB** were synthesized asymmetrically via enantioselective hydrophosphonylation of aldehydes using tridentate Schiff base **Al** (III) complexes as catalysts (Scheme 9.29).



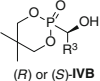
Scheme 9.29 Synthesis of optically active cyclic 1-hydroxyalkylphosphonates **IVB**

General procedure: Et₂AlBr (1 mmol) was added to a solution of ligand (**S**) or (**R**)-**L1-6** (1 mmol) in CH₂Cl₂ (4 mL) under nitrogen to form catalyst (**S**) or (**R**)-**Cat1-6**. After stirring at room temperature for 30 min, an appropriate aldehyde (10 mmol) in THF (6 mL) and silver carbonate (0.4 mmol) were added and stirred for another 30 min. Cyclic phosphonate **M18-2** (12 mmol) was added at -15 °C, and the reaction solution was stirred for 2 h. The reaction were quenched by diluted hydrochloric acid (*v/v* = 1/15). The optically active 1-hydroxyalkyl phosphonate **IVB** was afforded by column chromatography on silica gel (acetone/petroleum ether = 1/2). The enantiomeric excesses (*ee*) were determined by HPLC analysis on chiral DAICEL CHIRALPAK AS-H column at 210 or 230 nm, n-hexane/*i*-PrOH = 30/70 [33].

The structures, physicochemical data, and yields of optically active cyclic 1-hydroxyalkylphosphonates **IVB** are listed in Table 9.42.

Table 9.42 Structure and physicochemical data of optically active cyclic 1-hydroxyalkylphosphonates **IVB**

onates **IVB**



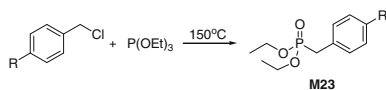
Compound	R ³	Appearance	mp (°C)	Yield (%) ^a	ee (%)	Conf ^b
(<i>R</i>)- IVB-1	Ph	White solid	154.1–155.3	81	99	<i>R</i>
(<i>S</i>)- IVB-1	Ph	White solid	154.1–155.3	82	99	<i>S</i>
(<i>R</i>)- IVB-3	4-ClPh	White solid	175.3–176.8	75	98	<i>R</i>
(<i>S</i>)- IVB-3	4-ClPh	White solid	175.3–176.8	75	99	<i>S</i>
(<i>S</i>)- IVB-4	2,4-Cl ₂ Ph	White solid	188.4–189.2	77	99	<i>S</i>
(<i>S</i>)- IVB-5	3,4-Cl ₂ Ph	White solid	189.8–191.5	76	99	<i>S</i>
(<i>S</i>)- IVB-6	4-MeOPh	White solid	186.4–187.9	79	92	<i>S</i>
(<i>R</i>)- IVB-7	4-MePh	White solid	170.3–172.1	84	99	<i>R</i>
(<i>S</i>)- IVB-7	4-MePh	White solid	170.3–172.1	84	99	<i>S</i>
(<i>S</i>)- IVB-10	Fur-2-yl	White solid	202.4–203.4	68	99	<i>S</i>
(<i>R</i>)- IVB-14	3-MePh	White solid	175.9–176.9	80	99	<i>R</i>
(<i>S</i>)- IVB-14	3-MePh	White solid	175.9–176.9	83	99	<i>S</i>
(<i>R</i>)- IVB-15	4-BrPh	White solid	189.1–191.6	81	98	<i>R</i>
(<i>S</i>)- IVB-15	4-BrPh	White solid	189.1–191.6	82	96	<i>S</i>
(<i>S</i>)- IVB-16	2,3-Cl ₂ Ph	White solid	193.1–194.5	72	99	<i>S</i>
(<i>S</i>)- IVB-17	Thien-2-yl	White solid	226.0–227.4	79	99	<i>S</i>

^a Yields refer to purified compounds

^b Generally, optical rotation of *R* form is dextrorotatory (+), but *S* form is levorotatory (–)

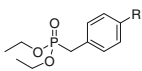
9.1.30 *O,O*-Diethyl (Substituted Benzyl)Phosphonates **M23**

O,O-Diethyl (substituted benzyl)phosphonates **M23** were prepared from substituted benzyl chlorides and triethyl phosphite via Arbuzov reaction (Scheme 9.30).

**Scheme 9.30** Synthesis of *O,O*-diethyl (substituted benzyl)phosphonates **M23**

General procedure: Triethylphosphite (20 mmol) and an appropriate substituted benzyl chloride (10 mmol) were added slowly into an oven-dried three-necked round-bottomed flask fitted with a condenser. The mixture was heated to 150 °C and maintained at this temperature, typically for 3 h until the reaction was complete as judged by TLC. The excess of triethylphosphite was removed under reduced pressure and the residue was purified by column chromatography on silica gel using ethyl acetate/petroleum ether (*v/v* = 2/1) as the eluent to give the desired *O,O*-

Table 9.43 Structure and physicochemical data of *O,O*-diethyl substituted benzylphosphonates

M23 

Compound	R	Appearance	Yield (%) ^a
M23-1	H	Colorless oil	87
M23-2	4-Me	Colorless oil	85
M23-3	4-MeO	Colorless oil	80
M23-4	4-Cl	Colorless oil	80

^a Yields refer to purified compounds

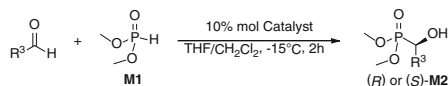
diethyl substituted benzylphosphonate **M23**. Several **M23** could be obtained by this procedure.

The structures, physicochemical data, and yields of *O,O*-diethyl substituted benzylphosphonates **M23** are listed in Table 9.43.

9.1.31 Optically Active 1-Hydroxyalkylphosphonates **M2**

9.1.31.1 Preparation via Enantioselective Hydrophosphonylation

1-Hydroxyalkylphosphonates **M2** were synthesized asymmetrically via enantioselective hydrophosphonylation of aldehydes using tridentate Schiff base Al(III) complexes as catalysts (Scheme 9.31).



Scheme 9.31 Synthesis of optically active 1-hydroxyalkylphosphonates **M2**

General procedure: Et_2AlBr (1 mmol) was added to a solution of ligand (**S**) or (**R**)-**L1-6** (1 mmol) in CH_2Cl_2 (4 mL) under nitrogen to form catalyst (**S**) or (**R**)-**Cat1-6**. After stirring at room temperature for 0.5 h, an appropriate aldehyde (10 mmol) in THF (6 mL) and silver carbonate (0.4 mmol) were added and stirred for another 0.5 h. Dimethyl phosphonate **M1-1** (12 mmol) was added at -15°C , and the reaction solution was stirred for 2 h. The reaction was quenched by diluted hydrochloric acid ($v/v = 1/15$). The corresponding optically active 1-hydroxyalkyl phosphonate (**S**) or (**R**)-**M2** was afforded by column chromatography on silica gel (acetone/petroleum ether = 1/2). A series of optically active (**S**) or (**R**)-**M2** could be obtained by this procedure. The enantiomeric excesses (*ee*) were determined by

Table 9.44 Structure and physicochemical data of optically active *O,O*-dimethyl 1-hydroxy-alkylphosphonates **M2**

Compound	R ³	Appearance	mp (°C)	Yield (%) ^a	ee (%)	Conf ^b
(<i>S</i>)- M2-24	Ph	Colorless crystal	60–61	82	98	<i>S</i>
(<i>R</i>)- M2-24	Ph	Colorless crystal	60–61	85	96	<i>R</i>
(<i>S</i>)- M2-25	4-MePh	Colorless crystal	64–65	83	95	<i>S</i>
(<i>R</i>)- M2-25	4-MePh	Colorless crystal	64–65	80	98	<i>R</i>
(<i>S</i>)- M2-29	4-MeOPh	Colorless crystal	67–68	78	97	<i>S</i>
(<i>R</i>)- M2-29	4-MeOPh	Colorless crystal	67–68	79	98	<i>R</i>
(<i>S</i>)- M2-33	4-ClPh	Colorless crystal	73–74	80	98	<i>S</i>
(<i>R</i>)- M2-33	4-ClPh	Colorless crystal	73–74	67	97	<i>R</i>
(<i>S</i>)- M2-37	Fur-2-yl	Yellow solid	54–55	75	98	<i>S</i>
(<i>R</i>)- M2-37	Fur-2-yl	Yellow solid	54–55	75	98	<i>R</i>
(<i>S</i>)- M2-38	Thien-2-yl	Yellow solid	58–59	76	98	<i>S</i>
(<i>R</i>)- M2-38	Thien-2-yl	Yellow solid	58–59	76	98	<i>R</i>

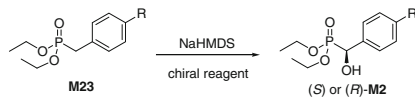
^a Yields refer to purified compounds^b Generally, optical rotation of *R* form is dextrorotatory (+), but *S* form is levorotatory (–)

HPLC analysis on chiral DAICEL CHIRALPAK AS-H column at 210 nm or 230 nm, n-hexane/*i*-PrOH = 30/70.

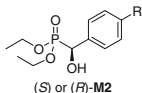
The structures, physicochemical data, and yields of optically active 1-hydroxyalkyl phosphonates **M2** are listed in Table 9.44.

9.1.31.2 Preparation via Enantioselective Hydroxylation

1-Hydroxy(substituted phenyl)methylphosphonates **M2** were prepared from *O,O*-diethyl (substituted benzyl)phosphonates **M23** reacted with NaHMDS and chiral reagent (Scheme 9.32).

**Scheme 9.32** Synthesis of optically active 1-hydroxyalkylphosphonates **M2**

General procedure: Under an inert atmosphere of nitrogen, NaHMDS (1 mmol) was added dropwise to a solution of the appropriate diethyl substituted benzylphosphonate **M23** (1 mmol) in THF (10 mL) at –78 °C and the resulting

Table 9.45 Structure and physicochemical data of optically active *O,O*-diethyl 1-hydroxy-1-(substituted phenyl)methylphosphonates **M2**

Compound	R	Appearance	Yield (%) ^a	<i>ee</i> (%)	Conf. ^b
(<i>S</i>)- M2-6	H	Colorless oil	47	88	<i>S</i>
(<i>R</i>)- M2-6	H	Colorless oil	50	88	<i>R</i>
(<i>S</i>)- M2-7	4-Me	Colorless oil	49	90	<i>S</i>
(<i>R</i>)- M2-7	4-Me	Colorless oil	48	90	<i>R</i>
(<i>S</i>)- M2-9	4-OMe	Colorless oil	54	99	<i>S</i>
(<i>R</i>)- M2-9	4-OMe	Colorless oil	52	98	<i>R</i>
(<i>S</i>)- M2-13	4-Cl	Colorless oil	36	93	<i>S</i>
(<i>R</i>)- M2-13	4-Cl	Colorless oil	40	93	<i>R</i>

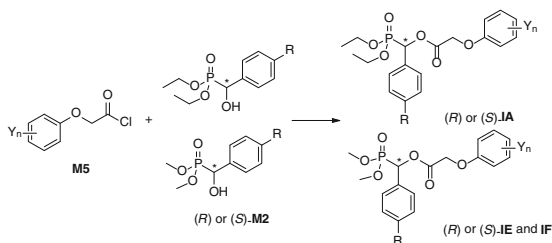
^a Yields refer to purified compounds^b Generally, the optical rotation of *R* form is dextrorotatory (+), *S* form is levorotatory (–)

solution was stirred for 0.5 h. A solution of (+) or (–)-8,8-(dichlorocamphor) sulfonyloxaziridine (2 mmol) in THF (10 mL) was added dropwise and the reaction was stirred for another 3 h, while the temperature was maintained at –78 °C (dry ice–acetone bath). The reaction was quenched by the addition of saturated NH₄Cl, and extracted several times with ethyl acetate. The combined organic fractions were washed with brine and then dried over anhydrous sodium sulfate. The crude product was purified by column chromatography on silica gel using ethyl acetate/petroleum ether (*v/v* = 2/1) as the eluent to give the desired optically active (*S*) or (*R*)-1-hydroxy-1-(substituted phenyl) methylphosphonate **M2**. A series of optically active (*S*) or (*R*)-**M2** could be obtained by this procedure. The enantiomeric excesses (*ee*) were determined by HPLC analysis on chiral DAICEL CHIRALPAK AS-H column at 210 nm, *n*-hexane/*i*-PrOH = 30/70.

The structures, physicochemical data, and yields of optically active 1-hydroxy-1-(substituted phenyl)methylphosphonate **M2** are listed in Table 9.45.

9.1.32 Optically Active (Substituted Phenyl) Methylphosphonates **IA**, **IE**, and **IF**

The typical procedure for the preparation of optically active *O,O*-dimethyl [1-(substituted phenoxyacetoxy)-1-(substituted phenyl)]methylphosphonates (Scheme 9.33) is described as follows.



Scheme 9.33 Synthesis of optically active *O,O*-dialkyl (substituted phenyl)methylphosphonates **IA**, **IE** and **IF**

General procedure: A solution of an appropriate substituted phenoxyacetyl chloride (22 mmol) in trichloromethane (10 mL) was added to a stirred mixture of corresponding optically active *O,O*-dimethyl 1-hydroxy-1-(substituted phenyl)methylphosphonate (20 mmol) and pyridine or triethylamine (22 mmol) in trichloromethane (25 mL) at 10–25 °C. The resultant mixture was stirred for 3–5 h at room temperature, and then for 1–2 h at 40–42 °C. The trichloromethane layer was washed with 0.1 M hydrochloric acid, saturated sodium hydrogen carbonate solution and brine, dried and concentrated. The residue was purified by column chromatography on silica gel and eluted with petroleum ether/acetone (2/1, *v/v*) to give the corresponding *O,O*-dimethyl [1-(substituted phenoxyacetoxy)-1-(substituted phenyl)]methylphosphonate **IE** or **IF**. Optically active *O,O*-diethyl [1-(substituted phenoxyacetoxy)-1-(substituted phenyl)]methylphosphonate **IA** could be synthesized by a similar procedure. Series of optically active **IA**, **IE**, and **IF** were obtained as the yellow liquids or colorless crystals in 52–89 % yields. The enantiomeric excesses (*ee*) were determined by HPLC analysis on a chiral DAICEL CHIRALPAK AS-H column at 254 nm or 230 nm, *n*-hexane/*i*-PrOH = 70/30.

The structures, physicochemical data, and yields of optically active **IA**, **IE**, and **IF** are listed in Tables 9.46 and 9.47.

Table 9.46 Structures and physicochemical data of optically active *O,O*-diethyl [1-(substituted

phenoxyacetoxy)-1-(substituted phenyl)]methylphosphonates **IA**

Compound	R	Y _n	Appearance	Yield (%) ^a	<i>ee</i> (%)	Conf. ^b
(R)-IA-13	H	2,4-Cl ₂	Yellowish liquid	85	88	<i>R</i>
(S)-IA-13	H	2,4-Cl ₂	Yellowish liquid	90	87	<i>S</i>
(R)-IA-14	Me	2,4-Cl ₂	Yellowish liquid	83	87	<i>R</i>
(S)-IA-14	Me	2,4-Cl ₂	Yellowish liquid	87	90	<i>S</i>
(R)-IA-21	Cl	2,4-Cl ₂	Yellowish liquid	87	92	<i>R</i>
(S)-IA-21	Cl	2,4-Cl ₂	Yellowish liquid	88	93	<i>S</i>

(continued)

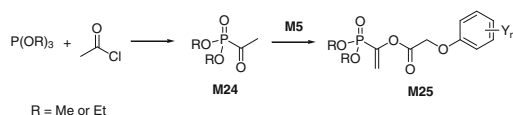
Table 9.46 (continued)

Compound	R	Y _n	Appearance	Yield (%) ^a	ee (%)	Conf. ^b
(<i>R</i>)- IA-25	MeO	2,4-Cl ₂	Yellowish liquid	81	87	<i>R</i>
(<i>S</i>)- IA-25	MeO	2,4-Cl ₂	Yellowish liquid	85	99	<i>S</i>
(<i>R</i>)- IA-26	Me	2-F,4-Cl	Yellowish liquid	75	88	<i>R</i>
(<i>S</i>)- IA-26	Me	2-F,4-Cl	Yellowish liquid	73	89	<i>S</i>
(<i>S</i>)- IA-27	Me	2-Cl,4-F	Yellowish liquid	72	90	<i>S</i>
(<i>R</i>)- IA-28	Cl	2-Cl,4-F	Yellowish liquid	72	90	<i>R</i>
(<i>S</i>)- IA-28	Cl	2-Cl,4-F	Yellowish liquid	76	87	<i>S</i>
(<i>S</i>)- IA-29	MeO	2-Cl,4-F	Yellowish liquid	78	99	<i>S</i>

^a Yields refer to purified compounds^b Generally, the optical rotation of *R* form is dextrorotatory (+), *S* form is levorotatory (–)

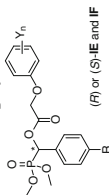
9.1.33 1-Keto Phosphonates **M24** and Vinylphosphonates **M25**

The Arbuzov reaction of trialkyl phosphite and acetyl chlorides gave α -keto phosphonates **M24**, which were then treated with various substituted phenoxyacetyl chlorides **M5** to afford *O,O*-dialkyl 1-(substituted phenoxy acetoxy)vinylphosphonate **M25** (Scheme 9.34).

**Scheme 9.34** Synthesis of 1-keto phosphonates **M24** and vinylphosphonates **M25**

General procedure: Acetyl chloride (2.5 mL, 35 mmol) was cooled to 0 °C in an oven-dried flask fitted with an addition funnel. Trimethyl phosphite (5 mL, 42 mmol) was added dropwise. A balloon was used to compensate for the released methyl chloride. When the addition was complete, the reaction was warmed to room temperature and stirred overnight. The mixture was concentrated under vacuum to remove volatile impurities and then the crude product of **M24** was taken directly to the next step. THF (40 mL) and substituted phenoxyacetyl chloride **M5** (5 mL, 28.2 mmol) were added to the crude product of **M24**, and the system was chilled to 0 °C. Et₃N (4.5 mL) was dissolved in 20 mL of THF, and this solution was then added slowly to the reaction mixtures. After being stirred for 45 min, the reaction mixture was warmed up to room temperature and stirred for another 3 h. The reaction mixture was diluted with EtOAc (200 mL), which was washed with saturated NaHCO₃, brine (75 mL), and then dried with MgSO₄. The solvent was

Table 9.47 Structures and physicochemical data of optically active *O,O*-dimethyl [1-(substituted phenoxyacetoxy)-1-(substituted phenyl)]methylphosphonates **IE** and **IF**



Compound	R	Y _n	Appearance	mp (°C)	Yield (%) ^a	ee (%)	Conf. ^b
(R)-IE-10	H	4-F	White solid	59.0–61.0	80	95	R
(S)-IE-10	H	4-F	White solid	59.0–61.0	82	93	S
(R)-IE-11	H	4-Cl	White solid	54.0–55.0	76	92	R
(S)-IE-11	H	4-Cl	White solid	54.0–55.0	75	97	S
(R)-IE-12	H	4-Br	White solid	63.0–64.0	80	95	R
(S)-IE-12	H	4-Br	White solid	63.0–64.0	75	92	S
(R)-IE-14	H	2-Me,4-Cl	Yellow solid	50.6–52.2	62	97	R
(S)-IE-14	H	2-Me,4-Cl	Yellow solid	51.6–53.4	70	96	S
(R)-IE-17	H	2,4-F ₂	White solid	64.0–65.0	83	92	R
(S)-IE-17	H	2,4-F ₂	White solid	64.0–65.0	80	92	S
(R)-IE-18	H	2-F,4-Cl	Yellow solid	46.7–48.4	61	96	R
(S)-IE-18	H	2-F,4-Cl	Yellow solid	47.8–49.4	67	95	S
(R)-IE-19	H	2-Cl,4-F	Yellow solid	60.4–62.8	66	94	R
(S)-IE-19	H	2-Cl,4-F	Yellow solid	61.4–63.3	67	95	S
(R)-IE-22	H	2,4-Cl ₂	Colorless crystal	49.4–51.9	62	96	R
(S)-IE-22	H	2,4-Cl ₂	Colorless crystal	50.6–52.5	66	96	S
(R)-IF-2	Me	4-F	White solid	60.0–61.0	82	96	R
(S)-IF-2	Me	4-F	White solid	60.0–61.0	80	95	S
(R)-IF-3	Me	4-Cl	White solid	63.0–64.0	82	95	R
(S)-IF-3	Me	4-Cl	White solid	63.0–64.0	82	95	S

(continued)

Table 9.47 (continued)

Compound	R	Y _n	Appearance	mp (°C)	Yield (%) ^a	ee (%)	Conf. ^b
(<i>R</i>)- IF-4	Me	4-Br	Colorless crystal	57.0–59.0	85	95	<i>R</i>
(<i>S</i>)- IF-4	Me	4-Br	Colorless crystal	57.0–59.0	82	95	<i>S</i>
(<i>R</i>)- IF-5	Me	2-Me,4-Cl	Yellow solid	44.3–46.1	61	95	<i>R</i>
(<i>S</i>)- IF-5	Me	2-Me,4-Cl	Yellow solid	45.6–47.5	66	96	<i>S</i>
(<i>R</i>)- IF-6	Me	2,4-F ₂	Colorless crystal	54.0–56.0	80	95	<i>R</i>
(<i>S</i>)- IF-6	Me	2,4-F ₂	Colorless crystal	54.0–56.0	85	99	<i>S</i>
(<i>R</i>)- IF-7	Me	2-F, 4-Cl	Yellow solid	60.4–62.2	62	95	<i>R</i>
(<i>S</i>)- IF-7	Me	2-F, 4-Cl	Yellow solid	60.3–62.2	71	95	<i>S</i>
(<i>R</i>)- IF-8	Me	2-Cl,4-F	Yellow solid	60.8–62.6	63	95	<i>R</i>
(<i>S</i>)- IF-8	Me	2-Cl,4-F	Yellow solid	61.6–63.4	70	96	<i>S</i>
(<i>R</i>)- IF-9	Me	2,4-Cl ₂	Yellow solid	55.7–57.3	60	95	<i>R</i>
(<i>S</i>)- IF-9	Me	2,4-Cl ₂	Yellow solid	56.4–57.9	67	96	<i>S</i>
(<i>R</i>)- IF-16	MeO	2-Me,4-Cl	Yellow solid	50.7–52.3	62	96	<i>R</i>
(<i>S</i>)- IF-16	MeO	2-Me,4-Cl	Yellow solid	51.3–53.1	70	96	<i>S</i>
(<i>R</i>)- IF-17	MeO	2,4-F ₂	White solid	67.0–68.0	78	95	<i>R</i>
(<i>S</i>)- IF-17	MeO	2,4-F ₂	White solid	67.0–68.0	80	93	<i>S</i>
(<i>R</i>)- IF-18	MeO	2-F,4-Cl	Yellow solid	64.6–66.1	65	96	<i>R</i>
(<i>S</i>)- IF-18	MeO	2-F, 4-Cl	Yellow solid	65.7–67.4	69	96	<i>S</i>
(<i>R</i>)- IF-19	MeO	2-Cl,4-F	Yellow solid	68.4–70.2	62	96	<i>R</i>
(<i>S</i>)- IF-19	MeO	2-Cl,4-F	Yellow solid	69.6–71.2	70	96	<i>S</i>
(<i>R</i>)- IF-20	MeO	2,4-Cl ₂	Colorless crystal	61.3–63.2	62	96	<i>R</i>
(<i>S</i>)- IF-20	MeO	2,4-Cl ₂	Colorless crystal	61.4–63.1	69	95	<i>S</i>
(<i>R</i>)- IF-28	Cl	2-Me,4-Cl	Colorless crystal	66.3–67.9	62	96	<i>R</i>

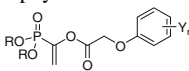
(continued)

Table 9.47 (continued)

Compound	R	Y _n	Appearance	mp (°C)	Yield (%) ^a	ee (%)	Conf. ^b
(S)-IF-28	Cl	2-Me, 4-Cl	Colorless crystal	67.3–68.9	66	96	S
(R)-IF-29	Cl	2-F, 4-Cl	Yellow solid	65.8–67.3	60	96	R
(S)-IF-29	Cl	2-F, 4-Cl	Yellow solid	66.7–68.4	67	96	S
(R)-IF-30	Cl	2-Cl, 4-F	Colorless crystal	66.3–68.1	62	95	R
(S)-IF-30	Cl	2-Cl, 4-F	Colorless crystal	67.4–69.2	65	96	S
(R)-IF-31	Cl	2,4-Cl ₂	Colorless crystal	49.6–51.5	61	96	R
(S)-IF-31	Cl	2,4-Cl ₂	Colorless crystal	50.6–52.4	65	95	S
(R)-IF-62	NO ₂	2,4-F ₂	Brown solid	48.0–49.0	85	91	R
(S)-IF-62	NO ₂	2,4-F ₂	Brown solid	48.0–49.0	80	90	S
(R)-IF-64	NO ₂	4-F	Brown solid	54.0–56.0	84	92	R
(S)-IF-64	NO ₂	4-F	Brown solid	54.0–56.0	85	92	S
(R)-IF-65	NO ₂	4-Cl	Brown solid	71.0–72.0	82	92	R
(S)-IF-65	NO ₂	4-Cl	Brown solid	71.0–72.0	78	94	S
(R)-IF-66	NO ₂	4-Br	Brown solid	65.0–66.0	85	91	R
(S)-IF-66	NO ₂	4-Br	Brown solid	65.0–66.0	82	92	S

^a Yields refer to purified compounds

^b Generally, the optical rotation of *S* form is dextrorotatory (+), *R* form is levorotatory (–)

Table 9.48 Structure and physicochemical data of *O,O*-dialkyl 1-(substituted phenoxyacetoxy)vinylphosphonates **M25**


Compound	R	Y _n	Appearance	mp (°C)	Yield (%) ^a
M25-1	Et	2,4-Cl ₂	Yellowish liquid	ND ^b	75
M25-2	Me	H	Yellowish solid	57–59	68
M25-3	Me	4-Me	Yellowish liquid	ND	87
M25-4	Me	3-CF ₃	Yellowish liquid	ND	62
M25-5	Me	4-F	Yellow liquid	ND	79
M25-6	Me	4-Cl	Yellowish solid	32–34	80
M25-7	Me	2,4-Cl ₂	White solid	78–80	59
M25-8	Me	2-Cl	Colorless liquid	ND	64
M25-9	Me	4-MeO	Yellow liquid	ND	75

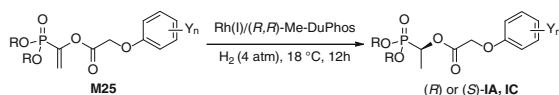
^a Yields refer to purified compounds^b No data

removed in vacuum to give yellow oil, which was purified on silica gel (EtOAc:petroleum ether = 1:1) to give corresponding *O,O*-dialkyl 1-(substituted phenoxyacetoxy)vinylphosphonate **M25**. A series of **M25** could be obtained by this procedure in 59–87 % isolated yield.

The structures, physicochemical data, and yields of vinylphosphonates **M25** are listed in Table 9.48.

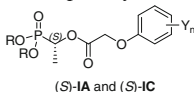
9.1.34 Optically Active 1-Substituted Ethylphosphonates **IA** and **IC**

Optically active substituted ethylphosphonates **IA** and **IC** were prepared from *O,O*-dialkyl 1-(substituted phenoxyacetoxy)vinylphosphonate **M25** asymmetrically hydrogenated using chiral Rh(I)-complexes as catalysts (Scheme 9.35).

**Scheme 9.35** Synthesis of optically active *O,O*-dialkyl 1-(substituted phenoxyacetoxy)ethylphosphonates **IA** and **IC**

General procedure: In a glove box, the Rh/Me-DuPhos complex was made in situ by mixing [Rh(COD)₂]BF₄ (2.0 mg, 0.005 mmol) and (*R,R*) or (*S,S*)-Me-DuPhos (1.7 mg, 0.0055 mmol) in MeOH (2.0 mL). After the mixture was stirred at room temperature for 10 min. An appropriate 1-(substituted phenoxyacetoxy)

Table 9.49 Structure and physicochemical data of optically active *O,O*-dialkyl 1-(substituted phenoxyacetoxymethyl)phosphonates **IA** and **IC**



Compound ^a	R	Y _n	Appearance	Conv. (%) ^b	ee (%)	Conf. ^c
(S)- IA-8	Et	2,4-Cl ₂	Yellowish liquid	>95	96	<i>S</i>
(S)- IC-2	Me	H	Yellowish liquid	>95	93	<i>S</i>
(S)- IC-4	Me	4-Me	Colorless liquid	>95	91	<i>S</i>
(S)- IC-5	Me	3-CF ₃	Yellow liquid	>95	92	<i>S</i>
(S)- IC-9	Me	4-F	Yellowish liquid	>95	94	<i>S</i>
(S)- IC-10	Me	4-Cl	Yellow liquid	>95	95	<i>S</i>
(S)- IC-22	Me	2,4-Cl ₂	Yellowish liquid	>95	94	<i>S</i>
(S)- IC-35	Me	2-Cl	Yellow liquid	>95	93	<i>S</i>
(S)- IC-36	Me	4-MeO	Yellowish liquid	91	95	<i>S</i>

^a The corresponding (*R*) forms were also achieved by using (*S,S*)-Me-DuPhos as a ligand

^b Conversions were determined by ¹H NMR

^c Generally, the optical rotation of (*S*) form is dextrorotatory (+)

vinylphosphonate **M25** (0.5 mmol) in MeOH (2.0 mL) was added by a syringe. The hydrogenation was performed at room temperature under 4 atm H₂ for 12 h. The reaction mixtures were concentrated and then passed through a silica gel plug using ethyl acetate and petroleum ether (3:1) as an eluant to give corresponding optically pure **IA** or **IC**. A series of (*S*)-**IA** or (*S*)-**IC** could be obtained using (*R,R*)-Me-DuPhos as a ligand by this procedure. The enantiomeric excess (*ee*) was determined on chiral HPLC.

The structures, physicochemical data, and conversions of (*S*)-**IA** and (*S*)-**IC** are listed in Table 9.49. The (*R*)-**IA** and (*R*)-**IC** could be also achieved by using (*S,S*)-Me-DuPhos as a ligand.

The structures of all title compounds were identified by elemental analysis and characterized by IR, ¹H NMR. Some of them were also characterized by MS, ³¹P NMR or ¹³C NMR spectra. The structures of some representative compounds were further confirmed by X-ray single-crystal diffraction. In addition, the optical rotations and enantiomeric excess (*ee*) of the optically active compounds were measured.

The general information of structural characterization is given in Sect. 9.2.

9.2 General Information of Structural Characterization

Melting points were measured on a hot-plate microscope apparatus and uncorrected.

¹H NMR spectra were recorded on a Varian Mercury-Plus 200 spectrometer at 200 MHz or on a Varian XL-300 spectrometer at 300 MHz, or on a Varian Mercury puls-400 spectrometer at 400 MHz, or on a Varian Mercury 600 spectrometer at

600 MHz. Chemical shifts were reported in δ (ppm) relative to tetramethylsilane (TMS) or residual solvent signals as the internal standard (CHCl_3 , $\delta = 7.26$, DMSO-d_6 , $\delta = 2.50$). Spectra data were presented as follows: Chemical shifts (δ ppm), multiplicity (s = singlet, d = doublet, t = triplet, q = quartet, m = multiplet), coupling constants (Hz), integration, and assignment.

^{13}C NMR spectra were collected on a Varian Mercury 600 spectrometer at 150 MHz or on a Varian Mercury puls-400 spectrometer at 100 MHz with complete proton decoupling. Chemical shifts were reported in ppm relative to TMS with the solvent resonance as internal standard (DMSO-d_6 , $\delta = 39.5$).

^{31}P NMR spectra were collected on a Varian Mercury 600 spectrometer at 243 MHz or on a Varian Mercury puls-400 spectrometer at 162 MHz with complete proton decoupling. Chemical shifts were reported in ppm referenced to 85 % phosphoric acid, which is assigned the chemical shift of 0.

Infrared spectra were obtained as a KBr disk on a Perkin-Elmer PE-983 infrared spectrometer or on a Nicolet Avatar 360 FT-IR spectrometer.

Mass spectra were measured on a Finnigan Trace MS spectrometer or on an API 2000 LC/MS spectrometer.

Elementary analyses were performed on a Vario EL III elementary analysis instrument. The results of elemental analyses for C, H, and N were within ± 0.5 % of the theoretical values.

The X-ray diffraction data were collected on a Bruker SMART AXS CCD diffractometer using graphite monochromated $\text{MoK}\alpha$ radiation ($\lambda = 0.071073$ nm). All data were corrected using SADABS program. The structure was solved by direct methods using SHELXS-97, all other calculations were performed with a Bruker SAINT system and Bruker SMART programs. All nonhydrogen atoms were refined on F^2 anisotropically by full-matrix least-squares method. Hydrogen atoms were observed and refined with a fixed value of their isotropic displacement parameter.

Optical rotations were measured on a JASCO P-1020 polarimeter and reported as follows: $[\alpha]_D^T$ ($c = \text{g}/100$ mL, solvent).

The enantiomeric excess (*ee*) of the product was determined by HPLC analysis on a chiral DAICEL CHIRALPAK AS-H column (at 254 nm) unless specially indicated.

9.3 Herbicidal Activity Assay

Herbicidal activity assessment is the first and most important step in developing novel herbicides. Test procedures and conditions must meet testing requirements of chemical screening. A series of test procedures has been developed for testing the biological activity of new compounds. Data from these tests will help us in assessing the herbicidal ability of new chemicals.

9.3.1 Test in Petri Dishes

This test is intended for use in developing data on the inhibitory activity of chemicals for herbicidal activity pre-evaluating. This section prescribes the test procedures and conditions using seeds of plants to develop data on plant stem/root inhibitory effect of chemicals.

9.3.1.1 Stem/Root Growth Inhibitory Activity Test

Test Plants: *Brassica napus L.* (rape) and *Echinochloa crusgalli* (barnyard grass).

Test Solution: Test chemicals were dissolved in *N,N*-dimethylformamide or acetone and a little of Tween 80 was added. The solution was then diluted with deionized or glass-distilled water until it reached the concentration required (e.g., 100 mg/L) for the test. The solvent and emulsifier should be used in the minimum amount required to dissolve or suspend the test chemical. The mixture of the same amount of water, solvent, and Tween 80 were prepared simultaneously as control.

Test Procedure: Seeds were separated into appropriate size classes, and the size class containing the most seeds should be used exclusively for the test. Damaged seeds should be discarded. Fresh test solution (5 mL) was added to Petri dishes (diameter = 9.0 cm) with a filter paper (diameter = 5.5 cm), and 10 rape or barnyard grass seeds were placed on the filter paper after soaking in deionized or glass-distilled water for 6 h. Petri dishes were placed in the growth chamber at $28 \pm 1^\circ\text{C}$ for 72 h with 10 h of lighting and 14 h in the dark. Test experiments were conducted in three replicates for each concentration and control.

Observation: The number of seeds that germinate should be counted and the root and stem lengths should be measured for each treatment and control.

Inhibitory potency: Inhibitory potency of tested chemicals against the growth of plants was measured as percentage change in the length of root or stem compared to that of the control, such as 0 % (no effect or not significantly different from control), and 100 % (completely inhibited). According to the corresponding inhibition percentage, the inhibitory potency was also expressed as the following four scales: A: ≥ 90 %, B: 70–89 %, C: 50–69 %, D: 1–49 %.

9.3.1.2 Determination of IC_{50} Values

The IC_{50} values of test compounds were determined against the preemergence growth of cucumber (*Cucumis sativa*). A defined amount of test compounds dissolved in acetone was poured on a filter paper (5.5 cm diameter) in Petri dishes (9 cm), and 10 cucumber seeds after soaking in water for 6 h were placed on the filter paper. The Petri dishes with cucumber seeds were placed in a lighting incubator at 28°C for 3 d with 10 h of lighting and 14 h in the dark. After 3 d of treatment, the inhibition percentage was calculated by corresponding control using

the length of the taproot or stem as an indicator. Three replications per concentration were performed. According to the average percentage of inhibition of cucumber root or stem at five concentrations for each test compound, the IC_{50} values for inhibition of cucumber root or stem were estimated by regression analysis using a logarithm of concentration and probit of corresponding inhibition percentage.

9.3.2 Test in Greenhouse

9.3.2.1 Herbicidal Activity Test

The preemergence and postemergence herbicidal activities of compounds were evaluated at different dosages in a set of greenhouse experiments.

Test plants: barnyard grass (*E. crusgalli*), crab grass (*Digitaria sanguinalis*), common amaranth (*Amaranthus retroflexus*), carrot (*Daucus carota*), clover (*Medicago sativa*), cucumber (*Cucumis sativus*), chingma abutilon (*Abutilon theophrasti*), spiny amaranth (*Amaranthus spinosus*), goosefoot (*Chenopodium album*), green bristlegrass (*Setaria viridis*), white eclipta (*Eclipta prostrata*), Siberian cocklebur (*Xanthium strumarium*), hairy bittercress (*Cardamine hirsuta*), purslane (*Portulaca oleracea*), cabbage type rape (*Brassica napus*), rice (*Oryza sativa*), wheat (*Triticum aestivum*), and maize (*Zea mays*) and some other plant species were chosen as the tested plants. All tested species are listed in the table of Test species.

Culture Method: Plastic pots were packed with sandy clay loam soil, and water was added up to 3 cm in depth. In the pot, about 15–20 seeds of plant were sown in the soil at a depth of 5 mm, and grown at 20–25 °C for a few days.

Preparation of Test Solution: Test compound was dissolved in *N,N*-dimethylformamide or acetone and a little of Tween 80 was added. The solution was then diluted with water until it reached a 1,000 L/ha spray volume. The mixture of the same amount of water, solvent, and Tween 80 were prepared as control.

Treatment: In the preemergence application, the diluted solution of each test compound was applied into pots before the emergence of seedlings. In the post-emergence application, the solution of the test compound was applied to the foliage of plants grown at the 2–3 leaves stage with a sprayer at the test rate with a spray volume of 1,000 L/ha. All treatments were replicated three times.

Observation: Test plants were harvested 20 days after treatment, and determined for fresh weight. The herbicidal activity against each weed was evaluated. The percentage of growth inhibition of roots and aerial parts were calculated in relation to the mass of the roots and aerial parts of the control, respectively. Weed numbers could be also counted as percentage change compared to that of the untreated control.

Inhibitory potency: The inhibitory potency of compounds on the growth of plants at a rate was measured as percentage change in each plant weight compared

to that of the control, such as 0 % (no effect or not significantly different from control), 100 % (completely killed); According to the corresponding inhibition percentage, the inhibitory effect was expressed as four scales: A: ≥ 90 %, B: 70–89 %, C: 50–69 %, D: < 50 %.

9.3.2.2 Crop Selectivity Test

Conventional rice, corn, cotton, soybean, rape, and wheat were, respectively, planted in plots (diameter = 12 cm) containing test soil and grown in a greenhouse at 20–25 °C. After plants reached the 4-leaf stage, the spraying treatment was conducted at different dosages by diluting the formulation of selected compounds. The visual injury and growth state of the individual plant were observed at regular intervals. The final evaluation for crop safety of selected compounds was conducted by visual observation in 30 days after treatment on the 0–100 scale.

References

1. McCombie H, Saunders BC, Stacey GJ (1945) Esters containing phosphorus. Part I J Chem Soc 93:380–382
2. Lv CX (2009) Preparation of organic intermediates. Beijing Chemical Industry, Beijing
3. Li YJ, He HW (2008) Synthesis and herbicidal activity of α -[2-(fluoro-substituted phenoxy) propionyloxy] alkyl phosphonates. Phosphorus Sulfur Silicon Relat Elem 183:712–713
4. Texier-Boullet F, Foucaud A (1982) Synthesis of 1-hydroxyalkane phosphonic esters on alumina. Synthesis 11:916
5. Texier-Boullet F, Foucaud A (1982) A convenient synthesis of dialkyl 1-hydroxyalkane phosphonates using potassium or caesium fluoride without solvent. Synthesis 1982 (2):165–166
6. Liu XF, He HW, Liu ZJ (1998) Reaction of 1-hydroxy alkyl phosphonate and chloroacetic chloride. J Centr Chin Norm Univ (Nat sci) 32:52–55
7. Deng XY, Liao GH, Long QW et al (2013) Synthesis and herbicidal activity of [(substituted phenoxyacetoxy)(substituted phenyl)methyl](methyl)phosphinates containing fluorine. Phosphorus Sulfur Silicon Relat Elem 188:663–671
8. Chen T, Shen P, Li YJ et al (2006) Synthesis and herbicidal activity of *O,O*-dialkyl phenoxyacetoxyalkylphosphonates containing fluorine. J Fluorine Chem 127:291–295
9. Chen T, Shen P, Li YJ et al (2006) The synthesis and herbicidal evaluation of fluorine-containing phenoxyacetoxyalkylphosphonate derivatives. Phosphorus Sulfur Silicon Relat Elem 181:2135–2145
10. Wang J, Chen XY, Liu XF et al (1999) The synthesis and biological properties of α -halogenated phenoxy carbonyloxy alkylphosphonic acids and esters. Chin J Chem Reag 21:301–303
11. He HW, Chen T, Li YJ (2007) Synthesis and herbicidal activity of alkyl 1-(3-trifluoromethylphenoxyacetoxy)-1-substituted methylphosphonates. J Pestic Sci 32:42–44
12. Wang T, He HW (2004) Simple and improved preparation of α -oxophosphonate monolithium salts. Phosphorus Sulfur Silicon Relat Elem 179:2081–2089
13. He HW, Yuan JL, Peng H et al (2011) Studies of *O,O*-dimethyl α -(2, 4-dichlorophenoxy acetoxy)ethylphosphonate (HW02) as a new herbicide. 1. Synthesis and herbicidal activity of

- HW02 and analogues as novel inhibitors of pyruvate dehydrogenase complex. *J Agric Food Chem* 59:4801–4813
14. Peng H, Wang T, Xie P et al (2007) Molecular docking and three-dimensional quantitative structure-activity relationship studies on the s of herbicidal 1-(substituted phenoxyacetoxy) alkylphosphonates to the E1 component of pyruvate dehydrogenase. *J Agric Food Chem* 55:1871–1880
 15. Wang T, He HW, Miao FM (2009) Synthesis, crystal structure and herbicidal activity of 1-(2,4-dichlorophenoxyacetoxy)-1-arylmethylphosphonates. *Chin J Org Chem* 29:1152–1157
 16. Meng LP, He HW, Liu ZJ (1998) Synthesis and biological activities of *O,O*-dimethyl α -(NO₂ substituted phenoxyacetoxy)alkylphosphonates. *Chin J HuBei Chem Ind (special issue)*:40–41
 17. He HW, Peng H, Wang T et al (2013) α -(Substituted-phenoxyacetoxy)- α -heterocyclmethylphosphonates: synthesis, herbicidal activity, inhibition on pyruvate dehydrogenase complex (PDHc), and application as postemergent herbicide against broadleaf weeds. *J Agric Food Chem* 61:2479–2488
 18. Xiao WJ, Ding MW, Wang JH et al (1994) A research on the synthesis process of Triazophos. *Chin J Pestic* 33:14–15
 19. He HW, Meng LP, Hu LM et al (2002) Plant growth regulatory activity of 1-(1-phenyl-1,2,4-triazole-3-oxyacetoxy)alkylphosphonates. *Chin J Pestic Sci* 4:14–18
 20. Wang T, Zou P, Peng H et al (2014) Synthesis and biological activity of *O*-alkyl α -(substituted phenoxyacetoxy)alkylphosphonate. *Chin J Org Chem* 34:215–219
 21. He HW, Wang T, Yuan JL (2005) Synthesis and herbicidal activities of methyl-1-(2,4-dichlorophenoxyacetoxy)alkylphosphonate monosalts. *J Organomet Chem* 690:2608–2613
 22. Wang T, He HW (2004) An efficient synthesis of α -(2,4-dichlorophenoxyacetoxy) aryl methyl phosphonate monosodium salts. *Synth Commun* 34:1415–1423
 23. Wang T, Wang W, Peng H et al (2013) Synthesis and herbicidal activities of potassium methyl 1-(substituted phenoxyacetoxy)alkylphosphonate. *Chem Res Chin U* 29:690–694
 24. Peng H, Long QW, Deng XY et al (2013) Synthesis and herbicidal activities of lithium or potassium hydrogen 1-(substituted phenoxyacetoxy)alkylphosphonates. *Phosphorus Sulfur Silicon Relat Elem* 188:1868–1874
 25. Long QW, Deng XY, Gao YJ et al (2013) Synthesis and herbicidal activity of sodium hydrogen 1-(substituted phenoxyacetoxy)alkylphosphonates. *Phosphorus Sulfur Silicon Relat Elem* 188:819–825
 26. Peng H, Deng XY, Gao L et al (2014) Synthesis and herbicidal activities of 2-methylpropan-2-aminium *O*-methyl 1-(substituted phenoxyacetoxy)alkylphosphonates. *Chem Res Chin U* 30:82–86
 27. Gao L, Deng XY, Tan XS et al (2013) Synthesis and herbicidal activities of 2-methylpropan-2-aminium methyl 1-(substituted phenoxyacetoxy)alkylphosphonates. *Phosphorus Sulfur Silicon Relat Elem* 188:989–994
 28. Li MQ, You GY, Peng H et al (2013) Synthesis and herbicidal activities of *O*-methyl methyl [1-(substituted phenoxyacetoxy)alkyl]phosphinates. *J Pestic Sci* 38:78–84
 29. Wang T, Peng H, He HW (2014) Synthesis and biological activity of *O*-methyl methyl 1-(substituted phenoxyacetoxy)-1-(thien-2-yl)methylphosphinates. *J Heterocycl Chem*. doi:10.1002/jhet.2143
 30. Wang T, He HW (2008) Synthesis and biological activity of α -oxo-2-pyridyl methyl phosphinates. *Phosphorus Sulfur Silicon Relat Elem* 183:1884–1891
 31. Wang T, He HW (2008) An efficient synthesis of sodium methyl α -(substituted phenoxyacetoxy)alkylphosphinates. *Phosphorus Sulfur and Silicon Relat Elem* 183:644–645
 32. He HW, Li MQ, Lu AH et al (2002) Synthesis and biological activities of methyl 1-(5-methyl isoxazol-3-oxy acetoxy) alkyl methyl phosphinates. *Phosphorus Sulfur Silicon Relat Elem* 177:1651–1655
 33. Wang CB, Xu C, Tan XS et al (2012) The asymmetric synthesis of chiral cyclic α -hydroxy phosphonates and quaternary cyclic α -hydroxy phosphonates. *Org Biomol Chem* 10:1680–1685

Index

A

Absolute configuration, 37, 271, 281, 284, 287, 290, 293, 294, 308, 313, 314
Acetyl Coenzyme A (Acetyl CoA), 10, 12–14, 336
Acetylphosphonate, 221
Active compound, 9, 33, 46, 179, 222, 279, 308, 314, 326
Active site, 14, 17–19, 21, 37, 324, 326
Acute aquatic toxicity, 37, 280, 310, 316–318
Acute toxicity, 252, 260, 316, 340, 377, 388, 390
Acylphosphinate, 20, 21, 24, 26, 30, 33, 38, 123, 179, 180, 323, 335, 347, 355
Acylphosphonate, 20, 21, 24, 26, 30, 33, 38, 47, 88, 91, 123, 179, 180, 323, 335, 347, 355
Agrochemical, 1, 5, 9, 22, 35, 124, 215, 324, 359
Al(III) complexes, 282–284, 431, 433
Alkali metal, 32, 123, 125–128, 133, 148, 154, 155, 164, 166, 407, 411
Alkylphosphonate, 26, 30–39, 45–54, 56, 58, 66, 67, 70, 82–84, 86, 89–91, 93, 116, 117, 119, 123–130, 134, 136–150, 152, 154, 155, 165–168, 172, 175, 177, 179, 180, 185, 197, 204–206, 221–223, 228–233, 241, 247, 259, 271, 279–283, 286, 287, 291–298, 300, 301, 303, 305, 306, 308–310, 313, 314, 316–318, 323, 335, 346, 347, 354, 381, 391–393, 398–400, 406–411, 413, 414, 423, 424, 426–428, 431–433
Alligatorweed, 255, 257
Al-Schiff base, 282, 291
Aluminium chloride, 415
Aluminium trichloride, 182, 183, 414
Ambient temperature, 361, 416
American sloughgrass, 305, 307, 382

Aminium salts, 33, 124, 172, 177, 413
Annual bluegrass, 305, 307, 365, 382
Antibacterial activity, 18
Aquatic toxicity, 37, 280, 310, 316–318
Arbuzov reaction, 289, 290, 311, 437
Aromatic ring, 188, 216, 234, 264
Asia minor bluegrass, 305, 307, 382
Asian copperleaf, 368, 373, 374, 376, 386
Asymmetric hydrogenation, 280, 310–312
Asymmetric hydrophosphonylation, 283, 284, 286, 287, 291, 292
Asymmetric synthesis, 37, 280, 282–284, 288, 290, 310
Auxin-type herbicide, 67, 347

B

Bactericidal activities, 18
Ball cabbage, 255, 257
Barnyard grass, 27, 33, 34, 65, 66, 68, 70–73, 75, 81, 89, 90, 102, 103, 106, 108, 110, 112, 119, 133–148, 151, 153, 159–165, 172, 174–177, 192–205, 211–213, 217, 228–230, 241, 243–249, 253, 254, 268–273, 269, 314, 318, 343, 347, 364, 365, 444, 445
Base-catalysis addition, 49
Binding conformational analysis, 37, 325
Binding mode, 37, 323, 325, 345
Bioactivity, 31, 35, 181, 221, 325
Bioassay, 9, 35, 38, 67, 71, 82, 90, 104, 108, 133, 138, 144, 159, 172, 179, 180, 201, 204, 211, 217, 221, 222, 228, 230, 231, 241, 244, 248, 253, 258, 268, 270, 271, 296, 305, 307, 314, 323, 382
Bioavailability, 18
Biochemical experiment, 323, 354
Biochemical test, 16
Biochemistry mechanism, 9

- Bioisosterism, 33, 123, 154, 179
Biological activity, 9, 24, 34, 37, 116, 181, 214, 221, 261, 279–281, 310, 324, 359, 391, 443
Biological evaluation, 391
Biorational design, 9, 10, 12, 23, 39
Black nightshade, 374
Bog chickweed, 382
Bristlegrass, 82, 159, 162, 164, 165, 175, 192, 197, 198, 200, 205, 241, 243, 244, 246, 247, 249, 368, 382, 445
Broadleaf plant, 89, 308, 348
Broadleaf weed, 1, 31, 38, 46, 89, 91, 113, 115, 116, 123, 125, 175–177, 335, 355
Broad-leaved weed, 221, 244, 247, 251, 254, 255, 260, 270, 271, 273, 275, 359, 367, 371, 373, 374, 376, 380, 381, 383, 389
2-bromopropionic acid ester, 233, 262, 425
Bunge's smartweed, 373, 374
- C**
Cabbage type rape, 133, 134, 136, 138, 139, 144, 145, 159–161, 172, 174, 192, 201–203, 205, 210–213, 228–230, 241, 244–246, 248, 253, 254, 268, 271–273, 445
Caged bicyclic phosphate, 35, 36, 221, 261–263, 268, 270–273, 275, 429, 430
Candidate herbicide, 22, 39, 359
Carboxylate, 19, 26, 117, 155
Carboxylic acid ester, 233, 263, 293
Carrot, 89, 90, 365, 445
Catalytic mechanism, 12, 14, 24, 52, 283
Chemical control, 1
Chemical modification, 26, 28, 48, 65, 88, 323, 342, 345, 354
Chemical screening, 443
Chickweed, 255, 257, 305, 307–309, 371, 376, 382
Chili, 255, 258
Chinese cabbage, 364
Chinese Ixeris, 296–298
Chinese spinach, 65, 66, 376
Chingma abutilon, 82, 84, 102, 104, 107, 108, 149, 151, 153, 192, 197–200, 205, 241, 243, 244, 246–249, 253–255, 257, 296–300, 302, 304, 305, 309, 364, 373, 374, 376, 382, 384, 445
Chiral carbon, 36, 279, 284, 293, 310
Chiral centers, 236
Chiral herbicide, 37, 279
Chiral HPLC, 290, 294, 312, 442
Chiral HPLC analysis, 290, 294
Chiral reagent, 281, 289, 292, 434
Chiral Rh(I)-complexes, 311, 441
Chiral selectivity, 305, 308, 309
Chirality, 37, 279, 296
Chloroacetic acid, 49, 50, 126, 185, 231, 393
1-(Chloroacetoxy)alkylphosphonate, 48, 116, 119, 393, 406
Chlorotrimethylsilane, 155, 166
Cis-Tetrahydrothiamin pyrophosphate, 16
Citric acid cycle, 10
Clacyfos, 30, 34, 36–38, 108, 123, 165, 166, 177, 179, 221, 244, 247, 249, 251, 253, 255, 260, 279, 296, 299, 300, 308, 310, 335, 354, 359–362, 364–367, 370–380
Clover, 68, 72, 74, 75, 89, 90, 102, 103, 106, 110, 134, 135, 138, 140–143, 146, 147, 365, 445
Coenzyme, 11, 12, 16, 20, 24, 324, 336
Column chromatography, 391–393, 398, 406, 411, 413, 416, 421, 431–433, 435, 436
Common amaranth, 27, 68, 72, 74, 75, 89, 90, 102, 103, 106–108, 110, 112, 113, 134, 135, 141–144, 146, 147, 149, 151, 153, 154, 159, 162–165, 172, 175, 176, 192, 197, 199, 200, 205, 241, 243, 244, 246–255, 257, 260, 270, 296–300, 302, 304, 305, 309, 343, 347, 363, 366–368, 376, 382–386, 445
Common nipplewort, 372, 376
Common purslane, 175, 176, 375, 376, 383–386
Common vetch, 27, 372, 382
Comparative molecular field analysis (CoMFA), 324
Comparative molecular similarity indices analysis (CoMSIA), 324
Competitive inhibitor, 14, 20, 38, 123, 179, 180, 205, 355, 359
Cotton, 1, 4, 8, 22, 175, 255, 258, 383, 390, 446
Crab grass, 33, 34, 68, 70–72, 74, 75, 81–83, 89, 90, 102, 103, 106, 110, 112, 119, 134, 135, 137, 140–144, 146–148, 159, 162–165, 172, 175, 192–200, 204, 205, 217, 241, 243, 244, 246, 247, 249, 270, 346, 364, 365, 382, 445
Creeping thistle, 372, 376
Crop protection, 5, 10
Crop safety, 31, 37, 175, 221, 279, 280, 310, 355, 365, 383
Crop selectivity, 39, 89, 258, 365, 446
Crop selectivity test, 446

- Crystal structure, 16, 17, 20, 63, 64, 98–101, 133, 169, 191, 226, 227, 239, 239, 266, 268, 285, 287, 288
- Cucumber, 27, 65, 83, 85, 87, 88, 119, 191–195, 198, 204, 217, 218, 255, 256, 345, 346, 444, 445
- Curled dock, 255, 257, 365, 382
- Cyclic 1-hydroxyalkylphosphonates, 224, 225, 230, 233, 234, 262, 284–286, 296, 427–429, 433, 434
- Cyclic phosphonate, 35, 36, 221, 231, 233, 241, 244, 247, 255, 259–261, 271, 273, 275, 279, 286, 291, 292, 423, 431
- D**
- 2,4-D, 1, 36, 67, 70, 71, 73, 75, 76, 81, 83, 87, 91, 104, 105, 108–111, 113–115, 228, 230, 251, 253, 255, 259, 305, 347, 355, 376
- Dayflower, 376
- Decarboxylation, 10, 11, 14, 15, 19–21, 23–25, 324
- Degradation product, 362
- Dialkyl phosphonates, 48, 49, 281, 283, 285, 393
- Dichloro(methyl)phosphine, 183, 184, 414, 415
- 2,6-dichlorophenolindophenol (2,6-DCIP), 353
- Dicotyledon, 31, 32, 36, 65, 70, 71, 73, 75, 76, 109, 111, 135, 138, 140, 142, 144, 146, 149, 165, 194, 198, 199, 241, 247, 248, 251, 253, 254, 259, 260, 270, 296, 323, 336, 338, 343
- Dicotyledonous weed, 143, 144, 159, 164–166, 172, 175, 259, 343, 365, 382, 384
- Diethyl phosphonate, 117
- Dimethyl phosphonate, 49, 118, 391
- E**
- Eclipta, 104, 108, 241, 243, 244, 247, 249, 253, 260, 299, 302, 304, 305, 309, 373
- Emulsifier, 444
- Enantiomer, 216, 279, 280, 292, 293, 296, 299, 300, 308–310, 314, 316–318
- Enantiomeric excess (EE), 280, 282, 290, 293, 308, 442, 443
- Enantiomeric purity, 290, 291, 294, 295
- Enantiomeric selectivity, 37, 279, 280, 310, 314, 316, 318
- Enantioselective catalysts, 282
- Enantioselective hydrophosphonylation, 281, 282, 431, 433
- Enantioselective hydroxylation, 289, 292, 434
- Enantioselectivity, 281, 283, 284, 286, 291, 292, 313, 314, 316, 318
- Environmental safety, 37, 279, 280, 316, 317
- Enzyme, 9, 14, 15, 17, 19, 20, 23, 179, 323, 324, 326, 336, 339, 345, 348, 350–353
- Enzyme activity assay, 323, 337
- Enzyme catalytic mechanism, 14
- Enzyme inhibition, 34, 180, 205, 339, 345, 348, 354, 355
- Enzyme-selective inhibition, 22, 25, 323, 340, 354, 355
- Enzyme solution, 350, 352
- Esterase, 347
- Ethyl bromoacetate, 50, 215, 396
- Exothermic reaction, 422
- F**
- Feather finger grass, 372
- Field bindweed, 372
- Field chickweed, 175, 176, 257, 382
- Field mustard, 257
- Field trial, 38, 359, 370, 371, 375, 376, 386
- Fungicidal activity, 18
- Fungicide, 13, 18
- Fur-2-Yl, 31, 38, 342, 346
- Furyl, 31, 91, 231, 244, 247
- G**
- Giant foxtail, 102, 110, 365
- Glyphosate, 1, 5, 8, 9, 113–115, 251, 253, 255, 260, 380, 383
- Goosefoot, 82, 84, 112, 113, 149, 175, 251, 255, 305, 373, 376, 383, 386
- Green bristlegrass, 83, 163, 172, 175, 192, 197, 205, 244, 247, 249, 382, 445
- Greenhouse, 26, 38, 67, 75, 389, 446
- Greenhouse tests, 347
- H**
- Hairy bittercress, 89, 90, 445
- Halopyruvate, 13
- Henbit deadnettle, 371
- Herbicidal activity, 22, 24, 26, 30–38, 45, 47, 48, 65, 67, 70, 71, 73–76, 81, 83, 87, 88, 90, 102, 104, 105, 111, 376, 381–384, 443–445
- Herbicidal activity assessment, 443
- Herbicidal spectrum, 89
- Herbicide, 1, 2, 5, 6, 8, 9, 11, 12, 20, 22–25, 32, 36, 38, 39, 45, 47, 65, 67, 82, 88,

- 89, 91, 112, 116, 123, 179, 180, 228, 251, 260, 279, 310, 324, 335, 343, 345, 348, 365, 375, 379, 381, 383, 385, 390, 443
- Herbicide-resistant weed, 6, 8
- Heterocyclymethylphosphonates, 92, 93, 102, 116
- Hit compound, 25, 45, 221, 335
- Homolog, 345
- HPLC, 284, 287, 288, 290, 431, 434–436, 443
- HW02, 30, 34, 36–38, 88, 114, 179, 197, 244, 247, 249, 251, 255, 260, 279, 296, 299, 308, 310, 335, 354, 359
- HWS, 31, 37, 38, 179, 221, 279, 335, 354, 359, 381–386, 388–390
- Hydrolysis, 50, 93, 117, 126, 185, 215, 347, 361, 362, 378, 396
- Hydrophosphonylation, 222, 281, 282, 285, 287, 291, 423
- Hydroxyalkylphosphonate, 36, 48–51, 90, 93, 117, 126, 222, 223, 228, 230–233, 247, 259, 280–283, 286, 287, 291, 293, 313, 392, 393, 398, 433
- Hydroxyethylidene-TTP, 12, 19
- I**
- In vitro, 323, 336, 343, 347, 350–355, 381
- In vivo, 21, 180, 205, 316, 318, 347, 355
- Indian toothcup, 387
- Inhibitor, 8–10, 12–25, 32–34, 37–39, 47, 65, 83, 87, 91, 123, 154, 180, 194, 200, 204, 205, 222, 279, 281, 323, 324, 329, 331, 337, 340, 347, 352–354
- Inhibitor-enzyme, 331
- Inhibitory activity, 17, 32–34, 65, 87, 119, 123, 135, 138, 140, 142–147, 154, 159, 161, 162, 166, 173, 193–195, 197–201, 204–206, 211, 213, 215, 217, 228, 230, 244, 246, 248, 258, 268, 273, 296, 305, 308, 309, 327, 341–343, 345, 347, 348, 376, 444
- Inhibitory effect, 13, 68, 119, 123, 125, 134, 135, 140, 142, 159, 164–166, 172, 175, 192, 199, 201–203, 210, 213, 218, 228, 241, 244, 245, 248, 253, 254, 268, 271, 273, 274, 308, 366, 373, 385, 444, 446
- Inhibitory potency, 33, 37, 65, 67, 72, 74, 75, 82, 83, 85, 87–89, 103, 106, 110, 113, 124, 136, 137, 139–141, 143, 145–149, 151, 153, 154, 160–165, 174–176, 180, 192–196, 198–200, 202–204, 210, 212, 213, 217, 229, 242, 243, 245, 246, 248–250, 254, 257–270, 272, 297–300, 302, 304, 305, 307, 309, 315, 323, 336–338, 340–343, 345–349, 354, 355, 360, 364, 365, 371–375, 381, 384, 385, 444, 445
- Integrated pest management (IPM), 1
- Intermediate, 12, 14, 15, 16, 19–21, 48, 167, 215, 222, 281, 290, 293, 311, 316–318, 391, 421
- Iodomethane, 183, 414
- Iodotrimethylsilane, 155, 410
- Irreversible inhibition, 345
- Isoxazole, 34, 179, 214–216, 420
- J**
- Japanese alopecurus, 372, 382
- Japanese cayratia, 367, 368
- K**
- Kinetic experiment, 323, 338, 339, 352, 354, 355
- Kinetic parameter, 23
- Knotgrass, 372, 376, 382, 386, 388
- L**
- LC50 values, 316, 317
- Lead compound, 9, 46, 26, 29, 38
- Lead structure, 25, 31, 36, 45, 46, 65, 231, 323
- Leaf mustard, 112–115, 159, 162–165, 172, 175, 176, 192, 197–200, 241, 243, 244, 246–251, 253, 255, 257, 270, 296, 299, 300, 302, 304, 305, 307, 309, 347, 365, 368, 371, 382
- Lettuce, 119, 192–195, 198, 204, 217, 218
- Ligand, 282–285, 311–313, 318, 324, 325, 327, 330, 431, 433, 442
- Ligand screening, 312
- Lithium bromide, 126, 127, 407
- Lithium iodide, 126, 149
- Lobedleaf parbitis, 379
- M**
- Maize, 1, 8, 31, 36, 38, 89, 112, 113, 116, 175–177, 258, 260, 359, 365, 367, 373, 374, 379, 383, 384, 386, 390, 445
- Metabolic pathway, 16, 347, 348
- Metabolic product, 347, 348, 355
- Methyl iodide, 182
- Methylphosphonate, 26, 31, 38, 55, 56, 65, 76, 91, 93, 94, 103, 105–110, 116, 130,

- 221, 281, 284, 289–294, 296, 308–310, 359, 381, 435, 436
- Mitochondria, 350–352
- Mode of action, 5, 9, 23, 24, 37, 39, 279
- Modification, 27, 30, 31, 34, 45–47, 71, 74, 76, 88, 109, 124, 138, 142, 180, 181, 206, 211, 222, 231, 247, 253, 259, 261, 273, 323
- Molecular docking, 37, 323, 324, 330, 331, 345
- Molecular structure, 63, 98, 100, 133, 171, 185, 190, 191, 226, 239, 266, 285, 287, 288, 331
- Monocot weeds, 32, 89, 164, 166, 175, 244, 247, 249, 270
- Monocotyledon, 32, 36, 71, 73, 75, 76, 81, 90, 104, 105, 110, 111, 135, 138, 140–144, 146, 147, 149, 159, 164, 172, 194, 198, 199, 247–249, 251, 253, 259, 260, 268, 270, 305, 323, 337, 338, 343
- Monocotyledon plant, 337
- Monosodium salt, 32, 149, 155, 166, 213, 341, 342, 411
- Morning glory, 113, 115, 250–252, 255, 257, 383
- Mung bean, 38, 336–338, 341, 343, 345, 346, 351, 360
- N**
- Non-cross-validated analysis, 334
- Nonselective herbicide, 1, 5
- Nucleophilic addition, 48, 92, 184, 415
- Nutgrass, 368
- O**
- Open-chain dimethylphosphonate, 253
- Optically active, 36, 37, 280–282, 286, 287, 290–294, 296, 299, 300, 305, 308–311, 313, 314, 316, 318, 431–436, 441, 442
- Optimization, 9, 24, 25, 28, 30–32, 36, 38, 39, 45, 47, 91, 286, 313, 323, 335
- Organic phosphorus compound, 24, 221
- Organophosphorus, 378
- Oxaziridine-mediated hydroxylation, 289, 291, 292
- Oxidase, 347
- P**
- Packing diagram, 63, 64, 98–101, 133, 134, 169, 171, 191, 227, 240, 267, 286, 289
- Partial least-square (PLS) methodology, 334
- PDHc, 8, 10–24, 89
- PDHc inhibitor, 13, 14, 18, 24, 38, 323, 338
- Pea, 336, 337, 340, 341, 343, 347, 350, 354, 355
- Petri dish method, 133, 134, 138, 144, 159, 201, 241, 246, 248, 253
- Phenoxyacetate, 32, 90
- Phenoxyacetyl chloride, 50, 92, 93, 126, 182, 184, 204, 231, 259, 263, 292, 293, 308, 310, 396, 398, 416, 426, 436
- Phenoxypropionyl chloride, 232, 262, 426, 429
- 1-Phenyl-3-Hydroxy-1,2,4-Triazole, 116, 117, 119, 406
- Phosphinate, 21, 24–26, 30, 33, 34, 91, 123, 126, 179, 180, 186, 191, 195, 197, 204, 206, 213, 216
- Phosphonate, 14, 24–26, 32–35, 37
- Phosphorus, 58, 60, 62, 88, 96, 118, 131, 138, 167–169, 180, 188, 208, 213, 216, 224, 236, 264
- Phosphorus oxychloride, 261, 262, 429
- Phosphorus trichloride, 126, 182, 183, 215, 223, 414, 415, 423
- Photodegradation, 362
- Physicochemical data, 392, 393, 396, 398, 401, 404, 406, 408, 411, 413, 416–418, 420, 422, 424–426, 428, 430, 431, 433–436, 438, 441, 442
- Phytotoxicity, 22, 24, 38, 180, 360, 365, 373, 376
- Pickeral weed, 255, 257
- Pig's knee, 368
- Pinkhead smartweed, 376
- Plant growth, 107, 124, 344, 366
- Post-emergence, 1, 21, 30–33, 36, 38, 68, 70, 71, 73, 76, 81–83, 88–90, 103, 108, 109, 111–115, 134, 135, 138, 142–144, 147, 149, 159, 164, 166, 175, 177, 192–194, 197, 198, 201, 204, 205, 244, 246, 249–251, 253, 260, 270, 275, 296, 300, 309, 335, 383
- Potassium iodide, 126, 127, 407
- Prediction of the activities, 324, 330, 334
- Pre-emergence, 34, 70, 71, 73, 75, 76, 81, 82, 104, 105, 110, 112, 135, 138, 140, 142, 144, 146–149, 192, 193, 195, 197, 199, 200, 204, 253, 271, 296, 308, 346, 444, 445
- Pre-emergence activity, 32, 110, 138, 195, 197, 299
- 1,3-Propanediol, 223, 422
- Prostrate false pimpernel, 387
- Pudovik reaction, 222, 230, 282, 283
- Purification, 353, 397, 411, 416, 421

- Pyridine, 51, 52, 93, 127, 224, 393, 398, 436
Pyridyl, 31, 91, 109, 111, 181, 204
Pyruvate, 10–16, 19, 21, 24
Pyruvate analog, 14, 323
Pyruvate dehydrogenase complex (Pdhc), 8, 10, 123
Pyruvic acid, 13–15, 32, 123
- R**
Racemate crystal, 100
Radish, 255, 258
Rape, 258, 268, 271, 273, 314, 318, 347, 365, 383, 446
Resistance, 5, 374
Rhodium-catalyzed Hydrogenation, 313, 314, 318
Rice, 336–338, 340, 341, 343, 346, 351, 354, 360, 365, 367, 383, 445
Ricefield flatsedge, 382
- S**
Safety evaluation, 258
Salts of alkylphosphonates, 32, 123, 166, 179, 413
Schiff base, 282–284
Schotten-Baumann condition, 293, 308
Sedge weed, 38, 359, 374, 376, 390
Selective demethylation, 124, 166
Selective enzyme inhibition, 339
Selective herbicide, 24, 113, 343, 381
Selective inhibition, 22, 23, 338–340, 343, 354
Selectivity, 13, 17, 25, 31, 33, 36, 38, 89, 116, 179, 194, 197, 198, 204, 221, 253, 258, 260, 364, 380
Setose thistle, 27, 119, 193, 197, 198, 217
Shepherd's purse, 371
Shortawn foxtail, 382
Siberian cocklebur, 89, 374, 445
Sickle senna, 175, 382
Single-crystal, 239, 287, 442
Site of action, 5, 6, 12, 13
Slender Amaranth, 112, 113, 373, 376, 383
Small goosefoot, 159, 163, 165, 172, 305, 382
Sodium iodide, 126, 127, 149, 391, 407, 410, 419
Sodium methylacetylphosphonate, 14, 15, 179
Sodium monomethylacetylphosphonate, 14, 15, 19
Solvent-free catalytic process, 49
Southern crabgrass, 382
Soybean, 1, 8, 175–177, 255, 258, 365, 383, 446
Spectrophotometer, 350, 352
Spectroscopic analysis, 20, 36, 56, 93, 155, 168, 208, 216, 234, 263
Spiny amaranth, 82, 84, 112, 383, 445
Spotted spurge, 387
Stereoselective hydroxylation, 281, 282
Structural characterization, 391
Structural optimization, 9, 36
Structure-activity, 36, 37, 155, 167, 206, 231, 271, 323, 324
Structure-activity relationship (3D-QSAR), 37, 324
Structure-activity relationship (SAR), 46, 271
Structure-herbicide activity relationship, 87, 111
Structure-inhibitory potency relationship, 341
Substituted benzylphosphonate, 292, 310, 432
Substituted phenol, 48, 49, 126, 232, 292, 393, 425
Substituted phenoxyacetic acid, 48–50, 93, 126, 184, 261, 347, 393, 397
Substituted phenoxyacetyl chloride, 48, 51, 90, 93, 116, 182, 186, 231, 261, 273, 280, 293, 297, 426, 429, 437
Substituted phenoxypropionic acid, 425
Substituted phenoxypropionyl chloride, 262, 273, 425
Sugar beet, 383
Superoxide dismutase, 339, 354
Synthetic procedure, 56, 155, 168, 186, 223, 234, 294, 313, 391
Synthetic strategy, 91
Systemic activity, 359
- T**
Tall buttercup, 376
Tall fescue, 374–376
Target enzyme, 12
Tautomeric form, 283
Tautomerism, 285
T-Butylamine, 124, 166–168, 413
Tetrabutylammonium, 117, 118, 406
Theoretical calculation, 323
Thiamine diphosphate, 324
Thiamin Pyrophosphate (TPP), 13, 16, 19
2-Thiazolone, 16, 19
2-Thiazolthione, 16
Thienyl, 31, 109, 181, 215
Thionyl chloride, 50, 184, 215, 262, 391, 396, 397, 421, 426

- TLC, 391, 411, 432
Tomato, 65, 66, 255
Toxicities, 316, 317
Toxicity, 37–39, 87, 279, 280, 310, 316–318, 340, 377, 388
Toxicity evaluation, 377, 388
TPP analog, 16, 17
TPP-dependent enzyme, 16
Trans-tetrahydrothiamin pyrophosphate, 16
Triazole, 17, 46, 116
1,2,4-triazole, 117, 405
Tricarboxylic acid cycle, 12
Triethylamine, 49, 92, 93, 168, 222, 232, 234, 262, 263, 391, 416, 423, 426, 429, 436
- U**
Ultraviolet-visible spectrophotometer, 352
Unit cell, 63, 98, 100, 133, 191
- W**
Water chickweed, 376
Water dropwort, 372
Water flea, 316–318
Water pepper, 376
Weeds control, 1, 22, 335, 343, 359, 374, 383
Weed spectrum, 255
Wheat, 8, 34, 36, 38, 65, 89, 176, 192, 194, 195, 197, 198, 204, 205, 215, 217, 258, 260, 367, 371, 376, 383, 389, 445
White eclipta, 89, 90, 102, 107, 108, 175, 241, 243, 246, 248, 249, 252, 254, 255, 260, 299, 300, 374, 382, 445
White mustard, 21
Wild oat, 21, 65, 66, 371
Wild vetch, 255, 257
Wolf's milk, 376
- X**
X-ray single-crystal diffraction, 64, 100, 101, 130, 187, 223, 227, 239, 263, 268
- Y**
Yellow bristlegrass, 368